Utilising Anionic Branched Polymerisation Techniques for the Synthesis of Novel Nanoparticles

Thesis submitted for the degree of Doctor of Philosophy by Tamara Alhilfi

February 2014

Declaration

Except where specific reference has been made to external sources, the work presented in this thesis is the work of the author. I hereby declare that this thesis has not been submitted, in whole or in part, in support of an application for another degree or qualification of this or any other University institutes of learning.

Signature: ..... Date: .....

Tamara K. Alhilfi

Abstract

Anionic polymerisation techniques have been optimised to develop a "one-pot", facile method to produce both linear and branched polystyrenes utilising the "Strathclyde" route to highly branched structures. ATRP was investigated as a possible method but anionic polymerisation was found to give much better control over the size and structure of polystyrenes produced.

Using this anionic polymerisation relatively monodisperse linear polystyrenes were synthesised with dispersity values as low as 1.03 for a polystyrene chain with a targeted degree of polymerisation (DP_n) of 100 monomer units. A number of different structures of branched polystyrene were synthesised, and their different physical properties examined by viscometry measurements and differential calorimetry scanning experiments. It has been found that very dense, highly branched materials (with approximations of 48 polymer chains branched together) can be synthesised with a targeted primary chain DP_n = 10 monomer units. Weight average molecular weight (M_w) values as high as 992,000 $gmol^{-1}$ for branched polystyrene can be synthesised with a primary chain length of DP_n =50 monomer units.

Functional polystyrenes were synthesised both by initiation with an amine containing compound and *sec*-BuLi, resulting in chain end functionalisation, and also post-functionalised by sulphonation of synthesised polystyrenes, resulting in a statistical distribution along the polymer chains pendant groups. The hydrophilicity could be

manipulated by the percentage of sulphonation. At over 30% sulphonation of the pendant polystyrene groups, the polymers become water soluble.

Polymer nanoparticles have been synthesised by a nanoprecipitation method from functionalised branched polystyrene synthesised by anionic polymerisation techniques. Nanoparticles synthesised from DP_n10 branched sulphonated polystyrenes were analysed by dynamic light scattering and found to be approximately 60nm with dispersity values as low as 0.15. They were found to be stable after 6 months ambienmt storage, and some preliminary testing on the encapsulation of Oil red suggests that the nanoparticles may be capable of encapsulating hydrophobic drugs.

Acknowledgments

I would like firstly to dedicate this thesis to my Mum, Dad, Nana, and sisters Jennan and Rhea. I feel extremely lucky to have had their continual love, help, advice and support throughout this entire process, and I am constantly thankful for the amazing family that I have.

I would like to thank my supervisor Steve Rannard at the University of Liverpool for the opportunities afforded to me over these four years, and also for his encouragement and positivity. I would like to thank all the members of the Rannard Group, particular thanks to Fiona Hatton for her help with SEM analysis, Jane Ford for her help with the sulphonated polystyrene studies and Pierre Chambon for his invaluable help, innovative ideas, advice and unwavering patience.

I would like to thank the technical staff at the University of Liverpool, and thanks to Sean Higgins of the Centre for Materials Discovery for his training and help with differential scanning calorimetry experiments.

Special mention to my friends within the department, who have made these last four years much easier, and made me feel welcome in a new city.

Table of Contents

List of Figures

Chapter 7

List of Tables

Chapter 4

Chapter 5

List of Schemes

Chapter 1

Chapter 7

Acronyms

ADPE	4,4'-vinylidenebis(N,N-dimethylaniline), often referred to as 1,1-bis(4-dimethylamino phenyl)ethylene
AIDS	Acquired Immunodeficiency Syndrome
ARV	Antiretroviral
ATRP	Atom Transfer Radical Polymerisation
BBB	Blood Brain Barrier
CMC	Critical Micelle Concentration
CNS	Central Nervous System
CRP	Controlled Radical Polymerisation
CTA	Chain Transfer Agent
DCE	Dichloroethane
DLS	Dynamic Light Scattering
DMSO	Dimethyl Sulphoxide
DNA	Deoxyribonucleaic Acid
DOX	Doxorubicin
DP_n	Degree of Polymerisation (related to M_n)
DP_w	Degree of Polymerisation (related to M_w)
DVB	Divinylbenzene
EPR	Enhanced Permeability and Retention effect
FDA	US Food and Drug Administration
FRP	Free Radical Polymerisation
g	Grams
GPC	Gel Permeation Chromatography
HAART	Highly Active Antiretroviral Therapy
HIV	Human Immunodeficiency Virus
mg	Milligrams

mL	Millilitres
M_n	Number Average Molecular Weight
M_w	Weight Average Molecular Weight
MRI	Magnetic Resonance Imaging
nm	Nanometers
NMP	Nitroxide-Mediated Polymerisation
NMR	Nuclear Magnetic Resonance
^{13}C NMR	Carbon Nuclear Magnetic Resonance
^{1}H NMR	Proton Nuclear Magnetic Resonance
PEG	Polyethyleneglycol
PS	Polystyrene
RAFT	Reversible Addition Fragmentation Chain Transfer Polymerisation
RNA	Ribonucleaic Acid
SCVP	Self-condensing Vinyl Polymerisation
***sec*-BuLi**	Secondary butyllithium
SEM	Scanning Electron Microscopy
***tert*-BuLi**	Tertiary butyllithium
TMEDA	*N*,*N*,*N*′,*N*′-Tetramethylethylenediamine
THF	Tetrahydrofuran
UNAIDS	United Nation & AIDS
VPOB	4-bis(4-vinylphenoxy)butane
VPODD	12-bis(4-vinylphenoxy)dodecane
VPOHEX	6-bis(4-vinylphenoxy)hexane
VPOOC	8-bis(4-vinylphenoxy)octane
VPOPARAX	4-bis(4-vinylphenoxy) *p*-xylene
VPOT	10-bis(4-vinylphenoxy)decane
WHO	World Health Organisation

Chapter 1

Introduction

1.1 Drug delivery by nanotechnology

Nanotechnology is defined as science, engineering, and technology conducted at the nanoscale, which is defined as ranging from 1 to 100 nanometers. [1] An important area within the nanotechnology field is nanomedicine, which, according to the National Institutes of Health (NIH) Nanomedicine Roadmap Initiative, refers to highly specific medical intervention at the molecular scale for diagnosis, prevention and treatment of diseases. [2]

Drug delivery is the process of transporting a pharmaceutical drug through the body to the site where it can deliver the desired therapeutic effects. There are many issues with the delivery of drugs to the body, including transport through the blood brain barrier, [3] and for oral therapeutics the absorption from the gastrointestinal tract. [4] However a significant issue with drug delivery is the solubility of the drug [5]. Even for drugs that easily cross the intenstinal mucosa, the onset of drug levels will be dependent on the time required for the drug to dissolve. We can define a drug as being 'poorly soluble' when its dissolution rate is so slow that dissolution takes longer than the transit time past its absorptive sites, resulting in incomplete bioavailability. [6] Poor bioavailabity of drugs is one of the biggest challenges regarding drug delivery. If drugs have a poor bioavailability this leads to higher dosages being needed, which can often lead to toxicological effects and unpleasant side effects in patients. [7]

Nanomedicine and nanotechnology has already made a significant impact on the development of drug delivery systems, such as the use of nanoparticles in gene therapy to treat cancer [8], and there are many different types of nanotechnology-based therapeutics currently being explored; these are considered briefly below.

1.1 1. Nanocrystals

Nanocrystals are crystals with a size in the nanometer range and are nanoparticles with a crystalline character. [9] Nanocrystals can be formed by building particles up from the molecular state, as in precipitation [10], or by breaking larger micron-sized particles down, by processes such as milling [11], [12].

The Elan milling process [13] is the most commonly used technology, however, recent advances in milling have been used to produce XPclad® nanoparticles [14]. Chen *et al* used planetary ball milling to generate particles of uniform size systemic, cutaneous, or oral administration of cancer drugs, vaccines, or therapeutic proteins. [15]

1.1.2 Nanosuspensions

An issue with many therapeutics is they are poorly soluble in water. Conventional approaches often attempt to solubilise insoluble drugs with the use of excessive amounts of co-solvents or surfactants, but this can pose toxicity problems, relating to the solvent or added surface active materials. An alternative way to overcome the poor solubility of many drugs is the formulation of nanosuspensions consisting of the water insoluble drug nanoparticles dispersed in a liquid media together with minimal quantities of surface stabilising agents. [16]

Nanosuspensions overcome delivery issues for these compounds by obviating the need to dissolve them, and by maintaining the drug in a preferred size that is sufficiently small for pharmaceutical acceptability. They can be prepared by different methods. For example Muller and Peters formulated nanosuspensions of poorly soluble intravenous drugs by high pressure homogenisation. [17] Meanwhile Na *et al* prepared suspensions of ethyl diatrizoate nanocrystals by wet milling in the presence of the surfactant poloxamine 908 [18] and Zhang *et al* prepared all-trans retinoic acid (ATRA) nanosuspensions by a modified precipitation method where the ATRA solution in acetone was injected into pure water by an air compressor under the action of ultrasonication. [19] Alternatively emulsion template freeze-drying [20] has been utilised to generate amorphous nanosuspensions for the treatment of HIV/AIDS. [21]

1.1.3 Magnetic Nanoparticles

Magnetic nanoparticles have traditionally been used as diagnostic agents such as contrast agents for MRI imaging, but they have recently received attention as targeted drug delivery systems. [22] Magnetic targeting has advantages for drug delivery, in particular, the ability to target a specific site, such as a tumour and enhancing the uptake at this target site could result in effective treatment at lower doses. Iron oxide nanoparticles have been synthesised and explored as drug delivery agents. [23], [24], [25] However, iron oxide has a relatively low magnetic moment. Alternatively cobalt nanocrystals produce high magnetic moment, but their biological applications are limited by their poor biocompatibility and resistance to oxidation.

To help achieve better biocompatibility and stability, more recently Bao and Krishnan synthesised gold coated, high magnetic moment cobalt nanocrystals with narrow size

distributions and controlled shapes. In addition, combined with well-established gold–thiol surface chemistry, these cobalt/gold core-shell nanocrystals can be functionalised further with proteins, DNA and other bio-molecules, thereby opening up possibilities in bio-labelling, magnetic separation and optical sensing. [26]

1.1.4 Liposomes

Phospholipids are composed of a hydrophilic head and two hydrophobic tails. The formation of vesicles, or liposomes, occurs in aqueous media due to the minimisation of interfacial tension between the water and the hydrophobic tails, combined with the hydrophilic interaction of the phospholipid head groups with water. Liposomes consist of simple lipid bilayers that resemble biological membranes, in the form of a spherical shell. They are regarded as good drug delivery systems [27] because of their ability to encapsulate drugs either in the phospholipid bilayer, in the entrapped aqueous volume [28] or at the bilayer interface [29].

Liposomes have the advantage of being non-toxic and biodegradable as they are composed of naturally occurring lipids [30] and they can also be modified to target specific sites. [31] For example, Ahmed *et al* entrapped the anti-cancer drug doxyrubicin in liposomes containing lipid derivatives of polyethylene glycol. Specific antibodies that targeted KLN-205 squamous cell carcinoma of the lung were attached at the liposome surface. [32]

1.1.5 Current Nanotherapies in use.

There are many US Food and Drug Administration (FDA) approved nanotechnologies currently being used to treat both chronic and acute diseases and symptoms. Table 1.1

gives a summary of some of these, taken from a more comprehensive list compiled in 2008 by Bawa. [33]

Table 1.1: Examples of FDA approved nanotechnologies currently being used therapeutically

Product/ Brand name	Nanoparticle drug component/ Active ingredient (s)	Delivery Route	FDA approved indication (s)
Doxil	Pegylated doxorubicin HCl liposomes	Intravenous (IV)	Metastatic ovarian cancer and AIDS related Kaposi's sarcoma
Abraxane	Paclitaxil bound albumin nanoparticles	IV	Metastatic breast cancer patients
Estrasorb	Estradiol hemihydrate micellar nanoparticles (emulsion)	transdermal	Reduction of vasomotor symptoms in menopausal women (hot flushes/ night sweats)
Abelcet	Amphoteracin B phospholipid complex	IV	Invasive fungal infections
Triglide	Nanocrystalline fenofibrate	Oral tablets	Lipid disorders

1.3 Nanotechnologies used as cancer therapeutics

One of the main areas currently of interest in nanotechnology research is the use of nanoparticles as cancer therapeutics. Cancer is a term used for diseases in which abnormal cells divide without control and are able to invade other tissues. Cancer cells can spread to other parts of the body through the blood and lymph systems. [34] Tumours arise due to accumulation of multiple genetic alterations (e.g. mutations, deletions, translocations) and epigenetic changes (e.g. promoter methylation) in cells. These changes result in abnormal (neoplastic) cell growth, forming a mass of tumour cells, that persists in the absence of the initiating causes. [35]

Most solid tumors possess unique pathophysiological characteristics [36] that are not observed in normal tissues or organs, such as:

- extensive angiogenesis; the physiological process through which new blood vessels form from pre-existing vessels, leading to an increased number or concentration of blood vessels
- defective vascular architecture
- impaired lymphatic drainage/recovery system

These anatomical and pathophysiological differences lead to a therapeutic opportunity through the phenomenon known as the enhanced permeability and retention (EPR) effect. The increased angiogenesis leads to high vascular density in solid tumours, large gaps can exist between endothelial cells in tumour blood vessels, and tumour tissues show selective leakage and retention of macromolecular drugs. [37]

This pathological uniqueness has been exploited in the research of cancer therapeutics and there have been many advances related to nanomedicines, using the EPR effect. Based on the EPR effect, many particulate drugs are being developed as a new class of antitumor agents include nanoparticles, polymer micelles and liposomes. [38]

Whereas in other nanotechnologies the focus has often been on specific targeting, such as the nanoparticles developed by Hilgenbrink and Low that targets the folic acid receptor which is overexpressed in various human carcinomas, [39] EPR is a passive targeting mechanism.

1.3 Nanomedicine and HIV/AIDS

Another therapy area where passive targeting could be of use is in the treatment of human immunodeficiency virus (HIV) and acquired immunodeficiency disorder (AIDS). HIV/AIDS is one of the leading causes of death in the world. According to the 2011 United Nations AIDS programme (UNAIDS) AIDS epidemic update, which use data supplied by the World Health Organisation, [40] the number of people living with HIV/AIDS in 2011 was estimated to be 34.2 million, with 3.4 million of those being children under 15 years of age. Additionally there were 1.7 million AIDS-related deaths, of which 230,000 were children under the age of 15 years. To put the impact of HIV and AIDS on the world into context, Weiss stated that in 2004 the death toll from HIV/AIDS worldwide was equivalent to three World Trade Centre attacks happening per day [41]. For a more local perspective it is important to note that the United Kingdom in 2010 had the highest percentage of new HIV infections in Europe.

People infected with HIV are now living longer largely due to the management of HIV by the use of antiretroviral drugs. The treatment of HIV has improved dramatically since the first therapies and the most common, and effective treatment utilises antiretroviral (ARV) drugs which can suppress the HIV virus and stop the progression of the HIV disease to AIDS. There are currently 9.7 million people globally who are currently receiving antiretroviral drug therapy. However, this is only 65% of the stated UN target of 15 million in June 2011. [42] This is illustrated in the UNAIDS and WHO map in Figure 1.1.

To understand the effect of these ARV drugs on the HIV virus, first the process of HIV replication must be discussed. HIV can be passed on through infected semen, vaginal fluids, [43] rectal secretions, [44] blood, or mother to child transmission. [45] The most

common ways HIV is passed on are through sex without a condom, or sharing infected needles, syringes or other intravenous drug equipment. [46]

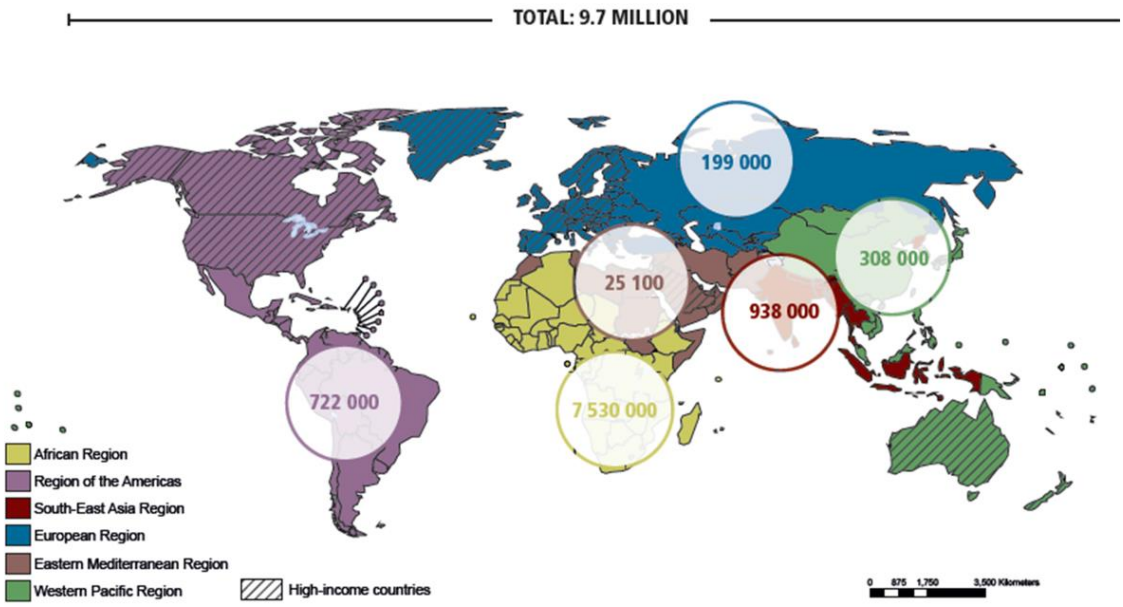

Figure 1. 1: UNAIDS and WHO map of patients currently receiving antiretroviral therapy [40].

Once a human is infected, the HIV viral capsid fuses to a host cell surface. The HIV ribonucleaic acid (RNA), reverse transcriptase, integrase and other viral proteins enter the host cell. Viral deoxyribonucleaic acid (DNA) is then formed by reverse transcription. Reverse transcription is the process of making a double stranded DNA molecule from a single stranded RNA template, through the reverse transcriptase enzyme.

The viral DNA is transported across the nucleus and integrates into the host DNA. New viral RNA is used as genomic RNA to make viral proteins which move to the cell surface and a new HIV viral capsid is formed. The virus matures by protease releasing individual HIV proteins. This entire process is illustrated in Figure 1.2.

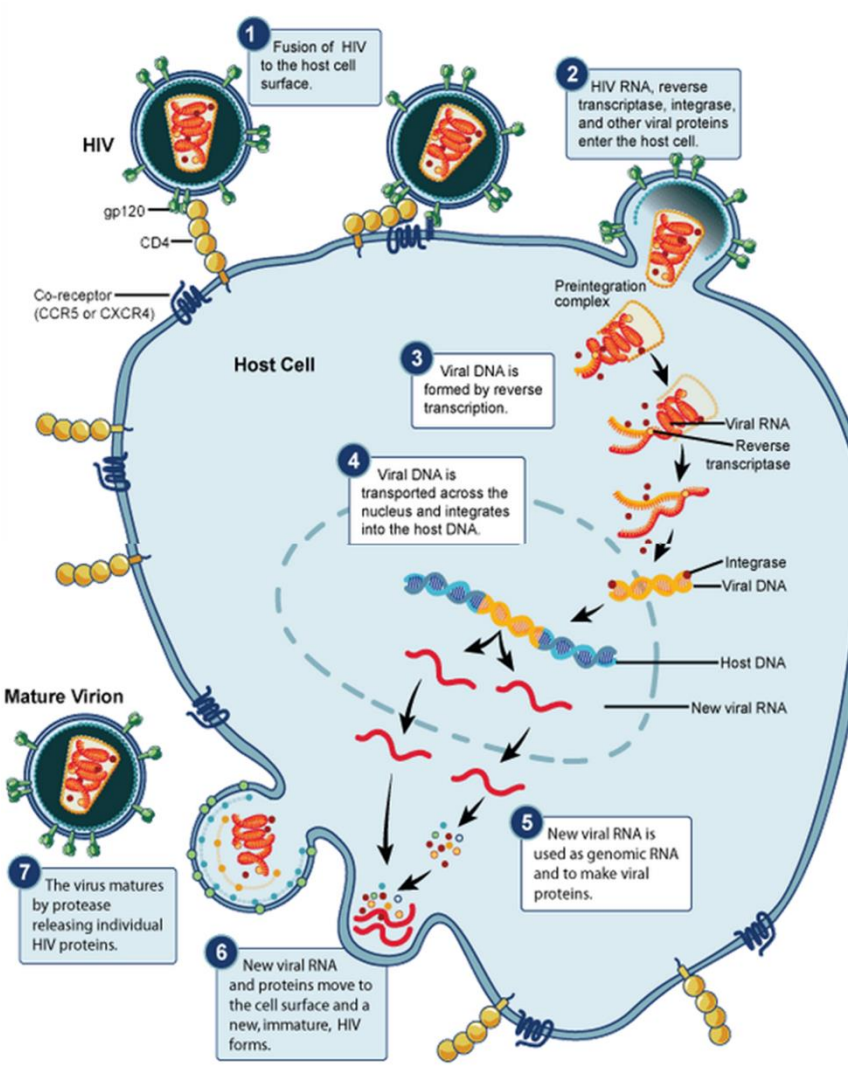

Figure 1.2: Schematic diagram of the HIV replication cycle [47]

Different ARV drugs have been developed to perform different tasks by targeting various aspects of the replication cycle to inhibit the HIV virus. There are many different types including;

- Integrase inhibitors which inhibit the integrase enzyme responsible for the integration of viral RNA into the DNA of the infected cell [48].
- Protease inhibitors block the viral protease enzyme necessary to produce mature virus particles upon cell division from the host membrane. [49]

- Nucleoside reverse transcriptase inhibitors (NRTI) and nucleotide reverse transcriptase inhibitors (NtRTI) are nucleoside and nucleotide analogues which inhibit reverse transcription. [50]
- Non-Nucleoside reverse transcriptase inhibitors (NNRTI) inhibit reverse transcriptase by binding to an allosteric site of the enzyme; where NNRTIs act as non-competitive inhibitors of reverse transcriptase. [51]
- Entry inhibitors (or fusion inhibitors) interfere with binding, fusion and entry of HIV-1 to the host cell. [52]

When several such drugs, typically three or four, are taken in combination, the approach is known as highly active antiretroviral therapy (HAART). [53] While these have proven to be effective in many cases, and help people infected with HIV live a longer, healthier life there are also many problems associated with HAART.

One of the main issues with these so called 'drug cocktails' is that large doses need to be taken due to the low bioavailability of the drugs, and this can lead to some very unpleasant side effects [54], [55] such as;

- nausea
- dizziness
- vomiting
- diarrhoea
- insomnia
- malaise
- taste abnormalities
- lipodystrophy
- skin rashes
- asthenia

Such side effects are often worse than the symptoms of HIV infection itself, which can lead to poor patient compliance when taking the HAART therapies. [56] It has been also found that as the complexity of the prescribed regimen increases, so do rates of non-adherence. [57] The long-term effectiveness of antiretroviral medication, is dependent upon strict adherence to the prescribed regimen, since HIV resistance to these drugs can develop with sub-therapeutic doses. [58] This can have a devastating effect on not only the individual's health, but also to public health as this can lead to strains of the virus that are resistant to antiretroviral drugs and therefore cannot be treated.

One key challenge in the treatment of HIV is to increase the bioavailability of ARV drugs so a decreased amount of drug can be taken, leading to a reduction in the unpleasant side effects, and hopefully better patient compliance with the therapy. It has been found that oral administration of therapeutic agents represents by far the easiest and most convenient route of drug delivery, especially in the case of chronic therapies [59]. However there are many challenges posed by adopting this method of administration. One of the most limiting steps can be the dissolution of the drug. In an attempt to overcome this problem there have been many reports of pure drug and polymer based nanotechnologies, which have been developed to target in particular increasing increased solubility, stability, bioavailability and targeting of anti-HIV drugs. [60]

Another major issue in HIV therapy is the existence of cellular and tissue-based viral sanctuary sites. Two possible sanctuary sites for HIV are the central nervous system (CNS), the testes [61] and the gut-associated lymphoid tissue (GALT). [62] Sanctuary sites are areas in the body that are poorly penetrated by dissolved molecules of the ARV

therapies. HIV is known to invade the CNS early in the course of the infection and primarily targets brain mononuclear macrophages. [63] It can enter the CNS through the blood brain barrier (BBB) in the form of infected white blood cells. Typically ARV drugs cannot cross the BBB so the brain can act as a sanctuary site for the HIV virus. The existence of sanctuary sites for HIV may potentially endanger the efficacy of ARV therapy in the long term and may even make eradication of HIV from the infected body impossible. [64]

As discussed earlier, in relation to cancerous cells and tumours, diseased cells can exhibit unusual properties and behave differently to normal cells. One area of specific interest within HIV research is the process of phagocytosis. Phagocytosis is the process of engulfing and ingestion of particles by the cell or a macrophage. [65] This is illustrated in Figure 1.3, which shows a scanning electron microscope image of two forms of phagocytosis of yeast cells (orange) by a strain of *T. Vaginalis* (green)

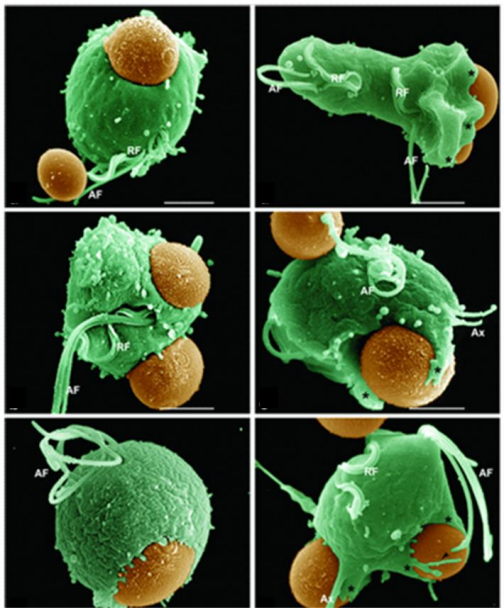

Figure 1.3: SEM image shown, illustrating two forms of phagocytosis of yeast cells (orange) by a strain of *T. Vaginalis* (green) [66]

It has been found that macrophages infected with HIV have enhanced phagocytic activity, and will uptake more particulate material by phagocytosis. [67] This could enable a similar type of passive targeting to that seen with the EPR effect in cancer therapies. If the phagocytic activity is increased in infected macrophages, they will be more likely to uptake particles than non-infected macrophages. If the particles are antiretroviral drugs, that have managed to cross the BBB then this leads to passive targeting where the infected macrophages are uptaking the drugs, leading potentially to lower doses and decreased side effects.

Nanotechnology has led to the ability to allow substances to permeate past the BBB. [68], [69] If a drug nanoparticle can be synthesised to be large enough to be engulfed by an infected macrophage this would have a huge benefit and lower the sanctuary sites available to the virus.

Another area that nanotechnology can offer novel technical solutions is the improved delivery of poorly water soluble drugs. There is great interest in this research as the antiretroviral drugs are very hydrophobic and therefore not water soluble. This may enable high dosing with reduced toxicity provided that toxic drug levels are not reached *in vivo*. If drugs are water soluble they may be small enough to diffuse into other cells, but they are not large enough to be engulfed by macrophages through the induction of phagocytosis. The aim of this PhD project is to synthesise a polymer nanoparticle containing antiretroviral drugs that is both stable in water, thus helping to overcome the issues of dissolution associated with the hydrophobic antiretroviral drugs, and also has a particle size large enough to be engulfed by macrophages during phagocytosis.

1.4 Polymer nanoparticles as drug delivery systems

Polymer nanoparticles can be produced by a range of routes including direct synthesis, for example in dendrimers, [70] or the synthesis of the components which then can either self assemble, in the case of vesicles or micelles, [71] or the components can react to form a single structure such as shell- and core-crosslinked micelles. [72]

1.4.1 Classic Polymer Micelles

Polymeric micelles often consist of a block copolymer with a hydrophobic block segment which constitutes the core and a hydrophilic block constituting the shell of the micelle. This arrangement facilitates their use as a drug delivery carrier and as a result, micelles are suitable for the solubilisation of poorly water soluble drugs, and offer protection against chemical degradation and metabolism and controlled release. Additionally, surface properties of micelles can be tailored by attaching hydrophilic blocks to antibodies or other ligands specific for the type of receptors present on the disease site. [73]

Molecules can be physically trapped in the hydrophobic inner core of functional micelles. Cammas *et al* physically entrapped doxorubicin (DOX) into the hydrophobic core of a polymeric micelle consisting of the block copolymer poly(α-hydroxy ethylene oxide-co-β-benzyl L-aspartate), (α-hyrdoxy PEO/PBLA). They determined the diameter of DOX-loaded *α*-hydroxy PEO/PBLA micelles to be approximately the same as the diameter of the corresponding empty micelles, at ca. 25 nm and showed that the DOX-loaded functional micelles were stable in solution, even in the presence of proteins. Furthermore, they found that the DOX-loaded α-hydroxy PEO/PBLA micelles had a higher cytotoxic effect against P388Dl leukemia cells than DOX-loaded

α-methoxy PEO/PBLA micelles, while both empty micelles were shown to be non-cytotoxic against P388Dl leukemia cells. [74]

Conversely Kwon *et al* developed an oil-in-water emulsion method to load poly(ethylene oxide)-*block*-poly(β-benzyl-L-aspartate) (PEO/PBLA) micelles with DOX. The level of DOX in PEO-PBLA micelles was 5–12% w/w. However they found the diameter of the micelle did increase with loading. The mean diameter of unloaded, PEO-PBLA micelles was ca. 19 nm and the mean diameter of PEO-PBLA micelles loaded with DOX was ca. 37 nm. Furthermore minimal chemical degradation of DOX occurred as a result of loading in PEO-PBLA micelles. In addition, DOX in PEO-PBLA micelles was shown to be less susceptible to chemical degradation than free DOX in aqueous solution. They also determined that it was possible to freeze-dry PEO-PBLA micelles loaded with DOX and obtain micelles loaded with drug upon reconstitution in water. The PEO-PBLA micelles were shown to release DOX slowly in contrast to other micellar systems. [75]

One of the important areas in HIV treatment where micelles could have a significant impact is in the transporting of drugs through the blood brain barrier (BBB). Poloxamers are nonionic triblock copolymers composed of a central hydrophobic chain of polyoxypropylene (poly(propylene oxide)) flanked by two hydrophilic chains of polyoxyethylene (poly(ethylene oxide)). [76] They are arranged in an A-B-A structure: EO_x-PO_y-EO_x. Due to their amphiphilic nature, these block copolymers are able to self-assemble into micelles in aqueous solutions above the critical micelle concentration (CMC) [77] and are also known as pluronic micelles. Pluronic micelles have been shown to be highly effective for BBB drug transport enhancement *in vitro* and *in vivo*. [78]

Kabanov and co-workers investigated the effect of Pluronic 85 on the BBB barrier by using polarised bovine brain microvessel endothelial cell (BBMEC) monolayers as an *in vitro* model of the BBB. They found that this block copolymer could increase membrane transport and transcellular permeability through BBMEC cells, suggesting benefits in the future design of formulations to increase brain absorption of selected drugs, such as antiretrovirals [79].

Lui *et al* synthesised polymeric micelles self-assembled from cholesterol-conjugated poly(ethylene glycol) (PEG) and anchored with transcriptional activator TAT peptide (TAT-PEG-b-Col) for delivery of antibiotics across the BBB. The antibiotic ciprofloxacin, which demonstrates a high bactericidal effect, was loaded into the micelles by a membrane dialysis method. These were characterised *via* dynamic light scattering (DLS) and scanning electron microscopy (SEM). Animal studies showed that these micelles crossed the BBB and entered the brain. They concluded that these TAT-conjugated micelles may be used to deliver antibiotics across the BBB for treatment of brain infections. [80]

Whilst it has been demonstrated that micelles can be effective drug delivery systems, one of the main disadvantages is related to the CMC. The CMC is the concentration of the amphiphillic block co-polymer above which micelles form. The conventional micelle drug delivery systems that are based on the linear amphiphilic copolymers suffer from instability *in vivo* the micelles are diluted in the bloodstream and tend to disassemble once the concentration falls below the CMC, thereby losing the benefits of the micelle and potentially resulting in the instant release of entrapped drug. [81]

1.4.2 Dendrimers

To overcome the disadvantage of classical micelles, unimolecular micelles/nanoparticles based on amphiphilic copolymers with dendritic or hyperbranched structure have been developed**.**

A dendrimer is a structure in which a central molecule branches repetitively. [82] There are several branching sites around the core units, arranged in a layer by layer fashion which defines the growth, size and the microenvironment within the dendrimer. [83] Dendrimers offer unique properties such as uniform particle size, poly-valency of the end groups which helps in binding to diverse receptors and an ability to bind a variety of targeting agents to their high density peripheral functional groups.

Drug molecules can be covalently attached onto the surface of dendrimers through the peripheral functional groups, to give dendrimer-drug conjugates. Malik *et al* conjugated *cis*-diaminedichloroplatinum(II), or cisplatin, the platinum-containing anti-cancer drug, to a polyamidoamine (PAMAM) dendrimer generation 3.5 with a sodium carboxylate surface. This gave a dendrimer-platinate (dendrimer-Pt; 20-25 wt% platinum) which was highly water soluble and released platinum slowly *in vitro*. *In vivo* the dendrimer-Pt and cisplatin were equally active against cancer cells. They also found that the dendrimer-Pt was also less toxic than cisplatin alone. [84]

Drug molecules can also be physically entrapped within the dendritic structure, giving rise to another way that dendrimers can be used as potential drug delivery systems. The nature of drug encapsulation within a dendrimer may be simple physical entrapment, or can involve non-bonding interactions with specific functionality within the dendrimer.

Johan *et al* synthesised dendritic 'boxes' by the construction of a chiral shell of protected amino acids onto poly(propyleneimine) dendrimers with 64 amine end groups. They captured guest molecules such as the Bengal Rose dye within the internal cavities of the 'boxes' when they were constructed in the presence of the guest molecules. They found that due to the bulky nature of the amino acid derivative they used for capping the dendrimer generated steric crowding and the presence of hydrogen bonding, the entrapped guest molecules were not able to diffuse out of the densely packed shell of the dendrimer into the surrounding solution. [85]

Another potential interaction between drugs and dendrimers involves electrostatic attachment due to the presence of large numbers of ionisable groups on the surface of the dendrimer structure. An example of this is the G4 polyamidoamine (PAMAM) dendrimer. Milhelm *et al* investigated the change in the solubility of the hydrophobic drug ibuprofen with an aqueous solution of polyamidoamine (PAMAM) G4 dendrimer and sodium dodecyl sulphate (SDS). They found that the PAMAM G4 dendrimer solution significantly enhanced the solubility of ibuprofen compared to 2% SDS solution alone, and that the solubility of ibuprofen in the dendrimer solution was directly proportional to dendrimer concentration and inversely proportional to temperature. They concluded that the influence of dendrimer solution pH on the solubility enhancement of ibuprofen suggested that it involved this electrostatic interaction between the carboxyl group of the ibuprofen molecule and the amine groups of the dendrimer molecule. [86]

A disadvantage of using dendrimers as highly branched polymer drug delivery systems is the synthesis of the structures, which is often complex and laborious. The greater the

generation of dendrimer, the more complicated the synthesis, often resulting in low yields [87].

1.4.3 Hyperbranched polymers

Hyperbranched polymers are highly branched polymers that are prepared through a one step polymerisation process. Many kinds of hyperbranched polymers have been investigated as novel macro molecules. [88] One method of producing polymers with both highly branched structures and numerous reactive groups is self-condensing vinyl polymerisation (SCVP). This method of producing hyperbranched polymer architectures was reported first by Frechet [89] in 1995 utilised an AB vinyl polymer to prepare a highly branched polymer. Scheme 1.1 outlines the basic concept of SCVP.

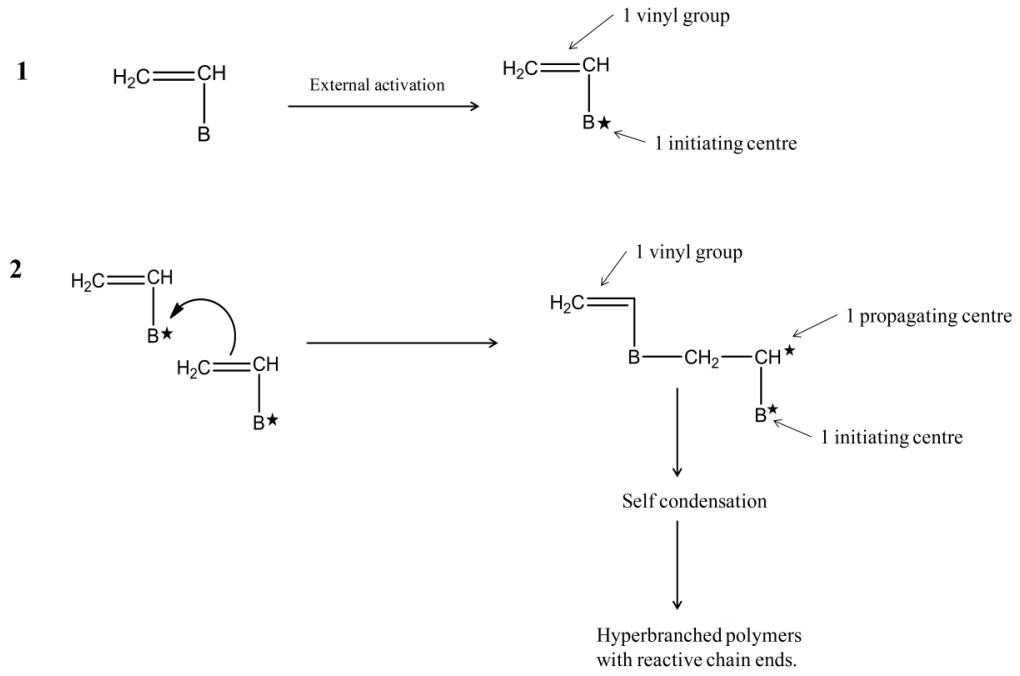

Scheme 1.1. Mechanism of self-condensing vinyl polymerisation. [89]

The vinyl AB monomer is chosen based on the ability of the B group to be activated to a B* moiety by an external activation stimulus. This activated B* is then itself capable

of initiating the polymerisation of a vinyl monomer by either radical or cationic polymerisation. The initiating B* group reacts with the double bond of another AB* monomer, giving the dimer shown in Scheme 1.1 (2). This dimer now has one initiating centre as well as a propagating centre, and the AB monomer has been turned effectively into an AB_2-type monomer. Highly branched, high molecular weight polymers are formed by the reaction of the activated AB* monomer, the dimer, and the larger oligomeric species produced by subsequent condensations.

Hawker *et al* utilised this principle, together with his earlier work regarding the use of well-defined uni-molecular initiators to initiate radical polymerizations with accurate control over molecular weights and chain ends, [90] to prepare hyperbranched polymers by controlled free radical polymerisation. [91]

1.5 Controlling polymer architecture

There are many different methods for synthesising varying architectures of branched polymers. One way of producing highly branched macromolecular structures involves coupling of end-reactive polymer molecules onto a multifunctional core. This is known as a "grafting onto" strategy and structures such as molecular brushes can be synthesised by this method.

Matyjaszewski and co-workers synthesised densely grafted polymers by the "grafting onto" method *via* a combination of atom transfer radical polymerisation (ATRP) and "click" reactions. Linear poly(2-hydroxyethyl methacrylate) (pHEMA) polymers were

synthesised first by ATRP. After esterification reactions between pentynoic acid and the hydroxyl side groups, polymeric backbones with alkynyl side groups on essentially every monomer unit (pHEMA-alkyne) were obtained. Five kinds of azido-terminated polymeric side chains (SCs) with different chemical compositions and molecular weights were used, including poly(ethylene glycol)-N3 (PEO-N3), polystyrene-N3, poly(n-butyl acrylate)-N3, and poly-(n-butyl acrylate)-b-polystyrene-N3. They found the alkyne functionality on backbones and azido functionality on polymeric SCs was very high. [92]

Another method is the "grafting from" strategy, which uses a multifunctional core as the initiator for a variety of "living"/controlled polymerisation reactions. This grafting-from strategy can also be used to grow a polymer from a solid surface, such as silica. Bottcher *et al* covalently bound the ATRP initiator (1,1'-chlorodimethylsilylundecyl)-2-chloro-2-phenylacetate to the surface of silica gel. ATRP grafting of styrene monomer from the silica surface was achieved and the grafts could be detached from the solid particles for analysis. After the polymerisation of a first generation of grafts, a second generation was grown showing that the chain ends of the grafts were still active to initiate a second monomer feed to further chain growth. [93] Similarly, Hawker and co-workers reported the ATRP grafting of methyl methacrylate from a silicon wafer surface using the ATRP initiator (5'-trichlorosilylpentyl)-2-bromo-2-methylpropionate. [94]

A common feature of the synthesis strategies summarised above is that they can result in multi-step polymerizations, end-group modifications and architectures that tether one or both polymer chain-ends to the growing macromolecule i.e. the polymer chain ends

constitute the branch points. In 2007 Rannard and co-workers [95] reported controlled polymerisation approaches that built on the Sherrington group work. The Sherrington group reported the introduction of combinations of chain transfer and divinyl branching monomers in the conventional free radical polymerisation of monovinyl monomers and the formation of high molecular weight branched polymers and branched block and graft copolymers. Gelation is avoided by the careful balance of the concentration of brancher and chain transfer agents in order to maintain less than one brancher monomer per primary polymer chain. [96], [97]

Figure 1.4 illustrates the "Strathclyde Route" for producing soluble, high molecular weight branched polymers by conventional free radical polymerisation.

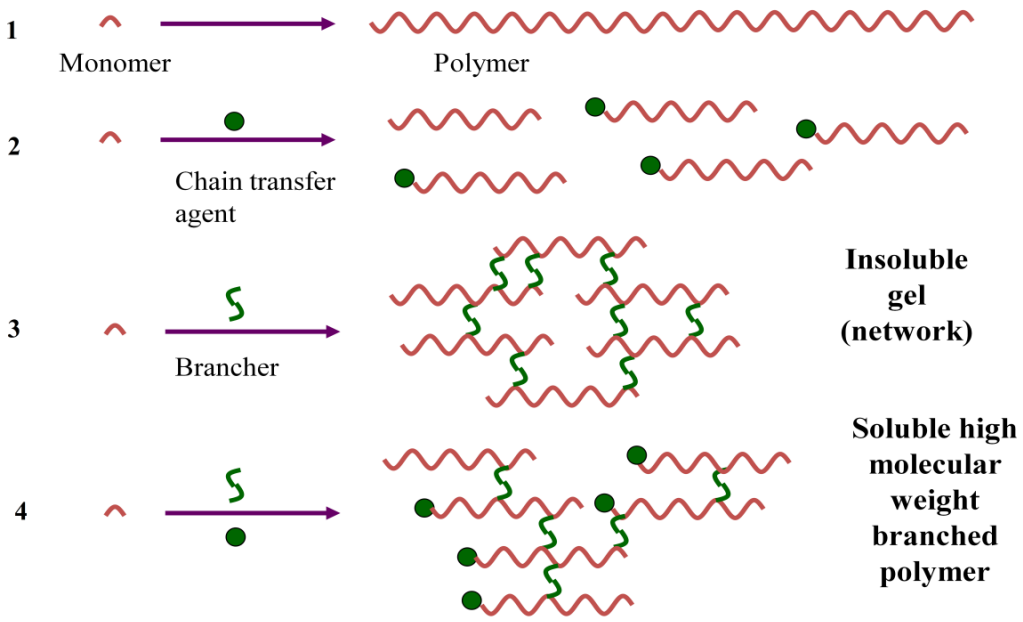

Figure 1.4: Illustration of the 'Strathclyde route' to branched polymers

As illustrated in stage 3 (in Figure 1.4) normally a monomer with a branching agent would result in an insoluble cross-linked 'gel' structure. However the use of a chain transfer agent illustrated in stage 2, in combination with a brancher in stage 4, results in

a soluble, high molecular weight, highly branched structure where both ends of each polymer chain are untethered and there is optimally less than one brancher per polymer chain.

Another branched polymer architecture of interest are star co-polymers. Star polymers consist of several linear polymer chains connected at one point. There are two general types of star polymers; regular star polymers, also known as homo-arm polymers, which have arms with the same chemical composition and similar molecular weights and mikto-arm star polymers, also known as heteroarm star copolymers, having two or more arms with different chemical compositions, and/or molecular weights and/or different peripheral functionality on the polymer chain ends. [98] They can be synthesised *via* different routes; core first, arm first or the coupling/ grafting-to approach. These are illustrated in Figure 1.5.

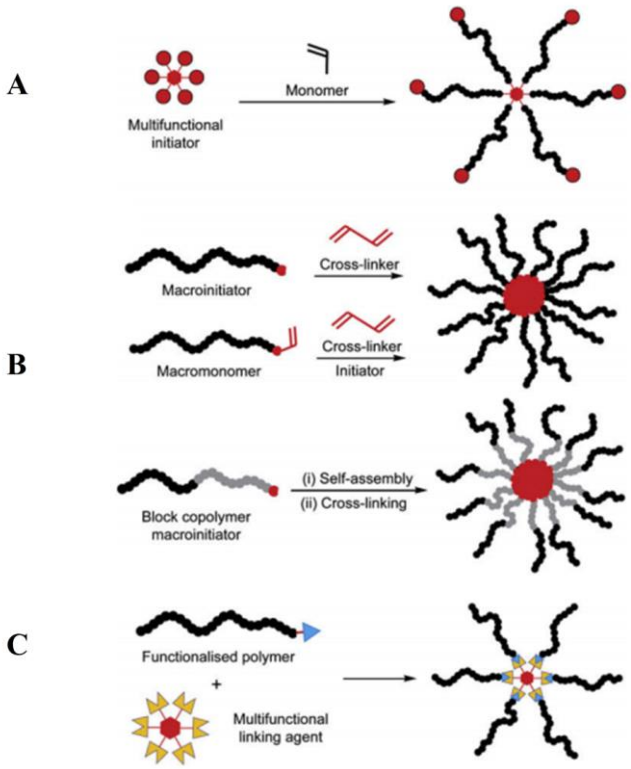

Figure 1.5: Synthetic approaches for the preparation of star polymers via controlled polymerisation techniques; (A) the core-first approach, (B) the arm-first approach and (C) grafting to-approach [98]

The ‘core-first’ approach has been employed by Sawamoto and co-workers who synthesised novel tri-, tetra-, hexa- and octafunctional dichloroacetate initiators and grew poly(methyl methacrylate) (PMMA) star polymers from these *via* ATRP [99]. Matyjaszewski and Gao have successfully synthesised poly(*tert*-butyl acrylate) *n*-poly(divinylbenzene-co-*tert*-butyl acrylate) using the ‘arm-first’ method in a one step process whereby linear *tert*-butylacrylate (*t*BA) was polymerised by ATRP methods, with divinylbenzene added as a core crosslinker, which co-polymerises with the remaining *t*BA and produced the target star copolymer [100].

1.6 Methods of polymersation

1.6.1 Free radical polymerisation

Most of the examples of synthesis of different structures and architectures of polymers discussed above utilised controlled radical polymerisation. Conventional free radical polymerisation (FRP) is the most versatile type of chain growth polymerisation as it can polymerise a wide range of monomers. It can be accomplished using emulsion polymerisation, [101] suspension polymerisation, [102] within a solvent (solution polymerisation) or without solvent. [103] It is also the more robust method commercially and it is relatively less sensitive to impurities.

Free radical polymerisation occurs when a radical is produced by an initiator by either thermal decomposition, [104] photolysis, [105] redox reaction, [106] or exposure to ionising radiation. [107] A chain carrier is formed from the reaction of the free radical and a

monomer unit and chain propagation proceeds rapidly by addition to the active chain end to produce a polymer.

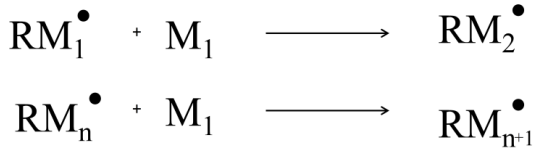

Scheme 1.2: Propagation in free radical polymerisation

Termination of the propagating chains can occur in many ways including by the reaction of an active chain end with an initiator radical, the interaction of two active chain ends, transfer of the active centre to another molecule (such as the solvent, initiator or monomer) and interaction with impurities such as oxygen or polymerisation inhibitors. [108]

The two most common routes of termination are combination, where two chain ends couple together to form one long chain, and disproportionation [109] where hydride abstraction occurs from one end to give an unsaturated group and two dead polymer chains. These are shown in Scheme 1.3.

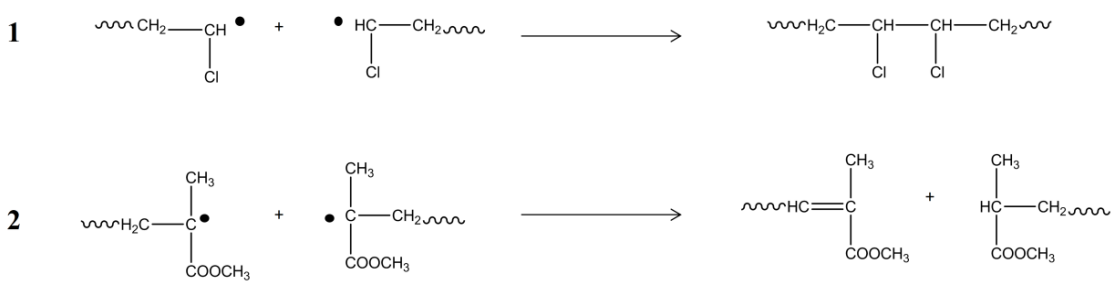

Scheme 1.3. Termination by (A) coupling of chains and (B) disproportionation

Although there are advantages to free radical polymerisation there are many limitations including a lack of control over the polydispersity of the polymers and the inability to

controllably synthesise well defined block co-polymers by this conventional method. Recent advances in polymer chemistry have tried to enable more control over the polymerisations, and these techniques are collectively known as controlled radical polymerisation (CRP).

1.6.2 Atom transfer radical polymerisation (ATRP)

ATRP is well documented as being one of the most widely used methods of controlled radical polymerisation and it offers a robust method to control the chemical composition and architecture of a range of polymers. One of the major advantages of ATRP is it can be tolerant to a wide range of functionalities and experimental conditions, compared to ionic polymerisation techniques. [110]

The general mechanism of ATRP is shown in Scheme 1.4, whereby Y is the pendant group of the monomer, Mt^zL_m is the transition metal complex, X is a halogen such as bromine (Br) or chlorine (Cl) and R is the initiator.

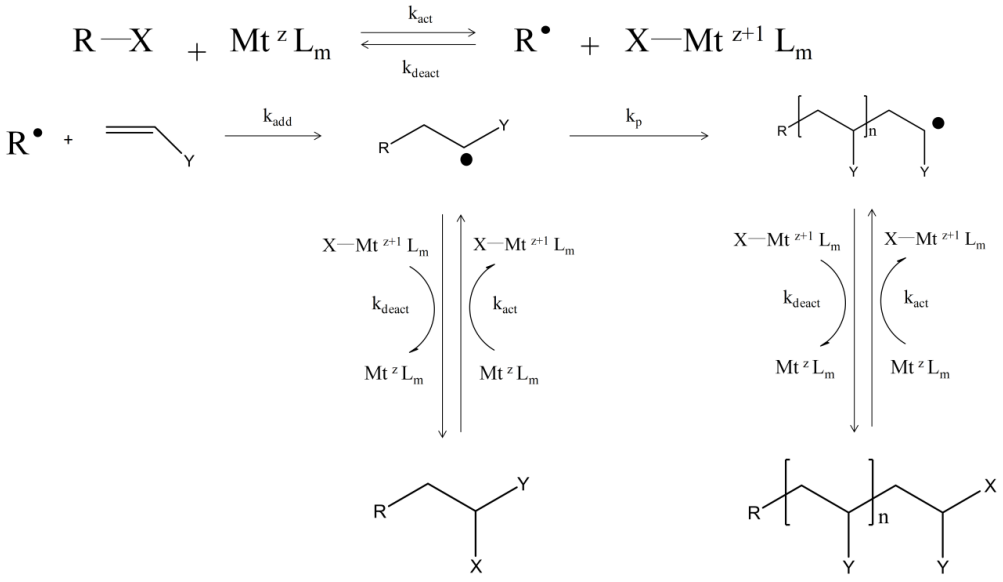

Scheme 1.4: Mechanism of metal complex-mediated ATRP [110]

ATRP is based on an inner sphere electron transfer process, which involves a reversible homolytic (pseudo) halogen transfer between a dormant species, an added initiator or dormant propagating chain end (R-X or R-P_n-X) and a transition metal complex in the lower oxidation state (Mt^z/L_m). The reaction results in the formation of propagating radicals and the metal complex in the higher oxidation state with a coordinated halide ligand (e.g. X-Mt^{z+1}/L_m). A simplified mechanism is shown in Scheme 1.5 whereby P is the polymer chain, Mt^n is the transition metal, L is the complexing ligand and again X is the halogen.

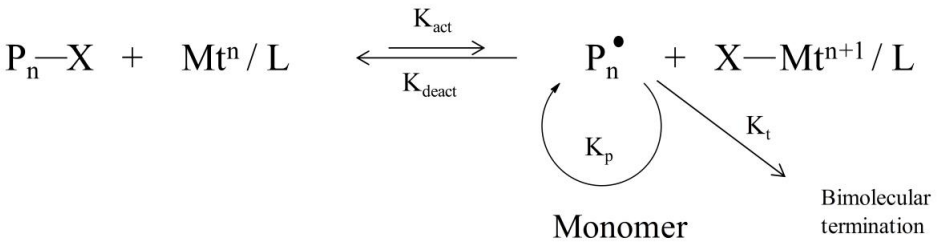

Scheme 1.5: Summary of the fundamental mechanism of ATRP [111]

The rate K_{act} can be affected by a number of variables, [112] one example being the type of ligand used. The ligand forms a complex with the transition metal to form the catalytic active species. The degree of control over the polymerisation reaction can be affected by the electron donating ability of the ligand as it can affect the reactivity of the metal centre in halogen abstraction and transfer.

ATRP also cannot be used for systems where the monomer being polymerised can interact with the metal catalyst or when the polymers being prepared are required to be free of trace metal contamination. This problem can be overcome with the use of the metal catalyst-free methods of polymerisation such as nitroxide-mediated

polymerisation (NMP) [113] and reversible addition fragmentation chain transfer polymerisation (RAFT). [114]

1.6.3 Nitroxide-mediated polymerisation (NMP)

NMP is also a controlled free radical polymerisation process and relies upon the reversible deactivation of active polymer radicals by a nitroxide functionality, such as 2,2,6,6-tetramethyl-1-piperidinyloxyl (TEMPO), to form a dormant alkoxyamine [115]. This dormant functionality regenerates the propagating radical and the nitroxide by thermal cleavage. This equilibrium presents the advantage of being a purely thermal process where neither catalyst nor bimolecular exchange is required [116]. The mechanism of this is shown in Scheme 1.6.

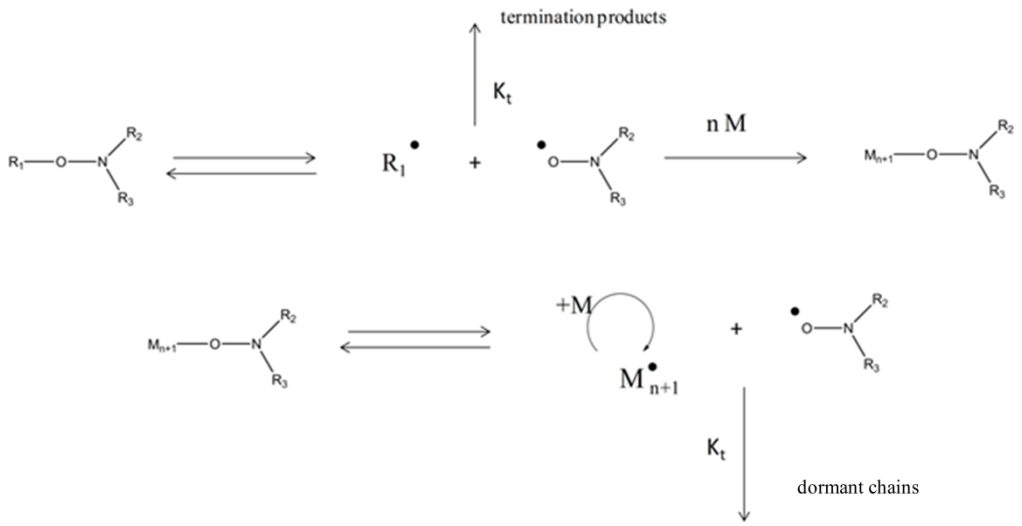

Scheme 1.6: General mechanism of NMR polymerisation

There are however limitations with this method of polymerisation. The three main issues are slow polymerisation kinetics that require high temperatures and lengthy polymerisation times, [117] the inability to easily control the polymerization of methacrylate monomers due to side reactions and/or slow recombination of the polymer

radical with nitroxide, and synthetic difficulties associated with nitroxide and alkoxyamine synthesis. [118] Additionally, other side and termination reactions that can limit molecular weight and broaden polymer molecular weight distributions can be problematic under certain NMP conditions. [119]

1.6.4 Reversible addition fragmentation chain transfer polymerisation (RAFT)

As discussed, one disadvantage of some CRP reactions is that the range of monomers they can polymerise can be fairly limited. Moad and co-workers in 1998 introduced the concept of a new controlled polymerisation method that could be used with a wide range of monomers and reaction conditions. [120] The RAFT process involves conventional free radical polymerisation of a substituted monomer in the presence of a suitable chain transfer agent (RAFT agent or CTA). Chain transfer occurs in polymerisations where the activity of a growing polymer chain is transferred to another molecule, shown in Scheme 1.7.

Scheme 1.7: Chain transfer reaction in a radical polymersation

By carefully designing the reactive molecule which undergoes chain transfer, it is possible to deliberately encourage reaction with the propagating polymer and stabilise the radical such that the resulting product is able to also act as a reactive chain transfer or RAFT agent. The general structure of a RAFT agent is shown in Figure 1.6.

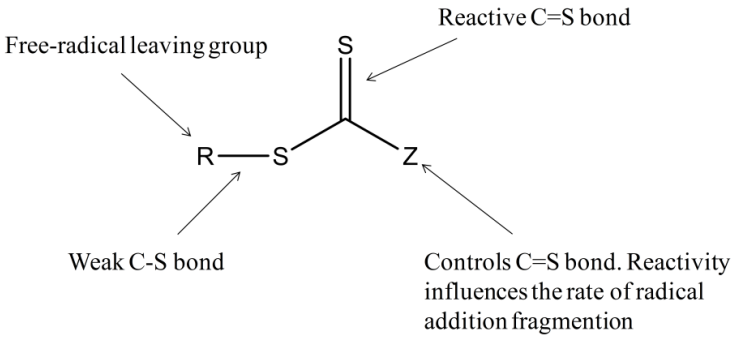

Figure 1.6: General structure of a RAFT agent.

The choice of the 'R' and 'Z' groups has a big impact on the polymerisation, and much research has focused on synthesising novel RAFT agents for specific polymerisations [121], [122]. The R group should be a good free-radical leaving group and as an expelled radical, R should be effective in reinitiating free-radical polymerisation. To ensure a high transfer constant, Z should activate (or at least not deactivate) the C=S double bond toward radical addition.

The main advantage of RAFT polymerisation is that it can be used with a wide range of monomers including functional monomers. It is also tolerant of functionality in the RAFT agent and the initiator compound allowing for the synthesis of polymers containing end or side chain functionality, without the need for secondary protection or deprotection reactions [123]. RAFT is also very compatible with a number of reaction conditions and can be conducted in bulk, organic or aqueous solution, and by emulsion, or suspension polymerisation methods [124].

The general mechanism that RAFT polymerisations proceed by is shown in Scheme 1.8.

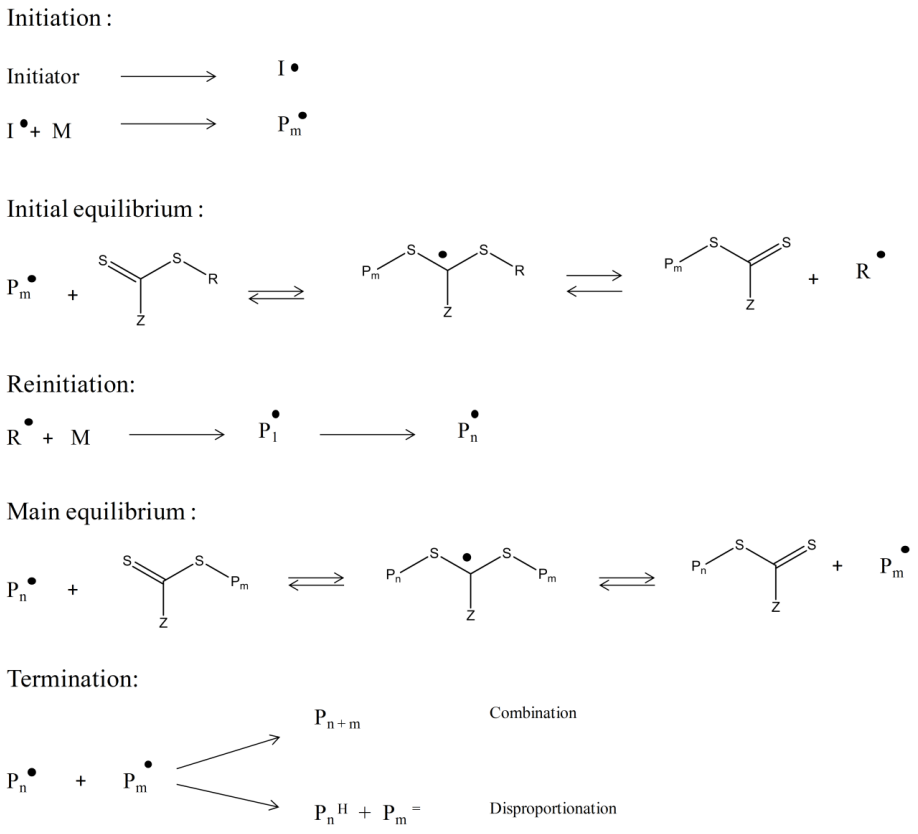

Scheme 1.8: General mechanism for RAFT polymerisation

1.6.5 'Living' anionic polymerisation

Anionic polymerisation was first reported in 1956 by Michael Szwarc. Most polymers at this time were typically initiated, grown by propagation and terminated by free radical polymerisation. However, he proposed that if there were no termination reactions the polymerisation would be "living" and would continue to propagate as more monomer was added. Styrene was the monomer initially explored and the polymerisation was initiated with sodium naphthalene. The solvent used was tetrahydrofuran (THF) and the reaction temperature was -78 ºC. [125] As the reaction can be terminated by the abstraction of a hydrogen atom from impurities such as water, great care was needed to exclude air and water from the reaction. The early reactions

were typically conducted under stringent high pressure, low temperature and vacuum conditions. Scheme 1.9 shows the reaction mechanism for the first anionic polymerisation of styrene.

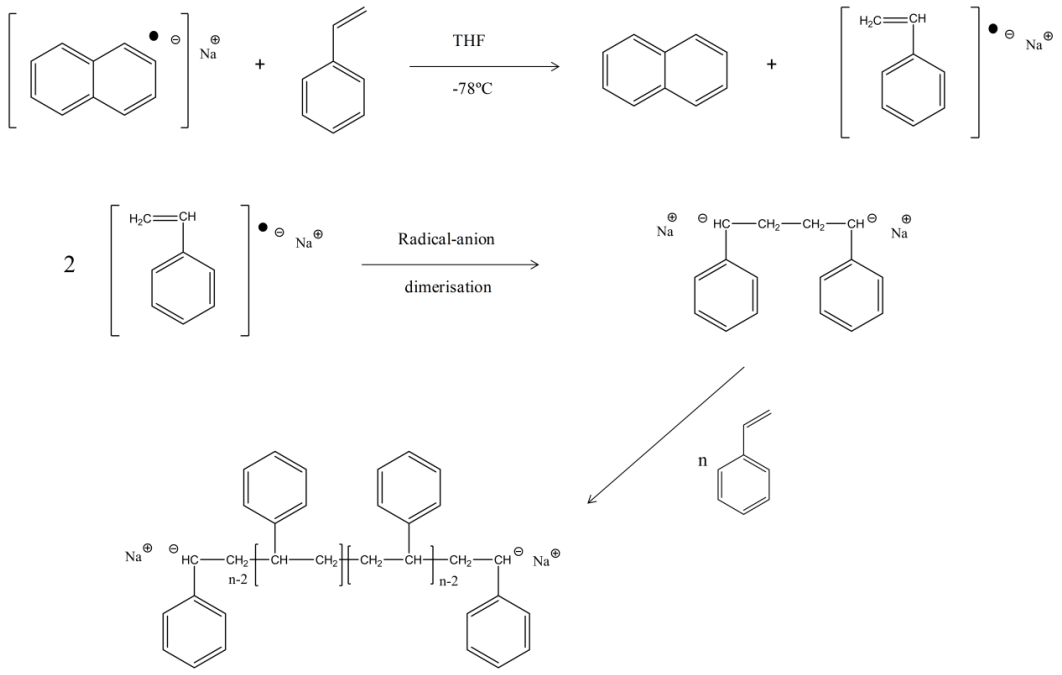

Scheme 1.9: Synthesis of polystyrene by anionic polymerisation [125]

In 1960 Worsford and Bywater investigated the kinetics of polystyrene by anionic polymerisation but at ambient temperature [126]. The reaction was performed under vacuum conditions at 30.3 ºC in the reactor vessel shown in Figure 1.7.

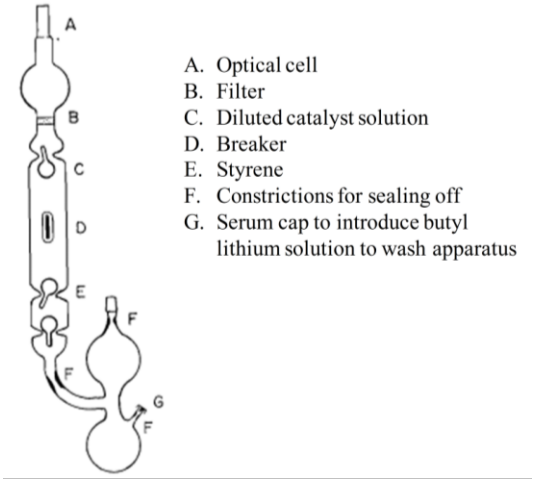

Figure 1.7: Reactor vessel used for anionic polymerisation initiated by *n*-butyllithium [126]

The polymerisation was initiated by *n*-butyllithium (*n*-BuLi) rather than sodium naphthalene and the solvent used was benzene. To prepare benzene suitable for use in an anionic polymerisation, it was stirred for a week in concentrated sulphuric acid, washed with water, dilute sodium hydroxide and then water again. The solvent was finally distilled from phosphorous pentoxide onto calcium hydride and stored under vacuum. The anionic polymerisation reaction progressed via the mechanism shown in Scheme 1.10.

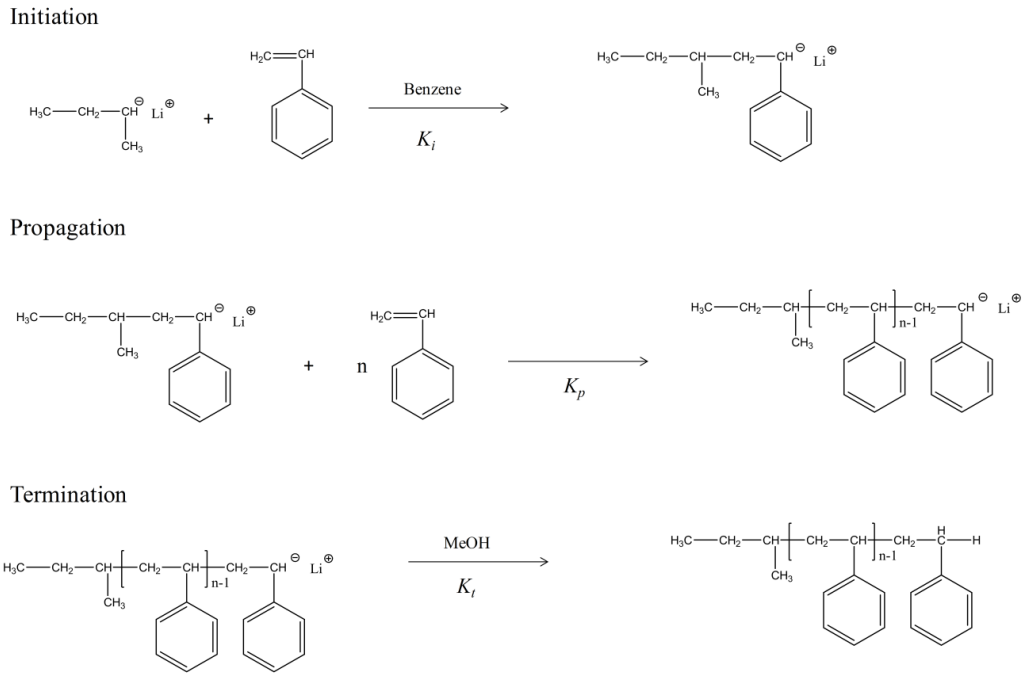

Scheme 1.10: Polymerisation of styrene by anionic polymerisation techniques, initiated by *n*-butyl lithium, in benzene solution.

1.7 Recent advances in anionic polymerisation.

Earlier in the Chapter the different complex architectures of highly branched polymers were discussed. In recent work, anionic polymerisation has been utilised to produce

highly branched, macromolecular structures with great control. Anionic polymerisation offers the ability to control the size of the polymers, and target different degrees of polymerisation (DP_n) with a level of accuracy that is not possible with controlled radical polymerisation. One particular class of architecture that has received considerable attention is the star co-polymers.

Altares *et al* synthesised star-type polystyrenes, polymers attached to a common multifunctional center, and comb-type polystyrenes, polymers with an average of *p* branches attached statistically to a polymeric backbone. The reactions used required the synthesis of polystyryllithium of narrow chain length distribution with appropriate *p*-functional molecules or with backbone polystyrene chains of narrow chain length distribution, containing the prerequisite number of benzylic-type chloromethyl groups. [127] However it was found that the coupling reaction with multifunctional benzyl halide derivatives was complicated by serious of side reactions such as metal-halogen exchange, benzyl proton abstraction, and single electron transfer reactions.

In the synthesis of styrene-methyl methacrylate or styrene-vinylpyridinezo block copolymers, where side reactions were also an issue, the reactivity of the polystyryl anion was modified by 'capping" the living polymer with a single 1,1-diphenylethylene (DPE) unit prior to adding the second monomer. Nucleophilic reactions leading to branching could therefore be avoided. This approach was used by Gauthier and Moller who reported that similar side reactions can be significantly reduced in the coupling reaction of chloromethylated polystyrene and polystyryllithium by end-capping polystyryllithium with DPE in the presence of THF. [128]

Following these reports, Hirao and co-workers have successfully synthesised several well defined star-branched polymers [129], [130], [131] by the coupling reaction of specially designed chain-functionalised polymers having a definite number of benzyl halide moieties with living anionic polymers of styrene, α-methylstyrene, and isoprene. The synthetic procedure involved three reaction stages as follows. The first stage was the preparation of precursor polymers that were functionalised with a defined number of anion-stable methoxymethylphenyl (MOM) groups by reacting an anionic living polymer with specially designed reagents. These MOM groups in the polymer chain are then quantitatively changed into reactive chloromethylphenyl groups in the second stage reaction. The star polymer is formed by the coupling of other living polymers. [132] This approach is illustrated in Scheme 1.11.

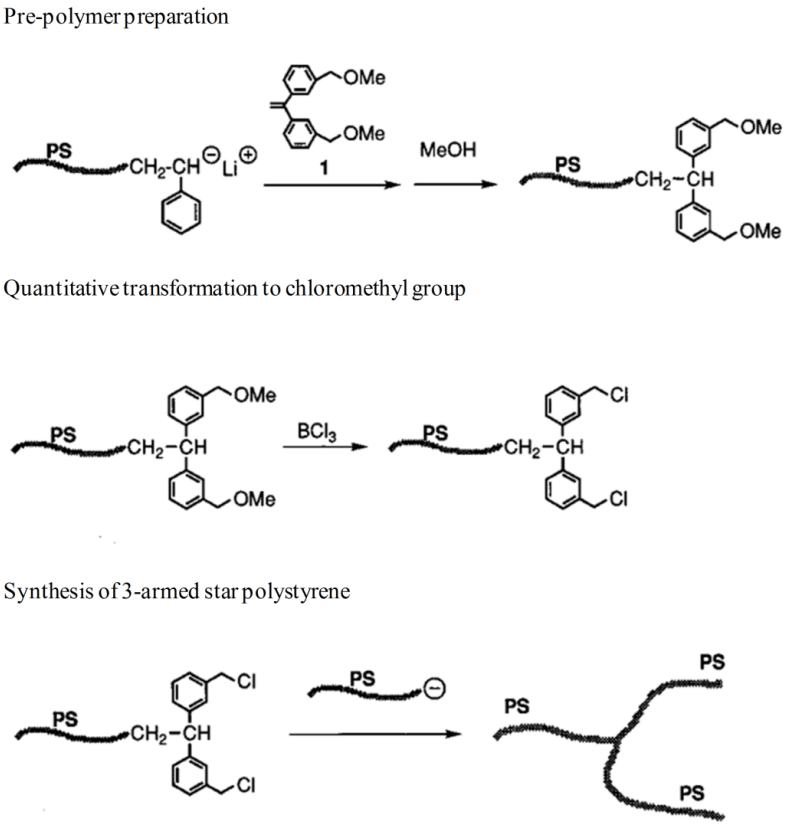

Scheme 1.11: Synthesis of 3-armed star polystyrenes [132]

Hajichristidis *et al* defines the three main methods for producing star polymers in their 2001 review [133] as; using multifunctional initiators (Figure 1.8.1), multifunctional linking agents (Figure 1.8.2), or difunctional monomers (Figure 1.8.3).

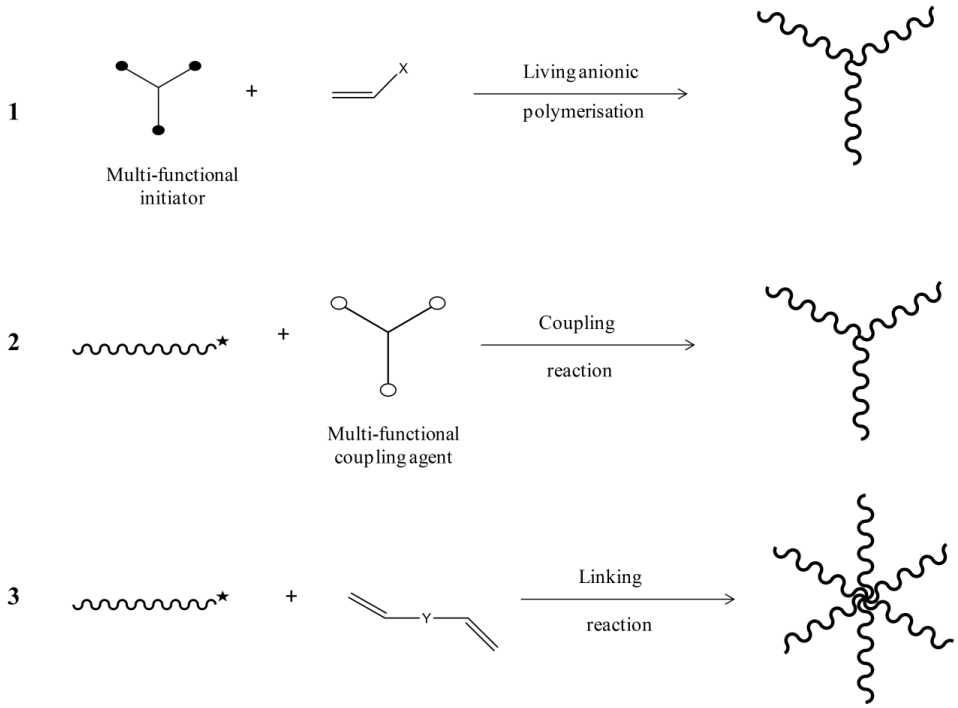

Figure 1.8: Methods of synthesising star co-polymers [133]

In the case of forming the star polymers by a multi-functional initiator, Remp and Lutz in 1988 polymerised divinylbenzene (DVB) with sodium naphthalene to give a short chain, low molecular weight polymer. [134] This resulting polymeric "core" exhibited a number of metalo-organic sites, and acted as a multifunctional initiator. In a subsequent step, these sites initiated the polymerisation of styrene to give a star co-polymer. They found high numbers of branches could be obtained. A major advantage of this "core first" method is that it allows functionalisation of the branches at their outer chain-ends.

Conversely, Eschway and Burchard anionically polymerised DVB in solution with THF at -78 ºC using *n*-butyl lithium (*n*-BuLi) as the initiator, resulting in densely cross-linked poly-DVB. These polymers bear a large number of living carbanionic groups

which are capable of polymerising styrene or other monomers giving star polymers. The size and functionality of the densely cross-linked poly-DVB was increased by increasing the ratio of DVB: *n*-BuLi and the overall concentration of DVB within the reaction. [135]

Another strategy to form multifunctional initiators is the polylithiation of multifunctional aryl halides. [136] By using lithium-halide exchange, polymerisation can be initiated from each aryl halide group present within a target molecule. However, there are inherent problems with this approach; polylithiations of multihalide organic molecules by reagents such as *tert*-butyllithium (*tert*-BuLi) or sec-butyllithium (*sec*-BuLi) are reported to result in moderate yields and can also give products with varying degrees of substitution. [137]

Another issue relates to the solubility of these compounds; polylithiated compounds have limited solubility in most organic solvents, as they can form insoluble aggregates, undergo α-lithium halide eliminations and/or intermolecular couplings between the lithiated reagent and the halide-substituted species. [138]

Gnanou and co-workers in 2005 reported a novel approach to the preparation of polylithium organic compounds by lithium/halogen exchange and their use as initiators for the synthesis of star polymers by ambient temperature anionic polymerisation techniques. [139] Polyarylhalides shown in Scheme 1.12 were synthesised and treated with a stoichiometric amount of *sec*-BuLi to generate the dilithiated, trilithiated and tetralithiated intitiators also shown in Scheme 1.12.

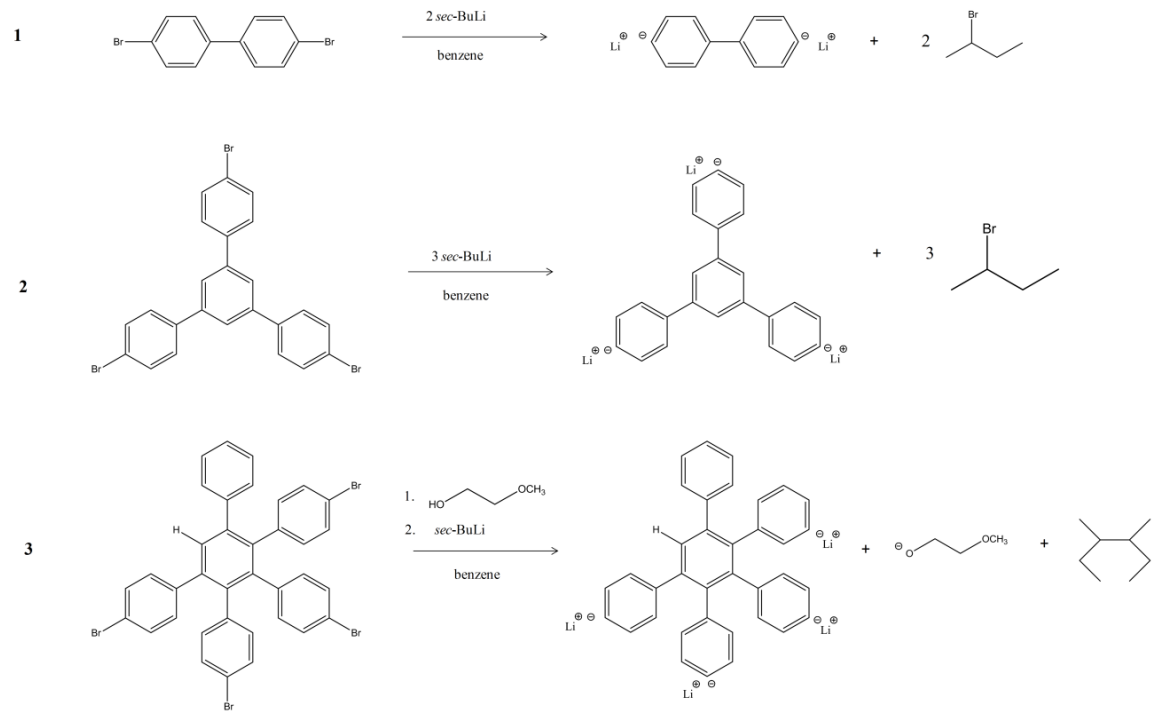

Scheme 1.12: Synthesis of (1) dilithiated (2), trilithiated and (3) tetralithiated initiators.

Anionic polymerisation proceeded after the addition of styrene and the synthesis of the four-armed polystyrene from the tetralithiated initiator (3) is shown in Scheme 1.13.

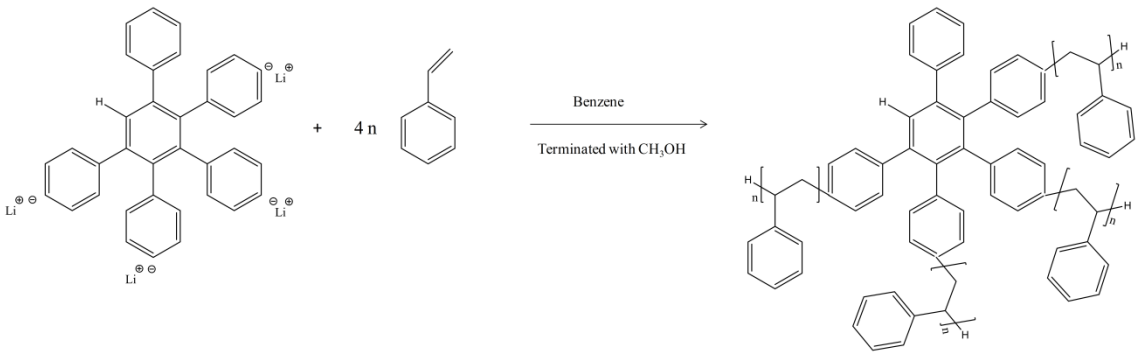

Scheme 1.13: Synthesis of four-armed star-polystyrene initiated by a multifunctional initiator, in benzene and terminated with CH_3OH.

The resulting polymers were analysed by gel permeation chromatography (GPC) and viscometry measurements and both linear and star polystyrenes showed an excellent agreement between the experimental and expected values for the molar masses.

In 2008 Matmour and Gnanou expanded upon their work to produce a new and versatile synthetic strategy that provides access to precisely defined and soluble multicarbanionic initiators. This synthetic strategy, shown in Scheme 1.14, is used to obtain, by divergent growth, dendrimer-like samples of polystyrene (PS) (up to the seventh generation) or polybutadiene (PB) and also asymmetric and miktoarm stars [140].

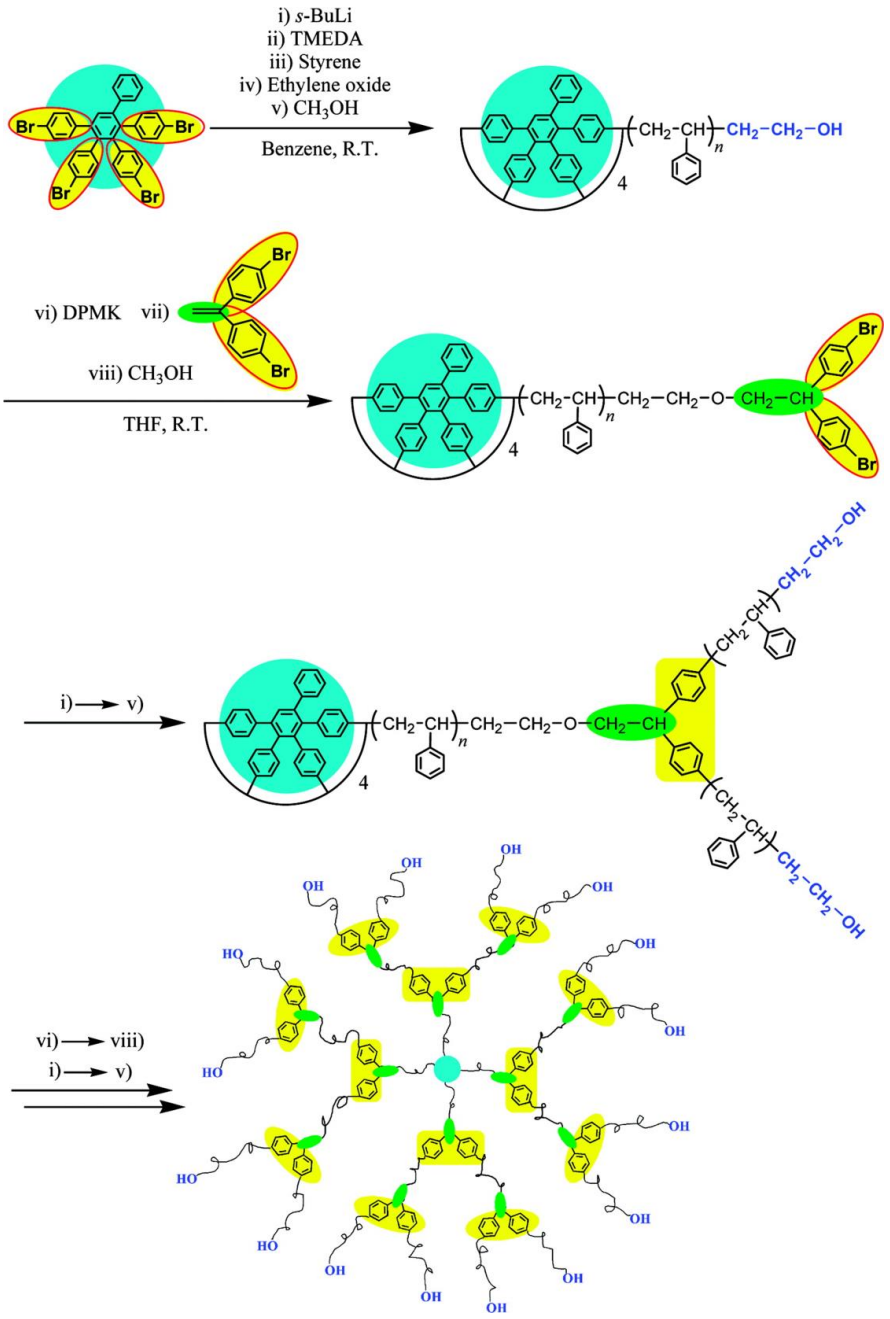

Scheme 1.14: Synthesis of seventh generation dendritic polystyrenes [140]

They successfully synthesised 7th generation material with M_n values as high as 1920 x10^{-3} gmol^{-1} and reported dispersity values of 1.04 for these large macrostructures. However, one point worth noting is that the polymer chain ends within the structure are tethered at both ends, and unavailable for any further functionalisation apart from at the surface of the material.

These reports are of particular relevance and importance to the work presented in the following Chapters. The methods used to produce polystyrene at ambient temperatures by anionic polymerisation techniques, and use of halide exchange reactions to synthesise multiple armed polystyrenes are explored and expanded upon.

1.10 Synthesis of nanoparticles

Polymer nanoparticles can be synthesised by a number of different methods. These can include preparation by polymerisation of monomers, or by the dispersion of preformed polymer. Examples include emulsion polymerisation, [141] microemulsion polymerisation, [142] and interfacial polymerisation. [143]. Polymeric nanoparticles can also be prepared by methods such as solvent evaporation, [144] nanoprecipitiation, [145], [146], [147] emulsification, [148] solvent diffusion, [149] salting out, dialysis, [150] and use of supercritical fluid. [151]

Nanoprecipitation is of particular relevance to this study and is the method used to synthesise the amphiphillic nanoparticles from the targeted polymer structures that have been synthesisied. Nanoprecipitation is a facile, mild, and low energy process for the preparation of polymeric nanoparticles. In the recent literature, a review has pointed out that the majority of the reported polymer systems [152] that are formed into nanoparticles

via nanoprecipitation are based on block copolymers since these systems usually possess amphiphilic character and form a core–shell structure due to their micelle-like behaviour. Nanoprecipitation is also called the solvent displacement method, and was first patented by Fessi *et al*. [153] A schematic diagram of the basic method is shown in Figure 1.9.

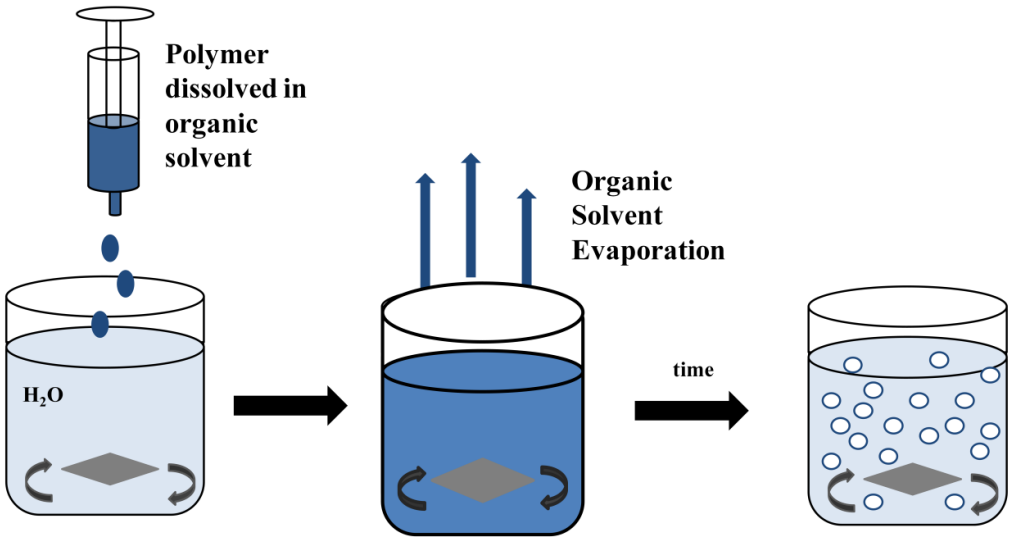

Figure 1.9: Schematic diagram outlining the process of nanoprecipitation

The aqueous solution may be neutral, acidic or basic and may contain a surfactant as a stabiliser. Polymer deposition on the interface between the water and the organic solvent, caused by fast diffusion of the solvent, leads to the instantaneous formation of a colloidal suspension.

Memisogul *et al* used nanoprecipitation to develop and characterize a highly loaded nanoparticulate system based on amphiphilic β-cyclodextrins (CDs) to facilitate the administration of the poorly soluble antifungal model drugs bifonazole and clotrimazole. [154] They found that amphiphilic *β*-CDs form highly loaded nanospheres

with lower hemolytic activity than that of natural CDs directly from inclusion complexes. As a result they enhanced solubility and subsequently therapeutic efficacy of the model drugs.

Nanoprecipitation is limited to water-miscible solvents, and therefore the polymer has to be soluble in a limited number of solvents. It is also an unsuitable method for water soluble drugs. Niwa *et al* studied the efficiency of this technique to synthesise nanoparticles containing 5-fluorouracil, a water soluble anti-cancer drug. They found that 5-fluorouracil was poorly encapsulated because of considerable leakage of drug into the aqueous phase during preparation. [155]

This effect was also seen by Barichello *et al* who accessed the relative advantages and drawbacks of the nanoprecipitation/solvent displacement method for a range of drugs with respect to the particle size and drug encapsulation in polylactic-co-glycolic acid (PLGA) nanoparticles. [156] They found that the results of the encapsulation efficiency analysis demonstrated that more lipophilic drugs, such as cyclosporin and indomethacin, did not suffer from the problems of drug leakage to the external medium, resulting in improved drug content in the nanoparticles. However the hydrophilic drugs, such as vancomycin and phenobarbital, were poorly encapsulated in PLGA nanoparticles.

1.11 Aims of the work

The use of nanoparticles for the delivery of therapeutics for HIV/AIDS is relatively under researched when compared to cancer therapeutics. However, there is great scope to exploit the passive targeting of macrophages by nanoparticles. As has been discussed, polymeric nanoparticles may offer therapeutic benefits to patients and drug delivery from branched polymers that have been nanoprecipitated is a potentially valuable area of research.

Branched polymers can be produced in many ways. One way is utilising the 'Strathclyde' route. This is typically used for controlled radical polymerisations, however, these do not allow the same degree of control as anionic polymerisation techniques. Recent work by Gnanou and co-workers has shown the ability to synthesise highly branched polystyrenes by ambient anionic techniques. Ambient anionic polymerisation within the Strathclyde strategy has not been studied, but this may offer the potential to synthesise branched polystyrenes with the ability to directly control the architecture of the branched polystyrenes. If hydrophilic character can be introduced to these controlled macromolecular architectures, then the formation of water stable polymer nanoparticles may be viable.

The primary aim of this work is to produce a carrier for the drug delivery of antiretroviral drugs that is both stable in water, thus helping to overcome the issues of dissolution associated with ARV drugs, and also produce a particle large enough to be engulfed by macrophages by phagocytosis. Figure 1.10 shows the basic structure of the target nanoparticle that we aim to synthesise.

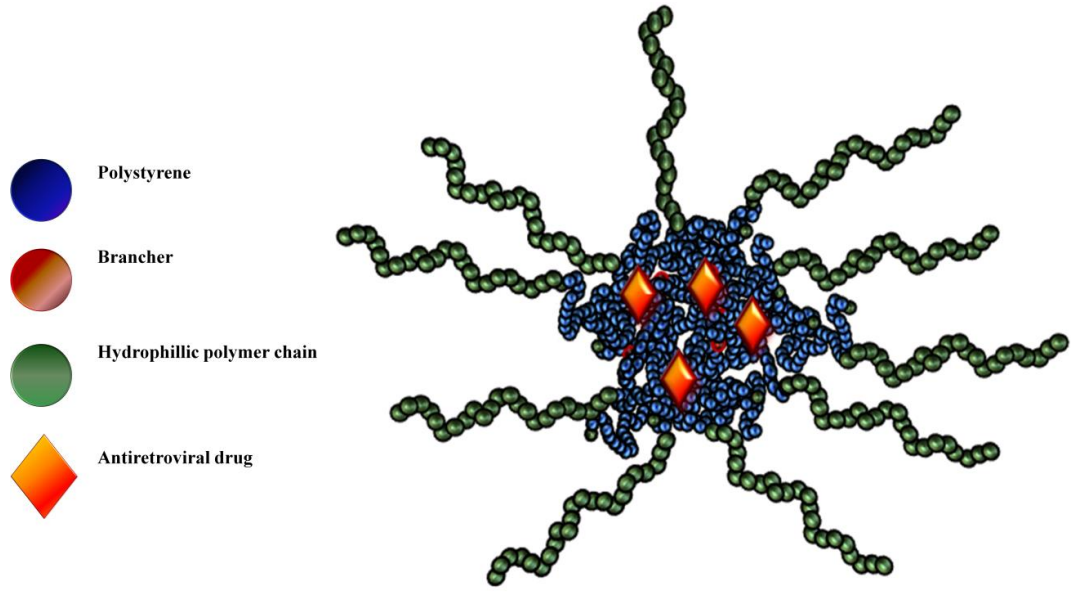

Figure 1.10: Proposed target nanoparticle.

The blue core is a highly branched hydrophobic polymer chain, which will potentially encapsulate the hydrophobic antiretroviral drug, shown in orange. Green symbolises the hydrophilic element of the particle. This is achieved either with a charged species, or linear hydrophilic polymer chains, as shown in Figure 1.10.

1.10 References

1. Sanchez, F.; Sobolev, K., *Constr. Build. Mater*., **2010**, *24*, 2060

2. Park, J., J. *Control. Release*., **2007**, *120*, 1

3. Chen, Y.; Liu, L., *Adv. Drug. Deliver. Rev*., **2012**, *64*, 640

4. Ensign, L.M.; Cone, R.; Hanes, J., *Adv. Drug. Deliver. Rev*., **2012**, *64*, 557

5. Alsenz, J.; Kansy, M., *Adv. Drug. Deliver. Rev*., **2007**, *59*, 546

6. Horter, D.; Dressman, J.B., *Adv. Drug. Deliver. Rev*., **2001**, *46*, 75

7. Heger, J.J.; Prystowsky, E.N.; Zipes, D.P., *Am. Heart. J*., **1983**, *106*, 931

8. Jain, K.K., *Technol. Cancer. Res. T*., **2005**, *4*, 407

9. Junghanns, J.A.H.; Muller, R.H., *Int. J. Nanomedicine*, **2008**, *3*, 295

10. Khan, S.; Matas, M.; Zhang, J.; Anwar, *J., Cryst. Growth. Des*., **2013**, *13*, 2766

11. Fecht, H.J.; Hellstern, E.; Fu, Z.; Johnson, W.L., *Metall. Trans. A*., **1990**, *21*, 2333

12. Peltonen, L.; Hirvonen, J., *J. Pharm. Pharmacol*., **2010**, *62*, 1569

13. Reed, R.G.; Czekai, D., System and method for milling materials, **2005**, US 6976647 B2

14. Chen, S.; Jang, B.Z.; Yang, J., High-energy planetary ball milling apparatus and method for the preparation of nanometer-sized powders, **2000**, US 6126097 A

15. Singha, R.; Lillard, J.W., *Exp. Mol. Pathol.*, **2009**, *86*, 215

16. Rabinow, B.E., *Nat. Rev*., **2004**, *4*, 407

17. Muller, R.H.; Peters, K., *Int. J. Pharm*., **1998**, *160*, 229

18. Wiedmann, T.S.; DeCastro, L.; Wood, R.W., *Pharm. Res*., **1997**, *14*, 112

19. Zhang, X.; Xia, Q.; Gu, N., *Drug. Dev. Ind. Pharm*., **2006**, *32*, 857

20. Campbell, J.; Long, B.; Duncalf, A.J.; Hopkinson, A.; Taylor, D.; Angus, D.; Cooper, A.I.; Rannard, S.P., *Nature Nano*. **2008**, *80*, 506

21. McDonald, T.O.; Giardiello, M.; Martin, P.; Siccardi, M.; Liptrott, N.J.; Smith, D., Roberts, P.; Curley, P.; Schipani, A.; Khoo, S.H., Long, A.J.; Rannard, S.P.; Owen, *A. Adv. Healthcare. Mater*., **2013**, *In Press*

22. Dobson, J., *Drug. Dev.Res*., **2006**, *67*, 55

23. Chertok, B.; Moffat. B.; David, A.E.; Yu, F.; Bergemann, C.; Ross, B.D.; Yang, V.C., *Biomaterials*, **2008**, *29*, 4887

24. Jain, T.K.; Morales, M.A.; Sahoo, S.K.; Peleky, L.; Labhasetwar, V., Mol. Pharma., 2005, 2, 194

25. Marcu, A.; Dumitrache, F.; Mocanu, M.; Niculite, M.; Gherhiceanu, M.; Lungu, C.P.; Fleaca, C.; Ianchis, R.; Barbut, A.; Grigoriiu, C.; Morjan, I., *Appl. Surf. Sci*., **2013**, *281*, 60

26. Bao, Y.; Krishnan, K.M., *J. Magn. Mater*., **2005**, *293*, 15

27. Gregoriadis, G.; Florence, A.T., *Drugs*, **1993**, *45*, 15

28. Ostro, M.J.; Cullis, P.R., *Am. J. Hosp. Pharm*., **1989**, *46*, 1576

29. Sharma, A.; Sharma, U., *Int. J. Pharm.*, **199**7, *154*, 123

30. Gregoriadis, G., Trends. Biotechnol., **1995**, *13*, 527

31. Blume, G.; Cevc, G.; Crommelin, M.D.J.A.; Bakker, I.A.; Kluft, C.; Storm, G., *BBA-Biomembranes*, **1993**, *1149*, 180

32. Ahmed, I.; Longenecker, M.; Allen, T.M., *Cancer Res*, **1993**, *57*, 1484

33. Bawa, R., *Nanotechnology, Law and Business*, **2008**, *5*, 135

34. www.cancer.gov/cancertopics/cancerlibrary/what-is-cancer

35. Cross, S.S., Underwood's Pathology; A Clinical Approach, **2013**, *6th Edition*, Churchill Livingstone

36. Maeda, H.; Wu, J.; Sawa, T.; Matsumura, Y.; Hori, *J. Control. Release*, **2000**, *65*, 271

37. Fang, J.; Nakamura, H.; Maeda, H., *Adv. Drug. Deliv. Rev*., **2011**, *63*, 136

38. Maedaa, H.; Bharatea, J.; Daruwallac, J., *Eur. J. Pharm. Biopharm*., **2009**, *71*, 409

39. Hilgenbrink. A.R.; Low, P.S., *J. Pharma. Sci*., **2005**, *94*, 2135

40. www.unaids.org/en/media/unaids/contentsassets/documents/unaidspublication/2011

41. Weiss, R.A., *EMBO Reports*, **2003**, *4*, 10

42. www.un.org/milleniumgoals/aids.shtml

43. Gray, R.H.; Wawer, M.J.; Brookmeyer, R.; Sewankambo, N.; Serwadda, D.; Quinn, T.C., *Lancet*, **2001**, *14*, 1149

44. Bozicevic, I.; Rode, O.D.; Lepej, S.Z.; Johnston, L.G.; Stulhofer, *AIDS. Behav*., **2009**, *13*, 303

45. De Cock, K.; Fowler, M.; Mercier, E.; Rogers, M.; Schaffer, N., *J. Am. Med. Soc*., **2000**, *283*, 1175

46. www.hivaware.co.uk

47. www.niaid.nih.gov/topics/HIVAIDS/understanding/hivreplicationcycle.aspx

48. Pommier, Y.; Johnson, A.A.; Marchand, C., *Nat. Rev. Drug. Discov*., **2005**, *4*, 236

49. Deeks, S.G.; Smith, M.; Holodniy, M.; Khan, J.O., *J. Am. Med. Soc*, **1997**, *277*, 145

50. De Clercq, E., *Antivir. Res*., **1998**, *38*, 153

51. Esnouf, R.; Ren, J.; Ross, C.; Jones, Y.; Stammers, D.; Stuar, D., *Nat. Struct. Biol*., **1995**, *2*, 303

52. Este, J.A.; Telenti, A., *Lancet*, **2007**, *370*, 81

53. Yeni, P., *J. Hepatol*., **2006**, *44*, 100

54. Cabrero, E.; Griffa, L.; Burgos, A., *AIDS. Patient. Car. St*., **2010**, *24*, 5

55. Luther, J.; Glesby, M., *Am. J. Clin. Dermatol*., **2007**, *8*, 221

56. Singh, N,; Squier, C.; Sivek, C.; Wagener, M.; Nyugen, M.; Yu, V.L., *AIDS. Care*., **1996**, *8*, 261

57. Mehta, S.; Moore, R.D.; Graham, N.M.H., *AIDS*, **1997**, *11*, 1665

58. Cinatl, J.; Rabenau, H.; Doerr, H.W.; Weber, B., *Intervirology*, **1994**, *37*, 307

59. Liu, L.; Venkatraman, S.S.; Yang, Y.Y.; Guo, K.; Kan, L., *Biopolymers*, **2008**, *90*, 617

60. Sharma, P.; Garg, S., *Adv. Drug. Deliver. Rev*., **2010**, *3*, 491

61. Swami, M., *Nat Med*, **2013**, *19*, 416

62. Walker, K.; Bowers, J.; Mitchell, R.J.; Potchoiba, M.J.; Schroeder, M.; Small, H.F., *Xenobiotica*, **2008**, *38*, 1330

63. Kerza-Kwiatecki, A.P.; Amini, S., J. *Neurovirol*., **1999**, *5*, 113

64. Hoetelmans, R.M., *Antivir. Ther*. , **1998**, *3*, 13

65. www.biology-online.org/dictionary/phagocytosis

66. Neves, P.; Benchimol, M., *Biol. Cell*, **2007**, *99*, 87

67. Pugliese, A.; Vidotto, V.; Beltramo, T.; Torre, D., *Clin. Diagn. Lab. Immun*., **2005**, *12*, 889

68. Kreuter, J.; Alyautdin, R.N.; Kharkevich, D.A.; Ivanov, A.A., *Brain. Res*., **1995**, *13*, 171

69. Schroder, U.; Sabel, B.A., *Brain Res*., **1996**, *26*, 121

70. Mortamet, A.C.; Pethrick, R.A., *J. Appl. Polym. Sci*., **2012**, *123*, 1539

71. Uchegbu, I.F.; Vyas, S.P., *Int. J. Pharm*., **1998**, *10*, 393

72. Zhang, L.; Lui, W.; Chen, D.; Stenzel, M.H., *Biomacromolecules*, **2008**, *9*, 3321

73. O'Brien, N.; McKee, A.; Sherrington, D.C.; Slark, A.T.; Titterton, A., *Polymer*, **2000**, *41*, 6027

74. Cammas, S.; Matsumoto, T.; Okano, T.; Sakurai, Y.; Kataoka, K., *Mat. Sci. Eng*., **1997**, *4*, 241

75. Kwon, G.; Naito, M.; Yokoyama, M.; Okano, T.; Sakurai, Y.; Kataoka, K., *J. Control. Release*, **1997**, *48*, 195

76. Dumortier, G.; Grossiord, J.L.; Agnely, F.; Chaumeil, J.C., *Pharm. Res*., **2006**, *23*, 2709

77. Alexandridis, P.; Holzwarth, J.A; Hatton, T.A., *Macromolecules*, **1994**, *27*, 2414

78. Wong, H.L.; Chattopadhyay, N.; Wu, Y.X.; Bendayan, R., *Adv. Drug. Deliver. Rev*., **2010**, *62*, 503

79. Batrakova, E.V.; Han, H.; Miller, D.W.; Kabanov, A.V., *Pharm. Res*., **1998**, *15*, 1525

80. Lui, L.; Venkatraman, S.S.; Yang, Y.Y., Guo, K.; Lu, J; He, B.; Moochala, S.; Kan, L., *Biopolymers*, **2008**, *90*, 617

81. Wang, F.; Bronich, T.K.; Kabanov, A.V.; Rauh, R.D.; Roovers, J., *Bioconjugate Chem*., **2005**, *16*, 397

82. Froehling, P.E., *Dyes Pigments*, **2001**, *48*, 187

83. Villalonga-Barber, C.; Micha-Screttas, M.; Steele, B.R.; Georopolous, A.; Demetzos, C., *Curr. Top. Med. Chem*., **2008**, *3*, 1294

84. Malik, N.; Evagorou, E.G.; Duncan, R., *Colloq. Inse*., **1999**, *10*, 767

85. Jansen, J.F.G.A.; Brabander-van den Berg, E.M.M.; Meijer, E.W., *Science*, **1994**, *266*, 1226

86. Milhelm, O.M.; Myles, C.; McKeown, N.B.; Attwod, D.; D'Emanuele, A., *Int. J. Pharm*., **2000**, *197*, 239

87. Rouhi, M., *Chem. Eng. News*., **2004**, *82*, 5

88. Jikei, M.; Kakimoto, M., *Prog. Polymer. Sci*., **2001**, 1233

89. Frechet, J.M.J.; Hemni, M., *Science*, **1995**, *269*, 1080

90. Hawker, C.J., *J. Am. Chem. Soc*., **1994**, *116*, 11185

91. Hawker, C.J.; Frechet, J.M.J., *J. Am. Chem. Soc*, **1995**, *117*, 10763

92. Gao, H.; Matyjaszewski, K., *J. Am. Chem. Soc*., **2007**, *129*, 6633

93. Bottcher, H.; Hallensleben, M.L.; Wurm, H., *Polym. Bull*., **2000**, *44*, 223

94. Husseman, M.; Malmstrom, E.E.; McNamara, M.; Mate, M.; Mecerreyes, D.; Benoit, D.G.; Hedrick, J.L.; Mansky, P.; Huang, E.; Russell, T.P.; Hawker, C.J., *Macromolecules*, **1999**, *32*, 1424

95. He, T.; Adams, D.J.; Butler, M.F.; Yeoh, C.T.; Cooper, A.I.; Rannard, S.P., *Angew. Chem. Intl. Ed*., **2007**, *46*, 9243

96. Chrisholm, M.; Hudson, N.; Viela, F.; Sherrington, D.C., *Macromolecules*, **2009**, *42*, 7745

97. Rannard, S.P.; Sherrington, D.C., Rogers, S.H.; Royles, B.; Graham, S.; Findlay, P.H., *Abstr. Pap. Am. Chem. Soc*., **2004**, *228*, 416

98. Blencowe, A.; Tan, F.T.; Goh, T.K.; Qiao, G.G., *Polymer*, **2009**, *50*, 5

99. Ueda, J.; Matsuyama, M.; Kamigaito, M.; Sawamoto, M., *Macromolecules*, **1998**, *31*, 557

100. Gao, H.; Matyjaszewski, K., *Macromolecules*, **2006**, *39*, 3154

101. Bon, S.A.F.; Bosveld, M.; Klumperman, B.; German, A.L., *Macromolecules*, **1997**, *30*, 324

102. Cunningham, M.F., *Prog. Polym. Sci*., **2008**, *33*, 365

103. Matyjazewski, K.; Patten, T.E.; Xia, *J., J. Am. Chem. Soc*., **1997**, *119*, 674

104.Stromberg, R.R.; Straus, S.; Achhammer, B.G., *J. Polym. Sci*., **1959**, *35*, 355

105. Amirzadeh, G.; Schnabel, W., *Macromol. Chem. Physic*., **1981**, *182*, 2821

106. Mino, G.; Kaisemann, S.; Rasmussen, E., *J. Polym. Sci*., **1959**, *134*, 393

107. Chedekel, M.; Land, E.; Thompson, A.; Truscott, G., *J. Am. Chem. Soc. Chem. Commun*., **1984**, 1170

108. Bamford, C.H; Dyson, R.W.; Eastmond, G.C., *Polymer*, **1969**, *10*, 885

109. Cowie, J.M.J; Arrighi, V., Polymers: Chemistry and Physics of Modern Materials, **2008**, *3rd Edition*, Taylor & Francis Group: Florida

110. Matyjaszewski, K., *Macromolecules*, **2012**, *45*, 4015

111. www.cmu.edu/maty/development-atrp/index.html

112. Kajiwara, A.; Matyjaszewski, K., *Macromolecules*, **1998**, *31*, 5695

113. Nicolasa, J.; Guillaneuf, Y.; Lefayb; Didier, B.; Charleux, B., *Prog. Polym. Sci*., **2013**, *38*, 63

114. Gregory, A.; Stenzel, M.H., *Expert Opin. Drug. Deliv*., **2011**, *8*, 237

115. Hawker, C.J.; Bosman, A.W.; Harth, E., *Chem. Rev*., **2001**, *101*, 3661

116. Kazmaier, P.M.; Daimon, K.; Georges, M.K; Hamer, G.K.; Veregin, R.P.N., *Macromolecules*, **1997**, *30*, 2228

117. Harth, E.; Van Horn, B.; Hawker, C.J., *Chem. Comm*. **2001**, 823

118. Sciannamea, V.; Jerome, R.; Detrembleur, C., *Chem. Rev*., **2008**, *108*, 1104

119. Grubbs, R.B., *Polym. Revs*., **2011**, *51*, 104

120. Chiefari, J.; Chiong, B.; Ercole, F.; Kristina, J.; Jeffrey, J.; Mayadunne, R.; Meijis, G.F.; Moad, C.L.; Moad, G.; Rizzardo, E.; Thang, S.H., *Macromolecules*, **1998**, *31*, 5559

121. Samakande, A.; Sanderson, R.D.; Hartmann, P.C., *Synthetic Comm*., **2007**, *37*, 3861

122. Lai, J.T.; Filla, D.; Shea, R., *Macromolecules*, **2002,** *35*, 6754

123. Moad, G.; Solomon, D.H., The Chemistry of Radical Polymerisation, **2006**, 2nd Edition, Elsevier: Oxford

124. Moad, G.; Rizzardo, E.; Thang, S.H., *Aust. J. Chem*., **2009**, *62*, 1402

125. Szwarc, M., *Nature*, **1956**, *178*, 1168

126. Bywater, S.; Worsfold, D.J., *Can. J. Chemistry*, **1960**, *38*, 1891

127. Altares, T.; Wyman, D.P.; Allen, V.R.; Meyersen, K., *J.Polymer. Sci. Part A*., **1956**, *3*, 4131

128. Gauthier, M.; Moller, M., *Macromolecules*, **1991**, *24*, 4548

129. Zhao, Y.;Higashihara, T.; Sugiyama, K.; Hirao, A., *J. Am. Chem. Soc*., **2005**, *127*, 14158

130. Hirao, A.; Tokuda, Y.; Morifuji, K.; Hayashi, M., *Macromol. Chem. Physic*., **2001**, *202*, 1606

131. Hirao, A.; Hayashi, M.; Haraguchi, N., *Macromol. Rapid Comm*., **2001**, *21*, 1171

132. Hayashi, M.; Kojima, K.; Hirao, A., *Macromolecules*, **1999**, *32*,

133. Hadjichristidis, N.; Pitsikalis, M.; Pispas, S.; Iatrou, H., *Chem. Rev*., **2001**, *101*, 3747

134. Lutz, P.; Rempp, P., *Macromol. Chem. Physic*., **1988**, *189*, 1051

135. Eschwey, H.; Burchard, W., *Polymer*, **1975,** *16*, 180

136. Matmour, R.; Gnanou, Y., *Prog. Polym. Sci*., **2013**, *38*, 30

137. West, R.; Carney, P.A.; Mineo, C., *J. Am. Chem. Soc*., **1965**, *87*, 3788

138. Maercker, A.; Theis, M., *Top. Curr. Chem*., **1987**, *138*, 61

139. Matmour, R.; Lebreton, A.; Tsisilianis, C.; Kallitsis, I.; Rodriguez, V.H.; Gnanou, Y., *Angew. Chem. Int. Ed*., **2005**, *44*, 284

140. Matmour, R.; Gnanou, Y., *J. Am. Chem. Soc*., **2008**, *130*, 1350

141. Mock, E.B.; Bruyn, H.; Hawkett, B.S.; Gilbert, R.G.; Zukoski, C.F., *Langmuir*, **2006**, *22*, 4037

142. Eastoe, J.; Warne, B., *Curr. Opin. Colloid. In*., **1996**, *1*, 800

143. Krauel, K.; Davies, N.M.; Hook, S.; Rades, T., *J. Control. Release*, **2005**, *106*, 76

144. Desgouilles, S.; Vauthier, C.; Bazile, D.; Vacus, J.; Veillard, M.; Couvreur, P., *Langmuir*, **2003**, *19*, 9504

145. Schubert, S.; Delaney, J.T.; Schubert, U.S., *Soft Matter*, **2011**, *7*, 1581

146. Bilati, U.; Allemann, E.; Doelker, E., *Eur. J. Pharm. Sci*., **2005**, *24*, 67

147. Minost, A.; Delaveau, J.; Bolzinger, M.A.; Fessi, H.; Elaissari, A., *Recent. Pat. Drug. Deliv. Formul*., **2012**, *6*, 250

148. Nagavarma, B.V.N.; Hemant, K.S.; Yadav, A.; Vasudha, A.A.; Shivakumar, H.G., *Eur. J. Pharm. Clin. Res*., **2012**, *5*, 16

149. Hu, F.Q.; Yuan, H.; Zhang, H.H.; Fang, M., *Int. J. Pharm*., **2002**, *239*, 121

150. Xie, J.; Wang, C.H., *Pharm. Res*., **2005**, *22*, 2079

151. Byrappa, K.; Ohara, S.; Adschiri, *Adv. Drug. Deliver. Rev*., **2008**, *60*, 299

152. Rao, J.P.; Geckeler, K.E., *Prog. Polym. Sci*., **2011**, *36*, 887

153. Fessi, H.; Puisieux, F.; Devissaguet, J.P., Devissaguet, *Eur. Patent*, **1987**, *274*, 961

154. Memis, E.; Bochot, A.; Ozalp, M.; Dunchene, D.; Hincal, A., *Pharma. Res*., **2003**, *20*, 1

155. Niwa, T.; Takeuchi, H.; Kunou, N.; Kawashima, Y., *J. Control. Release*, **1993**, *25*, 89

156. Barichello, J.M.; Morishita, M.; Takayama, K.; Nagai, T., *Drug. Dev. Ind. Pharm*., **1999**, *25*, 471

Chapter 2

Experimental

2.1 Materials

All chemicals were purchased from Sigma Aldrich, Alfa Aesar, and Acros Organics and used as received, unless otherwise stated. With the exception of divinylbenzene (80%) all purity grades were above 96%. Benzene was dried over molecular sieves for 24 hours, and styrene monomer was passed through a column of basic aluminium oxide to remove the inhibitor and then dried over anhydrous calcium hydride rocks for 24 hours

2.2 Measurements

2.2.1 Nuclear Magnetic Resonance Spectroscopy

^{1}H NMR spectra were recorded on both a Bruker 400 Ultrashield and a Bruker Avance 400 MHz system fitted with a 5 mm broadband inverse (BBFO) probe with automatic tuning and matching capability (ATM) and a SampleJet autosampler. Data was collected at 25 ^{o}C at a frequency of 400.13 MHz for ^{1}H. Deuterated solvents were used as obtained from Sigma-Aldrich and all spectra are referenced to specified standards.

2.2.2 Mass Spectroscopy

Mass spectoscopy spectra were recorded on a Micromass LCT mass spectrometer.

2.2.3 Gel Permeation Chromatography

Apparent molar masses of polymers were determined by triple detection gel permeation chromatography (GPC) using a Malvern Viscotek instrument. The GPC was equipped with a GPCmax VE2001 auto-sampler, two Viscotek T6000 columns (and a guard column), a refractive index (RI) detector VE3580 and a 270 Dual Detector (light scattering and viscometer) with a mobile phase of THF and a flow-rate of 1 mL min^{-1}.

All polymer samples were prepared at approximately 4 mg/mL, accurate concentrations noted and input into the software for each sample. Results were confirmed by comparing the dn/dc values calculated by the software with the standard dn/dc value of polystyrene in THF dn/dc = 0.185.

2.2.4 Dynamic Light Scattering

Dynamic light scattering (DLS) studies were performed at a scattering angle of 173° using a Malvern Zetasizer Nano ZS equipped with a 4 mW He-Ne laser at a wavelength of 633 nm.

2.2.5 Differential Scanning Calorimetry

Differential scanning calorimetry analysis was carried out using a TA Instruments Q2000 DSC. Samples were heated/cooled/heated at a rate of 10 °C /min over two cycles between 25 °C and 250 °C.

2.2.6 Scanning Electron Microscopy

Scanning electron microscopy SEM images were obtained using a Hitachi S-4800 FE-SEM. Samples were dropped onto a silicon wafer mounted on an aluminium stub with a carbon tab, dried overnight at ambient temperature then gold coated at 20 mA for 2 minutes.

2.3 Synthesis Methods

2.3.1 Synthesis of Brancher Compounds

2.3.1.1 Synthesis of 1,4-bis(4 vinylphenoxybutane) (VPOB)

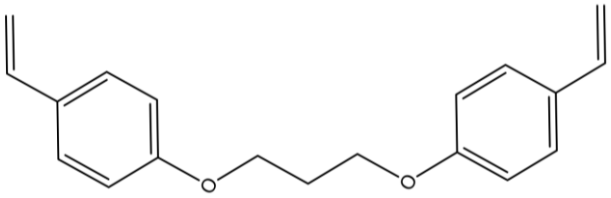

Figure 2.1: Structure of 1,4-bis(4-vinylphenoxybutane) (VPOB)

Method

5.19 g (31.9 mmol) of acetoxystyrene and 3.84 g (96 mmol) of sodium hydroxide in DMSO were stirred for one hour under nitrogen pressure at 75 ^{o}C. After one hour 3.45 g (15.9 m mol) dibromobutane in 20 mL DMSO was added dropwise under nitrogen over two hours. This was stirred at 75^{o}C for a further 5 hours, and then left to stir at room temperature overnight. The reaction mixture was poured into 100 mL of water and extracted up to eight times with a 3:1 v/v of diethylether/ toluene solution. The organic layer was washed 5 times with distilled water, dried over magnesium sulphate and the solvent removed under reduced pressure. The resulting white solid was repurified in chloroform and triturated with 500 mL ice-cold hexane. Typical recovered yield is 50 %. The typical purified recovered literature yield is 58 %.

Nominal mass spectroscopy: Expected: 294 m/z, Observed: 295 m/z $(M+ H)^{+}$

^{1}H NMR ($CDCl_3$) δ (ppm): 7.33 (d, 4 aromatic ^{1}H), 6.85 (d, 4 aromatic ^{1}H), 6.65 (d,d, 2 ^{1}H), 5.6 (d, 2 ^{1}H), 5.11 (d, 2 ^{1}H), 4.03 (t, 4 ^{1}H), 1.97(m, 4 ^{1}H), *^{13}C NMR* ($CDCl_3$) δ (ppm) : 158.8, 136.4, 130.4, 127.4, 114.6, 111.6, 67.6, 26.0

2.3.1.2 Synthesis of 6-bis(4-vinylphenoxy)hexane (VPOHEX)

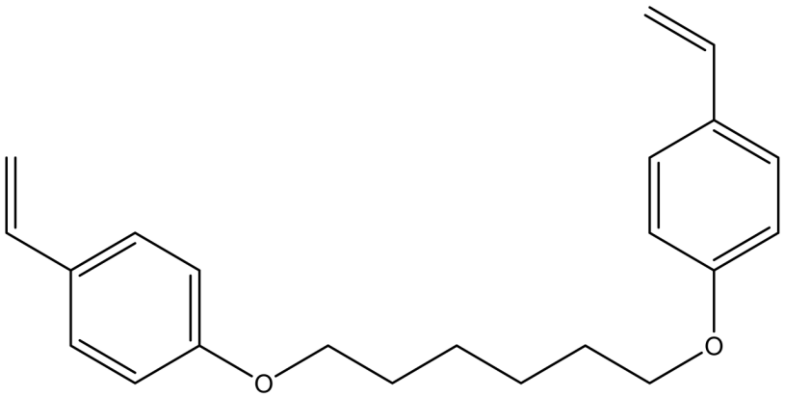

Figure 2.2: Structure of 1,6-bis(4-vinylphenoxyhexane) (VPOHEX)

5.19 g (31.9 mmol) of acetoxystyrene and 3.84 g (96 mmol) sodium hydroxide in DMSO was stirred for one hour under nitrogen at 75 ^{o}C. After one hour 3.88 g (15.9 mmol) 1,6 dibromohexane in 20 mL DMSO was added dropwise under nitrogen over two hours. This was stirred at 75^{o}C for a further 5 hours, and then left to stir at room temperature overnight. The reaction mixture was poured into 100 mL of water and extracted up to eight times with a 3:1 v/v of diethylether/ toluene solution. The organic layer was washed 5 times with distilled water, dried over magnesium sulphate and the solvent removed under reduced pressure. The resulting white solid was repurified in chloroform and triturated with 500 mL ice-cold hexane. Typical recovered yield is 60 %.

Nominal mass spectrometry: Expected: 323 m/z, Observed: 323 m/z $(M+ H)^{+}$

^{1}*H NMR* ($CDCl_3$) δ (ppm): 7.33 (d, 4 aromatic ^{1}H), 6.85 (d, 4 aromatic ^{1}H), 6.65 (d,d, 2 ^{1}H), 5.6 (d, 2 ^{1}H), 5.11 (d, 2 ^{1}H), 3.97 (t), 1.81 (q), 1.54 (m, 4 ^{1}H). ^{13}*C NMR* (CDCl3) δ (ppm): 158.8, 136.4, 130.4, 127.4, 114.6, 116.5, 67.8, 29.2, 25.9

2.3.1.3 Synthesis of 8-bis(4-vinylphenoxy)octane (VPOOC)

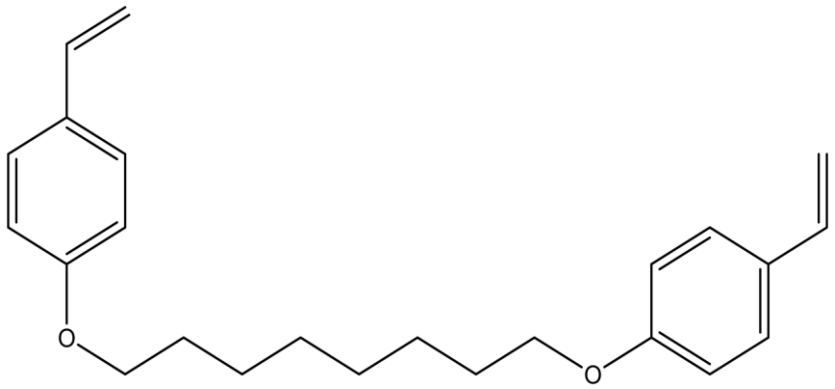

Figure 2.3: Structure of 1,8-bis(4-vinylphenoxyoctane) (VPOOC)

5.19g (31.9 mmol) of acetoxystyrene and 3.84g (96 mmol) sodium hydroxide in DMSO was stirred for one hour under nitrogen pressure at 75 ^{o}C. After one hour 4.33g (0.0159 mol) 1,8 dibromooctane in 20 mL DMSO was added dropwise under nitrogen over two hours. This was stirred at 75^{o}C for a further 5 hours, and then left to stir at room temperature overnight. The reaction mixture was poured into 100 mL of water and extracted up to eight times with a 3:1 v/v of diethylether/ toluene solution. The organic layer was washed 5 times with distilled water, dried over magnesium sulphate and the solvent removed under reduced pressure. The resulting white solid was repurified in chloroform and triturated with 500 mL ice-cold hexane. Typical recovered yield is 45 %.

Nominal mass spectrometry: Expected: 350 m/z Observed: 351 m/z (M+ H)

^{1}*H NMR* ($CDCl_3$) δ (ppm): 7.33 (d, 4 aromatic ^{1}H), 6.85 (d, 4 aromatic ^{1}H), 6.65 (d,d, 2 ^{1}H), 5.6 (d, 2 ^{1}H), 5.11 (d, 2 ^{1}H),, 3.95 (t), 2.17 (s), 1.78 (q), 1.55 (s), 1.46 (m, 6 ^{1}H), 1.39 (m). ^{13}*C NMR*: 159, 136.4, 130.4, 127.4, 114.6, 116.5, 67.8, 29.3, 29.2, 25.9

2.3.1.4 Synthesis of 10-bis(4-vinylphenoxy)decane (VPOT)

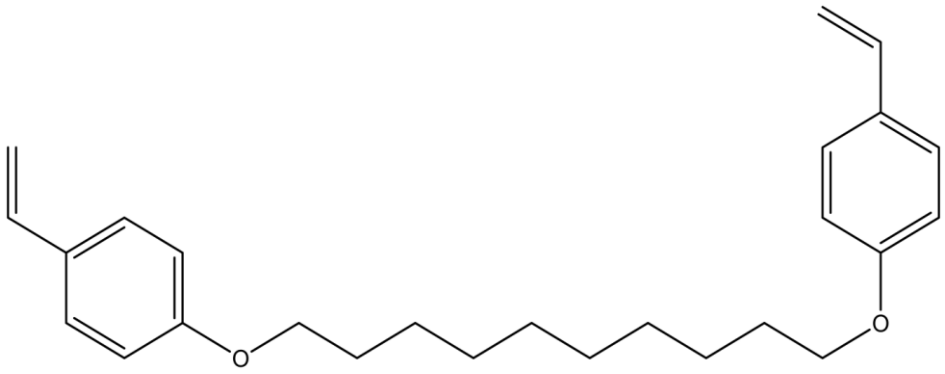

Figure 2.4: Structure of 1,10-bis(4-vinylphenoxydecane) (VPOT)

5.19g (31.9 mmol) of acetoxystyrene and 3.84g (96 mmol) sodium hydroxide in DMSO was stirred for one hour under nitrogen pressure at 75 ^{o}C. After one hour 4.77g (0.0159 mol) 1,10 dibromodecane in 20 mL DMSO was added dropwise under nitrogen over two hours. This was stirred at 75^{o}C for a further 5 hours, and then left to stir at room temperature overnight. The reaction mixture was poured into 100 mL of water and extracted up to eight times with a 3:1 v/v of diethylether/ toluene solution. The organic layer was washed 5 times with distilled water, dried over magnesium sulphate and the solvent removed under reduced pressure. The resulting white solid was repurified in chloroform and triturated with 500 mL ice-cold hexane. Typical recovered yield is 45 %.

Nominal mass spectrometry: Expected: 387 m/z, Observed: 379 m/z $(M+ H)^{+}$

^{1}H NMR ($CDCl_3$) δ (ppm): 7.33 (d, 4 aromatic ^{1}H), 6.85 (d, 4 aromatic ^{1}H), 6.65 (d,d, 2 ^{1}H), 5.6 (d, 2 ^{1}H), 5.11 (d, 2 ^{1}H), 3.95 (t), 1.76 (q), 1.54 (s), 1.45 (m, 8 ^{1}H), 1.33(m). *^{13}C NMR* (CDCl3) δ (ppm): 159, 136.4, 130.4, 127.4, 114.6, 116.5, 67.8, 29.4, 29.3, 29.2, 26.0

2.3.1.5. Synthesis of 12-bis(4-vinylphenoxy)dodecane (VPODD)

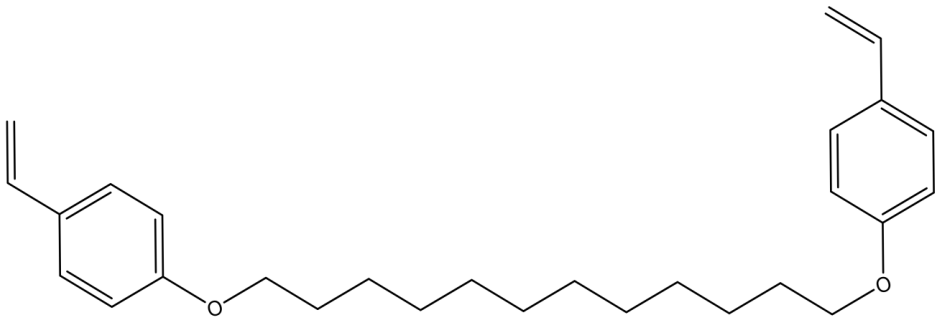

Figure 2.5: Structure of 1,12-bis(4-vinylphenoxydodecane) (VPODD)

5.19g (31.9 mmol) of acetoxystyrene and 3.84g (96 mmol) sodium hydroxide in DMSO was stirred for one hour under nitrogen pressure at 75 ^{o}C. After one hour 5.22 g (15.9 mmol) 1,12 dibromododecane in 20 mL DMSO was added dropwise under nitrogen over two hours. This was stirred at 75 ^{o}C for a further 5 hours, and then left to stir at room temperature overnight. The reaction mixture was poured into 100 mL of water and extracted up to eight times with a 3:1 v/v of diethylether/ toluene solution. The organic layer was washed 5 times with distilled water, dried over magnesium sulphate and the solvent removed under reduced pressure. The resulting white solid was repurified in chloroform and triturated with 500 mL ice-cold hexane. Typical recovered yields were less than 20 %.

Nominal mass spectrometry: 407 m/z, 424 m/z, 120 m/z. *^{1}H NMR* ($CDCl_3$) δ (ppm): 7.33 (d, 4 aromatic ^{1}H), 6.85 (d, 4 aromatic ^{1}H), 6.65 (d,d, 2 ^{1}H), 5.6 (d, 2 ^{1}H), 5.11 (d, 2 ^{1}H),, 3.95 (t), 3.6 (t), 1.77 (q), 1.55 (s), 1.45 (m, 8^{1}H), 1.28(m). *^{13}C NMR* (CDCl3) δ (ppm): 159, 136.3, 130.2, 127.4, 114.5, 111.4, 67.0, 29.6, 29.4, 29.3, 26.0

2.3.1.6. Synthesis of 1,4-bis(4-vinylphenoxy-*p*-xylene) (VPOPARAX)

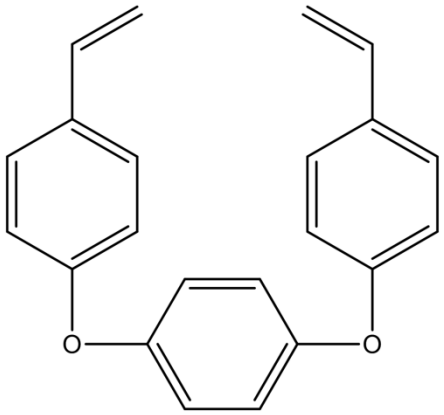

Figure 2.6: Structure of 1,4-bis(4-vinylphenoxydodecane) (VPOPARAX)

5.19 g (31.9 mmol) of acetoxystyrene and 3.84 g (96 mmol) sodium hydroxide in DMSO was stirred for one hour under nitrogen pressure at 75 ^{o}C. After one hour 4.19 g (15.9 mmol) of α, α' dibromo-*p*-xylene in 20 mL DMSO was added dropwise under nitrogen over two hours. This was stirred at 75 ^{o}C for a further 5 hours, and then left to stir at room temperature overnight. The reaction mixture was poured into 100 mL of water and extracted up to eight times with a 3:1 v/v of diethylether/ toluene solution. The organic layer was washed 5 times with distilled water, dried over magnesium sulphate and the solvent removed under reduced pressure. The resulting yellow solid was repurified in chloroform and triturated with 500 mL ice-cold hexane. Recovered yield was <20 %.

Analysis

Nominal mass spectrometry: Expected: 342 m/z, Observed: 343 m/z, $(M+ H)^{+}$

2.3.2 Synthesis of Linear Polystyrenes by Anionic Polymerisation Techniques

All glassware was dried in a hot oven for at least 24 hours prior to use. Benzene was dried over molecular sieves for 24 hours, and styrene monomer was passed through a column of basic aluminium oxide to remove the inhibitor and then dried over anhydrous calcium hydride rocks for 24 hours.

sec-Butylithium (*sec*-BuLi) was titrated to determine the accurate molarity using the method reported by Shapiro et al [21]. 291 mg (0. 768 mmol) of 1,3-Diphenylacetone *p*-tosylhydrazone was added to 8 mL of anhydrous THF under nitrogen pressure. *sec*-BuLi was added dropwise until a persistent yellow colour was observed.

Alternatively, the molarity of the *sec*-BuLi solution could also be determined by polymerising styrene: a known and accurate volume of *sec*-BuLi solution was added to a known and accurate amount of styrene in solution in benzene. After purification, the molecular weight of the polystyrene was determined by triple detection GPC and/or ^{1}H NMR. Knowing M_n of the polymer, the molar mass of styrene (MW = 104.15 g mol^{-1}) and the number of mol of styrene introduced (n_S) it is possible to assess the molarity of *sec*-BuLi by the equation: $n_{BuLi} = n_S / (M_n/M_w)$, where $(M_n/M_w) = DP_n$ is the degree of polymerisation of the polystyrene.

2.3.2.1 Synthesis of Polystyrene by Anionic Polymerisation initiated by lithium-halide exchange

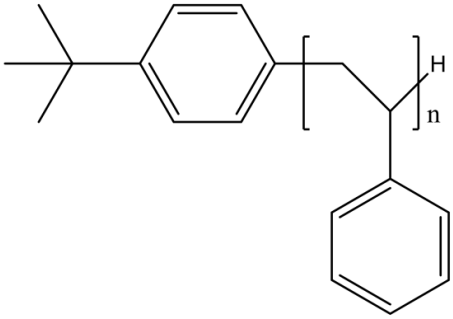

Figure 2.7: Structure of polystyrene initiated with a 1-bromo-4-*tert*-butylbenzene/*sec*-BuLi adduct, synthesised by anionic polymerisation techniques

The amount of initiators 1-bromo-4-*tert*-butylbenzene and *sec*-BuLi were calculated each time for different chain lengths of polystyrene using the equation;

$$DP_n = [M]/[I]$$

The amount of the stabilising compound N,N,N',N'-Tetramethylethylenediamine (TMEDA) was matched by the moles of initiator. 1-bromo-4-*tert*-butylbenzene was added to a dry 100 mL flask and purged with nitrogen for 15 minutes. 30 mL anhydrous benzene, TMEDA and *sec*-BuLi were added under nitrogen pressure and this was stirred for 30 minutes at ambient temperature to allow the lithium complex to form. Styrene was added and a colour change from "pale peach" to deep red was observed. The reaction was left to stir overnight under nitrogen pressure.

The reaction was terminated by the addition of methanol, and stirred until all the red colour had disappeared. The colourless solution was then added dropwise into cold, stirred methanol so as to precipitate the polystyrene. The product was recovered by filtration, redissolved in chloroform, and then precipitated a second time into cold

methanol. The resulting white precipitate was filtered and dried in a vacuum oven prior to GPC and NMR analysis.

2.3.2.2 Synthesis of Polystyrene by Anionic Polymerisation initiated by *sec*-butyllithium

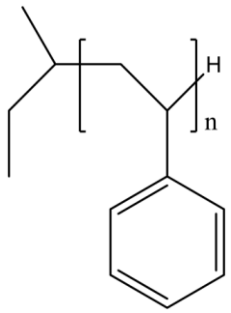

Figure 2.8: Structure of polystyrene initiated with *sec*-BuLi, synthesised by anionic polymerisation techniques

The amount of initiators was calculated each time for different chain lengths of polystyrene using DP_n=[M]/[I]. The amount of the the stabilising compound TMEDA was matched by the moles of initiator. Anhydrous benzene, TMEDA and styrene were added under nitrogen pressure. *sec*-BuLi was added and the colour change from colourless to deep red was observed. The reaction was left to stir for 1 hour under nitrogen pressure.

In a typical experiment such as a targeted DP_n= 50 monomer units amounts are as follows; 8 g of styrene (76.8 mmol), *sec*-BuLi (1.54 mmol), 0.14 mL TMEDA (1.54 mmol) and 30 mL benzene.

The reaction was terminated by the addition of methanol, and stirred until all red colour had disappeared. The colourless solution was then added dropwise into cold, stirred

methanol so as to precipitate the polystyrene. The product was recovered by filtration, redissolved in chloroform, and then precipitated a second time into cold methanol. The resulting white precipitate was filtered and dried in a vacuum oven prior to GPC and NMR analysis.

.

2.3.2.3 Synthesis of Polystyrene terminated with 4,4'-vinylidenebis(N,N-dimethylaniline) (ADPE)

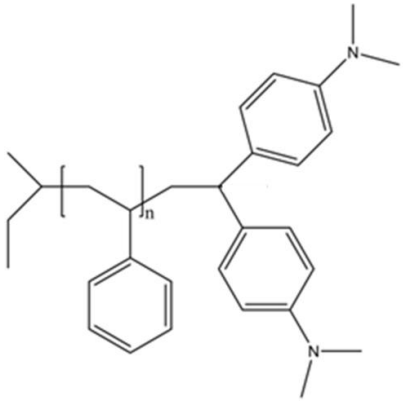

Figure 2.9: Structure of polystyrene initiated with *sec*-BuLi, terminated with ADPE synthesised by anionic polymerisation techniques

For a typical synthesis targeting a $DP_n = 50$ monomer units polystyrene, 4g of styrene (38 mmol) in 20 mL benzene were placed in a round bottomed flask and deoxygenated by nitrogen sparge for 10 minutes. The reaction was then initiated with 0.768 mmol of *sec*-BuLi and left to polymerise for 1 hour. The reaction was then terminated by the addition of 0.20g ADPE (0.768 mmol) in a mole ratio of 1:1 (ADPE:*sec*-BuLi) in benzene. In later experiments the solvent was changed and ADPE dissolved in THF was added. After termination had occurred, indicated by the absence of the red styrl anion colour, the white solution was then pipetted into cold, stirred methanol to give the

polystyrene precipitate. The colourless solution was then added dropwise into cold, stirred methanol so as to precipitate the polystyrene. The product was recovered by filtration, redissolved in chloroform, and then precipitated a second time into cold methanol. The resulting white precipitate was filtered and dried in a vacuum oven prior to GPC and NMR analysis.

.2.3.2.4. Synthesis of Polystyrene initiated with 4,4'-vinylidenebis(N,N-dimethylaniline) (ADPE)

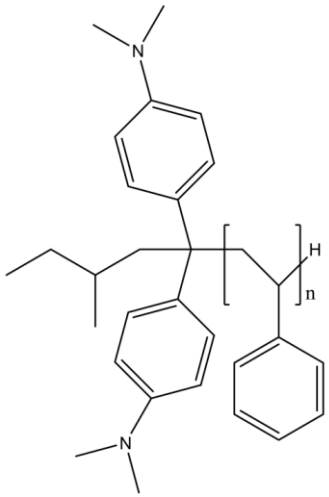

Figure 2.10: Structure of polystyrene initiated with a *sec*-BuLi/ADPE adduct, synthesised by anionic polymerisation techniques

The amount of the stabilising compound N,N,N',N'-Tetramethylethylenediamine (TMEDA) was matched by the moles of initiator. 4,4'-vinylidenebis(N,N-dimethylaniline) was added to a dry 100 mL two-necked flask with 30 mL anhydrous benzene, TMEDA and *sec*-BuLi were added under nitrogen pressure and this was stirred for 30 minutes at ambient temperature to allow the ADPE/*sec*-BuLi adduct to

form. Styrene was added and a colour change from orange to deep red was observed. The reaction was left to stir overnight under nitrogen pressure.

The reaction was terminated by the addition of methanol, and stirred until all the red colour had disappeared. The colourless solution was then added dropwise into cold, stirred methanol so as to precipitate the polystyrene. The product was recovered by filtration, redissolved in chloroform, and then precipitated a second time into cold methanol. The resulting white precipitate was filtered and dried in a vacuum oven prior to GPC and NMR analysis.

2.3.3 Synthesis of Branched Polystyrenes by Anionic Polymerisation

2.3.3.1 Synthesis of Branched Polystyrene by Anionic Polymerisation with DVB as brancher compound.

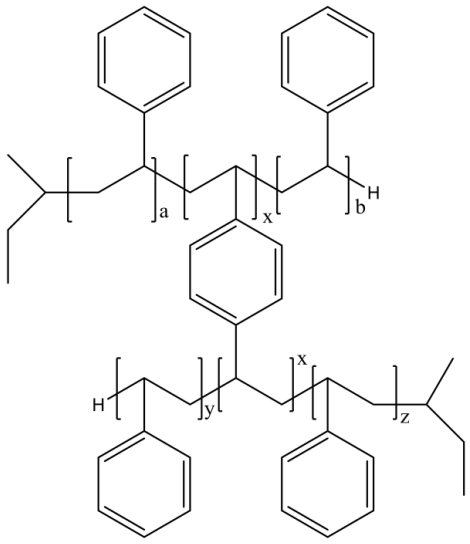

Figure 2.11: Structure of branched polystyrene initiated with *sec*-BuLi, DVB as brancher synthesised by anionic polymerisation techniques

The amount of brancher used was calculated at different moles due to different brancher:initiator ratios. DVB was added with anhydrous benzene, TMEDA and styrene to a 2-necked round bottomed flask under nitrogen pressure. Sec-butyllithium was then added and the colour change from colourless to deep red was observed. The reaction was left to stir for 3 hours under nitrogen pressure.

The reaction was terminated by the addition of methanol, and stirred until all red colour had disappeared. The colourless solution was then added dropwise into cold, stirred methanol so as to precipitate the polystyrene. The product was recovered by filtration, redissolved in chloroform, and then precipitated a second time into cold methanol. The resulting white precipitate was filtered and dried in a vacuum oven prior to GPC and NMR analysis.

2.3.3.2. Synthesis of Branched Polystyrene by Anionic Polymerisation with synthesised divinyl materials as brancher compounds

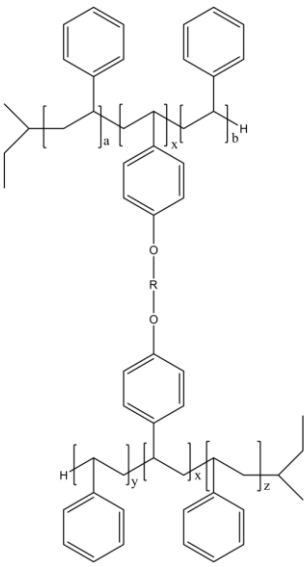

Figure 2.12: Structure of branched polystyrene initiated with *sec*-BuLi, divinyl compound as brancher synthesised by anionic polymerisation techniques

The following is a general synthetic method used for all brancher compounds. The amount of brancher used was calculated at different moles due to different brancher:initiator ratios. The brancher was added with anhydrous benzene, TMEDA and styrene to a 2-necked round bottomed flask under nitrogen pressure. Sec-butyllithium was then added and the colour change from colourless to deep red was observed. The reaction was left to stir for 3 hours under nitrogen pressure.

The reaction was terminated by the addition of methanol, and stirred until all red colour had disappeared. The colourless solution was then added dropwise into cold, stirred methanol so as to precipitate the polystyrene. The product was recovered by filtration, redissolved in chloroform, and then precipitated a second time into cold methanol. The resulting white precipitate was filtered and dried in a vacuum oven prior to GPC and NMR analysis.

2.3.4 Synthesis of Sulphonated Polymers

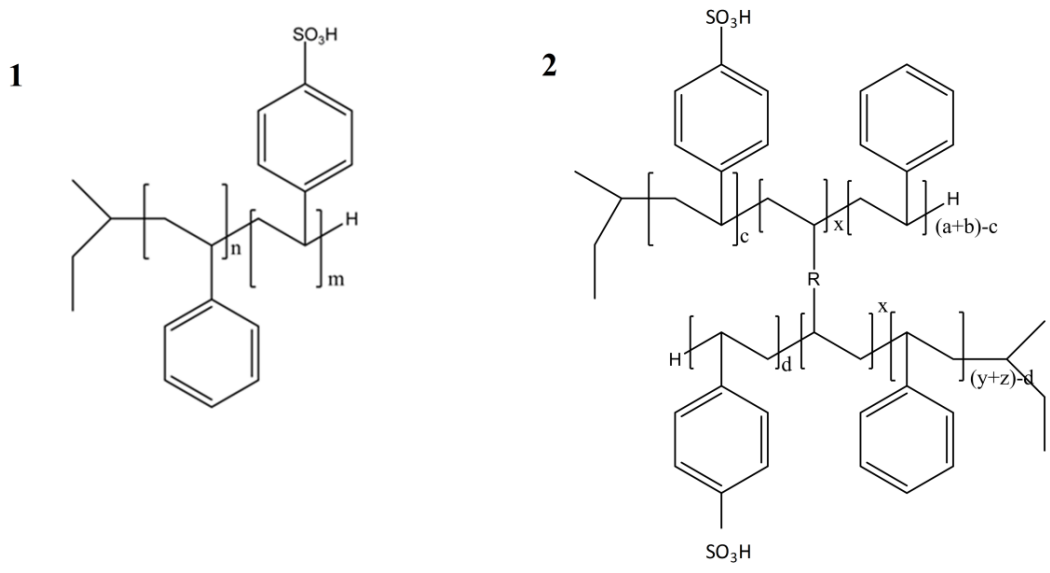

Figure 2.13: Structure of (1) linear and (2) branched sulphonated polystyrene

A 1.0 molar solution of acetyl sulphate was prepared in dichloroethane (DCE) was prepared. As the acetyl sulphate had to be prepared fresh before each synthesis different volumes were produced at different times. In a typical synthesis for 43 mL of a 1 M solution of acetyl sulphate the following amounts were used; 7.02 mL of acetic anhydride was added to 34ml of dichloroethane (DCE). The solution was cooled in ice to approximately 10 ºC and then 2.33 mL of concentrated sulphuric acid was slowly added. For the sulphonation of polystyrene, 1 g of synthesised polystyrene linear (1) or branched (2) material was dissolved in DCE, under nitrogen and heated to 50 ºC. Depending on the experiment different amounts of the acetyl sulphate was added by syringe under nitrogen pressure, and the reaction stirred at 50 ºC for 1 hour. The amount of acetyl sulphate added was varied each time to obtain a different level of sulphonation for specific polymers as follows;

1 g /104.15 gmol^{-1} = 0.00960154 mol of styrene repeat units.

So for '0.1 molar equivalents':

0.00960154 x 0.1 / 0.001 mol (moles per ml of acetyl sulphate solution) = 0.96 mL of acetyl sulphonate solution.

Amounts were calculated to be; 0.2 equivalents = 1.92 mL, 0.25 equivalents = 2.4 mL, 0.4 equivalents = 3.84 mL, 0.5 equivalents = 4.80 mL, 0.55 equivalents = 5.28 mL, 0.6 equivalents = 5.76 mL, 0.75 equivalents = 7.20 mL, 0.8 equivalents = 7.68 mL, 1 equivalent = 9.60 mL, 2 equivalents = 19.2 mL.

2.3.5 Synthesis of Sulphonated Polymers by Nanoprecitipation

Nanoprecipitation of sulphonated polystyrene requires the dissolution of each polymer in a suitable water-miscible solvent. The solvent used varied for different architectures of polymer and different sulphonation levels. At low sulphonation levels, such as those produced using 0.2 and 0.4 equivalents of acetyl sulphate, both linear and branched polystyrenes were soluble in either THF or MeOH. At higher sulphonation levels, the branched polymers were insoluble in a number of solvents, and therefore, unfortunately, nanoparticles could not be synthesised via nanoprecipitation.

To establish the best conditions for producing nanoparticles from the sulphonated polystryenes, solutions of both 10 mg mL^{-1} and 5 mg mL^{-1} were made for the different polymers in both MeOH and THF. 1 mL of the solutions were dropped by pipette into different volumes of stirred, ambient temperature water ; these being 1 mL, 2 mL, 5 mL and 10 mL. Initially, distilled water with a neutral pH was used, but in later experiments both basic (pH 9) and acidic (pH 5) water was evaluated. After the solutions were added dropwise with a pipette to water, the mixtures were left to stir at temperature overnight to allow evaporation of the organic solvent, yielding an aqueous dispersion of polymeric nanoparticles.

2.4 Nomenclature of Synthesised Polymers

2.4.1 Nomenclature of Linear Polystyrenes

Linear polystyrenes were synthesised with no brancher present and are named in relation to the targeted number of monomer units in the polymer chain or degree of polymerisation (DP_n) which relates to the number average molecular weight (M_n) value by the equation $DP = M_n / r$ where r is the mol weight of the repeat unit, ie. A chain of $DP_n = 10$ monomer units is so called DP_n10 or DP_n10 linear. For example;

DP_n25 or DP_n25 Linear	Linear polystyrene synthesised with a targeted $DP_n = 25$ monomer units

2.4.2 Nomenclature of Chain Extended Linear Polystyrenes

These polystyrenes synthesised with no brancher present and are named in relation to the targeted number of monomer units in the chain from the first batch of monomer added, plus the targeted number monomer units from the second batch of monomer added. So for a degree of polymerisation (DP) relating to the number average molecular weight (M_n) value, $DP_n = 10$ monomer units, followed with a targeted $DP_n = 40$ monomer units the polystyrene will be named DP_n10 plus DP_n40 or DP_n10 linear plus DP_n40 linear. For example:

DP_n10 plus DP_n90 or DP_n10 Linear plus DP_n90 linear	Linear polystyrene synthesised with a targeted $DP_n = 10$ monomer units followed by a second aliquot of styrene during the living anionic polymerisation equal to $DP_n = 90$ monomer units

2.4.3 Nomenclature of Branched Polystyrenes

For polystyrenes polymerised in the presence of a brancher monomer such as divinylbenzene or a synthesised distyrl compound, the nomenclature is related to the targeted chain length of the primary chain. The 'primary chain' is related to the degree of polymerisation of the linear polymer chain component that makes up the branched polymer, and will be the basis of the polymer structure. So a branched polymer with a targeted primary chain length of 10 monomer units will have an amount 'x' of DP_n =10 monomer units covalently bound by a branching monomer.

DP_n25 Branched	Branched polystyrene synthesised with a targeted primary chain length of DP_n = 25 monomer units

2.4.4 Nomenclature of Chain Extended Branched Polystyrenes

As above, polystyrenes polymerised in the presence of a brancher monomer, the nomenclature is related to the targeted chain length of the primary chain, and the branched polystyrene is named as described. The first part of the name relates to the polystyrene synthesised first plus the targeted number of monomer units in the second aliquot of monomer added. So for a degree of polymerisation (DP) relating to the number average molecular weight (M_n) value of the primary chain DP_n = 10 monomer units, followed with a targeted DP_n = 40 monomer units with brancher the polystyrene will be named DP_n10 linear plus DP_n40 branched.

DP_n10 linear plus DP_n40 branched	Linear polystyrene synthesised with a targeted DP_n = 10 monomer units followed by a second aliquot of styrene with brancher compound during the living anionic polymerisation with a targeted primary chain length equal to DP_n =40 monomer units

Chapter 3

Synthesis of Linear Polystyrenes using Controlled Polymerisation Techniques.

3.1 Target Molecules.

The primary aim of this work is to produce a carrier, to enhance the drug delivery of antiretroviral drugs, which is both stable in water, thus helping to overcome the issues of dissolution associated with the antiretroviral drugs, and is large enough to be engulfed by macrophages through phagocytosis. Macrophages act as sanctuary sites and infected macrophages could be important reservoirs outside the blood and as carriers of HIV to different organs. [1]

As discussed in the introduction, the use of nanoparticles as carriers for drug delivery has been of great scientific interest recently. Figure 3.1 shows the basic structure of the target nanoparticle that will be synthesised. The blue core is a highly branched hydrophobic polymer chain, which will potentially encapsulate the hydrophobic antiretroviral drug, shown in orange. Green symbolises the hydrophilic element of the particle. This is achieved either with a charged species, or linear hydrophilic polymer chains, as shown in Figure 3.1. Chapters 3, 4 and 5 shall focus on the synthesis of the highly branched hydrophobic polymer core.

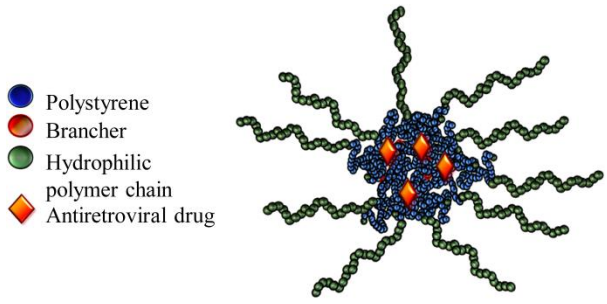

Figure 3.1: Illustration of the proposed nanoparticle to be synthesised

Previous work by Rannard and co-workers [2] has involved the generation of nanoparticles composed of a methacrylate based polymer core. Branched vinyl polymers of 2-hydroxypropyl methacrylate, *n*-butylmethacrylate [3], [4] ethylene glycol dimethacrylate were synthesised. From acetone or tetrahydrofuran (THF) solutions of these, nanoprecipitation or dialysis in water was employed to produce stable polymer nanoparticles. It was found that variations within the branched polymers led to considerable and unexpected stability to aqueous dilution, temperature, solvent addition and sonication suggesting that long term stability of the nanoparticles may be related to the architecture of the polymers.

Following from this work, branched polymers with different architectures have been synthesised within this study and nanoparticles have been generated in a similar process but with highly branched polystyrene based cores, rather than a methacrylate core. This will allow different properties to the methacrylate particles such as a higher glass transition temperature and different core environments to improve the encapsulation of varying antiretroviral drugs.

3.2 Synthesis of polystyrenes by anionic polymerisation

For the purpose of producing suitable highly branched polystyrenes for synthesis of polystyrene nanoparticles, there are many parameters that the method of synthesis and the polymers produced need to fulfil. One of the most important elements is there needs to be a very high percentage of monomer conversion to polymer, as branching has been shown to predominantly occur at high conversions (>85%) in many reported controlled branched vinyl polymerisations. It will be advantageous if this high conversion can be achieved in a relatively short time scale, definitely ideally less than 24 hours. This will

prove to be more important when block copolymers are produced, as less time taken for the first polymerisation to reach high conversion will allow a higher throughput of material within later studies.

Also related to the high conversion is the method of purification. If there is a high percentage of monomer left in the system this may prove difficult to remove and make purification difficult. Reactive vinyl monomers are known to be toxic and the removal of unreacted monomer is time consuming and costly. An ideal synthesis would not involve a lengthy and difficult purification of the system, either removing excess monomer, or in the case of many controlled radical polymerisations, removing residual metal catalyst.

The ability to control the polymerisation is also an important factor. If the number average degree of polymerisation, whereby the degree of polymerisation (DP_n) relates to the number of monomer units in the average polymer chain, can be controlled then it will be possible to target specific DP_n values, and therefore the polymer chain length for linear polystyrenes. For branched polystyrenes the ability to control the primary chain length will allow manipulation of the architecture, as shown in Chapter 5.1.

Linear polystyrene has previously been produced by a number of different controlled polymerisation methods such as nitroxide-mediated polymerisation [5], atom transfer radical polymerisation (ATRP) [6],[7],[8], stable free radical polymerisation (SFRP) [9], reversible addition-fragmentation chain transfer polymerisation (RAFT) [10], cationic polymerisation [11] and anionic polymerisation. [12]

The polymerisation of styrene by ATRP methods was attempted but deemed to be unsuitable. The results and discussion relating to these experiments can be found in the Supporting Information, Section 1.

One method that has proved in the literature to give excellent control over the degree of polymerisation is 'living' anionic polymerisation. 'Living' anionic polymerisation is a chain reaction polymerisation and unlike radical polymerisations such as ATRP there are no chain terminations, dormant chains or chain transfer reactions during the timescale of propagation. Under the right experimental conditions, it is assumed that there are no termination reactions. Although, in principle, this is identical to the control observed within ATRP, the reactive nature of the radicals that are generated, the establishment of the equilibrium of dormant and active chains, and the presence of reactive radicals at high conversions (with the potential for termination by combination) all present hurdles for high precision polymer synthesis by ATRP. Anionic polymerisation propagates via the reactive anions that are added to the reaction and the nature of the activity prevents anion-anion reaction and termination by combination which will allow for a high level of control over the M_n and DP_n.

3.2.1. Synthesis of linear polystyrenes.

As discussed in the introduction Chapter 1, both historically and more recently, anionic polymerisation is thought of as a technically difficult method of synthesis. Specialist reactors like the one illustrated in Figure 3.2 are often hand glass-blown in the laboratory by the polymer chemist.

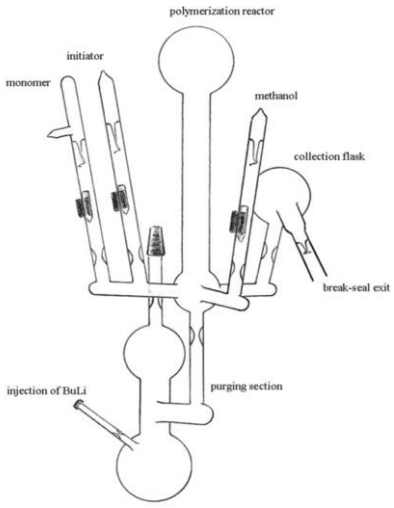

Figure 3.2: Example of an anionic polymerisation reactor vessel typically used in anionic polymerisations performed under vacuum conditions. [13]

Typically the reaction is performed under vacuum at an extremely low temperature of -78 °C to minimise side reactions. However, recent work by Matmour and Gnanou has demonstrated that anionic polymerisation can be undertaken successfully at ambient temperature to produce highly controlled polymers. [14]

Following from the related literature, low temperatures of -78 °C conditions were not adopted for the synthesis of polystyrene using anionic techniques within this study. Vacuum line techniques were not used, and standard reaction conditions were employed in early polymerisations (i.e no specialist laboratory procedures other than those required for water sensitive compounds); all glassware was dried in a hot oven for at least 24 hours prior to use, benzene was initially dried over molecular sieves for 24 hours, but in later work bottled anhydrous benzene was used as received from the supplier (Sigma Aldrich). Styrene monomer was passed through a column of basic aluminium oxide to remove the inhibitor and then dried over anhydrous calcium hydride rocks for 24 hours.

As the number of moles of initiator corresponds directly the DP_n of the polymer it is essential to accurately know the molarity of the organolithium initiator, *sec*-butylithium (*sec*-BuLi), in the purchased hexane solution. *sec*-BuLi was therefore titrated to help determine an accurate molarity using the method reported by Shapiro and co-workers.[15] This method uses the tosylhydrazone compound 1,3-diphenylacetone *p*-tosylhydrazone (DPTsH). Whilst all tosylhyrdrazone compounds give persistent coloured compounds upon anion formation, this compound was chosen as it gives a sharper end point than other similar compounds. A solution of 0.769 mol of DPTsH in 8mL of anhydrous tetrahydrofuran (THF) was cooled under nitrogen to approximately 0 ºC. s*ec*-BuLi was added slowly and accurately to the solution and an orange-yellow colour appeared and dissipated upon stirring. The end point is achieved when a persistent deep yellow/orange colour occurs. The end point has been missed if a deep orange/red colour occurs, as this indicates a high concentration of the dianion, generated after eqimolarity has been achieved. The titration reaction is illustrated in Scheme 3.1.

Whilst this does give an indication of the molarity and allows the number of moles to be calculated relatively accurately, there are problems with this method. The end point is very subjective as it progresses from colourless/pale to yellow/pale to orange/orange. It is difficult to generate concordant results and the titration has to be repeated many times. For the purpose of synthesising linear polymers this method is sufficient, however, in later work with branched polymers, a more accurate back calculation method is employed which is discussed further in Chapter 5. The amount of *sec*-BuLi was calculated each time for different chain lengths of polystyrene using $DP_n = [M]/[I]$. The amount of the stabilising compound N,N,N',N'-tetramethylethylenediamine (TMEDA) was matched by the moles of initiator.

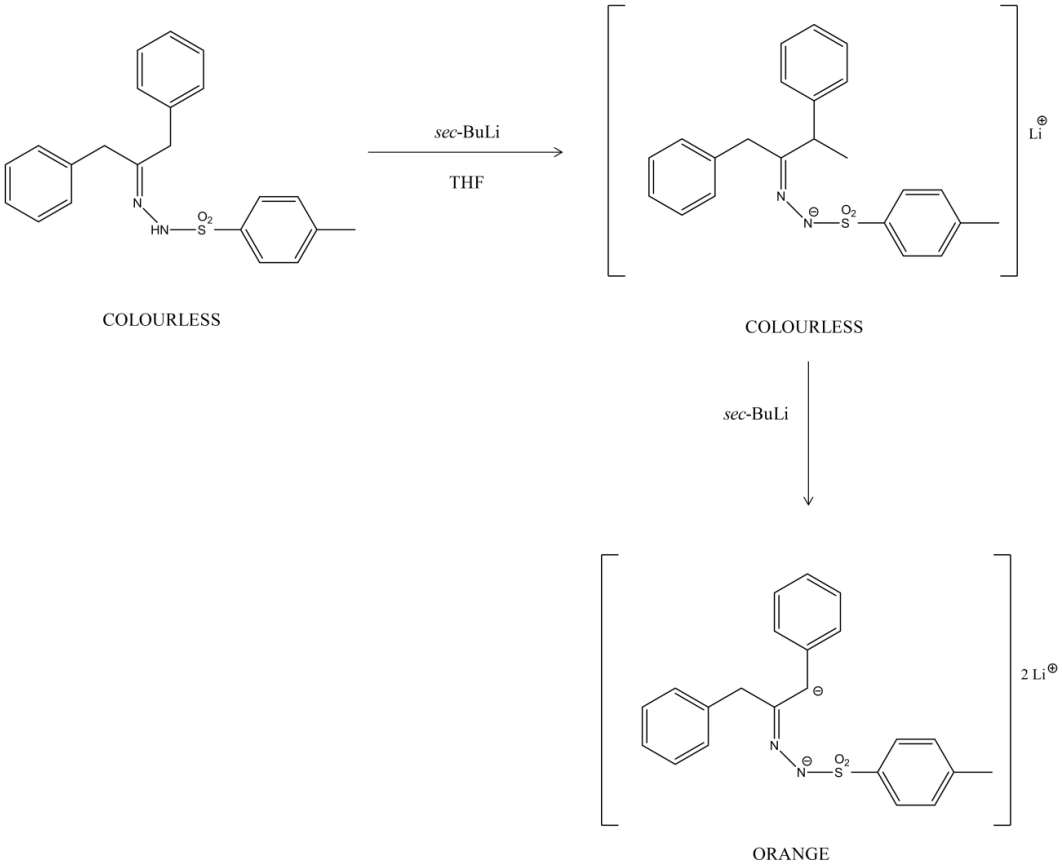

Scheme 3.1: Titration of *sec*-BuLi with 1,3-diphenylacetone *p*-tosylhydrazone whereby exceeding an equal molarity results in the formation of the coloured dianion shown. [17]

Anhydrous benzene, TMEDA and *sec*-BuLi were added by syringe under a positive nitrogen pressure. Nitrogen was dried through three separate drying agents; passed twice through powdered phosphorous pentoxide supported on vermiculite, and then through solid sodium hydroxide pellets to neutralise any acid generated by the phosphorous pentoxide treatment. Styrene was added rapidly under nitrogen by syringe and the colour change from pale peach to deep red was observed, indicating the presence of the styryl anion. A highly exothermic polymerisation reaction was observed, with temperatures reaching above 80 ºC as evidenced by the refluxing benzene. The reaction heated too rapidly to record the increase in temperature over time; the exothermic reaction is almost instantaneous when monomer is added. The

reaction was left to stir overnight under nitrogen pressure. The reaction Scheme is shown in Scheme 3.2, and a photograph of the experimental set-up is also shown in Figure 3.3.

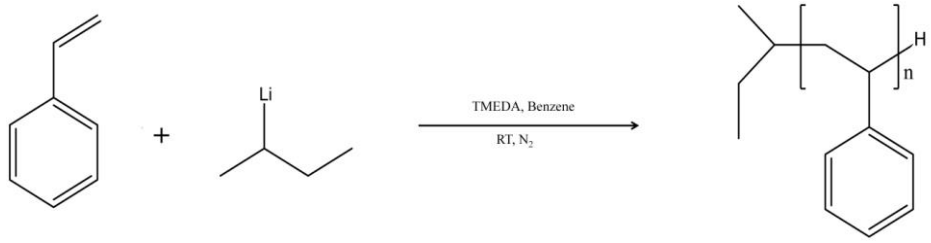

Scheme 3.2: Synthesis of linear polystyrenes initiated with *sec*-Buli

A series of linear polystyrenes of increasing chain lengths was synthesised using this approach. Different degrees of polymerisation were targeted for polystyrenes with DP_n values of 10, 25, 50, 100, 200 and 500 monomer units. Two approaches were used to determine the chain length and hence molecular weight of the polymers to provide comparative values; ^{1}H NMR and GPC. ^{1}H NMR spectroscopy shall be considered first.

Figure 3.3: Experimental method for synthesising polystyrene by anionic polymerisation, illustrating the colour change from the propagating reaction and the termination, resulting in the loss of the stryrl anion colour.

A ^{1}H NMR spectrum of polystyrene with a targeted DP_n of 50 monomer units in $CDCl_3$ is presented in Figure 3.4.

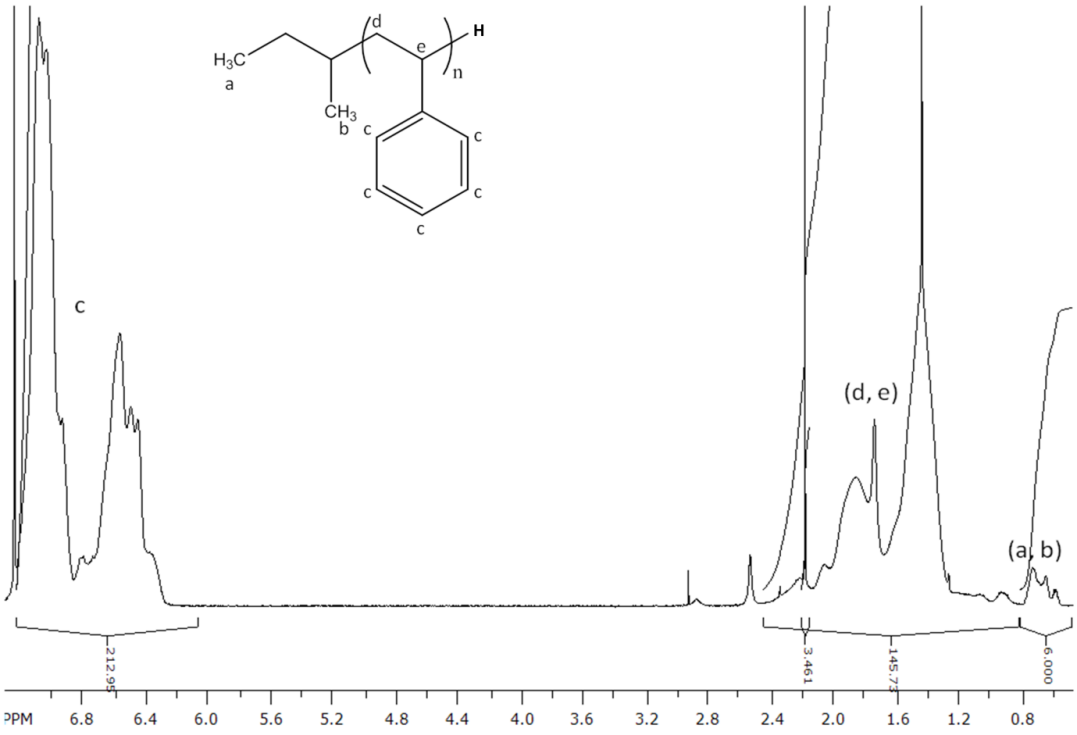

Figure 3.4: ^{1}H in $CDCl_3$ NMR spectrum of a targeted DP_n40 monomer units with an actual DP_n of 45 monomer units polystyrene synthesised by anionic polymerisation.

The signals due to the methyl groups of the *sec*-BuLi initiator are noticeable between 0.40 ppm and 0.80 ppm (labelled as A and B on Figure 3.4). Comparison of these integrated signals with those due to the five aromatic protons of the repeat unit between 6.20 ppm and 7.20 ppm (labelled C on Figure 3.4) or, alternatively, the three protons of the backbone between 0.80 ppm and 2.40 ppm (labelled D and E, Figure 3.4) allowed the DP_n to be estimated using the equation:

$$DP_n = I_{DE} / 3 \qquad or \qquad DP_n = I_C / 5$$

Where I_{DE} and I_C are, respectively, the integrals of the ^{1}H NMR signals between 0.80 ppm and 2.40 ppm (CH_3 of the initiator) and between 6.20 ppm and 7.20 ppm (aromatic protons of the repeat unit).

The signal of residual $CHCl_3$ in the ^1H NMR solvent at 7.26 ppm is overlapping slightly with the aromatic protons. If this is avoided in this integration, it is assumed that the resulting DP_n value will be underestimated by approximately 5 %. This is shown in the ^1H NMR spectrum in Figure 3.5, illustrating the area which will not be taken into account. Using the integrated signal of the polymer backbone between 0.80 ppm and 2.40 ppm would result in a similar error as this broad signal is covering the other protons of the initiator (CH_2 and CH) and is also likely to contain traces of methanol and other solvents used for the purification.

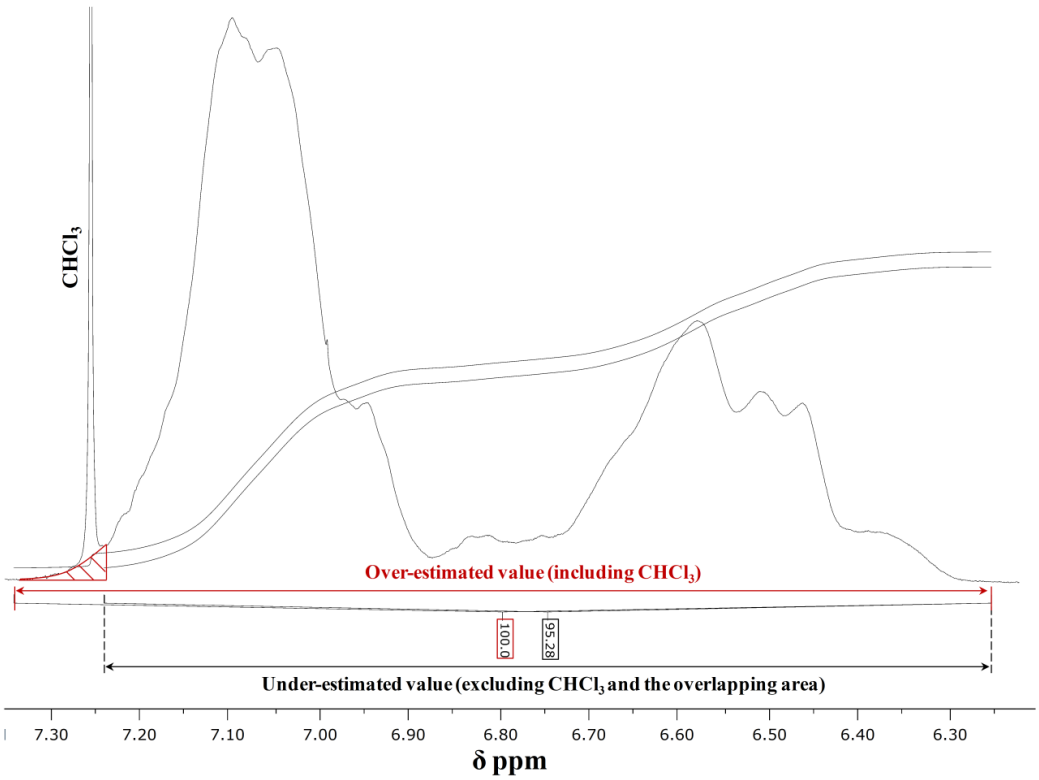

Figure 3.5: Representation of the rationale for omitting the $CHCl_3$ signal in calculations, using the ^1H NMR spectrum of polystyrene analysed in $CDCl_3$

In the example presented in Figure 3.4, the value of the DP_n calculated by ^1H NMR is 43 monomer units. This approach gives a DP_n that is close to the targeted value and correlates well with the values given by GPC as shown in Figure 3.6.

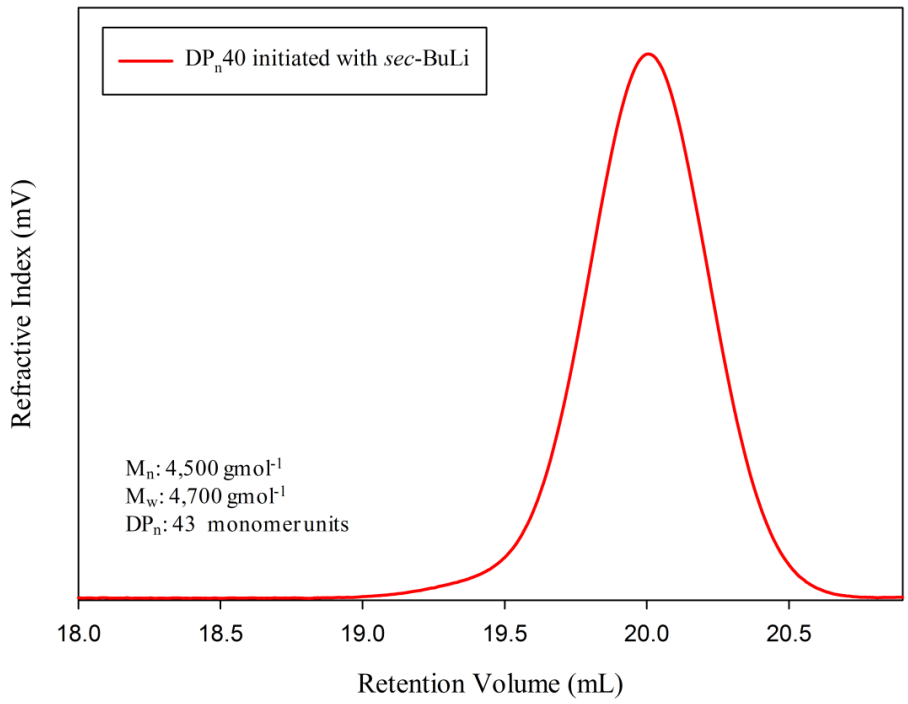

Figure 3.6: GPC chromatogram of a targeted DP_n40 polystyrene synthesised by anionic polymerisation.

This method not only allowed us to double check the molecular weight values given by GPC but also proved itself to be very useful when it comes to study complex chain-end functionalities, discussed later in Chapter 6.

For GPC analysis, the DP_n can be determined from the M_n by the equation:

$$DP_n = M_n / 104.15 gmol^{-1} (MW\ of\ styrene)$$

Shown in Figure 3.7 are the GPC chromatograms of polystyrenes with increased targeted DP_n values, ranging from 10 – 500 monomer units.

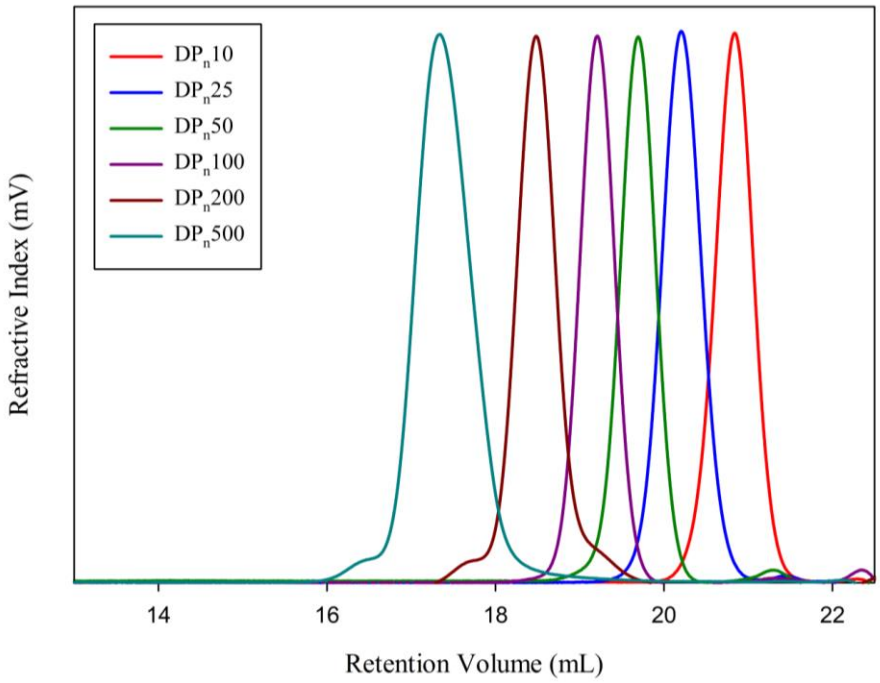

Figure 3.7: GPC chromatograms of different targeted chain length linear polystyrenes synthesised by anionic polymerisation techniques. DP_n10 (red), DP_n25 (blue), DP_n50 (green), DP_n100 (purple), DP_n200 (brown) DP_n500 (cyan).

The shape of the peaks from the refractive index detectors indicates that the polymers have relatively narrow polydispersities. In the longer chains, (target DP_n = 200 and 500 monomer units) a 'shoulder' is evident at lower elution times on each peak. This is thought to be due to some coupling of chains due to the oxoanion that can occur either due to some air (and therefore oxygen) getting into the reaction or during termination with methanol that has not been fully degassed to remove oxygen. Living anionic centres react readily with impurities and in the presence of oxygen a coupling reaction occurs readily after peroxidation of the polymer chain-end. [16] .The possible termination reactions are shown in Scheme 3.3 and the reaction that may result in the 'shoulder' seen on the GPC chromatograms is highlighted.

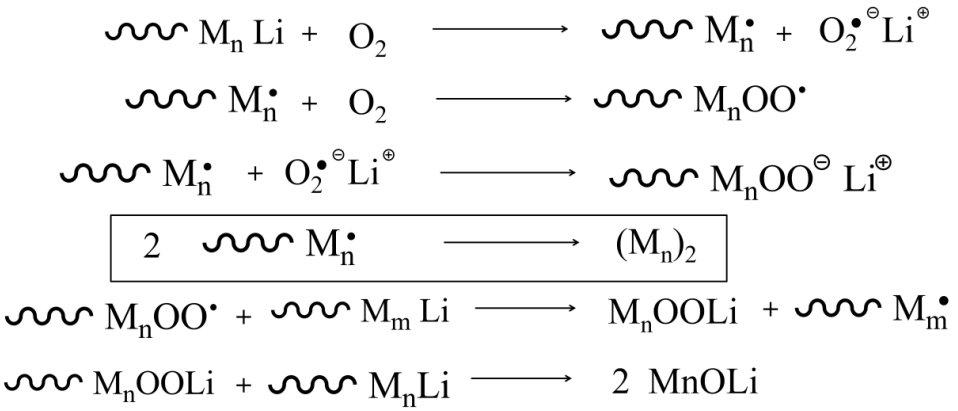

Scheme 3.3: Possible side reactions that may occur in the presence of oxygen [16].

The corresponding M_n and M_w values of these polymerisations are given in the Table 3.1. Theoretical M_n values (assuming 100% monomer conversion) are calculated by the following equation, whereby 57 $gmol^{-1}$ corresponds to the chain end resulting from the initiation by *sec*-BuLi.

$$Targeted\ M_n = (Targeted\ DP_n * 104.15 gmol^{-1}) + 57 gmol^{-1}$$

Table 3.1: Targeted and actual M_n and M_w values of polystyrenes produced by anionic polymerisation. Values determined by GPC.

Targeted DP_n	**Theoretical M_n ($gmol^{-1}$)**	**GPC**		
		M_n ($gmol^{-1}$)	**M_w ($gmol^{-1}$)**	**Đ**
10	1,098	1,000	1,100	1.11
25	2,660	2,400	2,500	1.04
50	5,264	4,500	4,700	1.04
100	10,472	11,300	11,700	1.03
200	20,887	19,600	22,700	1.16
500	52,132	53,100	59,300	1.17

As can be seen it is possible to control the chain length of the linear polystyrenes produced in a way that could not be readily achieved by ATRP. Anionic polymerisation offers superior control over the polymer synthesised, which will be important in later work in Chapter 5 where different architectures of polymer are explored. The ability to successfully target different polymer chain lengths is a big advantage for anionic polymerisation. Monomer to polymer conversion is also a key factor. ^{1}H NMR analysis of the crude reaction mixture after 24 hours showed that there was no monomer present in the system after this time. The ^{1}H NMR spectrum in Figure 3.4 illustrates the lack of vinyl signal present from the styrene monomer. This equates to a near 100% conversion of monomer to polymer which is a distinct improvement on ATRP methods.

3.2.2. Effect of changing the initiating system for anionic polymerisation

Lithium-halide exchange offers benefits for end group functionalisation, therefore the use of anionic polymerisation was studied under these different conditions. In later work *sec*-BuLi will be reacted with different compounds to create a bi-functional initiator (Chapter 3.2.2.2) and to create functionalised polystyrenes (Chapter 6).

To evaluate the effect that a lithium-halide initiation may have on the anionic polymerisation, two identical polymerisations of styrene were conducted, at a targeted chain length of 100 monomer units, with initiation by either *sec*-BuLi or a lithium-halide exchange reaction. In this instance, a molar ratio of 1:1 was used for 1-bromo-4-*tert*-butyl benzene and *sec*-BuLi and the amount of the stabilising compound TMEDA was matched to the moles of initiator. 1-bromo-4-*tert*-butylbenzene was added to a dry 100 mL flask and flushed with nitrogen for 15 minutes. 30 mL anhydrous benzene,

TMEDA and *sec*-BuLi were added under nitrogen pressure and this was stirred for 30 minutes to allow the lithium complex to form. Styrene monomer was added and the colour change from pale peach to deep red was observed. The reaction was left to stir overnight under nitrogen pressure, as before.

Figure 3.8 shows the overlaid GPC chromatograms of two linear polystyrene samples with target DP_n = 100 monomer units initiated either by the lithium halide or direct *sec*-BuLi methods.

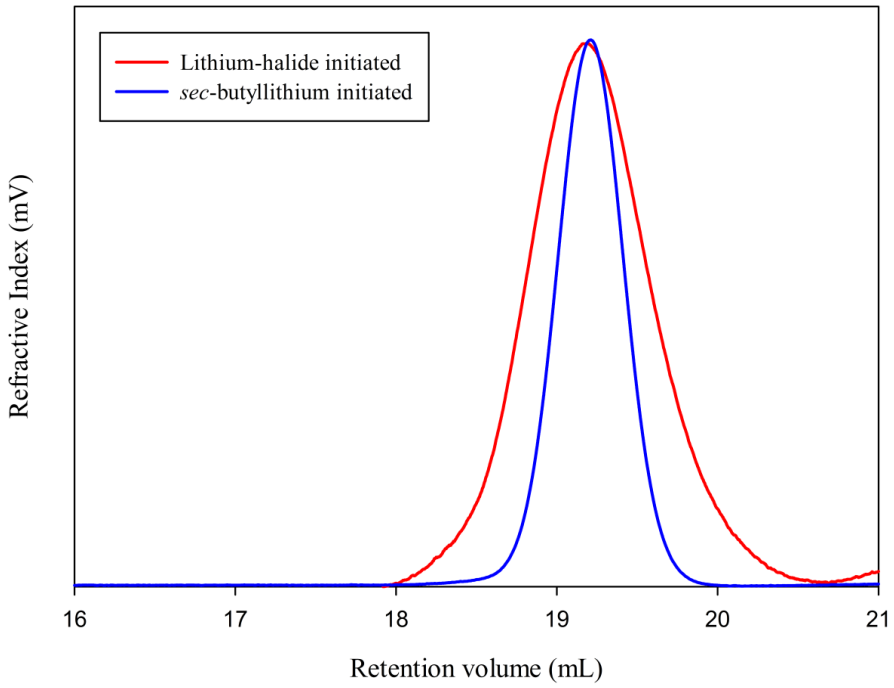

Figure 3.8: GPC chromatographs of DP_n100 monomer unit polystyrenes synthesised by anionic polymerisation techniques, initiated by lithium-halide exchange (red) and *sec*-BuLi alone (blue).

As can be seen, the peak of the molecular weight distribution is extremely similar in both chromatograms in Figure 3.8 suggesting good targeting of polymer chain lengths when using both initiating approaches, however, the noticeable difference is in the breadth of the molecular weight distributions; it would seem that initiation with just *sec*-BuLi results in a narrower dispersity. This is also seen in the M_n and M_w values in

Table 3.2. However, the polymerisation was still successful, reaching 100% conversion, and although the dispersity is higher than desired, it demonstrates that there can still be a level of control over the targeted polymer chain length when using lithium-halide exchange. As there appears to be no benefit to initiating in this way, and it also offers another potential contaminant into the system, all further experiments used *sec*-BuLi as the sole initiator, and lithium-halide exchange is only employed later where bi-functional initiation is explored (Chapter 3.2.2.)

Table 3.2: M_n, M_w and Đ values for polystyrenes with targeted DP_n100 = monomer units polystyrenes synthesised by anionic polymerisation techniques, initiated by lithium-halide exchange and *sec*-BuLi.

Initiator	**GPC**		
	M_n ($gmol^{-1}$)	**M_w ($gmol^{-1}$)**	**Đ (M_w/M_n)**
sec-Butyllithium	11,300	11,700	1.03
1-bromo-4-*tert*-butylbenzene	8,700	11,200	1.29

3.2.3. Effect of solvent concentration on anionic polymerisation.

The next variable to be investigated is whether increasing the amount of solvent, and thereby decreasing the solid content of the polymerisation and the concentration of initiating species, would have an effect on the polymerisation. This will also show any influence of solvent contaminants leading to unwanted termination, a factor that will be important when forming branched polymers.

A series of polymerisations was conducted where all conditions, except the volume of solvent, were kept the same; these being monomer amount (8g, 76.8 mmol), *sec*-BuLi

initiator (1.54 mmol, for a targeted DP_n = 50 monomer units) and TMEDA (1.54 mmol). All reactions were terminated after 24 hours. The amount of anhydrous benzene, bought from Aldrich and used as received without further purification, was increased in increments of 10 mL from 20 mL (styrene concentration = 0.4 gmL^{-1}) to 30 mL (styrene concentration = 0.27 gmL^{-1}), 40 mL (styrene concentration = 0.2 gmL^{-1}), 50 mL (styrene concentration = 0.16 gmL^{-1}) and 60 mL (styrene concentration = 0.13 gmL^{-1}). The resulting polymers were analysed by GPC and the RI traces are shown in figure 3.9.

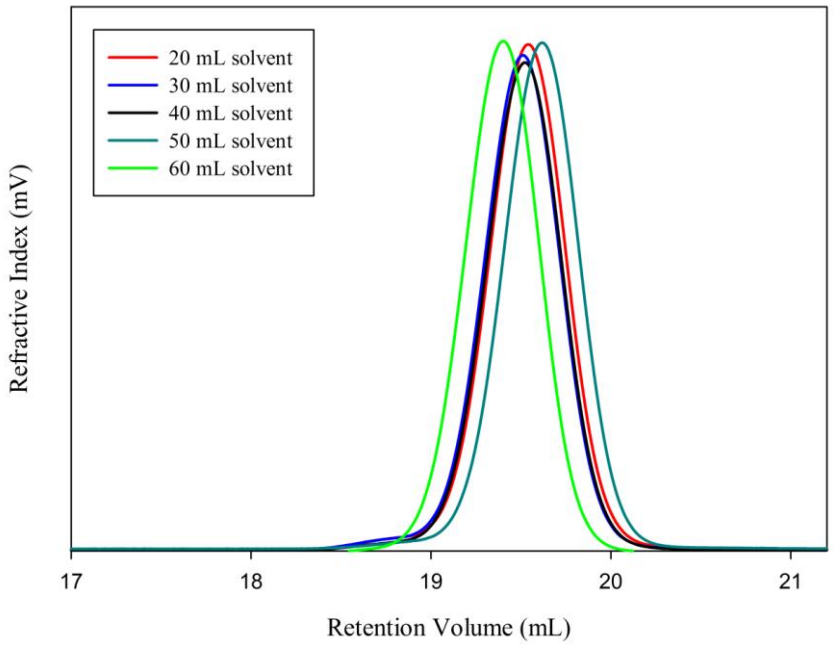

Figure 3.9: GPC chromatograms polystyrenes synthesised by anionic polymerisation techniques at different solvent concentrations; 0.4 gmL^{-1} (red), 0.27 g/mL (blue), 0.2 gmL^{-1} (black), 0.16 gmL^{-1} (cyan) and 0.13 gmL^{-1} (green).

As can be seen in Figure 3.9, there is very little difference between the polymers synthesised in benzene at varying concentrations. The M_n of the different polystyrenes varied from 9,400 - 10,200 $gmol^{-1}$, which is approximately 8 monomer units, and is within error of the titration and initiator/monomer additions. It was concluded that in

principle, variation of reaction concentration has no direct negative influence on the formation of linear polystyrene chains under these conditions. This also instils confidence that the anhydrous benzene from Sigma Aldrich is sufficiently dry for the anionic synthesis of polystyrene. It is not therefore necessary to distil the anhydrous benzene prior to polymerisation, provided the bottles are not stored after first use for prolonged periods of time. The effect of reaction concentration on the formation of branched polymers is explored further in Chapter 4.

3.2.4 Chain extension of linear polystyrenes polymerised by anionic polymerisation techniques.

Polystyrene chain extension was studied as the formation of block copolymers and the living nature of the chains is important in the formation of amphiphilic block copolymers, which could be used in the synthesis of polymeric nanoparticles.

For a living polymerisation, with no assumed termination, all initiated and propagating polymer chains should possess an 'active' anion after full monomer conversion that is ready to undergo further polymerisation with the addition of more monomer. The formation of a block copolymer was therefore attempted by first polymerising styrene using s*ec*-BuLi, as described previously, to achieve a target DP_n of 50 monomer units. After 24 hours a further volume of styrene, equivalent to 50 monomer units, was added and after another 24 hour period, another volume equivalent to 50 monomer units was added to the reaction mixture. Before each addition of monomer, samples of the reaction were taken and purified for analysis. The resulting polymer and samples were purified as before, and analysed by GPC under the same conditions previously

described. Figure 3.10 shows the GPC chromatographs of the final polymer, and overlaid are the samples of the polymer taken before each sequential addition of monomer.

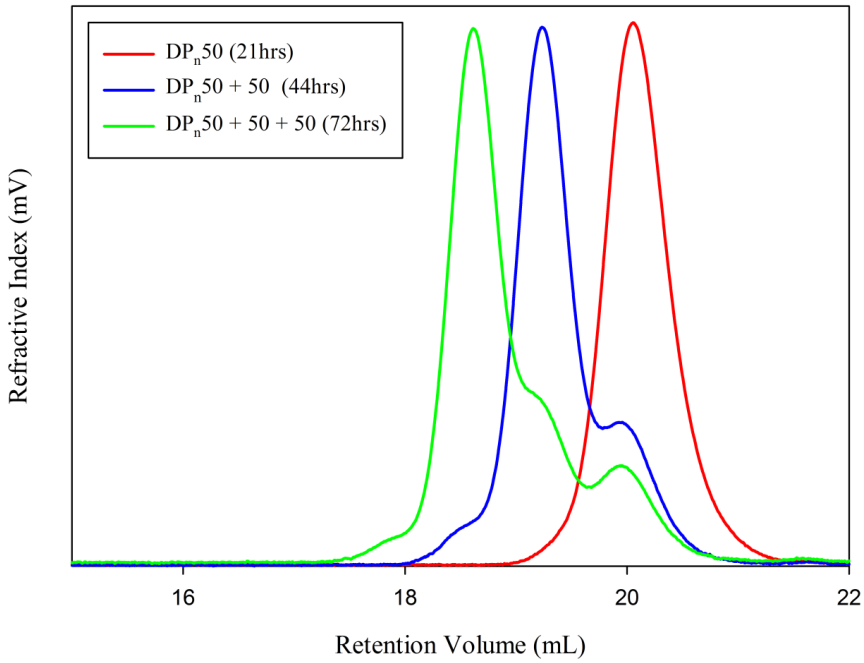

Figure 3.10: GPC chromatograms of the self blocking polymerisation of polystyrene. The M_n increases with the sequential addition of monomer so for DP_n50 the theoretical M_n is 5,200 $gmol^{-1}$ (red), DPn50 + 50 monomer units the theoretical M_n value is 10,400 $gmol^{-1}$ (blue) and DPn50 + 50 + 50 monomer units the theoretical M_n value is 15,600 $gmol^{-1}$.

As can be seen from Figure 15, the final polymer sample is multimodal with three defined species. As these appear to clearly overlay with the chromatograms of the samples with targeted DP_n = 100 and DP_n = 50 monomer units, it would appear that a significant amount of termination has occurred before each addition, and polystyrenes of varied chain lengths are present.

Termination may have happened during sampling, and adding the second and third batches of monomer as there is potential for air and therefore water to be introduced to the system. The time that the polymerisations were given to progress to full conversion (24 hours) may also have contributed to extra termination.

A study of the kinetics of the anionic polymerisation led to a dramatic change in the understanding of these polymerisations, and significantly changed the reaction time used experimentally for each polymerisation; a previous 24 hour reaction time was reduced to just 1 hour. With this change in synthetic method the previous chain extension experiment was repeated. A polystyrene of DP_n = 150 was initially targeted and the first addition of further monomer (equivalent to 50 monomer units) for the chain extension was added after 30 minutes, and the second monomer aliquot (equivalent to a further 50 monomer units) was added after another 30 minutes, giving a targeted polymer chain length of DP_n = 250 monomer units.. Figure 3.11 shows the GPC chromatographs of the final polymer, and overlaid are the samples of the polymer taken before each sequential addition of monomer.

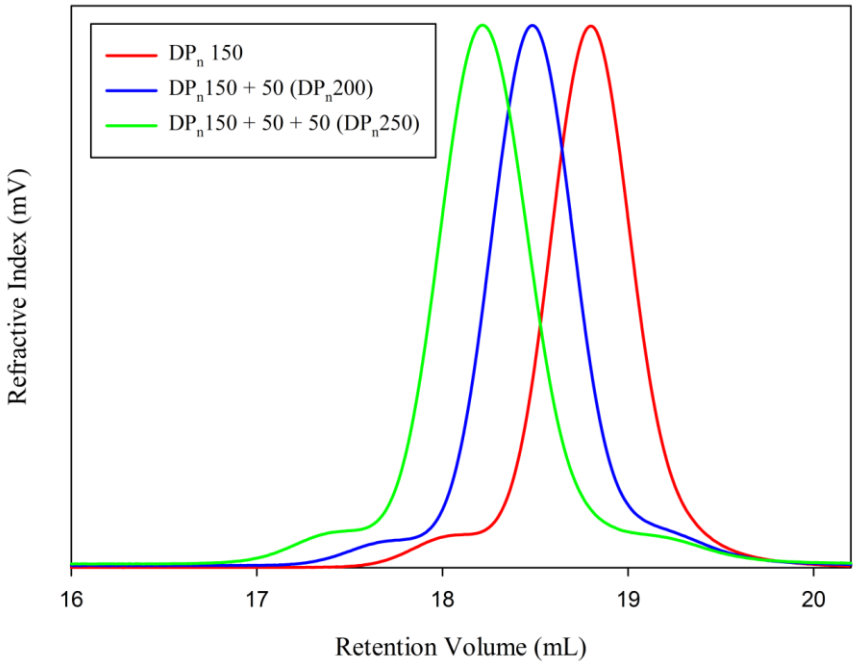

Figure 3.11: GPC chromatograms of the self blocking polymerisation. M_n increases with the sequential addition of monomer so for DP_{n1}50 the theoretical M_n is 15,600 $gmol^{-1}$ (red), DPn150 + 50 monomer units the theoretical M_n value is 20,800 $gmol^{-1}$ (blue) and DPn150 + 50 + 50 monomer units the theoretical M_n value is 26,000 $gmol^{-1}$.

Table 3.3 shows the values for the target M_n and the actual observed M_n values from GPC analysis and the dispersity value Đ of the chain extended polymer and the samples

taken before each addition. The GPC chromatogram obtained showed that the final polymer was essentially monomodal, with a polydispersity of 1.20.

Table 3.3: Target M_n, Actual M_n and Đ values determined by GPC

Target DP_n	**Target M_n ($gmol^{-1}$)**	**GPC**	
		Actual M_n ($gmol^{-1}$)	**Đ**
150	15,600	13,900	1.20
200	20,800	19,000	1.21
250	26,000	24,200	1.20

Each addition of monomer led to a linear increase in the polymer number average molecular weight as illustrated further in the graph in Figure 3.12.

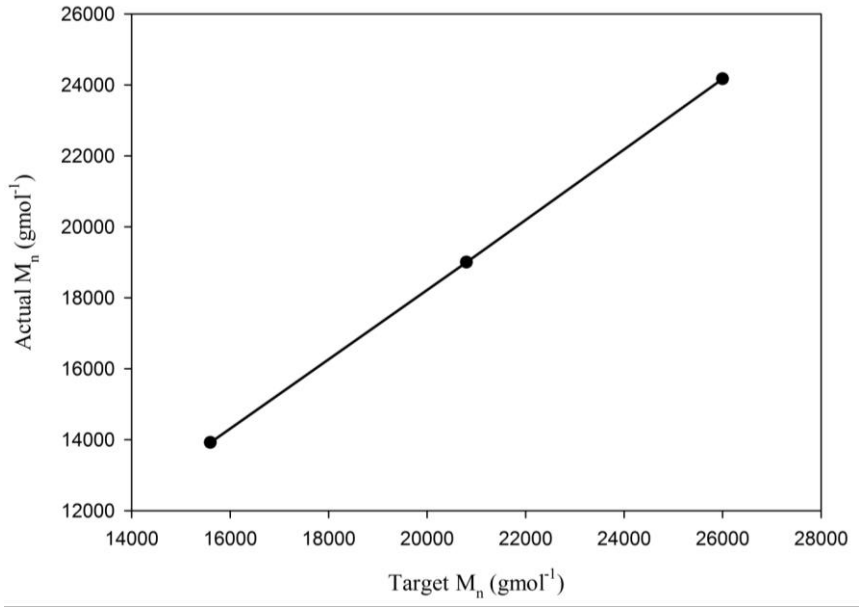

Figure 3.12: Graph of target M_n versus actual M_n, illustrating the linearity of chain extension growth.

To explore possible chain extensions further, which will be used in later experiments to significantly alter the architecture of branched polystyrene, a series of linear chain extension experiments were carried out. The following polystyrene DP_n values were targeted:

- Initial DP_n = 10 with the addition of 40 monomer units (final DP_n = 50 monomer units)
- Initial DP_n = 10 with the addition of 90 monomer units (final DP_n = 100 monomer units)
- Initial DP_n = 50 with the addition of 50 monomer units (final DP_n = 100 monomer units)

Table 3.4, is a table of the M_n and M_w values of the final polymers, as well as the M_n and M_w value of the sample taken before the second addition of monomer. This table and the GPC chromatographs of the final polymers overlaid in Figure 3.13 illustrates the success of the self-blocking experiments.

Table 3.4: M_n and M_w values of the pre-curser sample taken before additional monomer addition and M_n, M_w and Đ values for the final self-blocking polymer synthesised by anionic polymerisation techniques.

Targeted DP_n	**GPC**				
	M_n	**M_w**	**Final M_n ($gmol^{-1}$)**	**Final M^w ($gmol^{-1}$)**	**Đ**
DP_n10+DP_n40 (Total DP_n50)	1,000	1,100	5,320	5,540	1.04
DP_n10+DP_n90 (Total DP_n100)	1,000	1,100	11,100	11,500	1.04
DP_n50+DP_n50 (Total DP_n100)	4,810	5,070	9,280	11,100	1.09

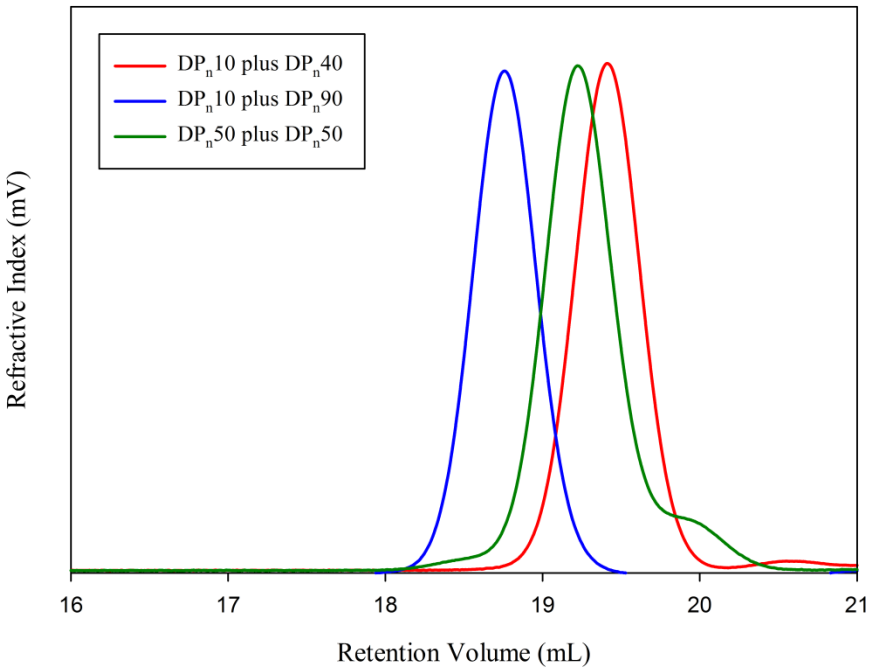

Figure 3.13: GPC chromatograms of the self blocking polymerisation of polystyrene by anionic polymerisation techniques.

3.2.5. Kinetic studies of linear polystyrene.

It was observed from ^{1}H NMR studies in Chapter 3.2.2.1 that after 24 hours the polymerisation had reached 100% conversion, however, the termination reactions observed during the chain extension syntheses led to an investigation of the reaction time of the polymerisation needed to obtain 100% conversion. One reason for the observed terminations may be the length of time the living chain is left at high conversion and in the absence of monomer.

Samples were taken throughout an anionic styrene polymerisation with a targeted chain length of DP_n = 100 monomer units. GPC analysis and ^{1}H NMR analysis in $CDCl_3$ were performed on the samples to follow the conversion. Figure 3.14 shows the GPC chromatograms of all the samples overlaid with the final polymer after 20 hours. The

reaction is highly exothermic and it was not possible to safely obtain samples during the first 10 minutes of the reaction.

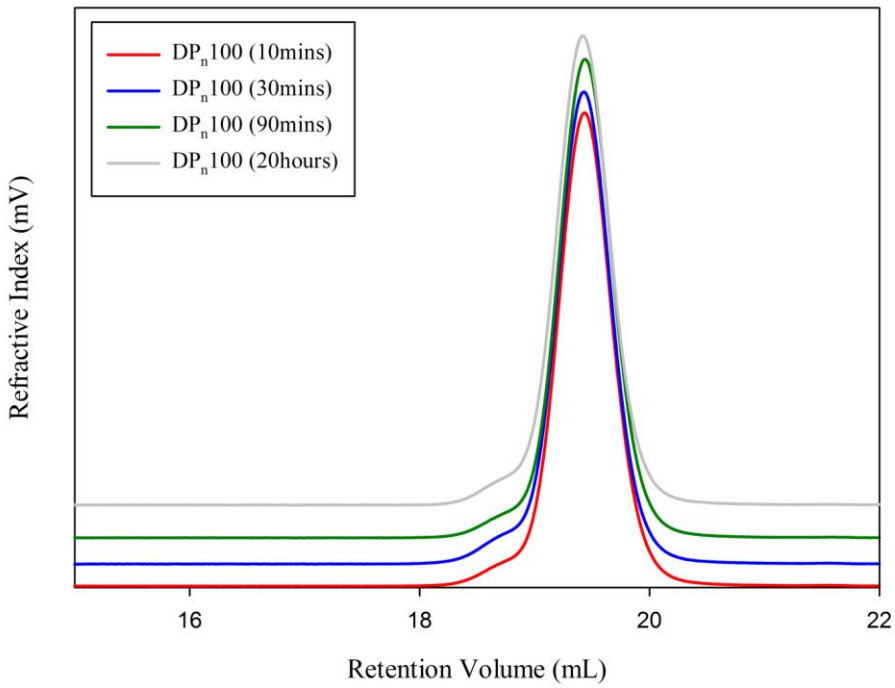

Figure 3.14: GPC chromatograms showing the progression over time of the anionic polymerisation of styrene at 10 minutes(red), 30 minutes (blue), 90 minutes (green) and 20 hours (grey).

The results appear to show that the reaction is complete after just 10 minutes, as the GPC chromatograms in Figure 3.14 show no difference in the samples over 20 hours. The ^{1}H NMR spectrum in Figure 3.15 shows clearly that after just 30 minutes there is no monomer present in the system, it has all been used during propagation and the reaction time is extremely fast.

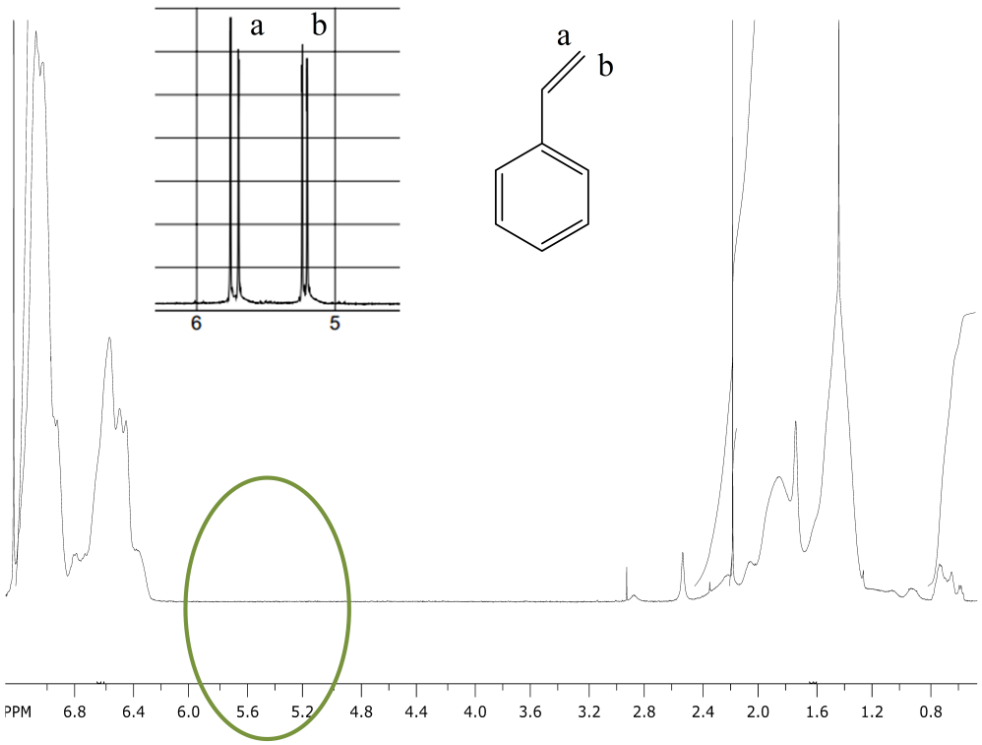

Figure 3.15: ^{1}H in $CDCl_3$ NMR spectrum of a polystyrene synthesised by anionic polymerisation. Reaction conditions; *sec*-BuLi initiator, 30 mL benzene. Highlighted is the absence of styrene protons.

This had a significant impact on the synthetic methods adopted, as it allows a higher throughput of polymerisations, and decreases the time taken in self-blocking polymerisations. It also offers synthetic benefits in that as 24 hours was not needed for complete conversion of monomer to linear polymer the challenge of maintaining anhydrous conditions was reduced, and therefore terminations could be minimised.

3.2.6 Linear polystyrenes by lithium-halide exchange.

In 2006 Gnanou and co-workers [17] successfully applied the halogen-lithium exchange reaction to generate a new dicarbanionic initiator from a dibromoaryl compound. This was the first example of dilithiated species initiating anionic polymerisation efficiently in the absence of another additive. It was found to be efficient enough to generate well-

defined polybutadiene telechelic polymers and styrene-butadiene-styrene (SBS) triblock copolymers with excellent mechanical properties. Scheme 3.4 outlines the synthesis of the SBS triblock copolymers.

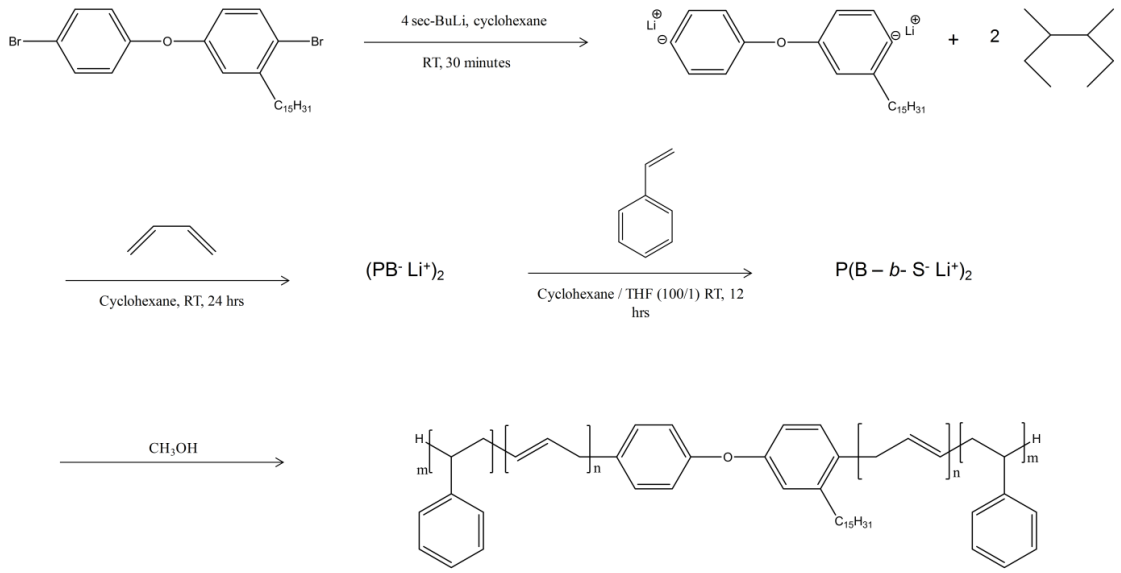

Scheme 3.4: Synthesis of SBS triblock copolymers [17]

Bifunctional initiation allowed the bidirectional growth of two polymer chains from one initiator leading to two hydrophobic polymer chains, such as polystyrene, being grown from one initiator. The synthesis of a hydrophillic polymer from the two active chain ends may yield an amphiphilic copolymer with potential benefits for producing the target amphiphilic nanopartices. As such, the potential for bifunctional initiation using dibromo compounds and the lithium-halide exchange reaction was investigated.

3.2.6.1 Synthesis of polystyrene initiated with bis(4-bromophenyl)ether

In this instance a molar ratio of 1:2 was used for bis(4-bromophenyl)ether and *sec*-BuLi. The amount of the stabilising compound TMEDA was matched to the moles of initiator. Bis(4-bromophenyl)ether was added to a dry 100 mL flask and flushed with nitrogen for 15 minutes. 30 mL of anhydrous benzene, TMEDA and *sec*-BuLi were added under nitrogen pressure and this was stirred for 30 minutes to allow the lithium complex to form. Styrene was added and the colour change from pale peach to deep red was observed. The reaction was left to stir overnight under nitrogen pressure, as before. The reaction scheme is shown in Scheme 3.5.

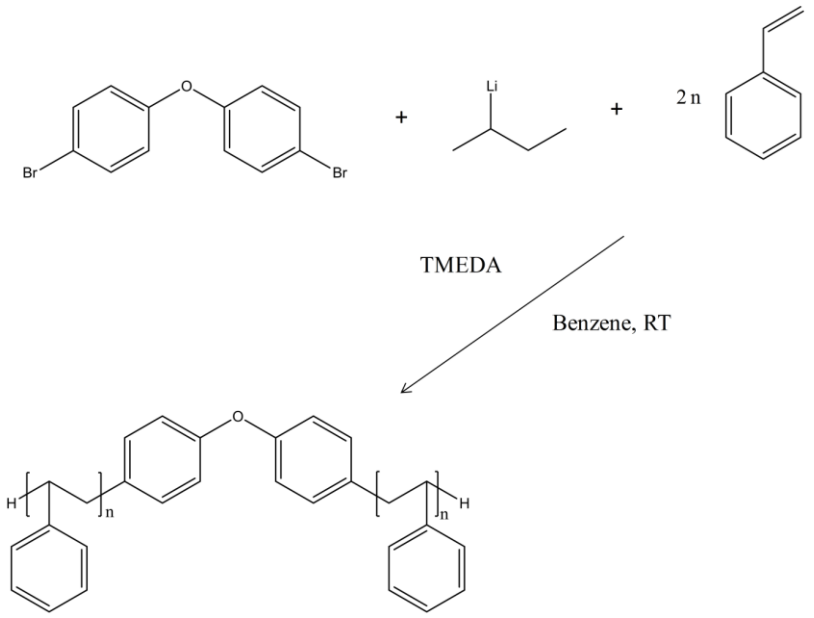

Scheme 3.5: Synthesis of bifunctionally initiated polystyrene by anionic polymerisation techniques, with bis(4-bromophenyl)ether as the diaryl compound.

In Figure 3.16 the GPC chromatogram of the bifunctionally initiated polymer (2 x DP_n100 = 200 monomer units) is shown, overlaid with a polystyrene with a targeted chain length of DP_n = 200 monomer units. As can be seen from the data, there are two separate peaks representing two different linear species.

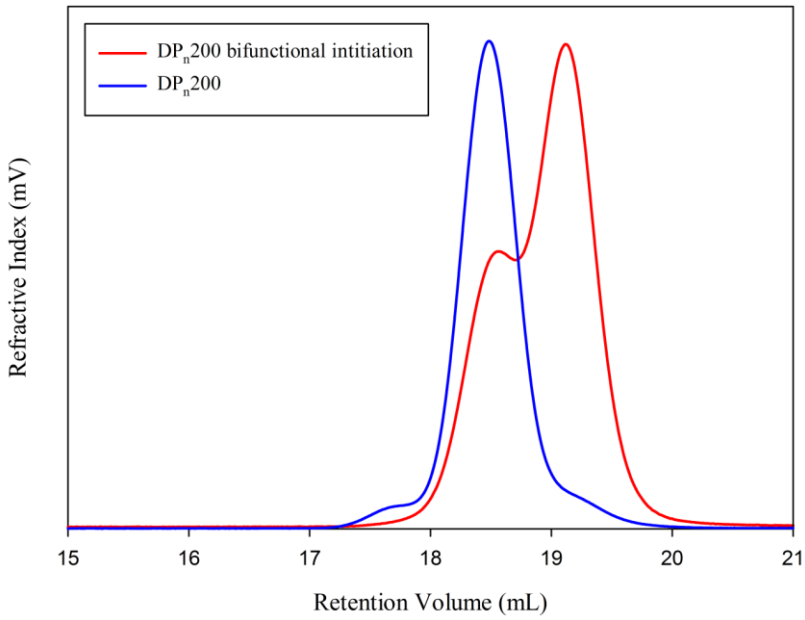

Figure 3.16: GPC chromatograms of a targeted DP_n (2 x 100) monomer units bifunctionally initiated polystyrene, with a typical DP_n200 monomer units polystyrene overlaid to illustrate the two separate species in the bifunctionally initiated polymer**.**

When a typical *sec*-BuLi-initiated linear polystyrene with a target DP_n of 200 monomer units is overlaid, one peak appears to correspond to a successful bifunctional initiation with successful propagation from each initiating site on the diaryl compound. However there appeared to be a higher concentration of a species that corresponds to a polystyrene with a DP_n = 100 monomer units, as shown further in the next comparison, see Figure 3.17, whereby a typical linear polystryrene with a target DP_n of 100 monomer units was overlaid. This indicates that there has been a significant amount of mono-initiation whereby only one side of the diaryl compound has reacted fully with the *sec*-BuLi and therefore there has not been a successful bifunctional polymerisation initiation.

Different variables were considered in an attempt to rectify this issue. The solvent was changed from benzene to cyclohexane but this was found to be unsuccessful and polymerisation did not occur. It was also considered that if an excess of *sec*-BuLi was

used the excess may fully ensure both sides of the compound were turned into initiating sites. Again, this was found to be unsuccessful as there was an even greater concentration of the lower molecular weight (DP_n = 100 monomer units) species. This is shown in Figure 21, where a small amount of bifunctional initiation can be seen to occur, but clearly the mono-initiated species is dominant.

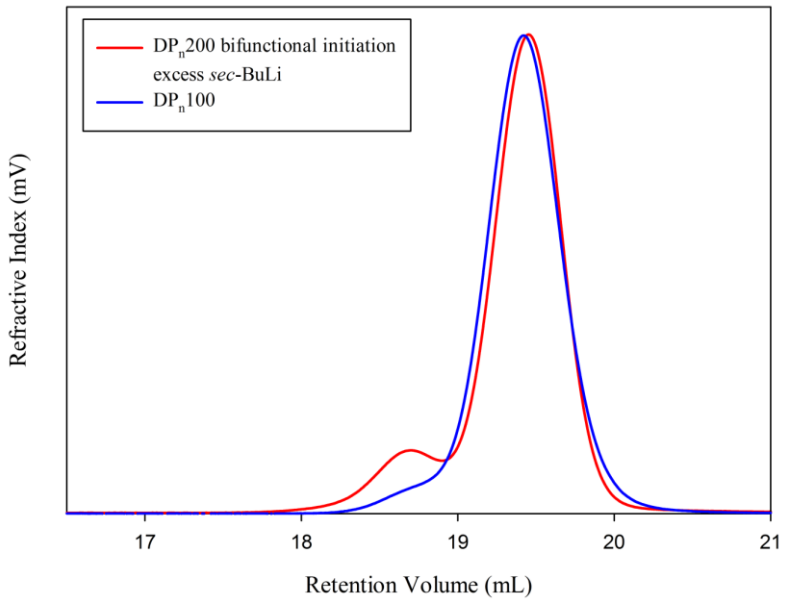

Figure 3.17: GPC chromatograms of a targeted DP_n (2 x 100) monomer units bifunctionally initiated polystyrene, with a typical DP_n100 monomer units polystyrene overlaid to illustrate the two seperate species in the bifunctionally initiated polymer.

A possible theoretical explanation of this is that the excess *sec*-BuLi was acting itself as an initiator for the styrene polymerisation. Bifunctional initiation was then attempted with an alternative diaryl compound.

3.2.6.2 Use of 2,7-dibromofluorene as diaryl compound

The synthesis of polystyrene by bifunctional initiation was carried out by the same method as described above, targeting a total of DP_n = 200 monomer units (chains with a targeted DP_n = 100 monomer units grown from each initiating site) but the diaryl compound used was 2,7-dibromofluorene. The scheme for the reaction is shown in Scheme 3.6 and typical GPC analysis results are shown in Figure 3.6.

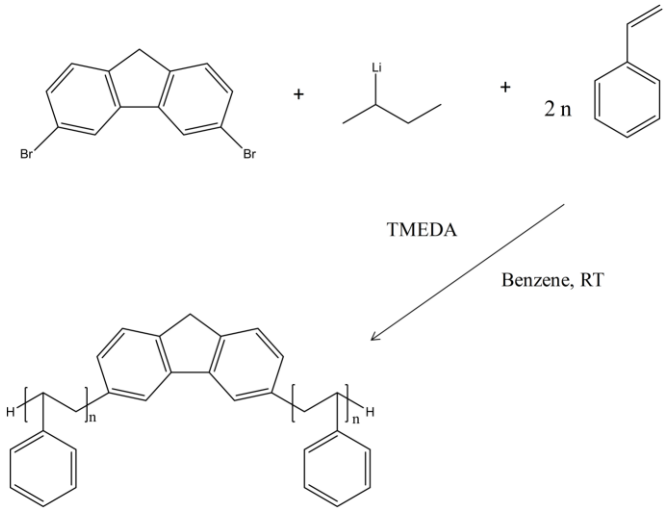

Scheme 3.6: Synthesis of bifunctionally initiated polystyrene by anionic polymerisation techniques, with 2,7 di-bromofluorene as the diaryl compound

As can be seen from the overlaid GPC chromatograms shown in Figure 3.18, there was a significant proportion of polystyrene with an apparent chain length of 100 monomer units, indicating the same issues that were problematic in the bifunctional initiation with bis(4-bromophenyl)ether. It is clear that successful bifunctional initiation under these reaction conditions was not trivial to achieve.

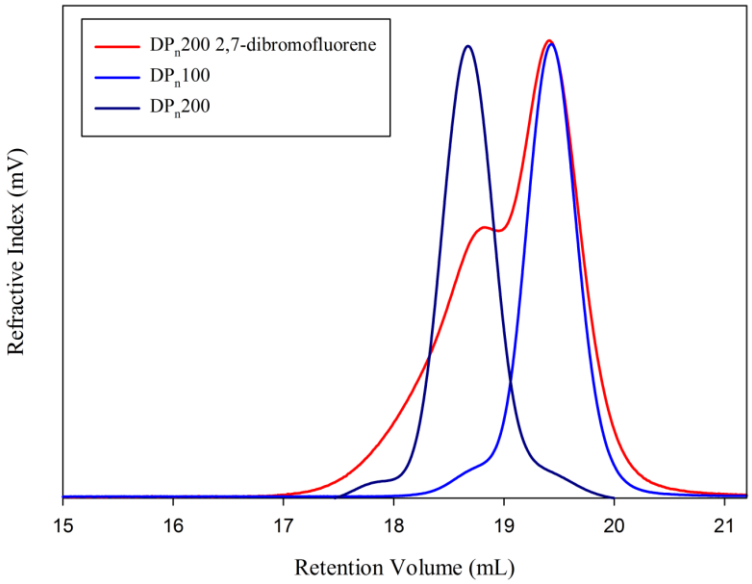

Figure 3.18: GPC chromatograms of a targeted DP_n (2 x 100) monomer units bifunctionally initiated polystyrene, with a typical DP_n100 and DP_n200 monomer units polystyrene overlaid to illustrate the two separate species in the bifunctionally initiated polymer.

3.3 Conclusions

Linear polystyrene chains have been synthesised by both ATRP (Supporting Information 1) and anionic polymerisation methods. The viability of ATRP as a method for synthesising controlled polymer chain length linear polystyrenes has been evaluated and rejected as a suitable method for synthesising the targeted complex architectures of the project due to poor control over chain length and low conversion of monomer to polymer within the observed extended reaction timescales.

Anionic polymerisation has been shown to be a viable method for producing linear polystyrenes at high conversion levels with excellent control over the chain length and the polydispersity. Very monodisperse polymers have been readily and reproducibly targeted with dispersity values as low as 1.02, without the specialist equipment and techniques conventionally employed for anionic polymerisation.

The kinetics of the reaction have been investigated, and the variables of the reaction have also been investigated to find the best conditions for the synthesis. It has been found that solvent volume has little or no effect on the polymerisation, and that 100% conversion of monomer to polymer can occur in less than 30 minutes.

The living nature of the polymers *in situ* has also been tested in a series of self-blocking experiments. It was found that block copolymers could be produced with a controlled chain length in a relatively short time.

Initiation by *sec*-BuLi alone and using lithium-halide exchange approaches has been explored. The latter has led onto the attempted synthesis of bifunctional initiators for anionic polymerisation but within the scope of this work it was found to be unsuccessful.

3.4 References

1. Weiss, R. A. *Science,* , **1993**, *260*, 1273
2. Slater, R. A.; McDonald, T. O.; Adams, D. Draper, E. R.; Weaver, J. V. M.; Rannard, S. P. *Soft Matter*, **2012**, *8*, 9816
3. He., T.; Adams, D.J.; Butler M.F.; Cooper, A.I.; Rannard, S.P, J. Am. Chem. Soc, 2009, 131, 1495
4. He, T.; Adams, D.J.; Butler, C.T.; Yeoh, C.T.; Cooper, A.I.; Rannard, S.P., Angew. Chem. Int. Ed, 2007, 46, 9243
5. Dias, R. S.; Goncalves, M. C.; Lona, L.M.F.; Vivaldo-Lima, E.; McMaunu, N. T.; Penlidis, A. *Chem. Eng. Sci*., **2007**, *62*, 5240
6. Gaynor, S. G.; Edelman, S.; Matyjaszewski, K. *Macromolecules*. **1996**, *29*, 1079
7. Xia, J.; Zhang, X.; Matyjaszewski, K. *Macromolecules*. **1999**, *32*, 4484
8. Sedjo, R.A.; Mirous, B.K.; Brittain, W. J. *Macromolecules*. **2000**, *33*, 1492
9. Fukanda, T.; Terauchi, T.; Goto, A.; Tsujii, Y.; Miyamoto, T. *Macromolecules*, **1996**, *29*, 3050
10. Chiefari, J. Chong; Y.K., Ercole, F.; Krstina, J.; Jeffery, J.; Le, T.P.T.; Mayadunne, R.T.A.; Meijis, G.F.; Moad, C.L.; Moad, G.; Rizzardo, E.; Thang, S.H. *Macromolecules*, **1998**, *31*, 5559
11. Ishihama, I.; Sawamoto, M.; Higashimura, T.; *Polym. Bull*., **1990**, *24*, 201
12. Worsfold, D. J.; Bywater, S., *Can. J. Chemistry*, **1960**, *38*, 1891

13. Matmour, R.; Gnanou, Y., *J. Am. Chem. Soc*., **2008**, *130*, 1350
14. Hadjichristidis, N.; Pitsikalis, M.; Pispas, S.; Iatrou. H., *Chem. Rev*., **2001**, *101*, 3747
15. Lipton, M.F.; Sorensen, C.M.; Sadler, A. C.; Shapiro, R.H., *J. Organomet. Chem*. **1980**, *186*, 155
16. Eastmond, G.C.; Ledwith, A.; Russo, S.; Sigwalt, P., Comprehensive Polymer Science: The synthesis, characterisation, reactions and applications of polymers, **1989**, *1st Edition*, Pergamon Press: Oxford
17. Matmour, R.; More, A.S.; Wadgaonkar, P. P.; Gnanou, Y., *J. Am. Chem. Soc*, **2006**, *128*, 8155

Chapter 4.

Branched Polystyrene

4.0 Introduction

As good linear polymers of varying chain lengths could be produced from both lithium-halide exchange reactions (single initiating sites) and solely from *sec*-butyl lithium (*sec*-BuLi) initiation, the formation of branched polymers from single initiating sites was investigated using the branched vinyl polymer strategy referred to as the 'Strathclyde approach'. The aim was to accurately and reproducibly form the branched hydrophobic core of the target nanoparticles, therefore it was necessary that the technique of synthesising branched polymers has to be investigated carefully.

With hyperbranched polymers produced using a mixture of mono and bifunctional vinyl monomers, there was a risk of cross-linking during synthesis, thereby forming an insoluble polymer gel. The challenges facing all branched vinyl polymerisations using controlled or 'living' conditions involves ensuring the very delicate ratio of initiator:brancher material remains at a level where cross-linking does not occur.

In this chapter variations of the conditions of the branched vinyl polymerisation of styrene using anionic polymerisation are discussed. Novel brancher compounds have also been synthesised and are evaluated. The kinetics of branched polystyrene synthesised by anionic polymerisation has been explored briefly, and conditions for optimum branching have been tested. Again, a balance has to be found between reaction time, brancher:initiator ratio, solvent concentration and primary chain length.

4.1 Synthesis of branched polystyrene by anionic polymerisation

The demonstration of considerable control of linear polystyrene synthesis using anionic polymerisation techniques suggests the potential to precisely control the individual primary chains of the architecture of branched polystyrenes produced under identical conditions, but in the presence of the brancher. The synthesis of branched polystyrenes by ATRP methods was also explored, and is presented in Supporting Information 1.2. DVB was initially used used as the brancher compound. DVB is well established as a suitable brancher for anionic polymerisation [1], [2], [3].

In a series of exploratory reactions, the number of moles of DVB was varied to generate different brancher:initiator ratios. In all experiments DVB was added with anhydrous benzene, an equimolar amount of TMEDA to the *sec*-BuLi initiator and 8 g (76.8 mmol) styrene to a 2-necked round bottomed flask under nitrogen pressure. *sec*-BuLi (15.4 mmol for a primary chain length of DP_n = 50 monomer units, 76.8 mmol for a primary chain length of DP_n =100 monomer units) was then added and the colour change from colourless to deep red was observed. The reaction was left to stir for 24 hours under nitrogen pressure. The reaction scheme for the anionic polymerisation of branched polystyrene with divinylbenzene (DVB) is shown in Scheme 4.1.

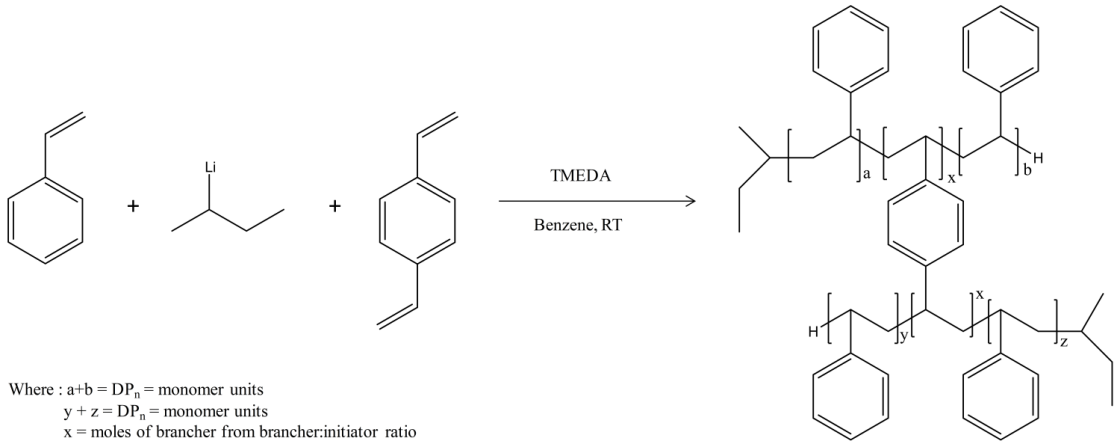

Scheme 4.1: Synthesis of branched polystyrene synthesised by anionic polymerisation methods. Reaction conditions: initiated with *sec*-BuLi, DVB as the brancher compound, benzene solvent in the presence of the stabilising compound TMEDA.

The actual *effective* concentration of *sec*-BuLi initiator can be affected significantly by water in the reaction and/or the molar concentration within the stock solution. This has the effect of increasing the *effective* ratio of brancher per initiating chain, and possibly causing the polymer to cross-link if this ratio exceeds one per chain. As such, a number of new experimental challenges are present within the branched anionic polymerisation of styrene, and a balance had to be found between reaction time, brancher:initiator ratio, solvent concentration and primary chain length.

4.2 Factors effecting branched vinyl polymerisations

4.2.1 Effect of solvent concentration.

As seen in Chapter 3 for the linear polystyrenes, an increase in solvent concentration has little effect on the success of the linear anionic polymerisation of styrene suggesting no direct loss of initiating sites due to solvent impurities. However, significant changes

and experimental anomalies were found when the amount of solvent (benzene) was increased or decreased during anionic branched polymerisations of styrene and DVB.

For branched polymers, the potential for intramolecular reaction becomes more significant if the reactions are conducted under dilute conditions, with the formation of loops rather than effective intermolecular branching between primary chains. This has been discussed previously in Chapter 1.

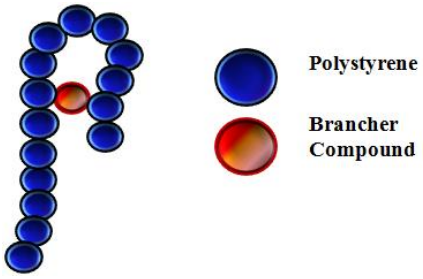

Figure 4.1: Illustration of the proposed 'looping' effect.

Loop formation affects the molecular weight of the branched polymer sample in several ways. Firstly there will be less brancher available to form intermolecular branches between groups of connected polymer chains, thereby limiting branched polymer growth; secondly, single linear chains with intramolecular loops will be formed, and these may have a reduced probability of becoming incorporated within a large branched polymer structure. It is possible such chains may have similar elution volumes as linear chains and will therefore appear within the population of linear chains at high elution volumes. Such material will affect the M_n of the overall polymer.

Dilution may also affect the kinetics of the reaction, resulting in a slower rate of propagation. As has been observed in the investigation into the kinetics of the

polymerisation reaction to form linear polystyrene in Chapter 3, the rate of the anionic polymerisation of styrene is very fast. To investigate the kinetics of the formation of branched polymers, samples were taken during two branched anionic polymerisations using DVB as the branching compound, the targeted linear primary chains had a DP_n 100, and the solids content was halved from 8 g of monomer (76.8 mmol) in 30 mL benzene (0.27 gmL^{-1}) to 8 g monomer in 60ml of benzene (0.13 gmL^{-1}).

The refractive index detector chromatograms from the GPC analyses are shown in Figure 4.2 for these studies. Table 4.1 details the individual calculation of molecular weights and molecular weight distributions of the samples taken during the kinetic investigation. It is important to note that virtually 100% conversion of styrene monomer is achieved within the first 30 minutes, as seen from linear polymerisation reactions in Chapter 3.

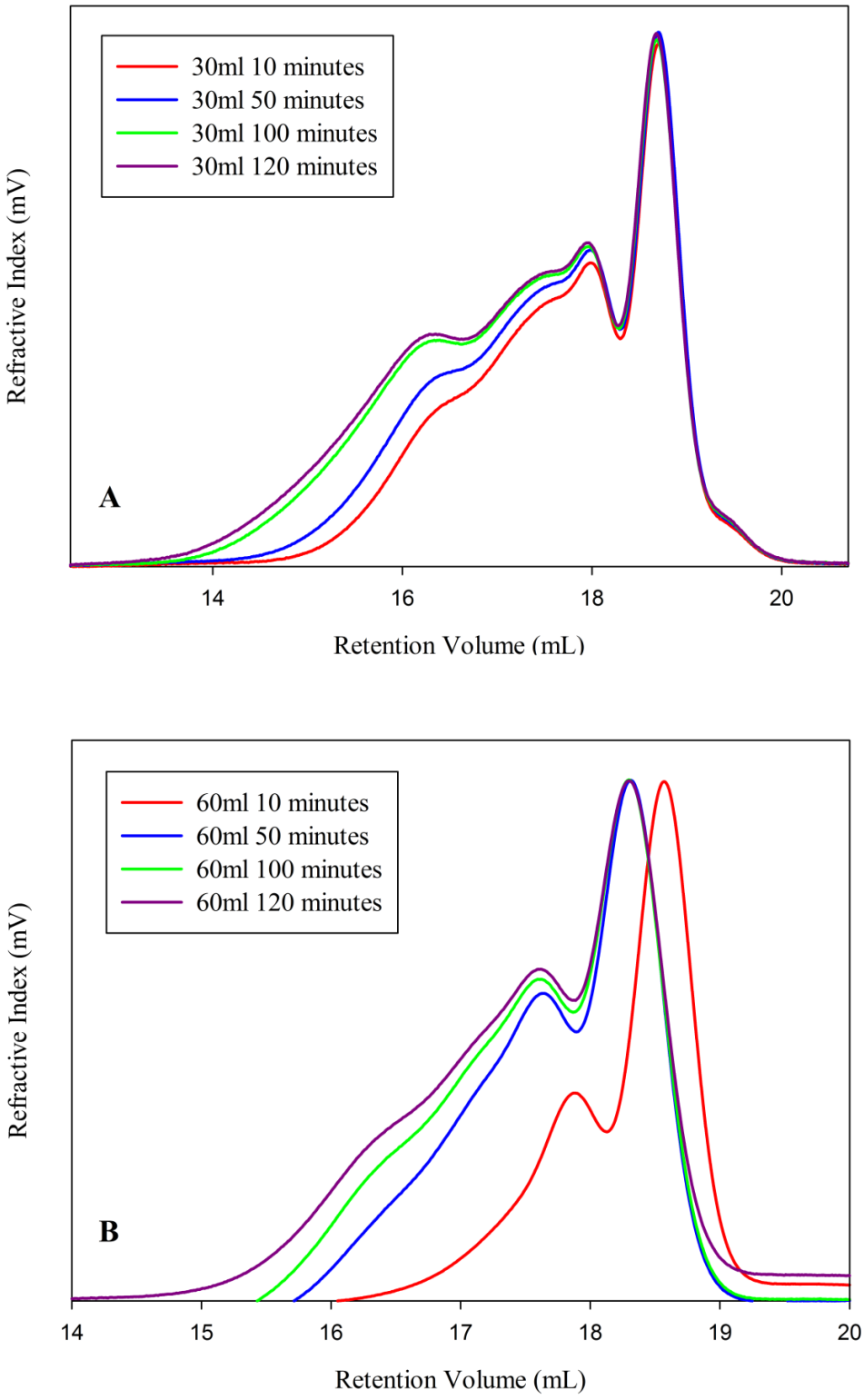

Figure 4.2: GPC chromatograms of samples taken throughout anionic polymerisations at solvent amounts of (A) 30 mL benzene (0.27 gmL^{-1}) and (B) 60 mL benzene (0.13 gmL^{-1}).

Table 4.1: Values of M_n, M_w and Đ of samples taken throughout anionic polymerisations at solvent amounts of 30 mL benzene (0.27 gmL^{-1}) and 60 mL benzene (0.13 gmL^{-1})

Benzene (mL)	Time (mins)	GPC		
		M_n ($gmol^{-1}$)	M_w ($gmol^{-1}$)	Đ
30	10	25,300	81,900	3.24
30	50	33,200	180,600	5.44
30	100	35,200	207,000	5.88
30	120	38,700	290,300	7.50
60	10	18,000	28,200	1.57
60	50	35,500	64,800	1.83
60	100	38,700	81,700	2.11
60	120	39,400	86,200	2.19

If the values in Table 4.1 are plotted, it allows the correlation between M_w, M_n and solvent concentration to be explored. This is shown in Figure 4.3.

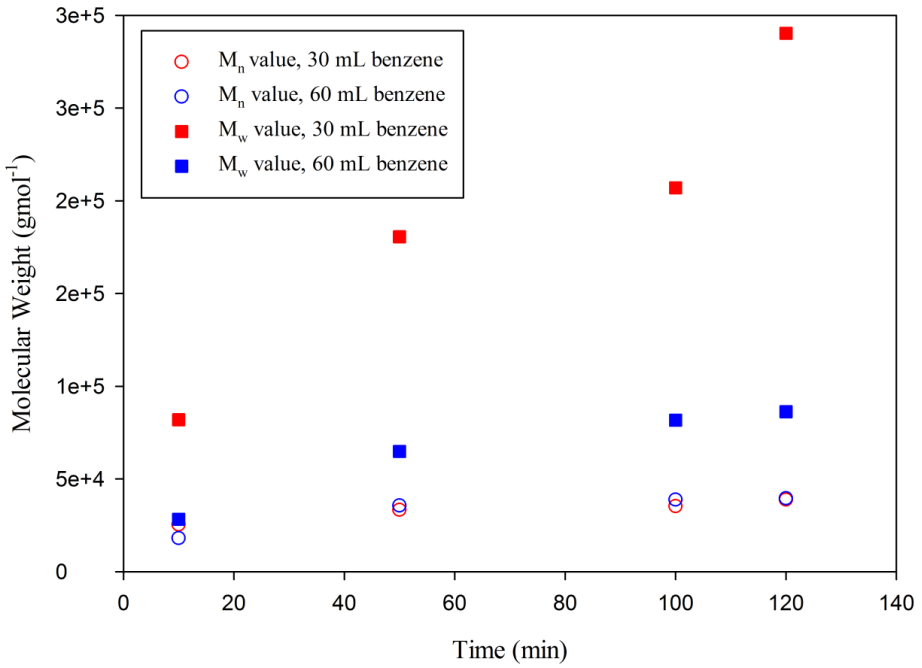

Figure 4.3: Plot of the change in M_w (shown as filled squares in Figure 4) and M_n (open circles) values over time for anionic polymerisations of at solvent amounts of (A) 30 mL benzene (0.27 g/mL), (red) and (B) 60 mL benzene (0.13 g/mL), (blue).

These results showed that in the initial stages of the polymerisation a higher concentration seemed to give more success with regards to speeding up the polymerisation and allowing highly branched polystyrene to be synthesised. The lower solid content polymerisation produced polymers which exhibited a much lower dispersity value, which suggests that the reaction mixture was too dilute to allow a high degree of intermolecular reaction, possibly leading to intramolecular cyclisation or 'looping' within the branched and linear polymer chains.

As this study was focussed on investigating the polymerisation during the first 120 minutes, and without variation of the brancher:initiator ratio (0.95:1), further work continued to determine the limits of the reaction concentration and its effects on the polymerisation. A series of experiments were conducted that also considered variations in the ratio of brancher to initiator. In this way, the maximum ratio of brancher that could be added to the system before the formation of an insoluble gelled polymer network was directly evaluated. A higher monomer concentration of 8 g monomer in 20 mL (0.4 gml^{-1}) of benzene was selected, and the brancher:initiator ratio was systematically increased from 0.9:1 in increments of 0.01:1. DVB was again used as the brancher material and results from this study are discussed further on in this Chapter.

Some interesting observations were made during these experiments. For example higher brancher:initiator ratios appeared to result in a gelled polymer matrix. A photograph of a gelled polymerisation is shown in Figure 4.4 of the ratio 0.97:1 and a targeted primary chain length of DP_n = 50 monomer units. The reaction flask is turned upside down to nearly a 180 º angle to illustrate the gelled, high viscosity nature of the reaction mixture. Despite the gel-like nature the reaction is still 'living' as it displays the classic deep red colour of the styryl anion.

Figure 4.4: Photograph illustrating the ‘gel’ like nature that occurs in a branched anionic polymerisation with 20 mL benzene

Originally discarded as being too high a brancher:initiator ratio, resulting in a polymer that was highly cross-linked, it in fact was observed that as the reaction was slowly terminated, seen by the colour change of red to orange to colourless seeping down through the gel over a prolonged time. During this process the ‘gel’ became a viscous colourless liquid. The material was then precipitated following procedures used for other polystyrene samples, using cold methanol, resulting in a polymer that could be analysed by GPC. When dissolved in tetrahydrofuran (THF) it was fully soluble with no microgel particles observed. This can be explained by reversible aggregation of the anions during anionic polymerisation.

This anionic association is lost as the reaction terminates and the number of anions decreases, returning the reaction mixture to its usual viscous state. However, due to the multifunctional nature of the branched anionic polymerisation, this means that rather than a small number of chains aggregating, as would be seen in a linear polymerisation, the large number of anions present on the branched polymer aggregated to form a physical cross-linking to produce a temporary and reversible gel formation.

To overcome the physical gel formation at these conditions, and add to the understanding of the importance of solvent concentration of the branched anionic polymerisation, an identical anionic polymerisation was conducted with a solvent volume of 40 mL of benzene, leading to a solid content of 0.2 gmL^{-1}. It was found that no 'gel' was formed under these conditions and, even over 24 hours, the reaction mixture stayed as a viscous liquid during the synthesis both before and after termination with methanol. GPC data for both of these polymerisations are shown in Figure 4.5.

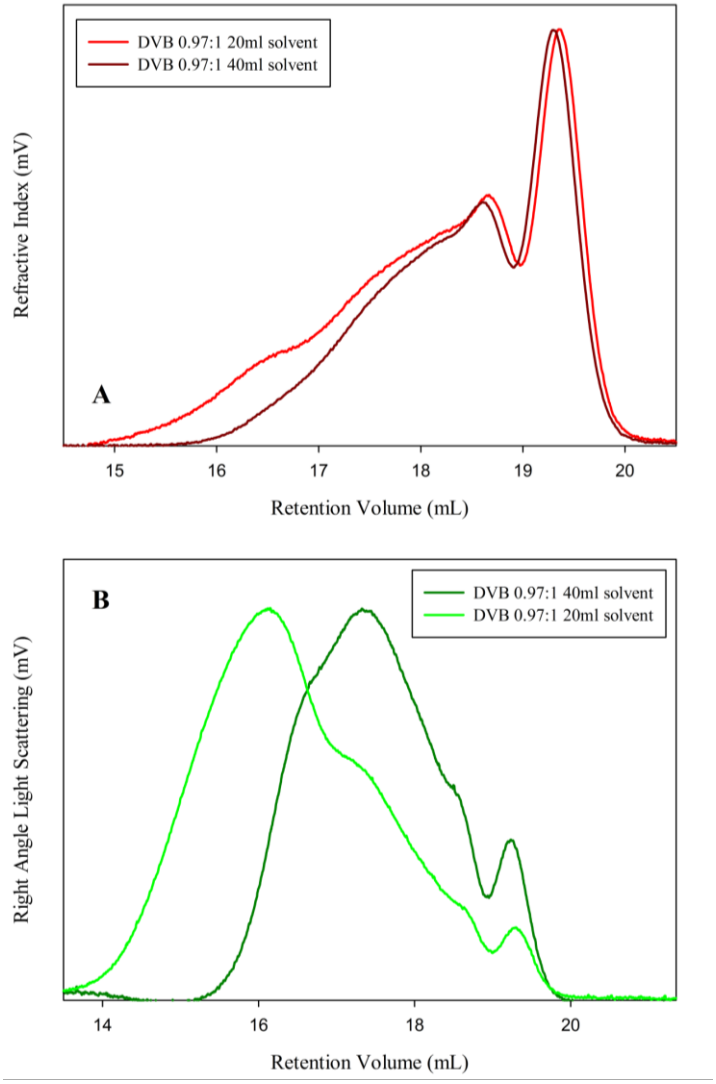

Figure 4.5: GPC chromatograms of the (A) RI detector of branched polystyrene synthesised by anionic polymerisation methods in 20 mL benzene (0.4 gmL^{-1}) (red) and 40 mL benzene (0.4 gmL^{-1}) (dark red) and (B) the RALS detector of polystyrene synthesised in 20 mL benzene (0.4 gmL^{-1}) (green) and 40 mL benzene (0.2 gmL^{-1}) (dark green).

As can be seen from the overlaid GPC RI chromatogram in Figure 6(A), there are much higher molecular weight branched polystyrene materials formed when the polymerisation is conducted in 20 mL of benzene. This is displayed more prominently if we take into consideration the signal from the right angle light scattering (RALS) detector that indicates the comparative sizes of the largest fraction of the polymer sample. There is clear fraction of the polymer distribution with very high molecular weight present in the polymerisation conducted at higher concentration even though the reaction gelled during polymerisation. This is shown further by the comparative M_n and M_w values shown in Table 4.2.

Table 4.2: Values of M_n, M_w and Đ of the final branched polymers of polystyrene synthesised by anionic polymerisation methods in 20ml benzene (0.4 gmL^{-1}) and 40ml benzene (0.4 gmL^{-1}).

Solvent (mL)	**GPC**		
	M_n ($gmol^{-1}$)	**M_w ($gmol^{-1}$)**	**Đ**
20	22,500	103,000	4.58
40	16,600	39,900	2.40

The data shown in Figure 4.5 and Table 4.2 reflects the trends found when investigating the effect of increasing the amount of solvent; decreasing the solid content two fold and thereby diluting the polymerisation has appeared to limit the formation of more highly branched polymer chains.

A possible way to overcome the ionic association at higher solid content levels is to decrease the number of anions on the branched polymer. As the brancher compound VPOB has to be synthesised, and can only be marginally scaled up in size due to the multi-step purifications, a method that offered an alternative to this would be advantageous. A novel method combining 'living' anionic polymerisation with a convergent growth process was reported by Knauss *et al* [3] who formed dendritically

branched polystyrene by using vinyl-functionalised reactants to produce macromonomers that react through their double bonds with 'living' polystyrene chain ends to give dimerised chains. The fast addition of vinylbenzenechloride (VBC) to an anionic polymerisation of styrene, and the effects on molecular weights of changing the solvent mixture, the amounts of VBC added and increasing the primary polystyrene chain length were investigated. Whilst these preliminary results appeared to demonstrate that branched structures can be synthesised from this divergent branching method, the methodology is more complex than branching from a one-addition synthesis with a distyrl branching monomer such as DVB or VPOB. The results of this study can be found in the Supporting Information, Section SI.4.

4.2.2. Increasing brancher:initiator ratio

As mentioned previously, the amount of brancher present within a branched vinyl polymerisation is critical and the determination of the optimum ratio of brancher to the number of primary polymer chains is required to generate high molecular weight material. Too little brancher will limit the number of branchers per chain, resulting in a less branched structure. Too high a ratio and cross-linking will lead to an insoluble gel network.

A series of experiments were performed whereby the brancher:initiator ratio for DVB was increased at increments of 0.01 moles. Figure 4.6 gives the GPC chromatograms of the polymer synthesised with the highest amount of DVB overlaid with the polymer synthesised with the least amount of DVB in the anionic polymerisation, to illustrate the effect of the increase in brancher had on the polymer.

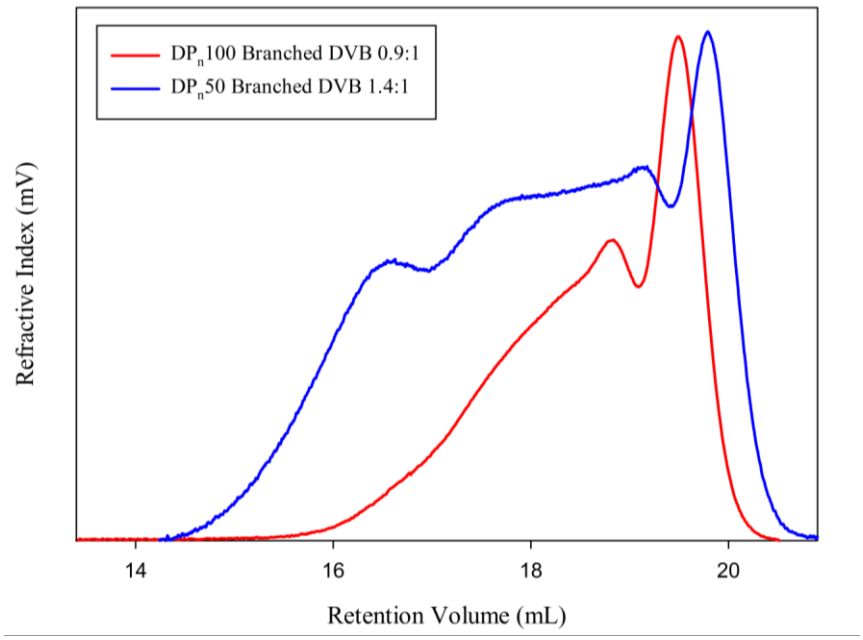

Figure 4.6: GPC chromatograms of branched polystyrene synthesised by anionic polymerisation methods. Reaction conditions (red): 8g styrene monomer (76.8 mmol), brancher :initiator ratio of 0.90:1 (DVB:*sec*-BuLi), 76.8 mmol *sec*-BuLi (for a targeted DP_n primary chain of 100 monomer units), 6.91 mmol DVB, 30 mL benzene. Reaction conditions (blue): 8g styrene monomer (76.8 mmol), brancher :initiator ratio of 1.14:1 (DVB:*sec*-BuLi), 15.4 mmol *sec*-BuLi (for a targeted DP_n primary chain of 50 monomer units), 17.6 mmol DVB, 30 mL benzene.

Whilst the GPC chromatograms in Figure 4.6 do give a good indication of the change that increasing the brancher concentration can have on the branched polystyrene, it is important to note that during these evaluation reactions, the target DP_n of the primary chains was varied although the solvent amount was generally maintained at 30 mL. For later experiments where the ratio was increased further (1.0-1.4) the solvent amount increased to 40 mL. All reactions were allowed to react for 3 hours, following an investigation of the kinetics. The relative M_n and M_w values for these polymers are given in Table 4.3.

Table 4.3: Values for M_n, M_w and the polydispersity value for polystyrene branched with DVB by anionic poylmerisation techniques under different conditions, outlined in the table.

Brancher: Initiator Ratio	Solvent (mL)	Targeted Primary chain length (monomer units)	GPC		
			M_n (gmol-1)	M_w (gmol-1)	Đ
0.9	30	100	17,700	49,500	2.79
0.91	30	100	15,800	36,800	2.33
0.92	30	100	21,100	52,500	2.49
0.93	30	100	21,700	53,900	2.48
0.94	30	100	55,200	141,200	2.56
1.0	30	50	8,209	47,400	5.77
1.2	30	50	10,300	67,500	6.55
1.4	30	50	14,300	187,900	13.14
0.97	20	100	22,500	103,100	4.58
0.97	40	100	19,100	56,400	2.95

Whilst the results in Table 4.3 cannot give a clear comparison due to changes in the variables such as solid content and primary chain length, it can still be seen from the dispersity values that the higher brancher:initiator ratios give a more polydisperse branched polymer as does the increase in reaction concentration.

4.2.3 Effect of reaction time

As was determined in earlier kinetics investigations of linear polymerisations, the anionic polymerisation of styrene is very fast, and 100% conversion can be reached in less than 30 minutes. The reaction time is a key parameter to understand within a branched vinyl polymerisation as a reaction that will ultimately lead to a cross-linked gel at the chosen brancher:initiator ratio may be inadvertently or deliberately terminated before the gel-point is reached, resulting in high molecular weight branched polymer synthesis. There could therefore be a potential to utilise time in such a way that a high amount of brancher could be used, and the polymerisation allowed to reach a very large molecular weight but terminated before it cross-links.

In order to investigate the kinetics of the anionic branched polymerisation of styrene over very long periods of time, a low brancher:initiator molar ratio of 0.95:1 (DVB:*sec*-BuLi) was chosen, and samples were taken throughout the polymerisation.

The very small samples that were taken from the reaction were purified to generate polymer sample for analysis by GPC. Figure 4.7 shows the GPC refractive index chromatograms of the reaction at each time interval.

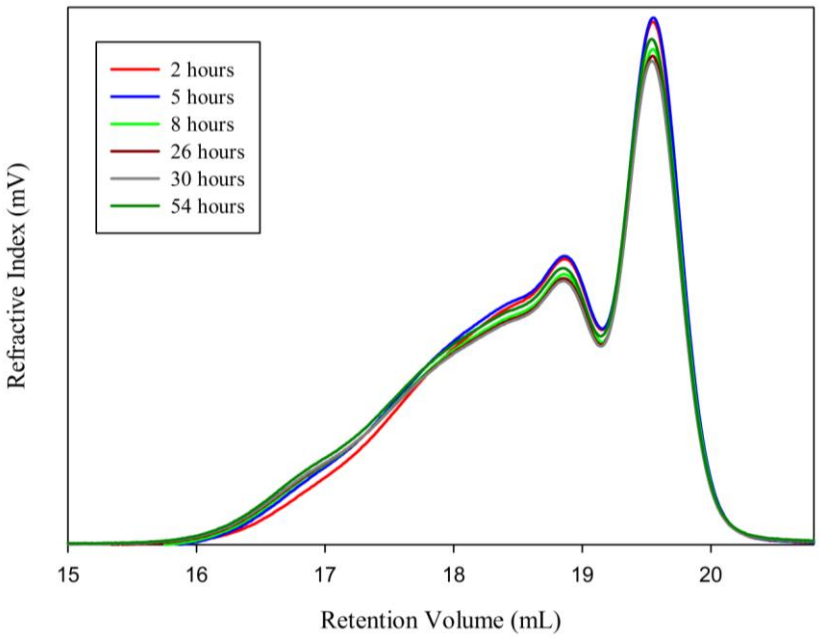

Figure 4.7: RI detector GPC chromatograms of kinetics samples taken over the polymerisation of branched styrene.

As can be seen from the Figure 8, there appeared to be little difference between the polymer after 2 hours or 54 hours. If the RALS detection is investigated, Figure 9, from the 2 hour and the 54 hour samples it can be seen that there actually is some significantly larger species in the samples left for long periods, however, they must be in very low concentration.

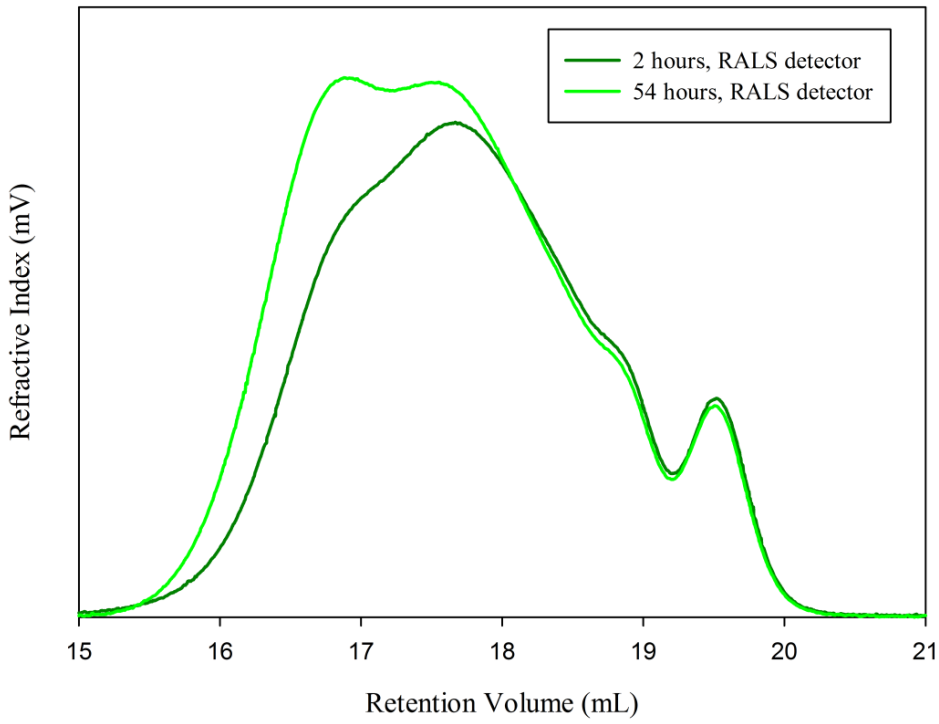

Figure 4.8: RALS chromatograms from the RALS detector of micro-samples taken at 2 hours (dark green) and 54 hours (bright green) during an anionic polymerisation of polystyrene branched with DVB at a ratio of 0.95:1 (DVB:*sec*-BuLi).

The same experiment was repeated twice with different brancher compounds (namely VPOB and VPOOC respectively, see Section 4.4) and the brancher:initiator ratio was increased further to 0.99:1 and fewer samples were taken, but the polymerisations were terminated after 100 hours. The results of these polymerisations are shown in Figure 4.9 and Table 4.4.

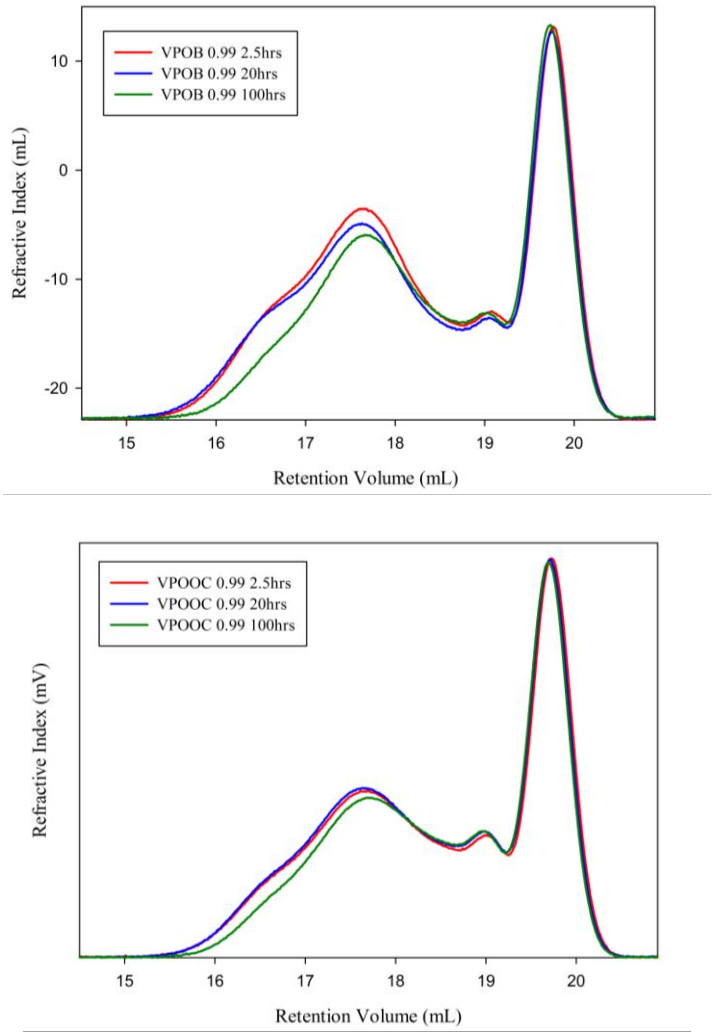

Figure 4.9: RI GPC chromatograms of kinetics samples taken during the anionic branched polymerisation of styrene; 2.5 hours (red), 20 hours (blue) and 100 hours (green).

Table 4.4: M_n, M_w and Đ values for of kinetics samples taken during the anionic branched polymerisation of styrene. Reaction conditions: 8g styrene monomer (76.8 mmol), 30 mL benzene, 76.8 mmol *sec*-BuLi (for a targeted DP_n primary chain of 100 monomer units), with (A) 76.8 mmol VPOB (0.99:1 VPOB:*sec*-BuLi ratio) and (B) 76.0 mol VPOOC (0.99:1 VPOOC:*sec*-BuLi ratio

Brancher Compound	Time (hours)	GPC		
		M_n (gmol^{-1})	M_w (gmol^{-1})	Đ
VPOB	2.5	13,000	87,900	6.77
VPOB	20	13,300	93,800	7.05
VPOB	100	12,209	64,300	5.27
VPOOC	2.5	11,400	62,200	5.47
VPOOC	20	12,400	65,400	5.25
VPOOC	100	11,700	53,000	4.52

From the results in Figure 4.9 and Table 4.4, it appears that there is a slight increase in M_n, M_w and dispersity between 2.5 hours and 20 hours, but after 100 hours the values drop significantly. This may suggest the formation of very high molecular weight materials the formation of microgel that is lost during sample preparation for the GPC measurements.

A standard timescale for all further branched anionic polymerisations of styrene was therefore chosen to be 3.5 hours to take into account the differences that may arise from termination at arbitrary times, the ability to directly compare reactions and the practical considerations such as available laboratory time.

4.3 Branching with alternative dystyrl brancher compounds

While DVB is an effective brancher there are several problems associated with its use. One of the main problems is, whilst it is commercially available, it is generally only 80% pure. It is known to also contain a mixture of ortho, meta and para-divinylbenzene and ethyl vinylbenzene, as shown in Figure 4.10.

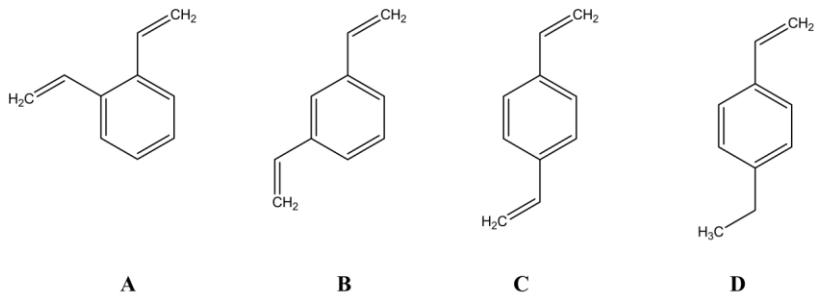

Figure 4.10: Variations in commercial DVB (A) *ortho*-DVB, (B) *meta*-DVB, (C) *para*-DVB and (D) *para*-ethyl vinylbenzene. Also present is *ortho* and *para*-ethylvinylbenzene not shown.

Also another important issue is that the reaction of one vinyl group leads to modification of reactivity of the pendant group. A more ideal brancher would be structurally more pure and have greater space between to the two vinyl groups to prevent modification of reactivity during polymerisation. Crivelo and Ramdas [4] investigated the synthesis of difunctional, aromatic vinyl aromatic ether analogues, and their use in photoinitiated cationic polymerisations to produce branched polymers.

A series of similar distyryl branchers were synthesised, increasing the space between the two styryl groups by extending the length of the carbon chain in the starting dibromo compound of the Crivelo and Ramdas synthetic strategy; 4-bis(4-vinylphenoxy)butane (VPOB), 6-bis(4-vinylphenoxy)hexane (VPOHEX), 8-bis (4vinylphenoxy)octane (VPOOC), 10-bis(4-vinylphenoxy)decane (VPOT), 12-bis(4-vinylphenoxy)dodecane (VPODD) and α-α'-dibromo-p-xylene (VPOPARAX).

The general method for synthesising the brancher compounds is as follows, shown in Scheme 4.2. 31.9 mmol of acetoxystyrene and 96 mmol sodium hydroxide in DMSO was stirred for one hour under nitrogen pressure at 75 $^{\circ}$C. After one hour 15.9 mmol of the corresponding dibromo compound (1,4-dibromobutane, 1,6-dibromohexane, 1,8-dibromooctane, 1,10-dibromodecane, 1,12-dibromododecane or *p*-xylene dibromide) in 20 mL DMSO was added dropwise under nitrogen pressure over two hours. This was stirred at 75 $^{\circ}$C for a further 5 hours, and then stirred at room temperature overnight. The reaction mixture was poured into 100 mL water and extracted four times with a 3:1 mixture of diethylether and toluene. The organic layer was washed 5 times with distilled water, dried over magnesium sulphate and the solvent removed under vacuum pressure. The white solid was repurified in chloroform and triturated with 500 mL ice-cold hexane.

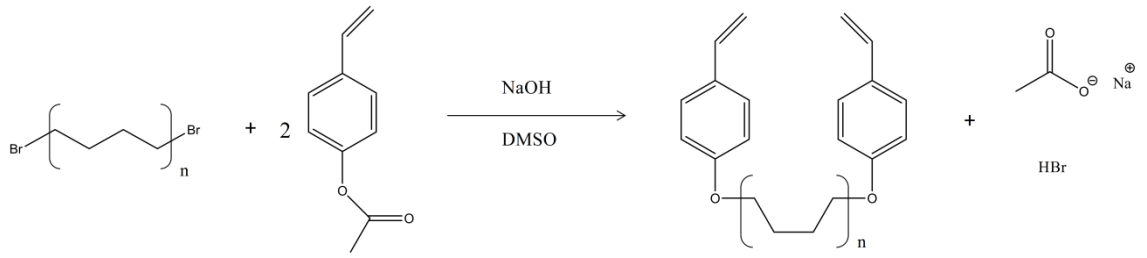

Scheme 4.2: General synthesis reaction of brancher compounds. Reaction: 31.9 mmol of acetoxystyrene, 0.0960 NaOH, 15.9 mmol of corresponding dibromo compound and 40 mL DMSO

The reaction was later scaled up by a factor of 0.75. Any higher and the work up of the products became very difficult. It was also found that increasing the number of extractions to 8 increased the yield, so average recovered yields of around 50 % were attained.

The brancher compounds synthesised are shown in Figure 4.11. The purified products were analysed by ^{1}H and ^{13}C NMR spectroscopy and mass spectrometry. Mass spectrometry was the preferred method of analysing the organic compounds as the difference in mass of each different brancher allowed identification of the compound.

Analytical confirmation of all the synthesised branchers is shown in Figures 4.12, 4.13, 4.14, 4.15, 4.16 and 4.17.

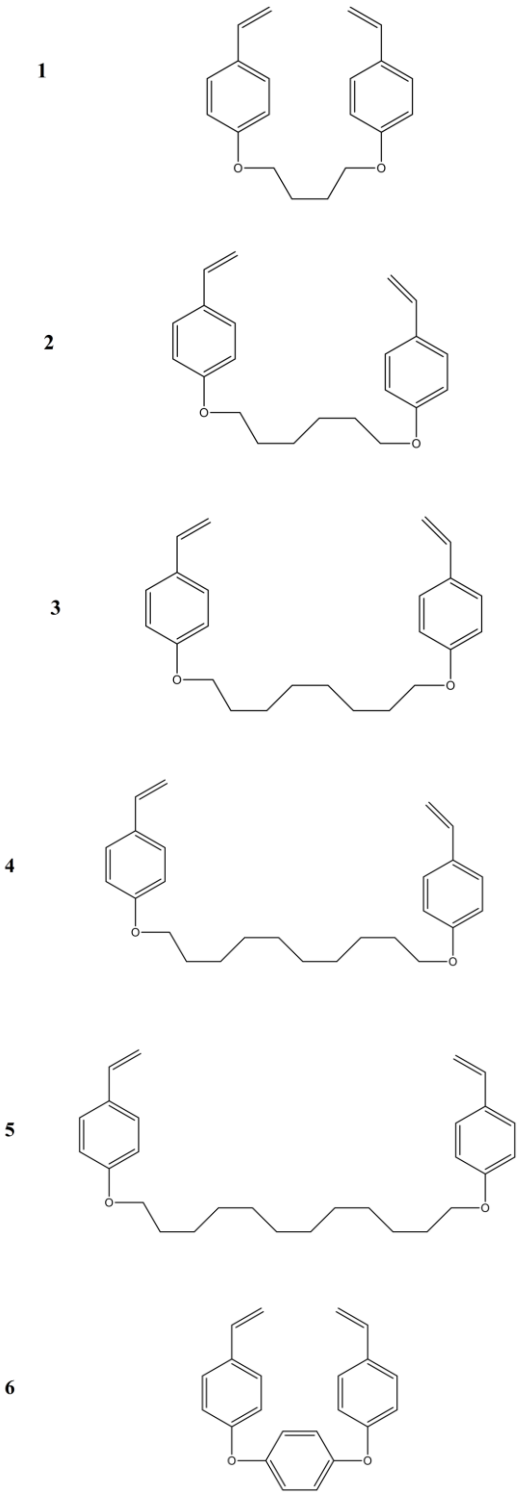

Figure 4.11: Brancher compounds synthesised by the reaction outlined in Scheme 3. (1) 4-bis(4-vinylphenoxy)butane, (2) 6-bis(4-vinylphenoxy)hexane and (3) 8-bis (4vinylphenoxy)octane. (4) 10-bis(10-vinylphenoxy)decane , (5) 12-bis(12-vinylphenoxy)dodcecane and (6) 4-bis(4-vinylphenoxy)*p*-xylene

A) ^{1}H NMR analysis

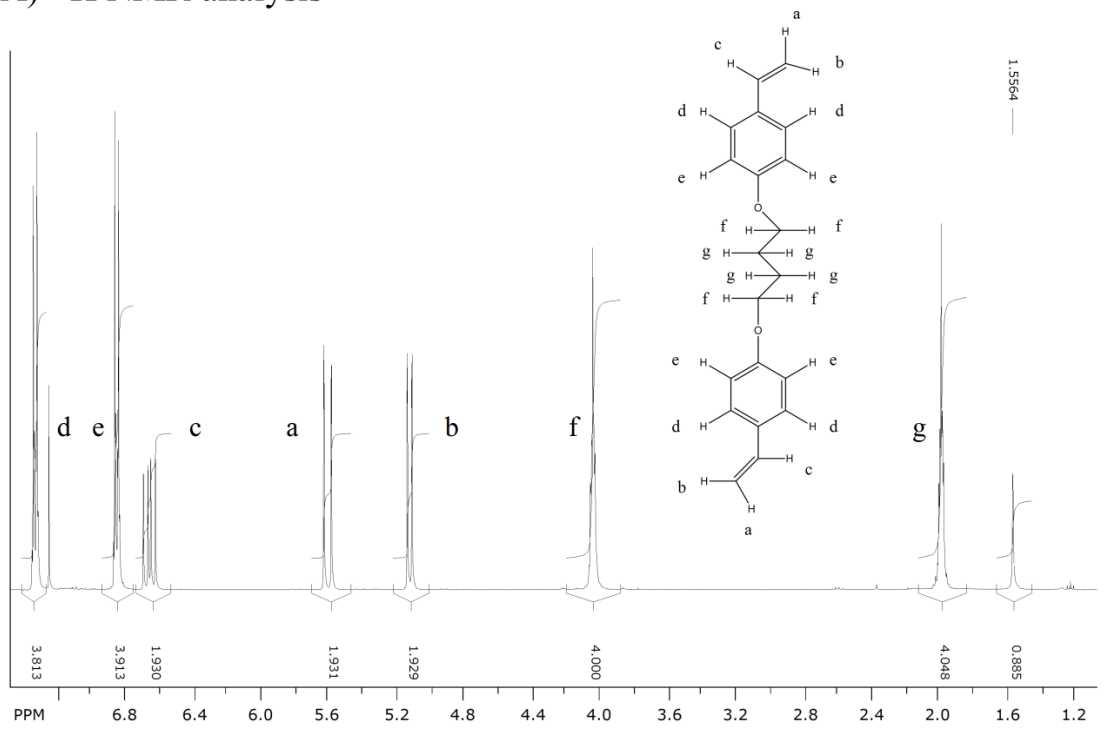

B) Mass Spectrometry analysis

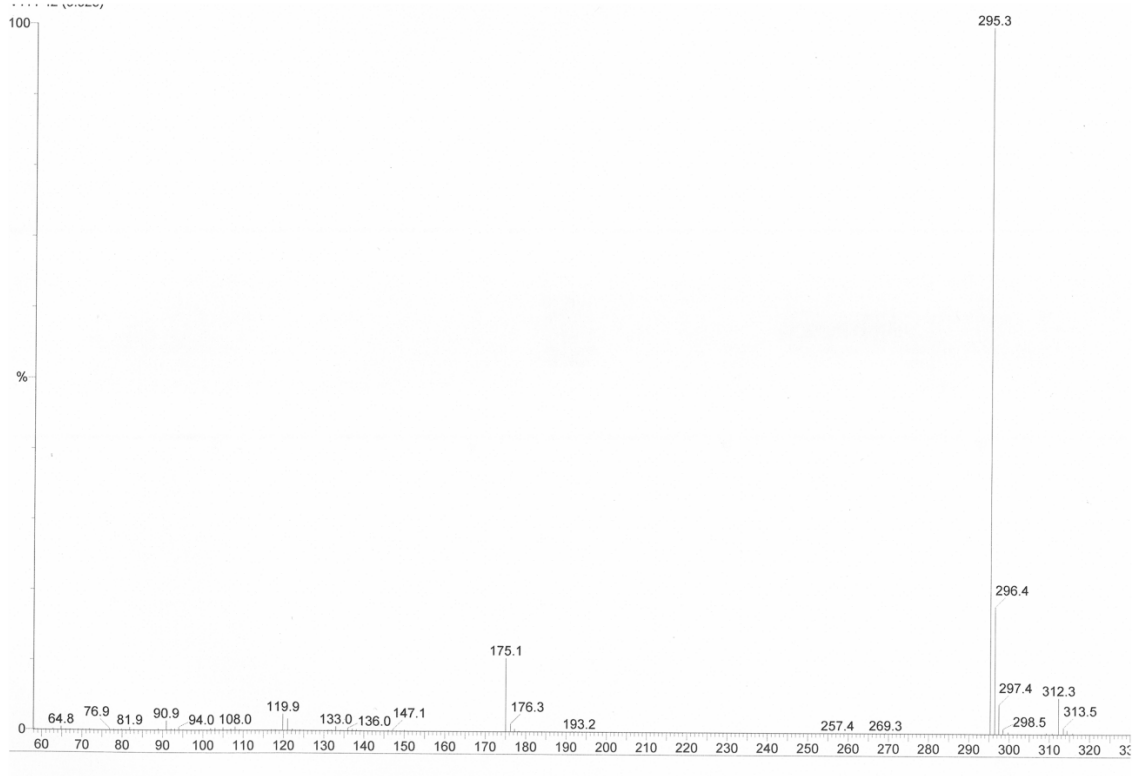

Figure 4.12: (A) ^{1}H NMR spectrum and (B) mass spectrum of 4-bis(4-vinylphenoxy)butane

A) ^{1}H NMR analysis

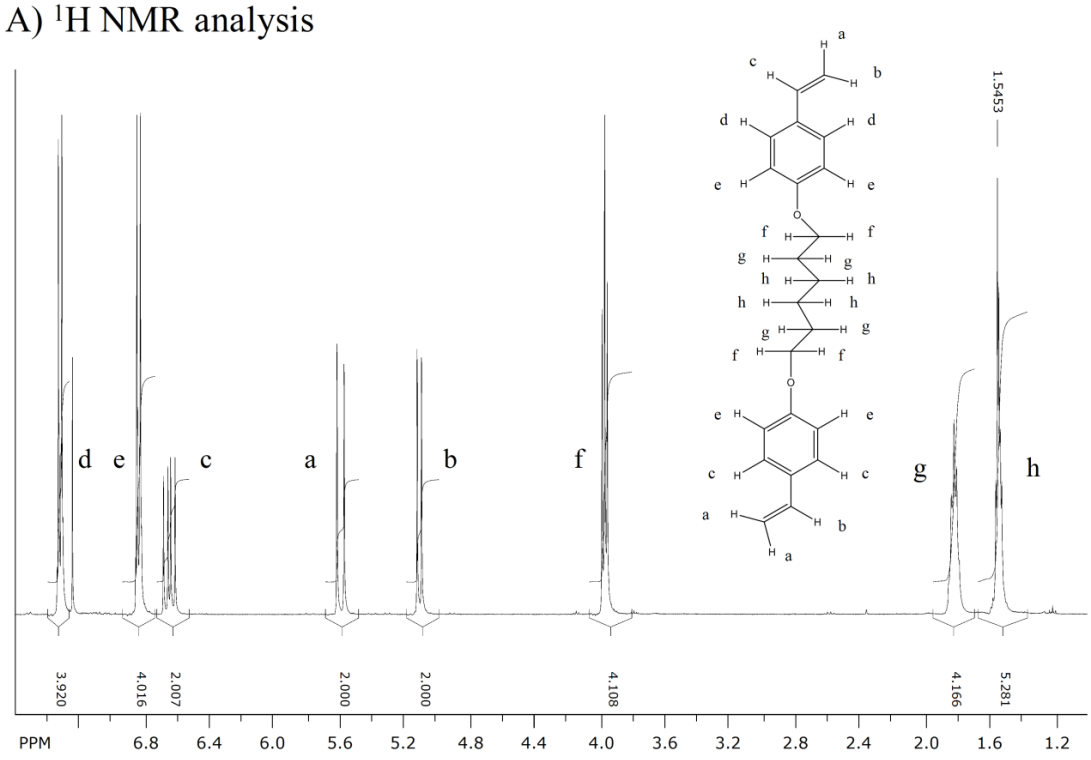

B) Mass Spectrometry analysis

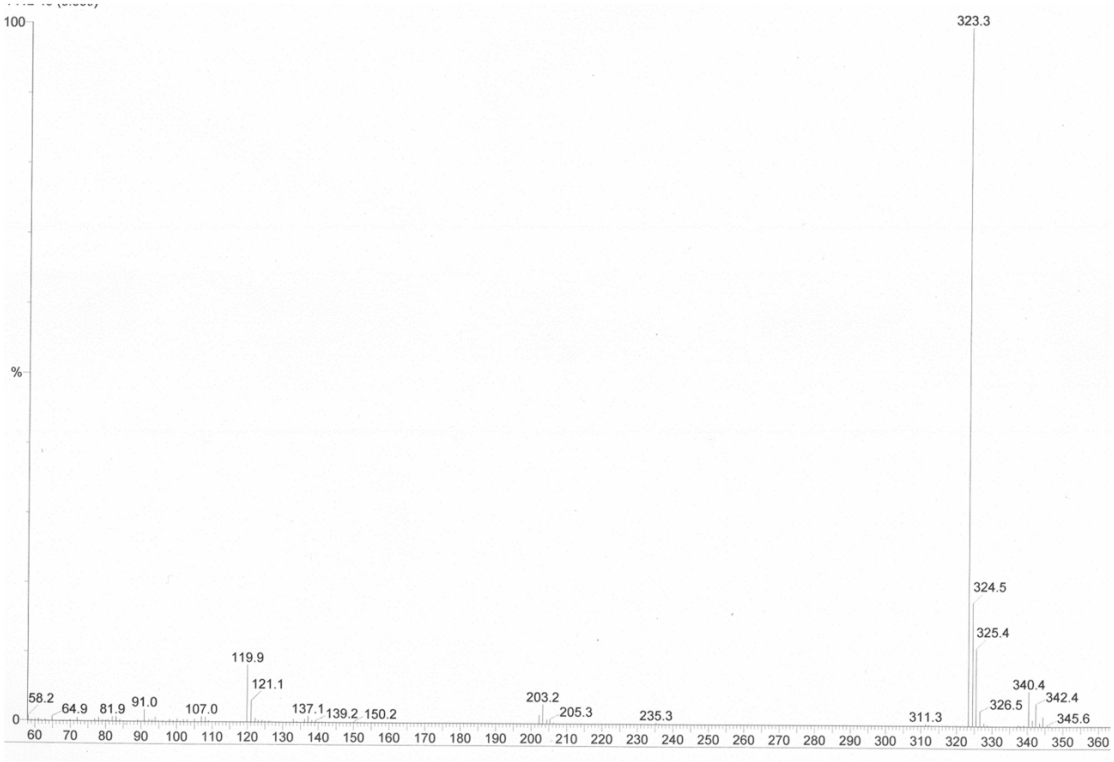

Figure 4.13: (A) ^{1}H NMR spectrum and (B) mass spectrum of 6-bis(6-vinylphenoxy)hexane

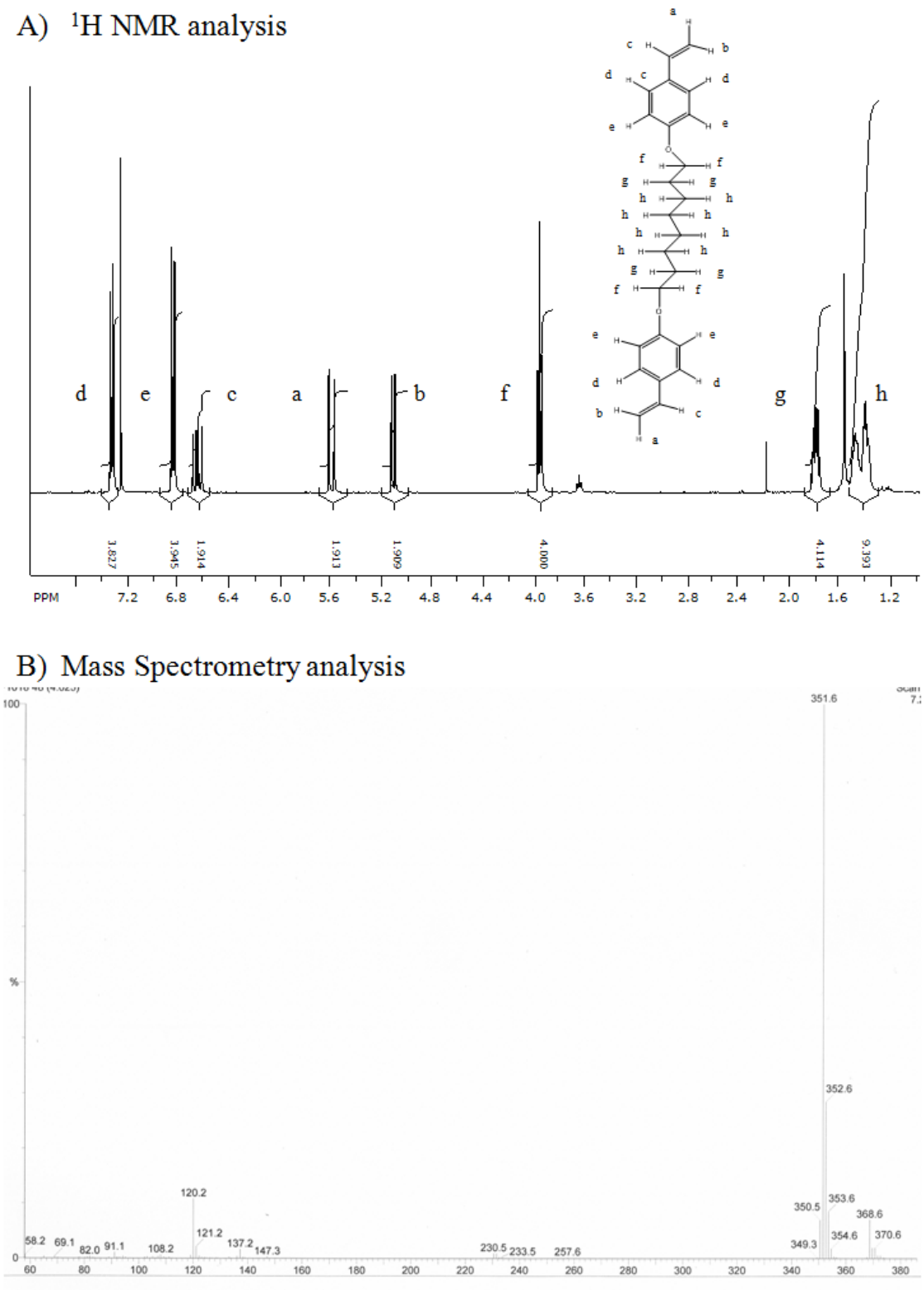

Figure 4.14: (A) ^{1}H NMR spectrum and (B) mass spectrum of 8-bis(8-vinylphenoxy)octane

A) ^{1}H NMR analysis

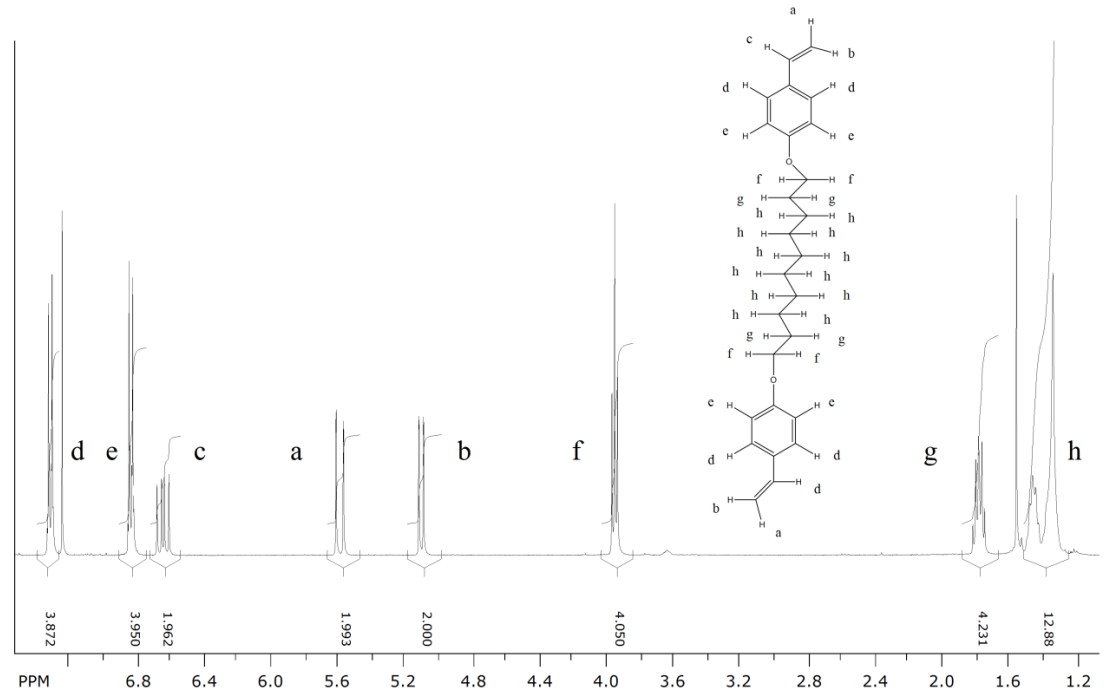

B) Mass Spectrometry analysis

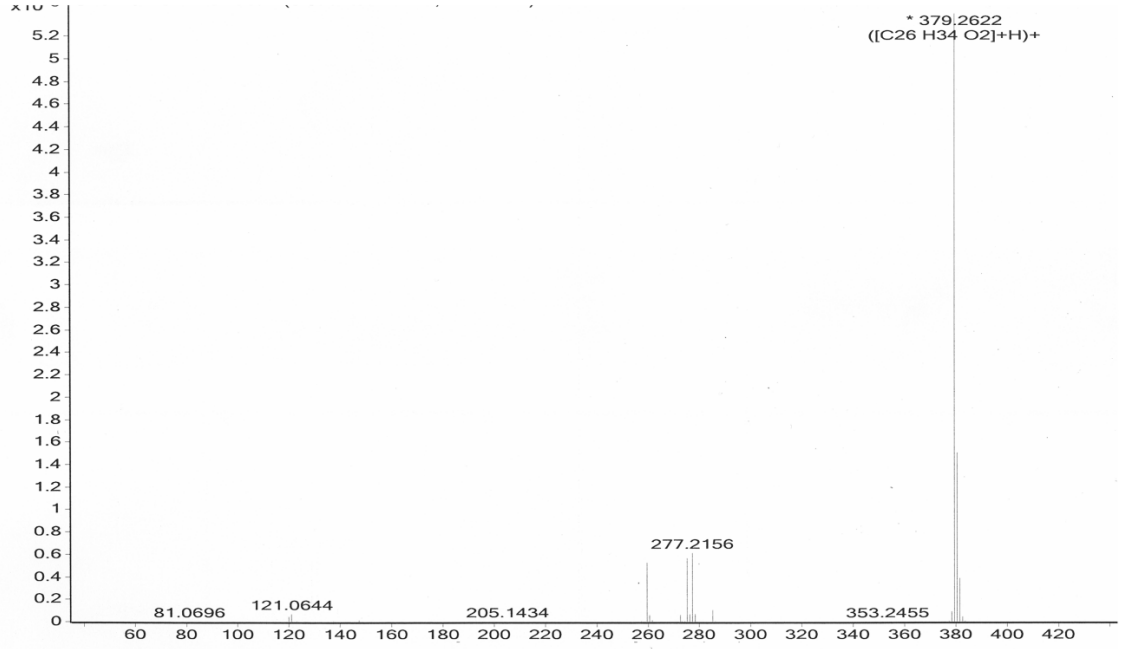

Figure 4.15: (A) ^{1}H NMR spectrum and (B) mass spectrum of 10-bis(10-vinylphenoxy)decane

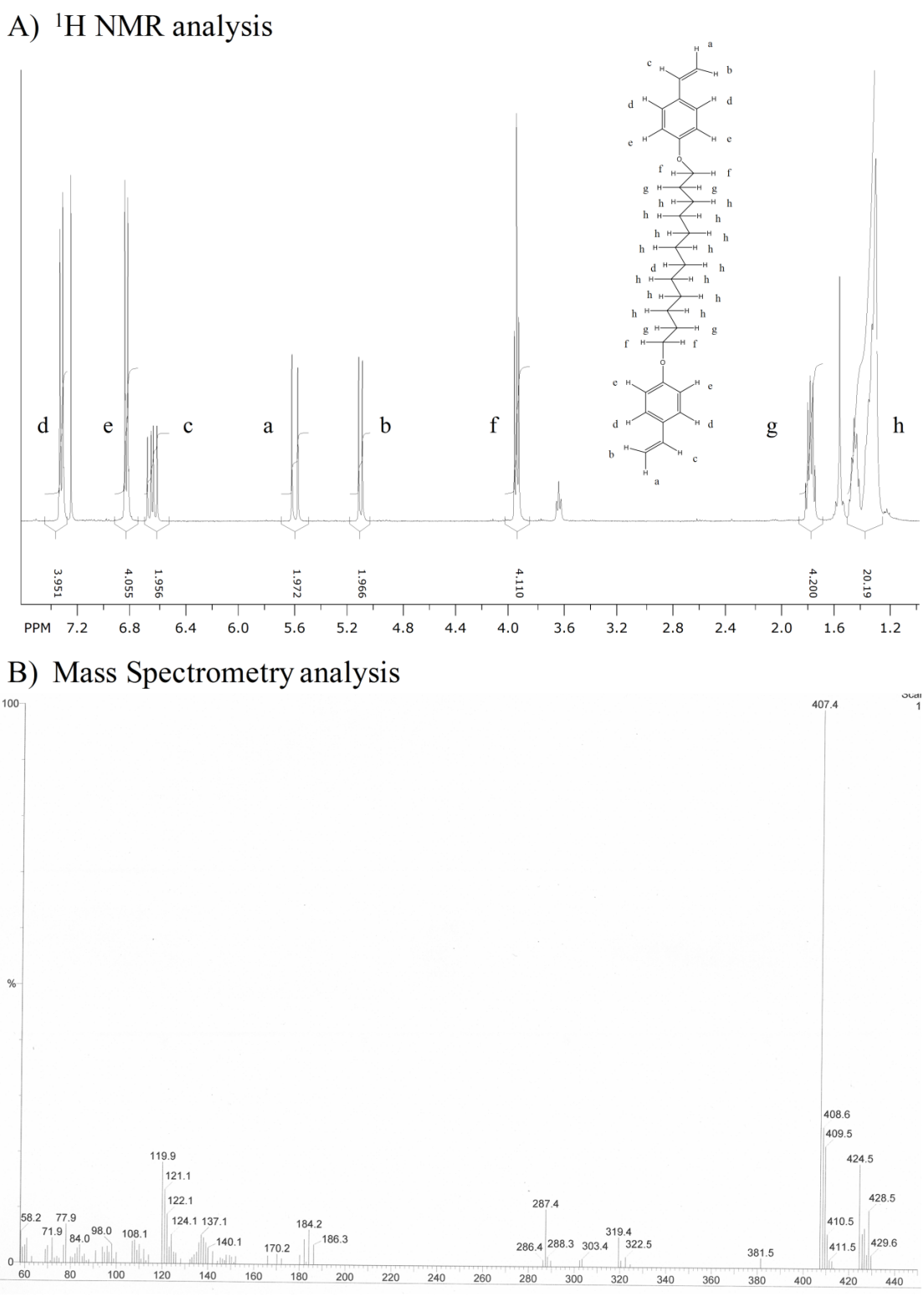

Figure 4.16: (A) ^{1}H NMR spectrum and (B) mass spectrum of 12-bis(12-vinylphenoxy)dodecane

A) ^{1}H NMR analysis

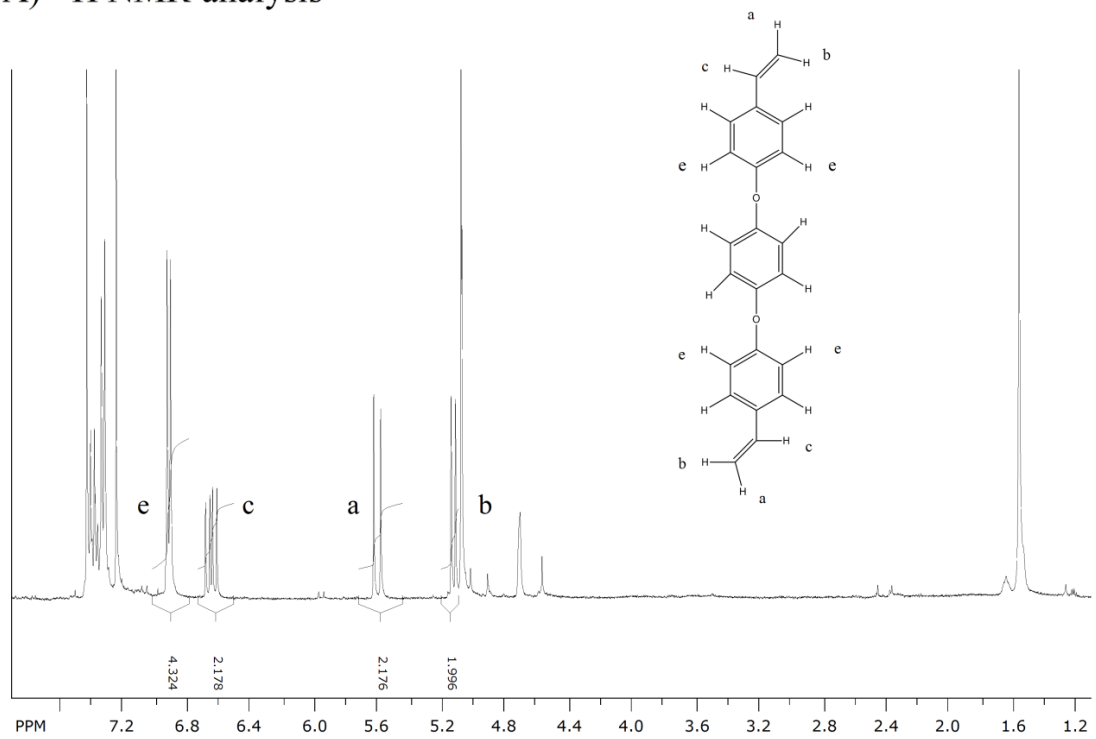

B) Mass Spectrometry analysis

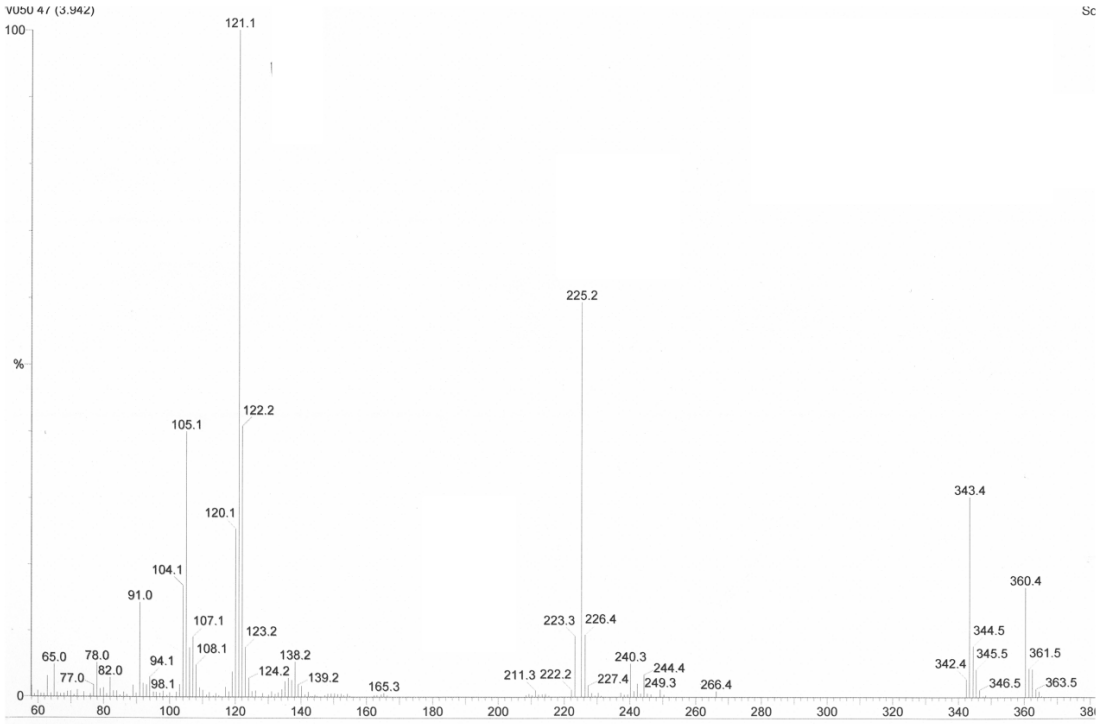

Figure 4.17: (A) ^{1}H NMR spectrum and (B) mass spectrum of 4-bis(4-vinylphenoxy)*p*-xylene

As can be seen, some of the integral calculations give a higher than expected number of protons. This can be explained by the presence of both diethylether, a chemical used in the extraction phase of the synthesis, and also the presence of water. Figure 4.18 illustrates the presence of water in the ^{1}H NMR spectra, and shows what should be two symmetrical quintets distorted by the presence of water at 1.56 ppm; the known chemical shift for water. [5]

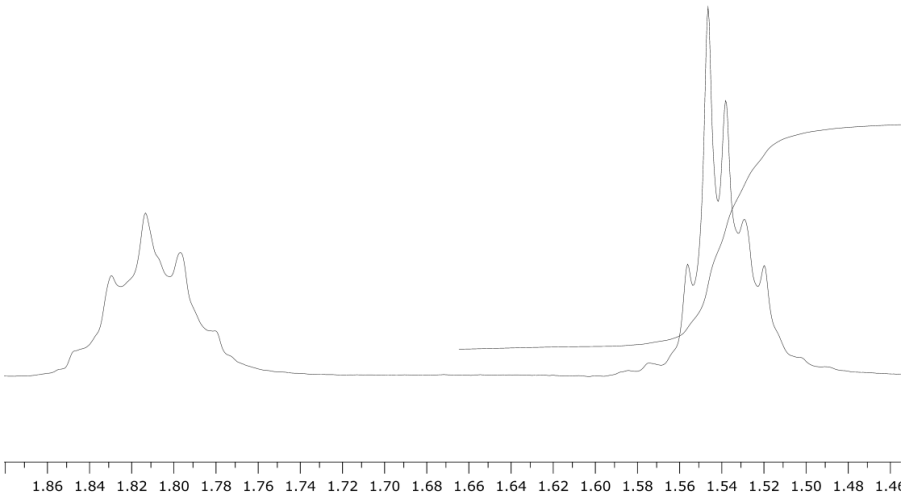

Figure 4.18: ^{1}H NMR spectrum of 6-bis(6-vinylphenoxy)hexane illustrating the presence of H_2O in the compound.

Due to this the branchers were stored in a vacuum oven prior to use in polymerisations. VPOPARAX was found to be too impure despite additional purification steps, and although a polymerisation was attempted it was unsuccessful so this was discarded as a possible brancher compound.

4.4. Increasing brancher:initiator ratio of synthesised dystyrl branchers.

4.4.1 4-bis(4-vinylphenoxy)butane (VPOB)

To study the potential improvement upon the branched anionic polymerisation of styrene using distyrl branchers other than DVB, a series of experiments similar to those

conducted with DVB as brancher were performed whereby the amount of brancher was increased. The experimental conditions were controlled as follows; 30 mL of benzene to 5 g (48 mmol) of styrene monomer, 0.96 mmol of *sec*-BuLi (for a targeted primary chain length of DP_n = 50 monomer units) and TMEDA (0.96 mmol). All experiments were terminated after 3 hours and the brancher used was VPOB.

The nature of the anionic polymerisation experimental practice makes it very difficult to accurately know the exact ratio of brancher:initiator. To reduce the experimental error that was observed during the titration of *sec*-BuLi and to gain a clear understanding of the *effective* molarity of the *sec*-BuLi initiator, an approach was developed that allowed the effective concentration within the anionic polymerisation of styrene to be determined, using the exact reagents and conditions of the intended branched polymerisation. Linear control polymers were synthesised at a reaction time of one hour immediately prior to the branched polystyrene experiments but under identical conditions. Rapid purification followed by GPC measurement of the linear polystyrene to determine M_n values allowed the calculations shown below to calculate the actual effective concentration of initiator that would present in an identical branched polystyrene reaction.

$$M_n\ 1^{st}\ injection + M_n\ 2^{nd}\ injection/\ 2 = Average\ M_n\ (gmol^{-1})$$

$$DP = Mn\ /\ MW\ of\ monomer\ (104.15gmol^{-1})$$

$$Mol\ of\ initiator\ [I]\ in\ a\ set\ volume\ of\ initiator = mol\ of\ monomer\ [M]\ /\ DP$$

The linear control polymers were utilised as a pre-experimental technique to allow increased accuracy when calculating the actual moles of initiator that were added to the

polymerisation and, therefore, the effective brancher:initiator ratio that was present within the polymerisation reaction. Whilst this does offer some improvement, the only outstanding impurities that are not accounted for are within the VPOB brancher, however, this was not considered to be an appreciable error. As can be seen in Table 4.5, the actual brancher:initiator ratio within each reaction was significantly lower than the ratios targeted using the stated molarity of the commercial *sec*-BuLi. M_n and M_w values of the branched polymers synthesised during this evaluation are also given in Table 4.5.

Table 4.5: M_n, M_w and Đ values for branched polystyrenes with increasing aamounts of brancher VPOB synthesised by anionic polymerisation techniques.

Targeted ratio(x:1)	**M_n of linear equivalent ($gmol^{-1}$)**	**Effective brancher ratio**	**GPC**		
			M_n of branched polymer ($gmol^{-1}$)	**M_w of branched polymer ($gmol^{-1}$**	**Đ**
1.6	4,500	1.9	Gel	Gel	Gel
1.5	4,500	1.77	Gel	Gel	Gel
1.4	4,500	1.66	Microgel	Microgel	Microgel
1.3	4,500	1.54	33,700	629,300	18.67
1.2	4,500	1.44	28,200	992,000	35.18
1.4	5,300	1.385	19,600	509,600	26.00
1.4	5,300	1.399	19,100	340,800	17.84
1.3	5,300	1.303	17,400	178,600	10.26
1.1	4,200	1.101	18,900	422,300	22.34
1.05	4,200	1.05	13,100	240,500	18.36
0.99	4,200	0.995	16,100	239,600	14.88
0.99	4,200	0.95	10,900	77,300	7.09
0.98	4,800	0.94	10,700	39,500	3.69
0.97	4,800	0.93	11,800	47,300	4.01
0.95	5,300	0.91	8,800	27,900	3.17

As can be seen in Table 4.5, there is a clear point where the concentration of brancher leads to the onset of gelation under these conditions. Figure 4.19 (A) shows a

photographic example of one such gel. It can also be seen that at an effective ratio of 1.54:1 there seems to be a decrease in the values from the 1.44:1 polymer. This is probably due to the formation of a small amount of insoluble microgel and therefore the highest molecular weight materials were not soluble and the soluble fraction, measured by the GPC, only includes lower molecular weight material. It is important to note that the number average molecular weights have continued to increase, as would be expected beyond the gel point. Figure 21 (B) shows a photographic example of microgel particles, highlighted by the arrow.

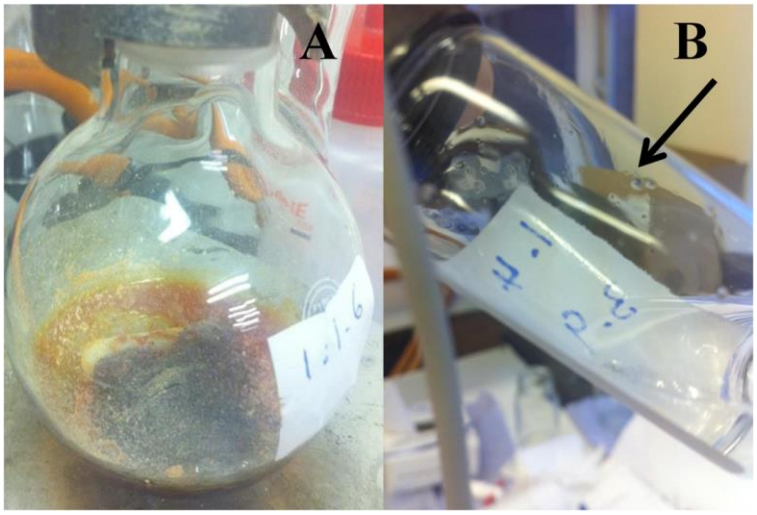

Figure 4.19: Photographs of (A) a gelled polystyrene, still 'living' and (B) a microgel in THF.

The weight average molecular weight increase is graphically represented in Figure 4.20. As can be seen from the graph, the M_w values increase steadily as the brancher:initiator ratio increases, but then at the highest brancher ratio it decreases sharply. This is not observed in the M_n values, however, a sharp decrease in dispersity is also seen at this level of brancher, Table 4.5. This is believed to indicate the onset of gelation and microgel particle formation as described above and shown in Figure 4.19 (B).

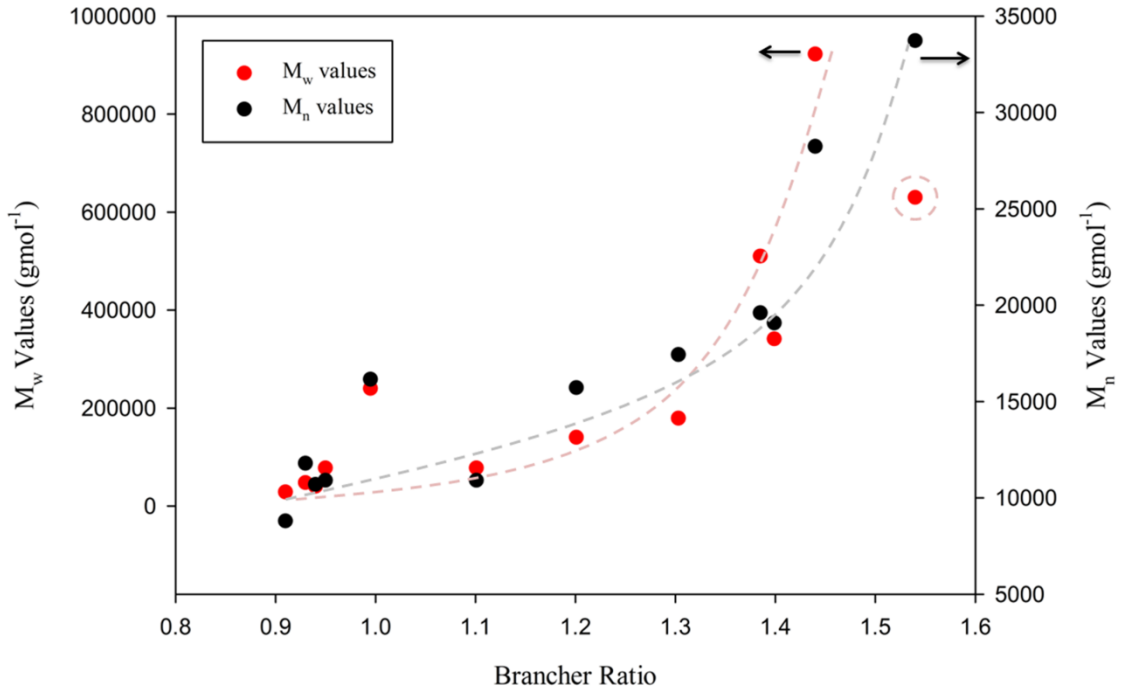

Figure 4.20: Graph of the brancher VPOB ratio to initiator *sec*-BuLi versus both M_n and M_w values of the polymers synthesised with an increasing amount of VPOB.

4.4.2 .1 6-bis (4vinylphenoxy)hexane (VPOHEX)

The series of experiments were repeated with VPOHEX as the brancher compound. The experimental conditions were controlled as follows; 30 mL of benzene to 5g (48 mmol) of styrene monomer, 0. 96 mmol of *sec*-BuLi (for a targeted primary chain length of DP_n = 50 monomer units) and TMEDA (0.96 mmol), all experiments were terminated after 3 hours and the brancher used was VPOHEX. Figure 4.21 shows the RI GPC traces of the VPOHEX:*sec*-BuLi ratios 1.2:1, 1.3: and 1.4:1, and Table 4.6 gives the M_n, M_w and dispersity values.

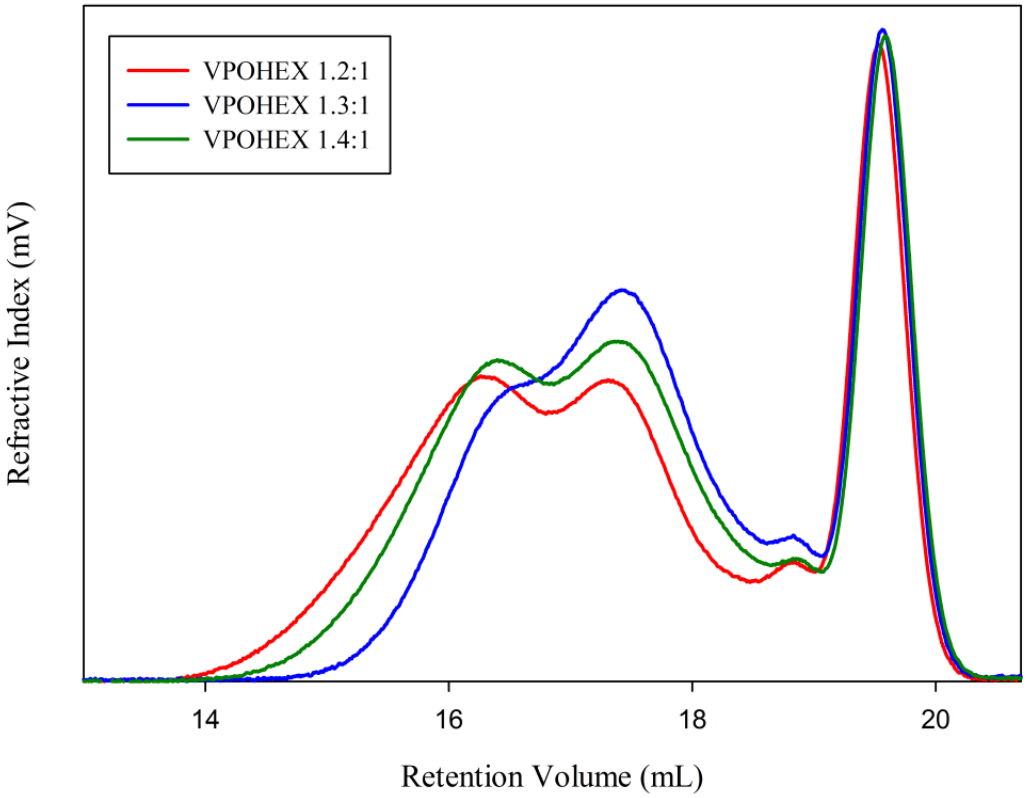

Figure 4.21: GPC chromatograms of branched polystyrenes synthesised by anionic polymerisation techniques with increasing amounts of VPOHEX.

Table 4.6: M_n, M_w and Đ values for of branched polystyrenes synthesised by anionic polymerisation techniques with increasing amounts of VPOHEX**.**

Targeted ratio	Calculated ratio	GPC		
		M_n (gmol^{-1})	M_w (gmol^{-1})	Đ
1.2:1	1.2	20,400	338,800	16.64
1.3:1	1.3	16,500	222,200	13.49
1.4:1	1.4	16,000	126,300	7.89

As can be seen from the results it appears that as the brancher amount is increased the Mw values decrease. This may be due to a similar effect seen in the VPOB experiments, the formation of insoluble microgel. However, unlike the polymerisations using VPOB the M_n values also decrease. Figure 4.22 shows the RALS detection GPC chromatograms for these polymers.

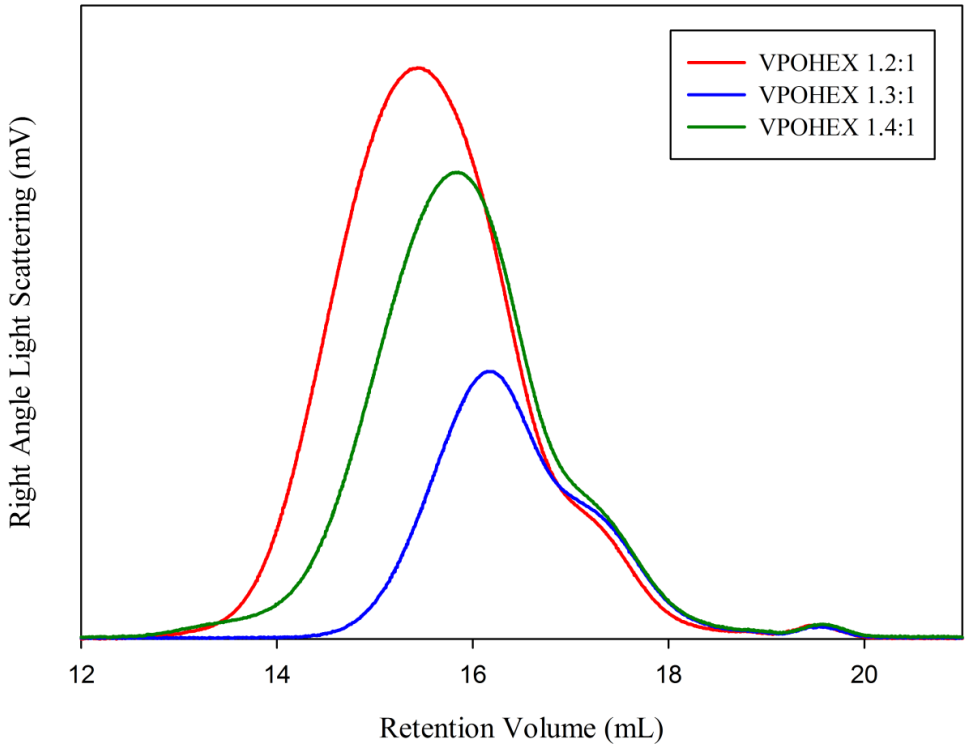

Figure 4.22: RALS GPC chromatograms of branched polystyrenes synthesised by anionic polymerisation techniques with increasing amounts of VPOHEX.

If we consider the RALS detection it can be seen that in the 1.2:1 ratio there are significantly larger species which would affect the M_n and M_w values significantly and a lower ability to reach high molecular weights is seen with increasing brancher.

4.4.3 8-bis (4vinylphenoxy)octane (VPOOC)

The anionic polymerisation experiments were repeated again, as outlined for VPOB and VPOHEX, but with VPOOC as the brancher compound. However the data presented in Table 4.7 is not directly comparable, as previous polymerisation experiments utilising VPOOC as the brancher compound have also been included for completeness, despite their different reaction conditions. Figure 4.23 shows the RI GPC chromatograms for all polymers synthesised with increasing amounts of VPOOC, and Table 8 gives the M_n, M_w and dispersity values.

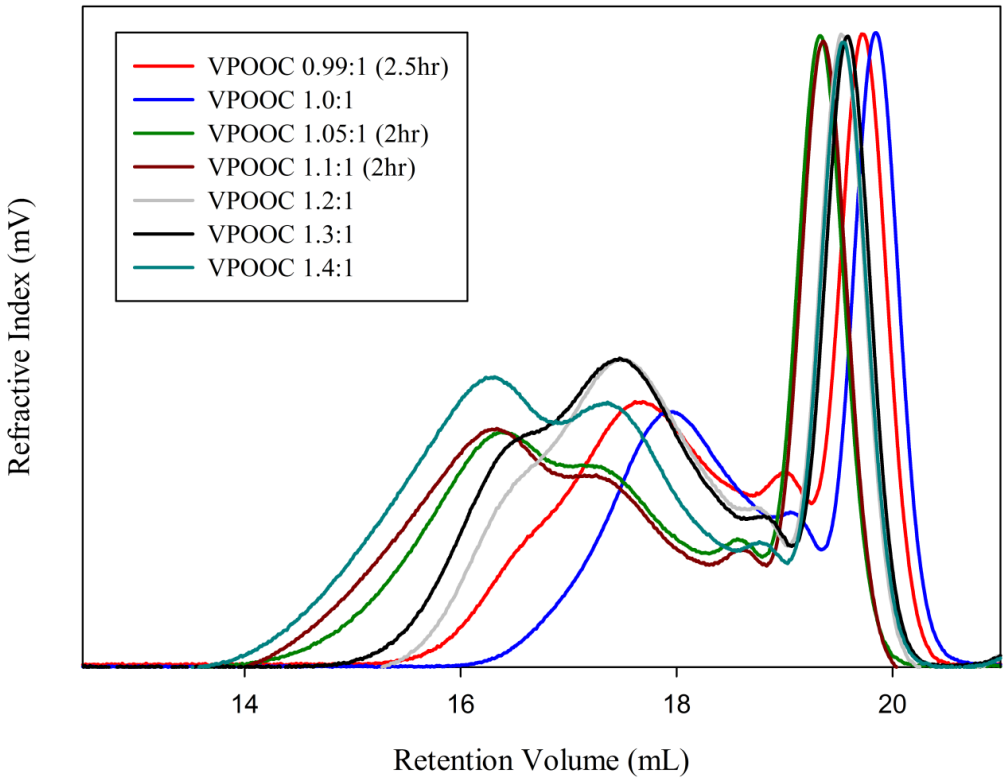

Figure 4.23: RI GPC chromatographs of branched polystyrene synthesised by anionic polymerisation techniques.

Table 4.7: M_n, M_w and Đ values for branched polystyrene synthesised by anionic polymerisation techniques.

Targeted ratio	Targeted Primary Chain Length	Calculated ratio	GPC		
			M_n (gmol^{-1})	M_w (gmol^{-1})	Đ
0.99	DP_n100	0.99	7,770	53,900	5.50
1.0	DP_n100	0.96	12,100	33,400	2.76
1.05	DP_n50	1.05	21,400	299,900	13.99
1.1	DP_n50	1.1	18,200	425,900	23.37
1.2	DP_n50	1.2	7,582	97,500	12.876
1.3	DP_n50	1.3	7,400	123,900	16.77
1.4	DP_n50	1.4	10,300	417,300	40.420

4.4.4 10-bis (4vinylphenoxy)decane (VPOT)

The series of experiments were repeated with VPOT as the brancher compound. The experimental conditions were controlled as follows; 30 mL of benzene to 5g (0.0480 mol) of styrene monomer, 0.96 mmol of *sec*-BuLi (for a targeted primary chain length of DP_n = 50 monomer units) and TMEDA (0.96 mmol), all experiments were terminated after 3 hours and the brancher used was VPOT. As it was found that the polymer gelled at a brancher:initiator ratio of 1.3:1, lower values were used; 0.98:1, 1.0:1 and 1.2:1. Figure 4.24 shows the RI GPC traces of the VPOHEX:*sec*-BuLi ratios 0.98:1, 1.0:1 and 1.2:1, and Table 4.6 gives the M_n, M_w and dispersity values.

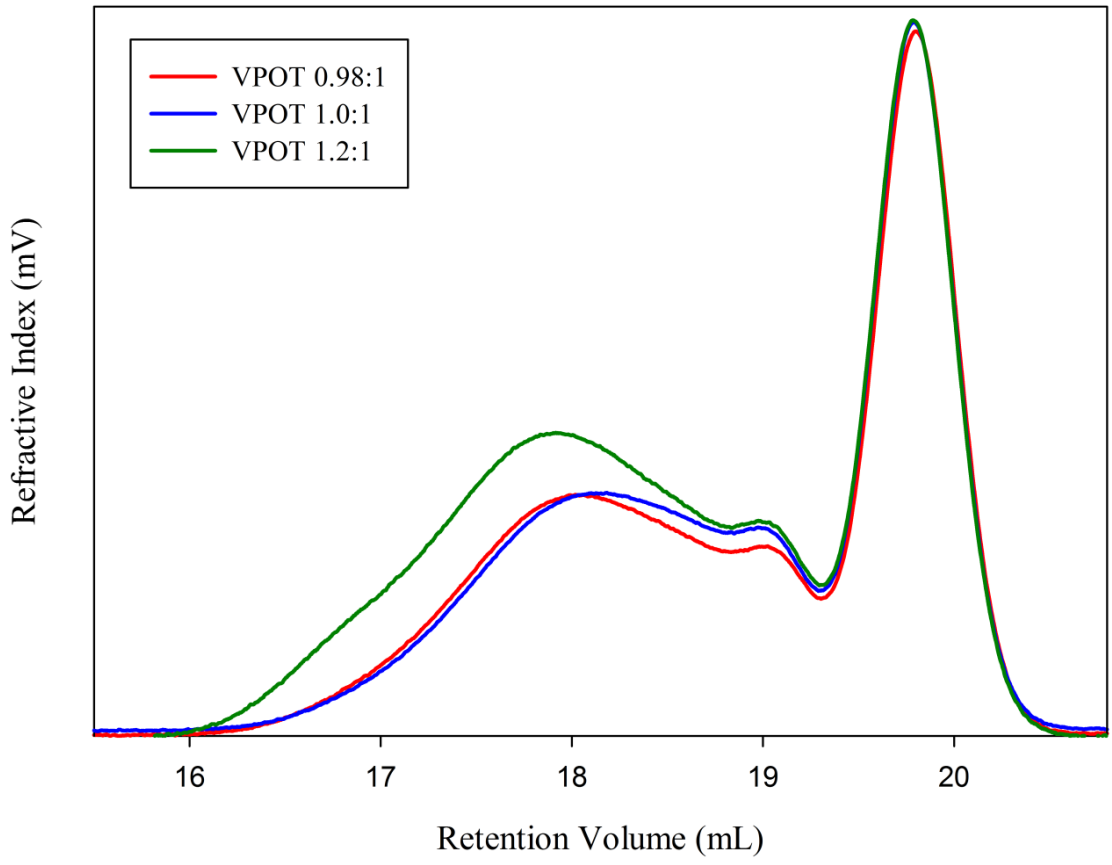

Figure 4.24: GPC chromatograms of branched polystyrenes synthesised by anionic polymerisation techniques with increasing amounts of VPOT.

Table 4.6: M_n, M_w and Đ values of branched polystyrenes synthesised by anionic polymerisation techniques with increasing amounts of VPOT.

Targeted ratio	Calculated ratio	GPC		
		M_n (gmol^{-1})	M_w (gmol^{-1})	Đ
0.98	1.05	5,900	38,300	6.49
1.1	1.07	7,000	36,400	5.15
1.2	1.28	6,900	57,300	8.30
1.3	1.34	GEL	GEL	GEL

4.4.5 12-bis (4vinylphenoxy)decane (VPODD)

The series of experiments was attempted with VPODD as the brancher compound. As the VPOT gelled at a lower level than VPOOC, VPOHEX and VPOB lower ratios were chosen; 1.0:1, 0.98:1 and 0.95: 1. However, it was found that a gel formed even at 0.95:1 so an additional polymerisation with a ratio of 0.90:1 was conducted, and the resulting polymer was analysed by GPC. The experimental conditions were controlled as follows; 30 mL of benzene to 5g (48 mmol) of styrene monomer, 0.96 mmol of *sec*-BuLi (for a targeted linear DP_n50 monomer units) and TMEDA (0.96 mmol), the experiment was terminated after 3 hours and the brancher used was VPODD (0.864 mmol for a 0.9:1 VPODD:*sec*-BuLi ratio). The RI GPC chromatogram is shown in Figure 27.

Table 4.7: M_n, M_w and Đ values for branched polystyrene synthesised by anionic polymerisation techniques.

Targeted ratio	Calculated ratio	M_n (gmol^{-1})	M_w (gmol^{-1})	Đ
0.90	1.05	5,900	38,300	6.49

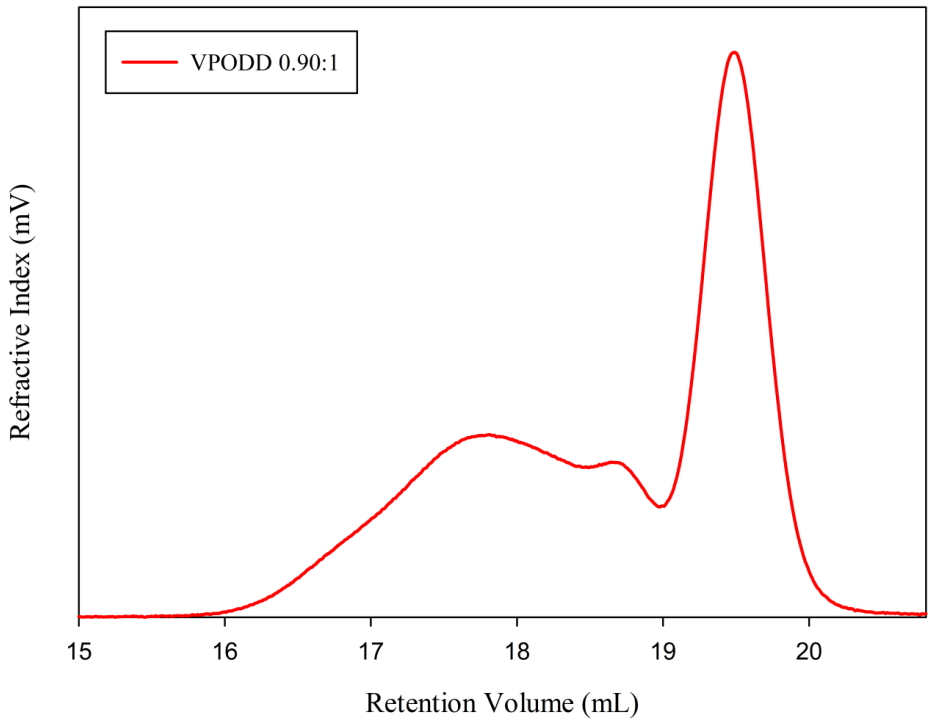

Figure 4.25: GPC chromatogram of branched polystyrene synthesised by anionic polymerisation techniques.

4.4.6 Comparison of distryl brancher compounds

As can be seen from the results of the different branched polymerisations utilising each synthesised brancher compound, the increasing ratios for each brancher were not as straight forward as planned, and the gel point varied significantly between the branchers. As the length of the distance between the reactive distyrl groups increased, specifically for VPOT and VPODD, a lower brancher:initiator ratio had to be used to avoid gellation. This may have been an effect of other anionic factors causing aggregation as they do not appear to reach high molecular weights before cross-linking, as seen in the other brancher compounds. A comparison of the same brancher to initiator ratio (1.2:1), with the exception of VPODD which is 0.9:1, can be seen in Figure 4.26.

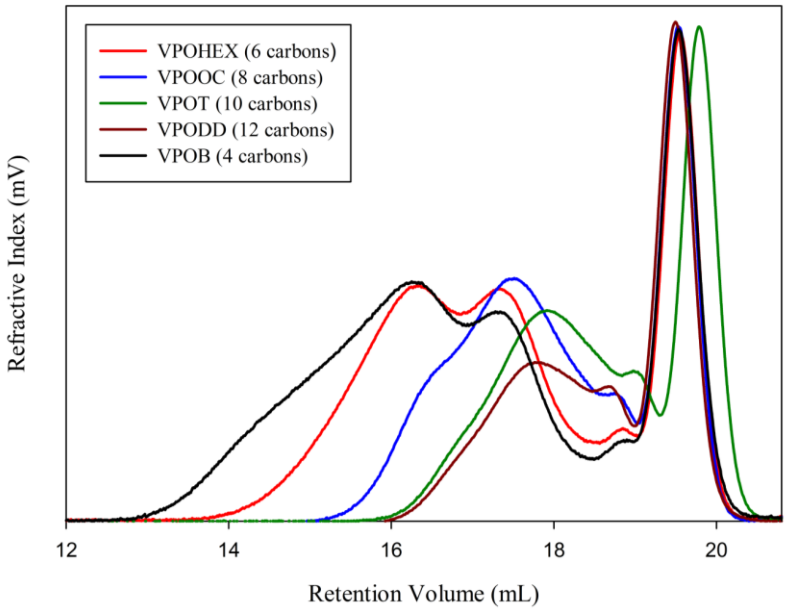

Figure 4.26: Comparison of RI GPC chromatograms of branched polystyrenes synthesised by anionic polymerisation techniques with different brancher compounds.

As can be seen it appears that the longer the space between the vinyl groups, the less branched the polymer becomes. Taking into account the difference in M_w values between the smaller compounds VPOB and VPOHEX, practical considerations such as availability and price of starting material resulted in VPOB being chosen as the preferred branching compound, and shall be used in all further branched polymerisation experiments.

4.5 Conclusions

Branched polystyrenes have been synthesised by ATRP and anionic polymerisation techniques. Different dystryl compounds have been tested as brancher compounds within anionic branched polymerisation and their relative suitabilities assessed. The commercially available DVB has been replaced with synthesised dystyrl compounds, allowing for greater control over the issues arising from the many isomers of DVB. A

series of compounds with increasing space between the two vinyl groups were synthesised to prevent modification of reactivity during polymerisation. Branched polystyrenes were produced from all of these compounds.

The conditions of the branched polymerisation were investigated, and many variables changed. From the results of this series of experiments a control experimental standard was set which included using 30 mL solvent (benzene), a reaction time of 3.5 hours and the brancher compound used was chosen to be VPOB.

4. 6 References

1. Funke, W.; Okay, O. *Macromolecules* **1991**, *24*, 2623
2. Lutz, P.; Rempp, P. *Macromol. Chem. Phys*., **1988**, *189*, 1051
3. Eschwey, H.; Burchard, W., *Polymer*, **1975**, 16, 180
4. Crivello, J. V., Ramdas, A. *J. Macromol. Sci. Pure*, **1992**, *9*, 753
5. Gottlieb, H.E.; Kotlyar, V.; Nuelman, A., *J. Org. Chem*., **1997,** *21*, 7512

Chapter 5

Changing the Architecture of Branched Polymers

5.0 Introduction

As shown in Chapter 4, branched polystyrenes were successfully synthesised using a branched anionic polymerisation strategy and the conditions of the reaction were investigated with optimum conditions derived.

In addition to the variables explored in Chapter 4, there are other factors that can affect the polymerisation, and changing these variables can significantly alter the architecture of the resulting polymer. Such variables as primary chain length, and the ability to produce branched block co-polymers with defined linear and branched character are discussed further in this chapter.

The ability to change the architecture of the branched polymer will potentially be of great benefit when synthesising the target amphiphillic nanoparticles, and will allow the manipulation of physical properties of the polymer.

5.1 Effect of primary chain length.

The target chain length of the primary chains that comprise the branched polystyrenes of Chapter 4 are expected to influence the polymerisation and the final properties of the resulting polymers as the distance between branch points (branching density) and the potential for the inclusion of brancher during synthesis will vary. In principle, one of the key factors within linear polymer properties is the overall molecular weight, or chain length, of the polymer chains. Within a branched polymer analogue, the molecular

weight of the macromolecule is a clear indication of the number of linear chains that have been intermolecularly conjugated; however, it is not a direct measure of the average architecture formed. Branched macromolecules of identical nominal molecular weight may have dramatically different architectures.

The effect of changing the primary chain length of the branched polystyrenes formed from the anionic branched polymerisation strategy was investigated, again, in a series of synthesis experiments in which the volume of monomer and amount of initiator were varied to provide the best experimental conditions for each chain length. Overall the brancher:initiator (VPOB:*sec*-BuLi) initiator ratio was kept constant at 1:1, and the primary chain length was varied. Targeted DP_n primary chain lengths of 10, 50,100, 250 and 500 monomer units were synthesised under the same conditions described in Chapter 3. Figure 5.1 shows the overlaid GPC chromatograms (RI detector response) for the increasing primary chain lengths.

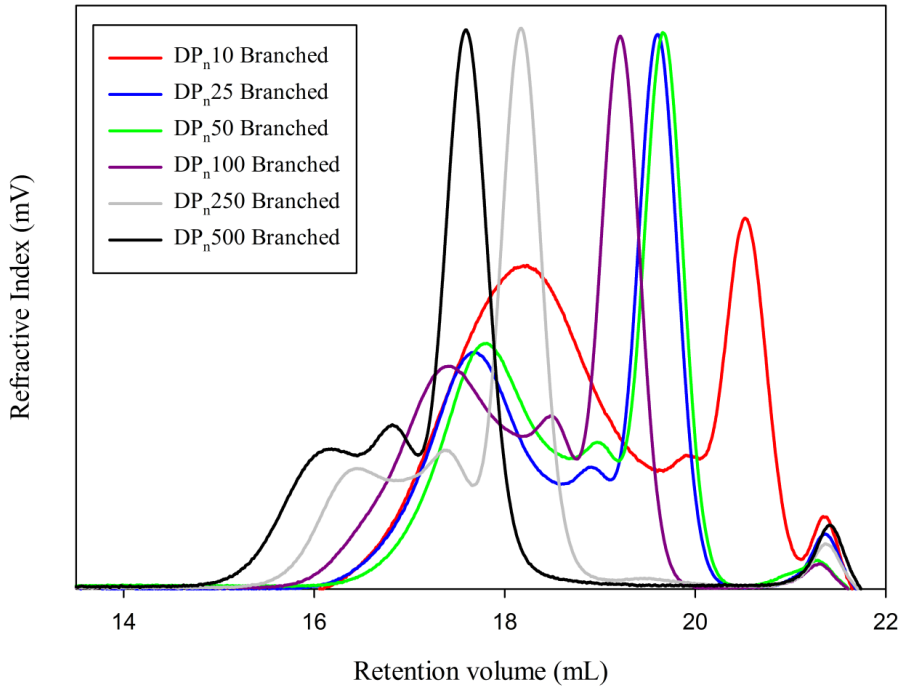

Figure 5.1: GPC chromatograms of branched polystyrene at different targeted primary chain lengths.

Table 5.1: M_n, M_w and Đ values for branched polystyrene with increasing primary chain lengths and the M_n values of the linear primary chain equivalents.

Target DP_n primary chain length (monomer units)	GPC				Approximate weight average number of chains per polymer
	Linear M_w ($gmol^{-1}$)	M_n ($gmol^{-1}$)	M_w ($gmol^{-1}$)	Đ	
10	1,100	6,400	48,900	7.64	44
25	2,500	9,700	39,500	4.07	16
50	4,700	8,400	29,800	3.55	6
100	11,700	13,400	43,400	3.24	4
250	27,700	30,800	65,700	2.13	2
500	59,300	54,700	106,200	1.94	2

As can be seen preliminarily from Table 5.1, it appears that the amount of branching is increasing as the primary chain length decreases. If the numbers are investigated further, as an example using DP_n500, it would appear that the weight average molecular weight of 106, 200 $gmol^{-1}$ indicates that there is an average of approximately two linear chains of $DP_w = 500$ ($M_w = 59{,}300$ $gmol^{-1}$) per branched polystyrene. If this is compared to the branched polymers with a targeted primary chain length of $DP_n = 10$ monomer units, taking into account the M_w of the linear chains (1,100 $gmol^{-1}$) it appears that the weight average branched polystyrene contains nearly 50 linear chains linked by the brancher compound. This is also very clearly indicated by the variation in dispersity which ranges from 7.64 – 1.94 as the targeted primary chain length increases under these conditions. Figure 5.2 shows the GPC chromatograms (RI detector) of the individual branched polymers overlaid with their respective linear counterparts, synthesised in the absence of the VPOB brancher but under identical conditions.

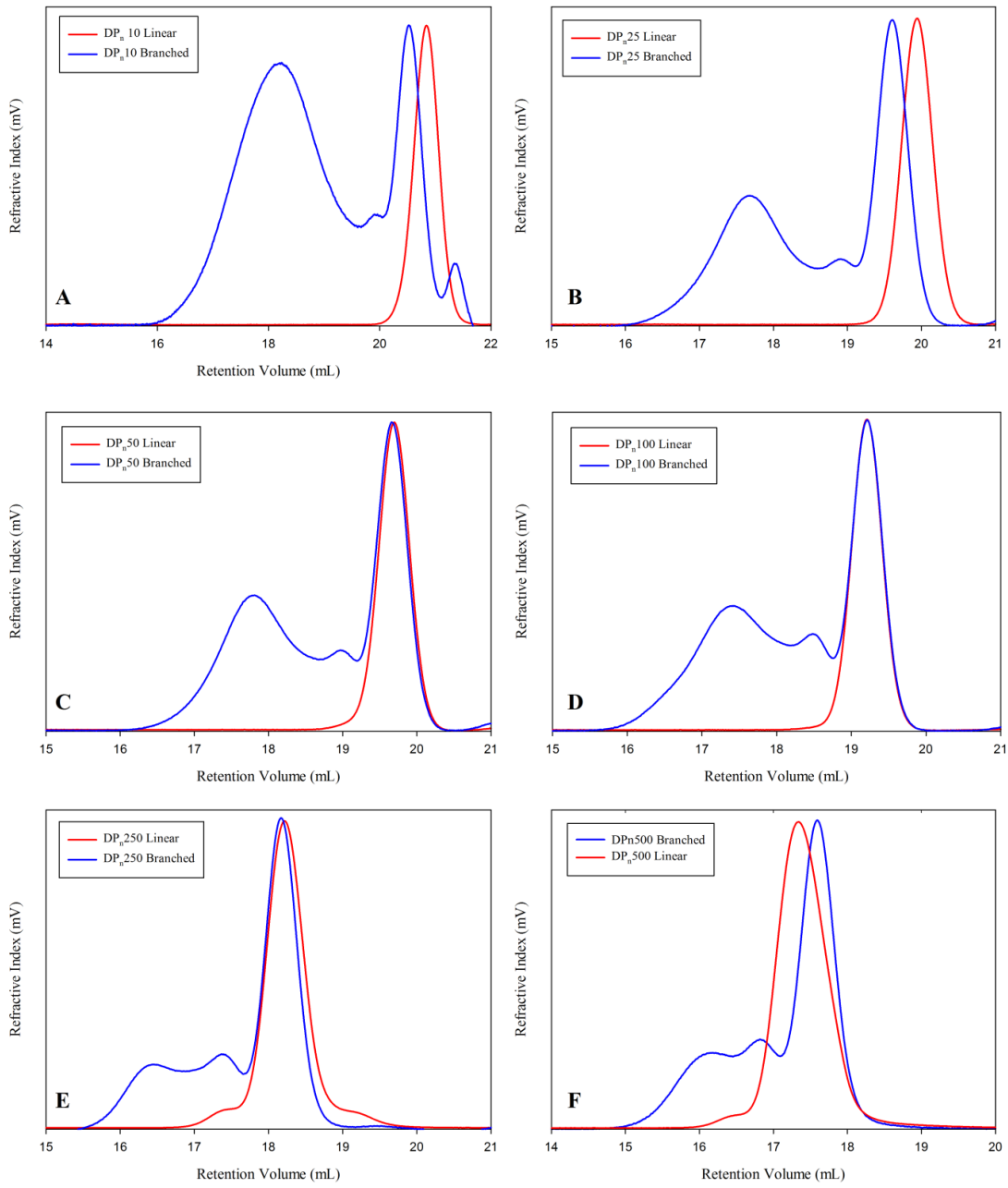

Figure 5.2: Overlaid GPC chromatograms (RI) of branched polystyrene samples (blue) with varying primary chain length, and the equivalent linear polystyrenes (red) synthesised without brancher.

As can be seen from the GPC chromatograms in Figure 5.2 there is a significant amount of linear polymer in all the branched polystyrene samples, for all the different primary chain lengths that were targeted. It can be seen that they overlay very well with the linear equivalent of the primary chains targeted.

For the results seen in Figure 5.2 (C) it can be assumed that the targeted primary chain of DP_n = 50 monomer units has been successfully synthesised as the linear proportion overlays almost exactly with the linear polystyrene (M_w = 4,700 $gmol^{-1}$), and it can be approximated that the weight average branched polystyrene is comprised of approximately six primary chains (29,800 $gmol^{-1}$ / 4,700 $gmol^{-1}$) of 50 monomer units.

The number of chains that form the weight average structure within each polymer sample can be calculated for all the branched polymers and is shown in Table 5.1. If this approximation is plotted against the targeted primary chain length, shown in Figure 5.3, then it can be seen that as the degree of branching decreases rapidly as the targeted primary chain length increases.

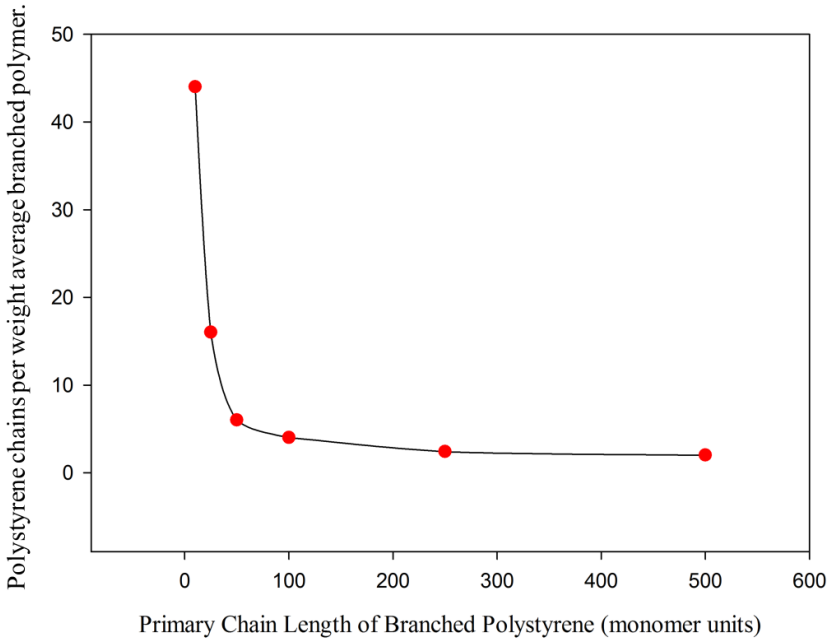

Figure 5.3: Graph of the relationship between the primary chain length and the degree of branching, this being the amount of polystyrene chains per weight average branched polymer.

If we consider an approximation of the structure of these branched polymers, the differences become more apparent. Figure 5.4 shows a cartoon of the different weight

average structures, drawn approximately to scale, of each synthesised branched polymer with increasing primary chain lengths.

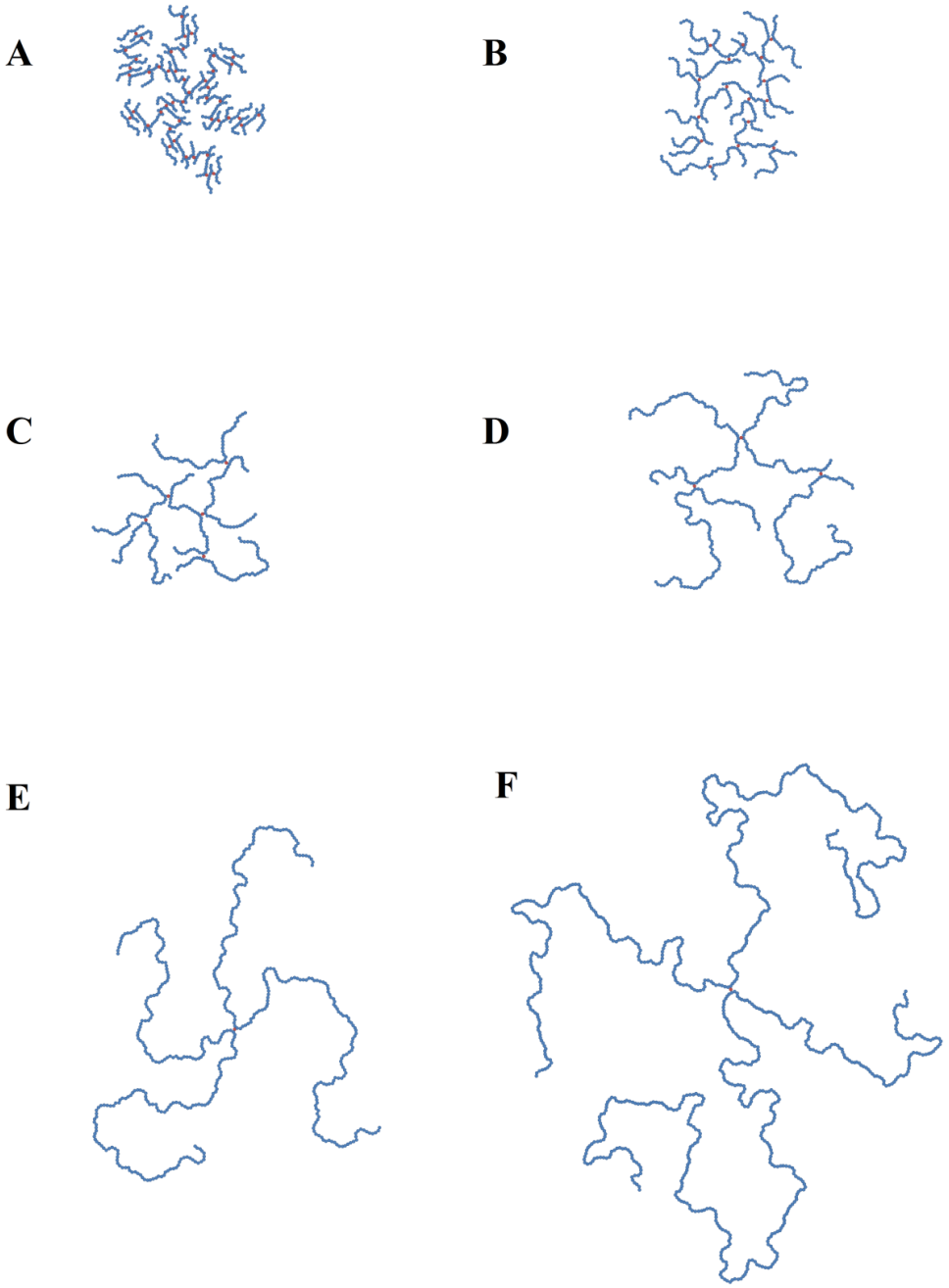

Figure 5.4: Schematic representations of (A) DP_n10 branched (approximate M_w = 48,900 $gmol^{-1}$), (B) DP_n25 branched (approximate M_w = 39,500 $gmol^{-1}$), (C) DP_n50 branched (approximate M_w = 29,800 $gmol^{-1}$), (D) DP_n100 branched (approximate M_w = 43,400 $gmol^{-1}$), (E) DP_n250 branched (approximate M_w = 65,700 $gmol^{-1}$) and (F) DP_n500 branched (approximate M_w = 106,200 $gmol^{-1}$)

However, these images are just approximations based on the M_w values of the polystyrenes. If we consider the RALS detector for each branched polymer with

increasing primary chain length is can be seen that there are some large species which cause a lot of light scattering. If they are considered in conjunction with the chromatograms from the RI detector, which relates to concentration, it can be seen that they are in very low amounts. Figure 5.5 shows the RALS detector signal for each branched polystyrene, overlaid with the respective RI detector signal.

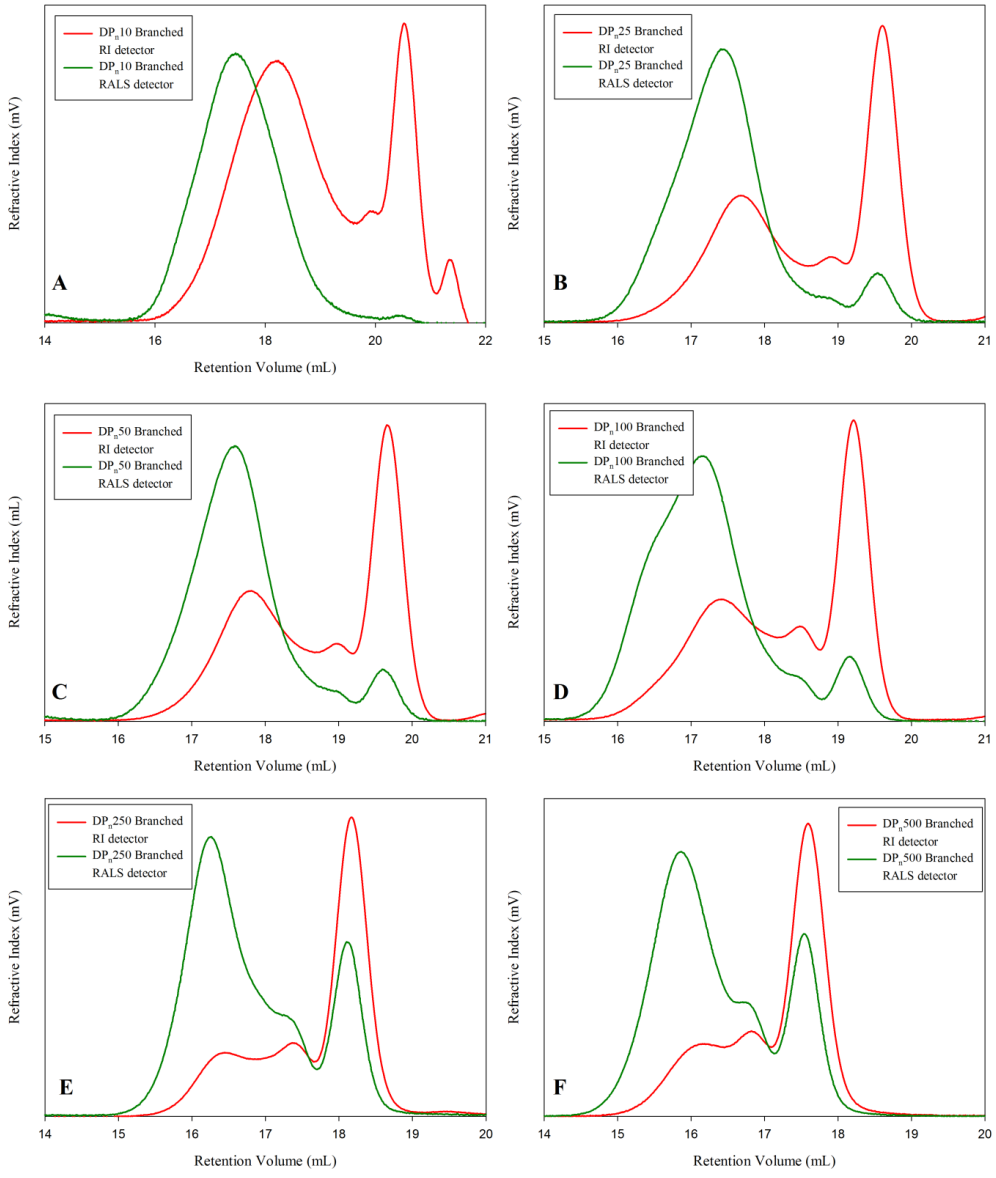

Figure 5.5: GPC chromatograms (RALS detector) of branched polystyrenes (green) with varying primary chain length, overlaid with their respective RI detector signal GPC chromatograms (red).

From these results it is clear that altering the primary chain length of the branched polystyrenes has a significant effect on the average structures and the architecture of the

polymers produced. This is explored further in Chapter 6, where the effect that this has on the physical properties is investigated through differential viscometry and differential scanning experiments.

5.2 Chain extension of branched polymers

As described in Chapter 3, during the studies of linear anionic polymerisation of styrene, chain extension was achieved through sequential monomer addition to form self-blocked linear polymers. Here, this strategy has been used to introduce mixtures of self-blocked polystyrenes with segments of linear and branched polystyrenes with different chain length combinations.

Block co-polymers were prepared by two methods; termed linear first and branched first. In the case of the so-called 'linear first', a linear polystyrene of a specific targeted DP_n (10, 40, 50, and 90 monomer units) was synthesised as follows; styrene, 30 mL of benzene, and TMEDA were stirred at temperature under nitrogen, followed by the addition of the intiator, *sec*-BuLi. In all cases the number of moles of each reagent was dependent on the targeted DP_n of the linear polymer, using the following equation:

$$\textit{Amount of styrene (g)} = \textit{moles of initiator} * \textit{targeted } DP_n * \textit{MW of styrene}$$

The reactions were allowed to polymerise for 1 hour to form the desired linear polymer chain, with an active anion chain-end capable of undergoing further anionic polymerisation. To exploit this, a branched polymer chain was grown from the linear polymer, therefore, after 1 hour a second batch of monomer was added together with an amount of the brancher, VPOB, at a ratio of 1:1 with the original moles of *sec*-BuLi.

The polymerisation was terminated after 3.5 hours and the resulting self-blocked, branched co-polymer was purified and analysed by GPC. For 'branched first' polymerisation the reverse of this method was applied. The effect of the different sequential monomer additions was to restrict the branching points within similar branched structures to specific parts of the primary chains.

With regards to nomenclature of these self-blocked, branched co-polymers, the first part of the names used herein refers to the type of polymer (ie. linear or branched) and the targeted DP_n of the polystyrene segment that was synthesised first (eg. DP_n10 monomer units). This is followed by the second part of the name which refers to the type of polymer (ie. linear or branched) and the targeted DP_n of the second addition (eg. DP_n 40 monomer units). The following block co-polymers were synthesised as a series.

- DP_n10 linear plus DP_n40 branched
- DP_n40 branched plus DP_n10 linear
- DP_n10 linear plus DP_n90 branched
- DP_n90 branched plus DP_n10 linear
- DP_n10 branched plus DP_n40 linear
- DP_n40 linear plus DP_n10 branched
- DP_n10 branched plus DP_n90 linear
- DP_n90 linear plus DP_n10 branched
- DP_n50 linear plus DP_n50 branched
- DP_n50 branched plus DP_n50 linear

The targeted macromolecules can be decribed as architectural or segmental block copolymers. Although the same monomer is used to form each segment of the complex material, there is a clear distinction between the two areas of the material; one that comprises a linear polystyrene and one that is covalently branched. This is fundamentally different to the statistcial inclusion of brancher throughout the polymerisation when both styrene and brancher are mixed and initiated through the anionic polymerisation. The materials were synthesised and analysed by GPC and

Differential Scanning Calorimetry (DSC) (discussed in Chapter 6.2) to assess the impact of varying the individual segment lengths of the architectural block copolymers and the overal length of the primary chains.

5.2.1 Self-blocked branched polystyrene co-polymers; all architectures with a primarychain length of DP_n = 100 monomer units

As described above, self-blocked branched co-polymers were synthesised via a 'linear-first' or a 'branched-first' approach. The architectures of these polymers can be compared to their equivalent branched polymers that are synthesised through the statistical incorporation of brancher throughout the primary chain. Within this section, all polymers can, therefore, be compared to the branched polystyrene with targeted primary chain of 100 monomer units. Theroretically the primary chain lengths within all structures within this section should have a DP_n = 100 monomer units.

The resulting polymers were purified and analysed by GPC and the results are shown in Figure 5.6 and Table 5.3.

- DP_n10 branched plus DP_n90 linear
- DP_n90 linear plus DP_n10 branched
- DP_n90 branched plus DP_n10 linear
- DP_n10 linear plus DP_n90 branched

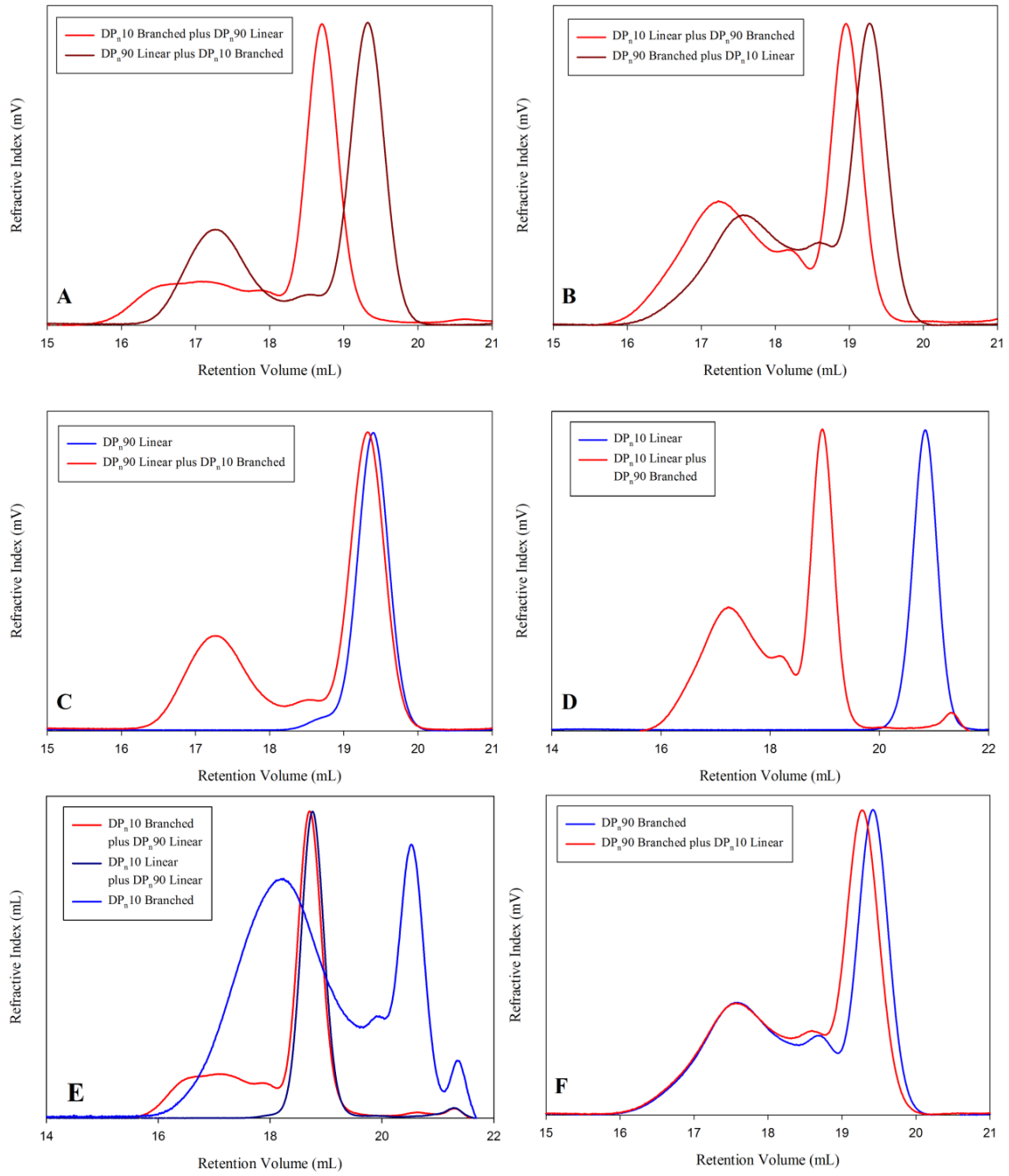

Figure 5.6: GPC chromatograms of (A) DP_n10 branched (br) plus DP_n90 linear (lin) overlaid with DP_n90 lin plus DP_n10 br (B) DP_n10 lin plus DP_n90 br overlaid with DP_n90 br plus DP_n10 lin (C) DP_n90 lin overlaid with DP_n90 lin plus DP_n10 br (D) DP_n10 lin overlaid with DP_n10 lin plus DP_n90 br (E) DP_n10 br overlaid with both DP_n10 br plus DP_n90 lin and DP_n10 lin plus DP_n90 lin (F) DP_n90 br overlaid with DP_n90 br plus DP_n10 lin.

From the GPC chromatograms (RI detector) seen in Figure 6, and the differences in M_w values, shown in Table 3, between the samples taken before and after the second aliquot

of monomer was added, it can be seen than block polymers have been successfully synthesised by this method.

Table 5.3: M_n, M_w and Đ values for branched polystyrene with different target architecture and the M_w values of the pre-cursor polymer before the second addition of monomer or monomer and brancher.

Polymer Architecture	**GPC**			
	M_w of precursor ($gmol^{-1}$)	**M_n ($gmol^{-1}$)**	**M_w ($gmol^{-1}$)**	**Đ**
DP_n10 branched plus DP_n90 linear	27,800	19,800	63,400	3.20
DP_n 90 linear plus DP_n10 branched	8,300	13,100	45,600	3.48
DP_n 10 linear plus DP_n90 branched	1,100	20,400	79,900	3.92
DP_n 90 branched plus DP_n 10 linear	41,700	15,400	46,200	3.00
DP_n100 branched	N/A	13,400	43,400	3.24
DP_n 90 branched	N/A	13,100	41,700	3.18
DP_n 90 linear	N/A	7,800	8,300	1.06

As can clearly be seen from the peaks within the GPC chromatograms at high retention volumes, attributed to the linear fraction of the polymer distributions, the linear polymer chains from the first addition are living, and the addition of further monomer results in the further propagation of these linear chains in addition to the growth of branched polymer chains.

In Figure 6 (D) there is a very significant shift from the DP_n10 linear before the addition of DP_n90 styrene units with brancher, and the final product. As can be seen in Figure 6 (E) the DP_n10 branched plus DP_n90 linear when overlaid with a DP_n10 linear plus DP_n90 linear, the linear peak clearly corresponds to a DP_n 100 linear polymer, rather than either a DP_n10 linear, or a DP_n90 linear, illustrating that the all the linear polymer chains have been chain extended as well as the branched polymer chains.

Wheras the previous block polymers were synthesised with starting DPn values of 10 monomer units or 90 monomer units, the same sythesis experiments were repeated but with DP_n50 as the starting targeted primary chain length for the synthesis to compare the effect on the architecture of the polymers produced.

- DP_n50 branched plus DP_n50 linear
- DP_n50 linear plus DP_n50 branched

The GPC analysis for the polymers synthesised by this DP_n50 monomer units plus a further DP_n50 monomer units are shown in Figure 5.7, and the M_n and M_w values are given in Table 5.4.

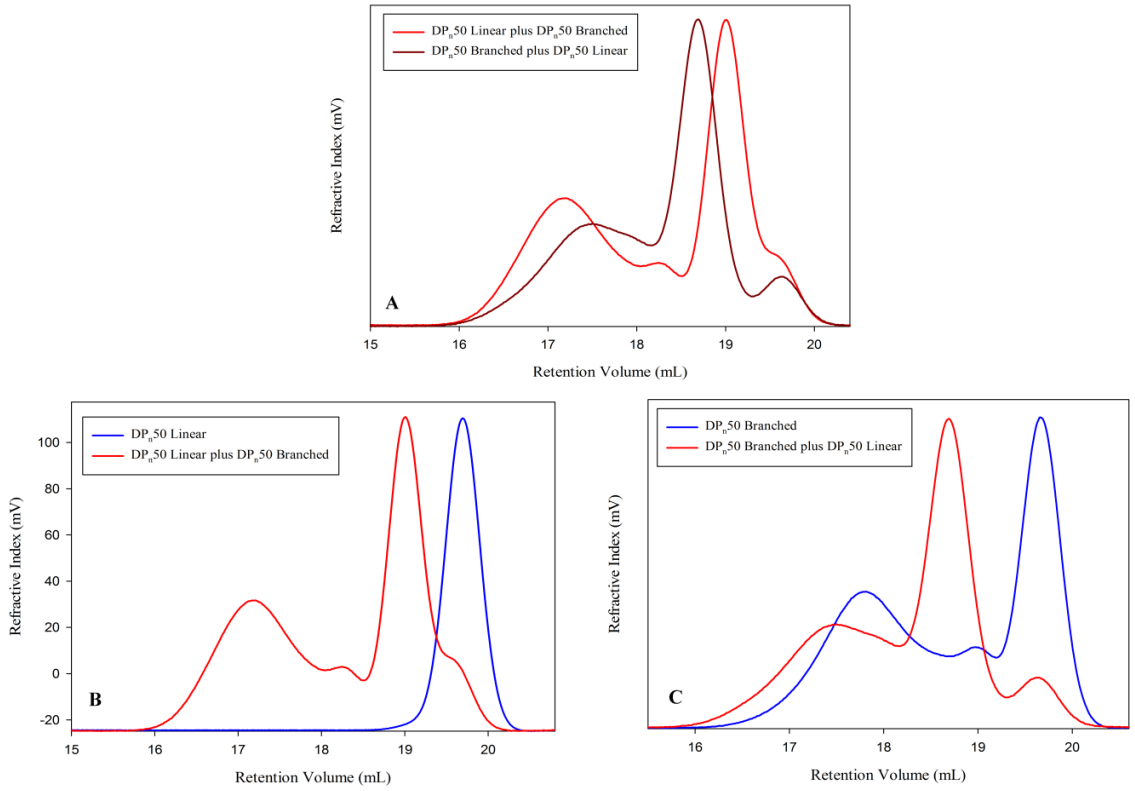

Figure 5.7: GPC chromatograms of (A) DP_n50 linear (lin) plus DP_n50 branched (br) overlaid with DP_n50 br plus DP_n50 lin (B) DPn50 lin overlaid with DP_n50 lin plus DP_n50 br (C) DP_n50 br overlaid with DP_n50 br plus DP_n50 lin.

As can be seen from the RI GCP chromatograms in Figure 5.6 (B) and (C) the linear DP_n50 chains propagate further to become DP_n100 linear. It can be seen that branching first can lead to some termination of the DP_n50 chains, illustrated in the small shoulder seen on Figure 5.6 (B) between 19 and 20 mL of the retention volume, that overlays with a DP_n50 linear polystyrene.

Table 5.3 gives the M_n, M_w and Đ values for these block polymers, with the M_w of the precursor sample, taken before the second batch of monomer was added.

Table 5.3: M_n, M_w and Đ values for branched polystyrene with different target architecture and the M_w values of the pre-cursor polymer before the second addition of monomer or monomer and brancher.

Polymer Architecture	**GPC**			
	M_w of precursor ($gmol^{-1}$)	**M_n ($gmol^{-1}$)**	**M_w ($gmol^{-1}$)**	**Đ**
DP_n50 linear plus DP_n50 branched	5,100	14,600	50,800	3.48
DP_n50 branched plus DP_n50 linear	29,800	16,000	42,700	2.67
DP_n100 branched	N/A	13,400	43,400	3.24
DP_n50 linear	N/A	4,800	5,100	1.06
DP_n50 branched	N/A	8,400	29,800	3.55

As can be seen from the results it appears that there is no significant impact on the M_n and M_w values if we compare the DP_n50 linear plus DP_n50 branched and the DP_n50 branched plus DP_n50 linear. However for the DP_n10 plus DP_n90 polymers there seems to be a definite increase in M_w values when DP_n10 is synthesised first, as seen in Table 5.3. The effect of synthesising the DP_n10 first shall be explored further in the following section.

5.2.2 Self-blocked branched polystyrene co-polymers; all architectures with a primarychain length of DP_n = 50 monomer units

As described in section 5.2, self-blocked, branched co-polymers were synthesised via a 'linear-first' or a 'branched-first' approach. Varying polymer architectures with a primary chain length of 100 monomer units were synthesised in section 5.2.1 and an analogous series was generated with an overall primary chain length of 50 monomer units. The resulting polymers were purified and analysed by GPC and the results are shown in Figure 5.8 and Table 5.5.

- DP_n10 branched plus DP_n40 linear
- DP_n40 linear plus DP_n10 branched
- DP_n40 branched plus DP_n10 linear
- DP_n10 linear plus DP_n40 branched

Table 5.4: M_n, M_w and Đ values for branched polystyrene with different target architecture and the M_w values of the pre-cursor polymer before the second addition of monomer or monomer and brancher.

Polymer Architecture	GPC			
	M_w of precursor ($gmol^{-1}$)	**M_n ($gmol^{-1}$)**	**M_w ($gmol^{-1}$)**	**Đ**
DP_n10 branched plus DP_n40 linear	36,600	9,400	35,400	3.77
DP_n40 linear plus DP_n10 branched	3,900	6,300	21,900	3.48
DP_n10 linear plus DP_n40 branched	1,100	9,000	26,600	2.96
DP_n40 branched plus DP_n10 linear	23,200	7,400	24,400	3.30
DP_n50 branched	N/A	8,400	29,800	3.55
DP_n40 branched	N/A	6,400	23,200	3.63
DP_n40 linear	N/A	3,700	3,900	1.05

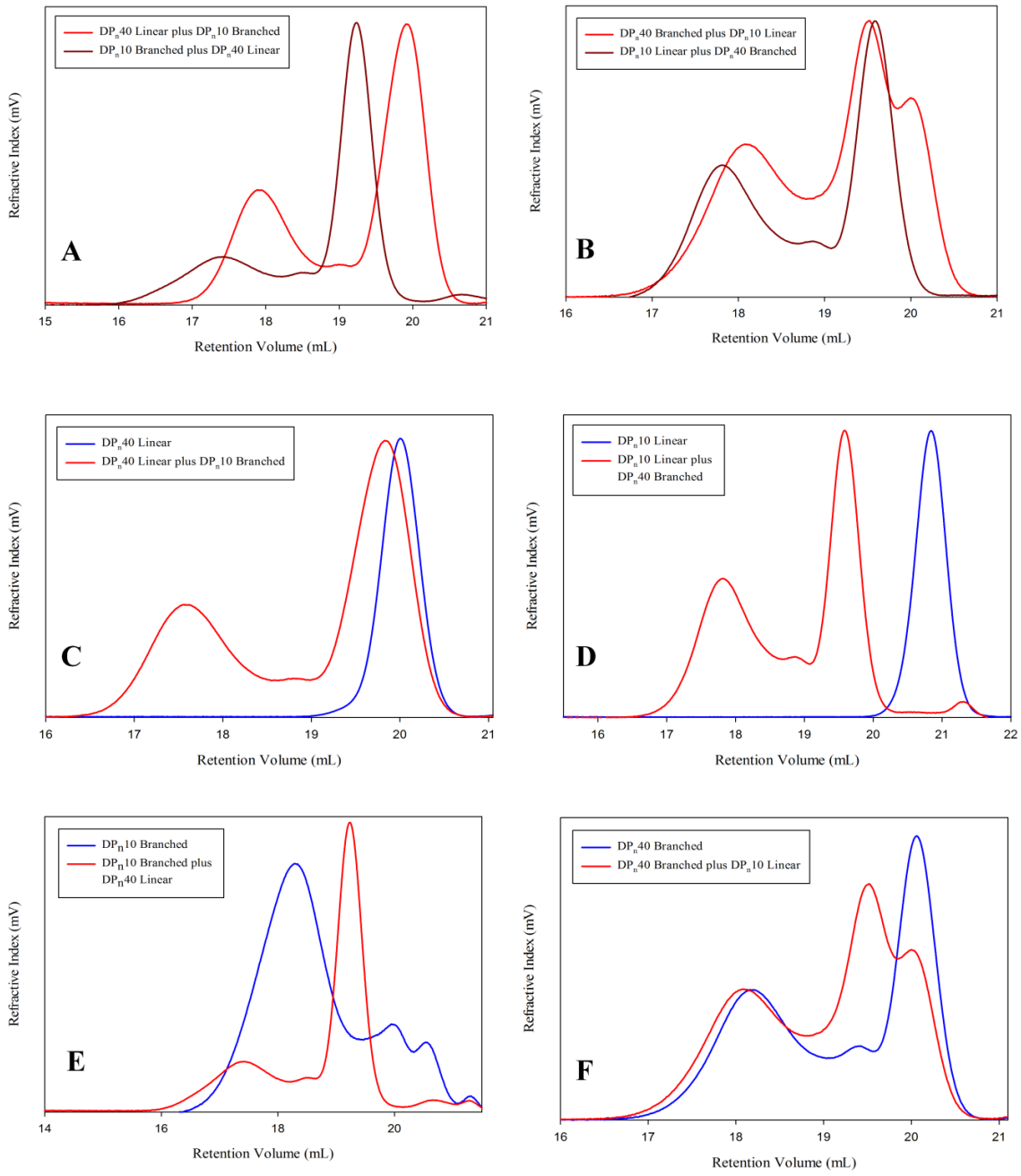

Figure 5.8: GPC chromatograms of (A) DP_n40 linear (lin) plus DP_n10 branched (br) overlaid with DP_n10 br plus DP_n40 lin (B) DP_n40 br plus DP_n10 lin overlaid with DP_n10 lin plus DP_n40 br (C) DP_n40 lin overlaid with DP_n40 lin plus DP_n10 br (D) DP_n10 lin overlaid with DP_n10 lin plus DP_n40 br (E) DP_n10 br overlaid with DP_n10 br plus DPn40 lin (F) DP_n40 br overlaid with DP_n40 br plus DP_n10 lin.

As can be seen from the chromatograms in Figures 5.8 (C) and (D) the branched co-polymers form in the same way as the DP_n =100 monomer units; the branched polystyrenes and the linear polystyrenes grow to be DP_n =50 monomer units. However

as seen from the overlays they only grow to the correct targeted length, indicating that there is growth from the branched chain ends as well, otherwise the DP_n of the linear components would be greater than the expected DP_n = 50 monomer units. Table 5.5 gives the M_w values of both the samples prior to the second batch of monomer addition and post addition, after purification of the resulting polymer. M_n and Đ values for the polystyrene are also given.

Also seen from the chromatograms in Figure 5.8, the branched co-polymers appear to display the same trends as the branched polymers with a primary chain length of DP_n = 100 monomer units. If we take the M_w values shown in Table 5.5 we can see that again it appears that starting with the DP_n10 branched polymer has the effect of increasing the final M_w value after the second addition of monomer. If we consider a cartoon of the conceptual structure of these polymers, Figure 9, the differences of the proposed architectures become clearer. All pictures show a structure of a model branched polymer (not based on values from synthesised polymers) with approximate molecular weights of 70,000 $gmol^{-1}$, for illustration purposes.

If we first consider the polymers that are equivalent to the DP_n100 branched polymers we can see the differences and certainly the similarities between them. For the DP_n90 branched plus DP_n10 linear, and the DP_n10 linear plus DP_n90 branched shown in Figure 5.9(B), the expected structures would be extremely similar to the DP_n100 branched, shown in Figure 5.9 (C). There is a slight difference between the DP_n50 branched plus DP_n50 linear (or DP_n50 linear plus DP_n50 branched), shown in Figure 5.9 (D), and the DP_n100 branched as the restriction of the branching to half of the primary chains starts to impact on the packing of the chains. This is not as significant as the extreme structural differences that can be seen for the DP_n10 branched

plus DP_n90 linear (or, again DP_n90 linear plus DP_n10 branched), shown in Figure 5.9 (A).

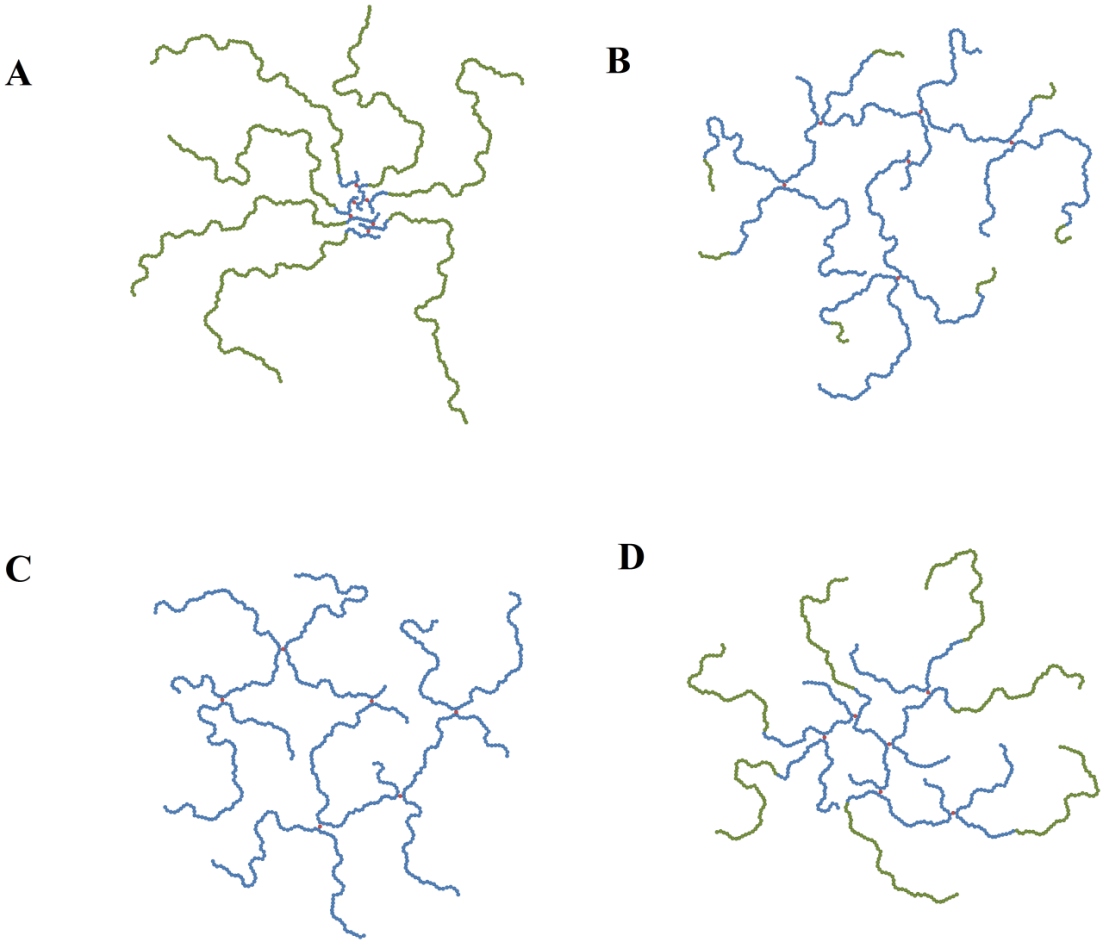

Figure 5.9: Cartoon representation of; (A) DP_n10 branched plus DP_n90 linear or DP_n90 linear plus DP_n10 branched, (B) DP_n90 branched plus DP_n10 linear or DP_n10 linear plus DP_n90 branched, (C) DP_n100 branched and (D) DP_n50 branched plus DP_n50 linear or DP_n50 linear plus DP_n50 branched

The same difference can be seen in the DP_n50 branched polymers; clearly the polymers with a DP_n10 branched core are structurally very different to their primary chain length equivalents. This cartoon representation is shown in Figure 5.10 (A), along with the DP_n40 branched plus DP_n10 linear, and the DP_n10 linear plus DP_n40 branched shown in Figure 10 (B), and the DP_n50 branched is also shown for comparison in Figure 5.10 (C).

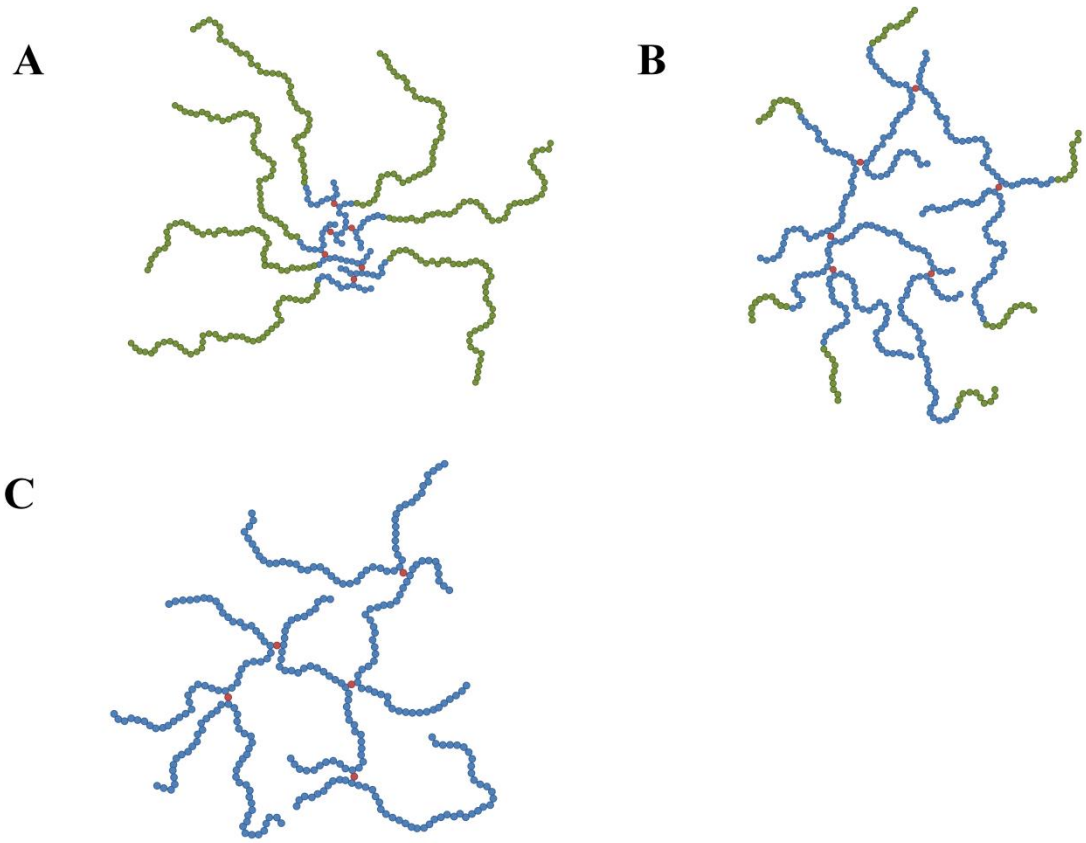

Figure 10: Cartoon representation of; (A) DP_n10 branched plus DP_n40 linear or DP_n40 linear plus DP_n10 branched, (B) DP_n40 branched plus DP_n10 linear or DP_n10 linear plus DP_n40 branched and (C) DP_n50 branched

As seen from the GPC results, and the cartoon representations the polymers synthesised with a DP_n10 branched are structurally very different to the other materials synthesised with modified architectures. The effect of this difference in structural architecture shall be studied further in the following Chapter where the physical properties of these synthesised polymers are analysed by differential scanning calorimetry and differential viscometry.

5.3 Conclusions

The architecture of branched polymers has been successfully manipulated by controlling the primary chain length of the polymer. It was found that the lower the primary chain length, the greater the degree of branching. This offers further control over the architecture of the branched polymers.

A series of self-blocked, branched co-polymers have been synthesised by anionic polymerisation techniques. The primary chain length of the polymer synthesised first as well as the primary chain length of the second batch of monomer has been controlled and the differences between these polymers compared to their total chain length equivalents.

It has been found that branched polystyrenes synthesised with a DP_n10 (DP_n10 branched plus DP_n90 linear and DP_n10 branched plus DP_n40 linear) core have higher M_w values than their equivalents (DP_n100 branched and DP_n50 branched respectively), suggesting both differences in their synthetic mechanism and the resulting architectures.

Chapter 6

Physical Properties of Branched Polymers

6.0 Introduction

The analysis of the polymers synthesised within this study has focused on the identification of the success of branching, and the number average molecular weight and weight average molecular weight of the resulting polymers. In the following chapter the physical properties of the branched and linear polymers will be studied and the differences between them and a series of differently synthesised architectures of the branched polymers will be explored.

6.1 Analysis of polystyrene chain branching by triple detection GPC

Linear polymer chains of identical chemistry but increasing chain length will follow a linear relationship of molecular weight (plotted on a logarithmic scale) *vs.* elution volume. [1] This relationship has been used for many years to provide calibration curves for single detection GPC (using RI detectors) using a series of known polymer standards. [2] By plotting the molecular weight distributions (logarithmic scale) of the various branched polystyrenes with increasing targeted primary chain length samples (these being DP_n10 branched, DP_n25 branched, DP_n50 branched, DP_n100 branched, DP_n250 branched and DP_n500 branched) *vs.* elution volume, the similarity or differences of the solvated polymer chains from different samples could be evaluated. The various linear relationships for each branched polymer sample can be seen in Figure 6.1.

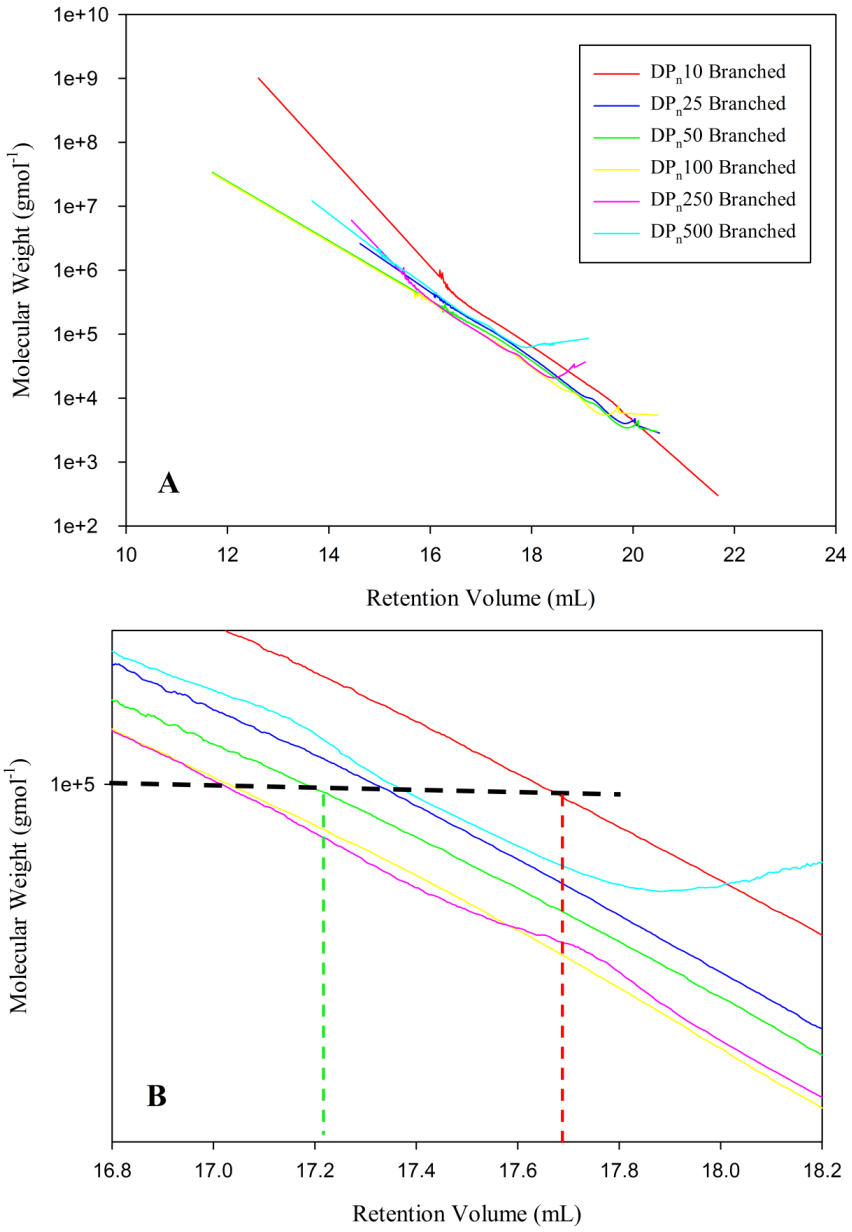

Figure 6.1: Graph of M_w (on a logarithmic scale) against retention volume for branched polystyrenes synthesised by anionic polymerisation techniques; DP_n10 branched (red), DP_n25 branched (dark blue), DP_n50 branched (green), DP_n100 branched (yellow), DP_n250 branched (pink), DP_n10 branched (light blue).

The graph in Figure 6.1 (A) is the total data from the detector, however, the molecular weights within each polymer distribution does not span the entire accessible range of molecular weights for the columns. The strong deviations that can be seen at the extremities of most of the curves are due to very low concentrations and insufficient data to allow accurate detection. Similarly, very straight lines are seen at the ends of the

curves, resulting from software extrapolation, rather than true data. For these reasons, Figure 6.1 (B) highlights the elution volumes between 16.8 mL and 18.2 mL, where good data is seen for all polymers studied.

As the targeted primary chain length of the branched polystyrenes increases, the slope of the individual relationships appears to be generally identical, Figure 6.1 (A), however, a clear downward shift in each relationship was observed. This provides an insight into the relative size of the branched polymers in the THF solution. Highlighted on Figure 6.1 (B) is an arbitrarily selected molecular weight of 100,000 $gmol^{-1}$ (black dashed line). Macromolecules with this molecular weight elute at a retention volume of approximately 17.2 mL if the targeted primary chain length of the branched polystyrene has a DP_n = 50 monomer units (green dashed line). Polymers with an identical molecular weight but synthesised by branching a targeted primary chain of DP_n = 10 monomer units, elute with at a retention volume of approximately 17.7 mL (red dashed line). The order of retention volumes for the varying targeted primary chain lengths at this arbitrary molecular weight follows the general order of the targeted primary chain lengths apart from branched polymers comprising the longest targeted chain length (DP_n = 500 monomer units). This relationship is more clearly observed when plotting the retention volume for polymers of 100,000 $gmol^{-1}$ against the targeted DP_n of the individual branched polymers, Figure 6.1(B).

The retention (or elution) volume is a direct indication of the size of the polymers in solution. The data clearly indicate a variation in the size of the solvated chains and, therefore, the variation of the density of branching as different primary chain lengths are targeted.

When targeting a primary chain length of DP_n = 10 monomer units, a highly branched and dense polymeric structure is clearly produced and the density of the polymer chains across the molecular weight distribution clearly decreases with increasing chain length. To put this into context, at the arbitrary molecular weight of 100,000 $gmol^{-1}$, the number of chains that are connected through interchain branching varies considerably. The branched polystyrene with primary chains of only 1000 $gmol^{-1}$ have 100 chains that are connected at the molecular weight, whereas the macromolecules produced from primary chains of 5000 $gmol^{-1}$ (primary chain DP_n = 50 monomer units) have 20 chains. At a primary chain length of 500 monomer units, only 2 chains are joined together. The variation of the number of chains incorporated in each polymer of 100,000 $gmol^{-1}$ is also shown in Figure 2 and follows a very similar trend to the observed decrease in retention volume. This analysis is only fully achievable through the knowledge that the anionic polymerisation generates highly monodisperse polymers.

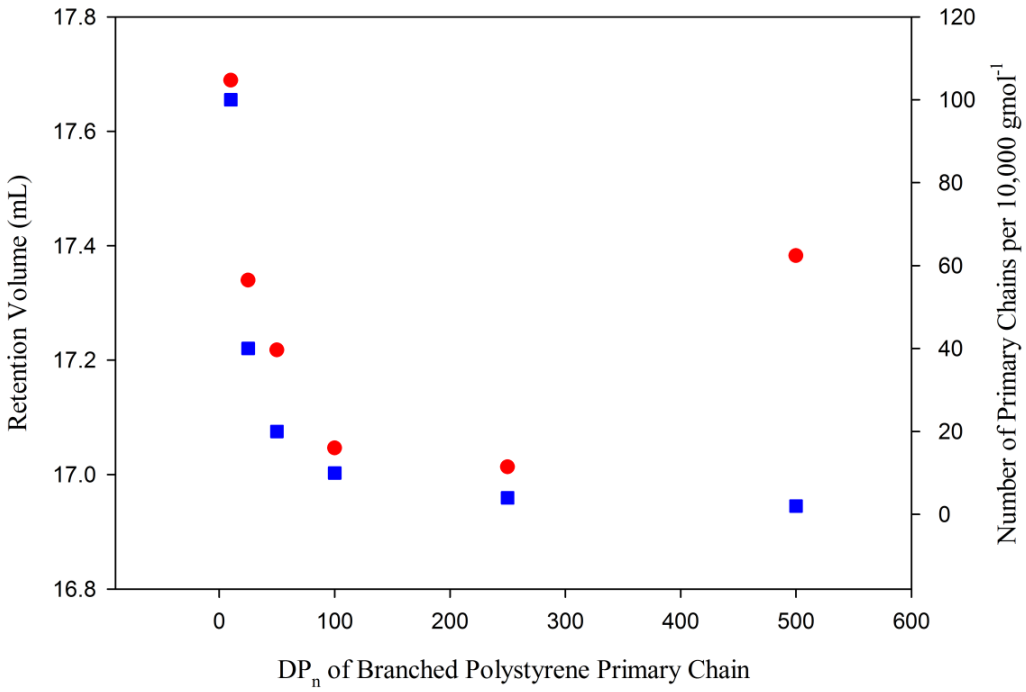

Figure 6.2: Graph illustrating the relationship between the retention volume against the targeted DP_n of the primary chain of branched polystyrenes (red circles) and the number of chains that would make up a polystyrene of molecular weight 10,000 $gmol^{-1}$ against the targeted DP_n of the primary chain of branched polystyrenes (blue squares).

Another comparison of the branched polymers that can be achieved is to study the materials that have the same total linear primary chain length but have been synthesised by different self-blocking polymerisations, as described in Chapter 5. An example of this is the range of materials that have a primary chain length of DP_n = 100 monomer units. As discussed earlier the following comparative polymers have been synthesised; DPn100 branched, DP_n10 branched plus DP_n90 linear, DP_n90 branched plus DP_n10 linear, DP_n10 linear plus DP_n90 branched, DP_n90 linear plus DP_n10 branched, DP_n50 branched plus DP_n50 linear and DP_n50 linear plus DP_n50 branched. Graphs of the molecular weight (plotted on a logarithmic scale) against retention volume for all of these polymers show the individual relationships for these materials. Figure 6.3 (A) shows the total data from the detectors, as previously, and Figure 6.3 (B) highlights the areas of the data where comparisons can be made with confidence.

As can be seen from the results, at the same molecular weight of 100,000 $gmol^{-1}$ all polymers elute at a similar time. There are two anomalous results DP_n90 branched plus DP_n10 linear and DP_n90 linear plus DP_n10 branched which appear to elute at a later time, therefore indicating a difference in their size and behaviour in solution. One possible explanation for this is that experimentally they were analysed at a separate time, after all others. It is possible that the difference falls within the error of the GPC detector, and this apparent difference can be discounted.

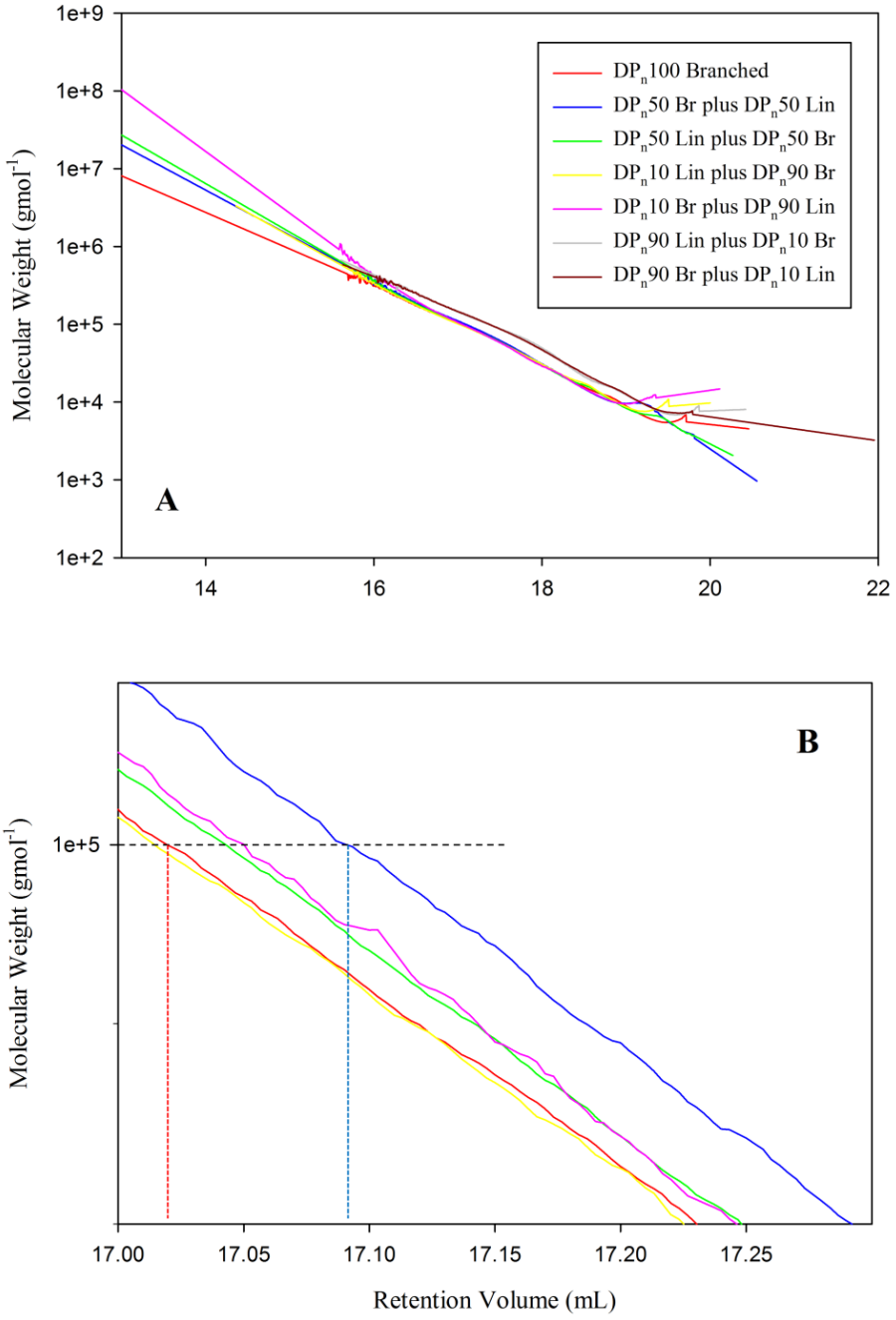

Figure 6.3: Graph of M_w (on a logarithmic scale) against retention volume for self- blocking branched polystyrenes synthesised by anionic polymerisation techniques; DP_n100 branched (red), DP_n50 branched plus DP_n50 linear (dark blue), DP_n50 linear plus DP_n50 branched (green), DP_n10 linear plus DP_n90 branched (yellow), DP_n10 branched plus DP_n90 linear (pink), DP_n90 linear plus DP_n10 branched (grey) and DP_n90 branched plus DP_n10 linear (brown).

An additional analysis technique that is available to determine in greater detail how different the structure of polymer molecules are is to compare polymers with relatively similar molecular weights, but very different dispersity values and different targeted

architectures. Examples of this is a comparison that can be made between a polystyrene branched with VPOB with a primary chain length of DP_n = 10 monomer units and an M_w of 48,900 $gmol^{-1}$ and value of 7.64, a branched polystyrene with a primary chain length of DP_n = 100 monomer units branched with a 0.99:1 VPOOC:*sec*-BuLi ratio, M_w = 53,900 $gmol^{-1}$, dispersity value; 5.50, a branched polystyrene with a primary chain length of DP_n = 50 monomer unitsbranched with a 1:1 DVB: sec-BuLi ratio, Mw = 47,400 $gmol^{-1}$, dispersity value; 5.77 and a mixed architecture polymer comprising a branched polystyrene core with a primary chain length DP_n = 10 monomer units, branched with VPOB at a 1:1 VPOB:*sec*-BuLi ratio with a subsequent linear polystyrene of DP_n = 90 monomer units synthesised from this core, Mw = 45,600$gmol^{-1}$ and dispersity; 3.48. Each of these polystyrenes have M_w values that lie within 9,000 $gmol^{-1}$.

Figure 6.4 (A) shows an overlay of the RI chromatogram of the branched polystyrene with a primary chain length of DP_n = 100 monomer units (branched with VPOOC at an initiator to brancher ratio of 1:0.99). As described previously, the data shown within the overlaid molecular weight vs retention volume curves that occurs after a retention volume of 19 mL is assumed to be derived from linear polymer chains and the data before 16.5 mL is extrapolation by the software.

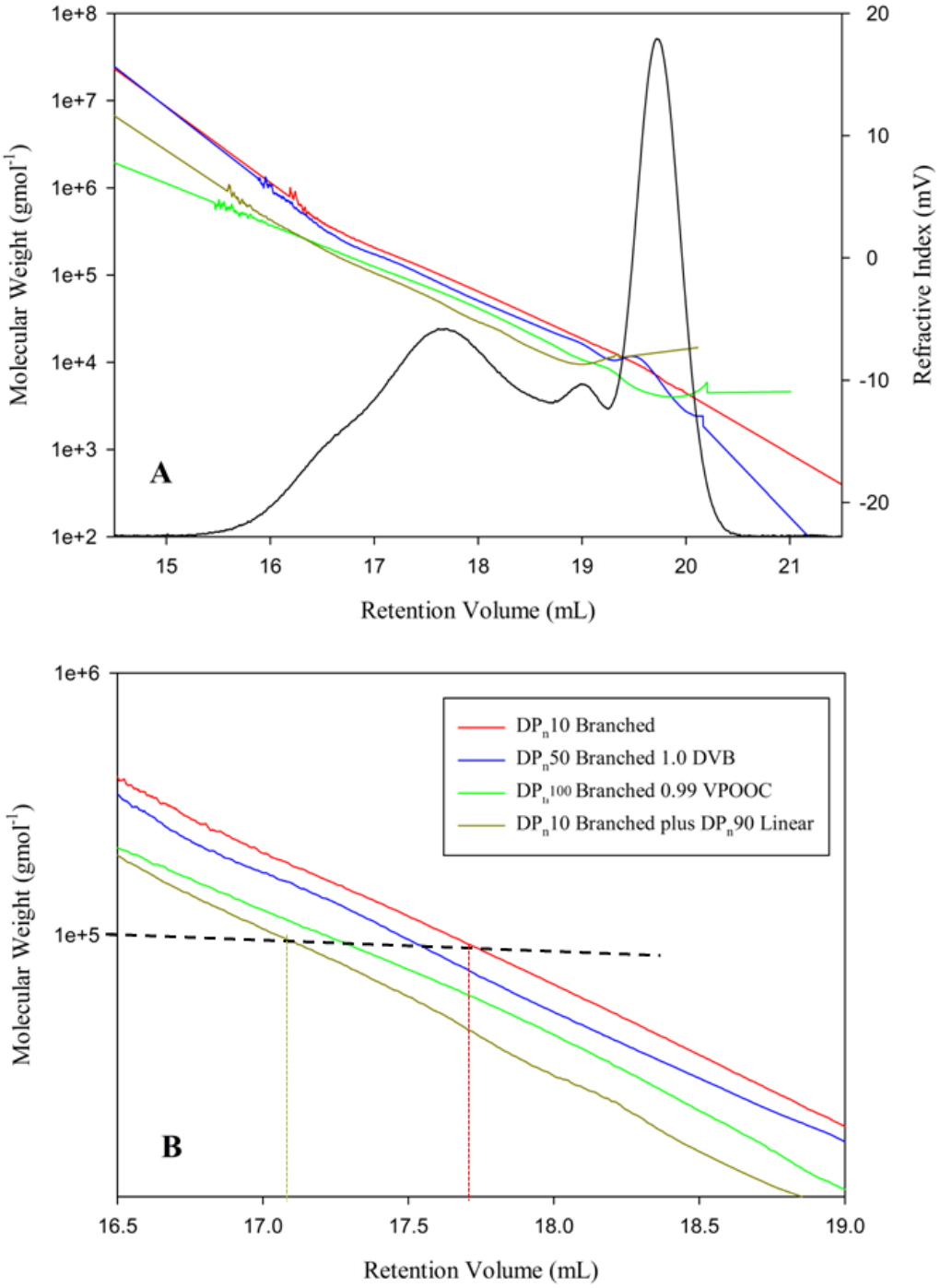

Figure 6.4: Graph of M_w (on a logarithmic scale) against retention volume for branched polystyrenes synthesised by anionic polymerisation techniques with M_w values of approximately 50,000 $gmol^{-1}$. DP_n10 branched, 1:1 VPOB:*sec*-BuLi (red), DP_n50 branched 1:1 DVB:*sec*-BuLi (blue), DP_n100 branched, 0.99:1 VPOOC:*sec*-BuLi (light green) and DP_n10 branched (1:1 VPOB:*sec*-BuLi) plus DP_n90 linear (dark green)

Figure 6.4 (B) is an expansion of the data between the retention volumes of 16.5 and 19 mL. As can be seen from the graph although the polymers have a similar weight

average molecular weight, at any molecular weight illustrated by the dotted line from 10,000 $gmol^{-1}$there is a clear difference between the density of the material comprising the branched polymer architectures with the branched polymer composed of primary chains with a target DP_n = 10 monomer units being the most densely branched materials. Interestingly, the formation of the linear chains from this polymer leads to a much lower density of material with polymers of identical molecular weight eluting at significantly lower retention volumes.

6.2 Differential viscometry measurement using triple detection GPC

All viscometry measurements were conducted using the triple detection GPC apparatus. Figure 6.5 is a schematic of the differential viscometer detector within the triple detector GPC that was used.

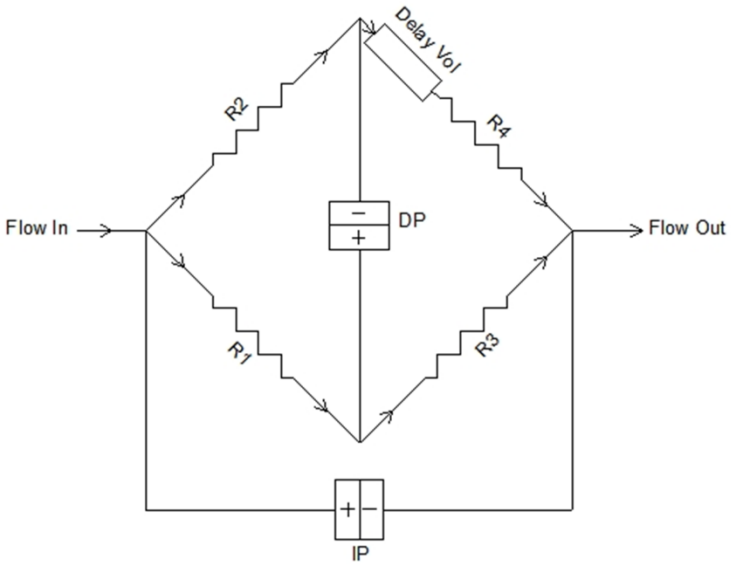

Figure 6.5: Schematic diagram of a differential viscometer GPC detector

Four capillary tubes R1 to R4, shown in Figure 6.5 are arranged in a balanced bridge configuration and differential pressure transducers measure the pressure difference (DP) across the midpoint of the bridge and the pressure difference (IP) from inlet to outlet. A delay volume is inserted in the circuit before capillary R4, in order to provide a reference flow of solvent through R4 during elution of the polymer sample. DP will respond to the viscosity of the sample as it elutes from the GPC.

As the flow into the capillary tubes and the flow out must be equal, the difference in flow of the polymer solution between the upper circuit and the lower circuits is detected. A polymer solution will have a measureable viscosity and the splitting of the flow of a viscous solution through the R1+R3 route and the R2+R4 route leads to a difference in the measured pressure as the inserted delay volume allows for a delay in the increase in pressure in the R2+R4 circuit. As the polymer sample that has been fractionated within the GPC columns passes into the viscometer, the pressure differences vary depending on the concentration and the molecular weight of the dissolved polymers. By overlaying this pressure difference onto the elution measurements from the refractive index and light scattering detectors it is possible to directly relate the viscous behaviour of the fractions of the polymer molecular weight distributions to the scattering and concentration detections from the other detectors and determine an accurate molecular weight of each sub-section of the polymer distribution.

The density of the polymer architectures are also defined in the Mark-Houwink plot in Figure 6.6 of intrinsic viscosity (log IV) vs. molecular weight (plotted on a log scale) for a range of branched polystyrenes including the branched polymer with a primary chain length of VPOB with a primary chain length of DP_n = 10 monomer units and an

M_w of 48,900 $gmol^{-1}$ (shown in red on Figure 6.6), a branched polystyrene with a primary chain length of DP_n = 50 monomer units branched with a 1:1 DVB: sec-BuLi ratio, M_w = 47,400 $gmol^{-1}$, and a mixed architecture polymer comprising a branched polystyrene core with a primary chain length DP_n = 10 monomer units, branched with VPOB at a 1:1 VPOB:*sec*-BuLi ratio with a subsequent linear polystyrene of DP_n = 90 monomer units synthesised from this core, M_w = 45,600$gmol^{-1}$.

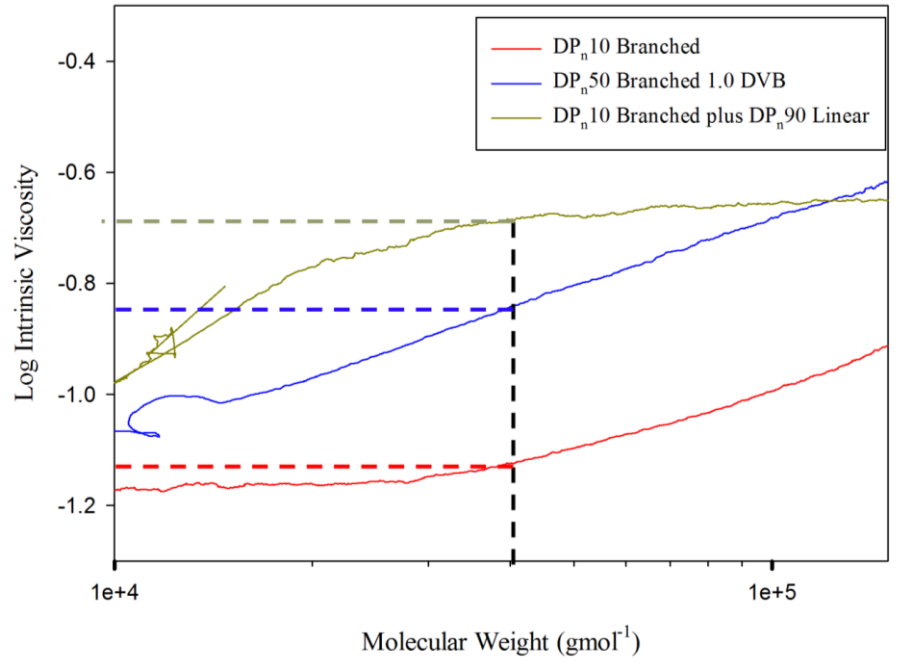

Figure 6.6: Graph of the log of the intrinsic viscosity against the molecular weight of branched polymers with different branched architectures synthesised by anionic polymerisation techniques.

For the same molecular weight the intrinsic viscosity changes as the density of the polymers increases. The branched polymer with a primary chain length of 10 monomer units is clearly more dense than the same architecture derived from primary chains of DP_n = 50 monomer units, and has a considerably lower intrinsic viscosity value. The addition of linear polymer chains to the highly dense core significantly increases the intrinsic viscosity above the value of the branched polymer with a primary chain length

of 50 monomer units. It is clear to see from these graphs that changing the architectiure of the branched polymers has a big effect on the density and size in solution of the polymers.

6.3. Glass transition temperature (T_g)

6.3.1 T_g of linear polystyrenes

In a recent report, Hitachi [4] studied the glass transition temperature *vs.* molecular weight relationship of polystrene using differential scanning calorimetry (DSC). The results of this application based study are shown below. They reported three separate values for the T_g, to include the onset temperature, mid-point temperature and the end temperature, given in Table 6.1.

Table 6.1: Literature values from a Hitachi investigation into the T_g versus M_w relationship of polystyrenes [4]

M_w of polystyrene ($gmol^{-1}$)	**T_g (^oC)**		
	Onset temperature	**Mid-point temperature**	**End temperature**
1,940	56.8	60.4	64.2
4,380	76.2	79.9	83.7
5,480	77.0	82.4	87.8
12,600	89.6	93.4	96.7
35,100	100.2	103.1	105.9
65,000	100.6	104.0	107.3
275,000	103.5	106.4	109.4
950,000	103.9	106.7	109.7

The Hitachi DSC analysis was repeated with the series of linear polystyrenes synthesised as described in Chapter 3. Experimentally, in the Hitachi work the temperature was raised at a rate of 10ºC a minute from room temperature to 160 ºC. A similar method was adopted within this study, but the temperature was increased at a rate of 10 ºC a minute to 250 ºC, cooled at a rate of 10 ºC a minute to 25 ºC and then heated at the same rate to 250 ºC. The heat-cool-heat cycle allows for all thermal history to be erased. Although all polymers were synthesised at temperature, the temperature during the reaction and the subsequent work up was not controlled. The results are shown in Figure 6.7a 6.7b.

The data shows a definite increase in the glass transition temperature as the molecular weight increases. Table 6.2 gives the T_g values for the onset, mid-point and end temperatures at increasing molecular weight

Table 6.2: Onset, mid-point and end T_g temperatures for polystyrenes of increasing M_w values. Analysis condtions: heated from a resting temperature of 25 ºC to 250 ºC, 1 minute isotherm, cooled to 25 ºC, 1 minute isotherm and heated again to 250 ºC. All cooling/ heating is at a rate of 10 ºC per minute

M_w of polystyrene ($gmol^{-1}$)	**T_g (^oC)**		
	Onset temperature	**Mid-point temperature**	**End temperature**
940	33	33	36
25,00	60	63	65
5,000	84	87	87
1,100	94	99	99
52,700	103	106	106

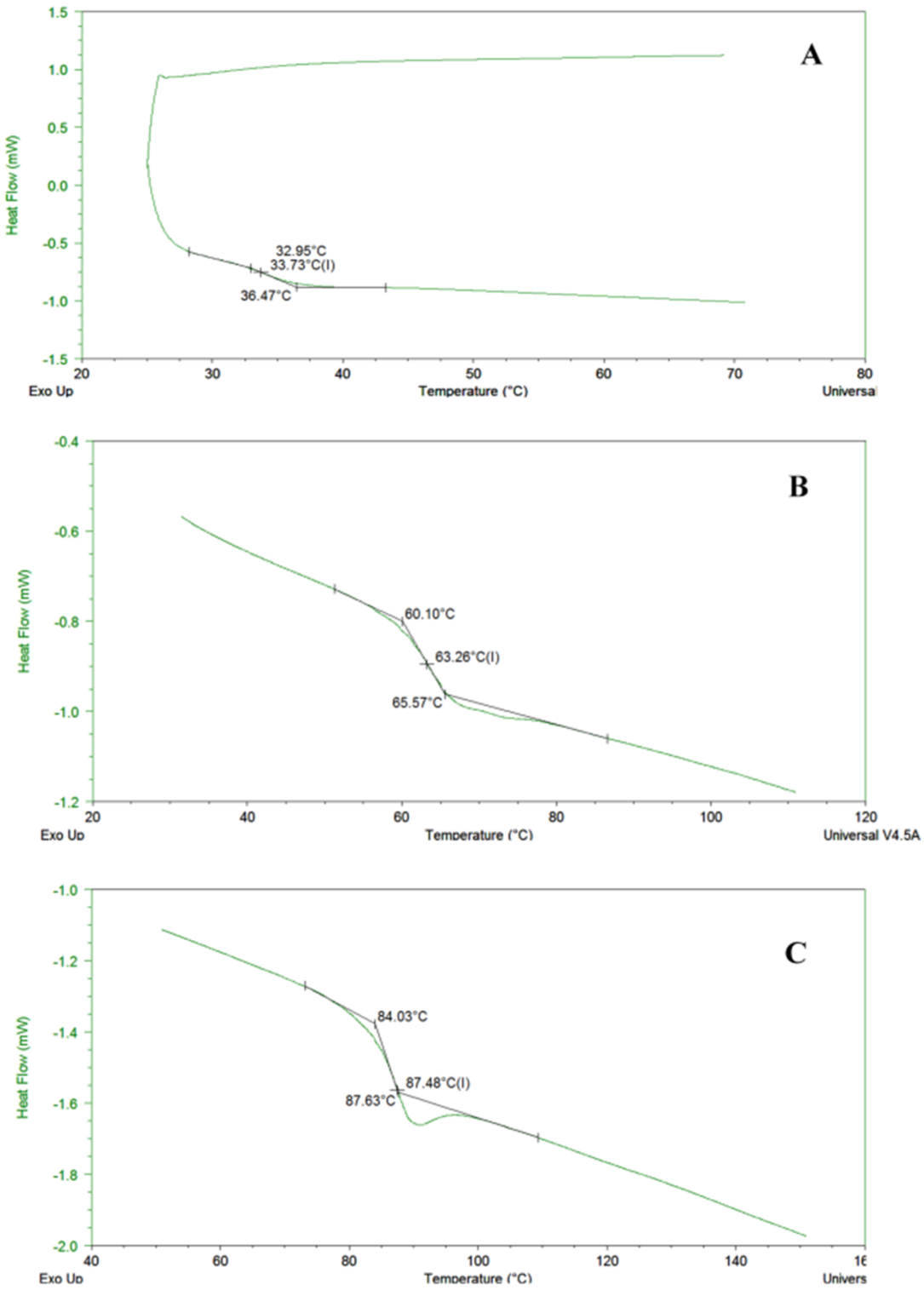

Figure 6.7a: Thermographs of DSC analysis of (A) DP_n10 linear, (B) DP_n25 linear, (C) DP_n50 linear.

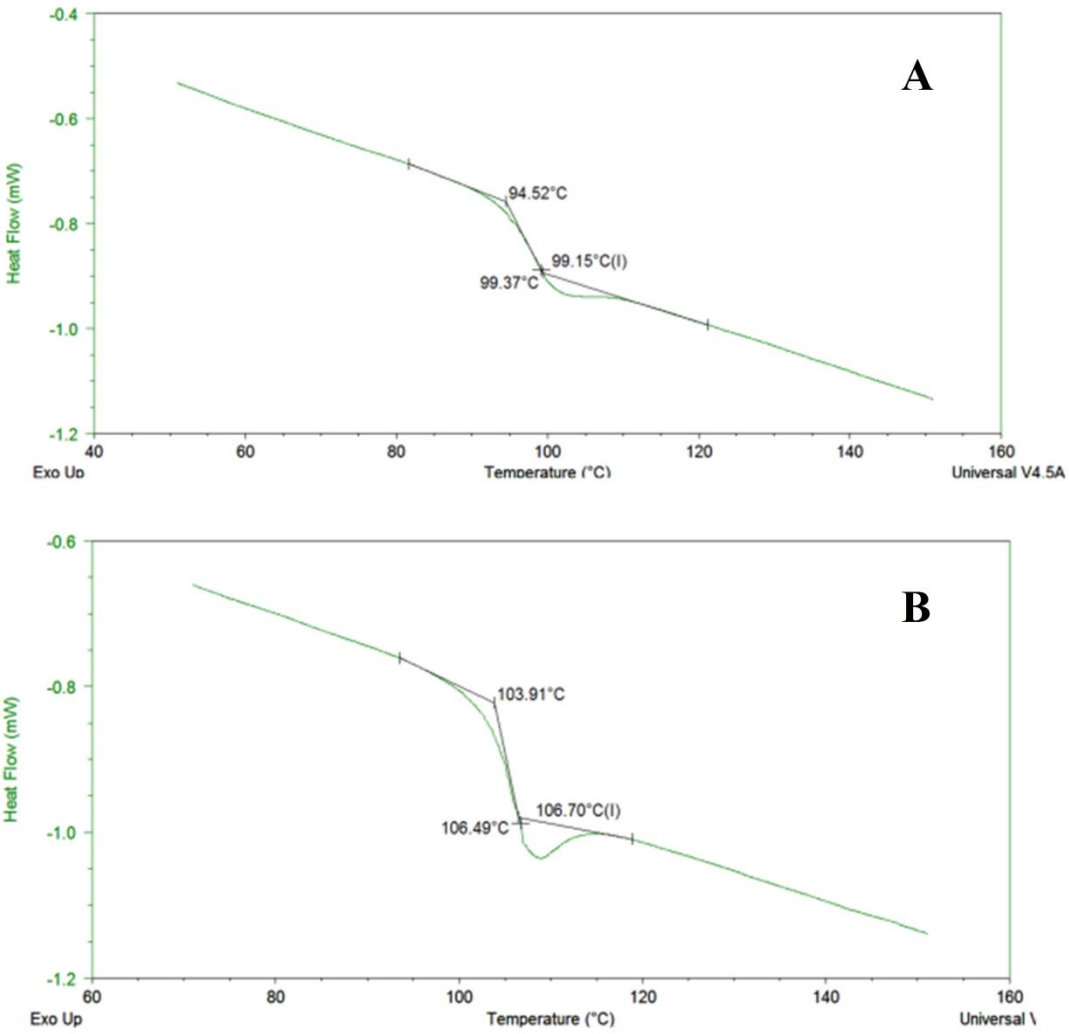

Figure 6.7b: Thermographs of DSC analysis of (A) DP_n100 linear and (B) DP_n500 linear polystyrenes.

All linear polystyrenes should have the same T_g versus molecular weight relationship, irrespective of the technique of synthesis. As we have seen in Chapter 3 the materials synthesised by anionic polymerisation are very monodisperse, with dispersity values as low as 1.02. This means that for the linear polystyrenes of this study the M_n and M_w are approximately the same values. This is not the case however for the branched polystyrenes; the M_n and M_w values are very different. As the branched polystyrenes comprise larger molecular weight materials containing varying numbers of monodisperse primary chains and a fraction of the molecular weight distribution that

relates to the unbranched linear primary chains, the actual values that properly describe the success of branching within each sample are the weight average molecular weights and so it is M_w that shall be considered within the discussion of the variation of T_g within this study. The Hitachi report and other reports [5] have determined the T_g versus M_w relationship and therefore the use of M_w rather than M_n within the branched polystyrenes is expected to show trends related to the higher molecular weight and, therefore, the branched nature of the polymers. To explore this relationship, the M_w values for the linear polymers synthesised within this study (appearing on the graph as open circles) are plotted with the M_w values for the literature Hitachi polymers (appearing on the graph as closed circles) against the T_g (mid-point temperature) data for both sets of polymers in Figure 6.8.

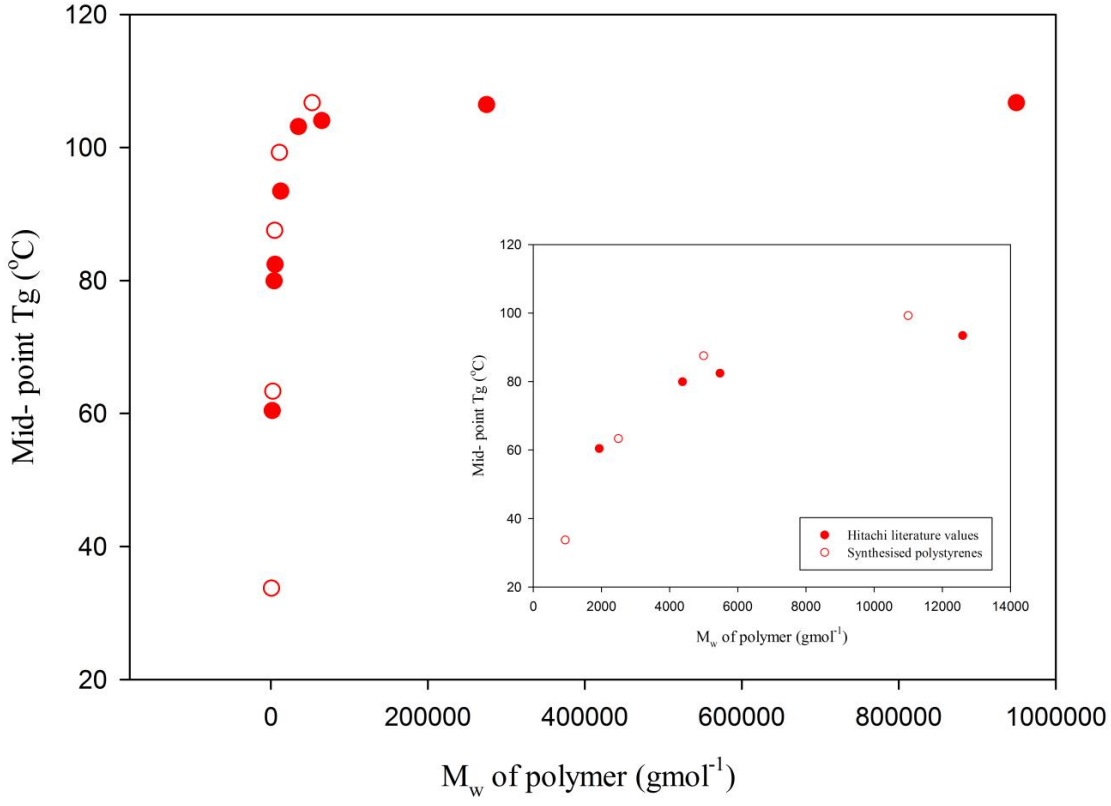

Figure 6.8: Graph showing the relationship between the M_w values of the Hitachi polystyrene (filled red circles) and synthesised polystyrenes (open red circles) and mid-point T_g values.

As can be seen from the graph in Figure 6.8 there is the same trend and same behaviour with increasing T_g directly correlated to molecular weight and reaching a plateau at a critical molecular weight value, which is normal for linear homopolymers. The smaller inset graph illustrates more clearly how similar the behaviour is at lower M_w values (< 14,000 $gmol^{-1}$).

6.3.2. T_g of branched polystyrenes

As was observed in earlier work, the degree of branching increased with a decreasing target primary chain length for the branched polystyrenes synthesised with VPOB. Therefore, to study how a more highly branched structure may have different thermal properties, the earlier DSC experiments were repeated with a series of branched polystyrene samples with varying target primary chain lengths as discussed in section 5.1 of Chapter 5. The data is tabulated in Table 6.3.

Table 6.3: Onset, mid-point and end T_g temperatures for branched polystyrenes of increasing primary chain length values.

Primary Chain Length	**M_w ($gmol^{-1}$)**	**Đ**	**T_g (^oC)**		
			Onset temperature	**Mid-point temperature**	**End temperature**
10	48,900	7.64	52.1	57.8	62.3
25	39,500	4.07	87.1	90.3	92.5
50	340,000	17.84	90.3	93.0	95.3
100	43,400	3.24	94.2	96.6	98.7
250	65,700	2.13	101.0	103.7	103.9
500	106,200	1.94	103.1	105.5	106.6

To determine whether a similar simple T_g versus M_w relationship also applies to the branched materials, the T_g values for the branched polymers were plotted onto the same

graph as their linear counterparts and this is shown in Figure 6.9. As can be seen, a simple T_g versus M_w relationship was not clear across the branched polymer samples.

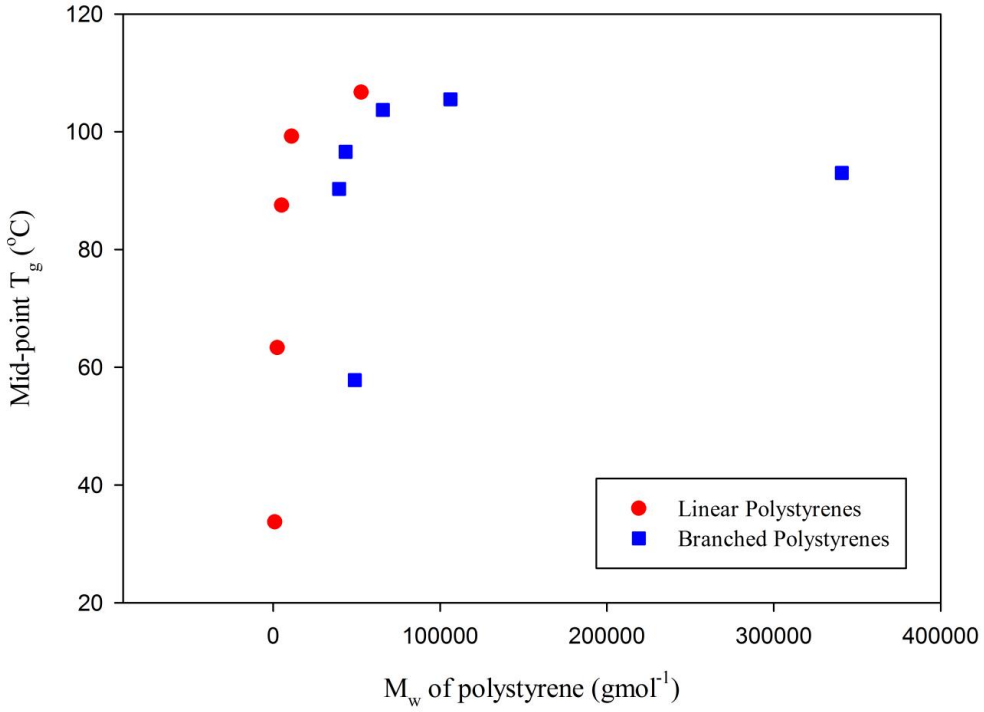

Figure 6.9: Graph showing the relationship between the M_w values of the synthesised linear polystyrenes (filled red circles) and synthesised branched polystyrenes (filled blue squares) and mid-point T_g values.

It appeared that the branched materials actually showed a much lower T_g at any particular weight average molecular weight. For any chosen T_g, it would seem that much higher M_w branched material can be generated within the range studied. A possible reason that it does not work as a simple M_w relationship is because the branched materials are not simple linear homopolymers and therefore the relationship is more complex. A large number of chain-ends within a branched polymer sample may increase the free-volume of the polymer and lead to a reduction in the observed T_g value.

A correlation was sought between the weight average chain length (DP_w) of the primary chains of the branched polymers and the observed T_g values. This was correlated to a T_g vs DP_w relationship of the linear polystyrene chains. In principle, as the anionic polymerisation produces very monodisperse polystyrenes, a T_g vs DP_w relationship should very closely resemble a T_g vs M_w relationship (as DP_w = M_w/monomer molecular weight) and the corresponding T_g vs M_n or T_g vs DP_n relationships for the linear materials. As the branched polymers are made of different numbers of these monodisperse primary chain components, any correlation between the T_g vs DP_w relationship of the primary chains within the branched polystyrenes and the relationship with the linear polystyrenes would be highly surprising. However, such a relationship was seen and is shown in Figure 6.10.

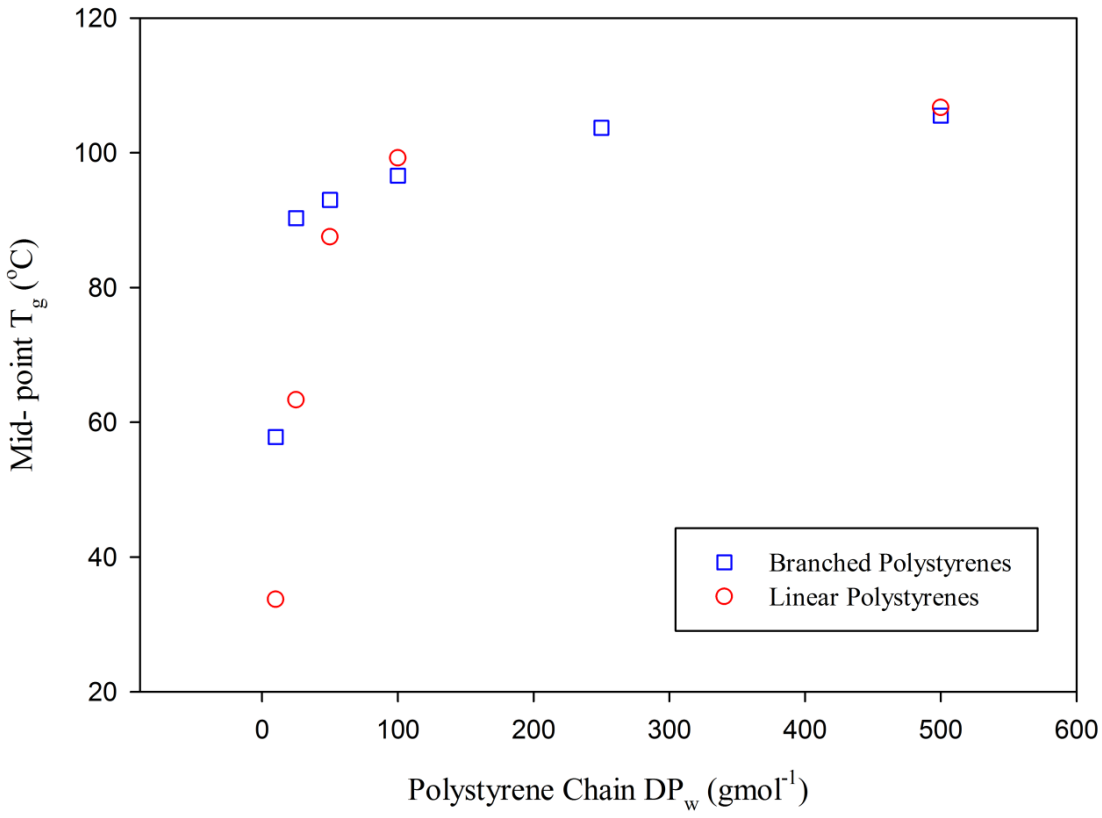

Figure 6.10: Graph showing the relationship between the DP_w values of the synthesised linear polystyrenes (open red circles) and synthesised branched polystyrenes (open blue squares) and mid-point T_g values.

From the graph in Figure 6.10, we can see clearly the relationship between the linear components of the branched polymers and the effect on the observed T_g. As shown earlier in the Chapter 5, the smaller the targeted DP_n of the primary chain (which is also taken as the assumed DP_w of the primary chain due to the nature of the anionic polymerisation producing monodisperse polymers in the absence of brancher) the greater the degree of branching. This results in very different architectures that appear to be affecting the observed T_g. When plotted against this scale, the T_g of the branched materials appears much higher for any given DP_w. However the M_w values of the branched materials are much higher so this would be expected. If we consider the basic structures of the branched polymers with different DP_w values for the primary chain, the differences in their architecture can be readily seen. A schematic representation of all polymers is shown in Figure 6.11.

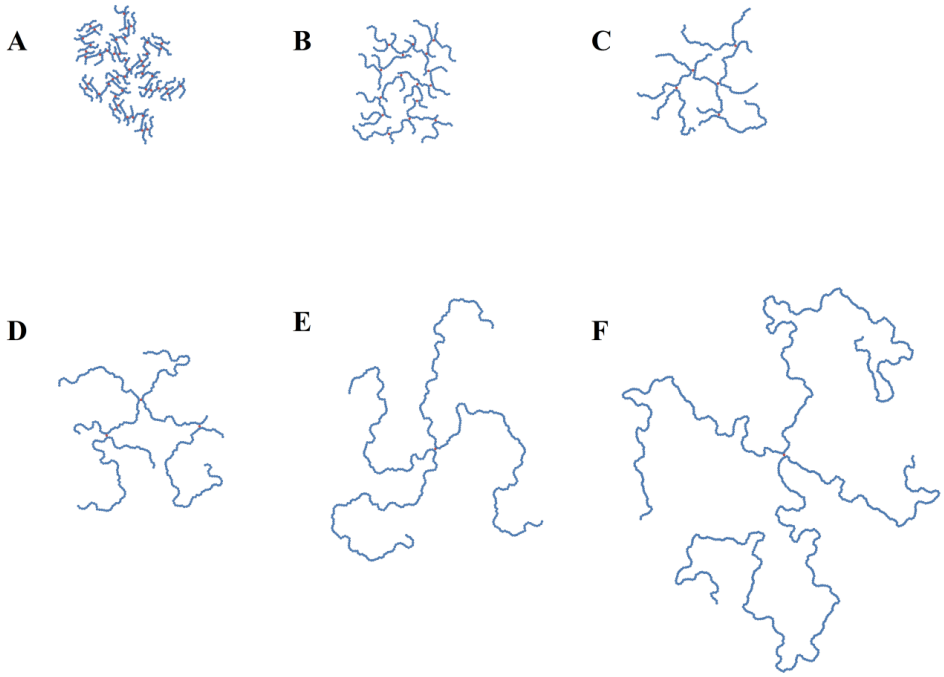

Figure 6.11: Cartoon representations of (A) DP_n10 branched (approximate M_w = 48,900 $gmol^{-1}$), (B) DP_n25 branched (approximate M_w = 39,500 $gmol^{-1}$), (C) DP_n50 branched (approximate M_w = 31,200 $gmol^{-1}$), (D) DP_n100 branched (approximate M_w = 43,400 $gmol^{-1}$), (E) DP_n250 branched (approximate M_w = 65,700 $gmol^{-1}$) and (F) DP_n10 branched (approximate M_w = 106,200 $gmol^{-1}$)

To better understand the effect of the extent of branching of the branched polymers the data shown in Chapter 4. needs to be considered. By considering the M_w values of the branched polymers, it can be seen that targeting longer primary chains leads to a significant decrease in the weight average number of chains that have branched, i.e fewer linear chains are joined together if the targeted molecular weight of the chains increases. So, for the branched polystyrenes with longer targeted primary chains (eg DP_n = 250 or 500 monomer units) it can be said that the weight average chains behave more like linear polymers and there will be less effect from architectural differences. I

f we consider the difference between the branched polystyrene with a primary chain of only 10 monomer units and the branched polystyrene comprising chains of 500 monomer units as a weight average structure, there are as many as 48 primary chains branched together in the structure comprising the shorter primary chains compared to just 2 chains within the material generated from larger chain lengths. The presence of a small number of branches in a big chain does not impact the polymer's architecture greatly and it can still behave very much as expected for a linear polymer. This is seen both in the T_g values and also the plotted relationship of the T_g versus the DP_w of the primary chain where eventually when a high DP_w for the primary chain is reached the polymer appears to act as linear polymer.

If the values in Table 6.3 are considered it can be seen that the DP_n50 branched has a much larger M_w value in comparison to the other branched polystyrenes, and a high dispersity value of 17.84. As discussed this is because the ratio of VPOB:sec-BuLi was raised to a maximum level of 1.4:1, resulting in a more highly branched structure with a high molecular weight (340,000 $gmol^{-1}$). The molecular weight of the DP_n50 branched

polystyrene is over three times the size of the DP_n500 branched polystyrene (106,200 $gmol^{-1}$) and yet it has a lower midpoint T_g value (DP_n50 branched = 93.0ºC, DP_n500 branched = 105.5ºC). This offers further proof to the reasoning that it is not a molecular weight relationship that affects the Tg, but rather the trend comes from the components that make up the branched polystyrene, namely the size of the primary chain length, or DP_w.

This correlates well with the viscometry data seen earlier in the chapter, where the branched polystyrene with a chain length of 10 monomer units was found to have a much higher intrinsic viscosity than the branched polymer comprising chains primary of DP_n = 250 monomer units despite having approximately the same M_w values.

A possible way to directly look at the effect of branching is to take polymers with similar molecular weights, but different architecture within the polymer and compare the differences or similarities in the physical properties. One example of this is the linear polystyrene sample with a targeted DP_n = 500 monomer units, with an M_w of 50,200 $gmol^{-1}$ and a dispersity value of 1.13 compared to a branched polystyrene with a targeted DP_n = 50 monomer units (initiator:VPOB ratio of 1:0.97) with an M_w of 47,300 $gmol^{-1}$ and dispersity value of 4.01 and a highly branched polystyrene with a targeted DP_n = 10 monomer units (initiator: VPOB ratio of 1:1) with and an M_w of 48,900 $gmol^{-1}$ and a dispersity value of 7.64. The thermogram results are shown in Figure 6.12.

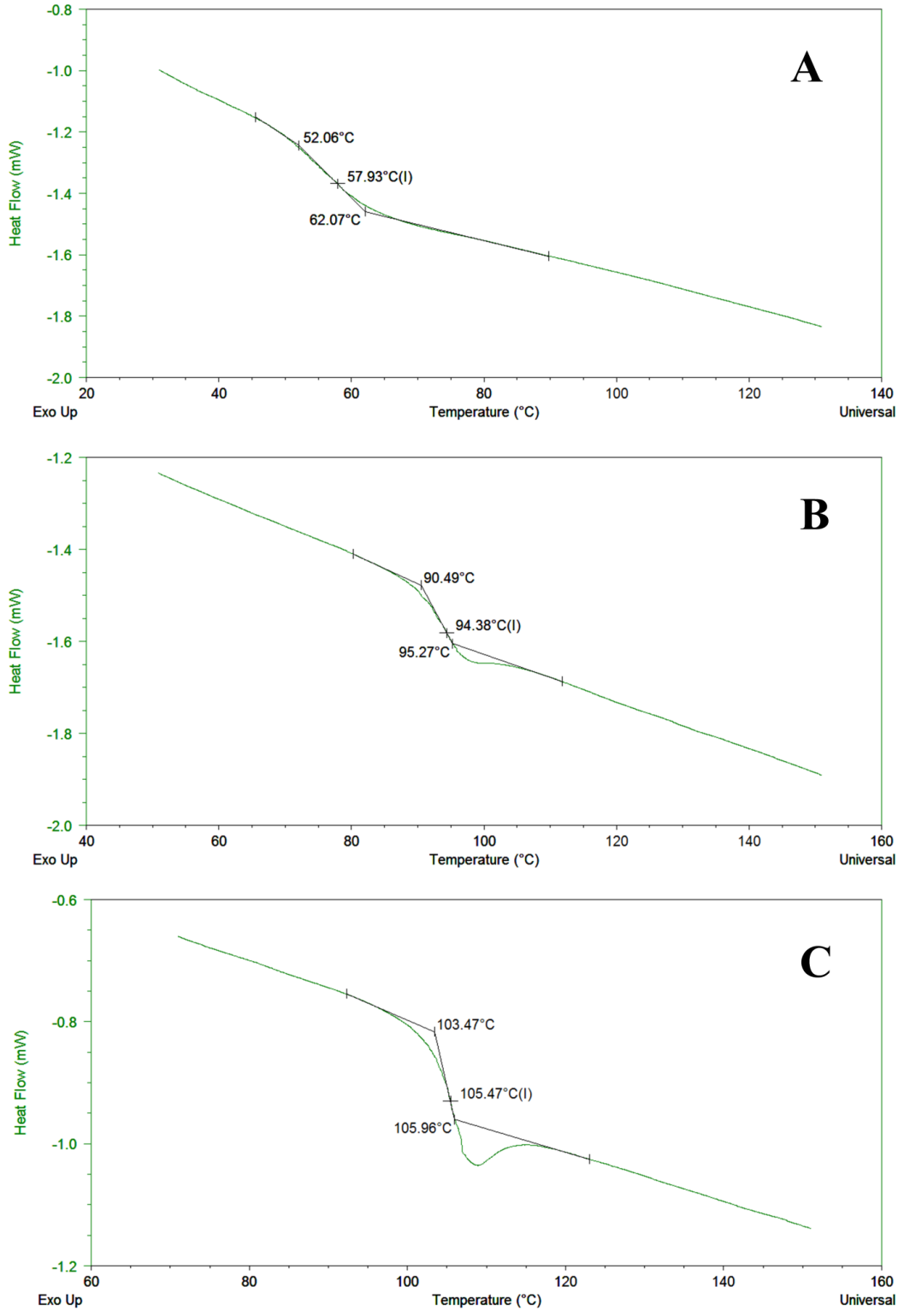

Figure 6.12: Thermograms of branched and linear polystyrenes with different architectures, but M_w values within a range of 2,900 $gmol^{-1}$; (A) DP_n10 branched (M_w = 48,900 $gmol^{-1}$), (B) DP_n50 branched (M_w = 47,300 $gmol^{-1}$) and (C) DP_n500 linear (M_w = 50,200 $gmol^{-1}$).

Table 6.4: Onset, mid-point and end T_g temperatures for branched and linear polystyrenes with different architectures, but M_w values within a range of 2,900 $gmol^{-1}$.

Architecture of Polymer	Đ	Tg (^oC)		
		Onset temperature	Mid-point temperature	End temperature
DP_n10 Branched	7.64	52.1	57.9	62.1
DP_n50 Branched	4.05	90.5	94.4	95.3
DP_n500 Linear	1.17	103.5	105.5	106.0

Although the polymers have a similar average molecular weight, the dispersity values decrease, showing the decrease in branching. As the branching increases the glass transition temperature decreases.

6.3.3 Effect of polymer architecture on T_g

Polystryenes synthesised with very different architectures, but have the same value of DP_w for the linear primary chains and therefore the linear proportion of the polymer molecular weight distribution can be investigated, such as the co-polymers synthesised shown below;

- DP_n10 linear plus DP_n90 branched
- DP_n90 branched plus DP_n10 linear
- DP_n10 branched plus DP_n90 linear
- DP_n90 linear plus DP_n10 branched
- DP_n50 linear plus DP_n50 branched
- DP_n50 branched plus DP_n50 linear

If we consider a cartoon of the conceptual structure of these polymers, shown in Figure 6.13, the differences of the proposed architectures become clearer. All pictures show a structure of a model branched polymer (not based on values from synthesised

polymers) with approximate molecular weights of 70,000 $gmol^{-1}$, for illustration purposes.

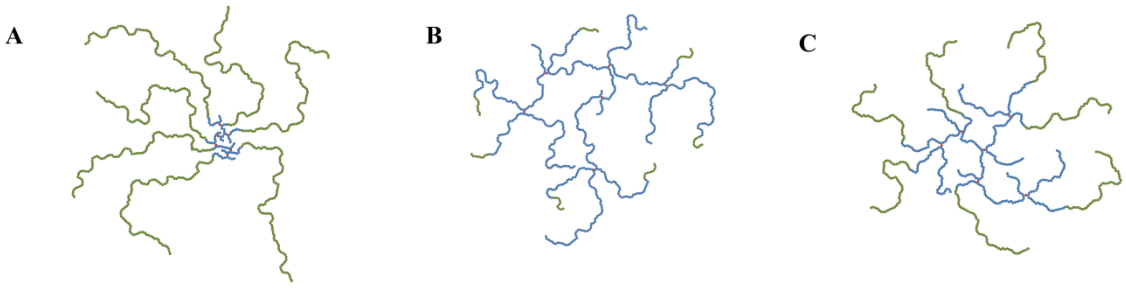

Figure 6.13: Cartoon representation of (A) DP_n10 branched plus DP_n 90 linear (or DP_n 90 linear plus DP_n10 branched), (B) DP_n90 branched plus DP_n 10 linear (or DP_n 10 linear plus DP_n90 branched) and (C) DP_n50 branched plus DP_n 50 linear (or DP_n 50 linear plus DP_n50 branched)

The same methodology was followed for the DSC experiments as described for the linear polystyrenes and branched polystyrenes previously. The results are shown in Table 6.5.

Table 6.5: Onset, mid-point and end T_g temperatures for branched polystyrenes with different architectures, but with a total DP_w value of 100 monomer units of the linear species.

Polymer Architecture	M_w ($gmol^{-1}$)	Tg (ºC)		
		Onset temperature	Mid-point temperature	End temperature
10 branched plus 90 linear	63,400	86.3	91.0	92.1
10 branched plus 90 linear (rpt)	45,600	87.1	91.0	92.1
90 linear plus 10 branched	79,900	94.1	97.1	98.7
10 linear plus 90 branched	46,200	96.5	100.3	101.0
90 branched plus 10 linear	50,800	75.6	79.0	81.5
50 linear plus 50 branched	42,700	95.4	98.0	99.8
50 branched plus 50 linear	35,400	94.1	97.1	98.1

As demonstrated earlier in the chapter, regardless of the order of synthesis or the different targeted DP_n values of each addition stage, all polymers where the total primary chain DP_n is 100 monomer units has only linear polymer with a DP_n = 100 monomer units present within the molecular weight distributions, and not smaller chains generated by termination or initiation during the different stages of monomer addition. For example, the polymer generated from a branched polymer with a target DP_n of 10 monomer units with an additional linear chain of DP_n = 90 monomer units added as a second stage of polymerisation, will have a low molecular weight linear fraction corresponding to a number average chain length of 100 monomer units and therefore no oligomers that are able to strongly influence the measured T_g. If we compare the T_g values of the linear polystyrene with a DP_n = 100 monomer units (Tg midpoint = 99 ºC with the complex architecture produced after synthesising a linear polystyrene with a target DP_n = 90 monomer units followed by branching a chain of 10 monomer units from these linear chains (T_g midpoint = 97 ºC), the T_g is 2 ºC lower for the branched polymer although the linear polymer fraction in both samples has a DP_n = 100 monomer units. There can also be a comparison between these two samples and the one-step branched polystyrene with a targeted primary chain length of 100 monomer units (T_g midpoint = 97 ºC), the complex architecture synthesised from a branched polystyrene of targeted chain length DP_n = 50 monomer units with an additional linear polymerisation of 50 monomer units (T_g midpoint = 97 ºC) and the alternative polystyrene synthesised by polymerising 50 monomer units in a linear chain followed an additional 50 monomer units in a branched polymerisation (T_g midpoint = 98 ºC). All of these have a measured T_g value that is less than the linear polymer with a chain length of 100 monomer units (T_g midpoint = 99 ºC).

A similar relationship can be seen if we consider all polymers where the total primary chain DP_n is 50 monomer units have only linear polymer with a DP_n = 50 monomer units present within the molecular weight distributions, and no smaller chains generated by termination or initiation during the different stages of monomer addition. For example, the polymer generated from a branched polymer with a target DP_n of 10 monomer units with an additional linear chain of DP_n = 40 monomer units added as a second stage of polymerisation, will have a low molecular weight linear fraction corresponding to a number average chain length of 50 monomer units and therefore no oligomers that are able to strongly influence the measured T_g. The DSC experiments were repeated as described but for the following synthesised polymers:

- DP_n10 branched plus DP_n40 linear
- DP_n40 linear plus DP_n10 branched
- DP_n10 linear plus DP_n40 branched
- DP_n10 branched plus DP_n40 branched

A schematic diagram of these polystyrene structures is shown in Figure 6.14. Results of the DSC experiments are given in Table 6.

Figure 6.14: Cartoon representation of (A) DP_n10 branched plus DP_n 40 linear (or DP_n 40 linear plus DP_n10 branched), (B) DP_n40 branched plus DP_n 10 linear (or DP_n 10 linear plus DP_n40 branched)

Table 6.6: Onset, mid-point and end T_g temperatures for branched polystyrenes with different architectures, but with a total DP_w value of 50 monomer units of the linear species.

Polymer architecture	M_w (gmol^{-1})	T_g (°C)		
		Onset temperature	Mid-point temperature	End temperature
10 branched plus 40 linear	21,900	85.4	87.9	89.2
40 linear plus 10 branched	26,600	82.3	83.9	85.8
10 linear plus 40 branched	24,400	88.6	92.0	93.5
40 branched plus 10 linear	24,400	83.5	87.6	89.0

Figure 6.15 shows the different branched structure architectures plotted as T_g against the M_w value of the polymers and a comparison with the relationship observed for the linear polystyrene samples.

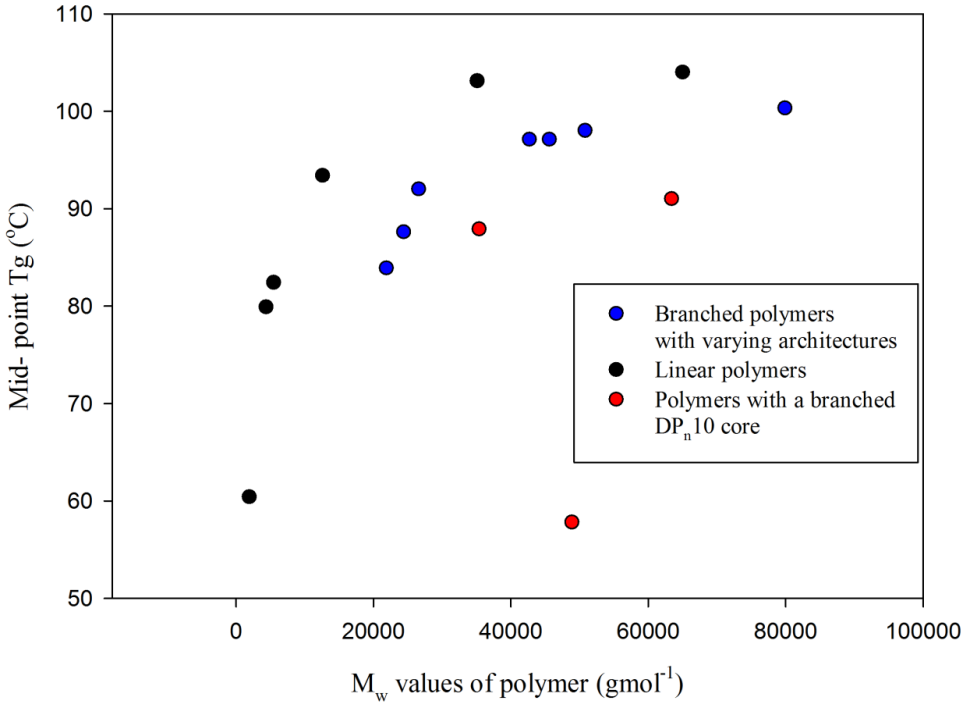

Figure 6.15: Graph showing the relationship between the M_w values of the branched co-polymers with different architectures (filled blue circles) , linear polystyrenes (filled black circles) and all polymers synthesised with a DPn10 branched core (filled red circles) against their respective mid-point T_g values.

As can be seen in Figure 6.15, there is clearly a T_g versus M_w relationship for the branched polymers with varying architectures (shown as blue circles in Figure 18) however it doesn't overlay with the T_g versus M_w relationship of the linear polystyrenes (black circles). It is therefore possible to generate polystyrene materials with the same T_g (as a low molecular weight polystyrene) from much higher M_w branched polymers.

Figure 6.16 shows a graphical summary of the discussed points regarding the relationship between T_g and M_w.

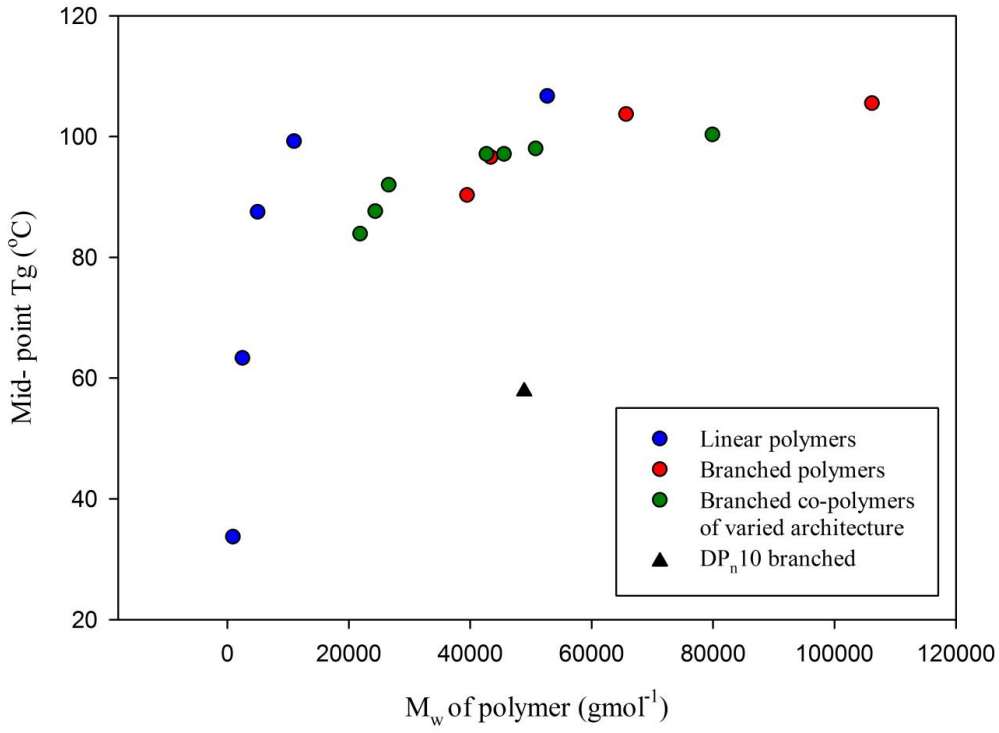

Figure 6.16: Graph showing the relationship between molecular weights of linear polystyrene (blue circles), branched polymers (red circles) and branched polymers with varied architecture (green circles) and the highly branched DP_n10 branched polystyrene (black triangle) and their respective mid-point T_g values.

As can be seen, a series of varying T_g vs M_w relationships exist across the branched polymers, apart from the architectures where the polymer contains the densely branched

primary chains of DP_n = 10 monomer units. The relationships appear to vary considerably depending on whether the branching is a statistical one-pot process or as part of an attempt to impart structural/architectural control.

6.3.4. Branched polystyrene architectures containing DP_n = 10 monomer units

As seen in the intrinsic viscosity measurements the branched polystyrene with a primary chain length of 10 monomer units was found to have a much higher intrinsic viscosity than the branched polymer comprising chains primary of DP_n = 250 monomer units despite having approximately the same M_w values. This leads to the conclusion that the branched DP_n = 10 monomer units polystyrene is much more dense, and highly branched. This has an effect on the glass transition temperature, with the DP_n10 branched polystyrene mid- point glass transition temperature being 57.9 ^oC, significantly lower than the different polymer architectures with similar molecular weight values.

One possible reason for the branched polymer with a primary chain length of DP_n = 10 monomer units having a much lower glass transition temperature could be the presence of small oligomers in the sample. As has been shown in the previous discussions regarding branched polymers there is a large proportion of unbranched, linear polymer chains of the chain length of the targeted primary chain length. This is illustrated in the GPC chromatogram in Figure 6.17 of a branched polystyrene with a targeted chain length of DP_n = 10 monomer units, with the linear proportion highlighted.

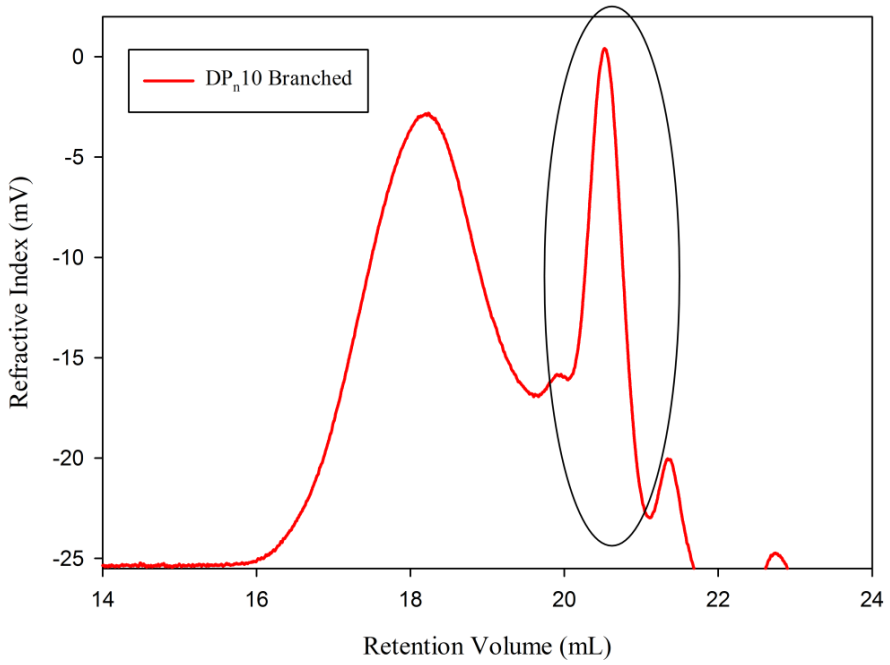

Figure 6.17: GPC chromatogram of a DP_n10 branched polystyrene (red) synthesised by anionic polymerisation techniques.

The area highlighted in black in Figure 6.17 indicates the presence of linear $DP_n = 10$ monomer units or smaller. The presence of these small polymer chains could be encouraging movement of the larger polymer chains and creating additional free volume which would lower the T_g.

If we take branched polymers that are derived from an initial polymerisation of styrene and VPOB with a target primary chain of 10 monomer units then the usual T_g to M_w relationship seen in Figure 6.15 is not observed. Figure 6.18 shows an interesting relationship of these three polymers where an increasing polystyrene chain is polymerised from the highly branched polymer, leading to increasing T_g values.

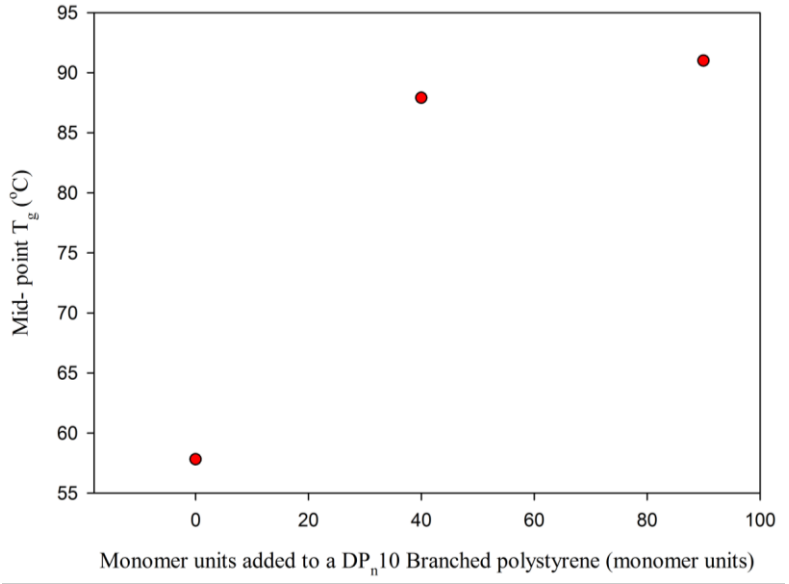

Figure 6.18: Graph showing the relationship between the amount of monomer units added to a DP_n10 branched polystyrene (i.e DP_n10 branched plus DP_n40 linear and DP_n10 branched plus DP_n90 linear) against their respective mid-point T_g values.

It is clear that branched polymers that are derived from an initial polymerisation of styrene and VPOB with a target primary chain of 10 monomer units, and branched polystyrenes with a primary chain length of DP_n = 10 monomer units behave in a different manner. These differences are exploited in the nanoparticle synthesis and discussed further in Chapter 7.

6.3.5 Effect of brancher compound on T_g

As described in Chapter 4, a series of novel brancher compounds of varying chain length were synthesised and evaluated within the branched anionic polymerisation of styrene. T_g is influenced strongly by free volume therefore the effect of changing the brancher on the glass transition temperature was studied. The range of branchers produced and discussed in Chapter 4 resulted in branched polymers with a difference of >12 carbon atoms between the polymer chains when comparing DVB and VPODD. A

DSC analysis was conducted on the series of branched polystyrenes with a targeted primary chain length of 50 monomer units but with the different brancher compounds, and these results are given in Table 6.7.

The brancher:initiator ratio for each polymer sample was not the same and the ratio that resulted in the most effectively branched polymer before the gel point was used, as described in Chapter 4 and listed below:

- DP_n50 branched, DVB:*sec*-BuLi = 1.6:1
- DP_n50 branched, VPOB:*sec*-BuLi = 1.4:1
- DP_n50 branched, VPOHEX:*sec*-BuLi = 1.4:1
- DP_n50 branched, VPOOC:*sec*-BuLi = 1.4:1
- DP_n50 branched, VPOT:*sec*-BuLi = 1.2:1
- DP_n50 branched, VPODD:*sec*-BuLi = 0.9:1

Table 6.7: Onset, mid-point and end T_g temperatures for branched polystyrenes with different brancher compounds used in the anionic synthesis.

Brancher compound	**Mw (gmol-1)**	**Đ**	**Tg (^{o}C)**		
			Onset temperature	**Mid-point temperature**	**End temperature**
DVB	187,900	13.14	98.5	101.8	103.8
VPOB	340,800	17.84	90.3	93.0	95.3
VPOHEX	338,800	16.64	88.8	92.0	94.4
VPOOC	417,300	40.42	90.3	93.3	96.1
VPOT	57,300	8.3	88.6	92.2	93.4
VPODD	38,300	6.49	87.9	91.2	93.0

If we take the mid-point glass transition temperature, the range of T_g values, with the exception of materials synthesised with DVB, is from 91.2 ^{o}C to 93.3^{o}C. It appears there is no large modification of the measured T_g values across the different brancher types. The exception to this is the materials produced using DVB, however the

polystyrene chains are held very closely together at the DVB branch points and the overall influence on the chain mobility may already be considerable with just four carbon atoms between the two styryl units of VPOB. Indeed, the decrease in T_g from the transition from DVB to VPOB is approximately 7 °C and further increases provide little additional benefit.

However if we plot the T_g against the carbon chain length, as shown in Figure 22, there is a very weak trend whereby the T_g appears to steadily decrease as the chain length of the brancher increases as would be expected.

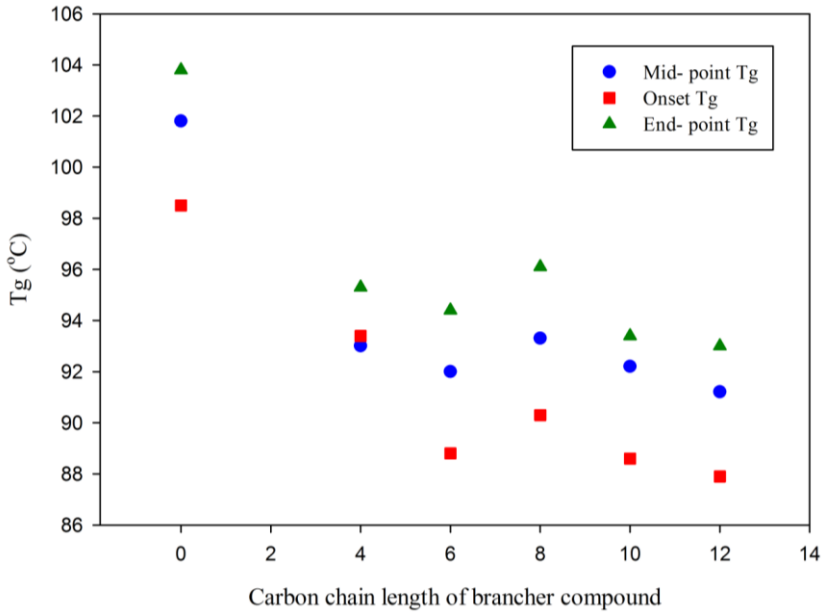

Figure 6.19: Graph of the midpoint Tg of branched polystyrenes synthesised by anionic polymerisation techniques, branched with synthesised distyrl branchers with increasing carbon chain length between reactive vinyl groups.

As can be seen from the T_g data the size of the primary chain length targeted has a significant effect on the T_g. It can be seen that there is no real relationship between M_w, but rather DP_w with regards to branched polymers and the architecture of the polymer affects the T_g significantly.

6.4 Conclusions

The effect of the primary chain length on the polymer architecture has been investigated by GPC analysis, and the analysis of physical properties by DSC. The behaviour in solution has also been examined by molecular weight and intrinsic viscometry *vs*. retention volume measurements. This has led to an interpretation of the extent of branching and how the size of the linear chain affects this. It has been found that as the primary chain length increases the degree of branching decreases. As a result of this decrease in branching less dense structures are formed. This has been confirmed by analysis of the intrinsic viscometry. It was found that the most highly branched structure had a primary chain length of DP_n10. The primary chain length was also found to have an important effect on the T_g of the branched structures. It was found that as the primary chain length increased the T_g increased, until a point of DP_n = 500 monomer units where the degree of branching became almost neglible and behaved as a linear polystyrene. A relationship between T_g and the M_w was also discounted.

6. 5 References

1. Runyon, J.R.; Barnes, D.E.; Rudd, J.F.; Tung, T., *J. Appl. Polym. Sci*., **1969**, *13*, 2359

2. Ouano, C. *J. Polym. Sci. A1*., **1972**, *10*, 2169

3. www.Malvern.com

4. www.hitachihitecscience.com/en/ thermal_analysis/application_TA_068e.pdf

5. Roth, C.B.; Pound, A.; Kamp

Chapter 7

Functionalisation of Branched Polystyrene.

7.0 Introduction

The target branched polystyrenes represent a material with a hydrophilic functionality, and this Chapter aims to introduce hydrophillic elements to the hydrophobic polystyrene, thereby allowing any nanoparticle formed from the polymers to be stable in water.

One way to achieve this would be to grow a hydrophilic polymer such as polyethyleneglycol (PEG) from the polystyrene. This would yield a block co-polymer with a branched, and thereby more dense, hydrophobic element and a hydrophilic element, illustrated in a simple model diagram in Figure 7.1.

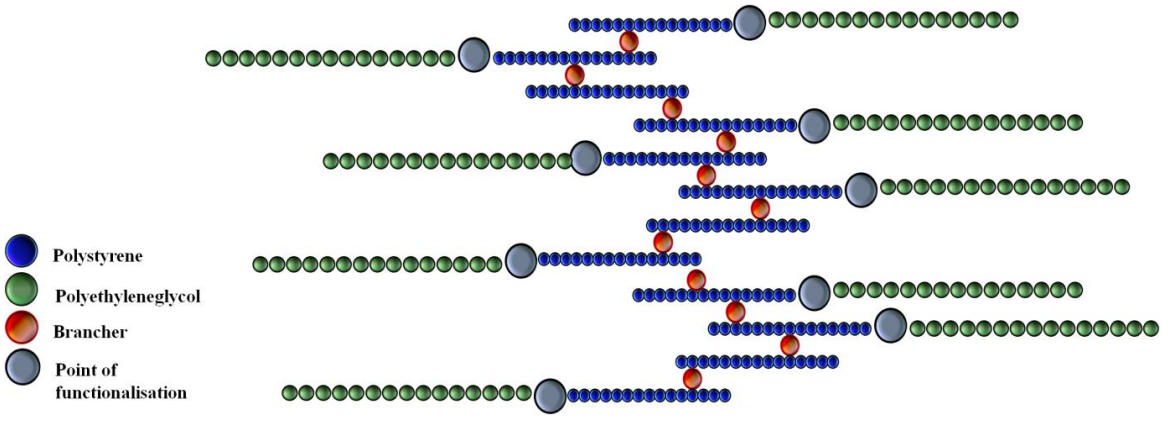

Figure 7.1: Illustration of proposed block co-polymer

Two general strategies exist for introducing the hydrophilic groups into branched polystyrenes; the polymer can be functionalised either *in-situ* as the polymer is

synthesised, or the polymer can be post-functionalised. Functionality can be added either at the chain ends, which can be achieved most readily during synthesis, or along the chain which can be also be achieved during synthesis but in this work is investigated as a post-synthesis procedure onto the branched polystyrene.

One way to functionalise polystyrene would be to add tertiary amine groups to the polystyrene chain ends that may be protonated, quaternised or used to conjugate other hydrophilic functionality. One strategy for the addition of tertiary amine groups to polystyrene would be to utilise an initiator that contained amine groups, or terminate an anionic polymerisation with an amine containing compound such as 4,4'-vinylidenebis(N,N-dimethylaniline), often referred to as 1,1-bis(4-dimethylamino phenyl)ethylene (ADPE) shown in Figure 7.2.

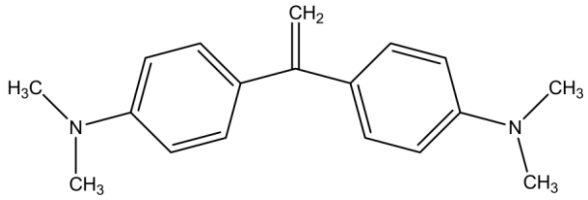

Figure 7.2: Structure of 4,4'-vinylidenebis(N,N-dimethylaniline), often referred to as 1,1-bis(4-dimethylanimophenyl)ethylene, abbreviated to ADPE in this work

7.1 Initiation with 4,4'-vinylidenebis(N,N-dimethylaniline)

A linear polystyrene was synthesised with ADPE and *sec*-BuLi as the initiator using a molar ratio of 1:1:1 of ADPE, *sec*-BuLi, and TMEDA; the three components were stirred in benzene for 30 minutes, to ensure reaction between APDE and *sec*-BuLi, and the styrene monomer was added to target a linear chain with a DP_n = 50 monomer units.

The reaction was terminated after 1 hour and a scheme for this synthesis is shown in Scheme 7.1.

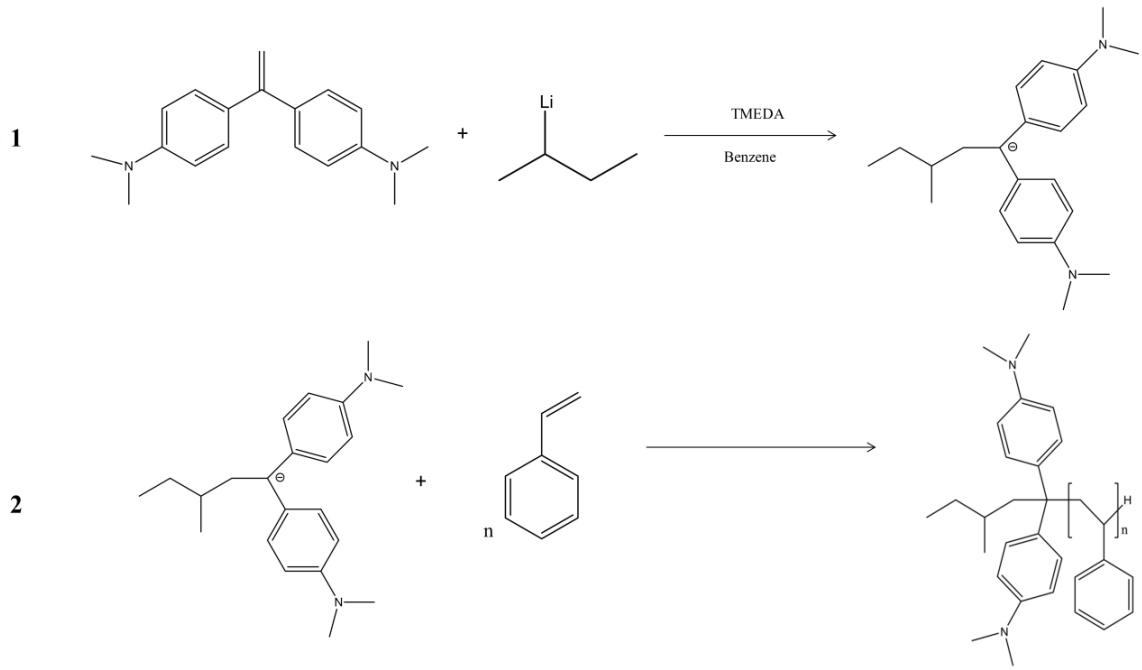

Scheme 7.1: Reaction scheme for (1) the formation of the sec-BuLi/ADPE adduct and (2) the susbsequent initiation of polystyrene from the initiation site.

To allow for a control experiment, another polymer was synthesised under identical conditions, however ADPE was omitted. The GPC chromatograms (RI) and the M_n and M_w values of both polymers are shown in Figure 7.3 and given in Table 7.1.

Table 7.1: M_w, M_n and Đ values of linear polystyrenes synthesised by anionic polymerisation techniques, initiated by *sec*-BuLi (blue) and a s*ec*-BuLi/ADPE adduct (red).

Initiator	Theoretical M_n ($gmol^{-1}$)	M_n ($gmol^{-1}$)	M_w ($gmol^{-1}$)	Đ
sec- BuLi	5,200	5,800	6,100	1.05
ADPE/*sec*-BuLi adduct	5,500	7,700	8,100	1.05

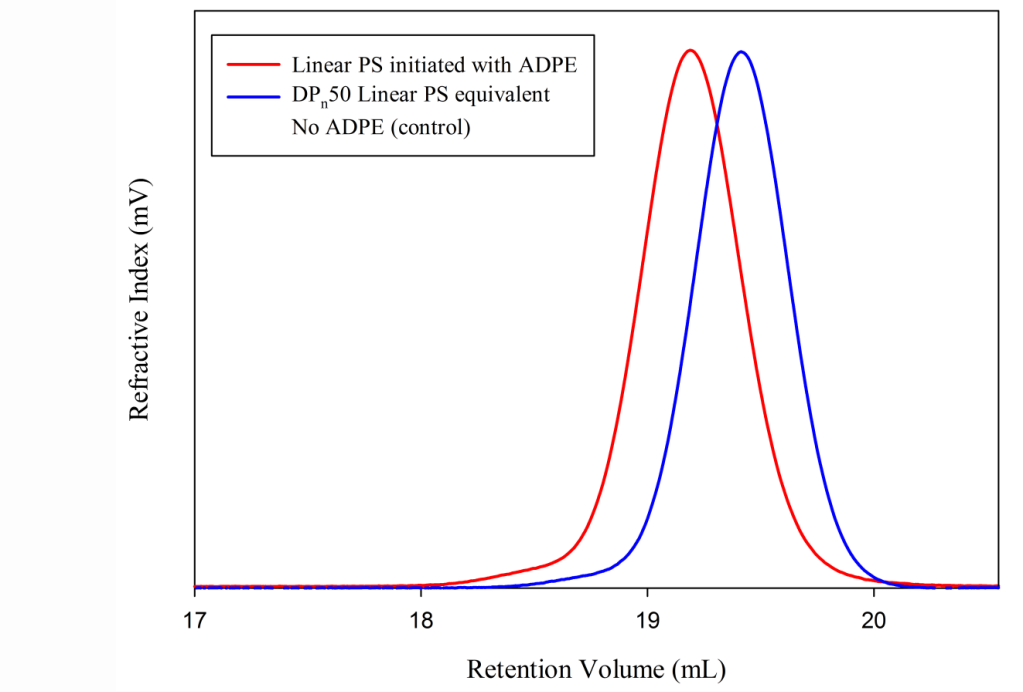

Figure 7.3: GPC chromatograms of linear polystyrenes synthesised by anionic polymerisation techniques, initiated by *sec*-BuLi (blue) and a s*ec*-BuLi/ADPE adduct (red).

As can be seen linear polystyrenes with a narrow dispersity value can be produced from initiation with the adduct of *sec*-BuLi and ADPE. A polystyrene chain length of 50 monomer units was targeted. However, the polystyrene initiated with the ADPE adduct has a larger than targeted DP_n of approximately 75 monomer units, indicating that there may have been less initiator available after reacting with *sec*-BuLi. This could be due to possible impurities in the commercial ADPE.

The initiation of branched polystyrenes from the ADPE/*sec*-BuLi adduct was then attempted. As described for the initiation of a styrene homopolymerisation a molar ratio of 1:1:1:1 was used for ADPE, *sec*-BuLi, TMEDA and VPOB respectively. The mixture of ADPE, *sec*-BuLi and TMEDA was stirred in benzene, to ensure the formation of the adduct followed by addition of the mixture of styrene and VPOB to generate a branched polymer with a primary chain length of $DP_n = 50$ monomer units. The reaction was

terminated after 3.5 hours, consistent with branched polystyrenes initiated with just *sec*-BuLi. The reaction scheme is shown in Scheme 7.2.

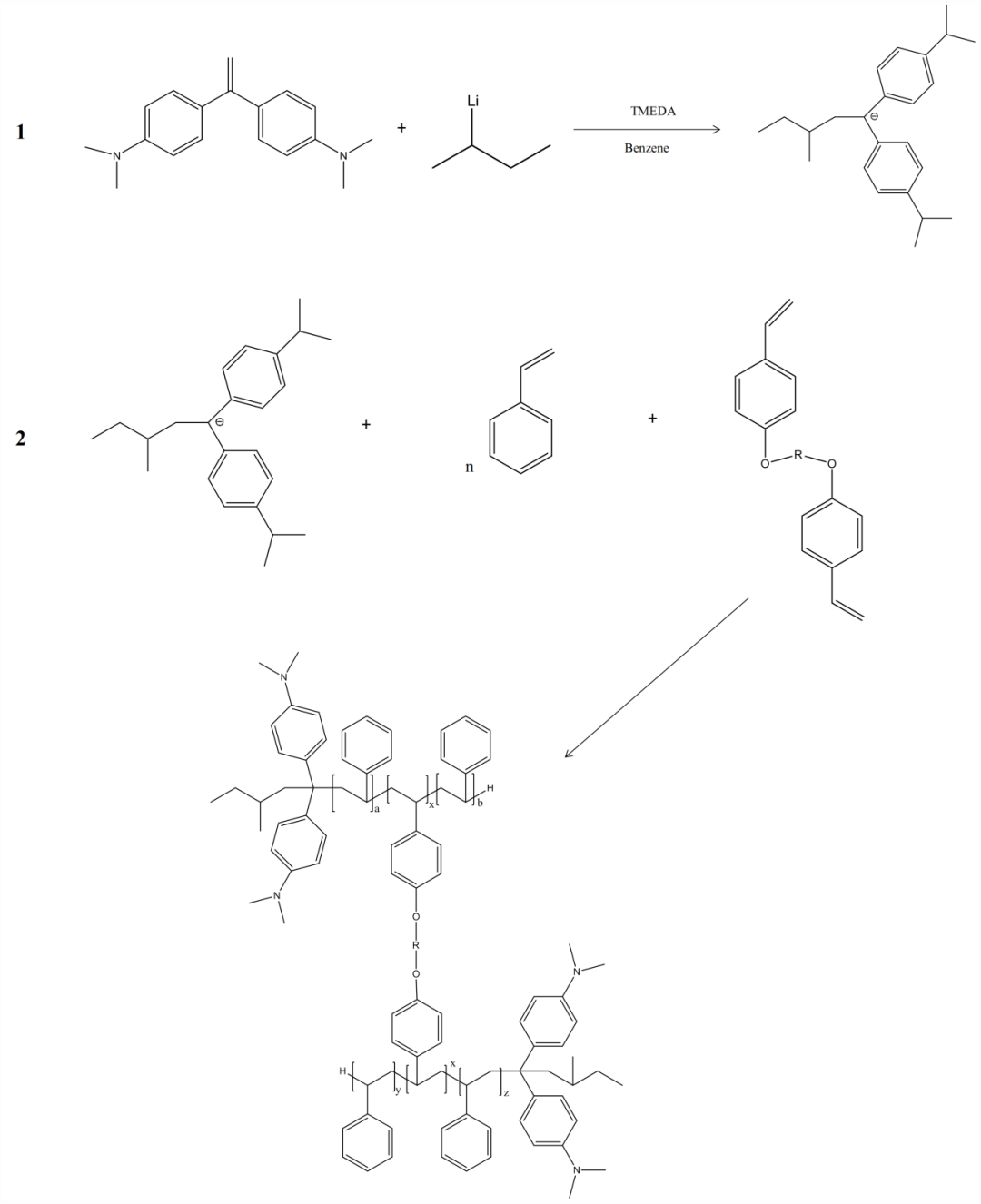

Scheme 7.2: Reaction scheme for the formation of the ADPE/ *sec*-BuLi adduct, followed by the branched polymerisation of polystyrene.

When the branched polystyrene synthesis was attempted in this way, it appeared to cross-link and form an insoluble gel within half an hour of monomer addition. The

reaction was terminated with methanol to rule out any aggregation effects caused by the anions, and the product was indeed found to be an insoluble gel. As seen within the analogous linear homopolymerisation, despite drying ADPE within a vacuum oven, a decrease in the number of initiating sites was observed when using ADPE, resulting in a higher than targeted linear polystyrene sample molecular weight. Within a branching polymerisation, this would result in increasing the effective initiator:brancher molar ratio much higher than the 1:1 ratio originally targeted. As shown in Chapter 4.3.2 even a small increase in the molar ratio of 0.01 beyond a limiting value can result in cross-linking occurring.

As a way to overcome this, an attempt was made to titrate out the ADPE impurities by the slow addition of *sec*-BuLi to the system. Once the orange-red colour ceased dissipating, a measured amount of *sec*-BuLi was added. A second reaction was conducted with ADPE and brancher omitted and this control was used to determine more accurate ratios of initiator:brancher, and initiator:ADPE molar ratios. From this, branched polystyrenes initiated with ADPE and *sec*-BuLi were synthesised. Both DVB and VPOB were used as brancher compounds and the resulting GPC chromatograms are shown in Figure 7.4.

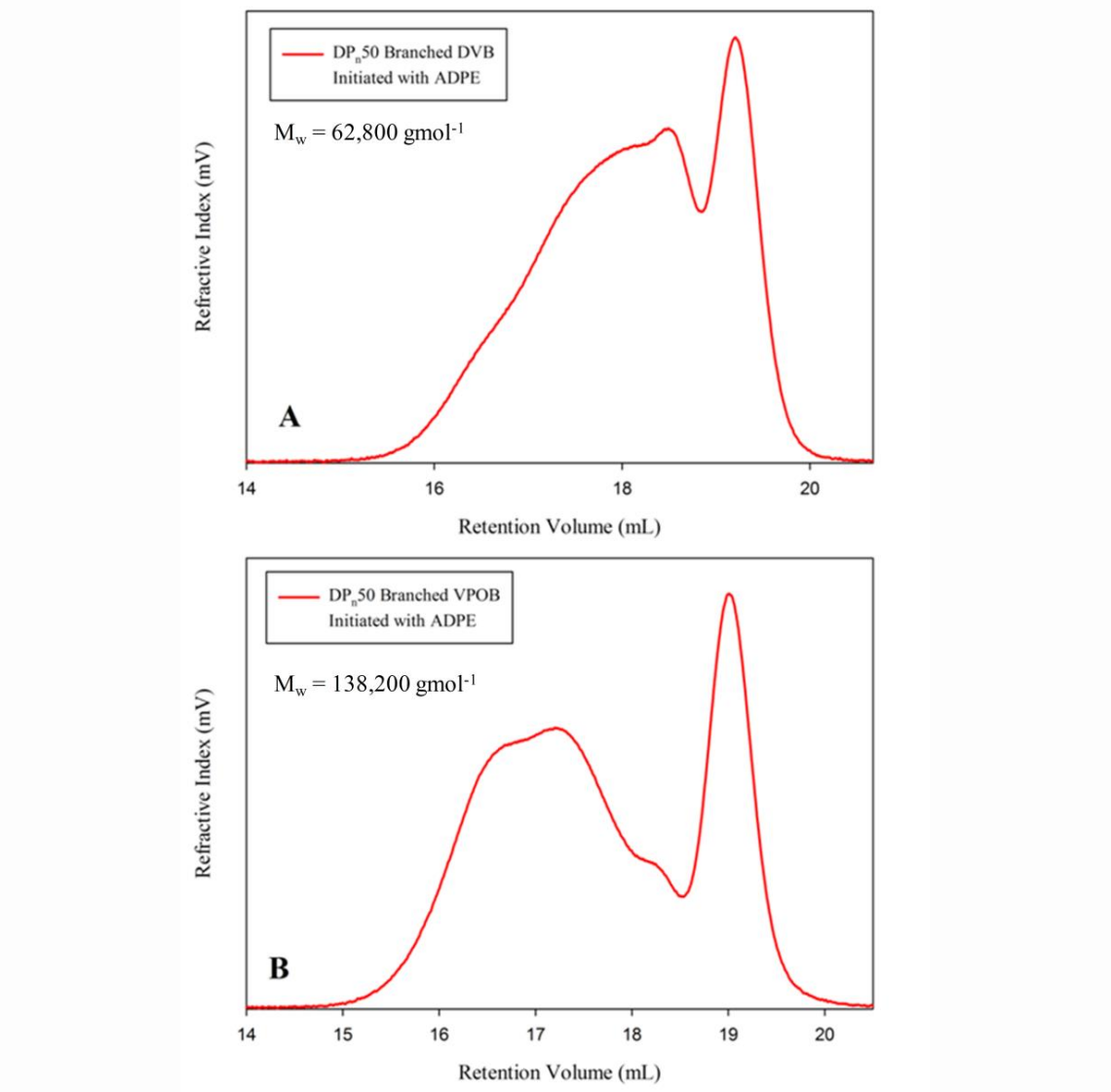

Figure 7.4: GPC chromatograms of branched polystyrenes initiated with ADPE/ *sec*-BuLi adduct formed as described in Scheme 3.

7.2 Terminating with 4,4'-vinylidenebis(N,N-dimethylaniline) (ADPE)

ADPE has been utilised in anionic polymerisation for several years [1], [2], [3]. Due to the hindered nature of the vinyl functionality, a propagating anionic chain end will react with the styrene-like vinyl group of ADPE, transferring the anionic centre to the ADPE monomer residue. However, the resulting anion is not able to propagate with further

ADPE molecules. This effectively terminates chain-growth with a single ADPE unit, even in a large excess, but maintains the anionic character and reactivity of the polymer in solution. To study the applicability of this termination reaction, a linear polystyrene was synthesised by anionic polymerisation techniques. A $DP_{n\,=}$ 50 monomer units was targeted, with 4g of styrene (0.038 mol) in 20ml benzene, initiated with 0.000768 mol of *sec*-BuLi and polymerised for 1 hour. Rather than terminating the reaction by the addition of methanol, ADPE was added in a molar ratio of 1:1 (ADPE:*sec*-BuLi) in benzene. The molar ratio of ADPE to initiator is 1:1, as it is assumed that there will be one ADPE to terminate each initiated polymer chain. The reaction is shown in Scheme 7.3.

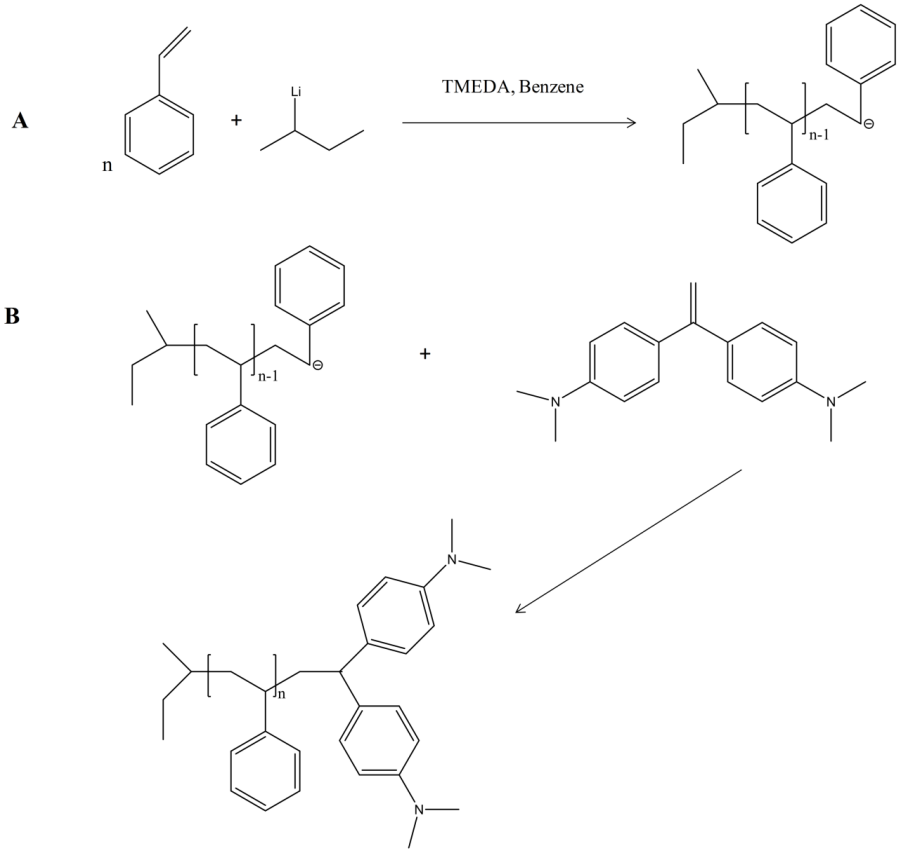

Scheme 7.3: (A) Initiation and propagation of a linear polystyrene and (B) termination with ADPE.

Branched polystyrenes terminated with ADPE were synthesised next. Branched polystyrenes with targeted DP_n = 50 monomer units within the primary chains were synthesised by the following conditions; 4g of styrene (0.038 mol) in 20ml benzene, initiated with 0.000768 mol of *sec*-BuLi, with an equimolar amount of TMEDA (0.000768 mol) and VPOB (0.000768 mol, 1:1 VPOB:*sec*-BuLi) and polymerised for 3.5 hours before termination with ADPE in THF.

An anomaly was found when terminating polystyrenes branched with VPOB as the system gelled when the ADPE was added to terminate the reaction. One possible explanation could be that the addition of THF was increasing the rate of polymerisation. The effect of the addition of THF on the rate of the anionic polymerisation of styrene has been investigated by Bywater and Worsfold [4]. They found that for small amounts of THF the propagation rate increased sharply. This could be leading to a more rapid consumption of brancher, causing the polymer to cross-link.

The influence of THF addition on the branched polystyrene synthesis was investigated by conducting a series of branched anionic polymerisations of styrene in benzene, with the addition of THF with a target primary chain length of DP_n = 50 monomer units with DVB as the brancher and at a brancher:initiator ratio of 0.9:1. Two such reactions were allowed to polymerise for three hours after which a sample was taken and purified. THF was added to just one of the reaction and both were left for a further 0.5 hours, terminated with methanol and then purified. This was then repeated with the brancher VPOB to evaluate the reproducibility of the results. The GPC chromatograms of all experiments are shown in Figure 7.5.

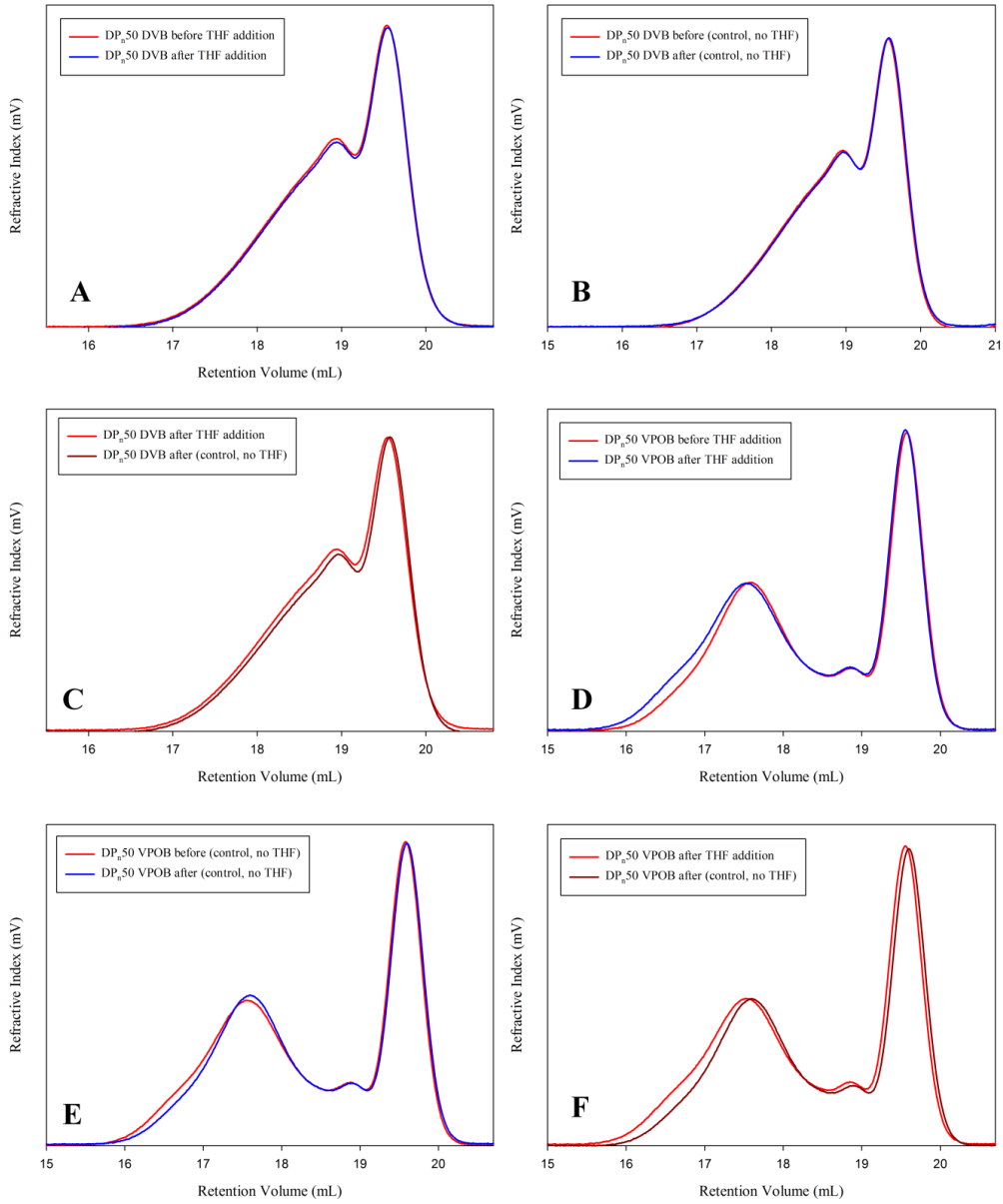

Figure 7.5: GPC chromatograms of samples taken during branched polymerisation synthesised by anionic polymerisation techniques. (A) relates to a sample taken prior to addition of THF (red) and after the addition of THF (blue), (B) is the corresponding samples in the control experiment, same reaction conditions, but no THF addition, (C) After THF addition (red) overlaid with the control (dark red), (D) relates to a sample taken prior to addition of THF (red) and after the addition of THF (blue), (E) is the corresponding samples in the control experiment, same reaction conditions, but no THF addition, (F) After THF addition (red) overlaid with the control (dark red)

As can be seen from the GPC chromatograms in Figure 7.5, the overlap of the analysis from the RI detectors indicates that the addition of THF is not significantly affecting the branching reaction.

7.3 Initiation and termination with 4,4'-vinylidenebis(N,N-dimethylaniline)

As an extension of the linear polymer functionalisation strategies in Sections 7.1 and 7.2, linear polystyrenes were synthesised whereby initiation by the ADPE/*sec*-BuLi adduct was accomplished, samples were taken for analysis and the polymerisation reaction was terminated by the addition of ADPE.

The GPC results of all linear polystyrenes initiated and terminated by ADPE are shown in Figure 7.6.

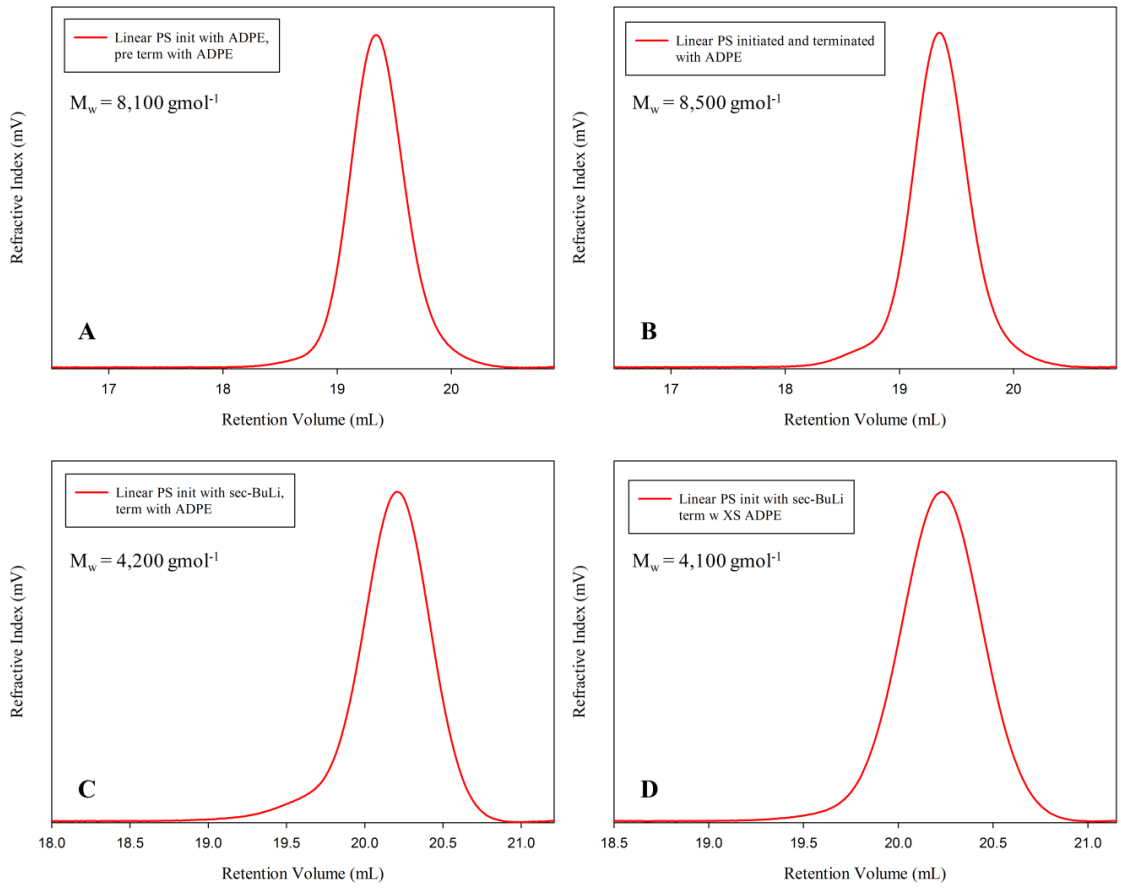

Figure 7.6: GPC chromatograms of linear polystyrenes (A) initiated with *sec*-BuLi/ADPE, pre-termination with ADPE, (B) initiated with *sec*-BuLi/ADPE and terminated with ADPE, (C) initiated with *sec*-BuLi only and terminated with ADPE at a molar ratio 1:1 initiator:ADPE and (D) initiated with *sec*-BuLi only and terminated with ADPE at a molar ratio 1:2 initiator:ADPE

Following the initial results from the attempts to functionalise both chain ends of a linear polystyrene with ADPE, attempts were made to direct the functional groups at each end of the primary chains of a branched polystyrene synthesis, using anionic polymerisation techniques, different branchers and different ratios of brancher to initiator. The results of a range of polymerisations are shown in Table 7.2.

Table 2: M_n and M_w values for branched polystyrenes initated, and initiated and terminated with sec-BuLi/ADPE and ADPE respectively. Reaction conditions: different variables are outlined in the table.

Brancher	Brancher: initiator ratio	Initiated / Terminated	Primary Chain Length	M_n ($gmol^{-1}$)	M_w ($gmol^{-1}$)
DVB	0.8	I	DP_n50	18,400	43,200
DVB	0.8	I, T	DP_n50	20,400	55,300
DVB	1.63	I	DP_n100	23,100	62,800
DVB	1.63	I,T	DP_n100	21,900	69,100
DVB	1.57	I	DP_n100	27,600	105,900
DVB	1.57	I,T	DP_n100	26,900	99,900
VPOB	0.8	I	DP_n50	23,900	73,500
VPOB	0.8	I, T	DP_n50	36,500	86,400
VPOB	1.68	I	DP_n100	32,400	138,200
VPOB	1.68	I, T	DP_n100	34,500	154,000
VPOB	1.62	I	DP_n100	44,100	227,200
VPOB	1.62	I, T	DP_n100	47,500	227,300

As can be seen both branched and linear polystyrenes have successfully been synthesised *via* the initiation with a *sec*-BuLi/ ADPE adduct, and reactions have been terminated in the presence of ADPE.

7.5 Quantification of incorporation of ADPE.

7.5.1 Terminating with ADPE analysis

Analysis of the polymer, to check if the termination with ADPE was successful, initially involved the synthesis of a small oligomer of polystyrene with a target DP_n of 15

monomer units and CHN microanalysis. However, this proved unsuccessful and no results were obtained that allowed a conclusion regarding the percentage of nitrogen, and therefore ADPE, that had been incorporated into the polymer chains. ^{1}H NMR spectroscopy was also utilised as a method to determine how successful the termination reaction had been. As discussed in Chapter 3, the resonances due to the methyl groups of the *sec*-BuLi initiator are noticeable on linear polystyrenes synthesised by anionic polymerisation, between 0.4 ppm and 0.8 ppm. Comparison of these integrated signals with the three protons of the backbone between 0.8 ppm and 2.4 ppm allows the DP_n to be estimated and to double check the targeted DP_n of the polymer with the GPC analysis. The calculation of the percentage of termination with ADPE can also be determined by the integration of the signal at 2.8-3.0 ppm corresponding to the methyl groups of the two dimethyl amino functionalities, and the ratio of this integration with the resonances from the *sec*-BuLi initiator fragment. The theoretical value for the integration should be 12, corresponding to the 12 methyl protons on the ADPE, all named 'a' on the spectrum in Figure 7.7.

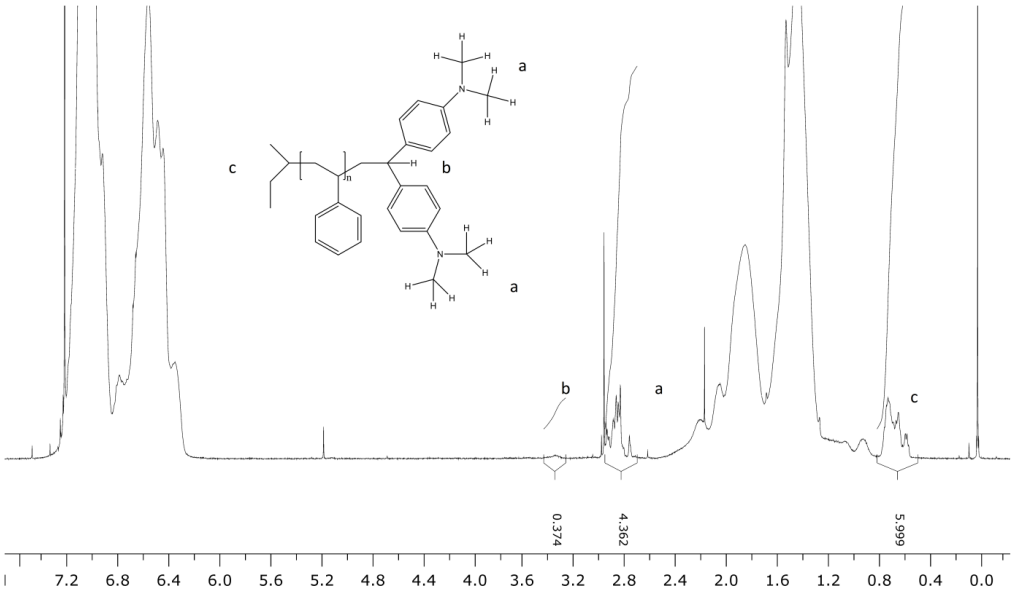

Figure 7.7: ^{1}H NMR spectra of polystyrene terminated with ADPE. Analysed in $CDCl_3$

The percentage of termination within a polystyrene sample that has been treated with ADPE, after normalisation with the 6 protons on the chain ends (‘c’ on the spectrum) can therefore be determined by the calculation:

$$\textit{Percentage of termination by ADPE} = (I_A / 12) * 100$$

For the example in Figure 7.7, the termination was calculated to be 36%.

The addition of THF was also tested to see if this would improve the amount of termination by ADPE. Figure 7.8, is the ^{1}H NMR spectrum for the most successful termination reaction conducted. This required a 1:2:50 molar ratio of initiator to ADPE and THF respectively.

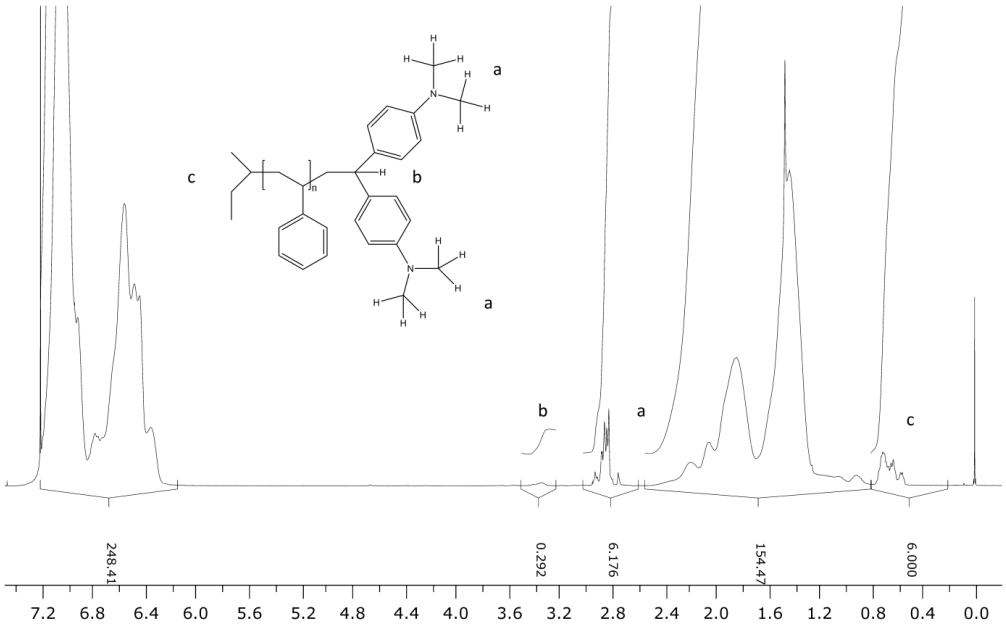

Figure 7.8: ^{1}H NMR spectra of polystyrene terminated with ADPE. Analysed in $CDCl_3$

It was found that the termination for linear polymers, even under these different and optimised conditions, was only 51 % successful. As a way to check the integrations above, the DP_n was calculated from ^{1}H NMR spectra using either the signal and

integration from the 5 aromatic protons of the repeat unit between 6.2 ppm and 7.2 ppm or the 3 protons of the backbone between 0.8 ppm and 2.4 ppm. Using the equation discussed in Chapter 3:

$$DP_n = I_{0.8\text{-}2.4ppm} / 3 \qquad or \qquad DP_n = I_{6.2\text{-}7.2ppm} / 5$$

Where $I_{0.8\text{-}2.4ppm}$ and $I_{6.2\text{-}7.2ppm}$ are respectively the integrals of the NMR signals between 0.8 ppm and 2.4 ppm (CH_3 of the initiator) and between 6.2 ppm and 7.2 ppm (aromatic protons of the repeat unit) then the above DP_n can be calculated to approximately 50 monomer units, which fits the targeted DP_n value.

7.5.2 Initiating with ADPE analysis

Analysis of the resulting polymer was conducted using ^{1}H NMR spectroscopy to determine the percentage of ADPE incorporation during the initiation step. As discussed in Chapter 3 resonances assigned to the methyl groups of the *sec*-BuLi initiator are noticeable on a ^{1}H NMR spectrum of *sec*-BuLi initiated polystyrene between 0.40 ppm and 0.80 ppm. After reaction with a single ADPE prior to addition of styrene, the environment of the *sec*-BuLi initiator residue has changed and these protons appear closer to 0.40 ppm - 0.60 ppm. The calculation of the percentage of initiation ADPE can still be determined by the integration of the signal at 2.80 -3.00 ppm, corresponding to the 12 methyl protons on the ADPE, all named ‘a’ on the spectrum in Figure 7.9.

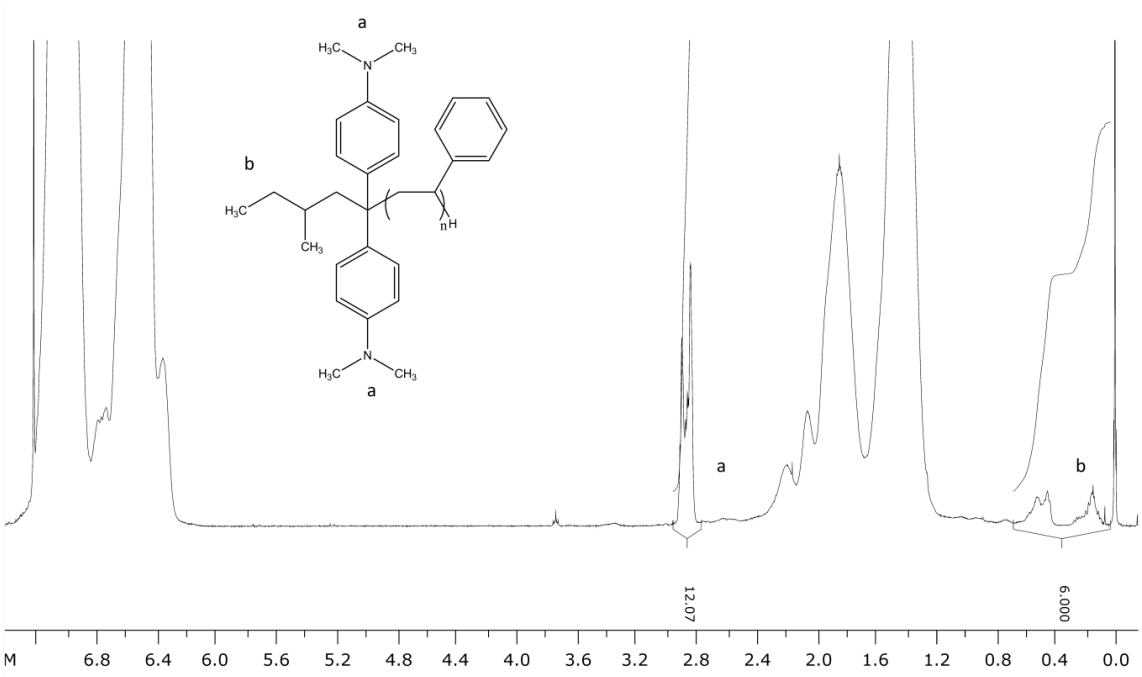

Figure 7.9: ^{1}H NMR spectrum of polystyrene synthesised by anionic polymerisation techniques, initiated a s*ec*-BuLi/ADPE adduct. Analysed in $CDCl_3$

If the signals are normalised to the chain end protons (labelled as 'b' on the spectrum) the percentage of initiation can be determined by the calculation:

$$\textit{Percentage of initiation by ADPE} = (I_A / 12) * 100$$

Where I_A is the integration of the 12 methyl protons, labelled 'a' on Figure 7.9. Using this equation, it was found that the initiation of polymer chains with the *sec*-BuLi/ADPE adduct was 100% successful and, if any were formed, an insignificant number of polystyrene chains were initiated solely by *sec*-BuLi.

The analysis showed that the introduction of amine functionality to the chain-end of a linear polystyrene could be achieved.

7.5.3. Initiating and terminating with ADPE analysis

The polymer and pre-termination sample were analysed to determine the percentage of initiation and termination with ADPE. The ^{1}H NMR analysis of the linear polystyrene initiated and terminated in this way is detailed in Figure 7.10.

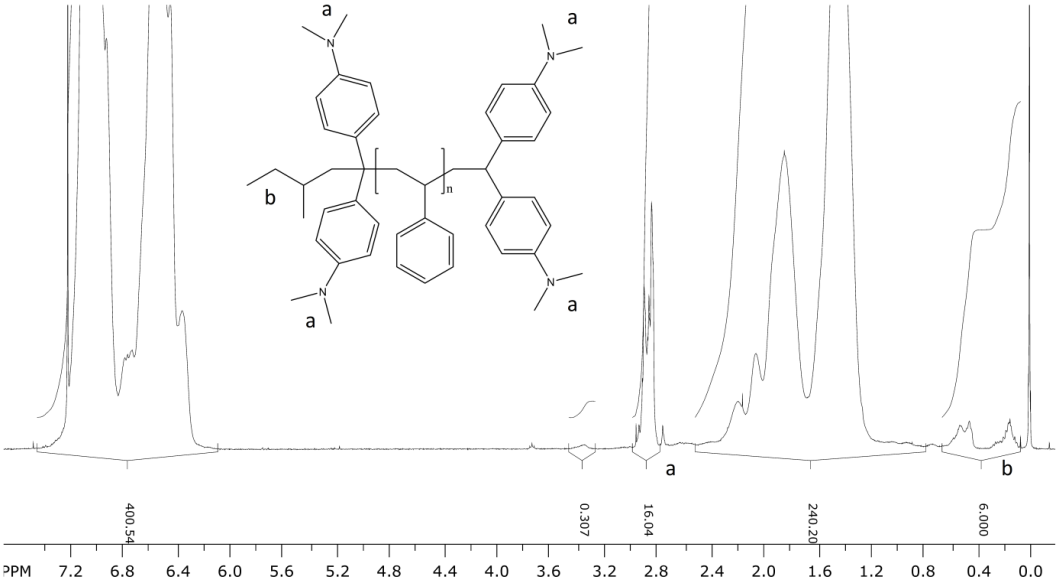

Figure 7.10: ^{1}H NMR spectrum of a linear polystyrene initiated with *sec*-BuLi/ ADPE adduct and terminated with ADPE. Analysed in $CDCl_3$

If the ADPE units have been successfully introduced at both ends of each polymer chain there will be twenty four protons corresponding the dimethyl amino groups per *sec*-butyl group on each chain. After normalisation against the *sec*-butyl chain ends, the percentage of ADPE incorporation can be calculated by the following:

$$Percentage\ of\ ADPE\ termination = (I_{Ait} - I_{Ai} / 12) * 100$$

Where I_{Ai} is the integral of the signal at 2.8ppm – 3.0ppm for the integration of the resonance on the initiation only ^{1}H NMR spectrum, and I_{Ait} is the intergral of the signal at 2.8ppm – 3.0ppm for the initiation and termination together. It was found that the

percentage of initiation was approximately 100%, therefore the termination could then be calculated as;

$$16\text{-}12\ /12\ *100 = 33\%.$$

Due to the lack of control over the chain-end functionalisation using APDE, an alternative method of producing amphiphillic nanoparticles was sought. One alternative is, as shown in Figure 7.11, where the point of functionalisation occurs statistically along the primary chains, rather than *via* a hydrophilic block copolymer polymer chain.

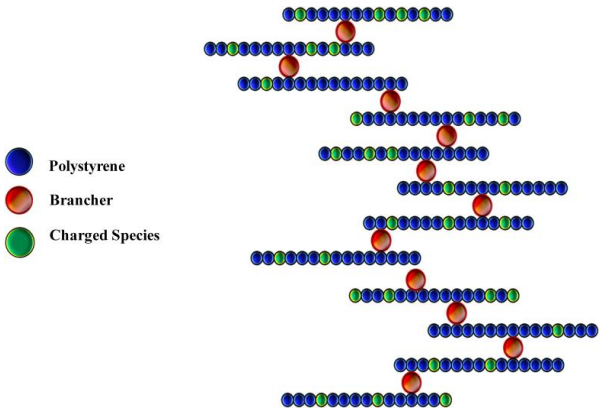

Figure 7.11: Diagram of proposed amphiphillic polystyrene

7.6 Post-functionalising with sulphonate groups.

Sulphonation of polystyrene can lead to a change in the properties of the polymer. Sulphonation of polymers can lead to better ion conductivity, higher hydrophilicity and improved solubility [5]. Shown in Figure 7.12 is the general structure of polystyrene sulphonate.

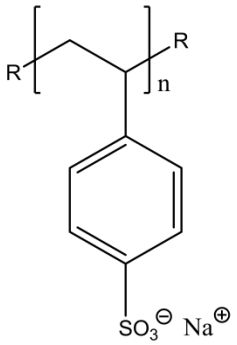

Figure 7.12: Structure of polystyrene sulphonate**.**

The degree of sulphonation of the polymer can have a big effect on the properties such as solubility and stability. For the purpose of the synthesis of the nanoparticles within this study, sulphonation is required to increase the hydrophillicity of the polystyrene, but not lead to water solubility. Polymers can be sulphonated with a range of different agents such as sulphur trioxide, and sulphuric acid. The relative strength of these agents can have an effect on the success of the post-sulphonation. For the following synthesis of post-functionalised polystyrenes, the work of Jancar and Kucera [6] was followed. They reported the homogenous sulphonation of polystyrene in a solution of dichloroethane (DCE) using acetyl sulphate as the sulphonating agent.

7.6.1 Synthesis of linear sulphonated polystyrenes

To evaluate the effectiveness of the sulphonation reaction, linear polystyrene samples were utilised in a series of model reactions A 1.0 molar solution of acetyl sulphate was freshly prepared for each reaction and was cooled in ice to approximately 10 ºC before 2.33 mL of concentrated sulphuric acid was slowly added. For the sulphonation of polystyrene, 1g of synthesised polystyrene was dissolved in dichloroethane (DCE) under nitrogen pressure and heated to 50 ºC. A measured amount of the acetyl sulphate

was added by syringe under nitrogen pressure, and the reaction stirred at 50 ºC for 1 hour. This reaction is shown in Scheme 7.4.

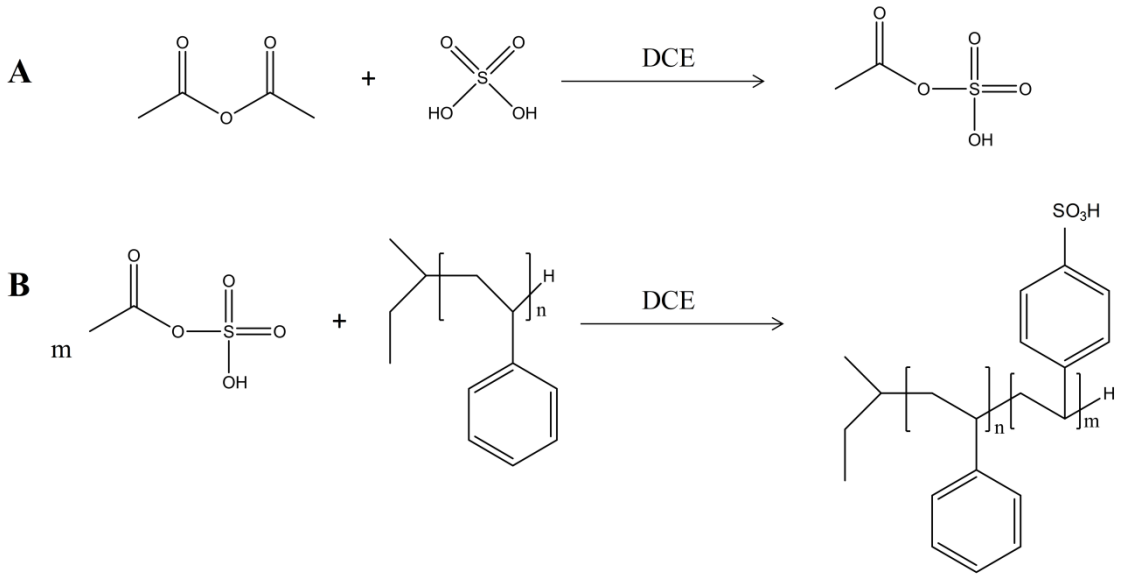

Scheme 7.4: (A) Preparation of acetyl sulphate solution and (B) its subsequent reaction with polystyrene

The amount of acetyl sulphate added was varied over a series of reactions to attempt to obtain a different level of sulphonation for specific polymers. So for 1 g of polystyrene:

1 g /104.15 gmol^{-1} = 0.00960154 mol of styrene repeat units.

For a reaction containing 0.25 equivalents of sulphonating agent:

0.00960154 x 0.25/0.001 mol (moles per ml of acetyl sulphate solution) = 2.4 ml of acetyl sulphonate solution.

In initial experiments, 1 g of a linear polystyrene sample with a target DP_n of 100 monomer units (9.6 x 10^{-3} mol of styrene monomer residues) was reacted with varying amounts of acetyl sulphate (2, 1, 0.5, 0.25 and 0.1 equivalents) while keeping the

reaction conditions and reaction time the same for each reaction. As different amounts of the sulphonating solution resulted in different levels, or degrees, of sulphonation, isolating the polymer samples with a single experimental procedure became problematic.

In Kucera and Jancar's [6] paper it stated that sulphonation levels below 15% per mole should result in no isolation problems, and the reaction mixture could be pipetted into cold water or methanol, in the same way as normal polystyrene, suggesting no significant change in polymer solubility. For sulphonation levels between 15-30%, problems with emulsion formation in water or methanol can arise, suggesting a quite considerable change in behaviour and the formation of amphiphilic materials. To overcome these issues, the report suggested evaporation of any solvent, and washing the powdered solid with water. For sulphonation levels higher than 30%, it was reported that the product was completely water soluble. Therefore the solvent, DCE, was evaporated and the polymer was subsequently purified by washing with a non-aqueous solvent. While these guidelines were followed to some degree within this study, the actual level of sulphonation for each sample was unknown, prior to purification, and the distribution of sulphonation across the sample may not have been truly homogeneous. With this in mind, the products from each reaction were treated in the same manner, starting with the removal of DCE by vacuum evaporation techniques. No further purification was attempted except on specific polymers for further testing. Purification by dialysis could be achieved on the water soluble products. The syntheses were repeated using different equivalents of acetyl sulphate and different chain lengths of linear polystyrene.

To get a better understanding of the levels of sulphonation achieved experimentally the percentage of sulphonation was calculated using ^{1}H NMR analysis.

7.6.2 Analysis of sulphonated linear polystyrenes

The percentage of sulphonation was calculated by analysis using ^{1}H NMR spectroscopy. Figure 7.13 shows the area of interest on the ^{1}HNMR spectrum (6.0 to 8.0 ppm) of an example sulphonated polystyrene, derived from a linear polystyrene with a target DP_n = 500 monomer units and the subsequent calculations are discussed.

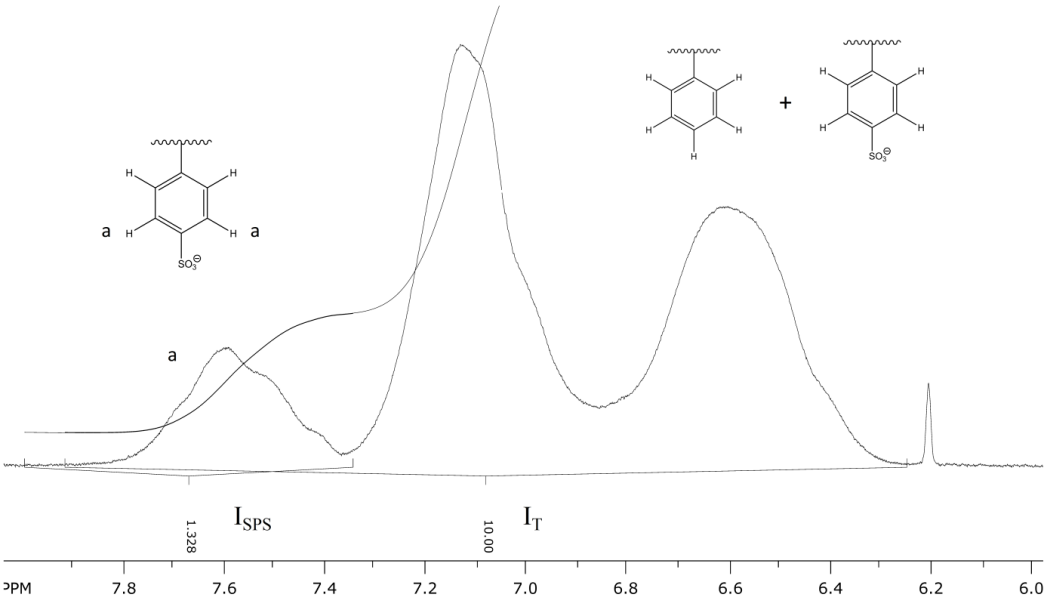

Figure 7.13: ^{1}H NMR spectra of sulphonated polystyrene. Analysis conditions: MeOD

In Figure 7.13 the integration between 6.2 ppm to 8.0 ppm is labelled IT and corresponds to the total integration of the aromatic protons on the pendant groups of the polymer. This total includes protons of normal and sulphonated polymer repeat units. The number of moles of styrene repeat units can therefore be expressed as:

$$n_T = \textit{no of moles of repeat unit of sulphonated polystyrene + no of moles of repeat unit of non-sulphonated polystyrene}$$

$$n_T = n_{SPS} + n_{PS}$$

Whereby:

$$n_{SPS} = x * n_T$$

$$n_{PS} = (1-x) * n_T$$

$$x = \text{mol fraction of sulphonated polystyrene} = n_{SPS} / (n_{SPS} + n_{PS})$$

On the spectrum in Figure 7.13, I_T and I_{SPS} are labelled where 5 relates to the 5 protons on the normal polystyrene in the equation, 4 in the equation relates to the 4 protons on the sulphonated polystyrene, and 2 relates to the 2 protons in a different environment, labelled 'a' and therefore their signal can be seen at 7.4 ppm to 8.0 ppm

So for the integrations I_T and I_{SPS}:

$$I_T = I_{1H} * 2 * x * n_T$$

$$I_{1H} * n_T = I_{SPS} / (2 * x) = Eq\ \#1$$

$$I_T = I_{1H} * \{ 4 * x * n_T + [5 * (1 - x) * n_T] \}$$

$$I_{1H} * n_T = I_T / [4* x + 5 * (1 - x)] = Eq\ \#2$$

$$Eq\ \#1 = Eq\ \#2$$

$$I_{SPS} / 2 * x = I_T / [4 * x + 5 * (1-x)]$$

Then, to extract x from the equation:

$$I_{SPS} * \{ (4 x + 5) - (5 * x)\} = I_T * 2 x$$

$$I_{SPS} (5 - x) = I_T * 2x$$

$$5 * I_{SPS} - x * I_{SPS} = I_T * 2x$$

$$5 * I_{SPS} = (I_T * 2x) + (x * I_{SPS})$$

$$5 * I_{SPS} = x * (2 * I_T + I_{SPS})$$

So, ultimately:

$$x = 5 * I_{SPS} / 2 * I_T + I_{SPS}$$

$$x * 100 = \text{percentage of successful sulphonation}$$

Using this method the percentage of sulphonation for some of the linear polystyrenes synthesised are shown in Table 7.3.

Table 7.3: Calculated percentage of sulphonation for increasing amounts of acetyl sulphate added in linear polymers with increasing DP_n primary chain values

DP_n (monomer units)	Equivalent amount of acetyl sulphate added	Percentage Sulphonation
25	0.8	31%
50	0.6	28%
50	0.8	32%
100	0.4	23%
100	0.6	29%
100	0.8	31%
500	0.8	31%

From the data presented in Table 7.3 it appears that as the amount of acetyl sulphate is increased the percentage of sulphonation increases which is beneficial as this will allow experimental control over the percentage of sulphonation, and therefore allowing the hydrophillicity to be controlled so that an extreme level, whereby full water solubility occurs, does not happen. It would appear that an increased molecular weight polystyrene, or a polystyrene with a higher number of monomer units targeted does not affect the sulphonation. This can be seen if the equivalents added is plotted against the percentage sulphonation for each different targeted DP_n, shown in Figure 7.14.

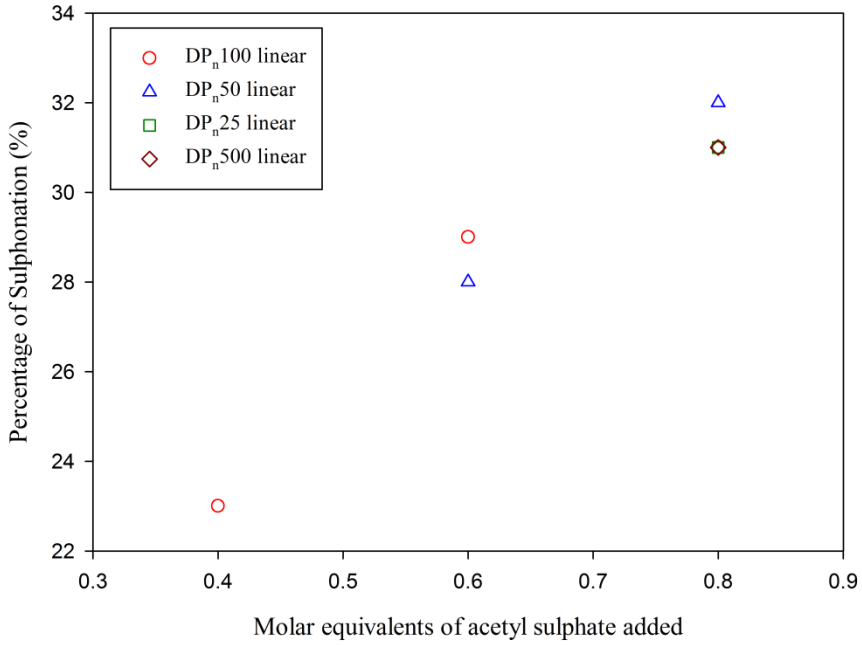

Figure 7.14: Graph of the calculated percentage of sulphonation against the amount of acetyl sulphate added in the sulphonation reaction for linear polystyrenes with increasing targeted DPn values; DP_n25 (green), DP_n50 (blue), DP_n100 (red) and DP_n500 (brown)

As can be seen there is a point where the number of equivalents of acetyl sulphate added (0.8) results in the same sulphonation percentage regardless of the DP_n of the linear polystyrene.

7.6.3 Properties of sulphonated linear polystyrenes

The level of sulphonation was found to have a big effect on the solubility of the polymers. One of the main differences was with regard to the solubility in methanol. Polystyrene is very insoluble in methanol, yet even at the lowest levels of sulphonation the sulphonated polystyrene became soluble in methanol. Figure 7.15 shows a linear DP_n100 polystyrene with no sulphonate groups in methanol (A) and a DP_n100 linear polystyrene reacted with 0.4 equivalents of acetyl sulphate (sulphonation percentage = 23%) (B).

Figure 7.15: Photograph of (A) DP_n100 polystyrene with no sulphonate groups in methanol and (B) DP_n100 linear polystyrene reacted with 0.4 equivalents of acetyl sulphate (sulphonation percentage = 23%)

Polystyrene is also very insoluble in water. Figure 7.16 shows a linear DP_n100 polystyrene with no sulphonate groups in H_2O (A) and a DP_n100 linear polystyrene reacted with 0.4 equivalents of acetyl sulphate (sulphonation percentage = 23%) (B) and a DPn100 linear polystyrene reacted with 0.8 equivalents of acetyl sulphate (sulphonation percentage = 31%) (C).

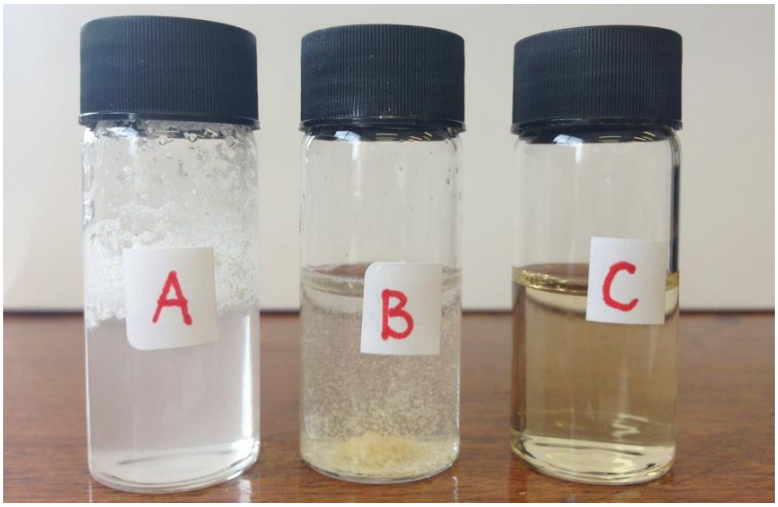

Figure 7.16: Photograph of (A) DP_n100 polystyrene with no sulphonate groups in H_2O, (B) DP_n100 linear polystyrene reacted with 0.4 equivalents of acetyl sulphate (sulphonation percentage = 23%) and (C) DP_n100 linear polystyrene reacted with 0.8 equivalents of acetyl sulphate (sulphonation percentage = 31%)

The hydrophobicity can be clearly seen as the polystyrene has more affinity for the glass vial than the water. As the level of sulphonation increases, the polymer becomes increasingly soluble in water, shown in the photo in Figure 7.17. At intermediate levels of sulphonation, a foam can be seen. The polymer has both hydrophilic and hydrophobic regions and therefore displays some surface activity, resulting in a foam at the air/water interface. A chart of the solubility in methanol and water is shown in Table 4 for the DP_n100 linear reacted with different equivalents of acetyl sulphate.

Figure 7.17: Photograph of (D) DP_n50 linear polystyrene reacted with 0.6 equivalents of acetyl sulphate (sulphonation percentage = 28%) in H_2O

Table 7.4: Table of the change in solubility behaviour as the percentage of sulphonation increases by increase of the molar equivalents of acetyl sulphate added to the linear DP_n = 100 monomer units polymer.

Equivalent	Percentage Sulphonation	Soluble in MeOH	Soluble in H_2O
0	0%	N	N
0.1	U*	Y	N
0.2	U*	Y	N
0.25	U*	Y	N
0.4	23%	Y	N
0.5	U*	Y	N
0.6	29%	Y	N
0.8	31%	Y	Y
1	>30%	Y	Y
2	>30%	Y	Y

U indicates gaps in the data whereby NMR spectroscopy could not be done, due in the majority to solubility issues in deuterated solvents.*

As can be seen from Table 7.4 the water solubility increases as the percentage of sulphonation increases. After 30%, the sulphonated polymer becomes water soluble, as described in the literature report the work is based on.

7.6.4 Synthesis and analysis of branched sulphonated polystyrenes

The introduction of sulphonate groups onto linear polystyrene using acetyl sulphate appeared to proceed without complication, therefore the synthesis of branched sulphonated polystyrene samples was attempted by following the same experimental procedure. The reaction is shown in Scheme 7.5.

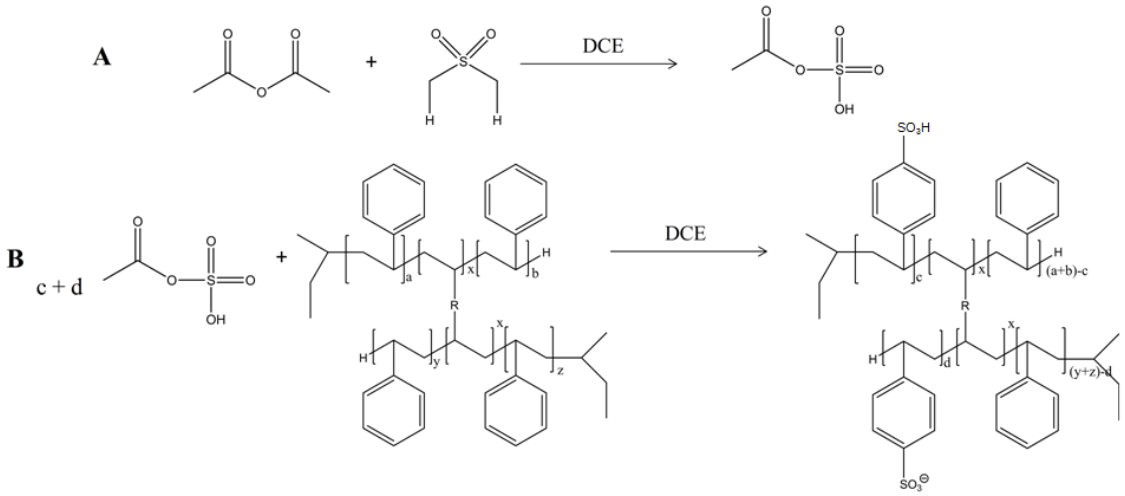

Scheme 7.5: (A) Preparation of acetyl sulphate solution and (B) its subsequent reaction with branched polystyrene

Initially 1 g of a DP_n100 branched polystyrene, with VPOB as the brancher compound, was reacted with varying equivalents of acetyl sulphate of 0.2, 0.4, 0.6, 0.8 per mole of styrene repeat unit. The results are shown in Table 7.5.

Table 7.5: Solubility data and percentage sulphonation for DP_n100 branched polystyrene at different experimental equivalents.

Equivalent	Percentage Sulphonation	Soluble in MeOH	Soluble in H_2O
0	0%	N	N
0.2	14%	Y	N
0.4	21%	Y	N
0.6	26%	Y	N
0.8	28%	Y	N

Compared to the sulphonation of linear polystyrene DP_n100 at 0.8 equivalents of acetyl sulphate, there is a lower degree of sulphonation for the reaction with the branched polymers resulting in different properties. The linear polystyrene reacted with 0.8 equivalents of acetyl sulphate is soluble in water and has a sulphonation percentage of 31%, which is concordant with the literature regarding mole percentages above 30% becoming water soluble. A further experiment was conducted where 2 equivalents of acetyl sulphate were used, in order to push the percentage of sulphonation up to a level where it would become water soluble. However this product, due to the possibly too large excess of acetyl sulphate used, was very impure and difficult to purify so no further analysis was conducted. It was found to be water soluble so it is likely to have reached a sulphonation percentage above 30%.

To investigate the effect of the architecture of the polymer on the level of sulphonation the experiments were repeated but using the self-blocking DP_n10 branched plus DP_n90 linear polystyrene. This has a similar linear chain building block component as the DP_n100 branched and has technically the same primary chain length. However, as seen in Chapter 5, it has a very different structure to the DP_n100 branched polymer. The DP_n10 branched polymer proportion contributes to a densely packed branched polymer

core, with DP_n90 linear chains from this. Again, acetyl sulphate equivalents of 0.2, 0.4, 0.6, 0.8 and 2.0 were used. The results are shown in Table 7.6.

Table 7.6: Solubility data and percentage sulphonation for DP_n10 branched plus DP_n90 linear polystyrene at increasing experimental equivalents.

Equivalent of acetyl sulphate added	Percentage Sulphonation	Soluble in MeOH	Soluble in H_2O
0.2	26%	Y	N
0.4	21%	Y	N
0.6	24%	Y	N
2.0	31%	Y	N

The sulphonation of the two-step, chain-extended, branched-linear polystyrene (branched polymer with targeted primary chains of 10 monomer units, plus a linear chain of 90 monomer units) follows a non-linear relationship that is slightly different to the single-stage one-pot branched polymer with a targeted primary chain length of 100 monomer units. This can be seen if the molar equivalent of acetyl sulphate added is plotted against the sulphonation percentage of the different branched polystyrenes, shown in Figure 7.18.

As can be seen from the graph in Figure 7.18 when 0.2 equivalents of acetyl sulphate is used, an abnormally high and probably anomalous result is observed. This may be as a result of the lack of solubility of this sample in methanol as a turbid solution was noticed immediately after ^{1}H NMR analysis. This issue with solubility was to prove problematic for a number of the branched sulphonated polymers, and many could not be analysed by ^{1}H NMR.

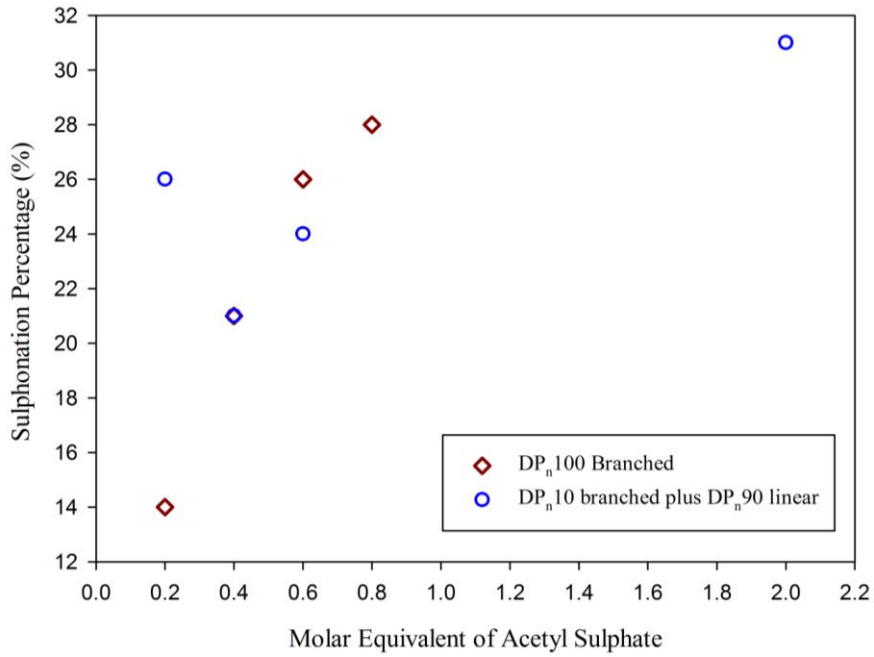

Figure 7.18: Graph illustrating the relationship between the amount of acetyl sulphate added (molar equivalent) and the percentage sulphonation for DP_n100 branched sulphonated polystyrene (brown open diamonds) and DP_n10 plus DP_n90 linear sulphonated polystyrene (blue open circles)

These reactions were repeated with branched polymers of different architectures including:

- DP_n10 branched
- DP_n25 branched
- DP_n50 branched
- DP_n50 branched plus DP_n50 linear
- DP_n50 linear plus DP_n50 branched

Again, analysis of these proved problematic. All samples that were generated from reactions with 0.2 equivalents of acetyl sulphate could not be analysed by ^1H NMR due to issues with turbidity, despite attempting various deuterated solvents, including DMSO and acetone; the sulphonated polymers appeared to react with acetone. For some samples, it was difficult to find a solvent for the different samples generated from the

reactions using varying concentrations of acetyl sulphate, making direct comparison impossible. For the two analogous branched polymers prepared with a targeted DP_n = 100 monomer units, but either from a branched polymer of 50 monomer units plus a linear chain of 50 monomer units or a linear chain of 50 monomer units plus a branched polymer of 50 monomer units a suitable solvent was not found. The photograph in Figure 7.19 shows a number of solvents that the polymers reacted with 0.8 equivalents of acetyl sulphate were insoluble in.

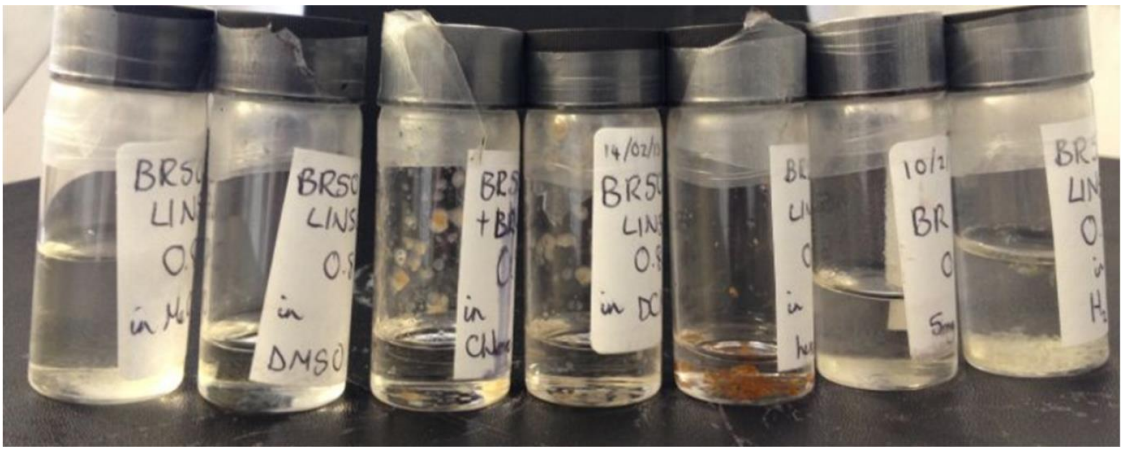

Figure 7.19: Photograph of sulphonated DP_n50 branched plus DP_n50 linear polystyrene in (L – R) methanol (MeOH), dimethylsulphoxide (DMSO), chloroform, dichloromethane (DCM), hexane, tetrahudrofuran (THF) and water (H_2O)

Table 7.7 summarises the range of sulphonated branched polymers synthesised, their changing solubility and where possible to analyse, their sulphonation percentage. THF solubility was also checked for later work involving the synthesis of nanoparticles.

Table 7: Solubility data and percentage sulphonation for all synthesised sulphonated polystyrenes of varied architecture.

Polymer Architecture	Molar Equivalent	Sulphonation Percentage	Solubility in H_2O	Solubility in MeOH	Solubility in THF
DP_n 10 branched	0.2	U*	N	N	Y
DP_n10 branched	0.4	U*	N	N	Y
DP_n10 branched	0.6	U*	N	Y	Y
DP_n10 branched	0.8	U*	N	Y	N

DP_n25 branched	0.2	U*	N	N	Y
DP_n25 branched	0.4	U*	N	N	Y
DP_n25 branched	0.8	U*	N	Y	N
DP_n 50 branched	0.2	U*	N	N	N
DP_n 50 branched	0.4	U*	N	N	Y
DP_n 50 branched	0.6	U*	N	Y	Y
DP_n50 branched	0.8	U*	N	Y	Y
DP_n50 branched DVB	0.4	22%	N	Y	Y
DP_n50 branched VPOOC	0.4	21%	N	Y	Y
DP_n10 branched VPODD	0.4	21%	N	Y	Y
DP_n100 branched	0.2	U*	N	Y	Y
DP_n100 branched	0.4	21%	N	Y	Y
DP_n100 branched	0.6	24%	N	Y	Y
DP_n100 branched	0.8	U*	N	Y	Y
DP_n100 branched	2	31	Y	Y	Y
DP_n10 branched plus DP_n90 linear	0.2	U*	N	Y	Y
DP_n10 branched plus DP_n90 linear	0.4	20.1%	N	Y	Y
DP_n10 branched plus DP_n90 linear	0.6	24%	N	Y	N
DP_n10 branched plus DP_n90 linear	0.8	U*	N	Y	N
DP_n10 branched plus DP_n90 linear	2	31%	N	Y	Y
DP_n50 branched plus DP_n50 linear	0.2	U*	N	N	Y
DP_n50 branched plus DP_n50 linear	0.4	U*	N	N	N
DP_n50 branched plus DP_n50 linear	0.6	U*	N	N	N
DP_n50 branched plus DP_n50 linear	0.8	U*	N	N	N
DPn50 linear plus DP_n50 branched	0.2	U*	N	N	Y
DPn50 linear plus DP_n50 branched	0.4	U*	N	N	N
DPn50 linear plus DP_n50 branched	0.6	U*	N	N	N
DPn50 linear plus DP_n50 branched	0.8	U*	N	N	N

U indicates gaps in the data whereby NMR spectroscopy could not be done, due in the majority to solubility issues in deuterated solvents.*

The next stage will be to synthesise sulphonated polystyrene nanoparticles from the synthesised sulphonated polymers.

7.7.1 Synthesis of linear polystyrene nanoparticles by nanoprecipitation

Polymer nanoparticles can be synthesised by a number of different methods, outlined in Chapter 1. The method used in this work is nanoprecipitation. Nanoprecipitation is also called the solvent displacement method, and this method was first patented by Fessi *et a.l* [7] It involves the precipitation of a preformed polymer from an organic solution and the diffusion of the organic solvent in the aqueous medium in the presence or absence of a surfactant. The polymer is dissolved in a water-miscible solvent, which is then added to a stirred aqueous solution. The solution may be neutral, acidic or basic and may contain a surfactant as a stabiliser. Polymer deposition on the interface between the water and the organic solvent, caused by fast diffusion of the solvent, leads to the instantaneous formation of a colloidal suspension.

Nanoprecipitation of sulphonated polystyrene requires the dissolution of each polymer in a suitable water-miscible solvent. The solvent used varied for different architectures of polymer and different sulphonation levels. At low sulphonation levels, such as those produced using 0.2 and 0.4 equivalents of acetyl sulphate, both linear and branched polystyrenes were soluble in either THF or MeOH. At higher sulphonation levels, the branched polymers were insoluble in a number of solvents, and therefore, unfortunately, nanoparticles were not synthesised from these sulphonated polymers.

To establish the best conditions for producing nanoparticles from the sulphonated polystryenes, solutions of both 10 $mgmL^{-1}$ and 5 $mgmL^{-1}$ were made for the different polymers in both MeOH and THF. 1 mL of the solutions were dropped by pipette into

different volumes of stirred, temperature water; these being 1 mL, 2 mL, 5 mL and 10 mL. Initially, distilled water with a neutral pH was used, but in later experiments both basic (pH 9) and acidic (pH 5) water was evaluated. After the solutions were added to water, the dispersions were left to stir overnight to allow evaporation of the organic solvent, yielding an aqueous solution of polymeric nanoparticles. A schematic illustration of this method is shown in Figure 7.20.

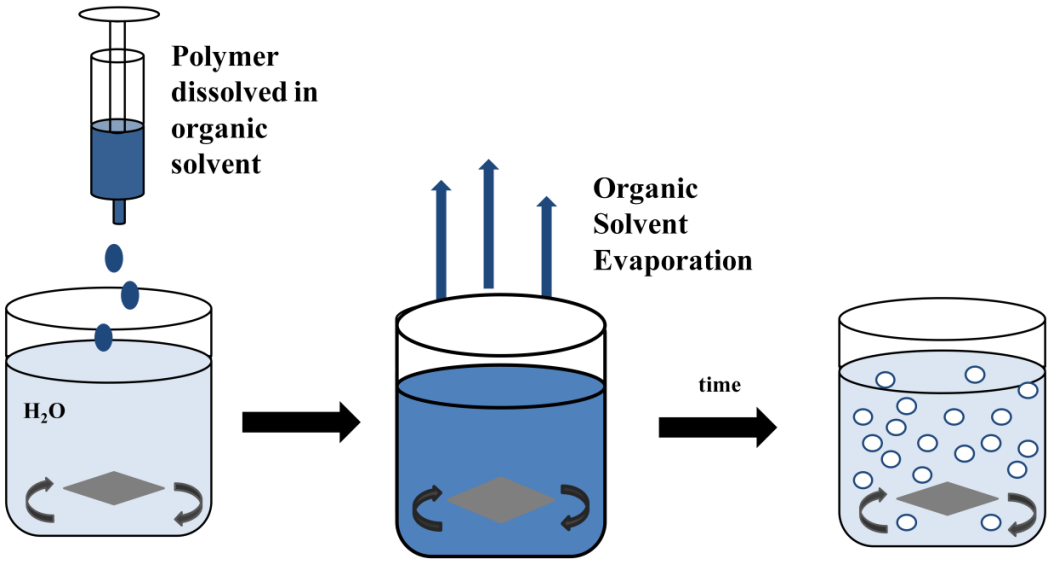

Figure 7.20: Schematic diagram of the nanaoprecipitaion method.

7.7.2 Analysis of linear polymer nanoparticles by dynamic light scattering (DLS)

Dynamic light scattering (DLS) is an analytical technique that is used to determine the size distribution of small particles in solution. The Brownian motion of particles or molecules in suspension causes laser light to be scattered at different intensities. Analysis of these intensity fluctuations yields the velocity of the Brownian motion and hence the particle size using the Stokes-Einstein relationship for diffusion of spherical particles through liquid [8].

$$D = k_B T/6\pi\eta r$$

Where D is the diffusion constant, k_B is the Boltzmann's constant, T is the absolute temperature, η is the viscosity and r is the radius of the spherical particle.

A large series of DLS measurements were conducted on all the nanoparticles synthesised from sulphonated linear polystyrenes. For the series of sulphonated linear polystyrene with a targeted DP_n = 100 monomer units, nanodispersions were prepared from initial solutions with concentrations of 10 $mgmL^{-1}$ and 5 $mgmL^{-1}$ and either 1 mL or 2 mL of these solutions were introduced dropwise into 1 mL or 10 mL of water to evaluate the conditions for nanoprecipitation. It was found that the nanoparticle sizes generated in this way are heavily influenced by both the amount of sulphonation, and the dilution factor. Almost no reproducibility of the size of the nanoparticles across a range of dilution factors was observed and the particle size distributions measured by DLS were rarely monodisperse in size.

The same nanoprecipitation and DLS analysis was repeated with all other primary chain lengths of the sulphonated linear polystyrene polymers, previously discussed in 7.6.1, using a single standardised approach (1 mL of a 5 $mgmL^{-1}$ solution of sulphonated polystyrene pippeted into 5 mL of neutral water). In an attempt to enhance the nanoparticle stability in water, all experiments were also repeated as dilutions into 5 ml of weakly basic (~pH 9) water. In all cases, the sulphonated polystyrene nanoparticles are not very monodisperse in size with the distributions becoming broader with increasing degrees of sulphonation. No specific trends in nanoprecipitate size could be dteremined with polymer chain length or degree of sulphonation. Table 8 gives the values of the z- average diameter, PDI and size of each peak for some of the better results obtained.

In general, the lower the degree of sulphonation the more likely the linear polystyrenes are to produce good nanoprecipitates. This is unsurprising as higher water solubility would be expected to lead to poor precipitation. The influence of precipitating into basic water (~pH 9) was also studied and the results are shown in Table 7.8.

Table 7.8: PdI and Z-average values for nanoparticles synthesised using linear polystyrenes with increasing targeted DP_n values, different aqueous conditions and increasing degress of sulphonation

Sulphonated Polymer	Aqueous Conditions	Peak 1(d.nm)	Peak 2 (d.nm)	PdI	Z-average (d.nm)
DP_n25 Linear 1:0.2 equiv.	Neutral H_2O	100.1 (89.5% intensity)	4,793	0.393	68.4
DP_n25 Linear 1:0.2 equiv. Repeat.	Neutral H_2O	83.3 (89.5% intensity)	5,440	0.407	70.72
DP_n100 Linear 1:0.2 equiv.	Neutral H_2O	193.6 (89.4% intensity)	30.47	0.438	279
DP_n500 Linear 1:0.4 equiv.	Neutral H_2O	70.6 (97.3% intensity)	4,957	0.372	55.16
DP_n25 Linear 1:0.2 equiv.	pH9 H_2O	78.4 (97.5% intensity)		0.277	63.91
DP_n50 Linear 1:0.2 equiv. Repeat.	pH9 H_2O	136.6 (70% intensity)	30.0	0.307	134.70
DP_n500 Linear 1:0.2 equiv.	pH9 H_2O	259.8 (74% intensity)	53.58	0.441	190.9

From these studies it would seem that linear polystyrenes do not produce good nanoparticles.

7.8 Nanoprecipitation of sulphonated branched polystyrenes.

With the failure of the linear sulphonated polystyrenes to produce monodisperse nanoprecipitated particles, a series of experiments were also attempted with a selection

of sulphonated branched polystyrene. The level of sulphonation across a series of branched polystyrenes was chosen (materials produced using 0.8 equivalents of acetyl sulphonate) and the DP_n values of the primary chains and block polymer architecture was varied. To establish any influence of initial solvent, both methanol and THF were tested and again both neutral and basic water was used in repeated experiments. Initial concentrations of 5 $mgmL^{-1}$ and 10 $mgmL^{-1}$ of polymer in water miscible solvent were used and preparations using 1 mL of these solutions were dropped into either 5 mL or 2 mL of water to vary the dilution range.

As mentioned previously there were solubility issues with a large proportion of the sulphonated polymers synthesised, as a result nanoparticles could not be synthesised from a number of these architectures.

It was found from the large number of DLS experiments performed that nanoparticles produced from the sulphonated highly branched DP_n10 branched polystyrenes displayed good PDI values, and reproducible z-average diameter values. The DLS results are tabulated in Table 9, and the DLS traces are shown in Figure 7.21.

Table 9: PdI and Z-average values for nanoparticles synthesised using DP_n10 branched sulphonated polystyrenes with different aqueous conditions and increasing degress of sulphonation

Sulphonated Polymer	Molar equivalent of acetyl sulphate	Aqueous Conditions	Peak 1(d.nm)	PDI	Z-average (d.nm)
DP_n10 branched	0.2	pH9 H_20	66.6	0.27	60.8
DP_n10 branched	0.4	pH9 H_20	59.7	0.15	54.4
DP_n10 branched	0.6	pH9 H_20	53.2	0.23	41.2
DP_n10 branched	0.2	neutral H_20	64.6	0.27	59.46
DP_n10 branched	0.4	neutral H_20	58.6	0.24	48.3
DP_n10 branched	0.6	neutral H_20	52.1	0.24	42.84

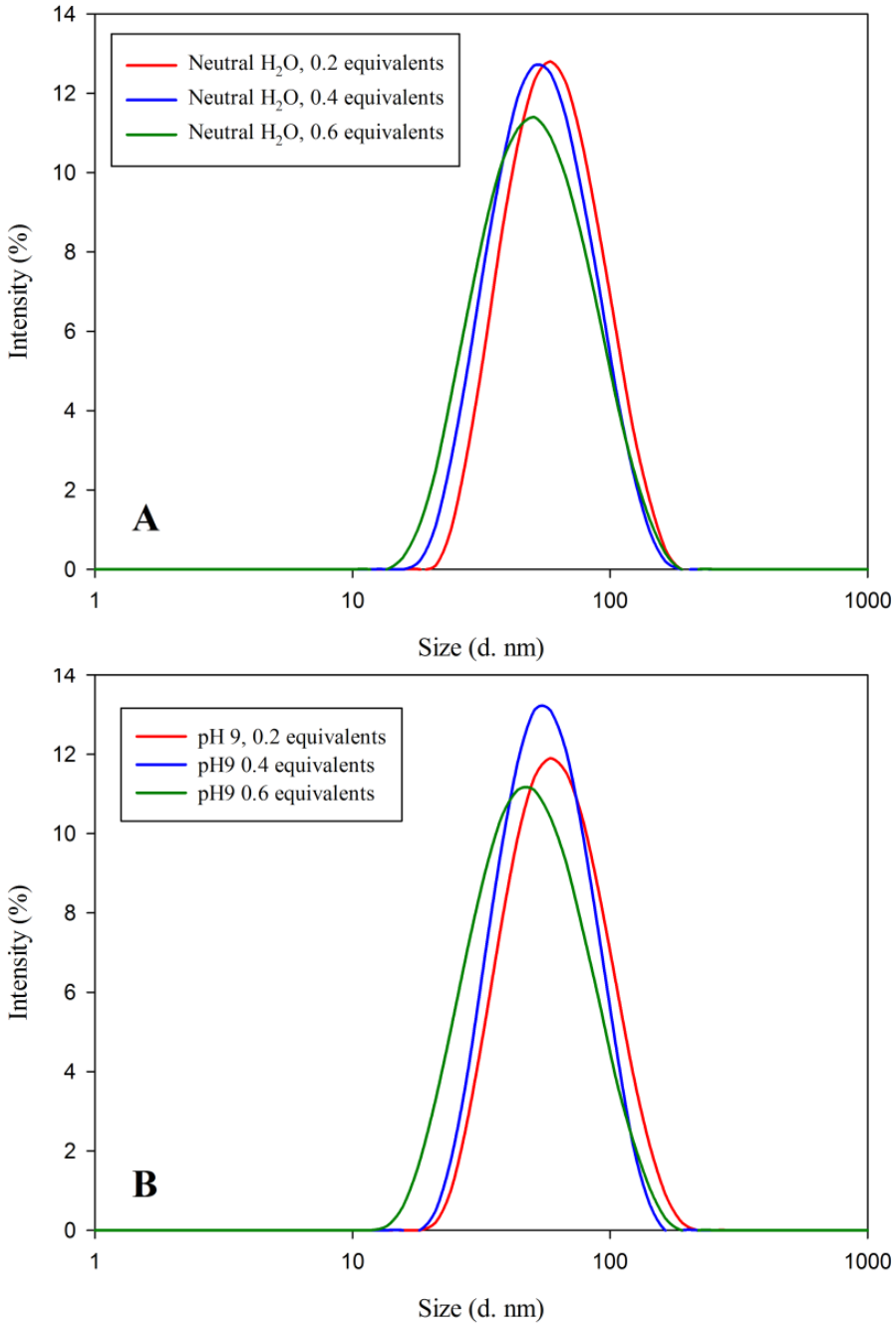

Figure 7.21: DLS particle size distribution for DP_n10 branched, sulphonated polystyrene nanoparticles in (A) neutral H2O and (B) basic pH9 H_2O

As can be seen from Table 7.9, the z-average diameters of the nanoprecipitates produced from the sulphonated polymers derived from branched polystyrene with a target primary chain length of 10 monomer units are of a similar size with a general

trend of decreasing nanoparticle size with increasing sulphonation and nanoprecipitation into weakly basic water, seen in Figure 7.22.

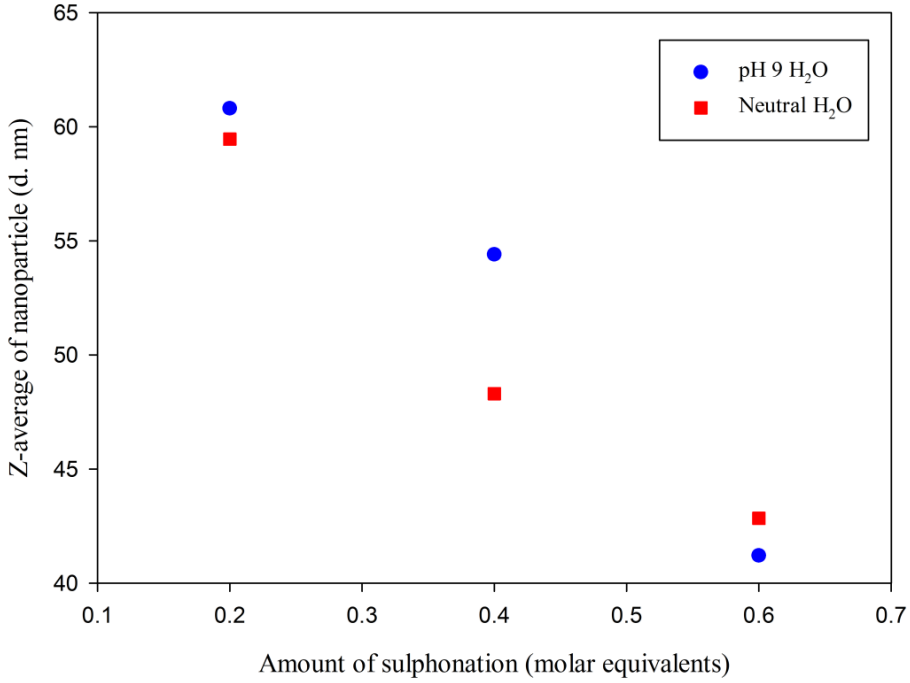

Figure 7.22: Graph showing the relationship between the Z-average of the DP_n10 branched sulphonated polystyrene nanoparticles with increasing amounts of sulphonation in neutral aqueous conditions (red squares) and basic (pH9) conditions (blue circles)

It can be seen that as the amount of sulphonation increases, the size of the particles decreases. This is due to the extra stability the higher sulphonation affords, and therefore the nanoparticles are colloidally stable at lower particle sizes. To test the relative stabilities of the nanoparticles the DLS experiments were repeated on the same nanoparticles that had been stored in conditions for 6 months. It was found that the nanopatricles synthesised from the sulphonated DP_n10 branched polystyrenes were still relatively monodisperse, and the Z-average values were very similar to the ones at t = 0, this being immediately after nanoparticle formulation. Table 7.10 gives the results of what are believed to be the most stable nanoparticles.

Table 7.10: PdI and Z-average values for nanoparticles synthesised from branched DPn10 sulphonated polystyrenes, after 6 months, and compared to t = 0 values also shown in the table.

Sulphonated Polymer	Molar equivalent of acetyl sulphate	Aqueous Conditions	PDI	z-average (d.nm) at t = 0	z-average (d.nm)
DP_n10 branched	0.2	Neutral H_20	0.24	59.46	56.5
DP_n10 branched	0.4	neutral H_20	0.20	48.3	48.9
DP_n10 branched	0.4	pH9 H_20	0.32	54.4	58.5
DP_n10 branched	0.6	pH9 H_20	0.31	41.2	42.27

7.9 Analysis of sulphonated polystyrene nanoparticles by scanning electron microscopy (SEM)

A scanning electron microscope (SEM) is a type of electron microscope that produces images of a sample by scanning it with a focused beam of electrons. The SEM uses a focused beam of high-energy electrons to generate a variety of signals at the surface of solid specimens. Figure 7.23 shows some images obtained from the stable DP_n10 branched sulphonated polystyrene nanaoparticles after drying from water onto a surface.

From the images in Figure 7.23 it appears that the nanoparticles form films. If we zoom in on the images, while there is some resolution lost there may be some structures visible. If we take the image in Figure 7.24 (A) on a micron scale the surface looks very flat and film-like. However if we look on a 500nm scale (B) , and even further on a 50nm scale (C) there may be some particles visible, indicated by the arrows in Figure 7.24 (C). These images are not satisfactory to conclude definitely that nanoparticles can be seen, and further work is needed, and discussed in Chapter 8.

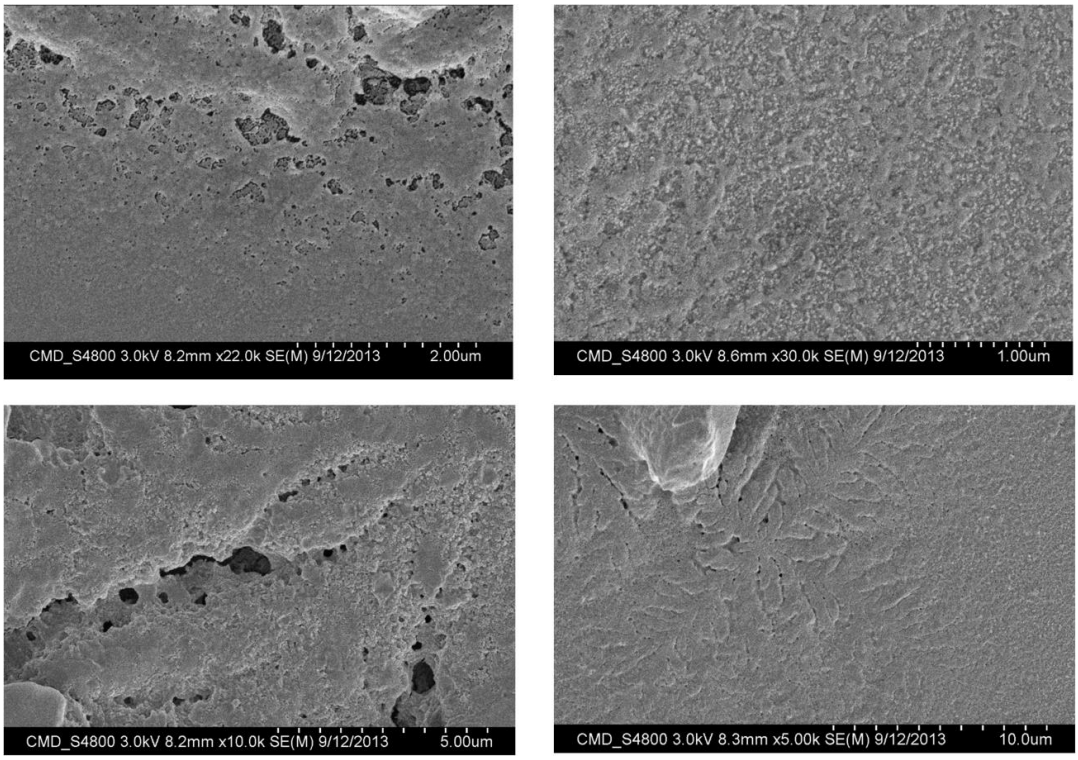

Figure 7.23: SEM images of nanoparticles synthesised from sulphonated DP_n10 branched polystyrenes

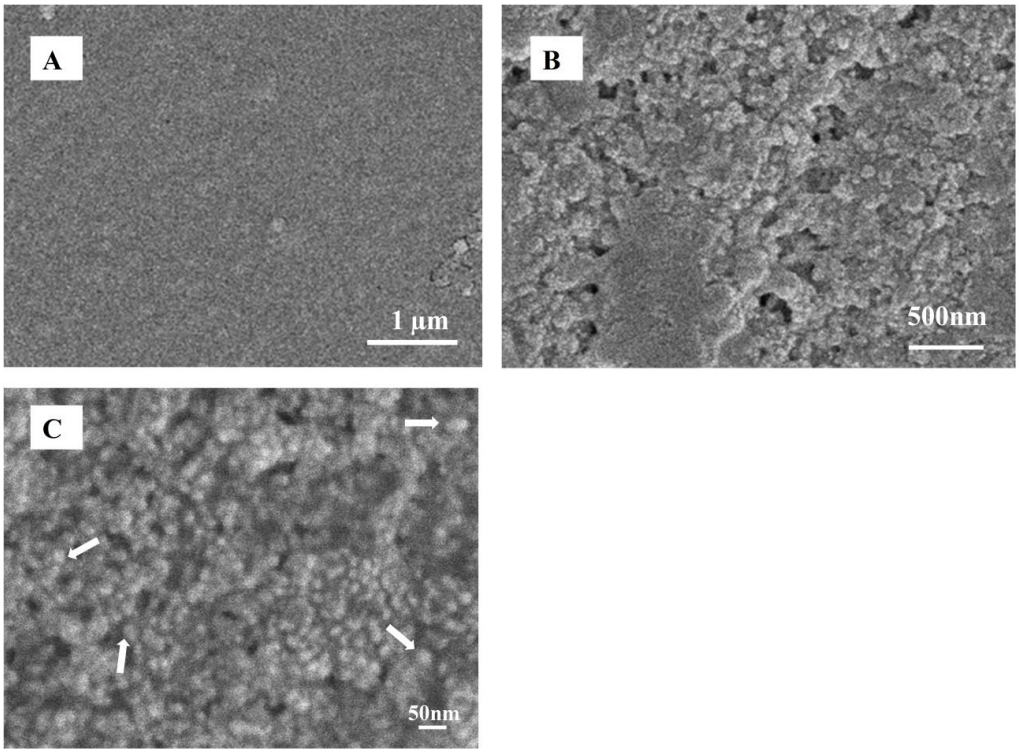

Figure 7.24: SEM images of nanoparticles synthesised from sulphonated DP_n10 branched polystyrenes on a (A) 1 µm scale, (B) 500 nm scale and (C) 50 nm scale.

7.10 Conclusions

The functionalisation of polystyrene has been investigated in order to introduce hydrophilicity into the range of branched polystyrene architectures, synthesised in previous Chapters, to enable the synthesis of polymer nanoparticles *via* nanoprecipitation techniques

Attempts to place an amine containing compound at both chain ends of the primary chains of branched polymers showed that initiation with *sec*-BuLi and ADPE could achieve close to 100% functionalisation of the initiating chain end. Unfortunately, termination by ADPE did not reach a satisfactory level. Due to this, the planned further work whereby the amine groups would be post-functionalised and a hydrophilic polymer grown from these sites was not carried out.

An alternative method to introduce hydrophilicity to the branched polystyrenes was sought, and the sulphonation of polymers of different architectures was investigated at different levels of sulphonation. Although there were experimental issues with the analysis of the sulphonated polymers, trends could be observed within the different architectures and it appears to be more difficult to sulphonate branched polymers than their linear equivalents.

From these sulphonated polymers, nanoparticles were synthesised by a nanoprecipitation method. These were analysed by DLS and the sulphonated branched polystryenes from a target primary chain of 10 monomer units produced nanoparticles in neutral and basic water with monodisperse size distributions that remained stable after storage for at least 6 months.

7.11 References

1. Jungahn, K.; Kwakl, S.; Kim, K.U.; Kim, K.H.; Cho, C.C., Jo, W.H.; Kim, D., *Macromol. Chem. Phys*., **1998**, *199*, 2185

2. Gnanou, P.; Lutz, P., *Makromol. Chem*.**1989**, *190*, 577

3. Quirk, R.P.; Lynch, T., *Macromolecules*, **1993**, *26*, 1206

4. Kucera, F.; Jancar, J., *Chem. Papers*, **1996**, *4*, 224

5. Fathima, N.N.; Aravindhan, R.; Lawrence, D.; Yugandhar, U.; Moorthy, T.S.R.; Nair, B.U., *J. Sci. Ind. Res*., **2007**, *66*, 209

6. Mock, E.B.; Bruyn, H.; Hawkett, B.S.; Gilbert, R.G.; Zukosi, C.F., *Langmuir*, **2006**, *22*, 4037

7. Fessi, H.; Puisieux, F.; Devissaguet, J.P., Devissaguet, *Eur. Patent*, **1987**, *274*, 961

8. www.malvern.com

Chapter 8

Conclusions and Further Work

8.1 Conclusions

Linear polystyrene chains have been synthesised by both ATRP and anionic polymerisation methods. The viability of ATRP as a method for synthesising controlled polymer chain length linear polystyrenes has been evaluated and rejected as a suitable method for synthesising the targeted complex architectures of the project due to poor control over chain length and low conversion of monomer to polymer within the observed extended reaction timescales.

Anionic polymerisation has been shown to be a viable method for producing linear polystyrenes at high conversion levels with excellent control over the chain length and the polydispersity. Very monodisperse polymers have been readily and reproducibly targeted with dispersity values as low as 1.02, without the specialist equipment and techniques conventionally employed for anionic polymerisation.

The kinetics of the reaction have been investigated along with a series of reaction variables to ascertain the best conditions for the synthesis. The living nature of the polymerisation *in situ* has also been tested in a series of self-blocking experiments. It was found that self-blocked polymers could be produced with a controlled chain length in a relatively short time. Initiation by *sec*-BuLi alone and using lithium-halide exchange approaches has been explored. The latter has led onto the attempted synthesis of bifunctional initiators for anionic polymerisation but within the scope of this work it was found to be unsuccessful.

Branched polystyrenes have been synthesised by ATRP and anionic polymerisation techniques. Different dystryl compounds have been tested as brancher compounds and their relative suitability assessed. The commercially available DVB has been replaced with synthesised dystyrl compounds, allowing for greater control over the issues arising from the many isomers of DVB. A series of compounds with increasing space between the two vinyl groups were synthesised to prevent modification of reactivity during polymerisation. Branched polystyrenes were produced from all of these compounds.

The conditions of the branched polymerisation were investigated, and many variables changed. The architecture of branched polymers has been successfully manipulated by controlling the primary chain length of the polymer, and also through a series of self-blocking polymerisations that ensure the branching is limited to specific areas of the primary chains. It was found that the lower the primary chain length, the greater the degree of branching. This offers further control over the architecture of the branched polymers.

The effect of the primary chain length on the polymer architecture has been investigated by GPC analysis, and the analysis of physical properties by DSC. The behaviour in solution has also been examined by differential viscometry measurements. This has led to an interpretation of the extent of branching and how the size of the linear chain affects this. It has been found that as the primary chain length increases, the degree of branching decreases, at least when considering the weight average macromolecules synthesised over a series of polymerisation conditions. As a result of this decrease in branching, less dense structures are formed. This has been confirmed by analysis of the intrinsic viscometry. It was found that the most highly branched structure had a primary chain length of $DP_n = 10$ monomer units.

The functionalisation of polystyrene has been investigated in order to introduce hydrophilicity into the range of branched polystyrene architectures, to enable the synthesis of polymer nanoparticles *via* nanoprecipitation techniques. Attempts to place an amine containing compound at both chain ends of branched showed that initiation with *sec*-BuLi and ADPE could achieve close to 100% functionalisation of the initiating chain end but, unfortunately, termination by ADPE failed to reach a satisfactory level. Hydrophilicity was introduced to the branched polystyrenes by the sulphonation of polymers of different architectures, and different levels of sulphonation were investigated. Although there were experimental issues with the analysis of the sulphonated polymers, trends could be observed within the different architectures and it appears to be more difficult to sulphonate branched polymers than their linear equivalents.

From these sulphonated polymers, nanoparticles were synthesised by a nanoprecipitation method. These were analysed by DLS and the sulphonated branched polystyrenes from a target primary chain of 10 monomer units produced nanoparticles in neutral and basic water with monodisperse size distributions that remained stable after ambient storage for at least 6 months. Attempts to image the nanoparticles were relatively unsuccessful and so further work is needed.

8.2 Further work

8.2.1 Alternative method of synthesising branched polystyrene by anionic polymerisation.

As discussed in the solvent concentration results in Chapter 4, a gel can form from the association of the ions present at the end of each polystyrene chain. This ionic association was found to be greater at higher solid content levels. A way to overcome one of these effects is to decrease the number of anions on the branched polymer.

As the brancher compound VPOB has to be synthesised, and can only be marginally scaled up in size due to the multi-step purifications, a method that offered an alternative to this would be advantageous. A novel method combining 'living' anionic polymerisation with a convergent growth process was reported by Knauss *et al* [1] who formed dendritically branched polystyrene by using vinyl-functionalised reactants to produce macromonomers that react through their double bonds with 'living' polystyrene chain ends to give dimerised chains.

In a further study, the fast addition of VBC to an anionic polymerisation of styrene, and the effects on molecular weights of changing the solvent mixture, the amounts of VBC added and increasing the primary polystyrene chain length were investigated. The difference between the step-wise addition of styrene and VBC and the consecutive addition of a mixed VBC/styrene monomer feed was also considered. The preliminary results appeared to demonstrate that branched structures can be synthesised from this divergent branching method, the methodology is more complex than branching from a one-addition synthesis with a distyrl branching monomer such as DVB or VPOB. Further work is needed to optimise these conditions. The results of this further work are given in the Supporting Information 3.

8.2.2 Encapsulation of substances within the nanoparticles

As the aim of the nanoparticle synthesis was to ultimately produce materials to act as a vehicle to transport antiretroviral drugs through the body, the ability to encapsulate these drugs is of great importance.

Preliminary experiments to explore the ability to encapsulate compounds were accomplished using the nanoparticles deemed the most stable, and forming the most monodisperse nanoparticles. As discussed in Chapter 7 this was the sulphonated DP_n10 branched polymer nanoparticles.

The sulphonated polymers were dissolved in the water miscible solvent THF, together with the hydrophobic diazo dye Oil red. This resulting solution was dropped into stirred ambient water, as with the previous nanoprecitipations. This was repeated for DP_n10 branched sulphonated polymers, produced using 0.4 equivalents of acetyl sulphate, into both neutral and basic (pH 9) water. Photographs of the resulting nanoparticle solutions are shown in Figure 8.1 (A) and 8.1 (B) respectively. Controls were also formulated; Figure 8.1 (C) shows a DP_n100 linear polystyrene with no sulphonate groups and Figure 8.1 (D) shows a DP_n10 branched polystyrene, with no sulphonate groups.

As can be seen, it appears that unsulphonated linear polystyrenes do not form nanoparticles and cannot encapsulate oil red. Branched, unsulphonated polystyrenes form a very turbid solution, indicating that this is also unsuccessful. The sulphonated polymers nanoparticles appear to encapsulate the oil red dye, however this may be an effect of the stabilising nature of the nanoparticles acting as a surfactant. Further work is needed to explore the encapsulation abilities of these nanoparticles.

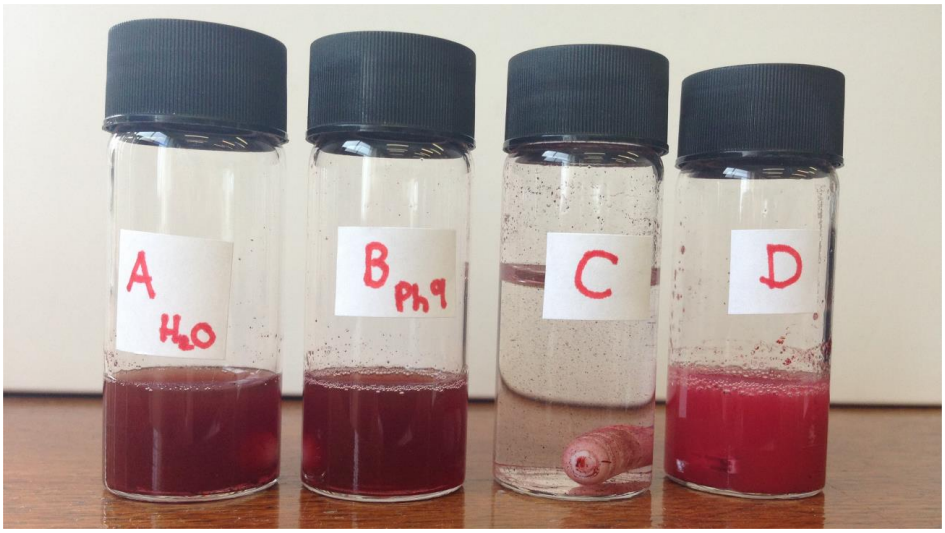

Figure 8.1: Photograph of the attempted encapsulation of oil red in polystyrene nanoparticles. Reaction conditions: (A) 5 $mgmL^{-1}$ solution of DP_n10 branched polystyrene sulphonated with 0.4 equivalents of acetyl sulphate in THF with 0.01mg oil red dye dropped into 5 mL of stirred ambient neutral water, after solvent evaporation. (B) 5 $mgmL^{-1}$ solution of DP_n10 branched polystyrene sulphonated with 0.4 equivalents of acetyl sulphate in THF with 0.01mg oil red dye dropped into 5 mL of stirred ambient pH 9 water, after solvent evaporation. (C) 5 $mgmL^{-1}$ solution of DP_n100 linear polystyrene in THF with 0.01mg oil red dye dropped into 5 mL of stirred ambient neutral water, after solvent evaporation. (D) 5 $mgmL^{-1}$ solution of DP_n10 branched polystyrene n THF with 0.01mg oil red dye dropped into 5 mL of stirred ambient neutral water, after solvent evaporation.

8.2.2 Imaging of the nanoparticles

As was seen with the SEM images that were obtained, further work is needed to obtain better images of the nanoparticles, and their structures. One option for this is transmission electron microscopy (TEM). TEM is a powerful and unique technique for structure characterisation.

Wang has reported the successful imaging of shape controlled nanocrytsals. [2] The most important application of TEM is the atomic-resolution real-space imaging of nanoparticles. By forming a nanometer size electron probe, TEM is unique in identifying and quantifying the chemical and electronic structure of individual nanocrystals. In a conventional TEM, a thin specimen is irradiated with an electron beam of uniform current density. [3] An image is formed from the interaction of the

electrons transmitted through the specimen; the image is magnified and focused onto an imaging device, such as a fluorescent screen, on a layer of photographic film or to be detected by a sensor such as a charge coupled device camera. In further work, this technique could be utilised to obtain images of the nanoparticles synthesised.

8.3 References

1. Knauss, D. M., Al-Muallem, H.A., Huang, T., Wu, D.T.; *Macromolecules*, 2000, *33*,3557

2. Wang, Z. L., J. *Phys. Chem. B,* 2000, *104*, 1153

3. Relmer, L.; Kohl, H., Transmission electron microscopy: Physics of image formation, 2008, 5th Edition, Springer: New York

Supporting Information

Table of Contents

List of Figures

List of Tables

List of Schemes

Appendix 1

GPC Chromatograms

Chapter 3

3.2.1 Atomic Transfer Radical Polymerisation (ATRP)

3.2.2.1. Synthesis of linear polystyrenes at ambient temperature.

3.2.2.1.1 Effect of changing the initiating system for ambient anionic polymerisation

3.2.2.1.2 Effect of solvent concentration on ambient anionic polymerisation.

Chapter 5

5.1 Effect of primary chain length

5.2 Chain extension of branched polymers

5.2.1 Equivalent to DPn100

5.2.2 Equivalent to DPn50

Chapter 8

8.2.3 Alternative method of synthesising branched polystyrene by ambient anionic polymerisation.

8.2.2 Branching from branched structures *in situ*.

Appendix 2

DSC Thermograms

Chapter 6

6.3.1 T_g of linear polystyrenes

6.3.2. T_g of branched polystyrenes

6.3.3 Effect of polymer architecture on T_g

6.3.4 Effect of brancher compound on T_g

Appendix 3

^{13}C NMR Specta

Chapter 4

4.4 Branching with alternative dystyrl brancher compounds

Supporting Information

SI.1 Atomic transfer radical polymerisation (ATRP)

SI. 1.1 Synthesis of linear polystyrenes by ATRP methods

ATRP is well documented as being one of the most widely used methods of controlled radical polymerisation (CRP) and it offers a robust way to control the chemical composition and architecture of polymers. ATRP was chosen here due to its relatively simple experimental procedure. One of the major advantages of ATRP is it can be tolerant to a wide range of functionalities and experimental conditions, compared to ionic polymerisation.

As discussed previously the ability to reach high monomer conversions is important in the synthesis of the polymers using a branched vinyl polymerisation strategy. A number of variables can affect the polymerisation. One of these variables is reaction temperature. For example Sawamoto and co-workers [1] found that at ambient temperature the rhenium catalysed polymerisation of styrene reached 83% monomer conversion but this took 27 days to achieve. Increasing the temperature was found to significantly increase the rate of reaction and the conversion.

Another variable that can influence the polymerisation is the ligand used within the chosen catalyst system. The ligand forms a catalyst complex with the transition metal and the degree of control over the polymerisation reaction can be affected by the

electron donating ability of the ligand as it can affect the reactivity of the metal centre in halogen abstraction and transfer.

ATRP is based on an inner sphere electron transfer process, which involves a reversible homolytic (pseudo)-halogen transfer between a dormant species, an added initiator or dormant propagating chain end (R-X or R-P_n-X) and a transition metal complex in the lower oxidation state (Mt^z/L_m), resulting in the formation of propagating radicals and the metal complex in the higher oxidation state with a coordinated halide ligand (e.g. X-Mt^{z+1}/L_m). A simplified mechanism is shown below in Scheme SI.1, whereby P is the polymer chain, Mt^n is the transition metal, L is the complexing ligand and X is the halogen.

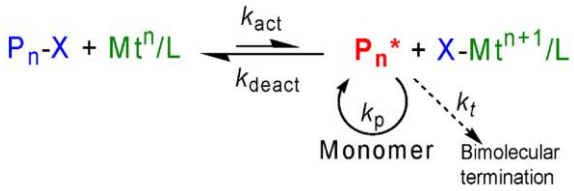

Scheme SI.1: Summary of the fundamental mechanism of ATRP [2]

As the rate of polymerisation can be affected by the variables discussed above, such as ligand type and reaction temperature, a number of different experiments were undertaken within this study in order to investigate the viability of ATRP in the formation of branched polystyrene and to find the best conditions with the highest conversion for this polymerisation. A series of variables were altered as outlined below.

- Ligand: four different amine ligands were employed, namely 2,2'bipyridine, *N*,*N*,*N*′,*N*″,*N*″-Pentamethyldiethylenetriamine (PMDETA), tris[2-(dimethyl amino) ethyl]amine (Me6 [TREN]), 4'4'di-n-nonyl 2,2'bipyridine
- Temperature: three different temperatures were used, namely ambient, 60 °C and 90°C

- Solvent: two different solvents were studied, namely benzene and toluene

In the initial experiments, 0.0739 g (0.747 mmol) of copper chloride powder and 0.233 g (13.6 mmol) of 2,2'-bipyridine were added to a round bottomed flask. In order to enhance the accuracy of the volume of initiator, 100 μL of the initiator ethyl α-bromoisobutyrate was added each time. The amount of monomer was calculated accordingly to allow for a targeted DP_n of 50 monomer units. The reported stoichiometries suggested for monomer:initiator:catalyst:ligand is 1:1:1:2 respectively, although experimentally 1:1:1.1:2.2 was used to allow for a slight excess of ligand. 20 mL of benzene was added (this was later changed in following experiments to 4mL of toluene) and the system degassed for 10 minutes under bubbled nitrogen purging to remove any oxygen from the system. For a polymer with a target DP_n of 50 monomer units it was calculated that 339.7 mmol of monomer was needed, therefore 3.98 mL (339.7 mmol) of styrene and 100 μL of the initiator ethyl α-bromoisobutyrate was therefore added. A colour change to brown/red was observed and the reaction was left to stir at ambient temperature for 24 hours.

When the reaction was fully terminated due to the introduction of oxygen into the system, the colour changed to a blue/green and the copper catalyst had to be removed by column chromatography, by passing through basic alumina. The resulting solution was then precipitated into cold methanol to yield the polystyrene product. The reaction scheme is shown in Scheme SI.2.

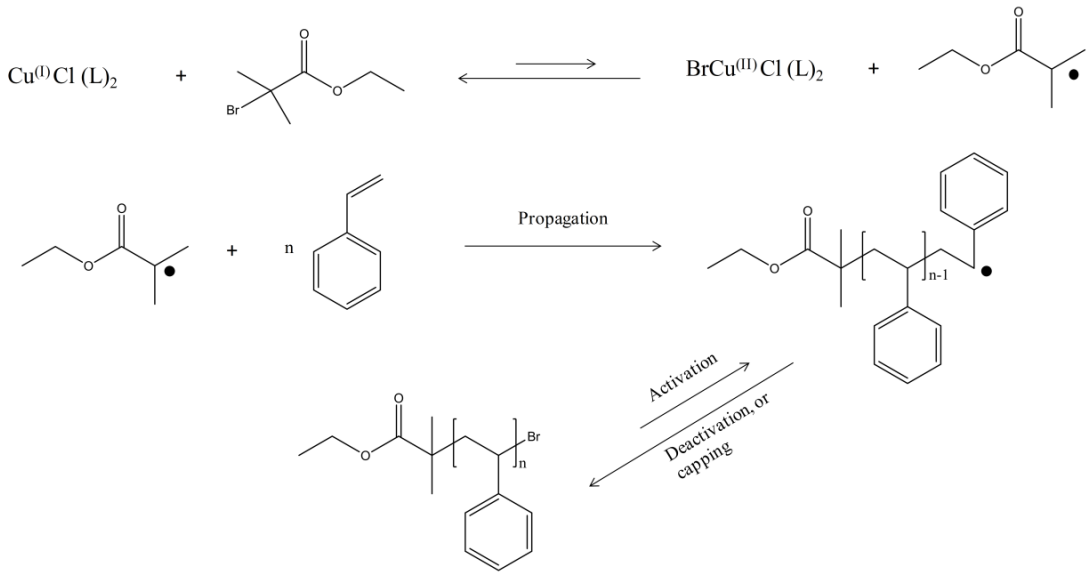

Scheme SI.2: General reaction scheme for the ATRP of polystyrene, initiated with ethyl α-bromoisobutyrate, metal catalyst is Cu(I)Cl and whereby L is the ligand used. See Figure 3 for the different ligands used.

The monomer conversion (i.e. the percentage of monomer introduced which has been converted into polymer) could be determined by proton nuclear magnetic resonance spectroscopy in $CDCl_3$ (^1H NMR) on a crude sample of the reaction medium. An example ^{1}NMR spectrum is shown below in Figure SI.1 for illustration of the method of calculation, whereby PMDETA was the ligand and toluene was the reaction solvent.

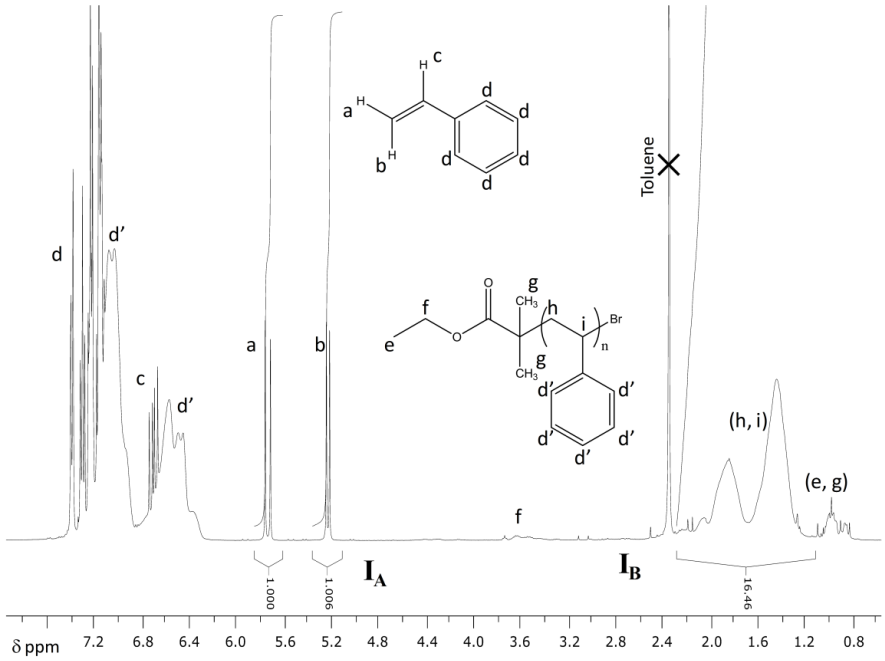

Figure SI.1: ^{1}H NMR spectrum of polystyrene synthesised by ATRP. Reaction conditions; ethyl α-bromoisobutyrate initiator, $Cu^{(I)}Cl$ metal catalyst, toluene as solvent, 50ºC, 24 hours. ^{1}H NMR analysis in $CDCl_3$

The vinyl protons (labelled a and b in Figure SI.1) due to the residual monomer can clearly be seen at approximately 5.20 ppm and 5.80 ppm. Comparison of these integrated signals with those due to the polystyrene backbone (labelled h and i in Figure SI.1) between 1.00 ppm and 2.30 ppm allowed the conversion to be estimated using the following equation:

$$Conversion = ((I_B / 3) / [(I_B / 3) + (I_A / 1)]) * 100$$

Where I_B (labelled on the spectrum in Figure SI.1) is the integral between 1.00 and 2.30 ppm and I_A is the integral of the ^{1}H NMR signals at 5.20 ppm. Confirmation of the conversion can also obtained by utilising the signal at 5.80 ppm as this is also indicative of unreacted monomer. The signal of the reaction solvent (toluene in this case) can be seen at 2.50 ppm and the signals of the catalytic system and ATRP initiator (<1.00 ppm)

overlay slightly with the signal of the polystyrene backbone. This may increase the error of the calculated conversion.

The initial experiments were conducted in benzene at ambient temperature and utilised 2,2'-bipyridine as the complexing ligand. It was found that the percentage conversion was below 50% after 24 hours. The reaction was repeated at 60 ºC, but again the conversion after 24 hours under these conditions was very low, below 50%. A series of experiments, whereby the complexing ligand was changed, was conducted. The temperature of the reaction was also raised to 90ºC and, as benzene boils at ~80 ºC, toluene was employed as the reaction solvent; all of the complexing ligands were soluble in toluene and it has a boiling point of 111 ºC so this was used as the solvent in all further ATRP experiments.

The complexing ligands investigated are illustrated in Figure SI.2. Spectra from these ATRP reactions using these ligands are shown in Figure SI.3 and the GPC analysis of the purified polymers (refractive index chromatograms) are shown in Figure SI.4.

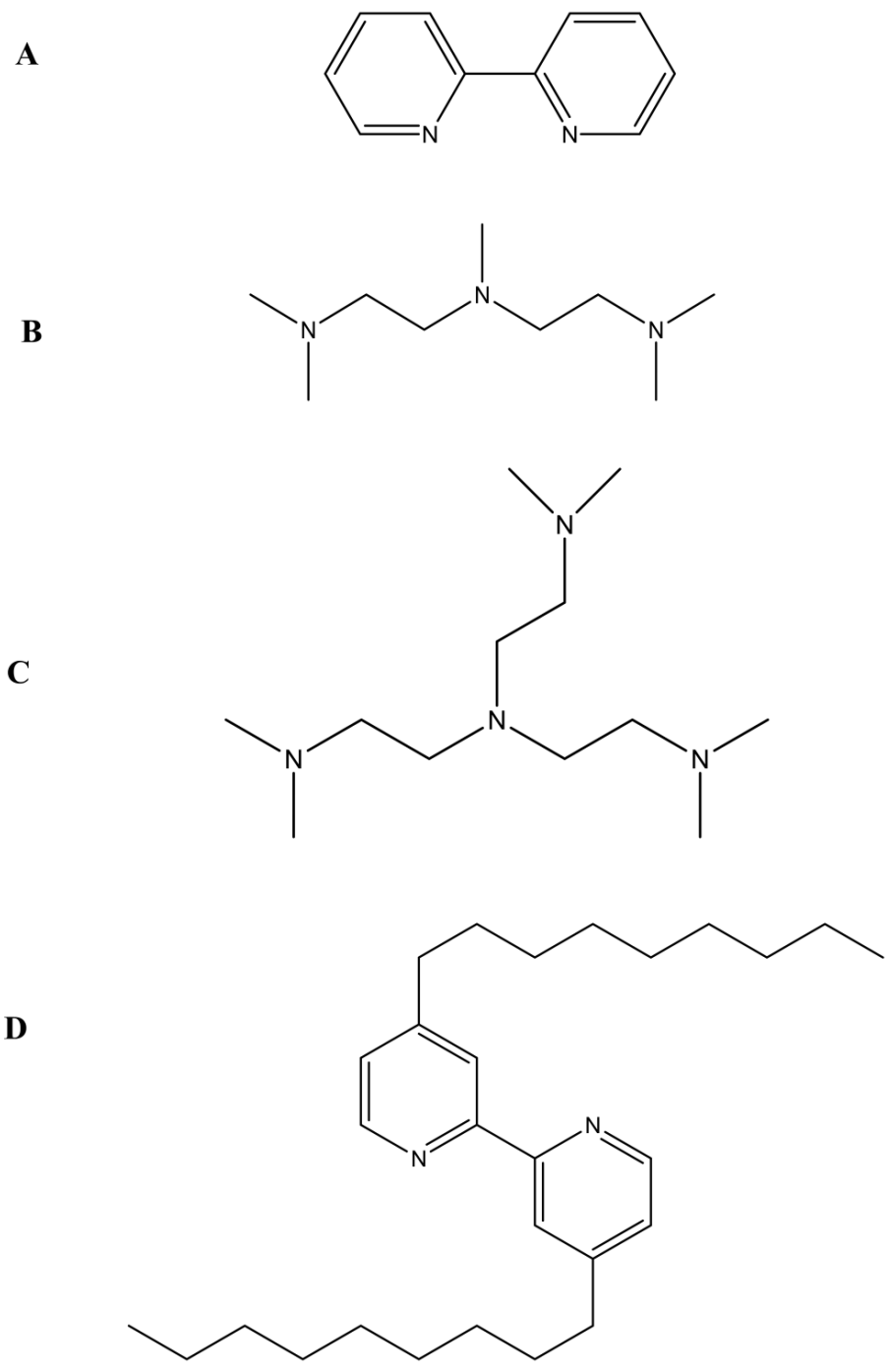

Figure SI.2: Ligands used in ATRP polymerisations of styrene (A) 2,2'bipyridine (B) *N*,*N*,*N*′,*N*″,*N*″-Pentamethyldiethylenetriamine (PMDETA) (C) tris[2-(dimethylamino) ethyl]amine (Me6 [TREN]) and (D) 4'4'di-n-nonyl 2,2'bipyridine

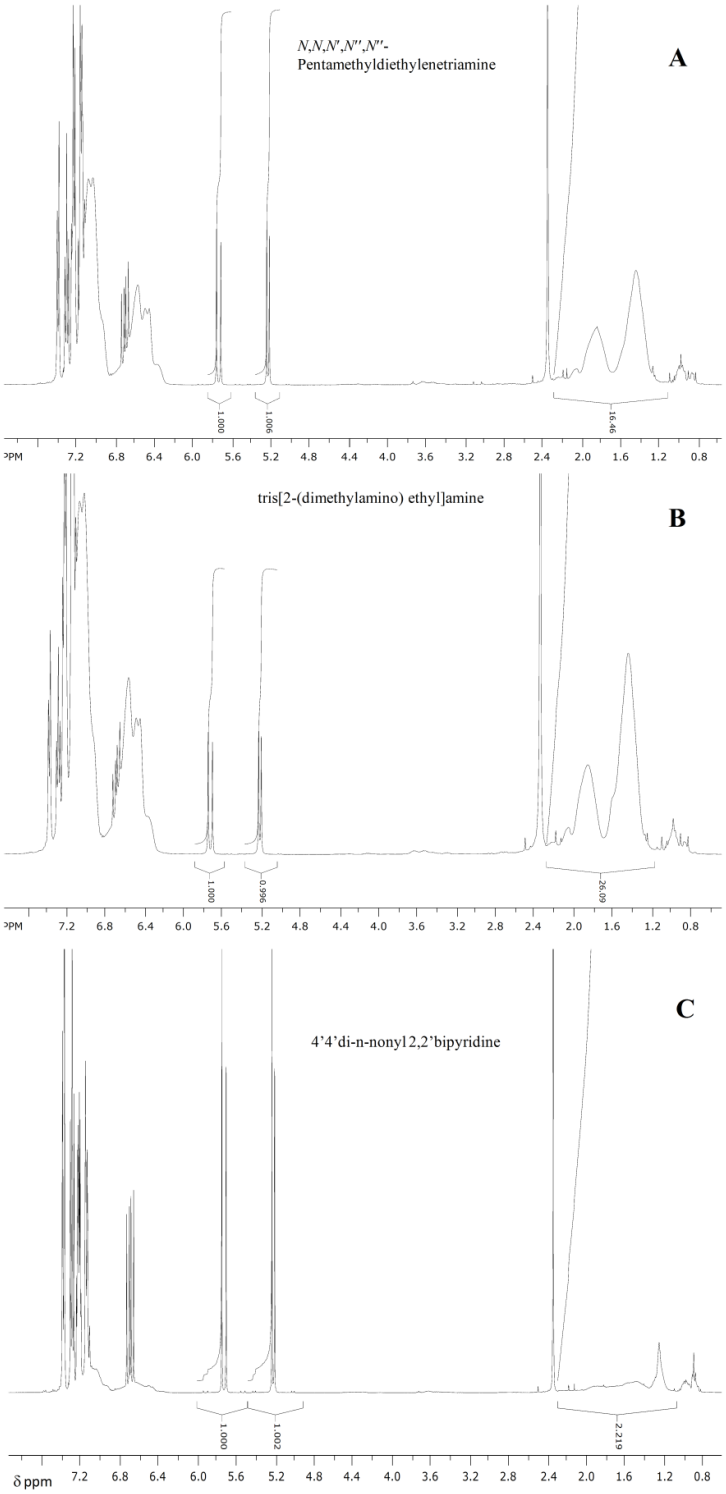

Figure SI.3: NMR spectra for linear polystyrene synthesised by ATRP. Reaction conditions; ethyl α-bromoisobutyrate initiator , $Cu^{(I)}Cl$ metal catalyst, toluene as solvent, 50ºC, 24 hours. ^{1}H NMR analysis in $CDCl_3$. The following ligands were employed (A) *N*,*N*′,*N*″,*N*″-Pentamethyldiethylenetriamine (PMDETA) (B) tris[2-(dimethylamino) ethyl]amine (Me6 [TREN]) and (C) 4’4’di-n-nonyl 2,2’bipyridine

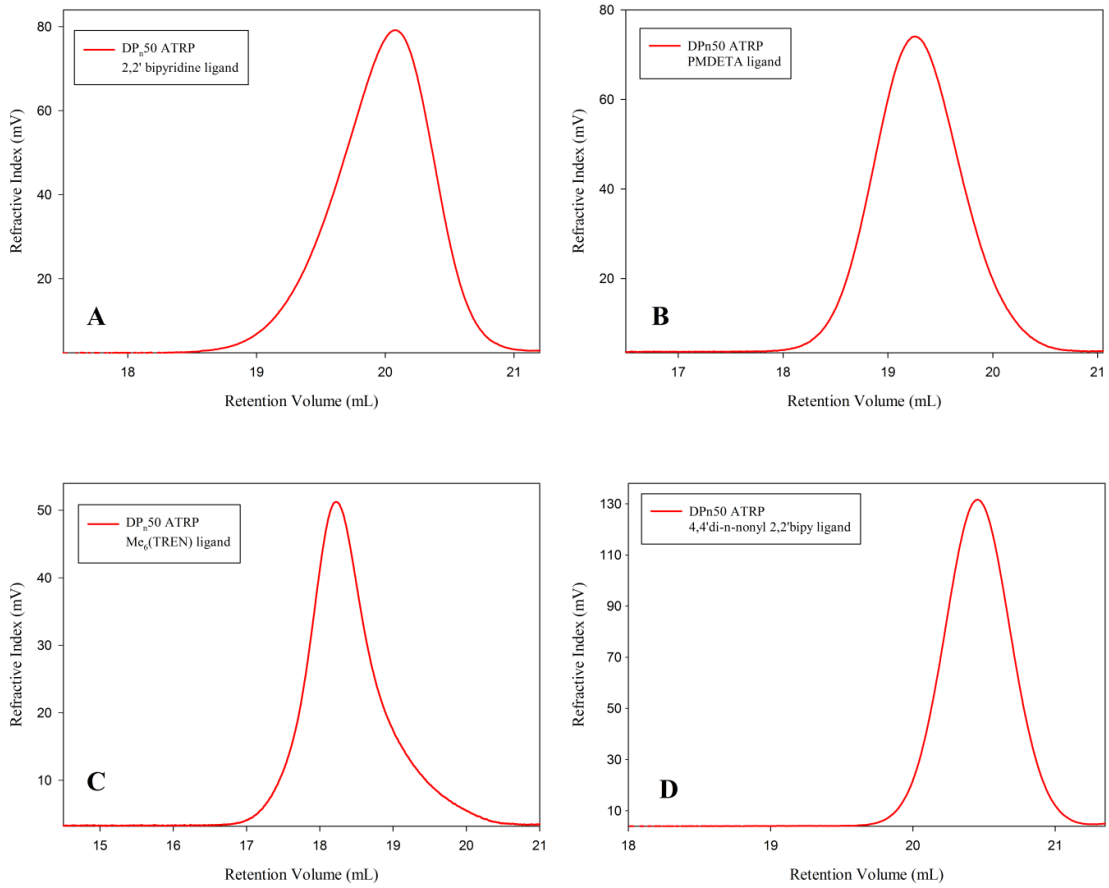

Figure SI.4: GPC chromatograms of polymers synthesised by ATRP with the corresponding ligand. ethyl α-bromoisobutyrate initiator , $Cu^{(I)}Cl$ metal catalyst, toluene as solvent, 50ºC, 24 hours. (A) 2,2'bipyridine (B) *N*,*N*,*N*′,*N*″,*N*″-Pentamethyldiethylenetriamine (PMDETA) (C) tris[2-(dimethylamino) ethyl]amine (Me6 [TREN]) and (D) 4'4'di-n-nonyl 2,2'bipyridine

Table SI.11 below summarises the results of the series of ATRP experiments under varying conditions. In all cases the target DP_n was 50 monomer units, the reaction time was 24 hours, and the monomer: initiator: catalyst: ligand ratio was 1:1:1.1:2.2 respectively.

Table SI. 1: M_n, M_w, Đ and monomer conversion percentage values for polystyrenes synthesised by ATRP under the conditions specified for each polymer in the table. The targeted DP_n was 50 monomer units, therefore the theoretical M_n value is 5,200 $gmol^{-1}$

Ligand	**Temp (^oC)**	**Solvent**	**M_n ($gmol^{-1}$)**	**M_w ($gmol^{-1}$)**	**Đ**	**Conversion (%)**
2,2'-bipyridine	Ambient	Benzene	3,000	3,700	1.23	< 50
2,2'-bipyridine	60	Benzene	3,600	4,700	1.31	< 50
N,N,N'-penta methyldiethylene triamine	90	Toluene	18,200	25,100	1.38	85
tris[2(dimethyl amino) ethyl]amine	90	Toluene	1,900	2,300	1.21	~90
4,4'-dinonyl-2,2'-bipyridine	90	Toluene	7,500	9,400	1.25	42

From the results it would it would appear that, despite changing a number of variables, the ATRP polymerisation of styrene under these conditions gave consistently relatively low monomer conversions, poor targeting of DP_n and required lengthy polymerisation times.

The conditions (ie. ligand, solvent and temperature) that gave the highest percentage of monomer to polymer conversion also gave a low M_n. For a target DP_n of 50 monomer units the target M_n value is approximately 5,000 $gmol^{-1}$, and the observed results when using tris[2-(dimethylamino)ethyl]amine showed a very low M_n of 1,900 $gmol^{-1}$ (roughly a DP_n of 20 monomer units) suggesting a lot of chain transfer. *N,N,N'*-pentamethyldiethylenetriamine gave a very high M_n value of 18,200 $gmol^{-1}$ which corresponds to a DP_n of approximately 175 monomer units. Even in the cases where the percentage conversion was below 50% the M_n values ranged from 3,000 $gmol^{-1}$ to

7,500 $gmol^{-1}$ which is greater than 50% of the target M_n, indicating that even at full conversion the M_n and DP_n would still be greater than the targeted values.

These results present a serious problem as it appears that there is very little control available over the chain length of the polymer when using ATRP in this way. This will prove even more of a problem in later branching work as it will not be possible to control the length of the primary chains within the branched structuress, which will affect the architecture of the polymer.

Time is also an issue; 100% conversion, which would be the ideal, does not occur in less than 24 hours in any of the reactions evaluated. Due to this, no further kinetics experiments were conducted to analyse the reaction rate as it was deemed 24 hours would not be an appropriate length of time to produce the polymers, and subsequent block polymers in later work.

All ATRP polymerisations also require a time consuming purification step to remove the catalyst. The purity of the polymer is also an issue as despite the purification method used there may still be some metal residue in the polymer. This may prove problematic in later pharmacological evaluation and potential cell toxicity.

SI. 1.2 Synthesis of branched polystyrene by ATRP

Although there were many disadvantages to using ATRP as the method of polymerisation for synthesising linear polystyrenes, there are examples in the literature of branched styrenic polymers produced by ATRP using a range of different conditions and branching molecule. These include the copolymerisation of *p*-(chloromethyl)styrene

with styrene, [3] the preparation of star-shaped polystyrenes by the coupling of polystyrene macroinitiators in the presence of divinylbenzene (DVB), [4] the formation of tethered diblock copolymer brushes by sequential 'living'/controlled radical polymerisation techniques using reverse atom transfer radical polymerisation (RATRP) [5] and the synthesis of polytetrahydrofuran /poly(1,3-dioxepane)/polystyrene ABC miktoarmstar copolymers by combination of cationic ring-opening polymerization (CROP) and ATRP. [6]

Quiang *et al* synthesised branched polystyrene using ATRP of styrene in the presence of DVB as branching comonomer. [7] The synthesis was completed *via* a facile one pot approach with a molar ratio of styrene to DVB in range of 5:1–30:1 employed to obtain soluble polymers. (1-bromoethyl)benzene (BEB) was used as the initiator and copper (I) bromide and the ligand anisole formed the metal ligand complex. The growth of molecular weight was monitored by GPC. The authors claimed that the results indicated the branched polymers were formed by self-condensing vinyl polymerization (SCVP) of an AB macromonomer that is formed *in situ* and drew a schematic to suggest that the chains were tethered at one end, however, it is now thought that this is an incorrect interpretation and this report is potentially one of the first ATRP syntheses of branched polystyrene under the conditions of the Strathclyde approach. Branched polystyrene reached M_w values = 38,000 $gmol^{-1}$ and a dispersity value (Đ) of 6.87, however, low overall conversions were reported for the styrene component of the polymerisation (50% after 9.5 hours) and low recovered yields (maximum of 58.8%).

DVB is well documented as a versatile cross-linking agent, used in the manufacture of a range of products including adhesives, plastics, elastomers, speciality polymers, pharmaceuticals and ion-exchange resins. However, if small amounts are used to avoid

cross-linking, highly branched polymer structures can be synthesised. Similarly Gong *et al* initially prepared hyperbranched polymers through ATRP polymerisation of an inimer formed *in situ* from an ATRP initiator and DVB. [8] However they found high amounts of cross-linking and a low double bond conversion of less than 60%. [9]

Due to its commercial availability, DVB was used initially as the brancher compound within this study, in an evaluation of ATRP for the branched vinyl polymerisation of styrene under the conditions of the Strathclyde approach. The reaction scheme is shown below in Scheme SI.3.

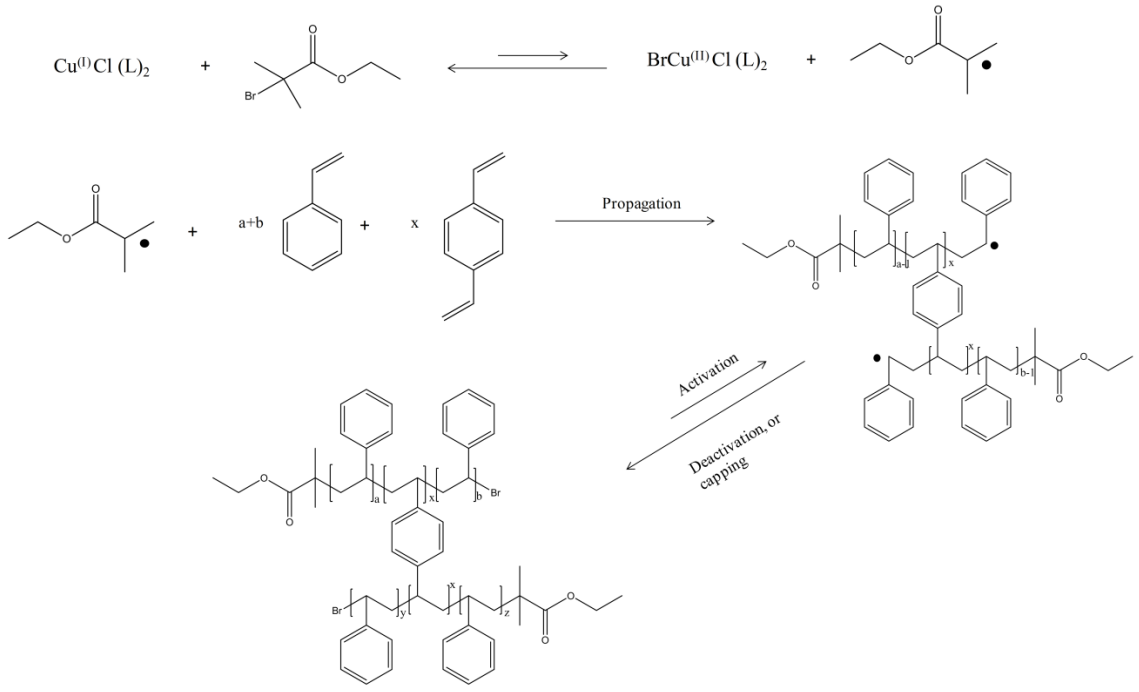

Scheme SI.3: Synthesis of polystyrene branched with DVB by ATRP methods. Reaction conditions: copper (I) catalyst (0.000747 mol), ligand (0.00136 mol), 8 mL toluene, DVB as brancher (0.0006114 mol), 100 µL of initiator ethylbromoisobutyrate and styrene monomer (0.3397)

In a typical ATRP reaction, 0.0739 g (0.747 mmol) of copper chloride powder and 0.233 g (1.36 mmol) of 2,2'-bipyridine were added to a round bottomed flask. The reported reaction stoichiometry for monomer:initiator:catalyst:ligand within a linear ATRP polymerisation is often 1:1:1:2 respectively, although experimentally 1:1:1.1:2.2

was used to allow for a slight excess as discussed previously. 8 mL of toluene was added, and the system was degassed for 10 minutes under bubbling nitrogen pressure to remove any oxygen from the system. For a polymer with a primary chain length target DP_n of 50 monomer units, it was calculated that 339.7 mmol of monomer was needed. 100 µL of the initiator ethylbromoisobutyrate was added followed by 3.98 mL (339.7 mmol) of styrene and 87 µL (0.6114 mmol) of DVB were added together. The reaction was left to stir at 60 ºC for 24 hours, before sampling and then left for a further 24 hours before termination. The sample after 24 hours and the resulting polymer after 48 hours were purified and analysed by gel permeation chromatography (GPC). The resulting refractive index detector responses for each sample are overlaid in Figure SI.5.

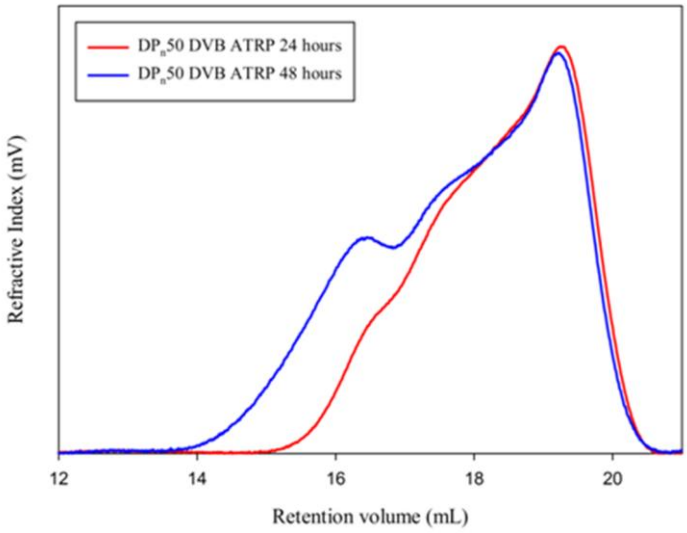

Figure SI.5: RI trace GPC chromatograms of micro-samples of branched polystyrene sampled at 24 hours (red) and 48 hours (blue) during an ATRP synthesis. Reaction conditions: copper (I) catalyst (0.747 mmol), ligand (1.36 mmol), 8 mL toluene, DVB as brancher (0.6114 mmol), 100 µL of initiator ethylbromoisobutyrate and styrene monomer.

Table SI.2: M_n, M_w and Đ values for samples taken during a branched polystyrene synthesis by ATRP methods with DVB as the branching compound. Reaction conditions: copper (I) catalyst (0.000747 mol), ligand (0.00136 mol), 8 mL toluene, DVB as brancher (0.0006114 mol), 100 µL of initiator ethylbromoisobutyrate and styrene monomer (0.3397)

Time (hours)	GPC		
	M_n (gmol^{-1})	M_w (gmol^{-1})	Đ
24	15,700	66,700	4.25
48	26,200	217,200	8.29

Although, as can be seen from the values in Table SI.2, and the GPC chromatograms in Figure SI.5, in 48 hours a branched polymer has been successfully synthesised, there still remains the same problem with the linear polystyrenes in that the primary chain length cannot be controlled and therefore aspects of the architecture cannot be controlled. Anionic polymerisation of linear polystyrene offered excellent control of linear polymers and therefore offers advantages for branched vinyl polymerisations.

SI. 2 Branching from branched structures *in situ*.

As seen in Chapter 5 branched architectures were produced successfully from the chain extension of linear polystyrene from branched polystyrene, and branched from linear polymers, it is proposed that even bigger and more complex architectures could be synthesised if branched polystyrene was synthesised, forming an anionic macroinitiator and then further monomer and brancher was added *in situ* to synthesise a highly branched polystyrene from this already branched polystyrene.

Preliminary work was undertaken to assess the possibility of this being successful, or if the system would simply cross link or form aggregates. A branched polystyrene with a DP_n of 50 and a very low ratio initiator:brancher 1:0.25 VPOB was first synthesised, followed by the *in-situ* addition of futher monomer and VPOB at a higher ratio of 1:1. Although a lot of termination was observed (colour change from deep red to a bright orange), a second addition of further monomer and VPOB occoured, this time at the original low ratio of 50 monomer units of styrne with 1:0.25 ratio of VPOB. Due to the large amount of termination observed the experiment was repeated. The results of both

block polymerisations are shown in Figure SI.6. Table SI.3 gives the M_n and M_w values of the resulting self-blocking polymerisations.

Table SI.3: M_n, M_w and Đ values for the branched self blocking polymerisations of polystyrene by anionic polymerisation techniques.

Architecture of Polymer	**GPC**		
	M_n (gmol^{-1})	**M_w (gmol^{-1})**	**Đ**
DP_n50 1:0.25 VPOB	6,700	9,600	1.43
DP_n50 1:0.25 VPOB (repeat)	4,300	6,700	1.57
DP_n50 1:0.25 plus DPn50 1:1	16,400	184,000	11.22
DP_n50 1:0.25 plus DPn50 1:1 (repeat)	15,300	80,700	5.27
DP_n50 1:0.25 plus DPn50 1:1 plus DPn50 1:0.25	19,400	230,300	11.87
DP_n50 1:0.25 plus DPn50 1:1 plus DPn50 1:0.25 (repeat)	27,000	258,300	9.57

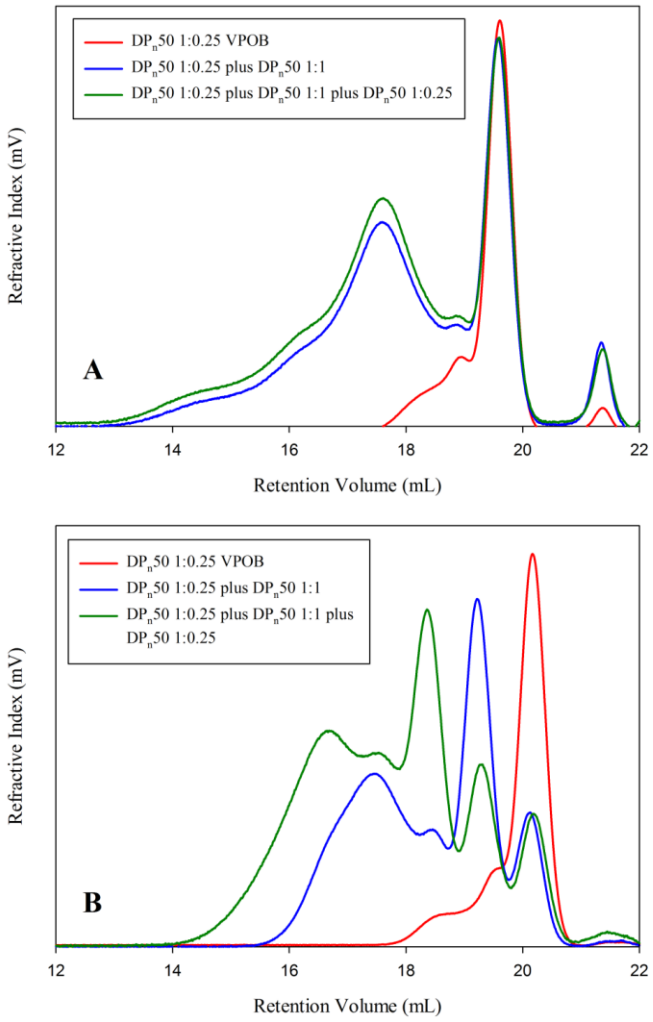

Figure SI.6: GPC chromatograms of the first repeat (A) and second repeat (B) of self blocking branched polystyrene.

As can be seen there has clearly been some successful branching onto a branched polymer, and polymers with a high molecular weight have been produced. As this had involved branching a small amount and then attempting a higher level of branching, the next experiment involved a significantly higher initial initiator:brancher ratio of 1:1, followed by a 1:0.5 ratio. In theory, the same total amount of brancher but with less monomer and hopefully less termination in the two sampling and monomer addition steps compared to three. The results are shown in Figure SI.7 and Table SI.4. The first GPC chromatogram in (A) explores the reproducibility of a DP_n50 1:1 ratio branched polymer, and the linear peak.

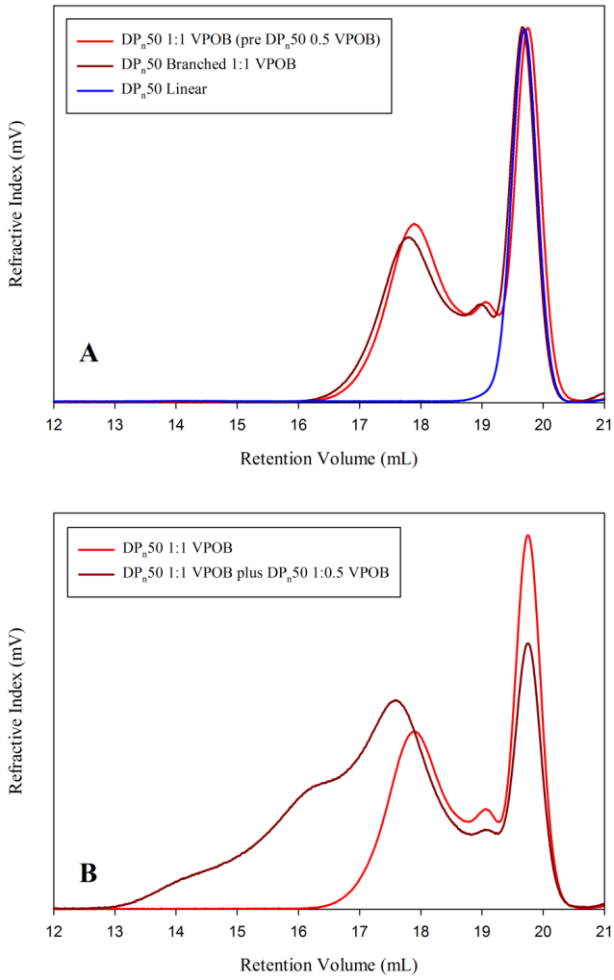

Figure SI.7: GPC chromatograms of (A) the first addition illustrating the reproducibility of synthesising branched polymers and (B) after the addition of a further 50 monomer units and 1:0.5 ratio of the brancher VPOB.

Table SI. 4: M_n, M_w and Đ values for a branched self-blocking polymerisation of polystyrene by anionic polymerisation techniques.

Architecture of Polymer	**GPC**		
	M_n (gmol^{-1})	**M_w (gmol^{-1})**	**Đ**
DPn50 1:1 VPOB	7,500	26,500	3.81
DPn50 1:1 VPOB (pre second addition)	9,100	30,600	3.36
DPn50 1:1 plus DPn50 1:0.5	21,600	363,000	16.81

This preliminary work has demonstrated that it is possible to synthesise branched polystyrenes and then grow further branched polystyrene from these by ambient anionic polymerisation techniques.

There is a lot of improvement needed to follow on from these initial experiments. A lot of termination was observed so further work is needed to optimise the anhydrous conditions. The issue could be with the brancher, and there may be further work needed to further dry and purify the compound.

The conditions of the ambient reaction also needs to be investigated. The solvent concentration, brancher:initiator ratio and targeted linear chain length can all undergo further series of experiments to find the best conditions for the reaction and the best conditions for producing the chain extended branched polystyrenes.

SI. 3 Alternative method of synthesising branched polystyrene by anionic polymerisation.

As discussed in the solvent concentration results in Chapter 4, a gel can form from the association of the ions present at the end of each polystyrene chain. This ionic association was found to be greater at higher solid content levels. A way to overcome one of these effects is to decrease the number of anions on the branched polymer.

As the brancher compound VPOB has to be synthesised, and can only be marginally scaled up in size due to the multi-step purifications, a method that offered an alternative to this would be advantageous. A novel method combining 'living' anionic polymerisation with a convergent growth process was reported by Knauss *et al* [10] who

formed dendritically branched polystyrene by using vinyl-functionalised reactants to produce macromonomers that react through their double bonds with 'living' polystyrene chain ends to give dimerised chains. This method has been used previously by Bronn and Silva [11] to make branched block copolymers of polystyrene and polyisoprene. Knauss and co-workers have investigated the use of vinylbenzyl chloride (VBC) [12] 4-(chlorodimethylsily)styrene (CDMSS) and 4-vinylstyrene oxide 20 (VSO) [13] as the coupling agents.

The reports from Knauss and co-workers investigated the slow addition of a stoichiometric amount of VBC alone to a living polymerisation of polystyrene and also its addition together with styrene. As shown in Figure SI.8, VBC can either terminate the reaction or add to the polymerisation as a monomer.

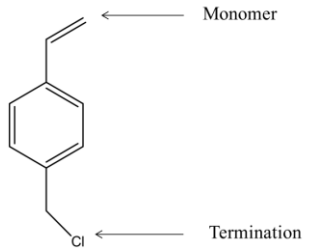

Figure SI. 8: Structure of vinylbenzlchloride

The bifunctional and orthogonal nature of the reactivity of VBC can result in the simultaneous termination of growing anionic polymer chains and the formation of macromonomers that can react with un-terminated propagating chains. This leads to the formation of side chains extending from a single propagating chain The structure becomes more complex as larger polymer chains are terminated and become macromonomers which can react with other branched and linear propagating chains.

Within this study, the fast addition of VBC to an anionic polymerisation of styrene, and the effects on molecular weights of changing the solvent mixture, the amounts of VBC added and increasing the primary polystyrene chain length were investigated. The difference between the step-wise addition of styrene and VBC and the consecutive addition of a mixed VBC/styrene monomer feed was also considered.

Initially a reaction was carried out whereby linear polystyrene was synthesised by anionic polymerisation to a targeted chain length of DP_n = 50 monomer units in 30 mL of benzene solvent. VBC was added in a 0.25:1 VBC:*sec*-BuLi ratio 1 hour after initiation of the polymerisation and the reaction mixture was left for one hour. This reaction is shown is Scheme SI. 4 below.

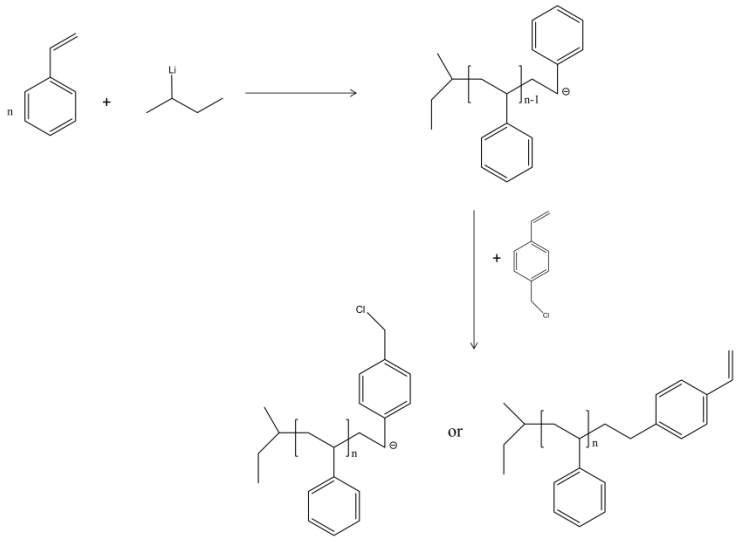

Scheme SI.4: Addition of VBC to a living anionic polymerisation of styrene and the resulting possible products.

The divergent branching occurs as shown in Scheme SI.5.

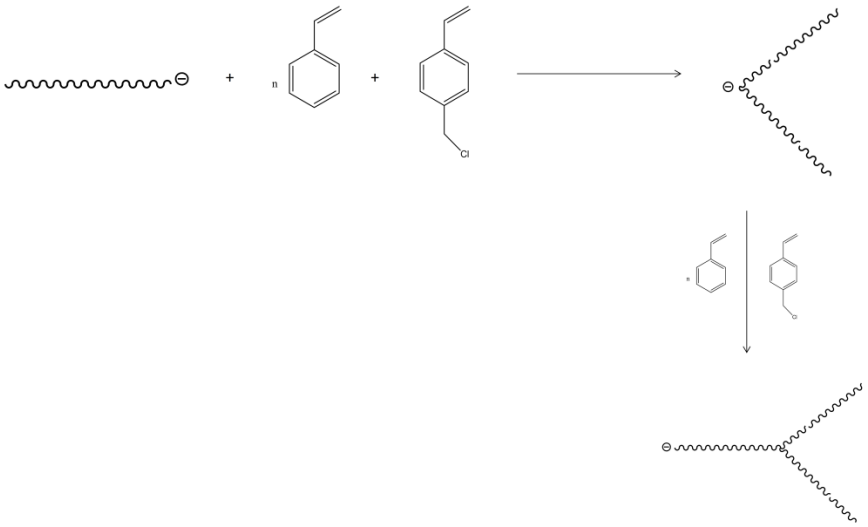

Scheme SI. 5: Representation of the divergent branching scheme by the addition on VBC to a living anionic polymerisation of polystyrene.

The polymeric products that result from the addition of VBC to an anionic polymerisation were analysed by GPC. Both benzene and a mixture of tetrahydrofuran and benzene in a 30:70 ratio were used as solvents for the reaction involving VBC addition. The GPC chromatography results are compared and shown in Figure SI. 9.

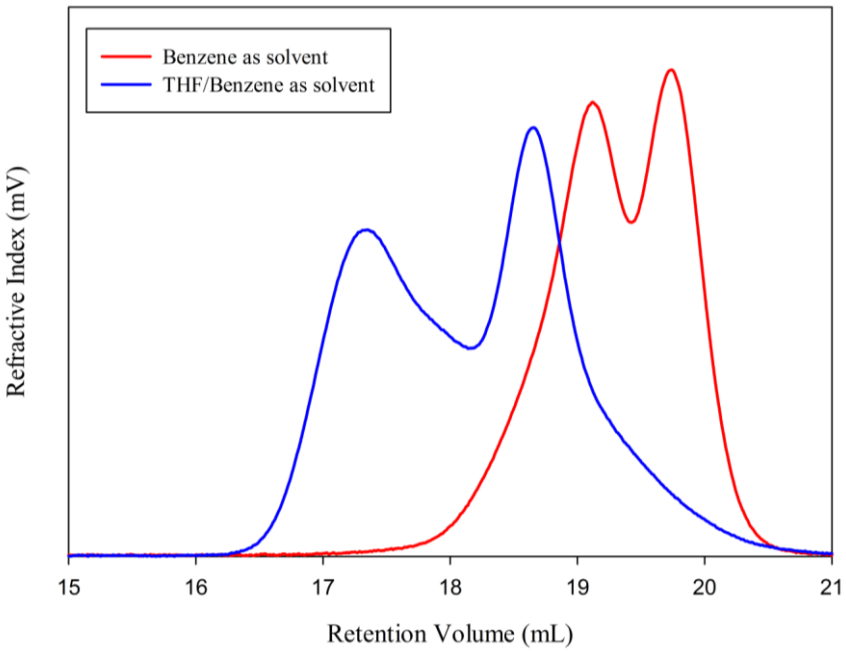

Figure SI.9: GPC chromatogram of polystyrene branched with VBC by anionic polymerisation techniques.

The sequential independent addition of styrene and VBC was then studied. A linear chain was synthesised followed by the sequential addition of an amount of VBC, addition of a second aliquot of styrene monomer, further VBC, a third batch of styrene, and finally VBC with 1 hr between each addition. The amount of VBC added was varied between additions, first a ratio of 0.5:1 VBC:*sec*-BuLi or 50% of the initiator concentration was added at three different times over 8 hours, and the results compared to additions of first 50% (0.5:1 VBC:*sec*-BuLi) of the initiator concentration of VBC, followed by 25% (0.25:1 VBC:*sec*-BuLi)and 12.5% (0.125:1 VBC:*sec*-BuLi). The GPC chromatograms of both final products are shown in Figure SI.10.

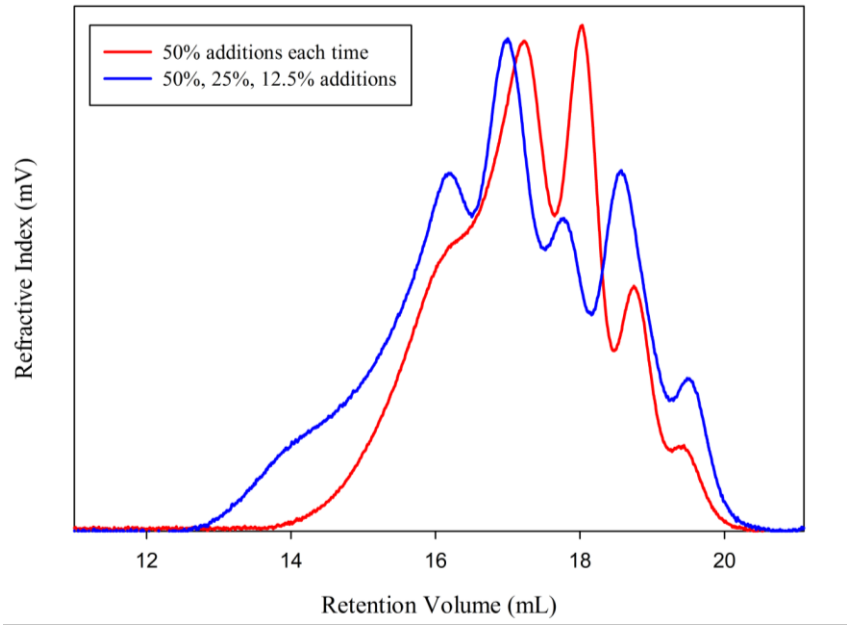

Figure SI. 10: GPC chromatogram comparing differences in amount of VBC added at each addition to an anionic polymerisation of styrene.

The ^{1}H NMR spectra of the final reaction mixtures and samples taken to monitor the reaction over time showed that the polymerisation had not reached full conversion. In order to avoid excess styrene monomer being present, a comparison of adding VBC into the polymerisation with the styrene monomer and conversely separate from the styrene monomer was undertaken. It was found from ^{1}H NMR analysis that adding styrene

separately resulted in excess monomer present in the reaction. In order to overcome this in further experiments, the addition of the VBC and styrene together was considered. A ratio of 0.5:1 VBC:*sec*-BuLi was added together with styrene, followed by two further additions of 0.25:1 and 0.125:1 as before. While the excess styrene is no longer present in the ^{1}H NMR spectra the molecular weights are not as high when the VBC is added with the styrene, seen in Table 1. The effect of the length of the primary polystyrene was also investigated. It was found that a DP_n= 50 monomer units resulted in the highest molecular weight as can be seen in Table SI.4, which gives a summary of all results.

Table SI.4: Table of M_n, M_w and Đ values for all polystyrenes synthesised with VBC as a branching agent by anionic polymerisation techniques. All conditions vary and these are outlined in the table.

Brancher: Initiator Ratio	**Monomer addition**	**Solvent**	**Chain Length**	**GPC**		
				M_n ($gmol^{-1}$)	**M_w ($gmol_{-1}$)**	**Đ**
50	Separate	Benzene/THF	50	21,000	43,900	2.09
50	Separate	Benzene	50	8,000	12,400	1.54
25,25,25	Separate	Benzene	50	39,800	170,000	4.37
50,25,12.5	Separate	Benzene	50	54,300	490,000	8.99
50,25,12.5	Separate	Benzene	50	41,500	430,000	10.45
50,25,12.5	Together	Benzene	50	46,000	150,000	3.26
50,25,12.5	Together	Benzene	25	26,800	120,000	4.33
50,25,12.5	Together	Benzene	100	26,100	30,000	1.16
50,25,12.5	Together	Benzene	200	31,400	48,700	1.55

Whilst these preliminary results appear to demonstrate that branched structures can be synthesised from this divergent branching method, the methodology is more complex than branching from a one-addition synthesis with a distyrl branching monomer such as DVB or VPOB. Further work is needed to optimise these conditions

SI. 4 References

1. Kotani, Y.; Kamigaito, M.; Sawamoto, M., *Macromolecules*, **1999**, *32*, 2420
2. www.cmu.edu/maty/chem/fundamentals-atrp/atrp.html
3. Gaynor, S. G.; Edelman, S.; Matyjaszewski, K. *Macromolecules*. **1996**, *29*, 1079
4. Xia, J.; Zhang, X.; Matyjaszewski, K. *Macromolecules*. **1999**, *32*, 4484
5. Sedjo, R.A.; Mirous, B.K.; Brittain, W. J. *Macromolecules*. **2000**, *33*, 1492
6. Feng, X., Y.; Pan, C., Y. *Macromolecules* **2002**, *35*, 2084
7. Qiang, R.; Fanghong, G.; Chunlin, L.; Guangqun, Z.; Bibiao, J.; Chao, L.; Yunhui, C. *Eur. Polym. J*., **2006**, *42*, 2573
8. Gong, F. H.; Tang, H. L.; Liu, C. L.; Jiang, B. B.; Ren, Q.; Yang, Y.; Chen, J. H., *J. Appl. Polym. Sci*., **2006**, *101*, 850
9. Tang, H.; Gong, F.; Lui, C.; Ren, Q.; Yang, Y.; Jiang, B.; Liu, C.; Chen, J. *J. Appl. Polym. Sci*., **2007**, *105*, 332
10. Knauss, D. M., Al-Muallem, H.A., Huang, T., Wu, D.T.; *Macromolecules*, 2000, *33*,3557
11. 4. Bonn, R., Silver, S.F.; *Polym. Prepr. (Am. Chem. Soc., Div. Polym. Chem)*, 1994, *35*, 572
12. 5. Knauss, D.M., Al-Muallem, H.A.; *Polym. Chem*., 2000, *38*, 4289
13. 6. Bender, J.T., Knauss, D. M.; *Macromolecules*, 2009, *42*, 2411

Appendix 1

GPC Chromatograms

Chapter 3

3.2.1 Atomic Transfer Radical Polymerisation (ATRP)

DP_n 50 monomer units, ligand; 2,2'bipyridine

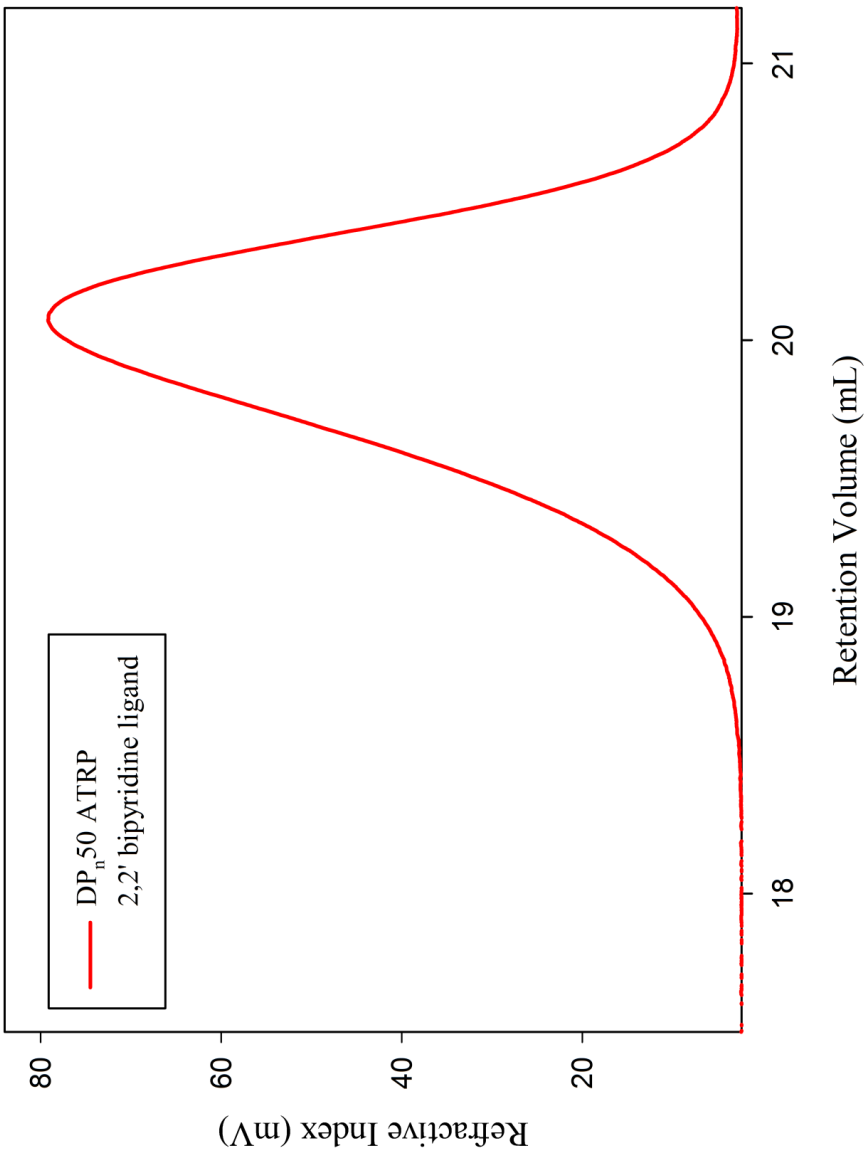

DP_n50 ligand; tris[2-(dimethylamino) ethyl]amine (Me6 [TREN])

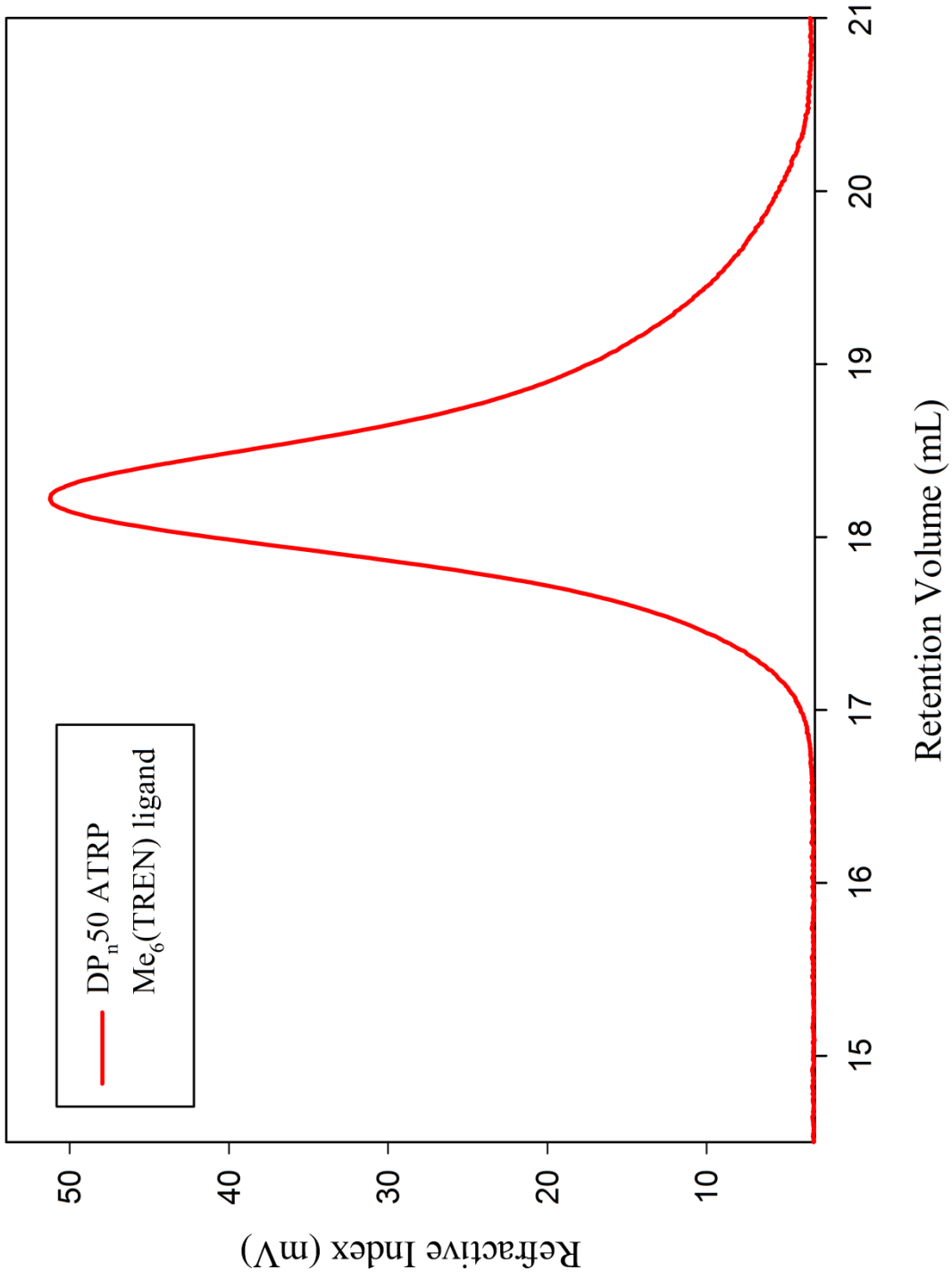

DP_n50, ligand; *N*,*N*′,*N*″,*N*‴-Pentamethyldiethylenetriamine (PMDETA)

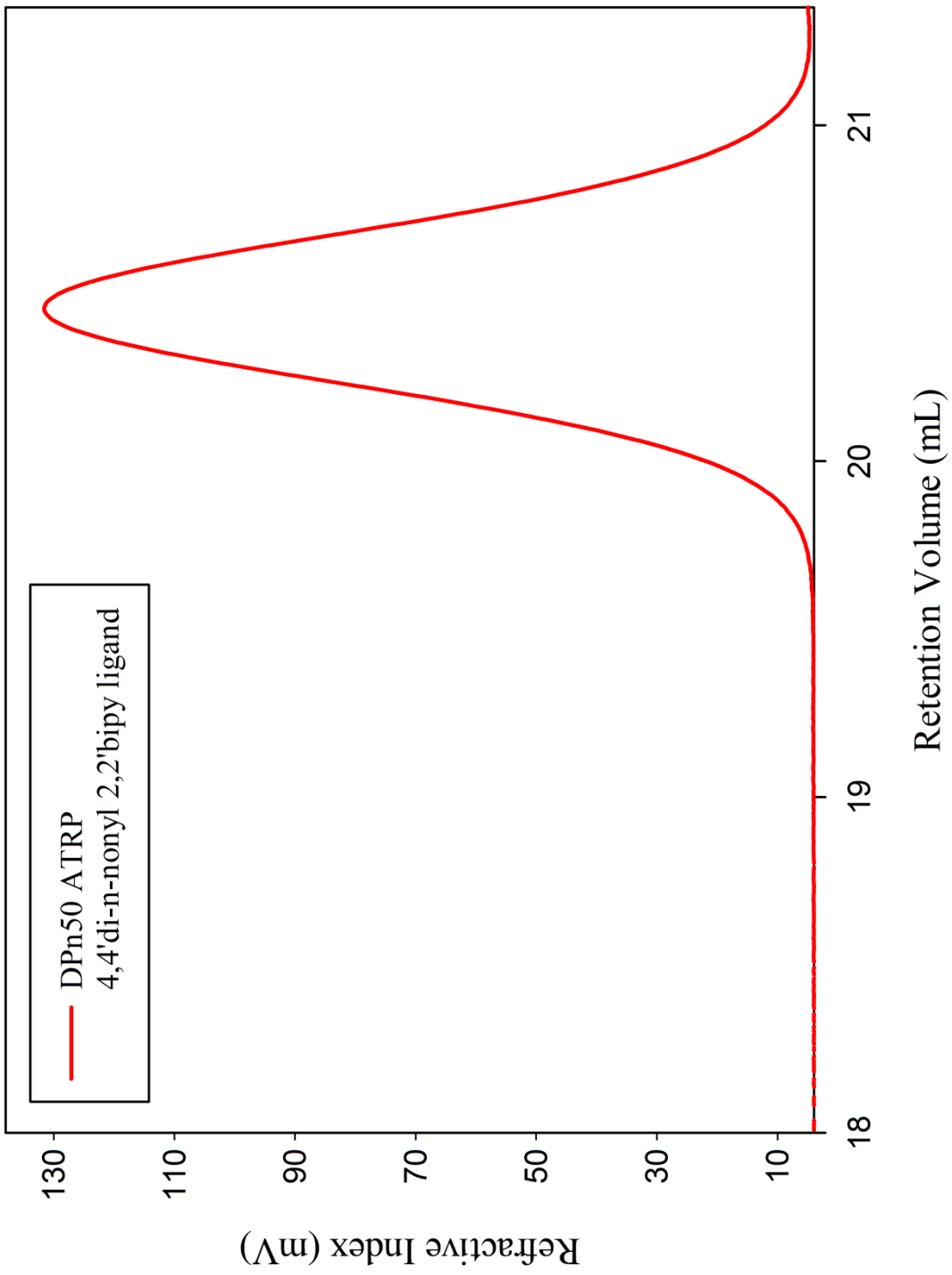

DP_n50, ligand; 4’4’di-n-nonyl 2,2’bipyridine

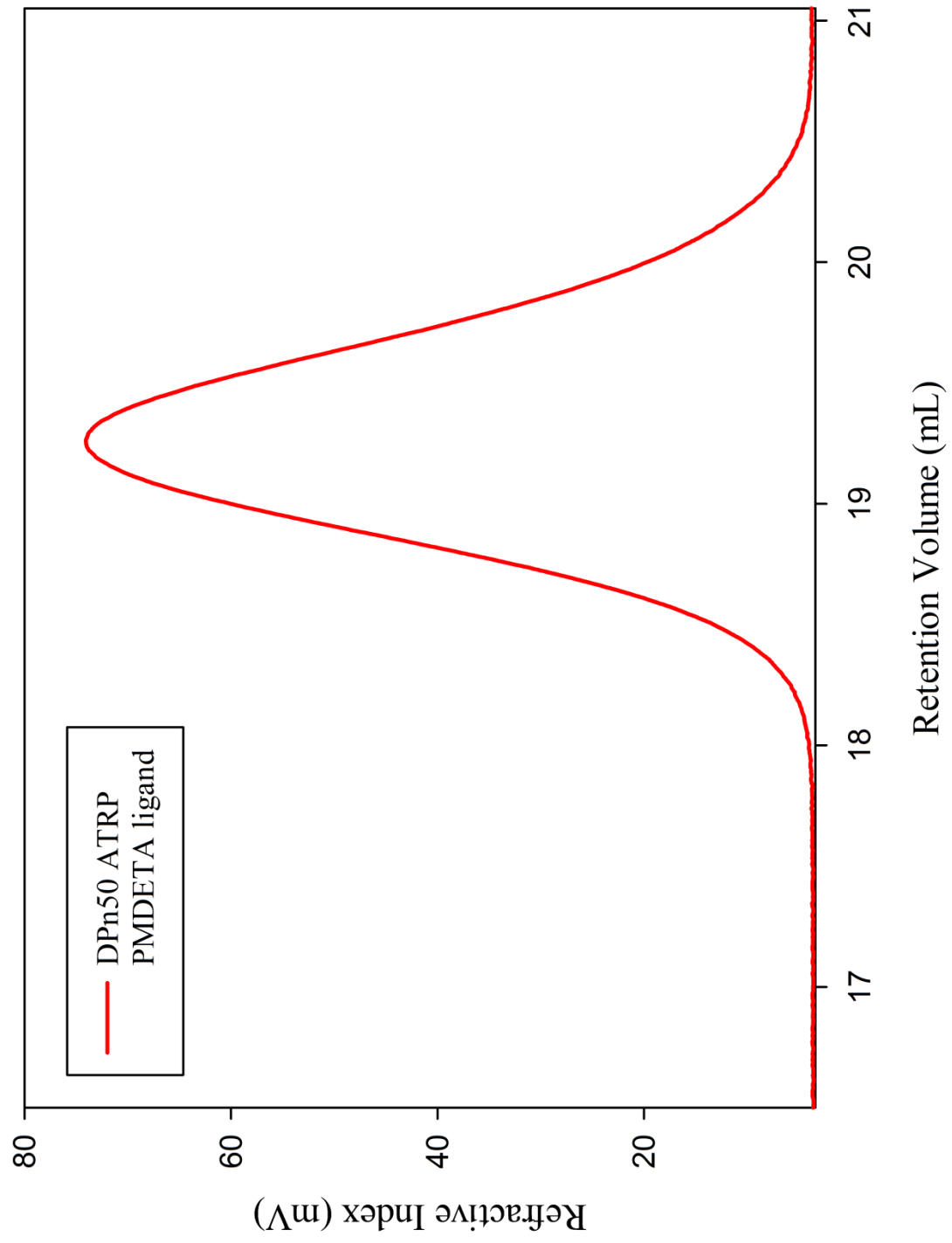

3.2.2.1. Synthesis of linear polystyrenes at ambient temperature.

DP_n10 linear

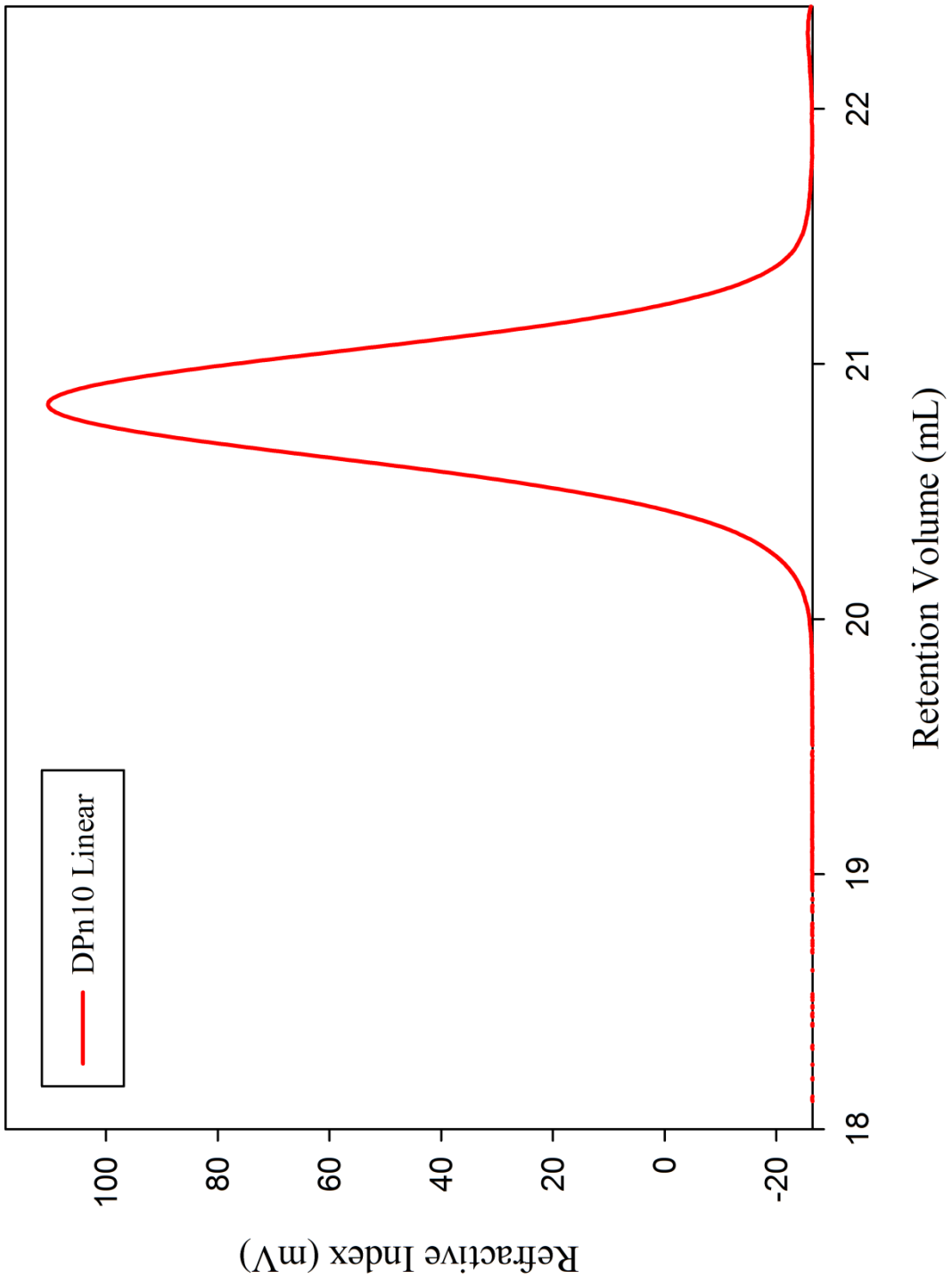

DP_n25 linear

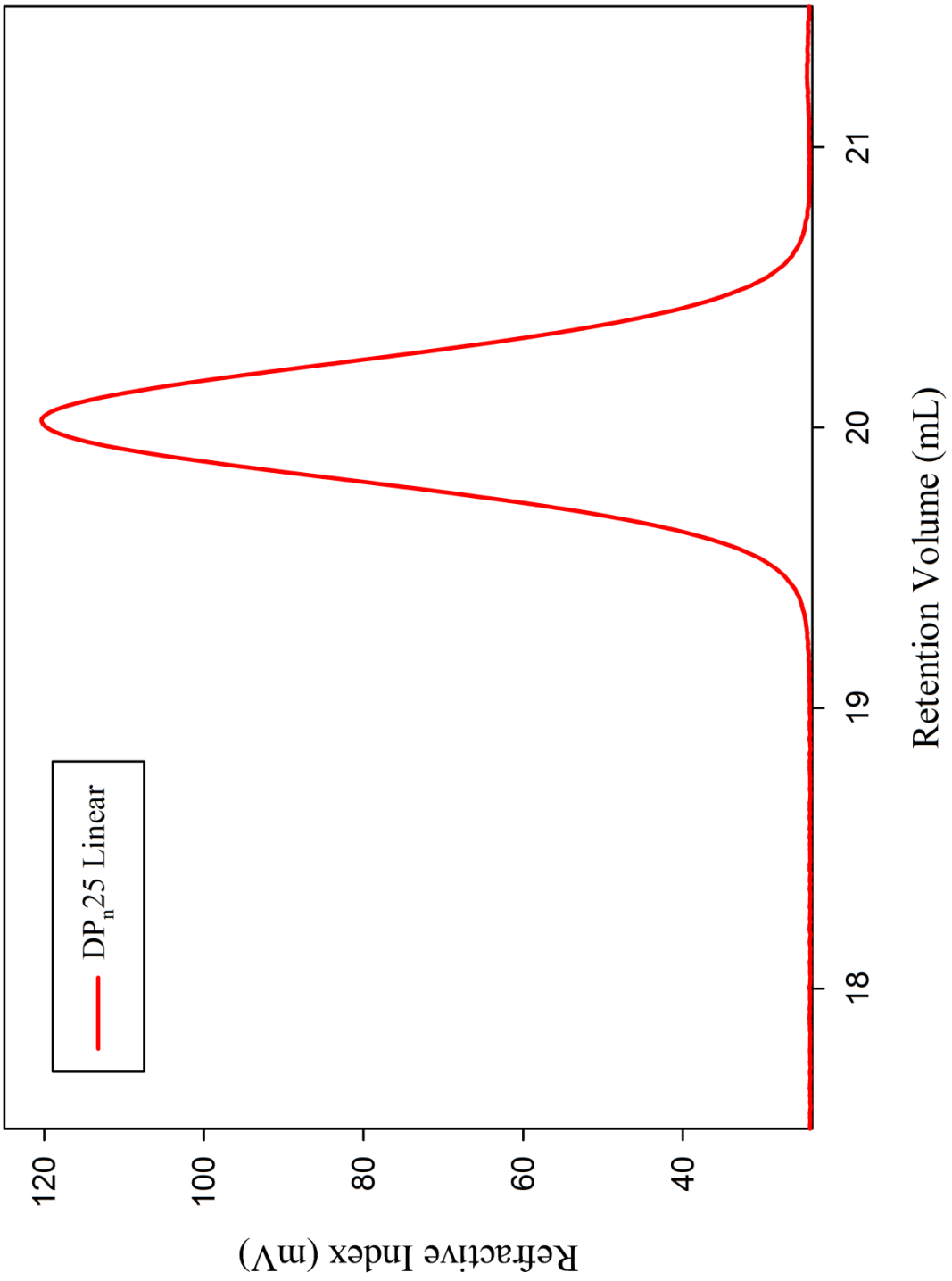

DP_n 50 linear

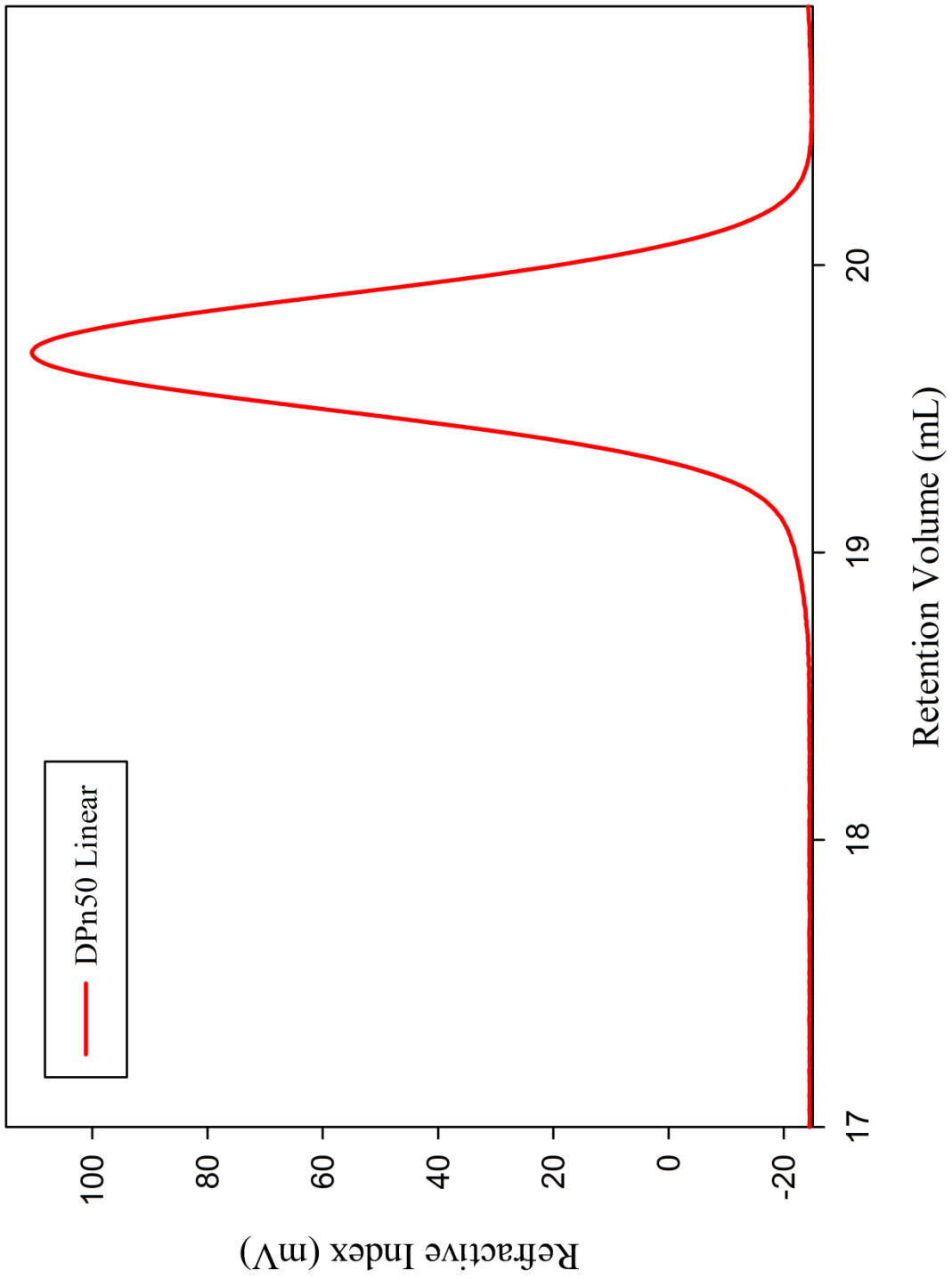

DP_n 100 linear

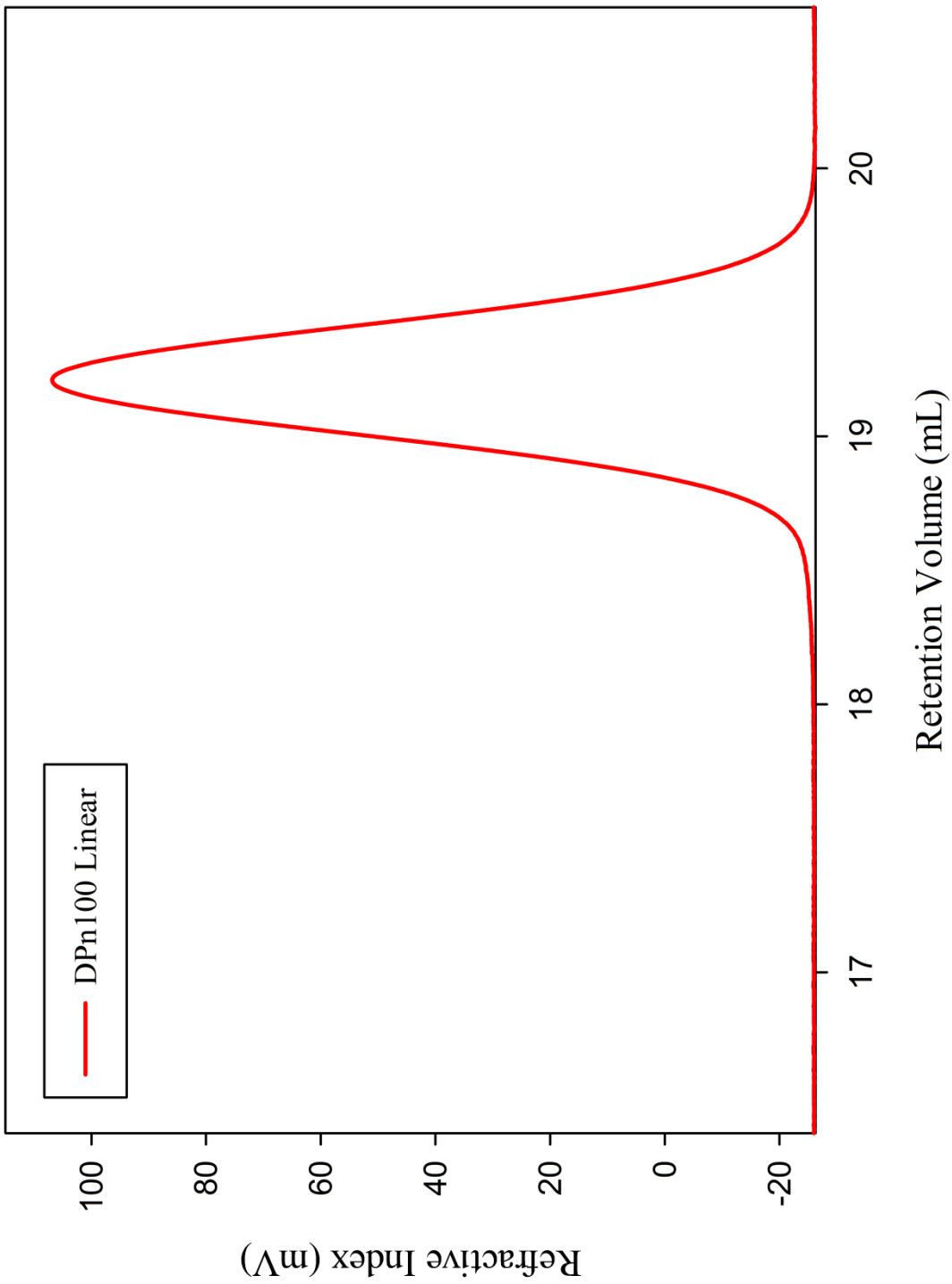

DP_n 250 linear

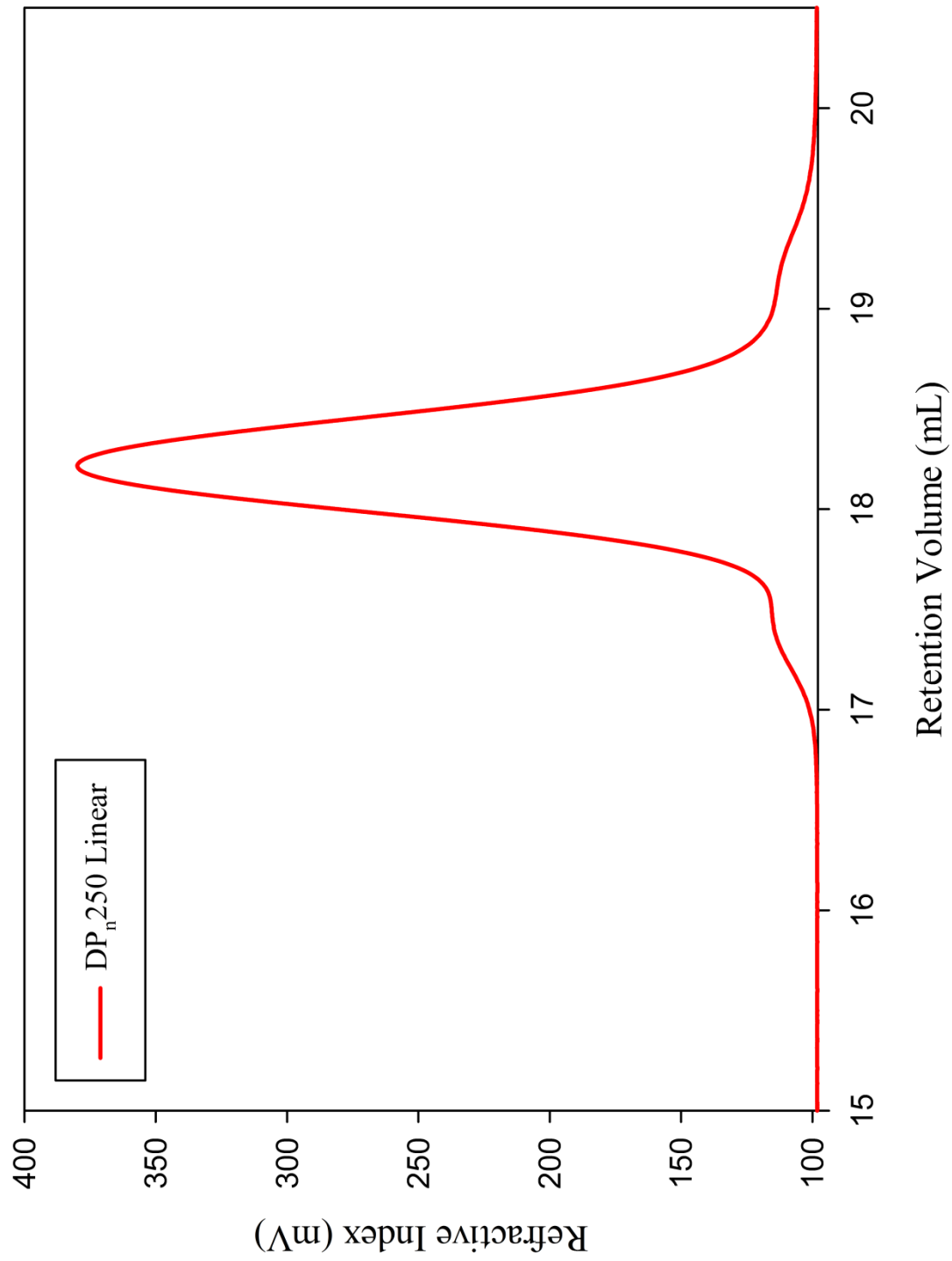

DP_n 500 linear

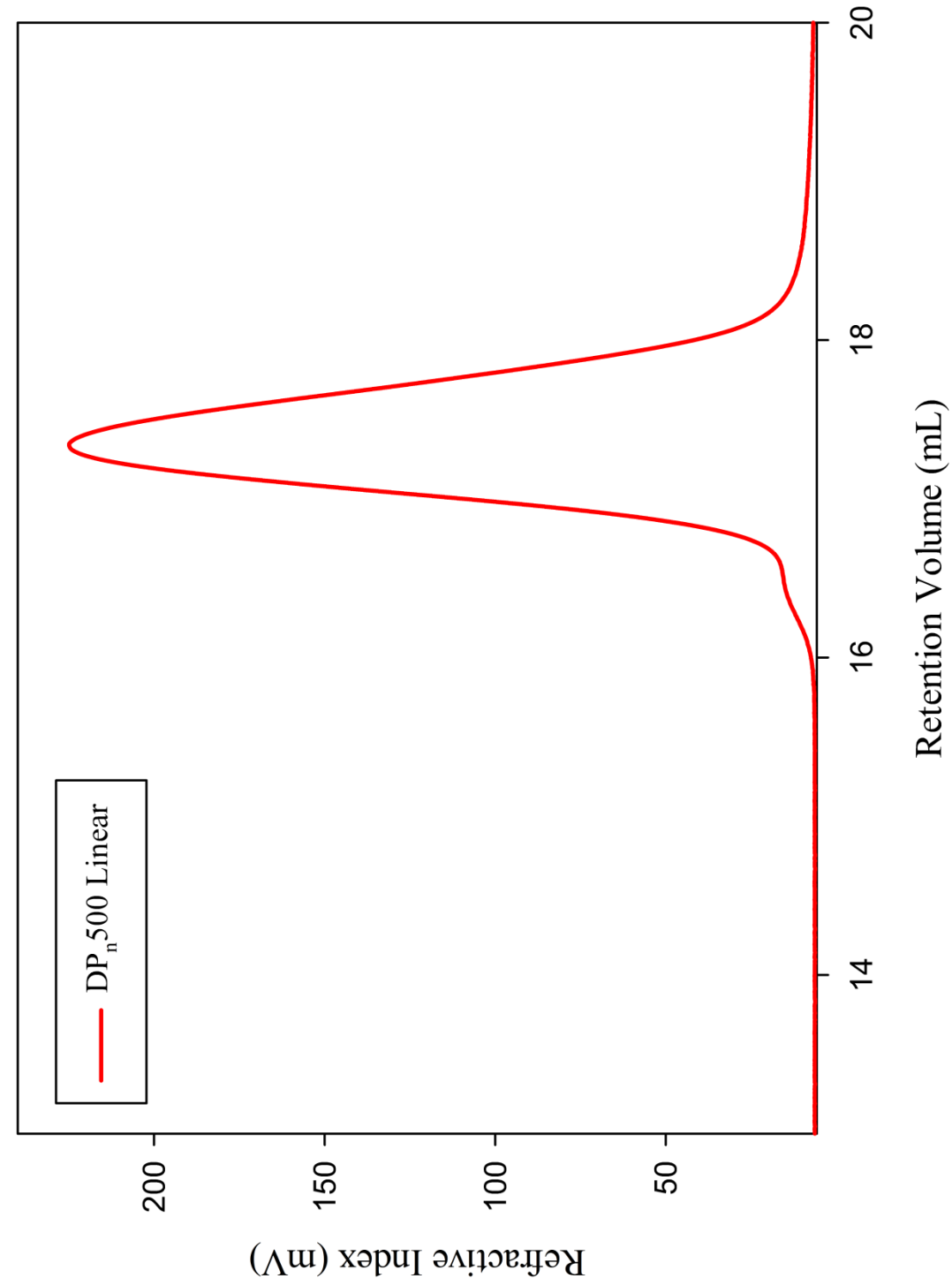

3.2.2.1.1 Effect of changing the initiating system for ambient anionic polymerisation

DP_n100, initiator; 1-bromo-4-*tert*-butylbenzene/ *sec*-BuLi adduct

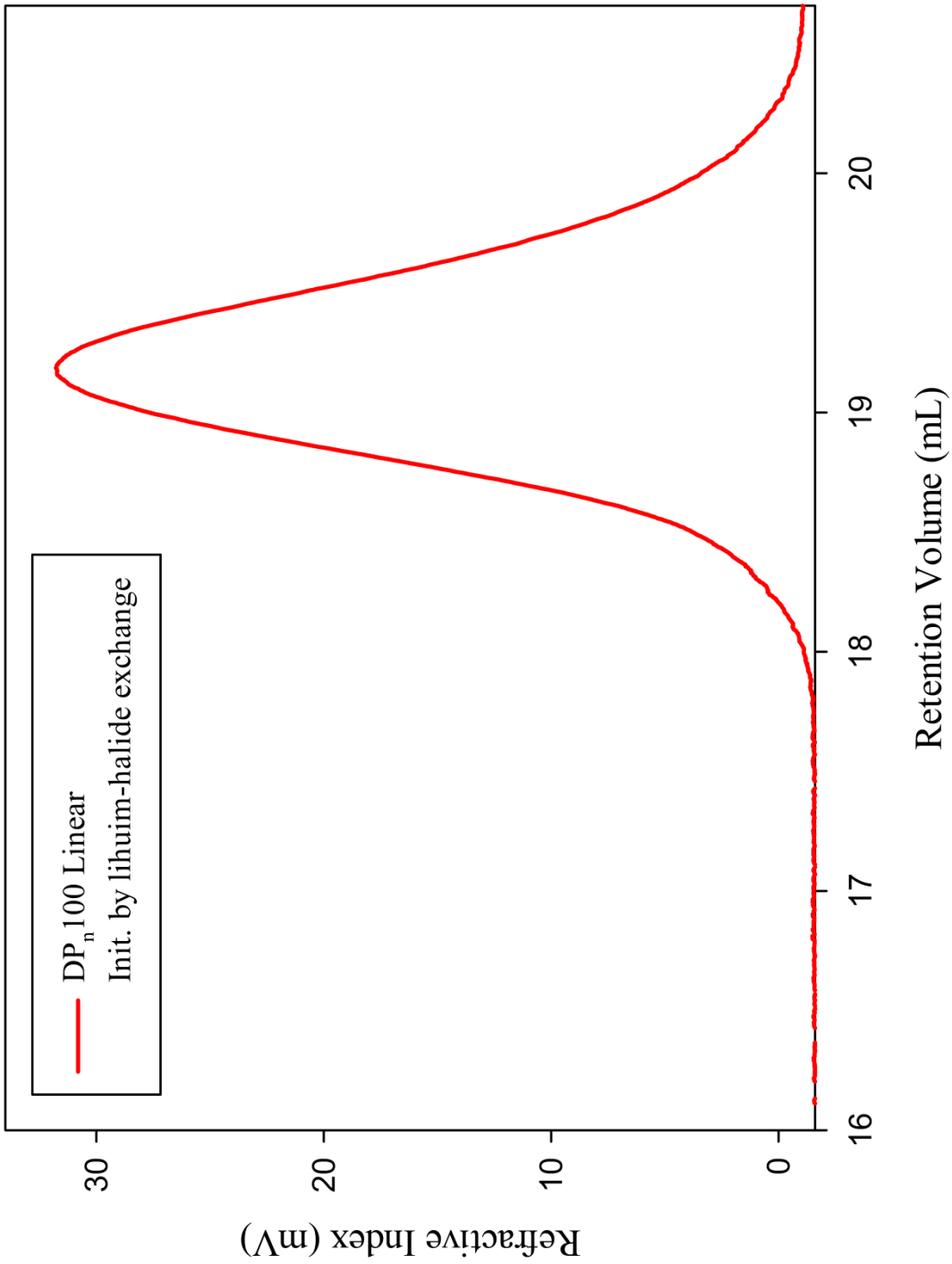

3.2.2.1.2 Effect of solvent concentration on ambient anionic polymerisation

DP_n50, benzene = 20 mL

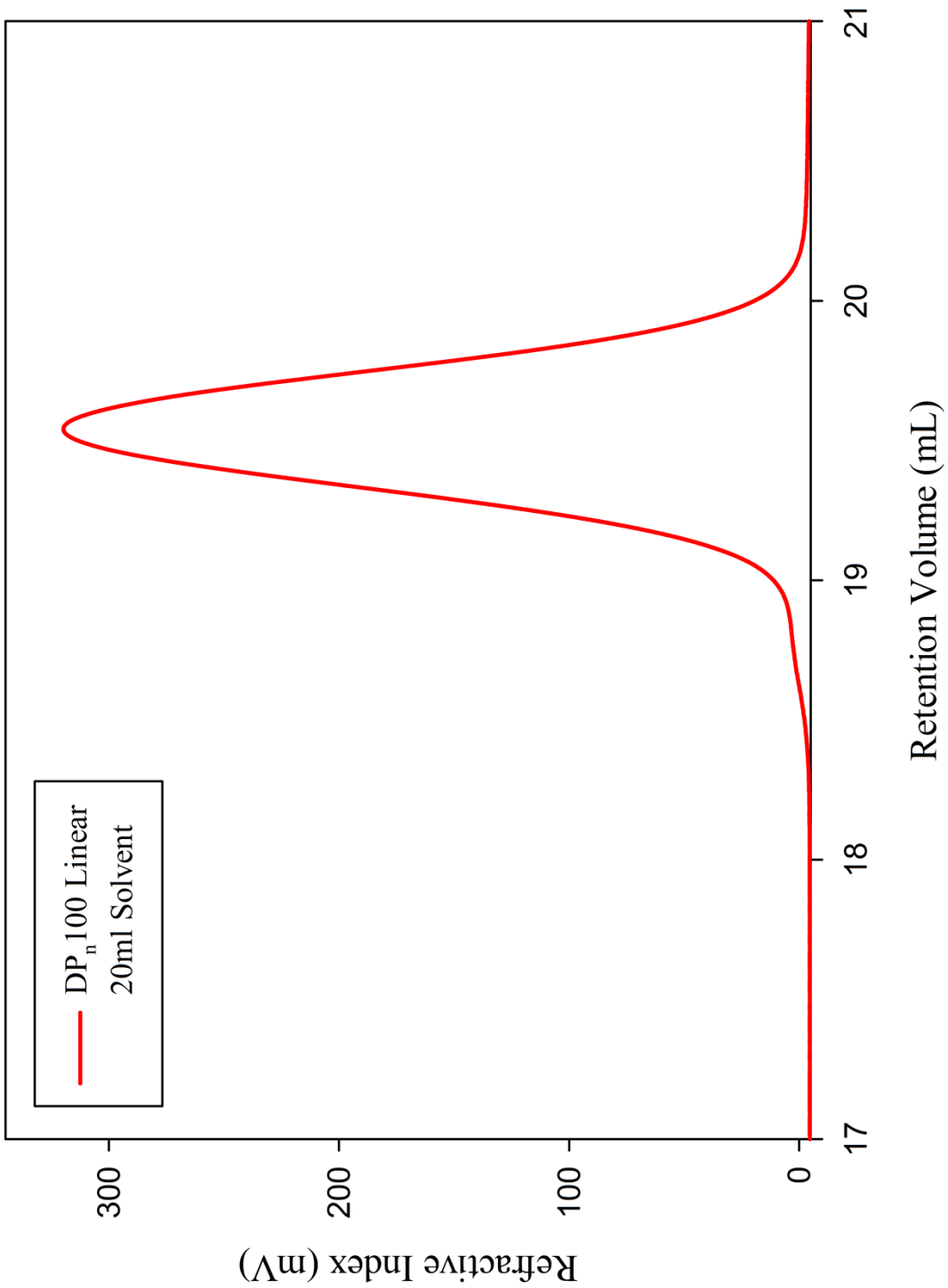

DP_n50, benzene = 30 mL

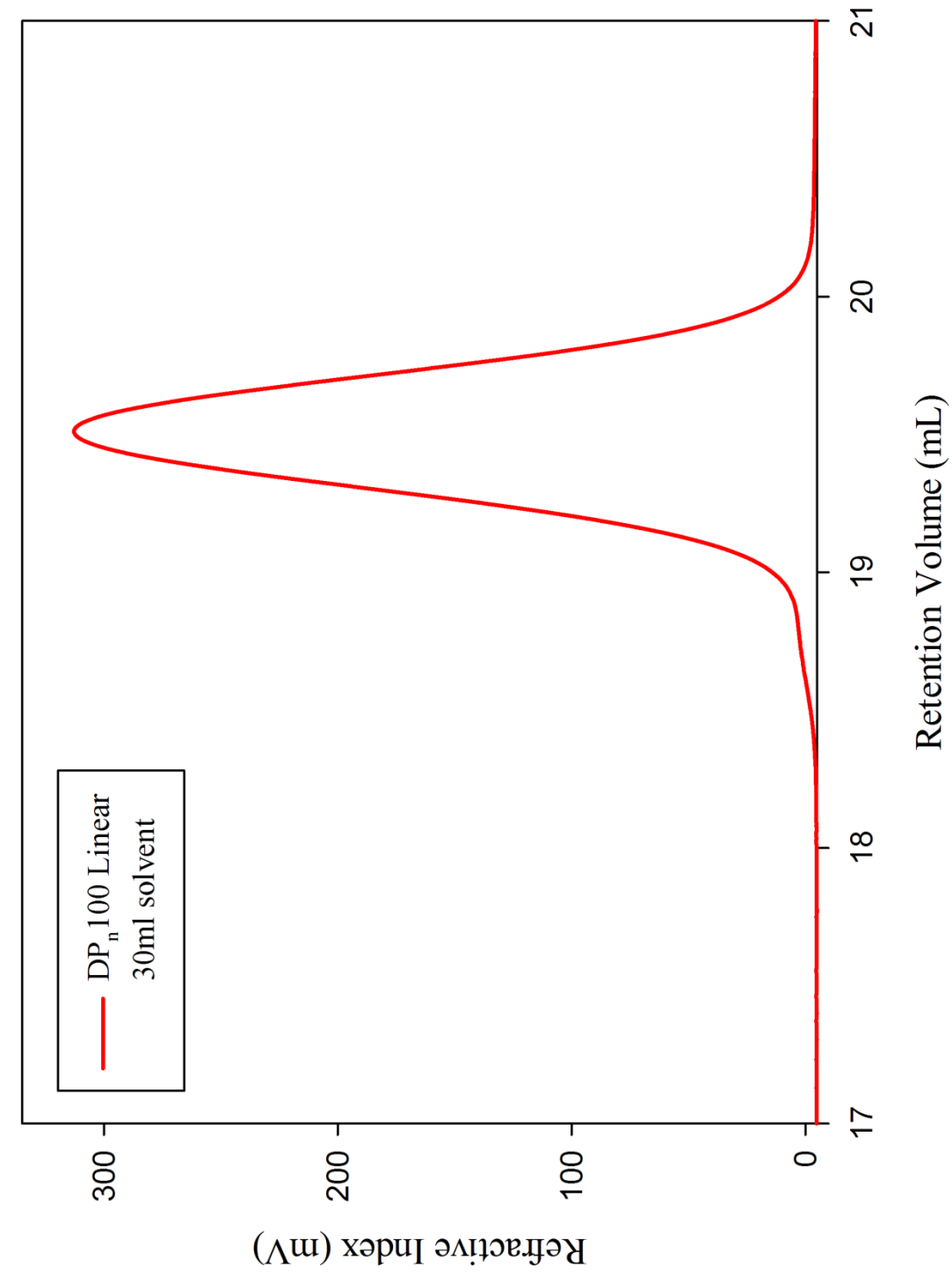

DP_n50, benzene = 40 mL

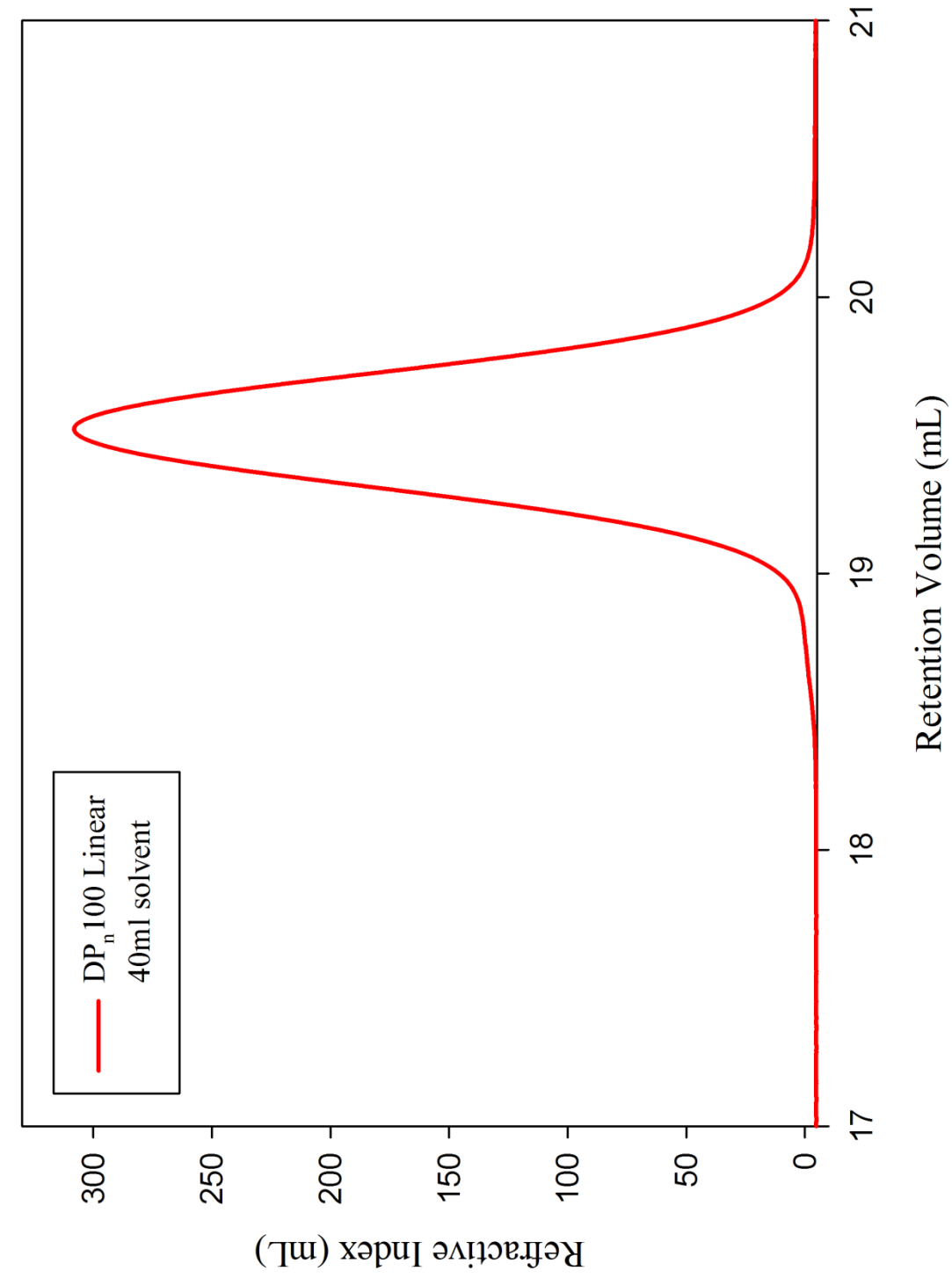

DP_n50, benzene = 50 mL

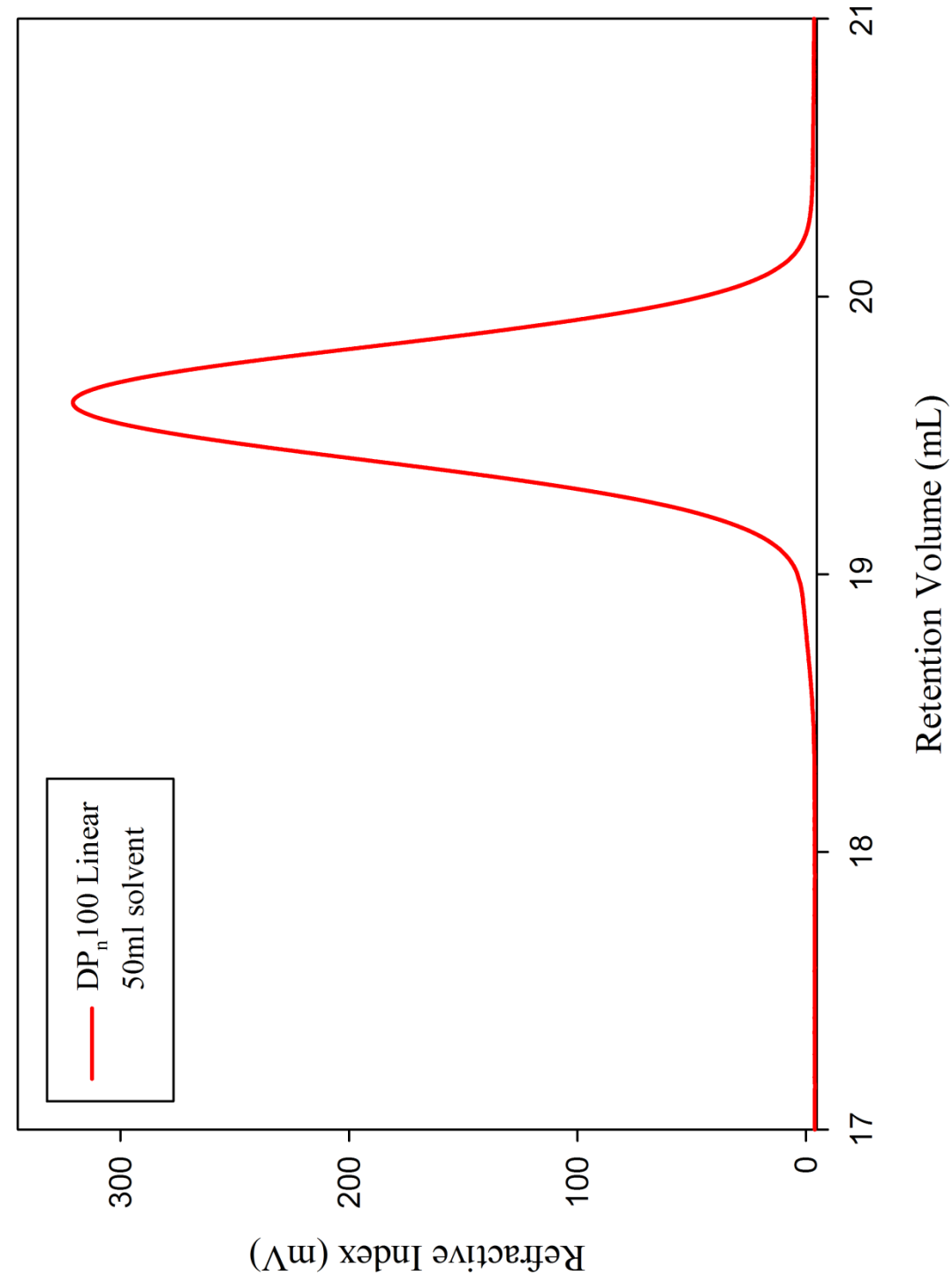

DP_n50, benzene = 60 mL

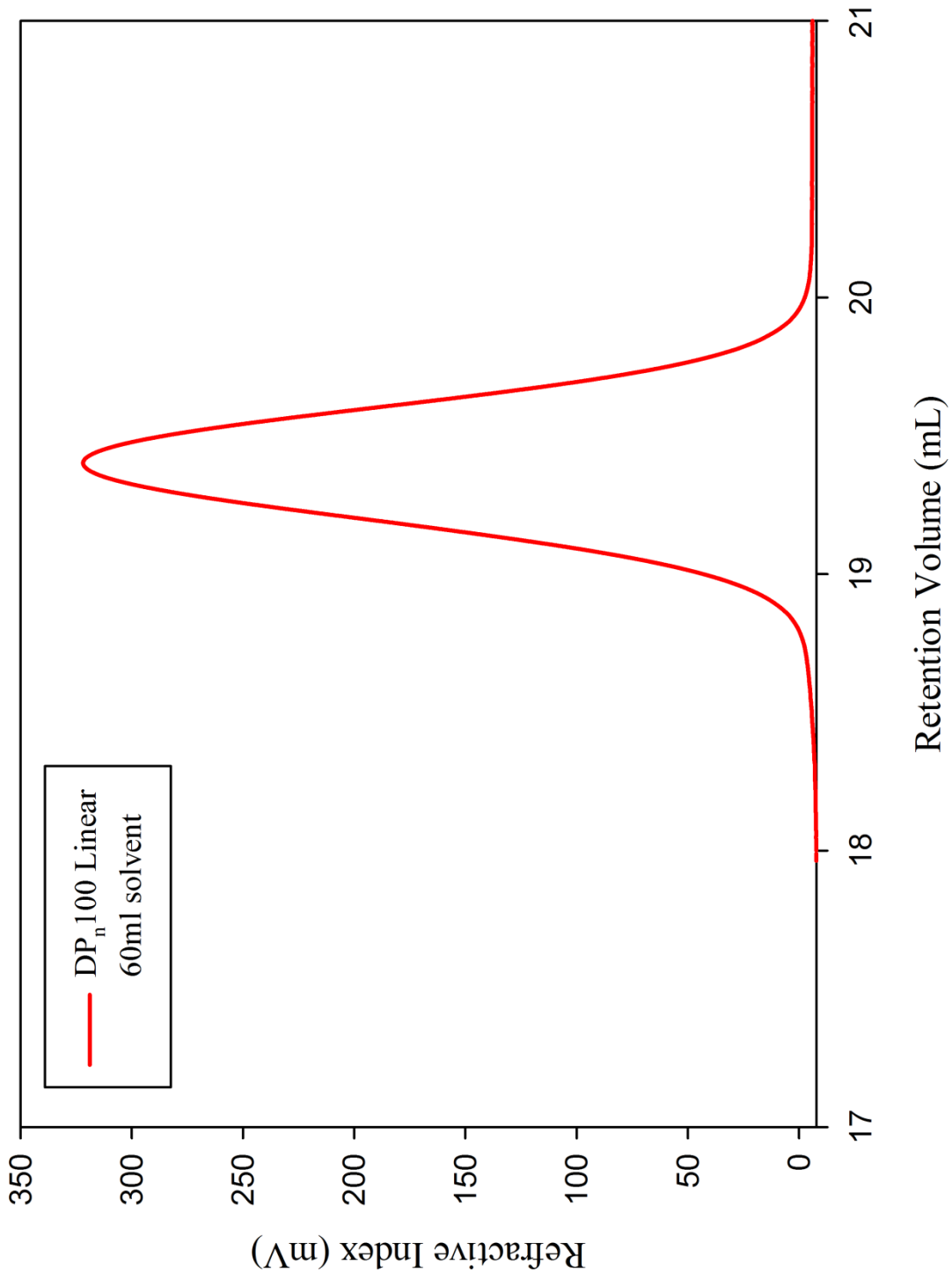

3.2.2.2 Chain extension of linear polystyrenes polymerised under ambient anionic conditions

DP_n50 linear

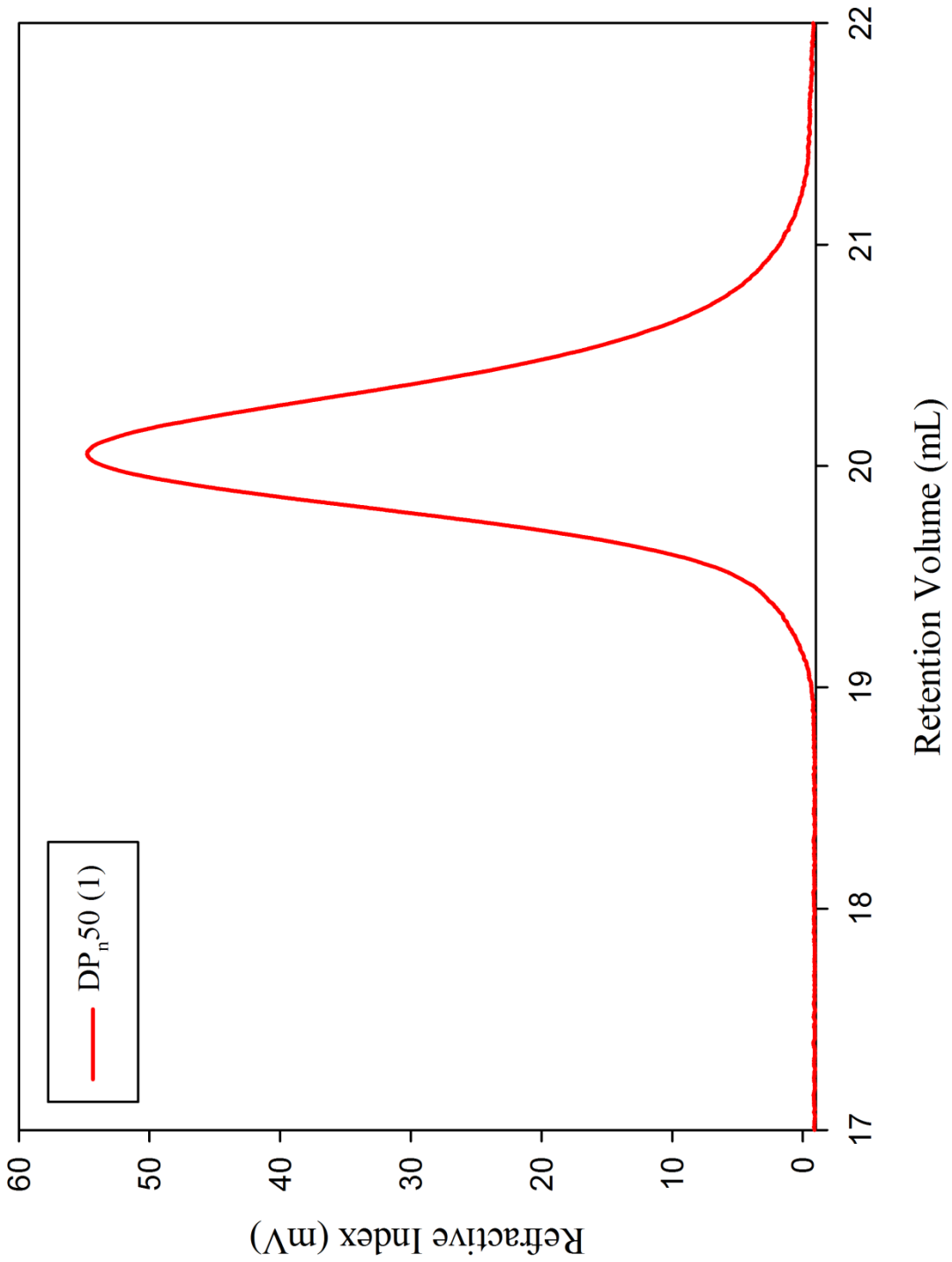

DP_n50 linear plus DP_n50 linear

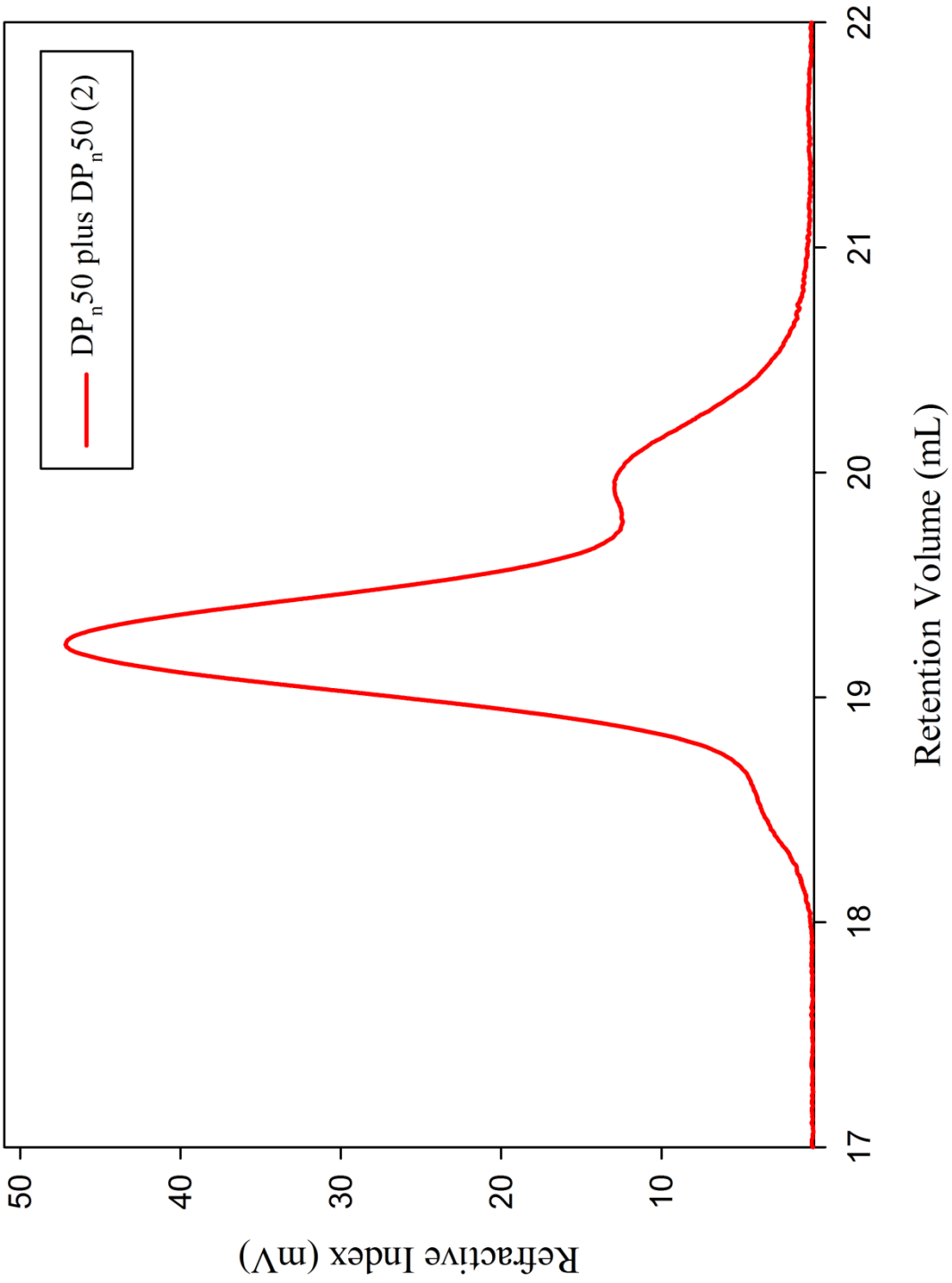

DP_n50 linear plus DP_n50 linear plus DP_n50 linear

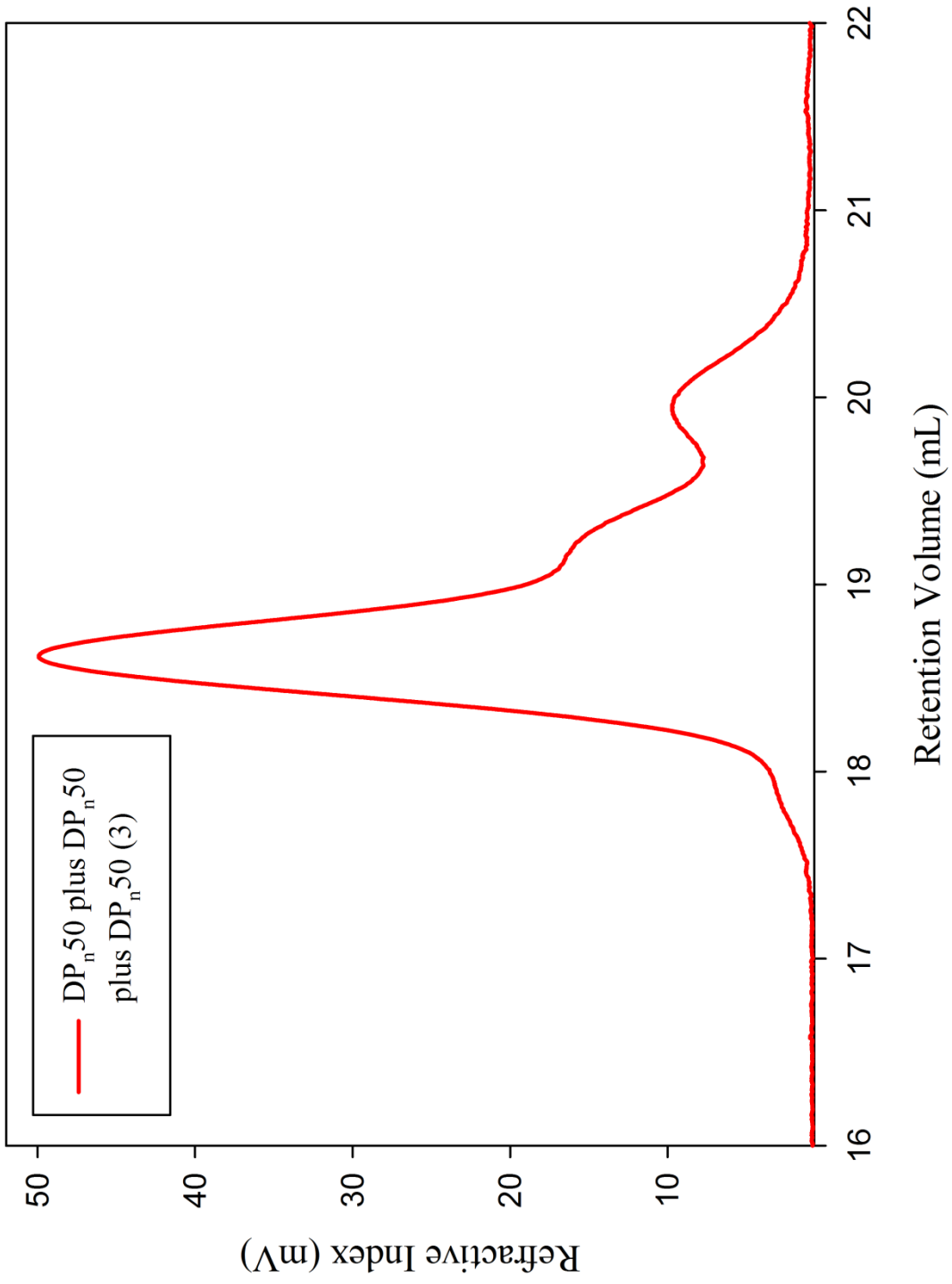

DP_n150 linear

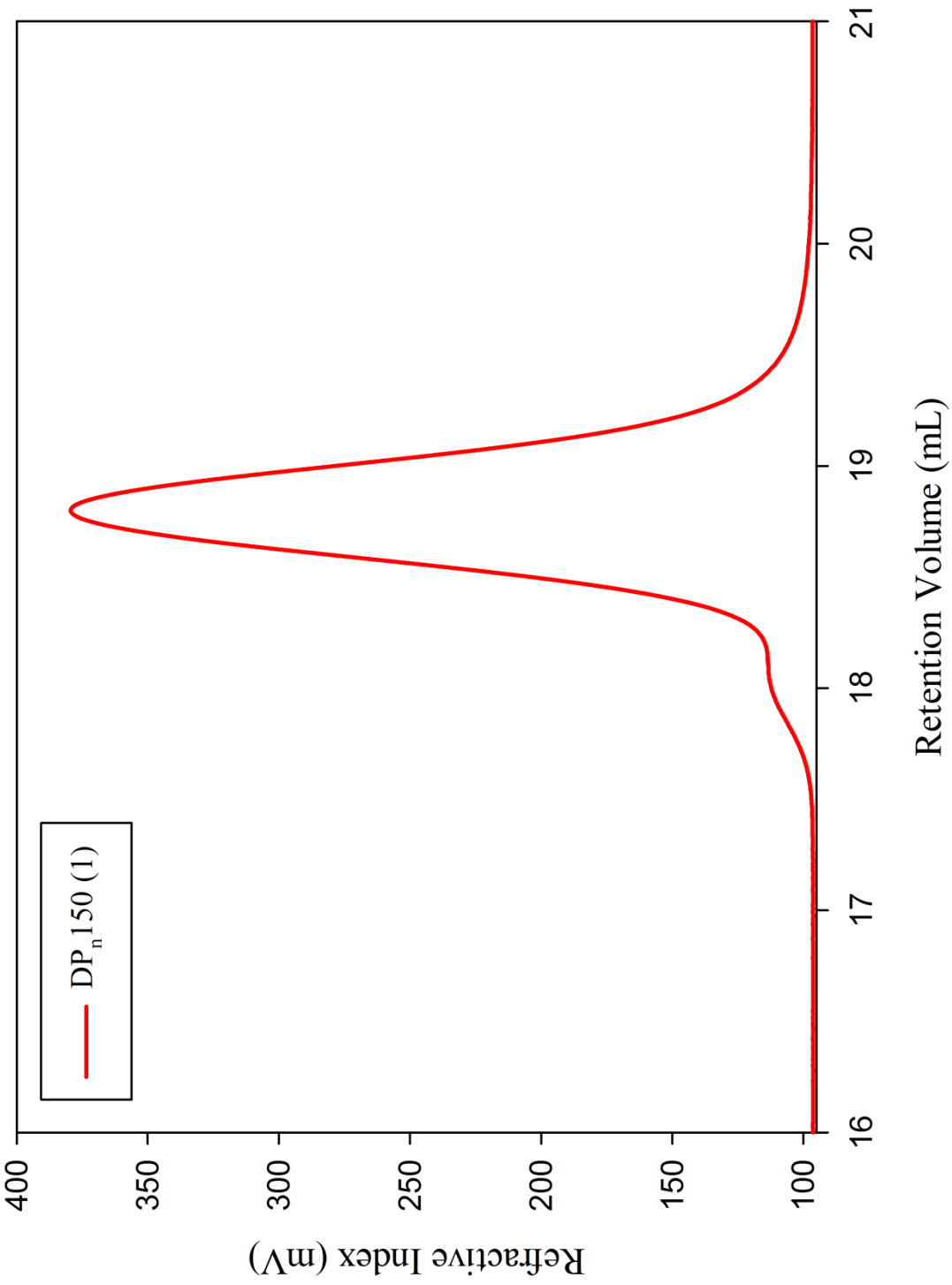

DP_n150 linear plus DP_n50 linear

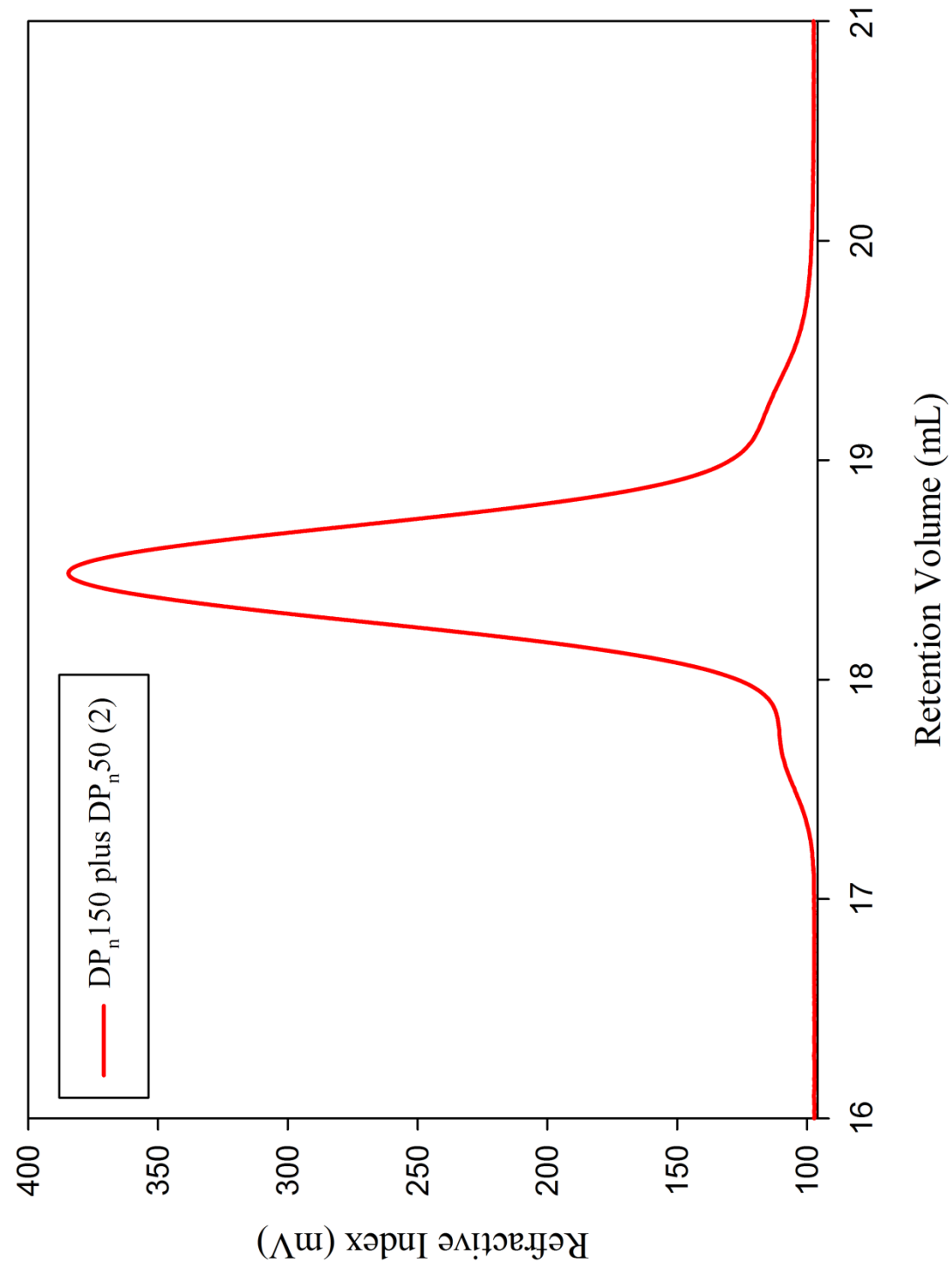

DP_n150 linear plus DP_n50 linear plus DP_n50 linear

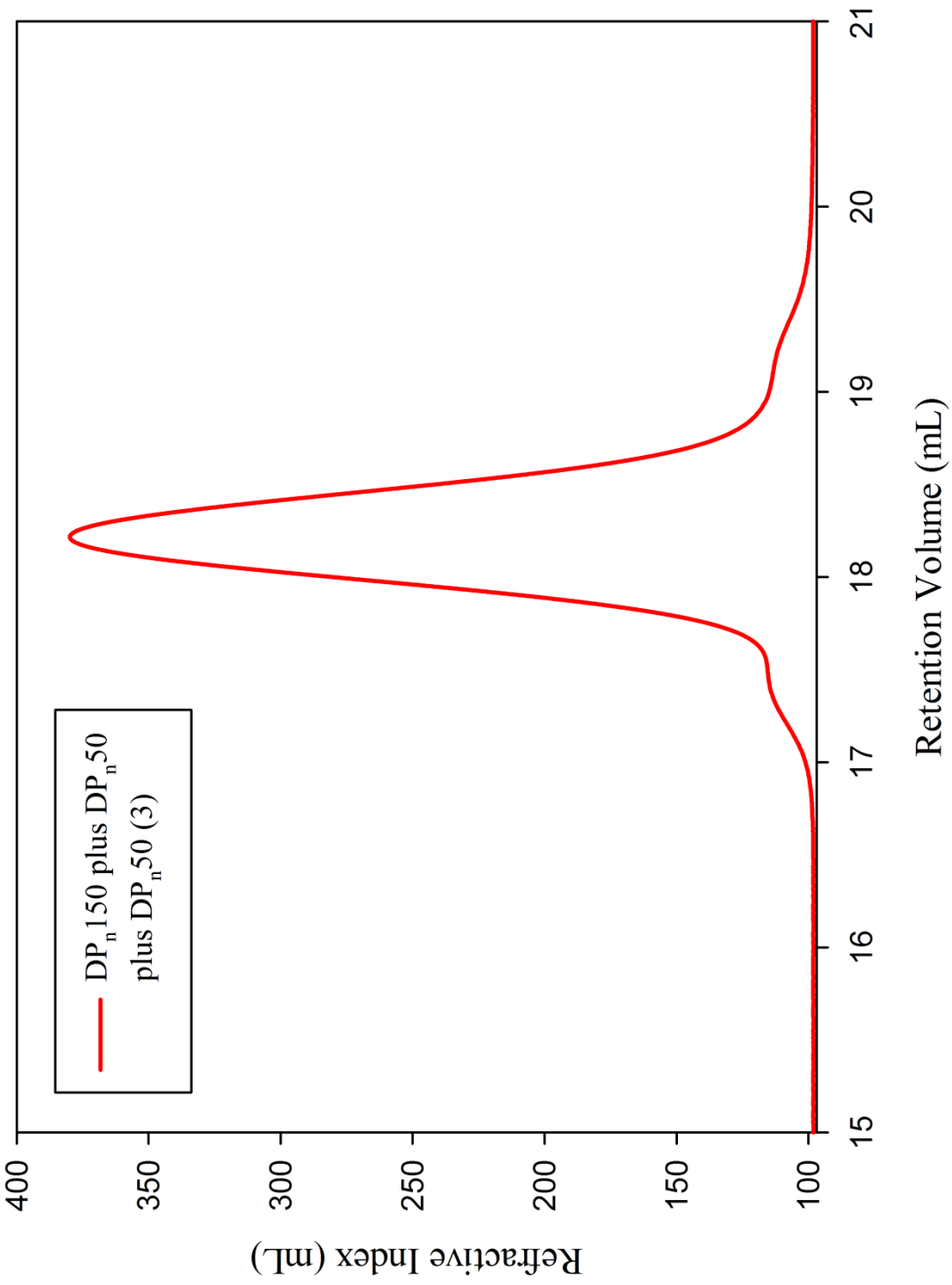

DP_n10 linear plus DP_n40 linear

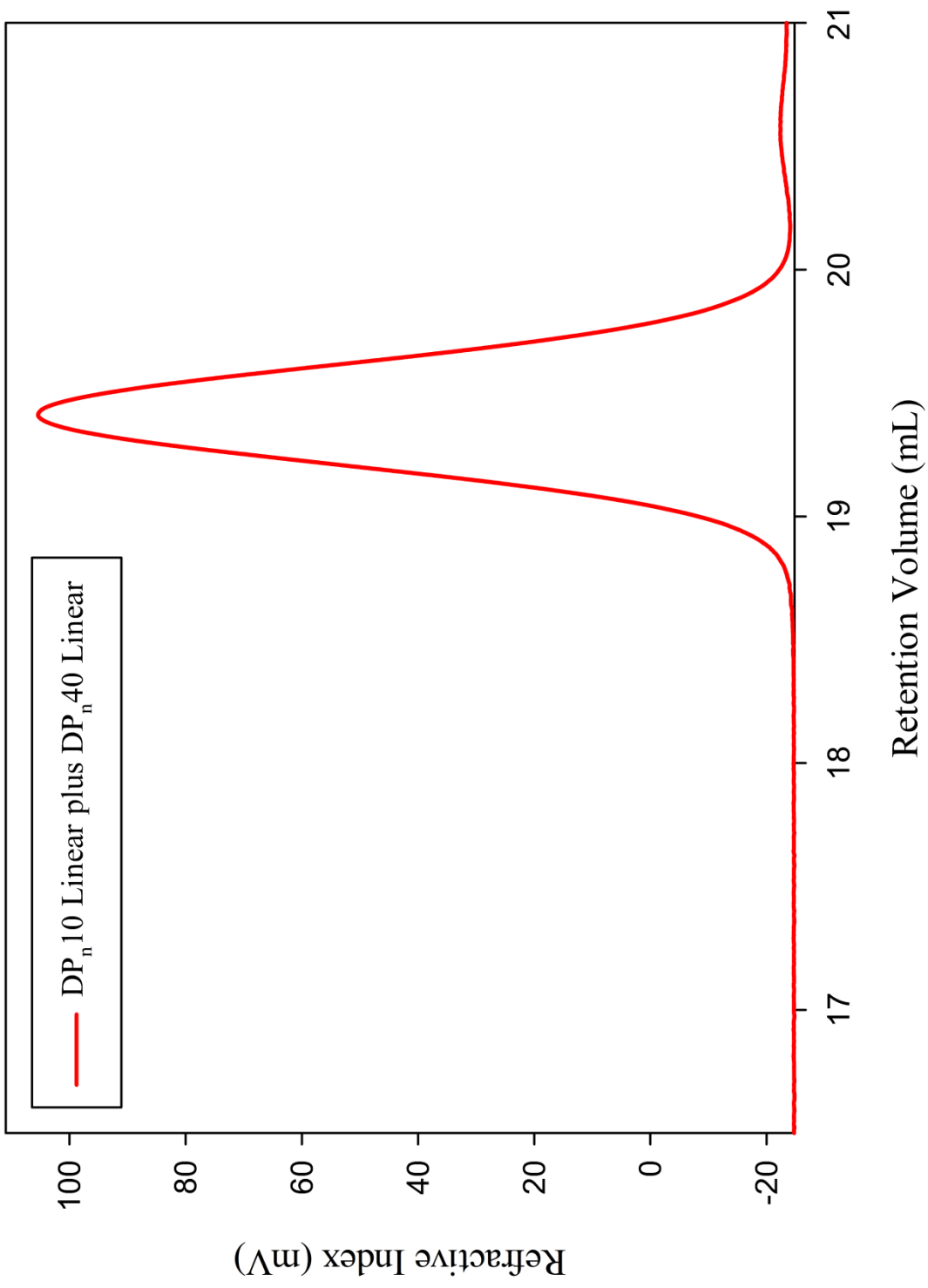

DP_n10 linear plus DP_n90 linear

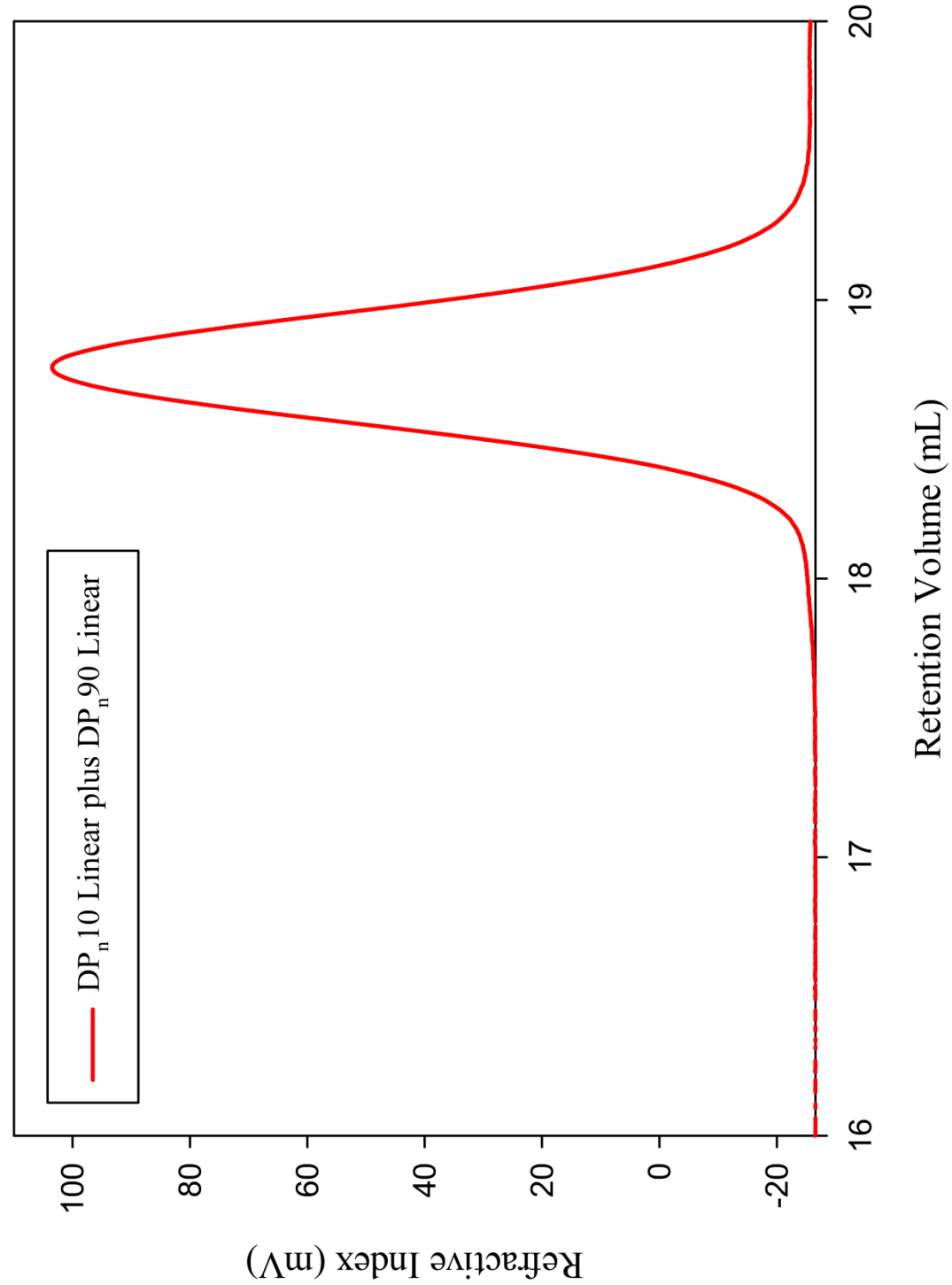

DP_n50 linear plus DP_n50 linear

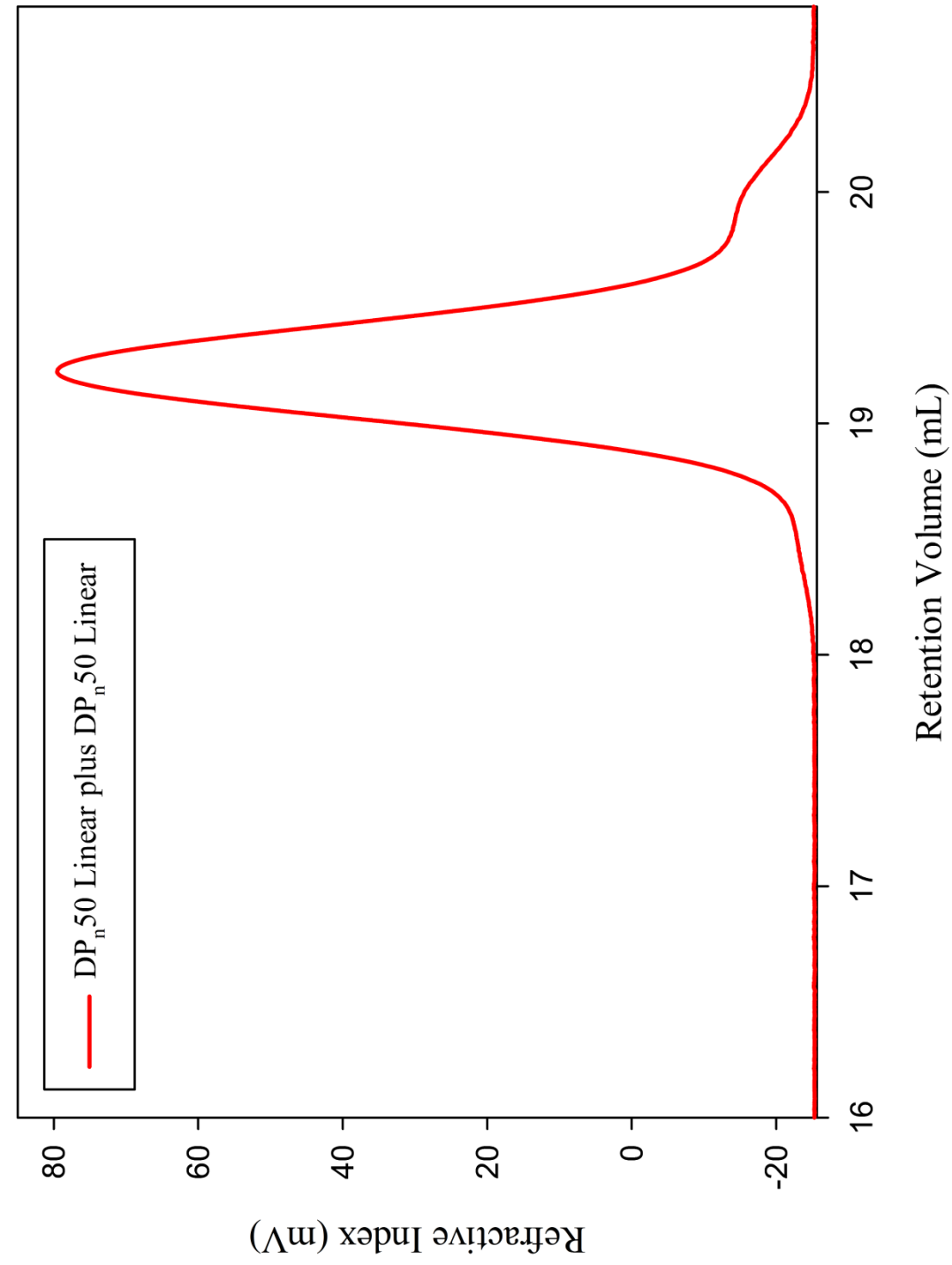

3.2.2.3. Kinetic studies of linear polystyrene.

DP_n100, time = 10 minutes

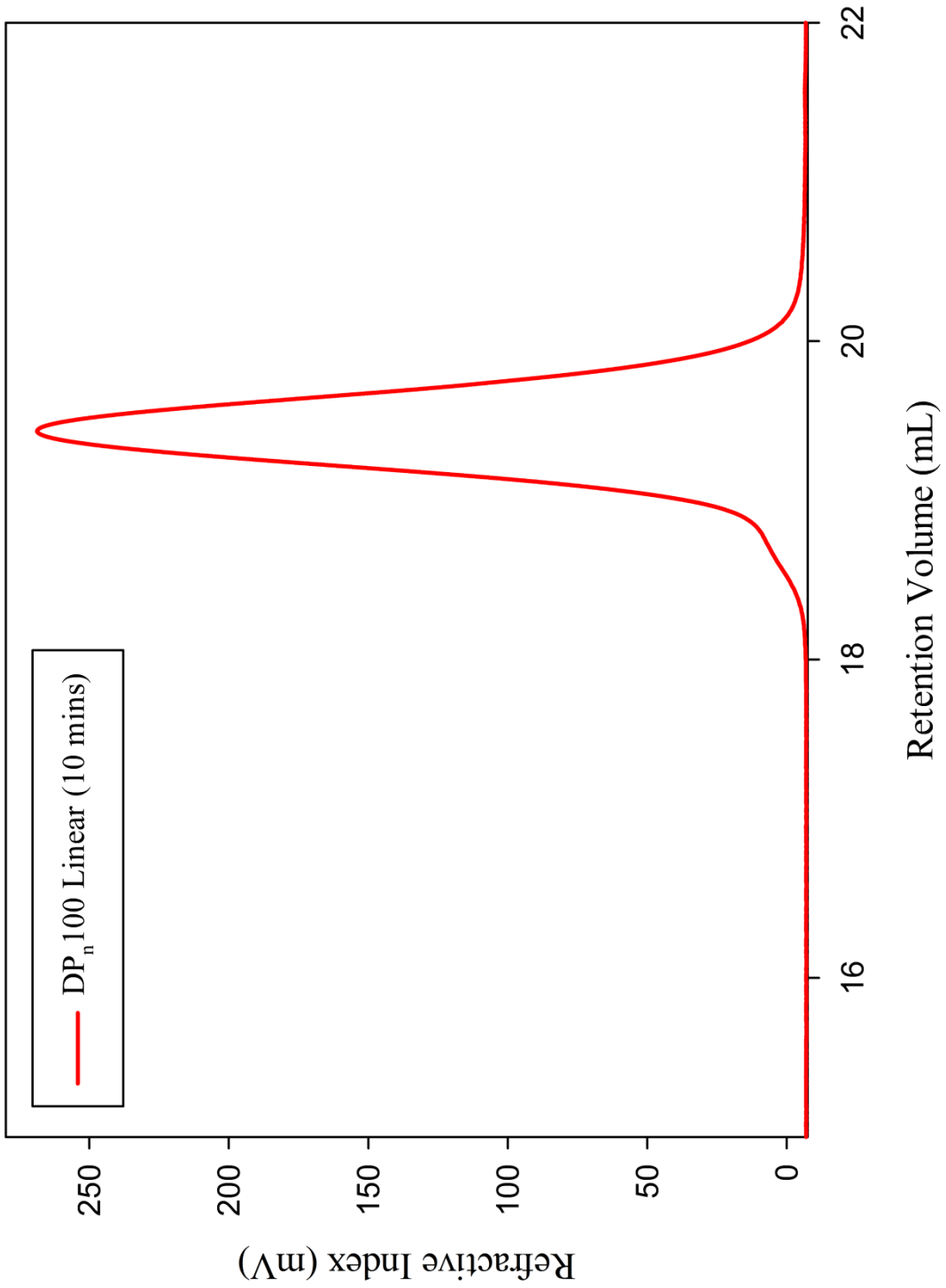

DP_n100, time = 30 minutes

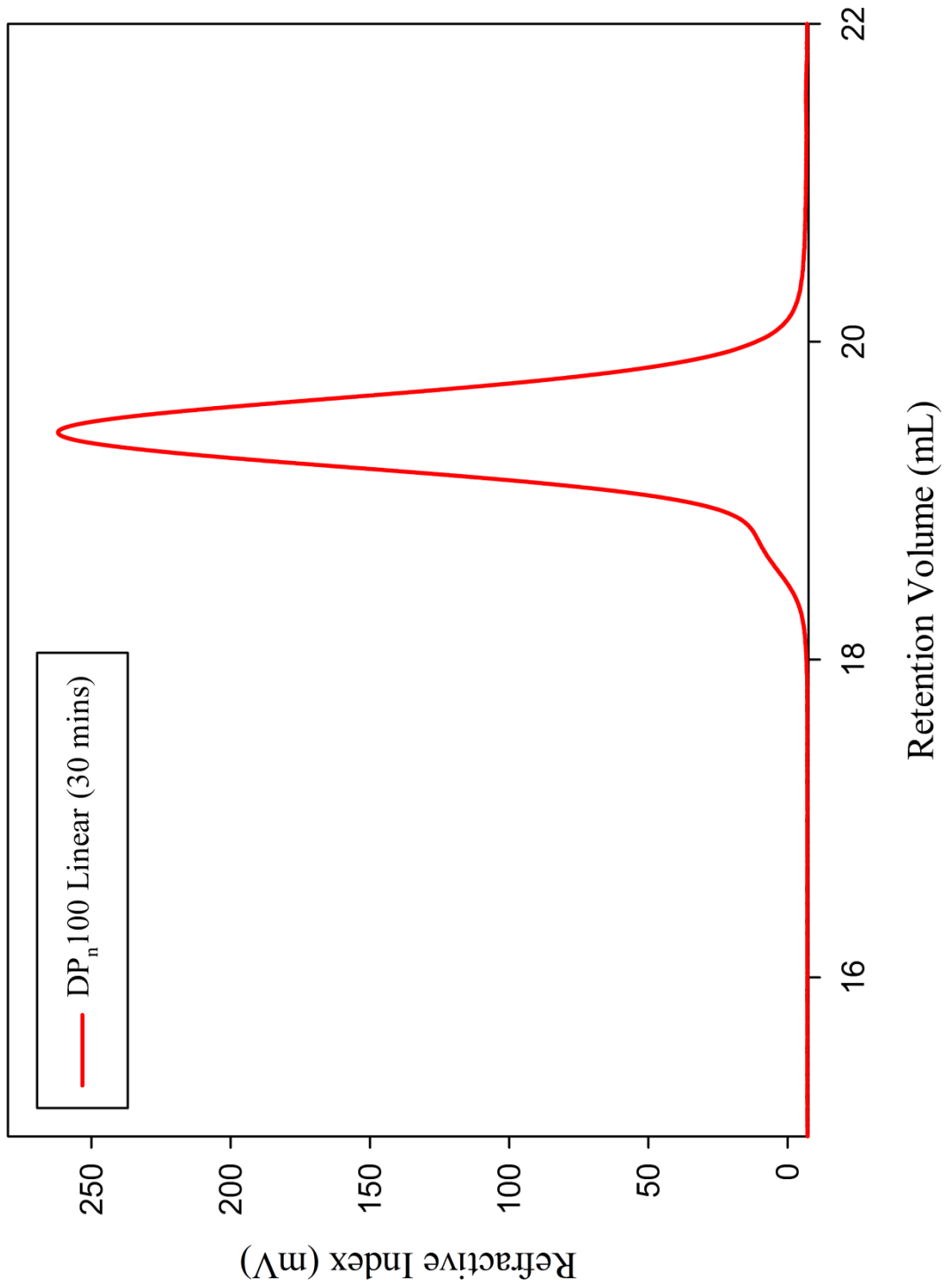

DP_n100, time = 90 minutes

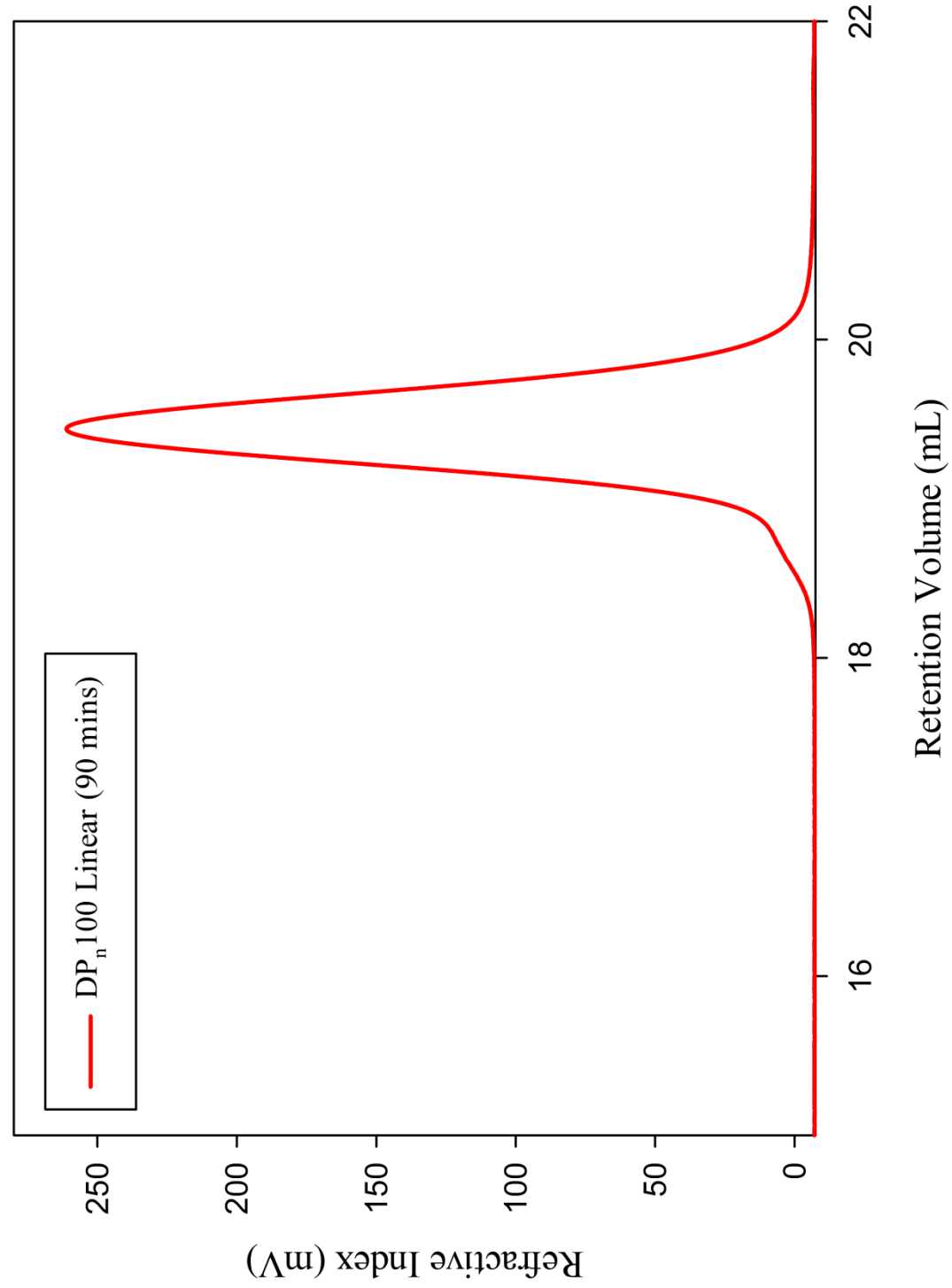

DP_n100, time = 20 hours

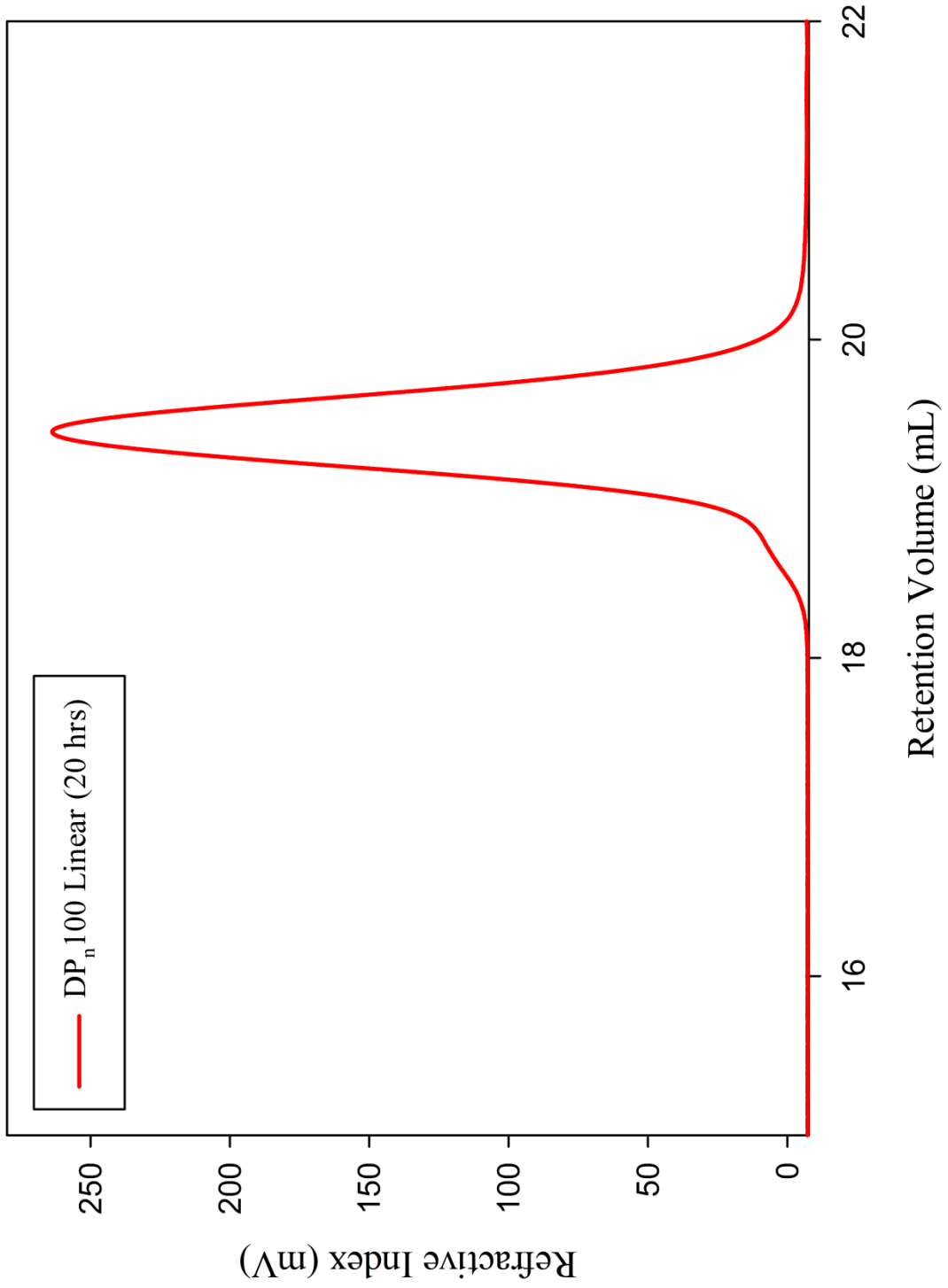

3.2.2.2.1 Synthesis of polystyrene initiated with bis(4-bromophenyl)ether

DP_n200, initiator; bis(4-bromophenyl)ether/ *sec*-BuLi adduct

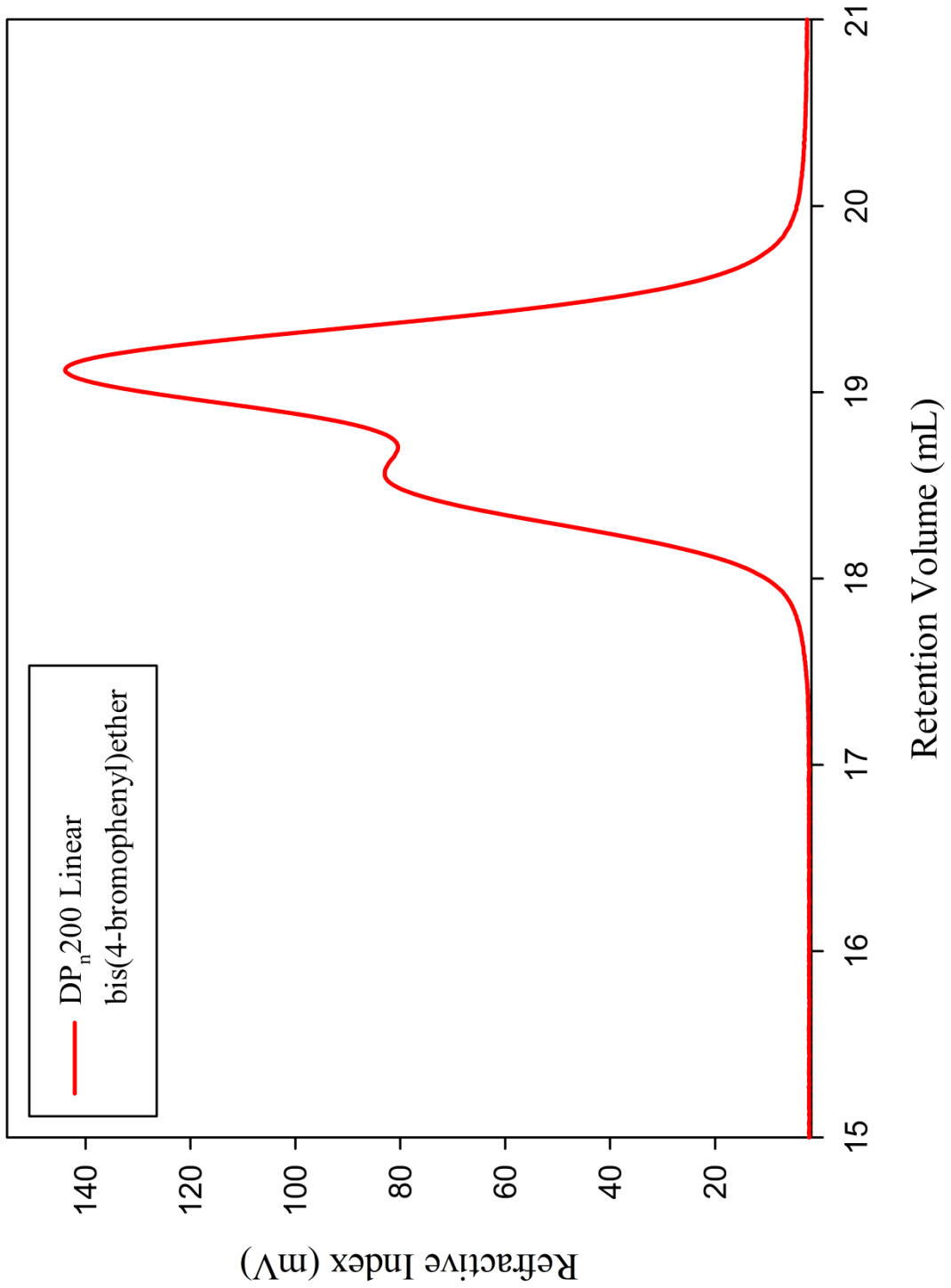

DP_n200, initiator; bis(4-bromophenyl)ether/ excess *sec*-BuLi adduct

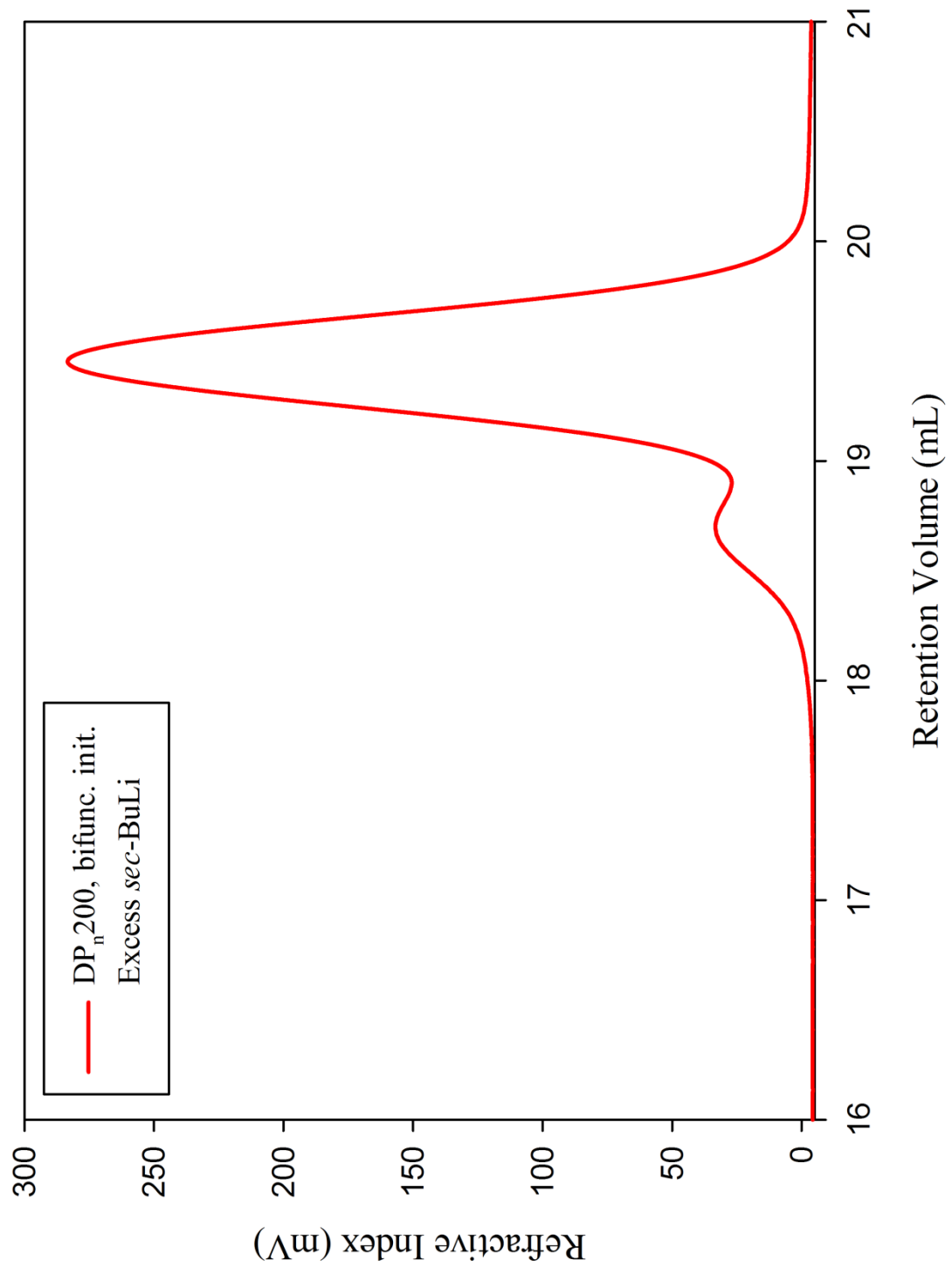

3.2.2.2.2 Use of 2,7-dibromofluorene as diaryl compound

DP_n200, initiator; 2,7-dibromofluorene/ *sec*-BuLi adduct

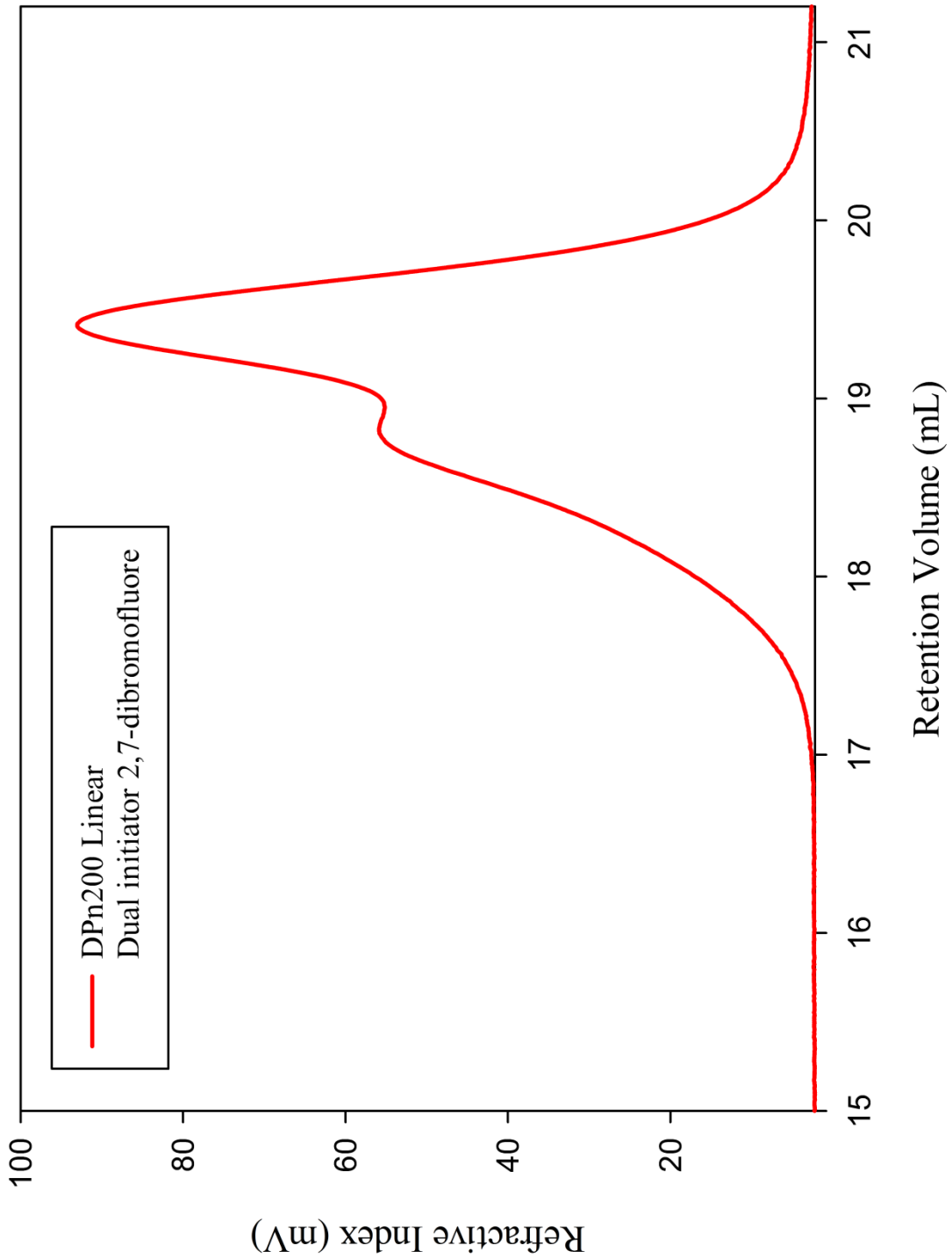

Chapter 4

4.1 Synthesis of branched polystyrene by ATRP

DP_n50 branched, ATRP, 24 hours

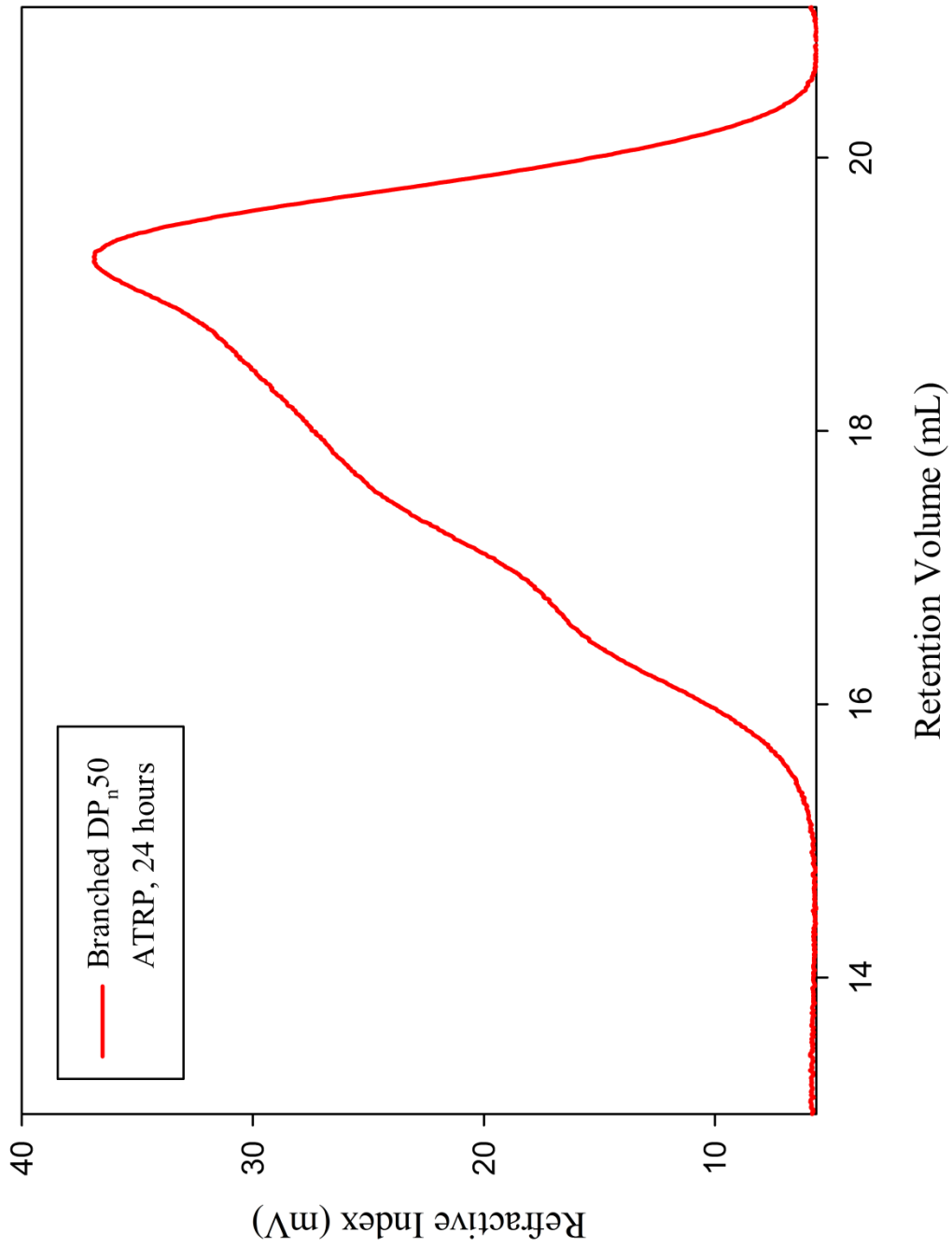

DP_n50 branched, ATRP, 48 hours

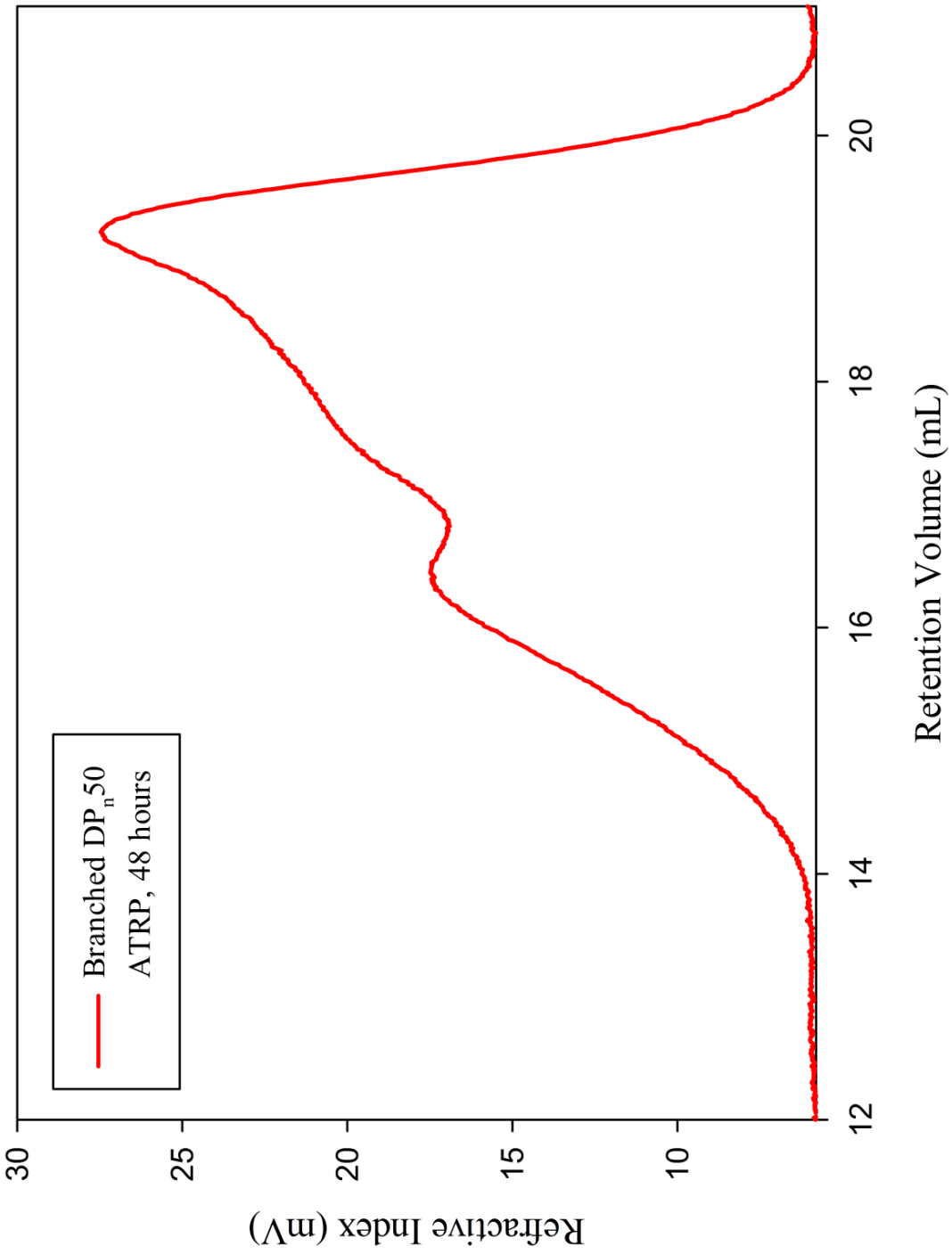

4.3.1 Effect of solvent concentration.

DP_n100 branched, DVB, 30ml (t= 10 min)

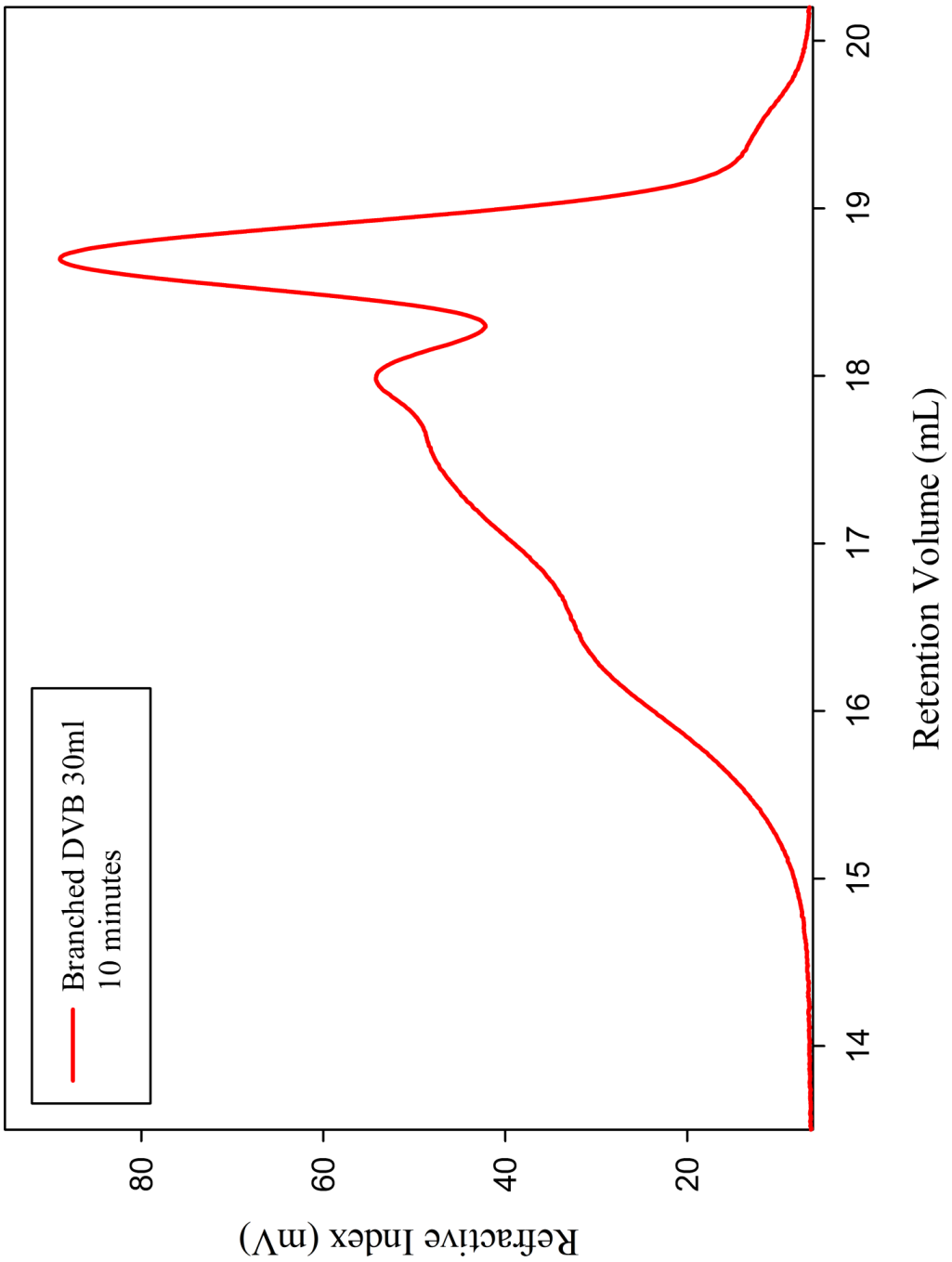

DP_n100 branched, DVB, 30ml (t= 50 min)

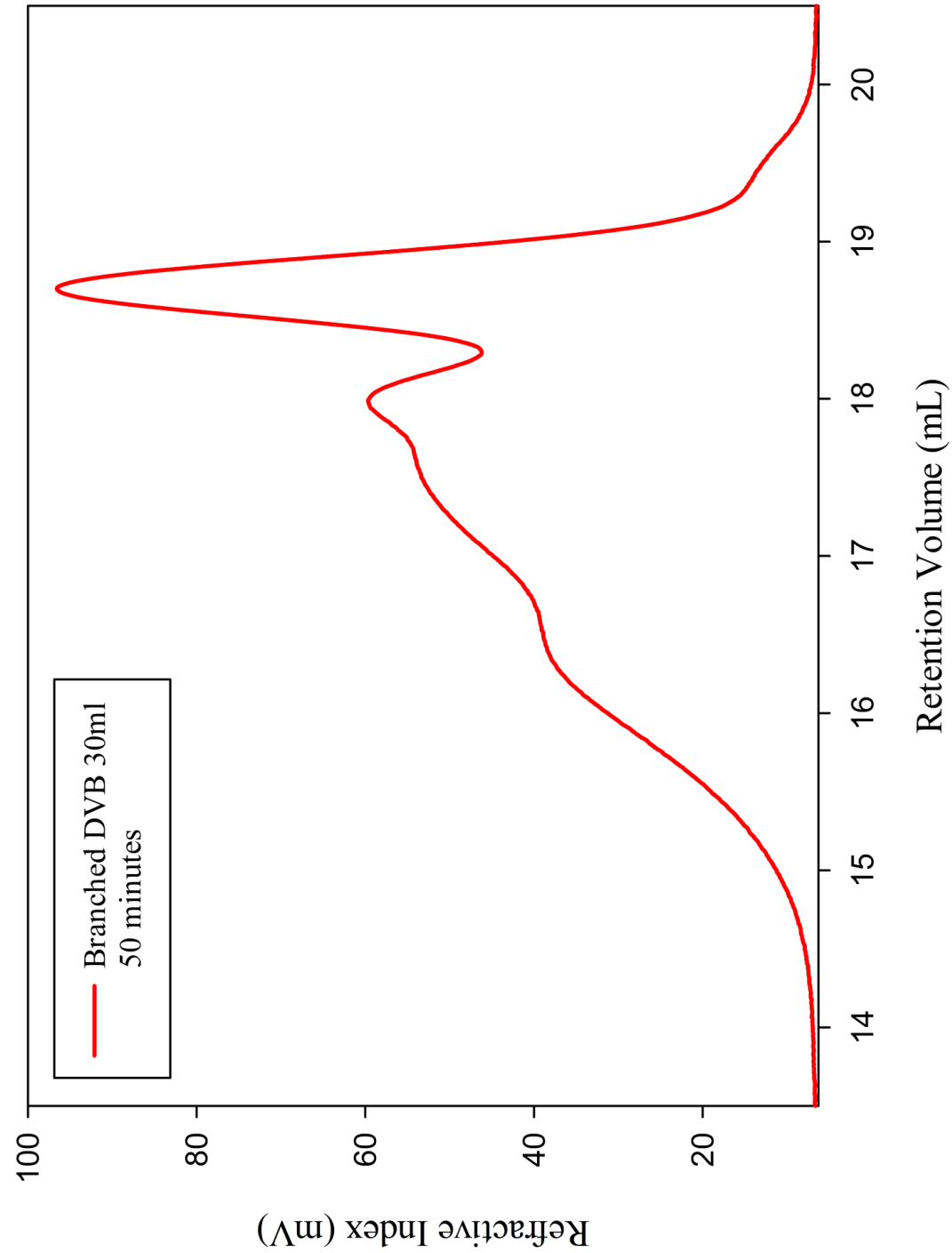

DP_n100 branched, DVB, 30ml (t= 100 min)

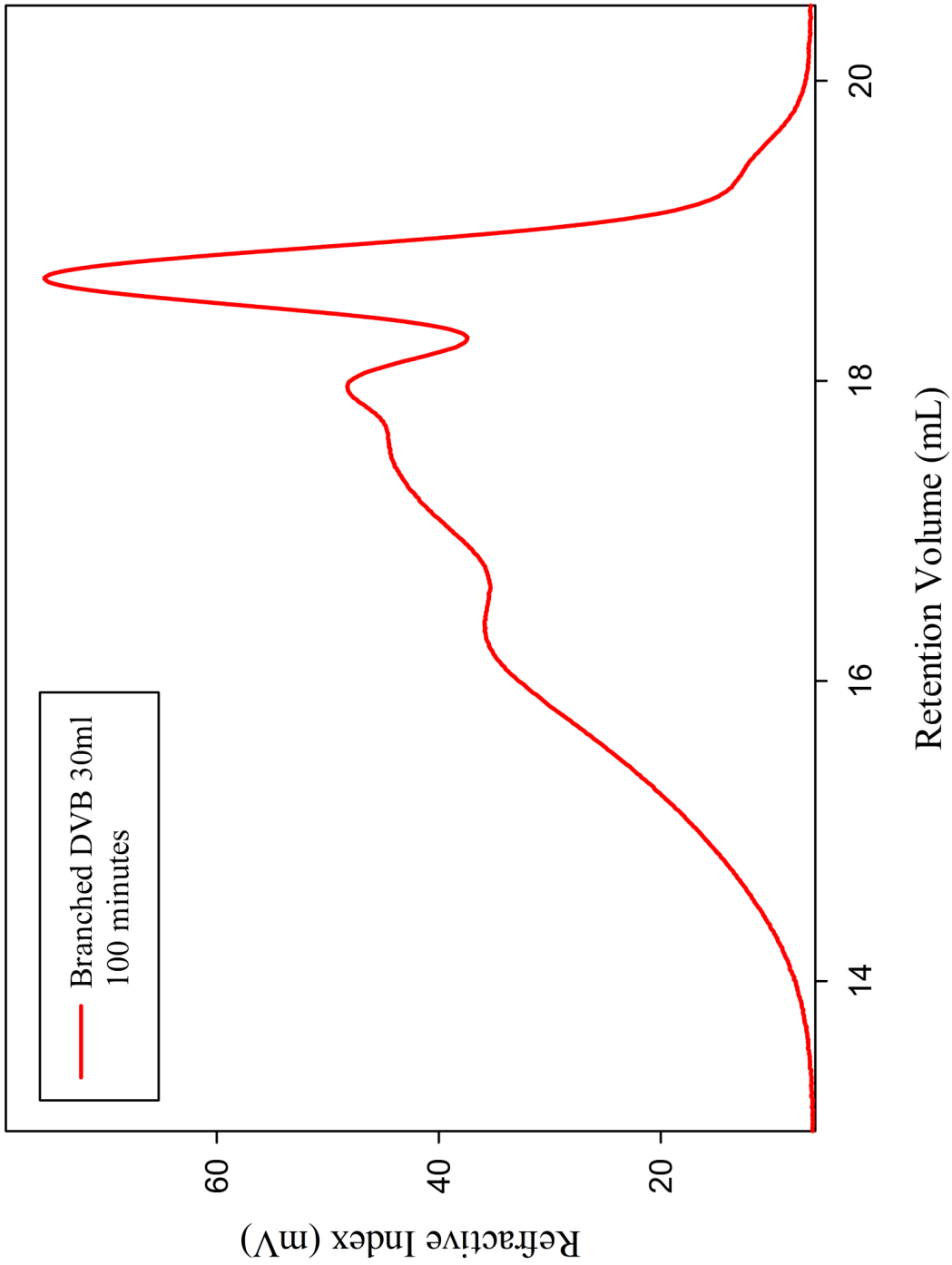

DP_n100 branched, DVB, 30ml (t= 200 min)

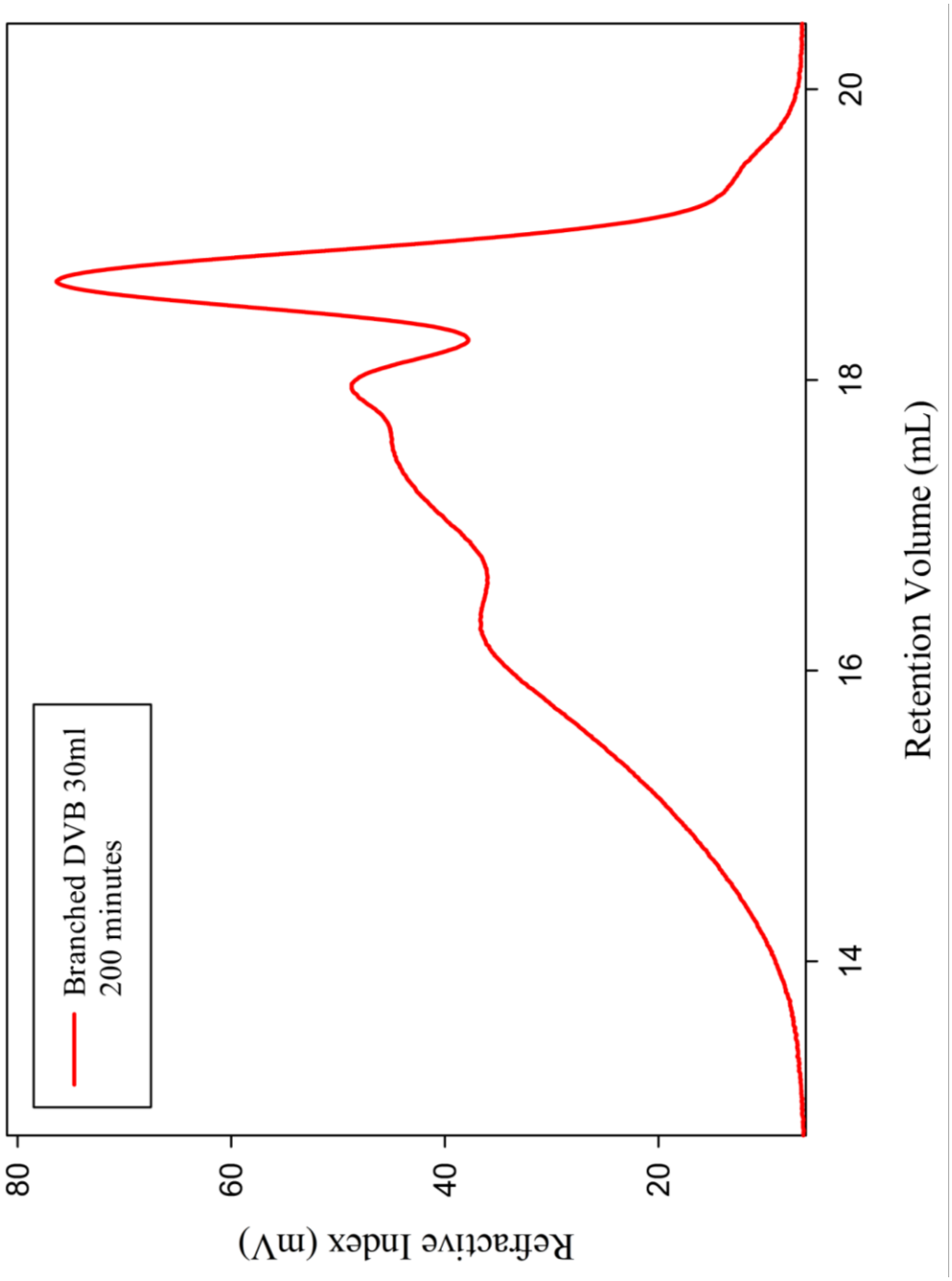

DP_n100 branched, DVB, 60ml (t= 10 min)

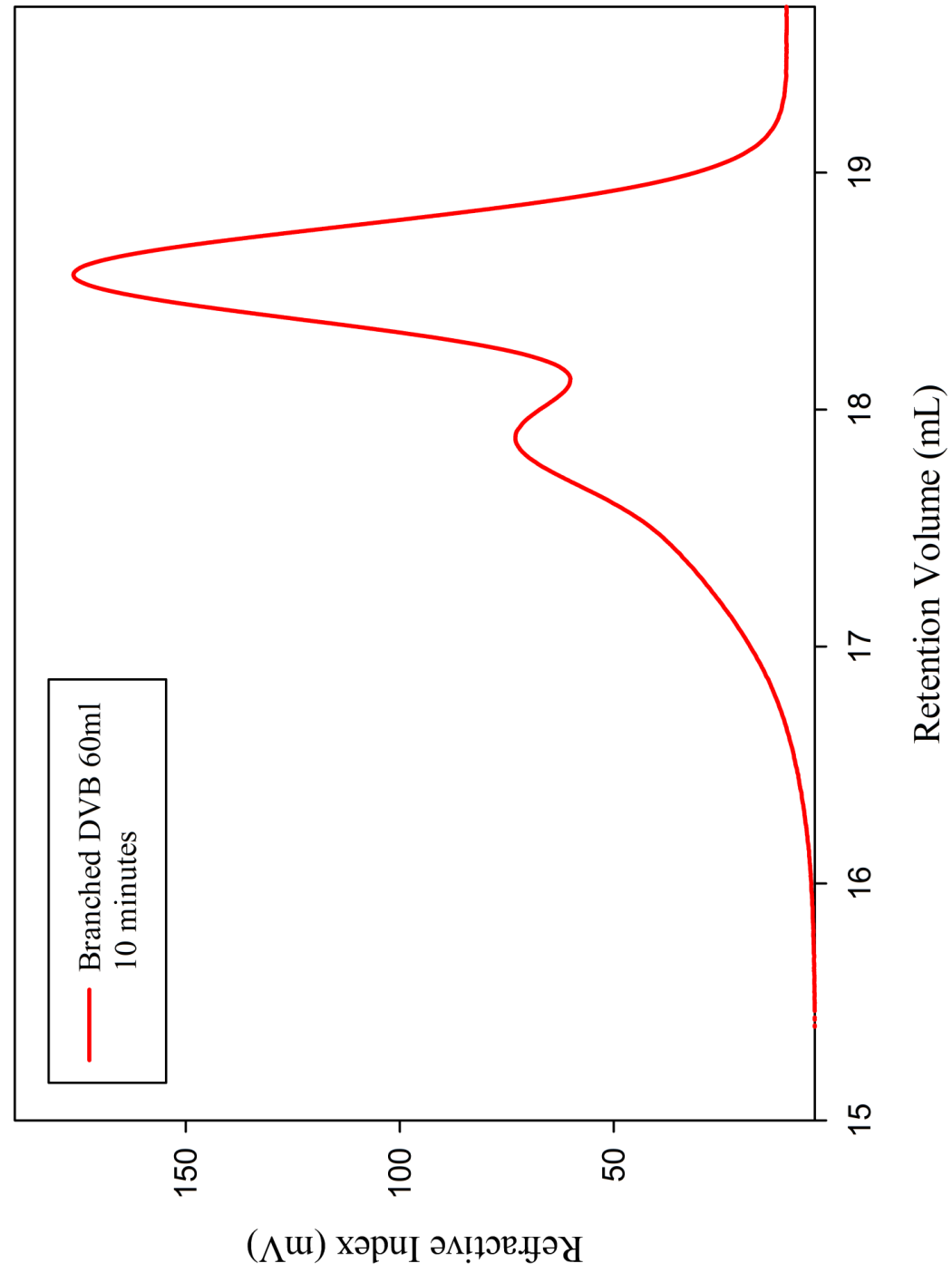

DP_n100 branched, DVB, 60ml (t= 50 min)

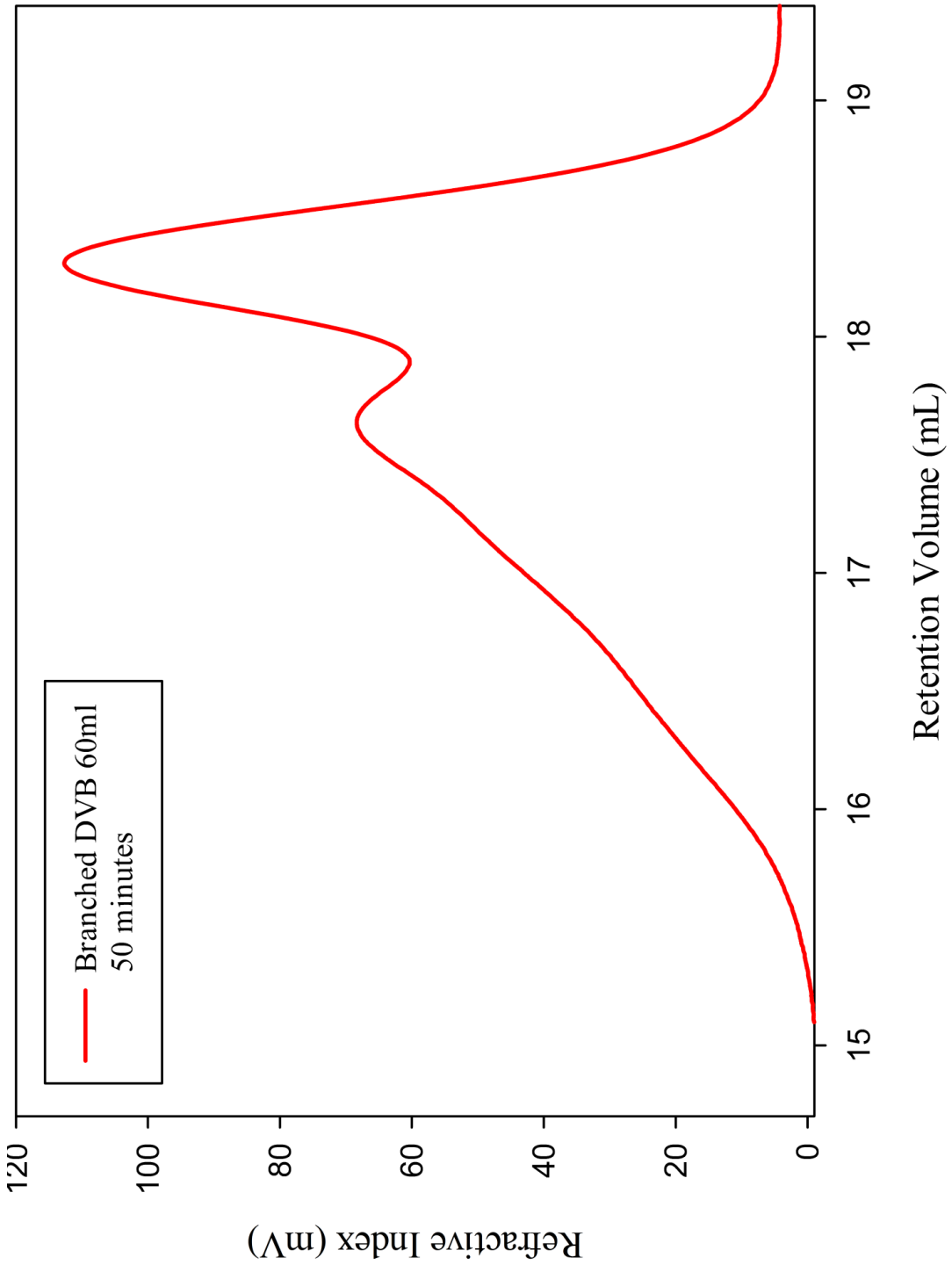

DP_n100 branched, DVB, 60ml (t= 100 min)

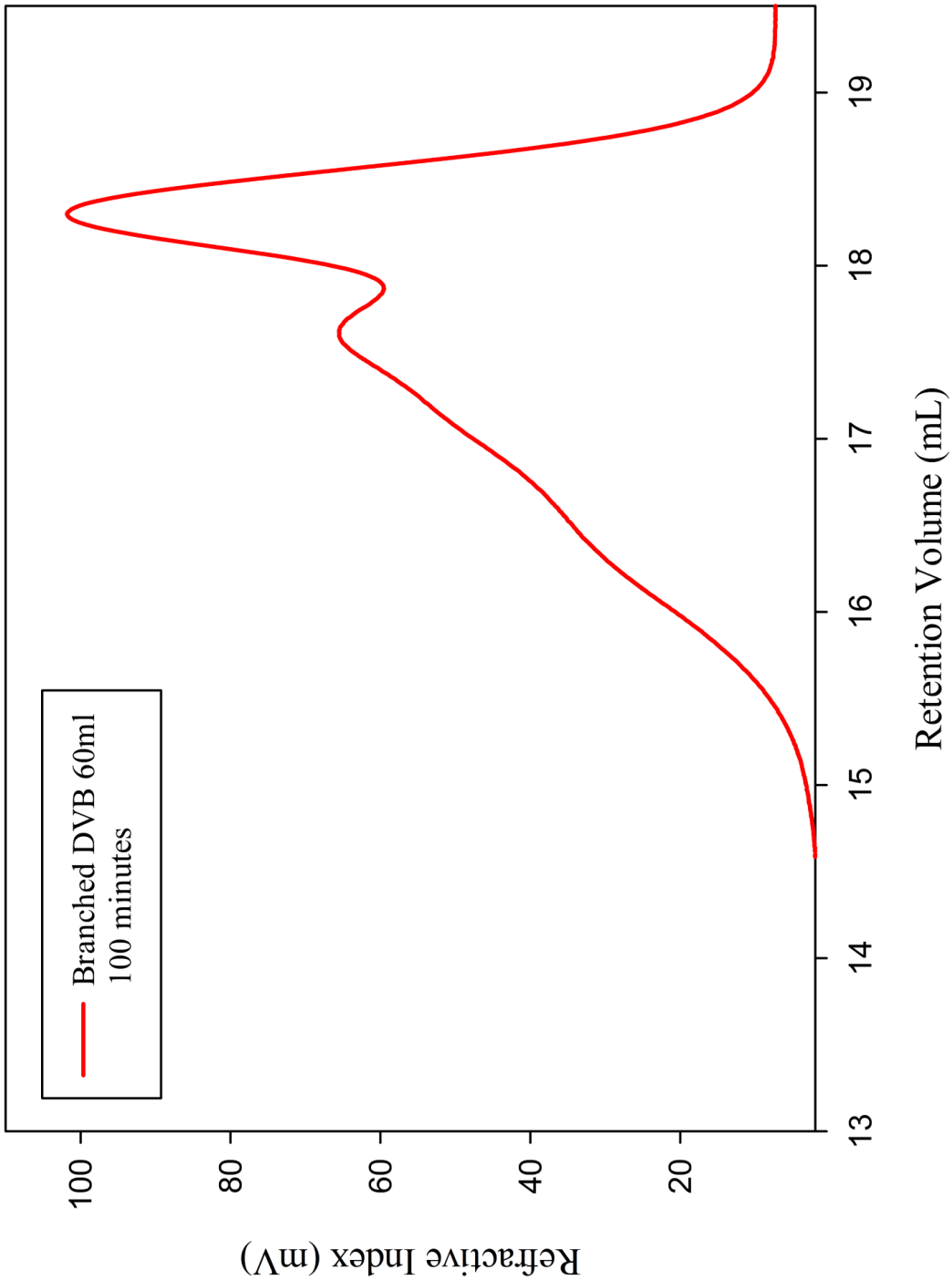

DP_n100 branched, DVB, 60ml (t= 200 min)

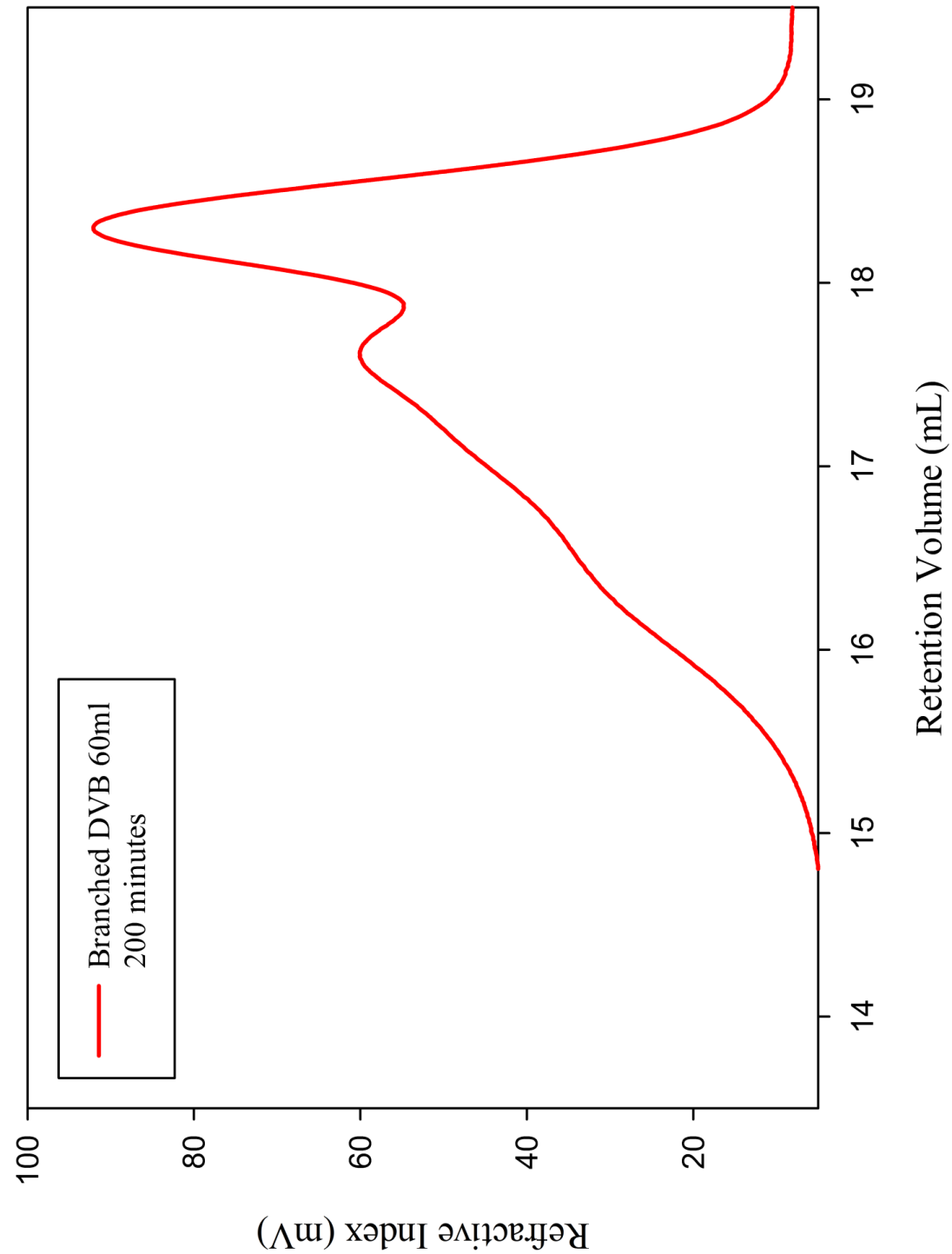

DP_n50 branched DVB, 0.97:1, 20ml

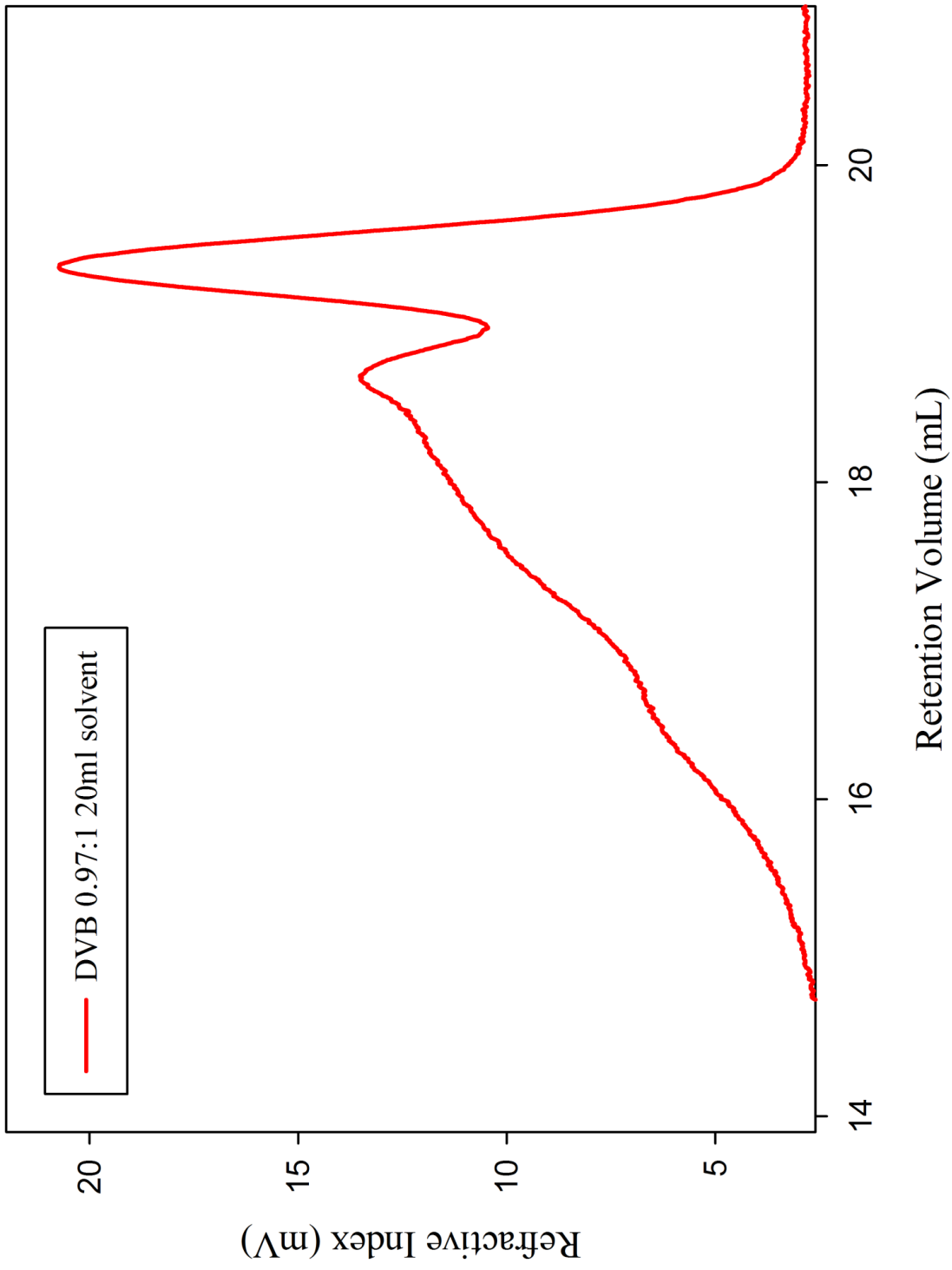

DP_n50 branched DVB, 0.97:1, 40ml

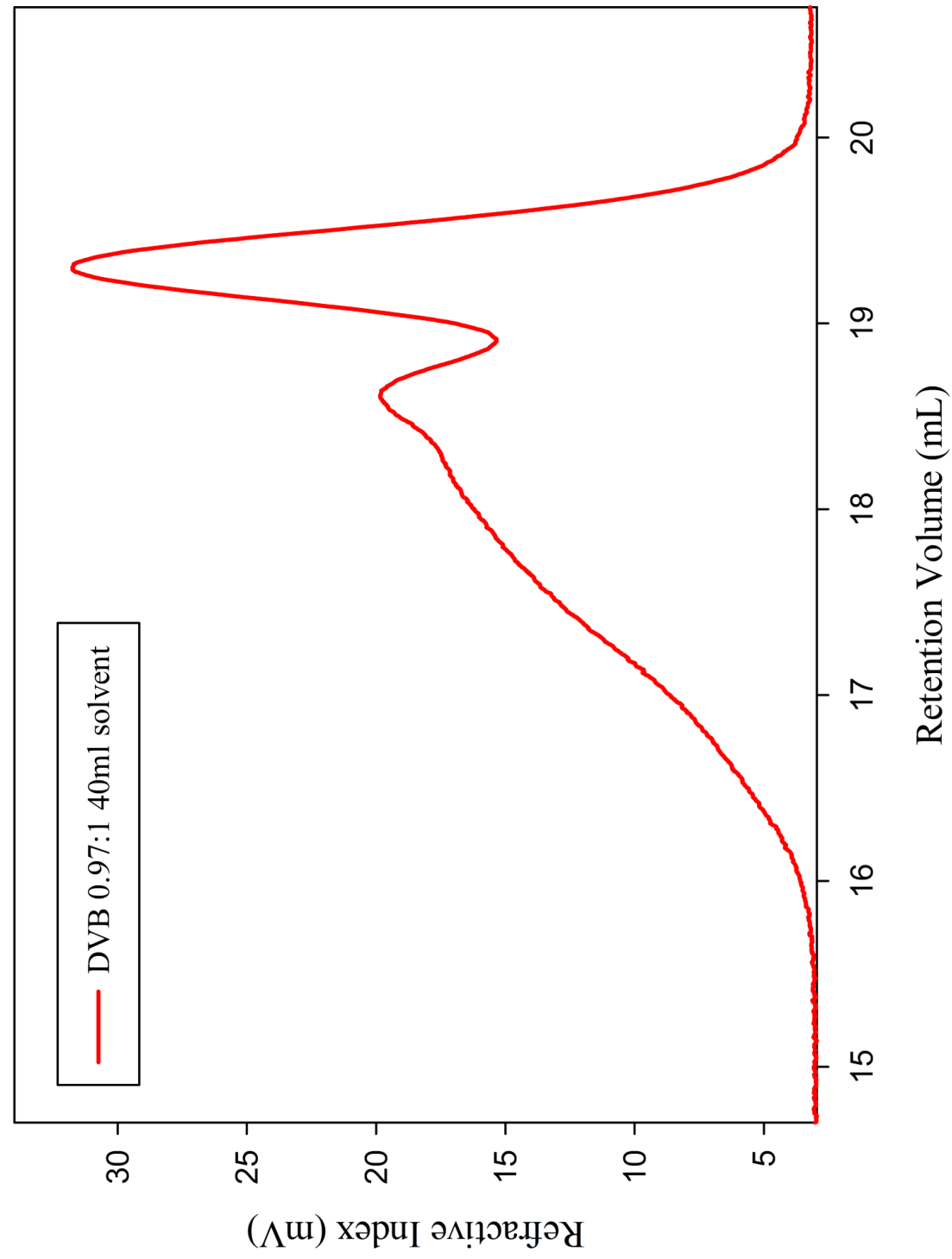

4.3.2 Increasing brancher ratio

DP_n 100 branched, DVB, 0.90:1

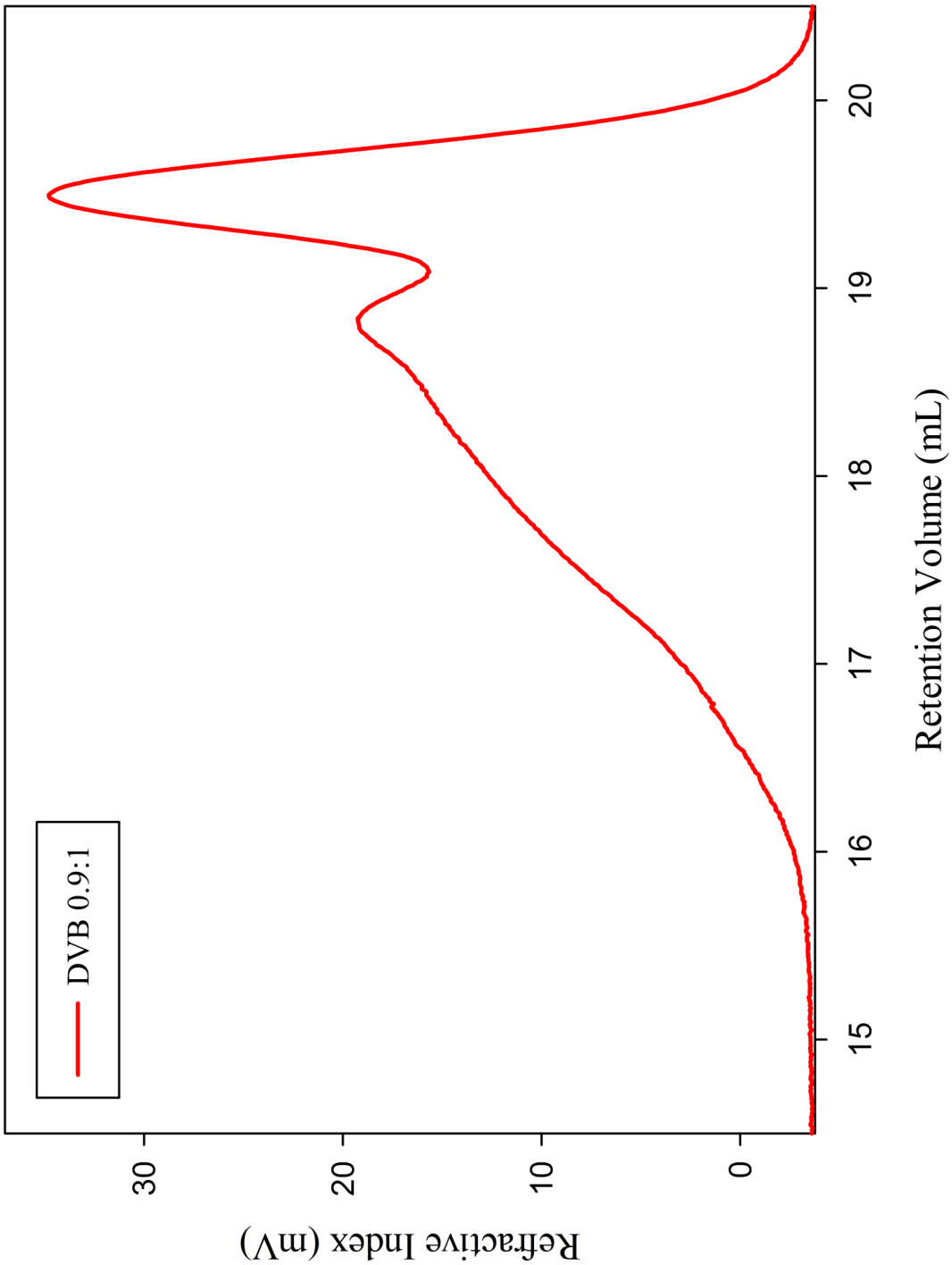

DP_n 100 branched, DVB, 0.91:1

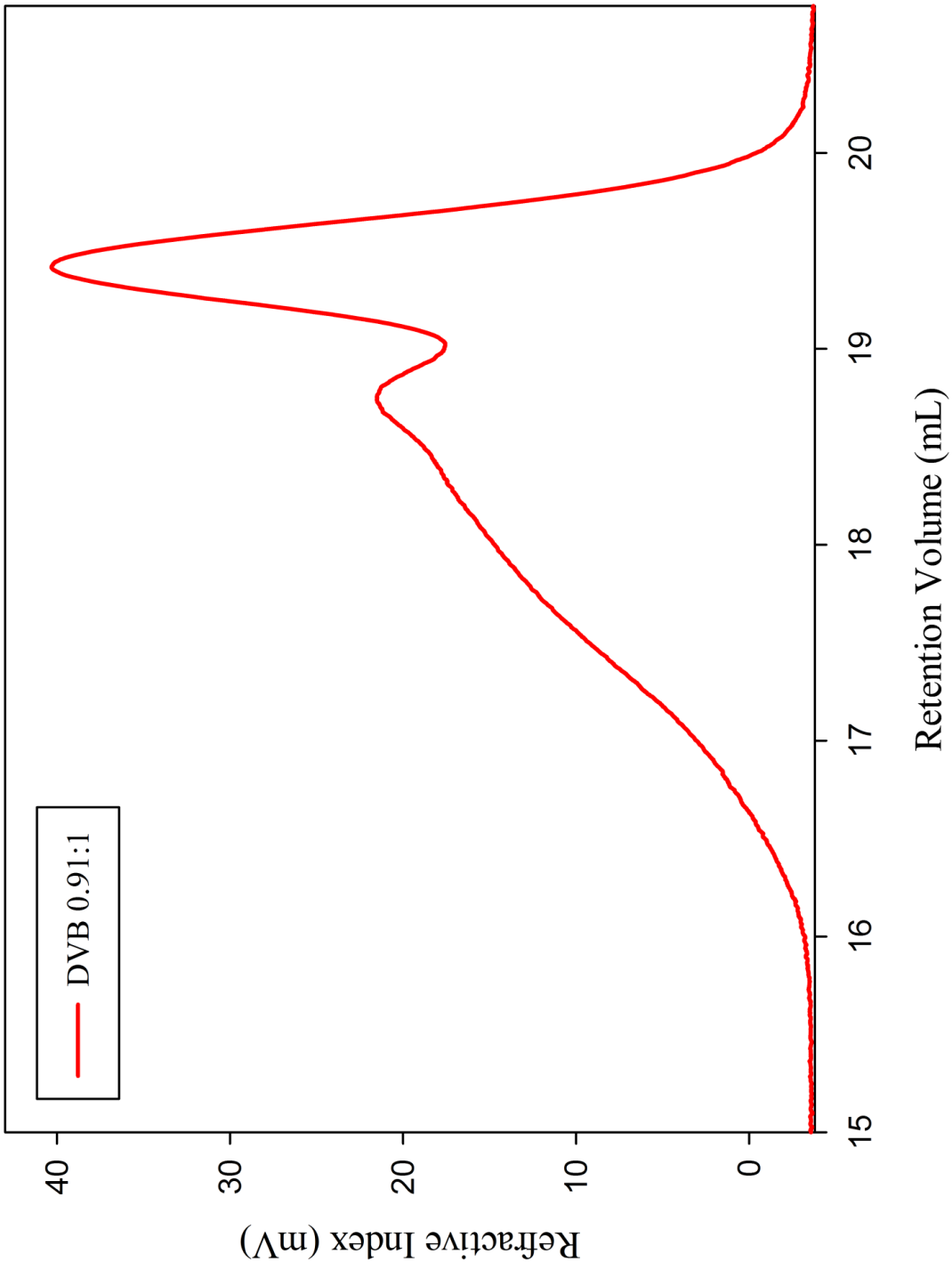

DP_n 100 branched, DVB, 0.92:1

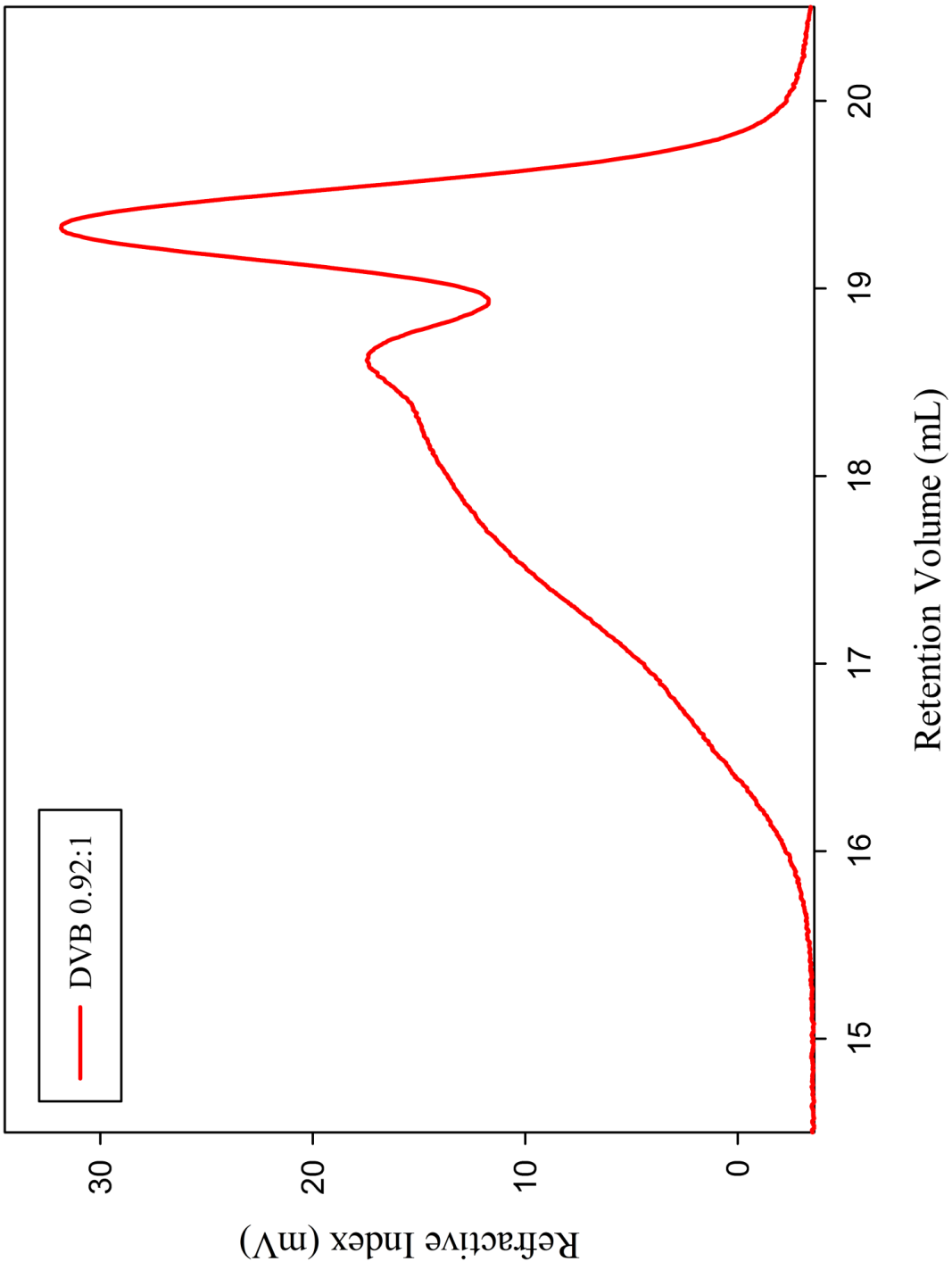

DP_n 100 branched, DVB, 0.93:1

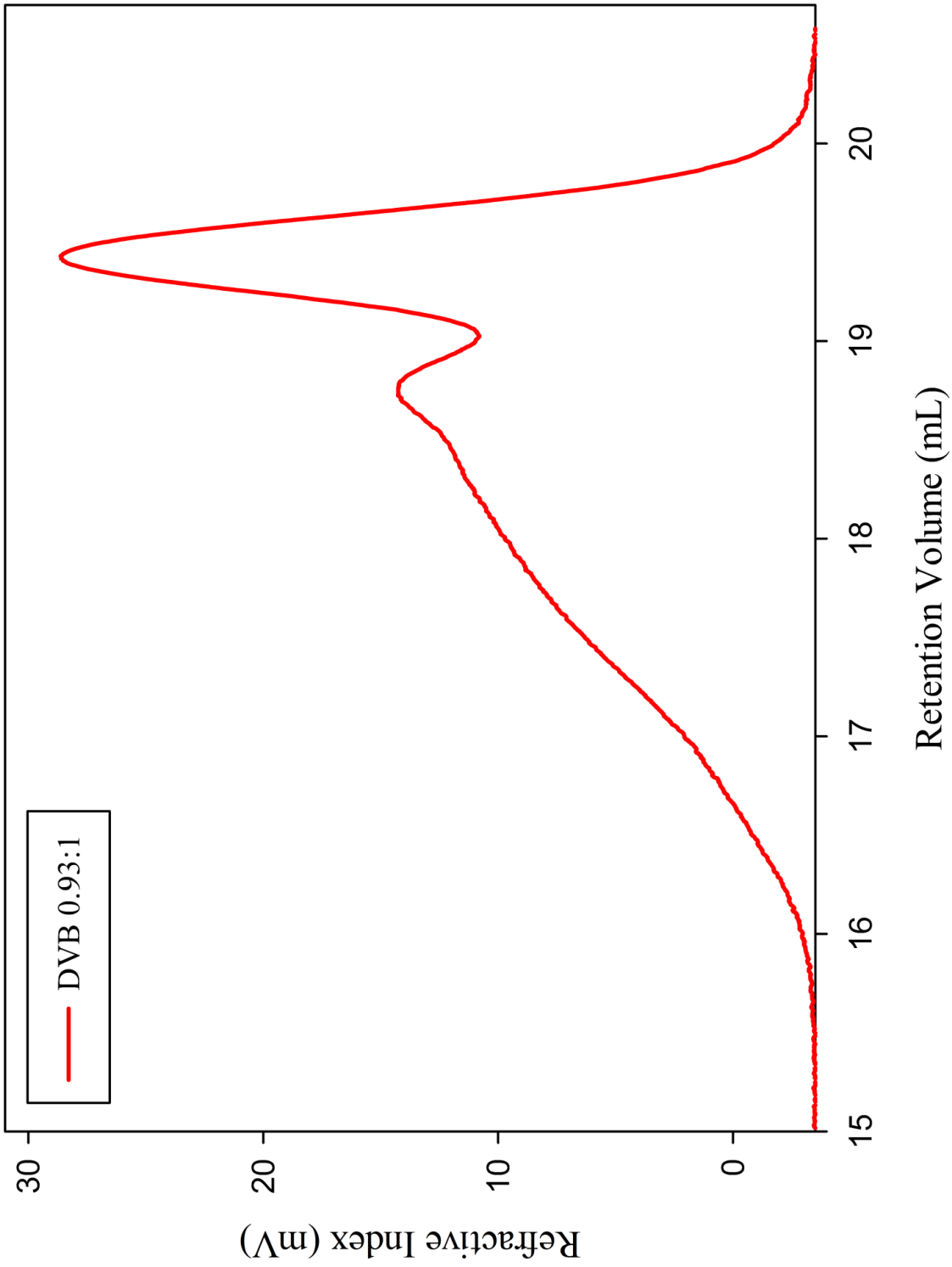

DP_n 100 branched, DVB, 0.94:1

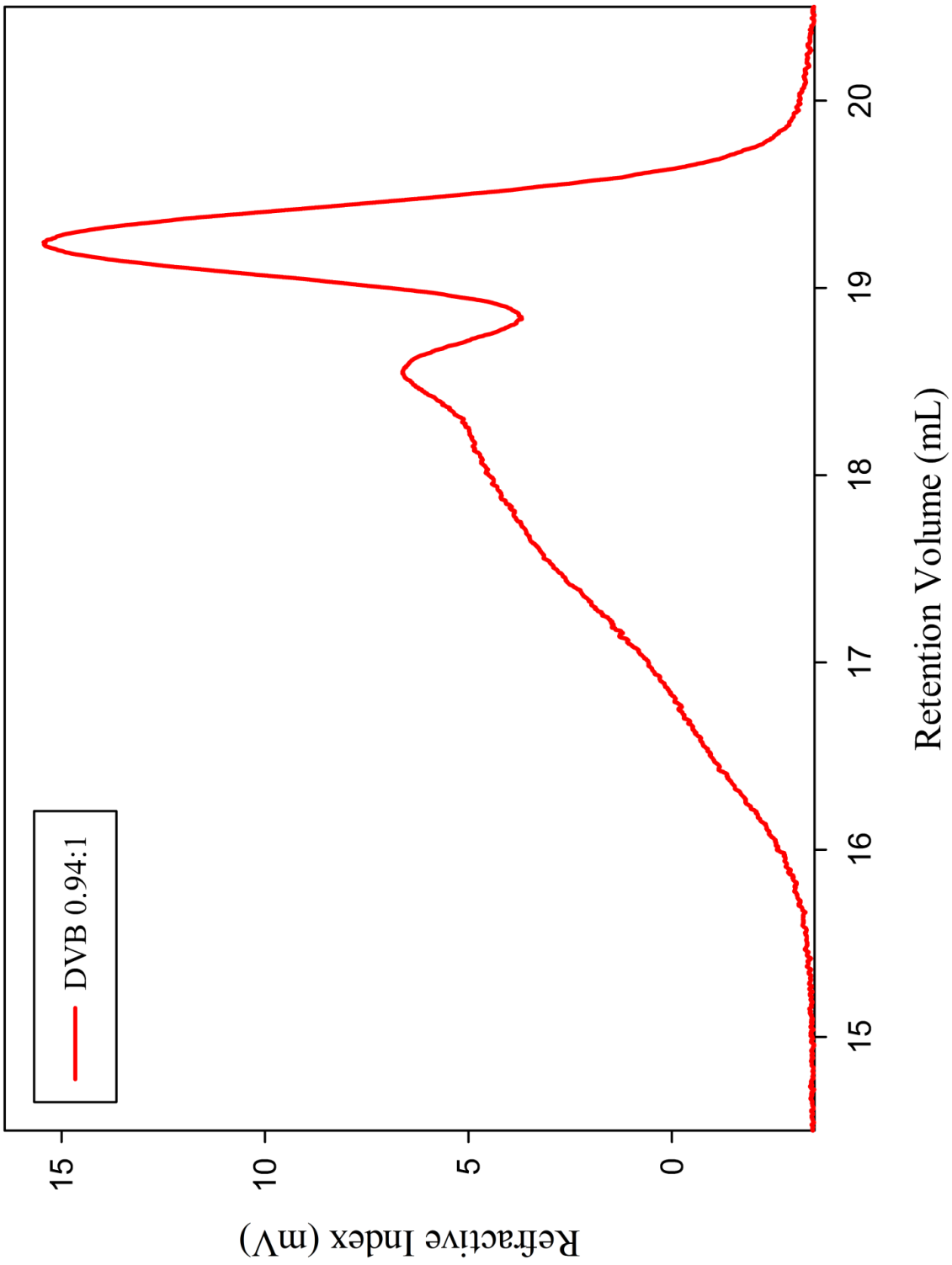

DP_n 50 branched, DVB, 1:1

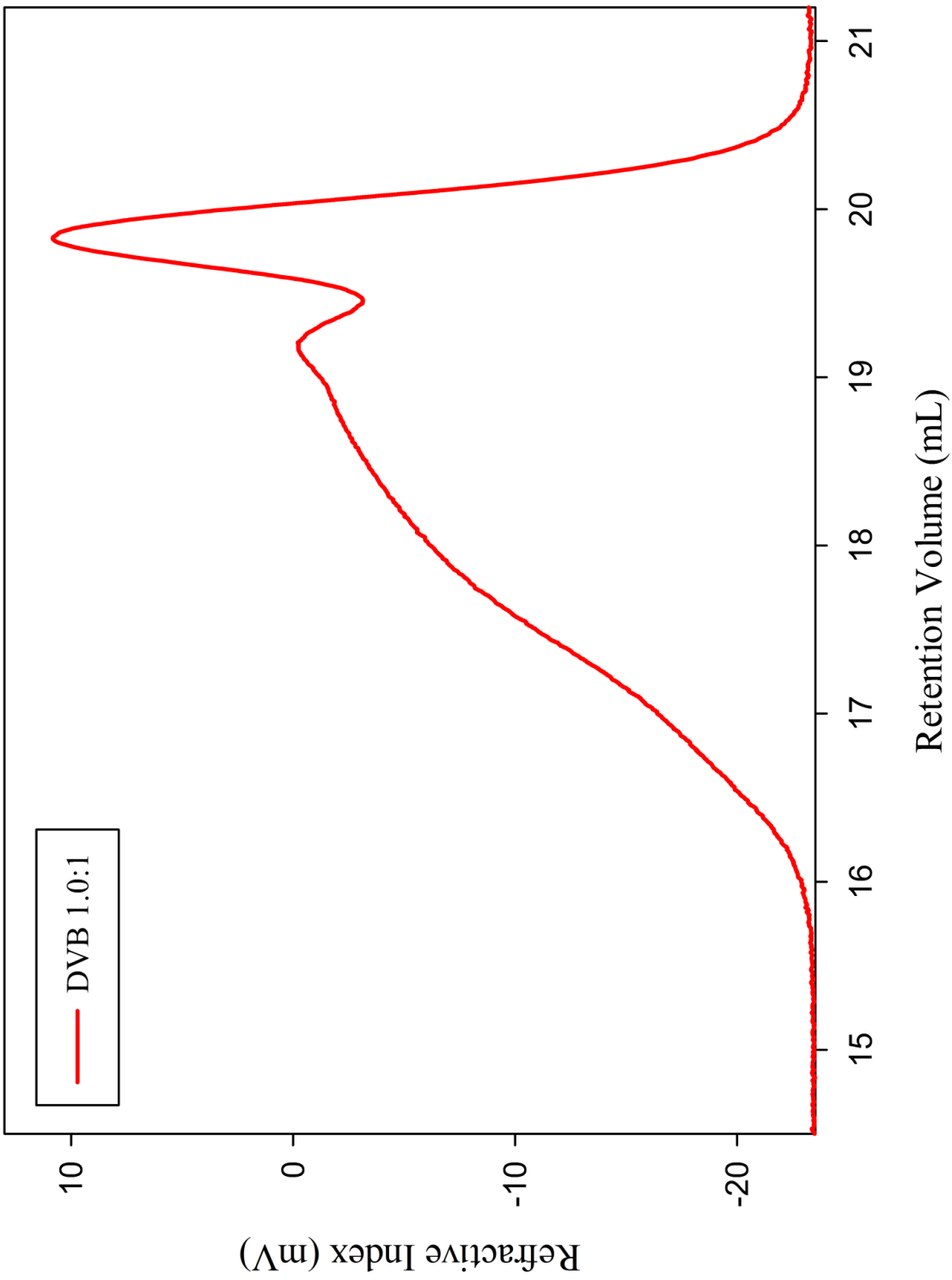

DP_n 50 branched, DVB, 1.2:1

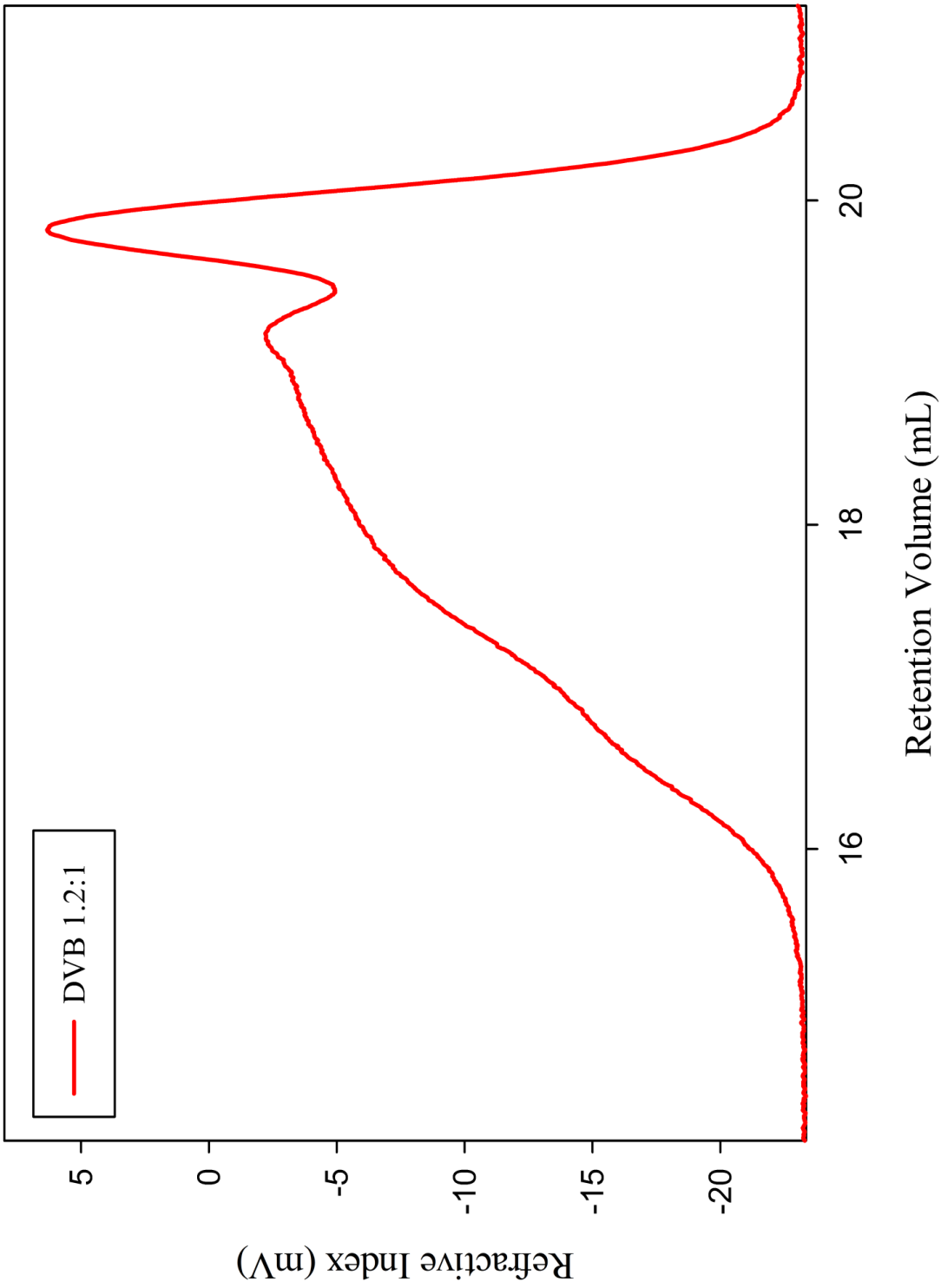

DP_n 50 branched, DVB, 1.4:1

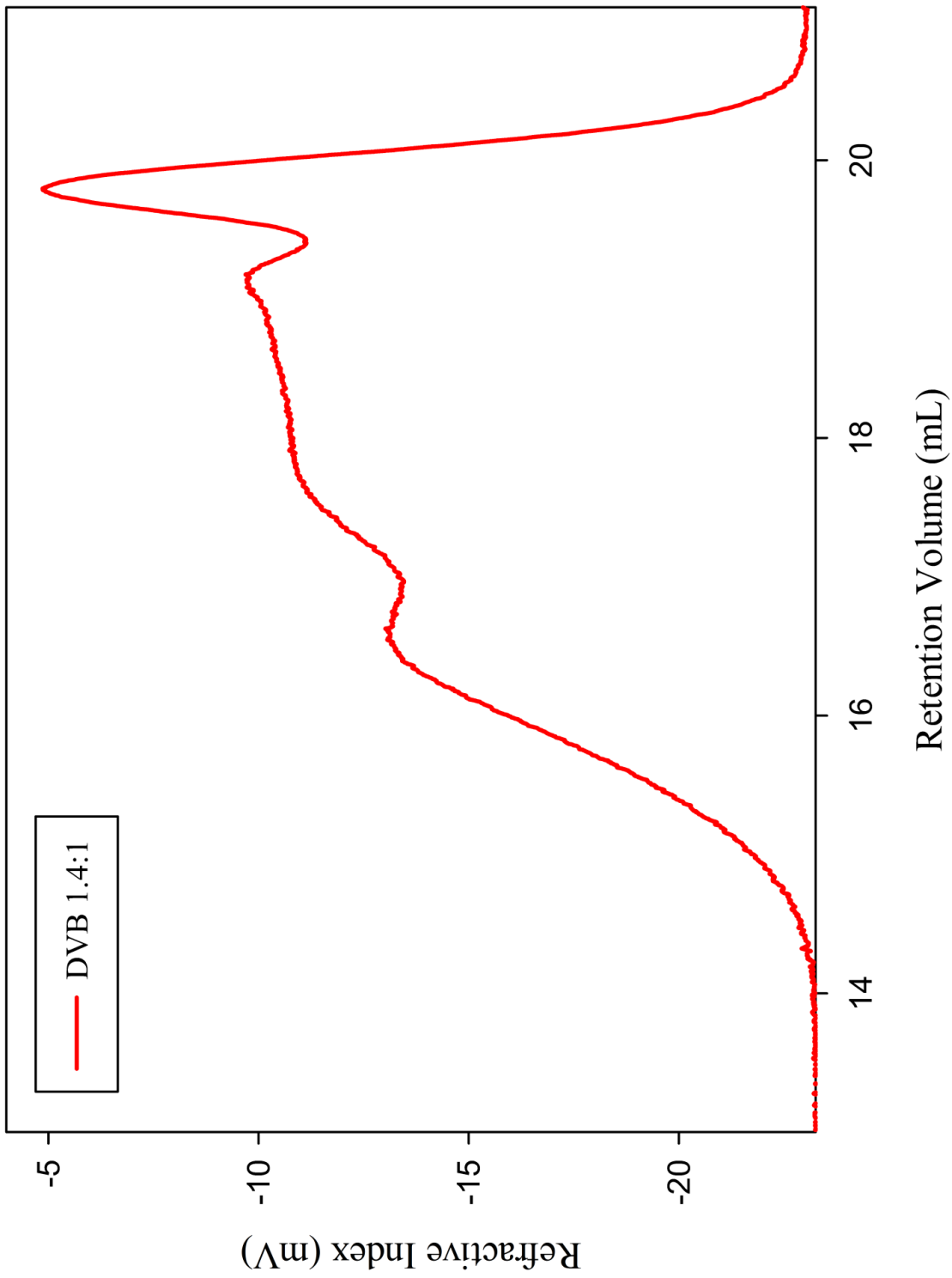

4.3.4 Effect of reaction time

DP_n100 branched, DVB, kinetics, t = 2 hours

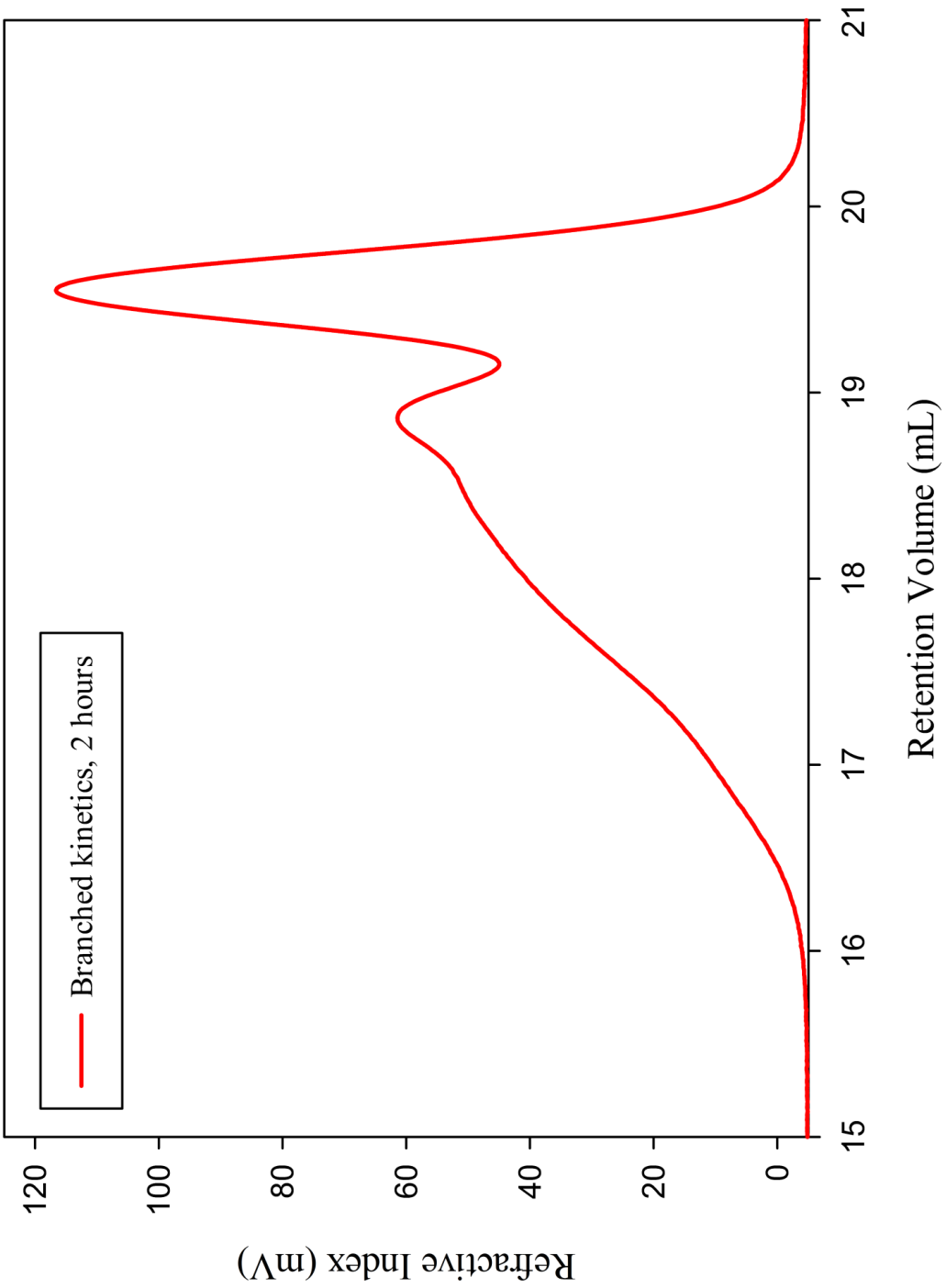

DP_n100 branched, DVB, kinetics, t = 5 hours

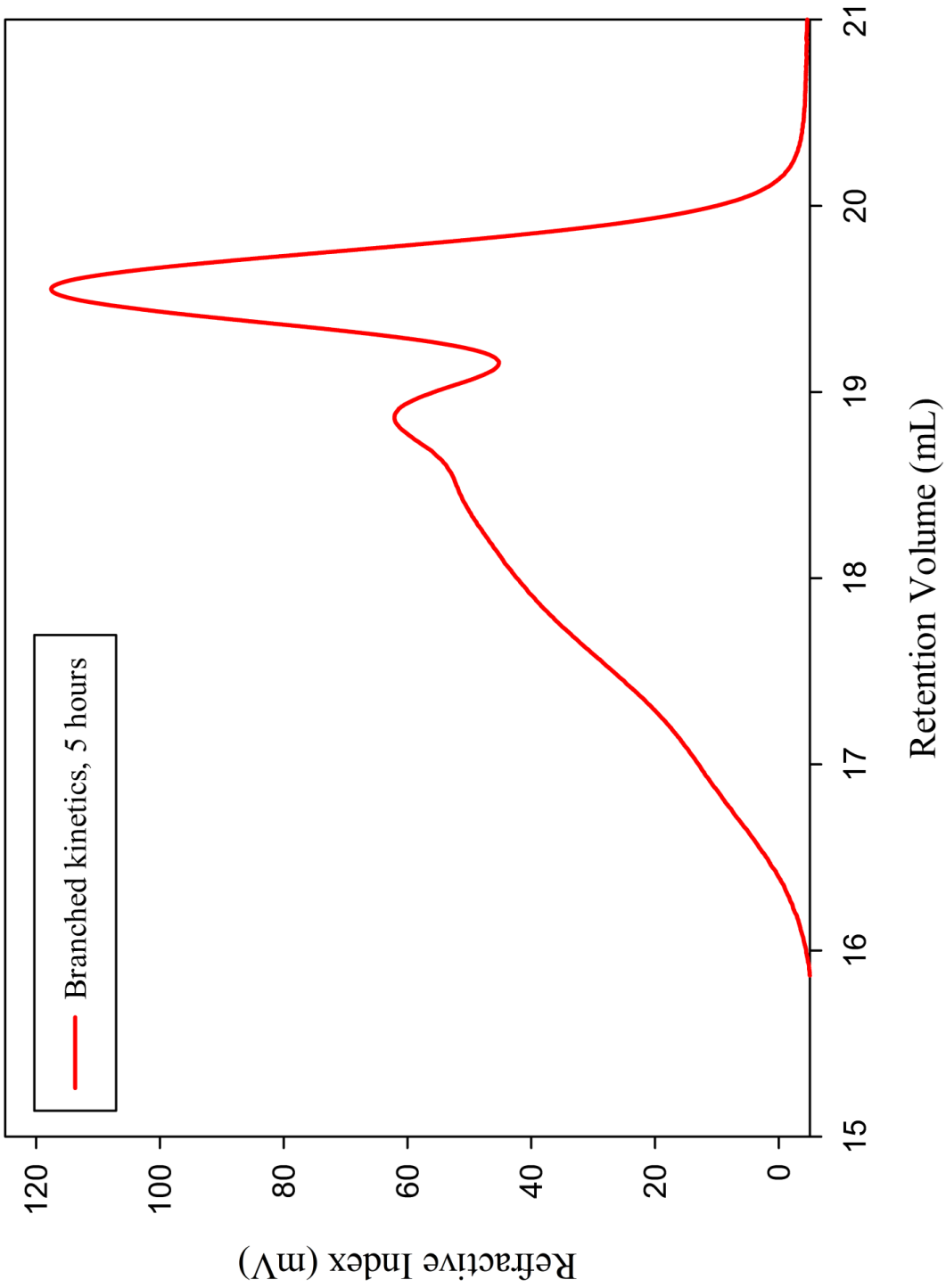

DP_n100 branched, DVB, kinetics, t = 8 hours

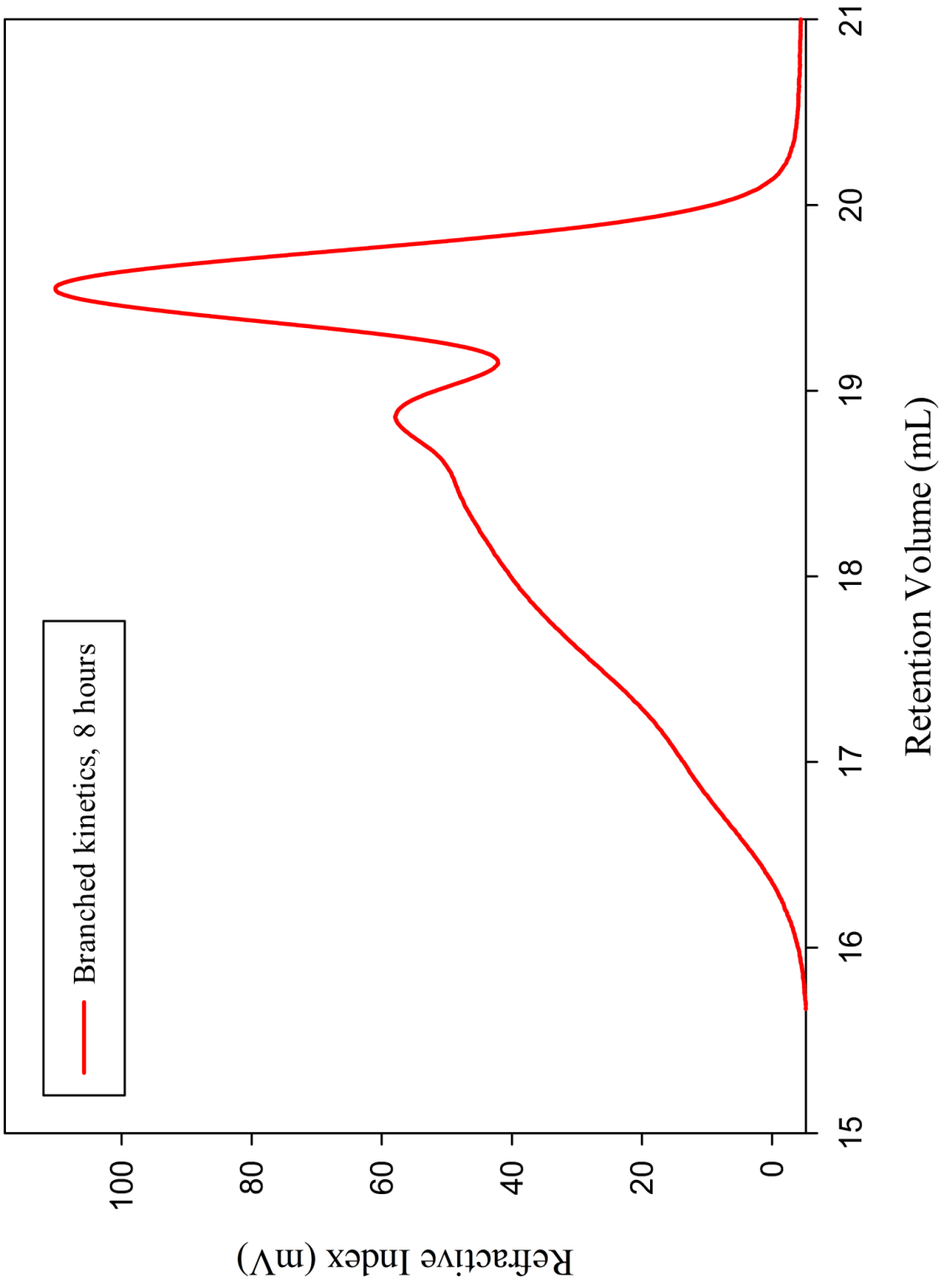

DP_n100 branched, DVB, kinetics, t = 26 hours

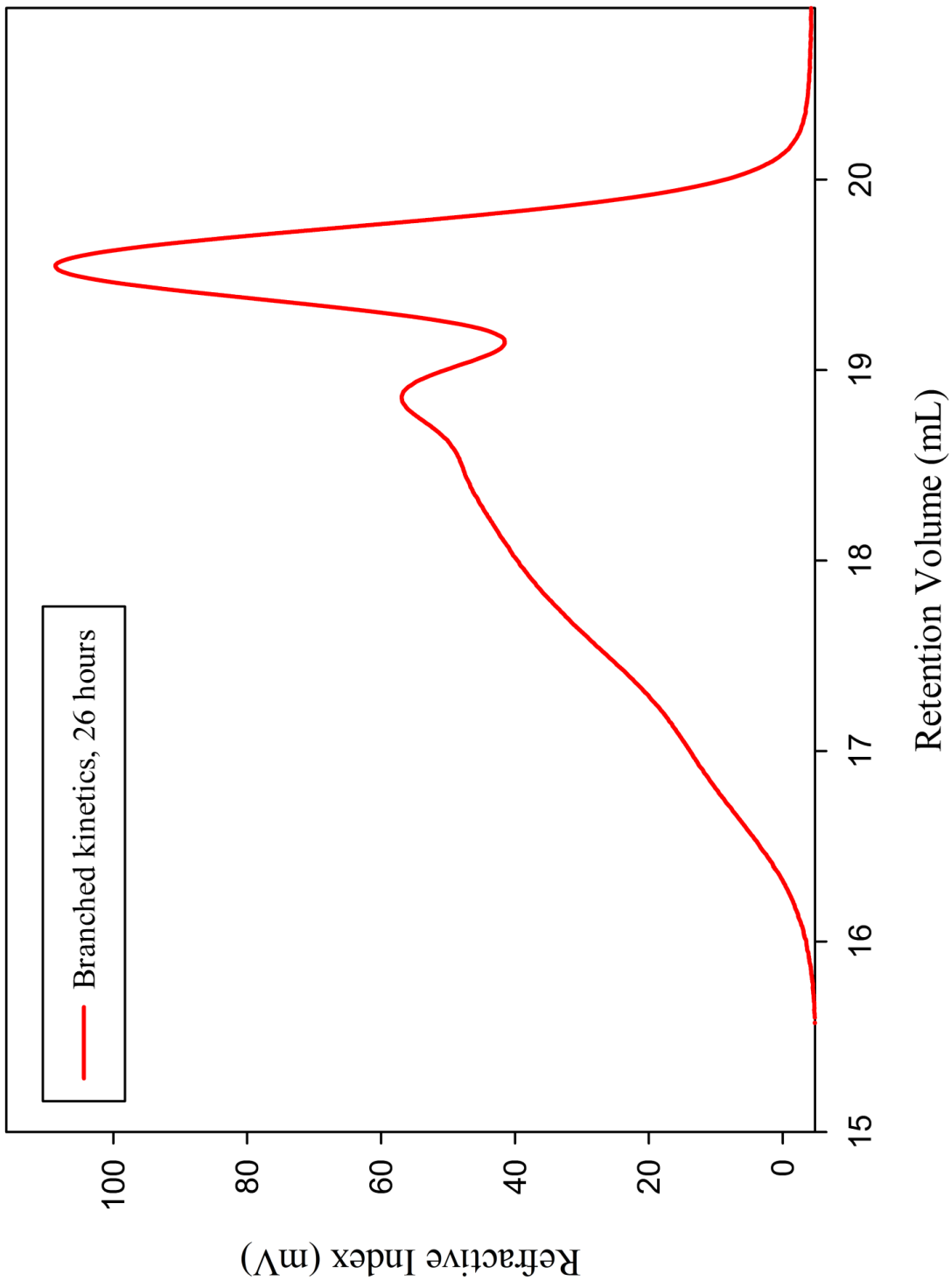

DP_n100 branched, DVB, kinetics, t = 30 hours

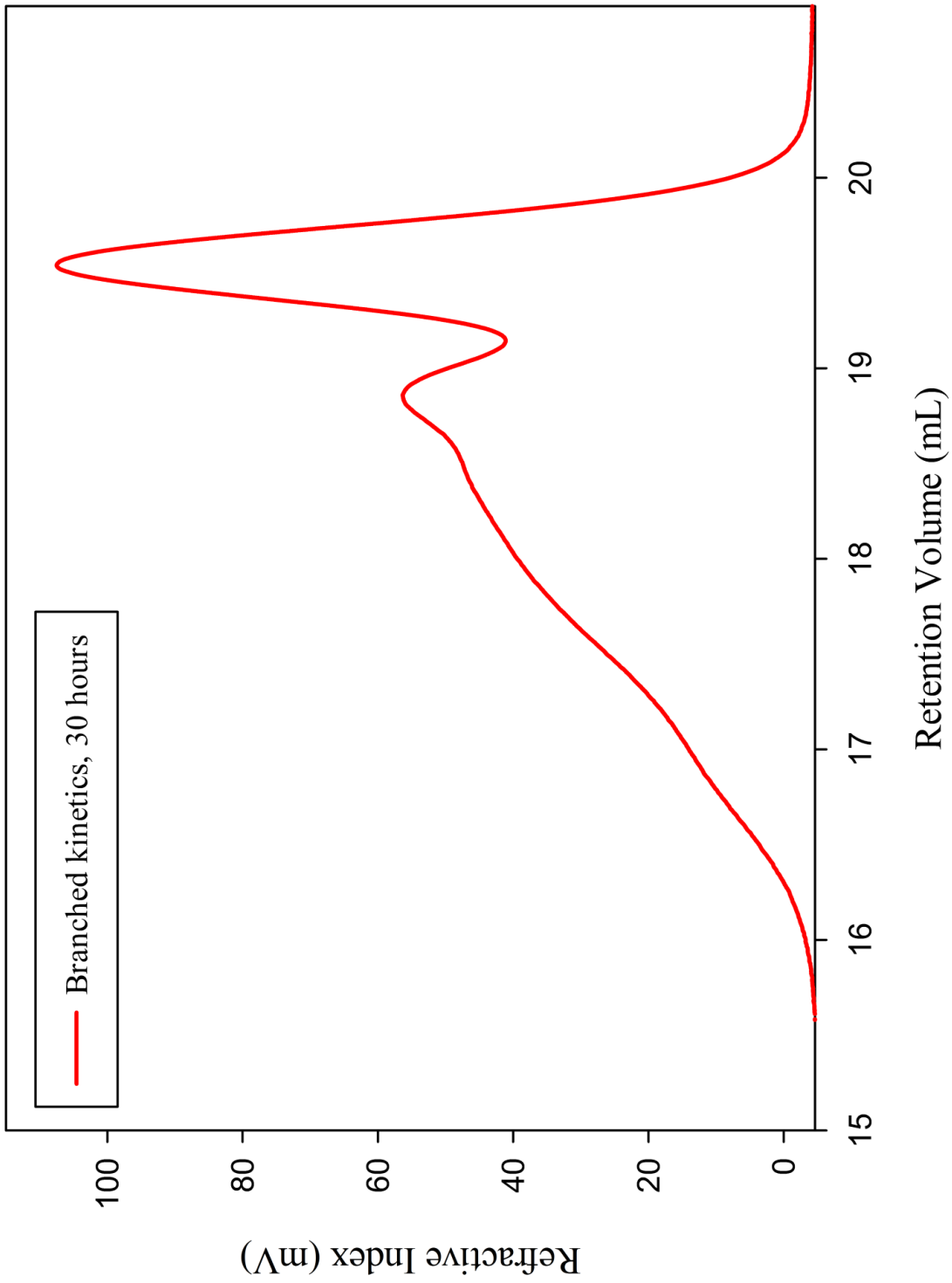

DP_n100 branched, DVB, kinetics, t = 54 hours

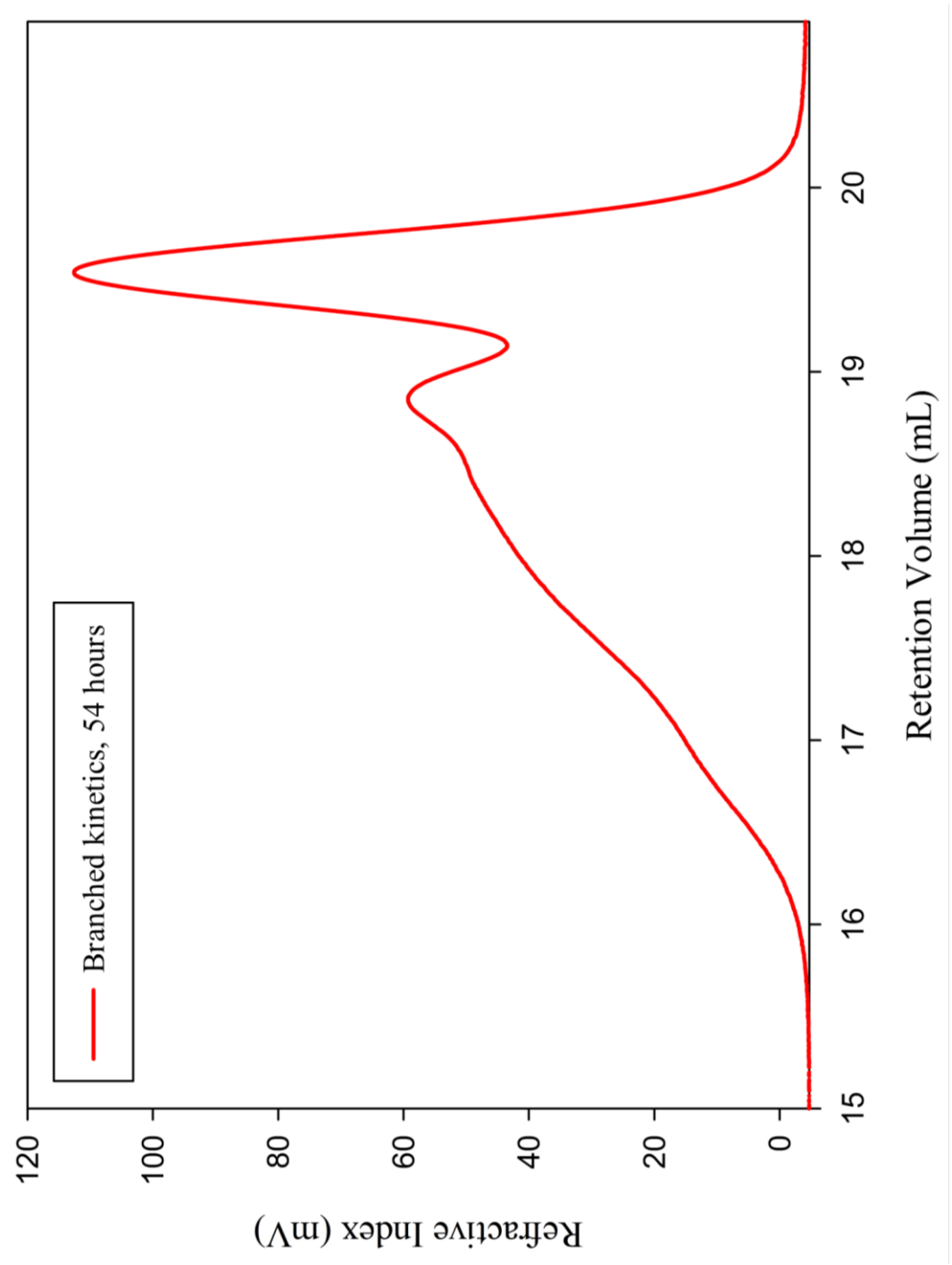

DP_n100 branched, VPOB, kinetics, t = 2.5 hours

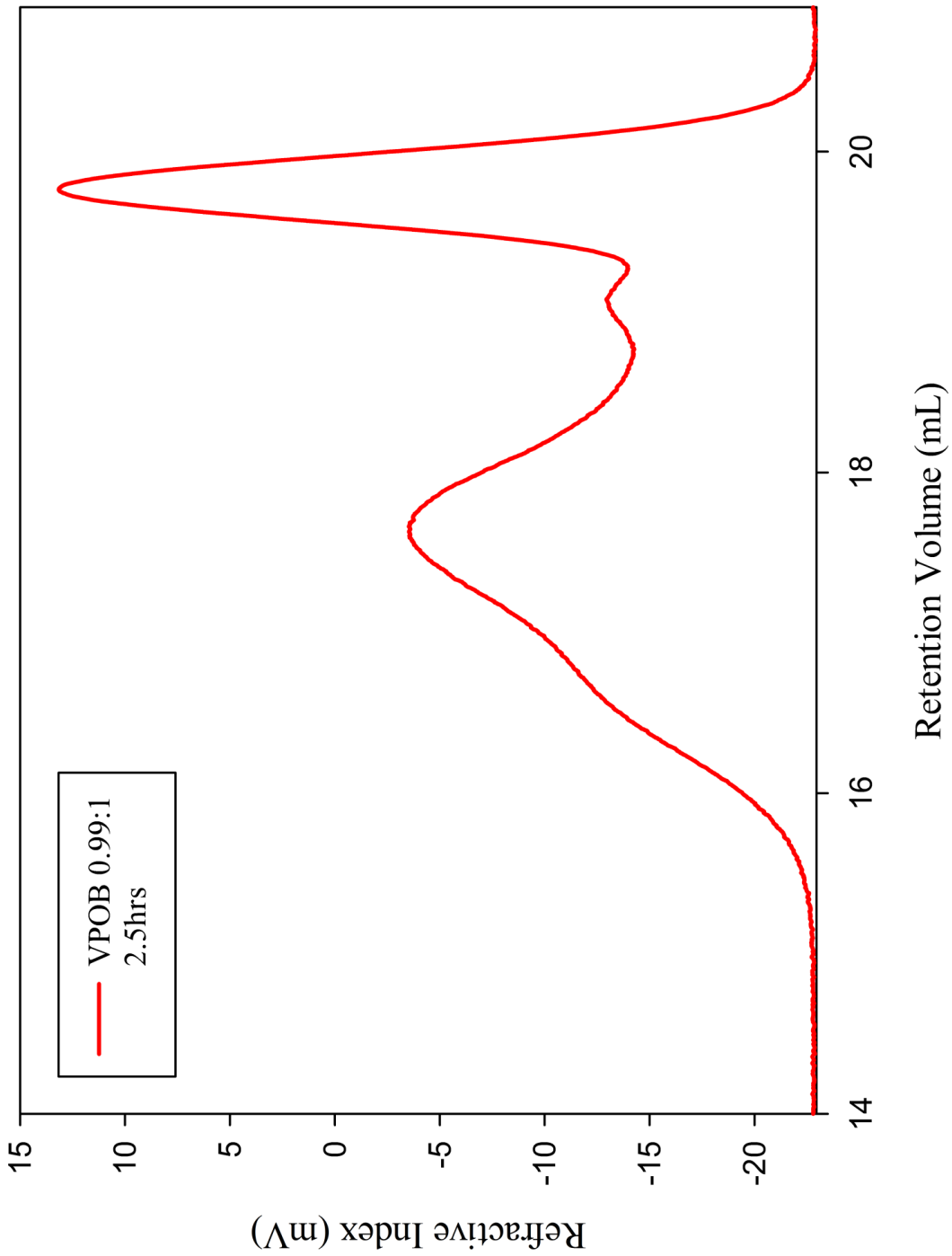

DP_n100 branched, VPOB, kinetics, t = 20 hours

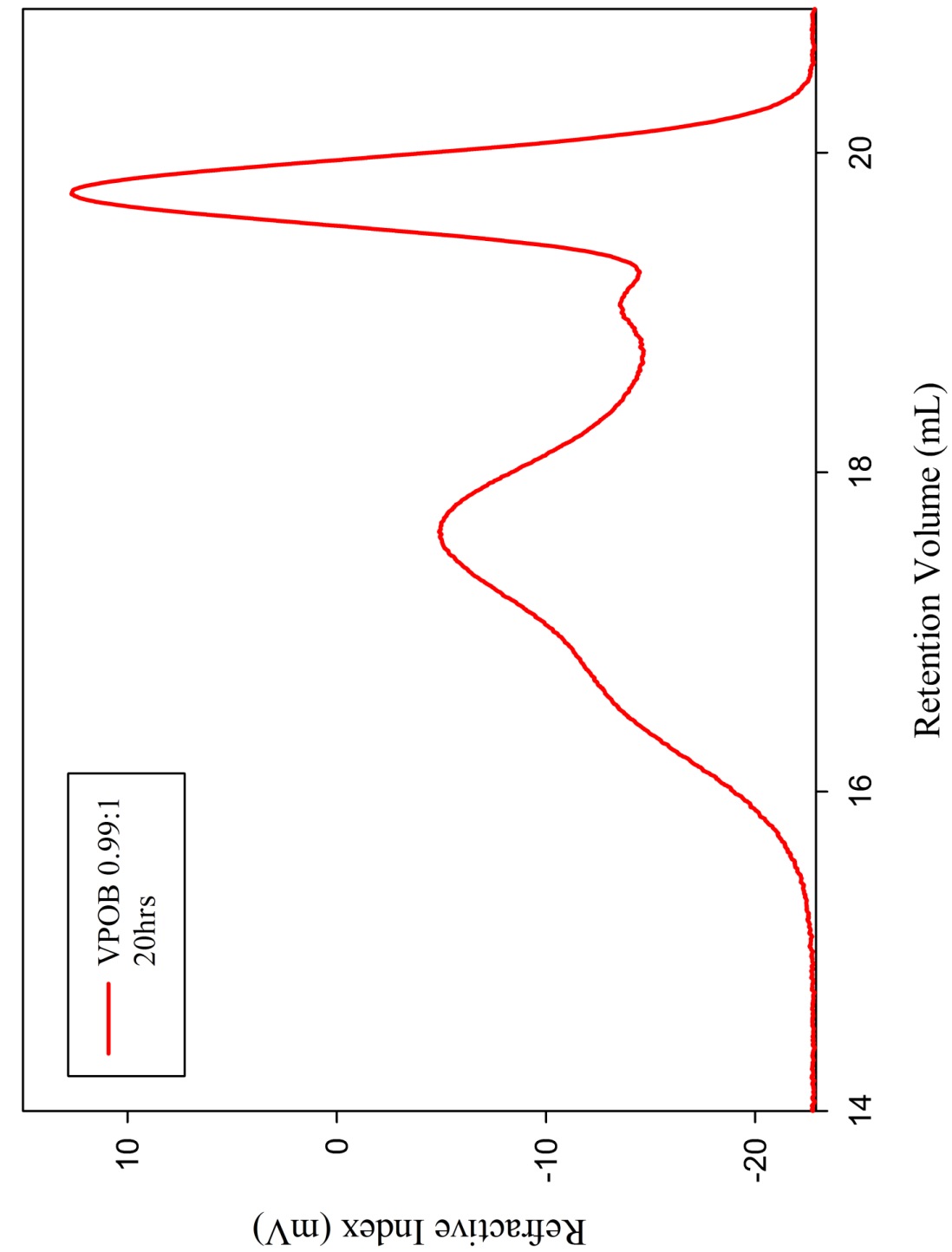

DP_n100 branched, VPOB, kinetics, t = 100 hours

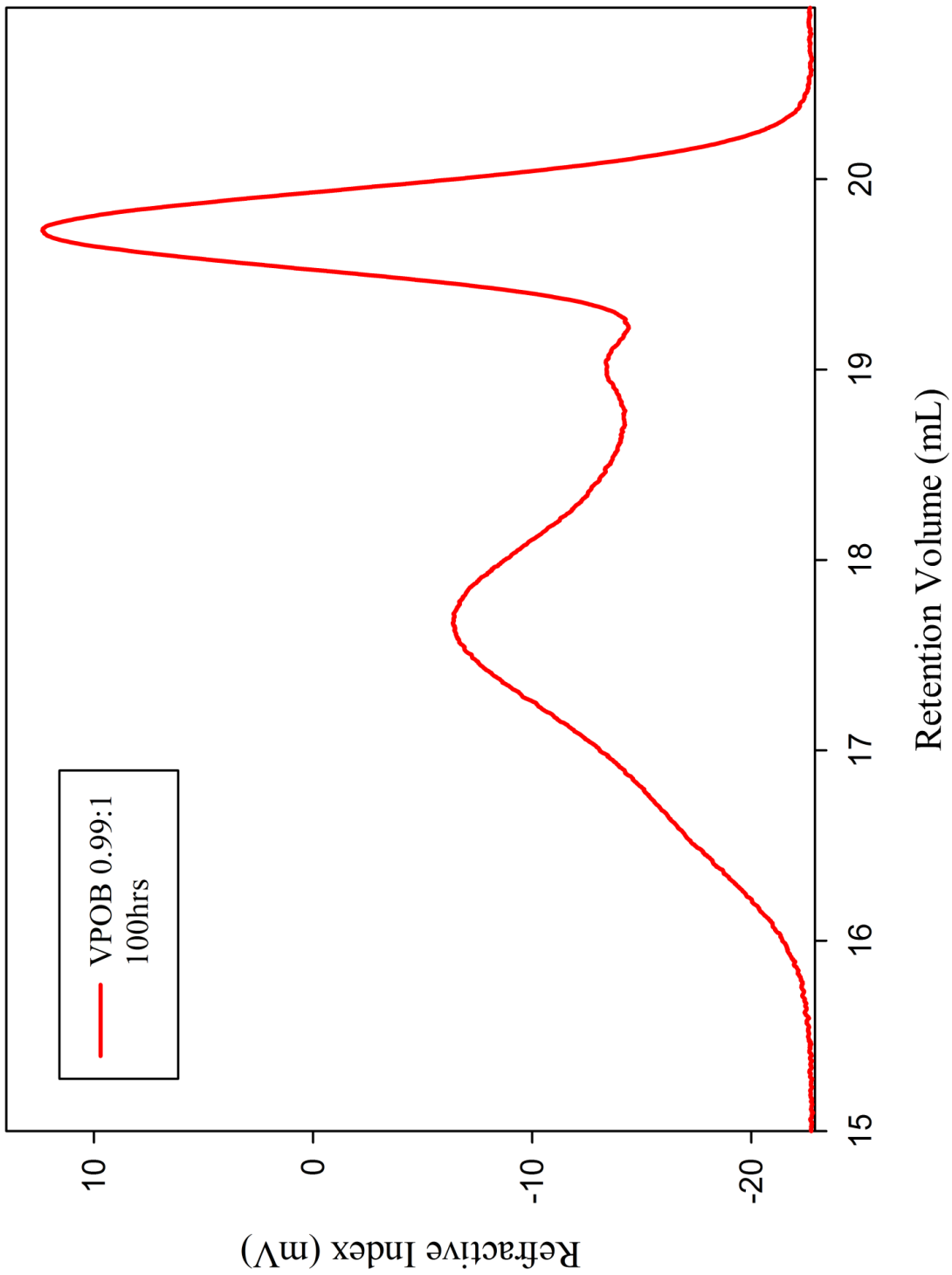

DP_n100 branched, VPOOC, kinetics, t = 2.5 hours

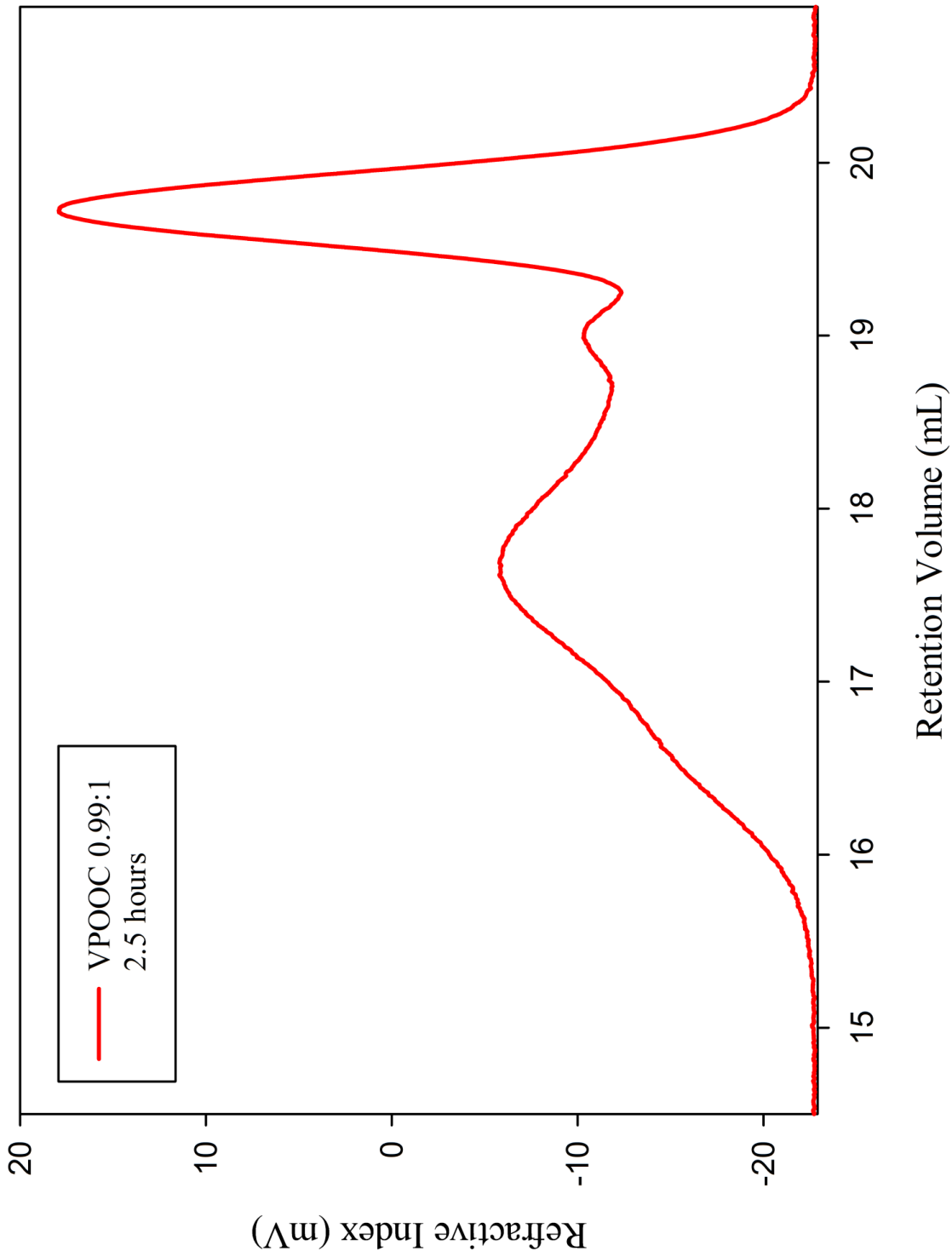

DP_n100 branched, VPOOC, kinetics, t = 20 hours

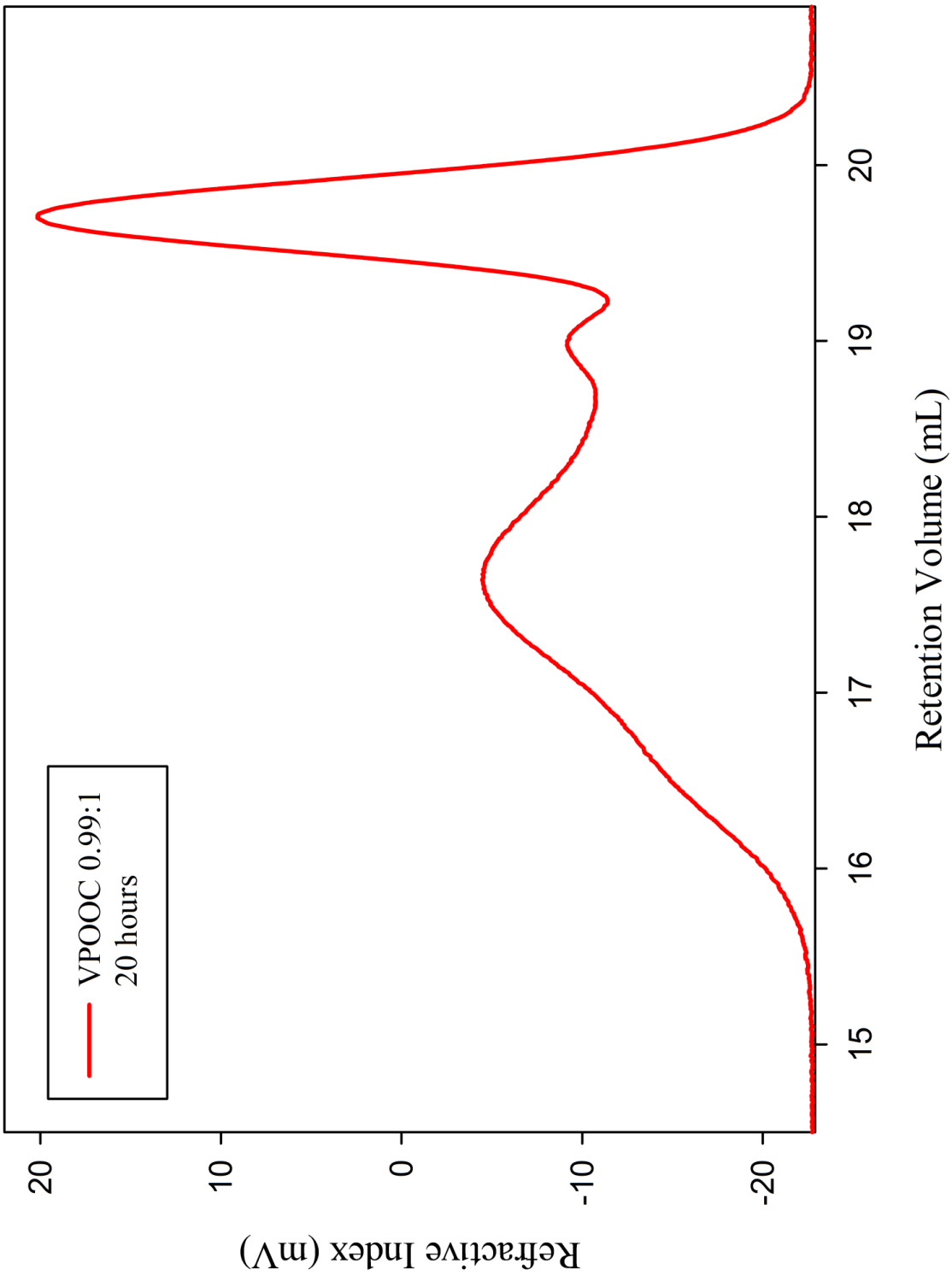

DP_n100 branched, VPOOC, kinetics, t = 100 hours

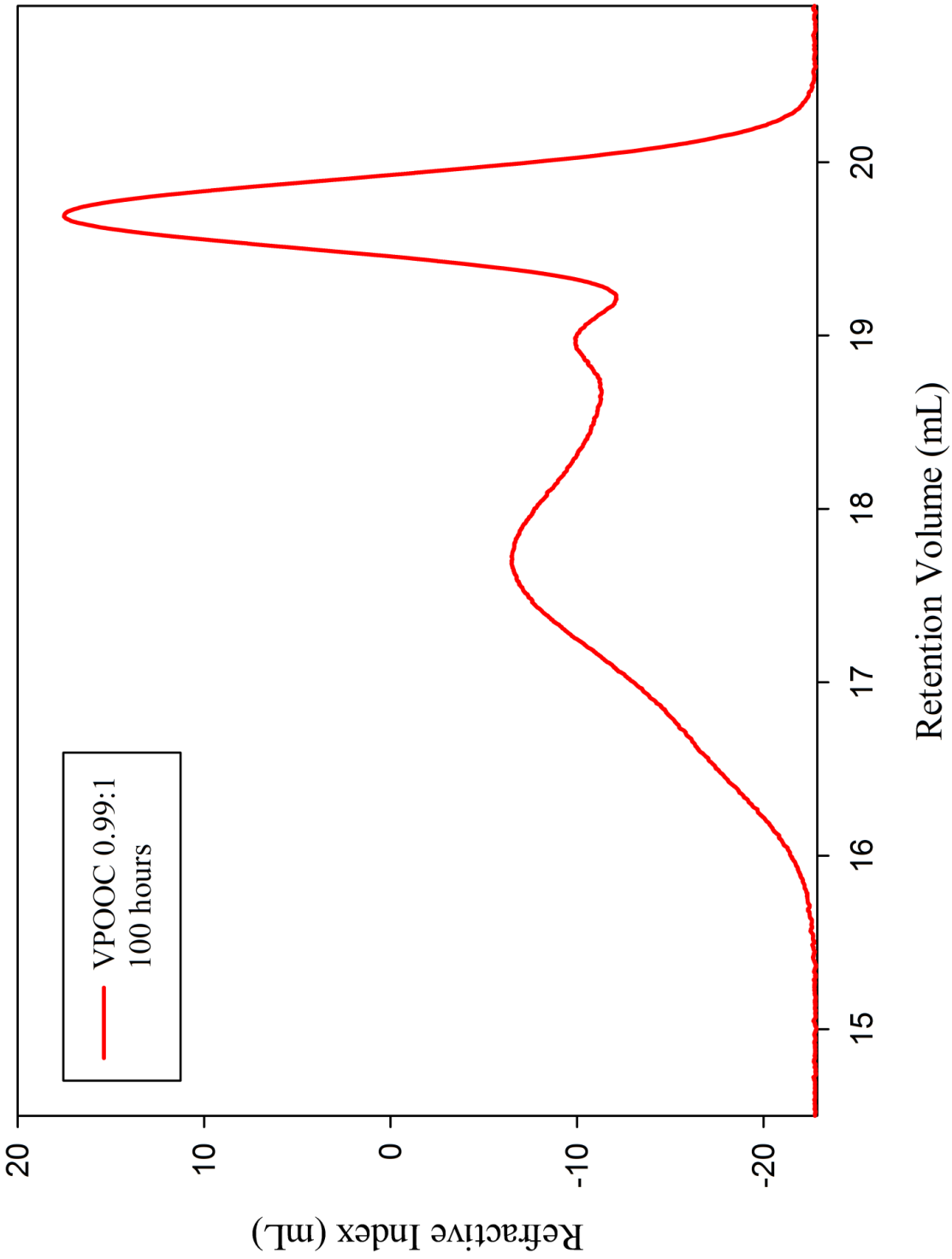

4.5. Increasing brancher:initiator ratio of synthesised dystyrl branchers.

4.5.1 4-bis(4-vinylphenoxy)butane (VPOB)

DP_n50 branched, VPOB, 0.95:1

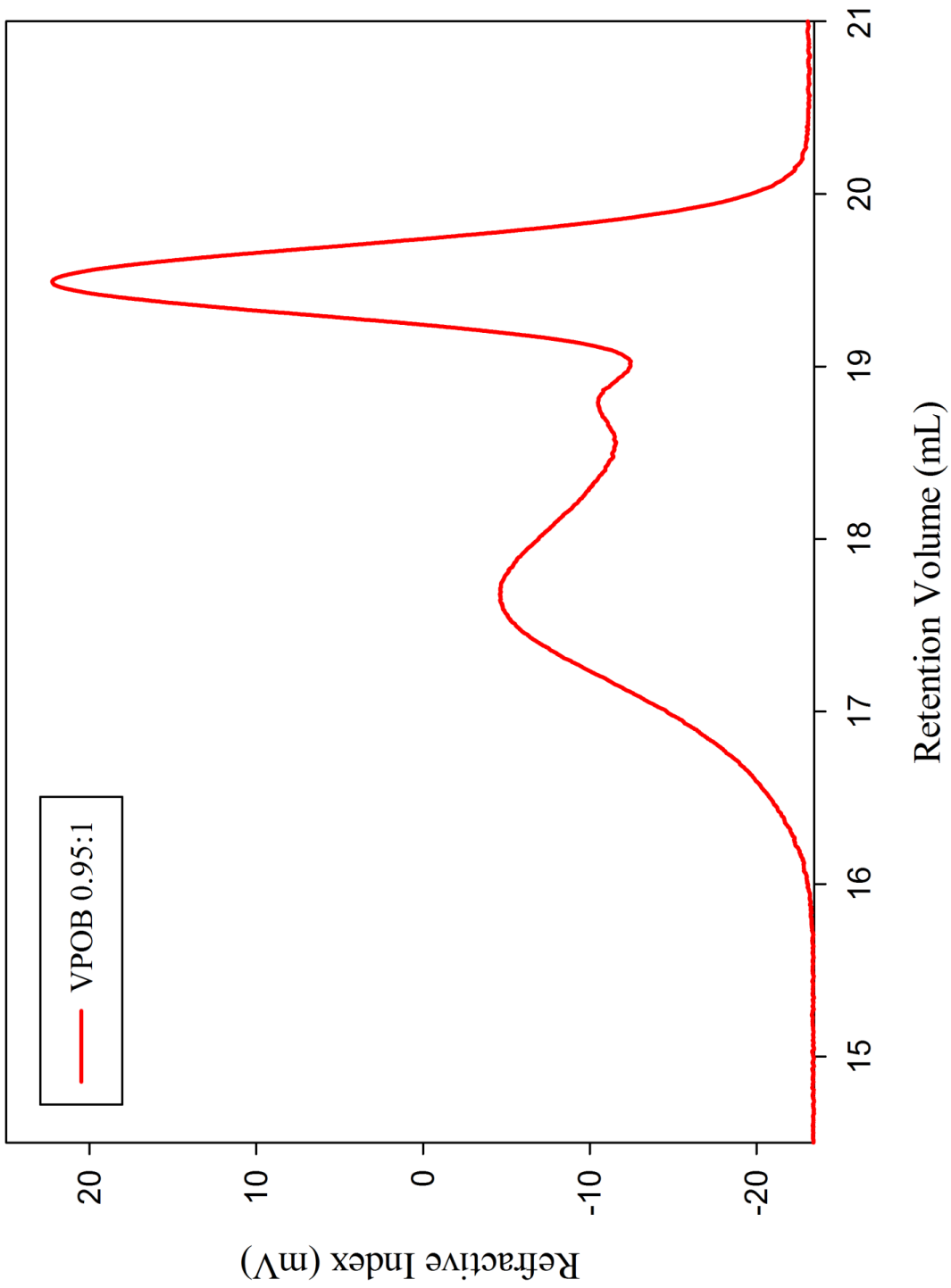

DP_n50 branched, VPOB, 0.99:1

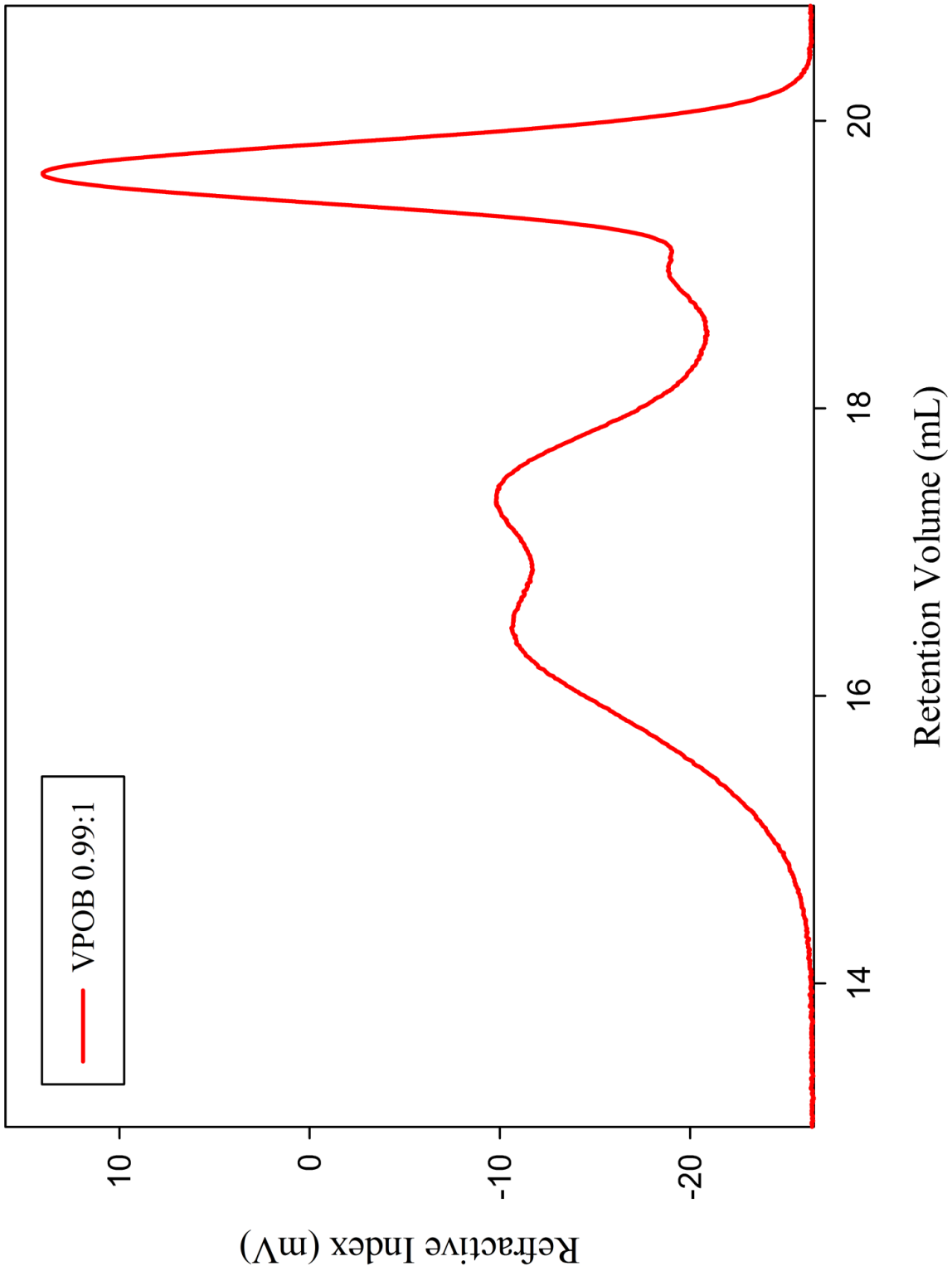

DP_n50 branched, VPOB, 1.05:1

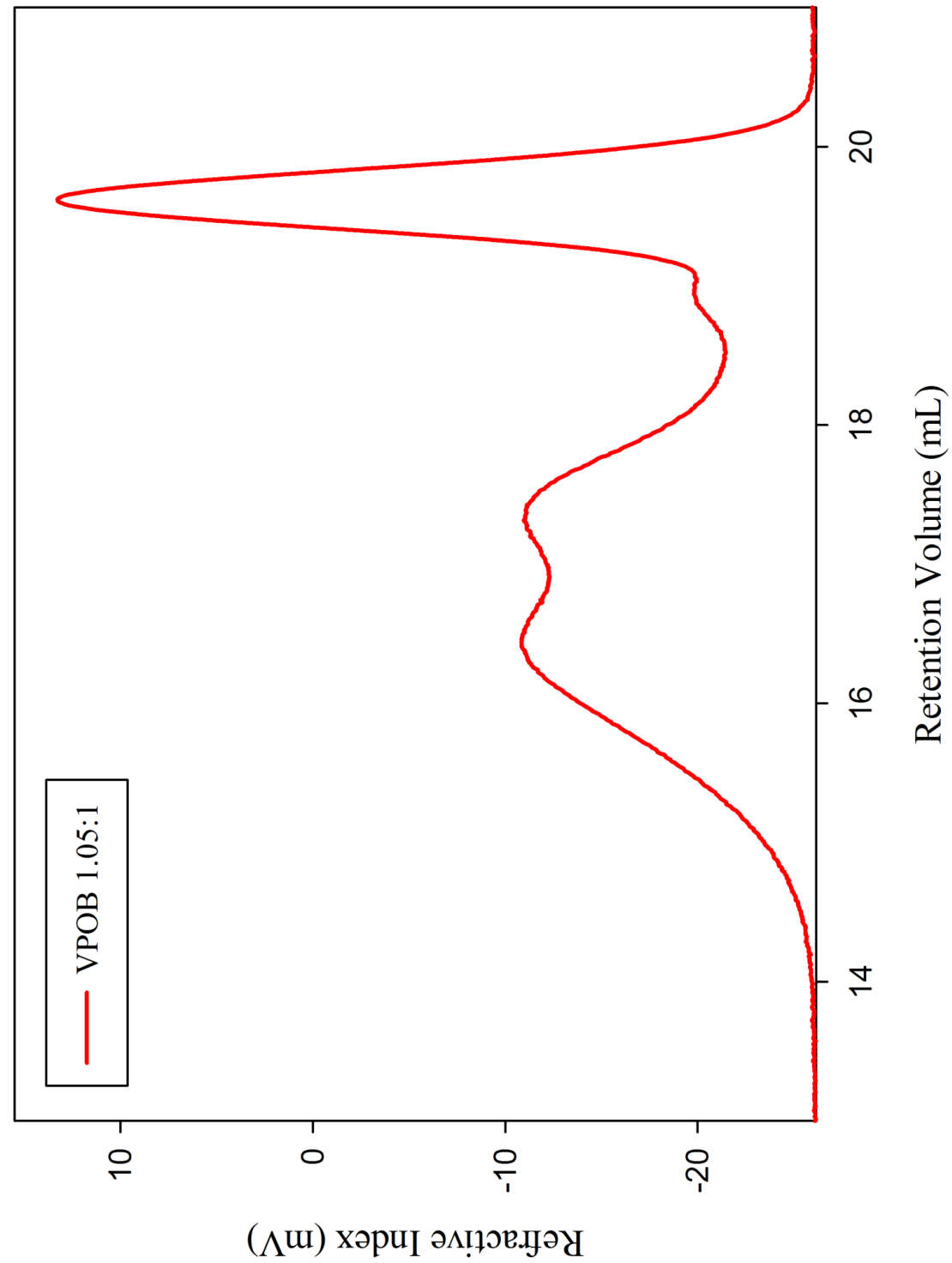

DP_n50 branched, VPOB, 1.1:1

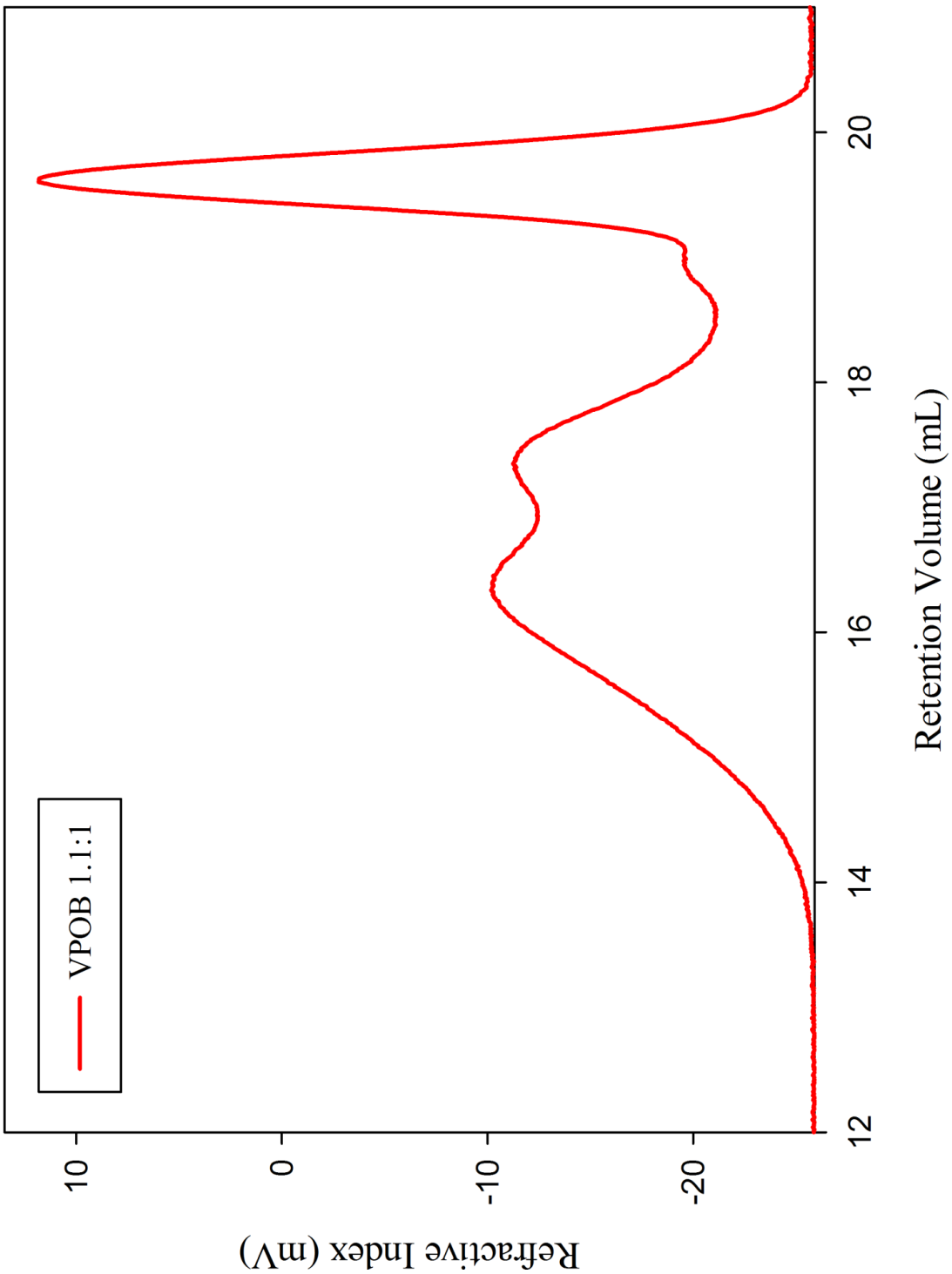

DP_n50 branched, VPOB, 1.2:1

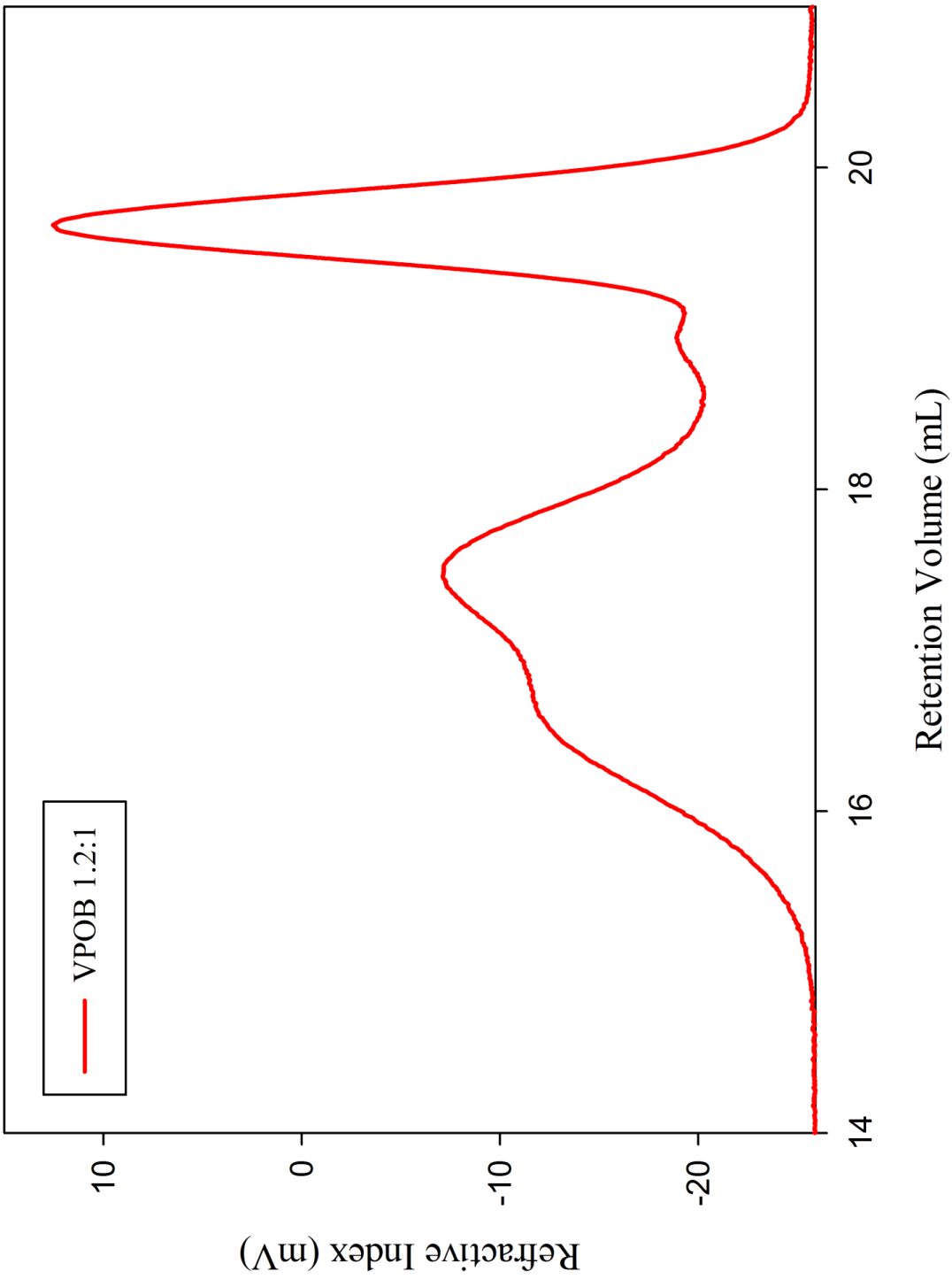

DP_n50 branched, VPOB, 1.3:1

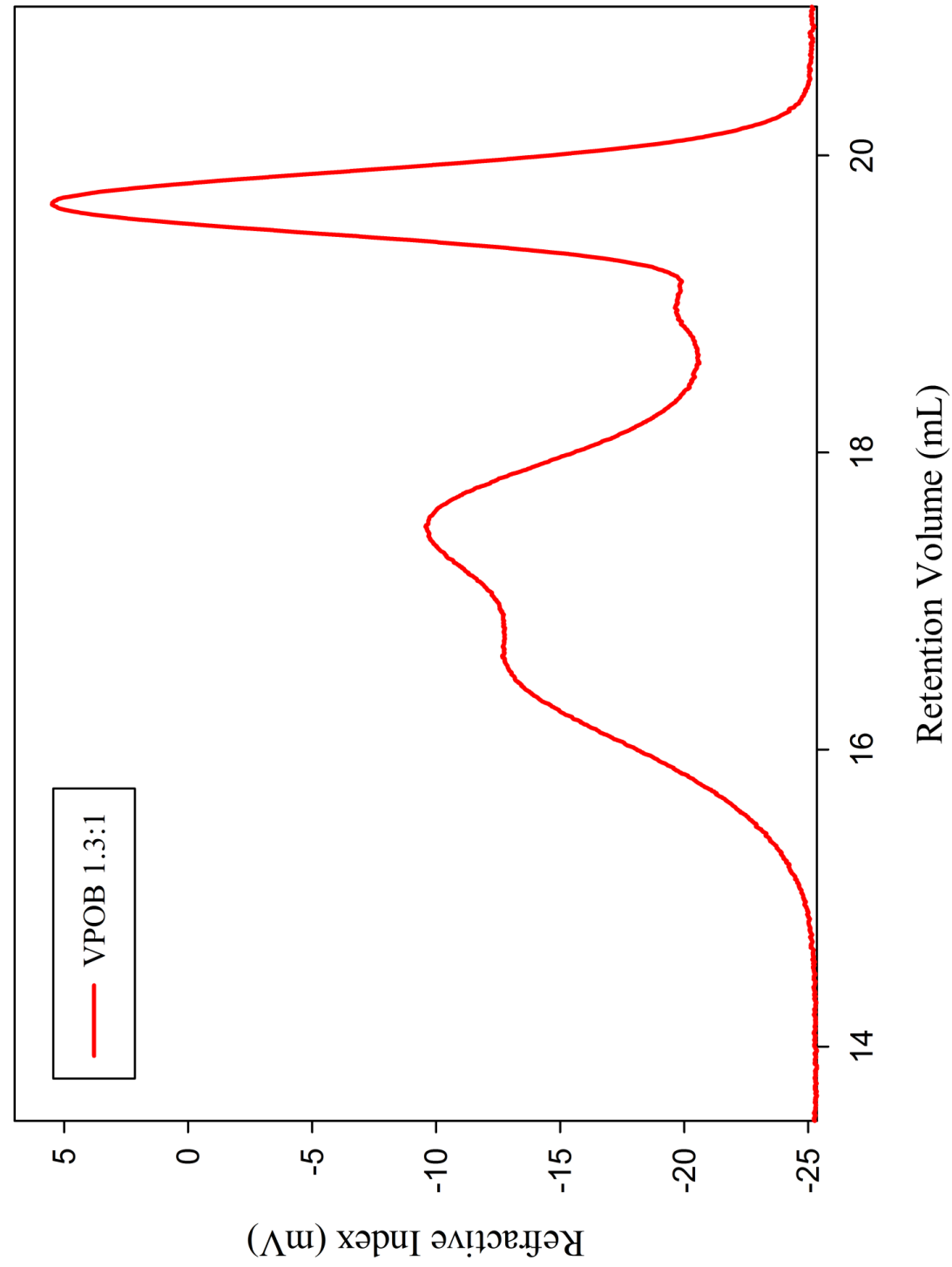

DP_n50 branched, VPOB, 1.4:1a

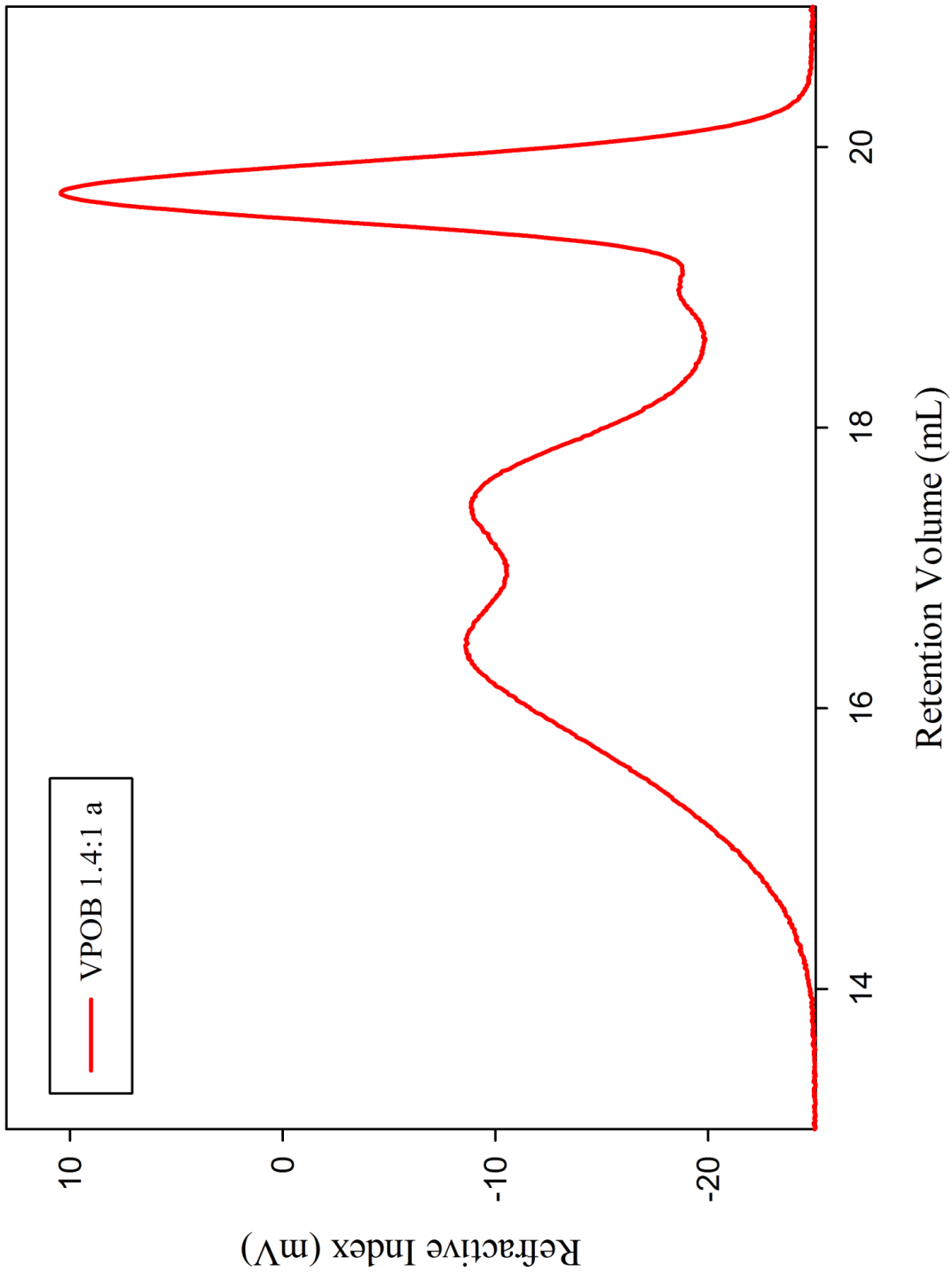

DP_n50 branched, VPOB, VPOB, 1.4:1b

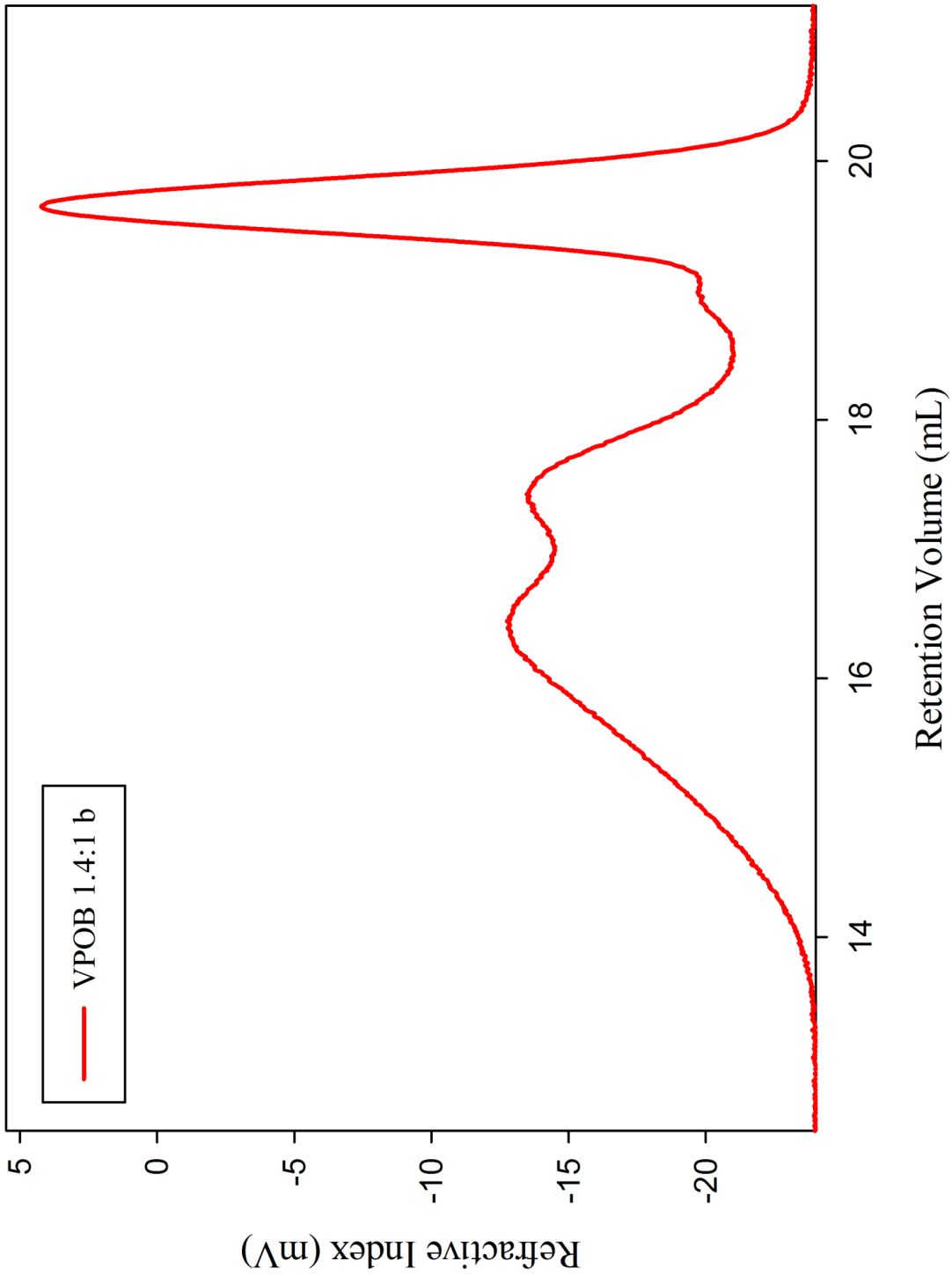

4.5.2 6-bis (4vinylphenoxy)hexane (VPOHEX)

DP_n50 branched, VPOHEX, 1.2:1

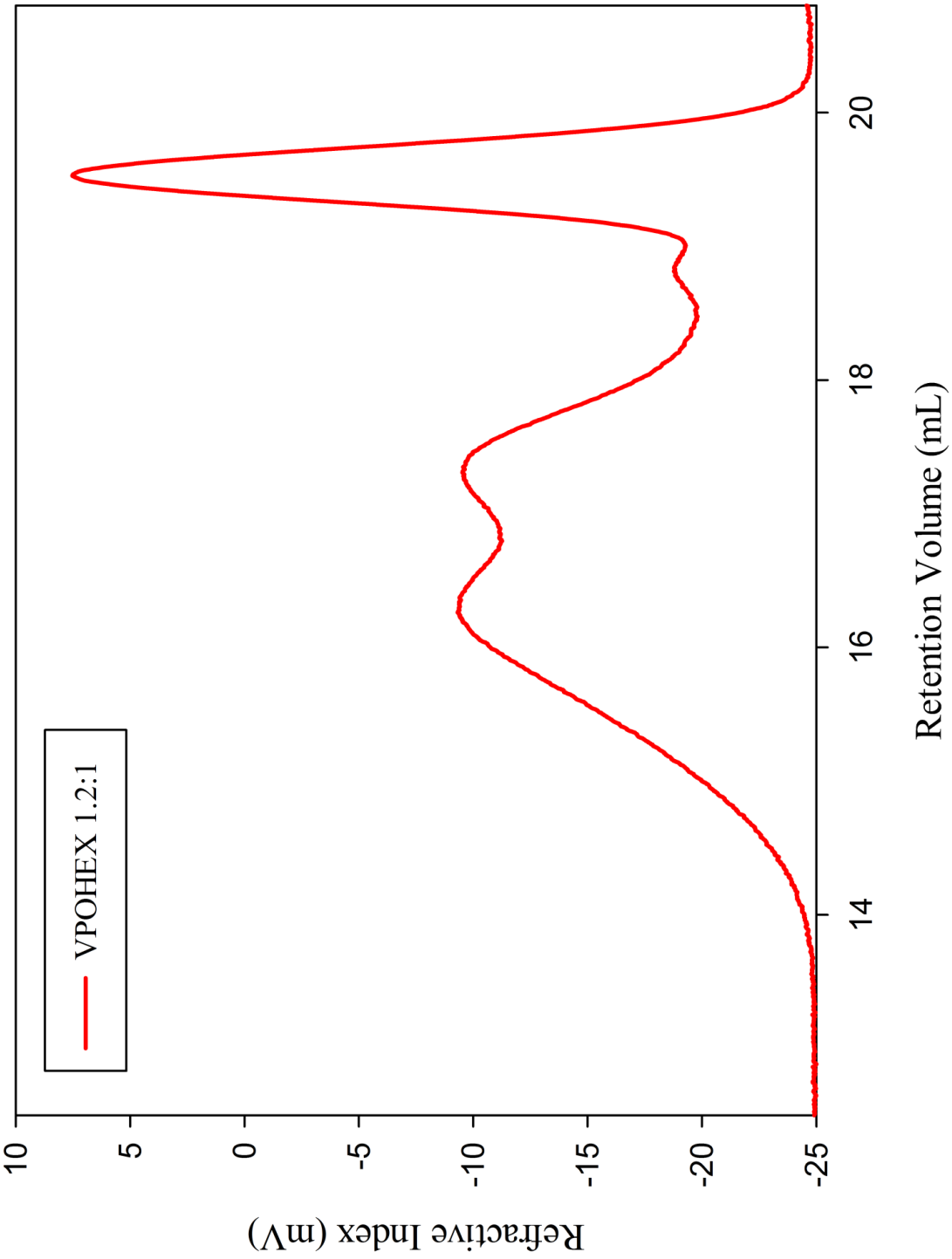

DP_n50 branched, VPOHEX, 1.3:1

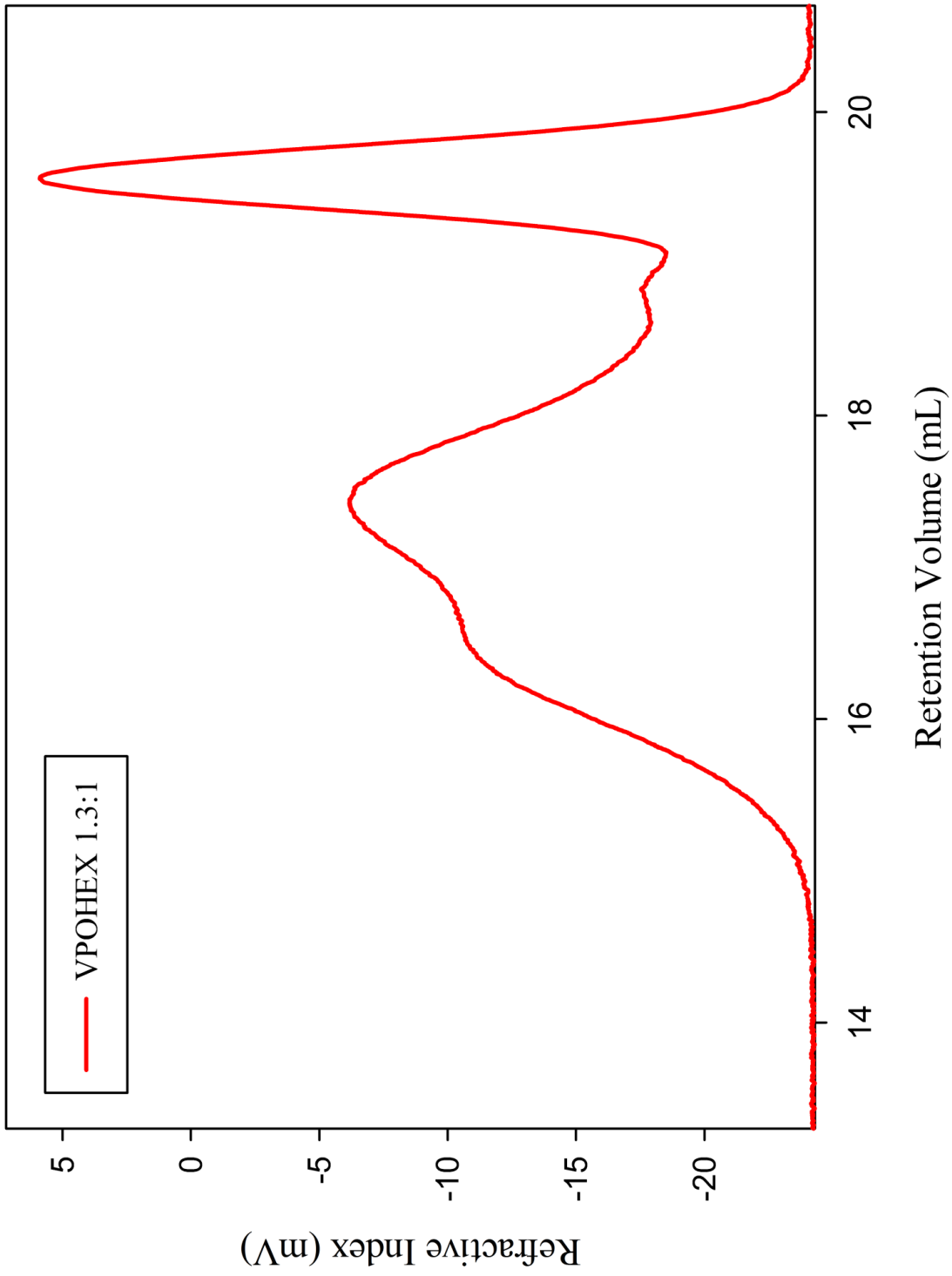

DP_n50 branched, VPOHEX, 1.4:1

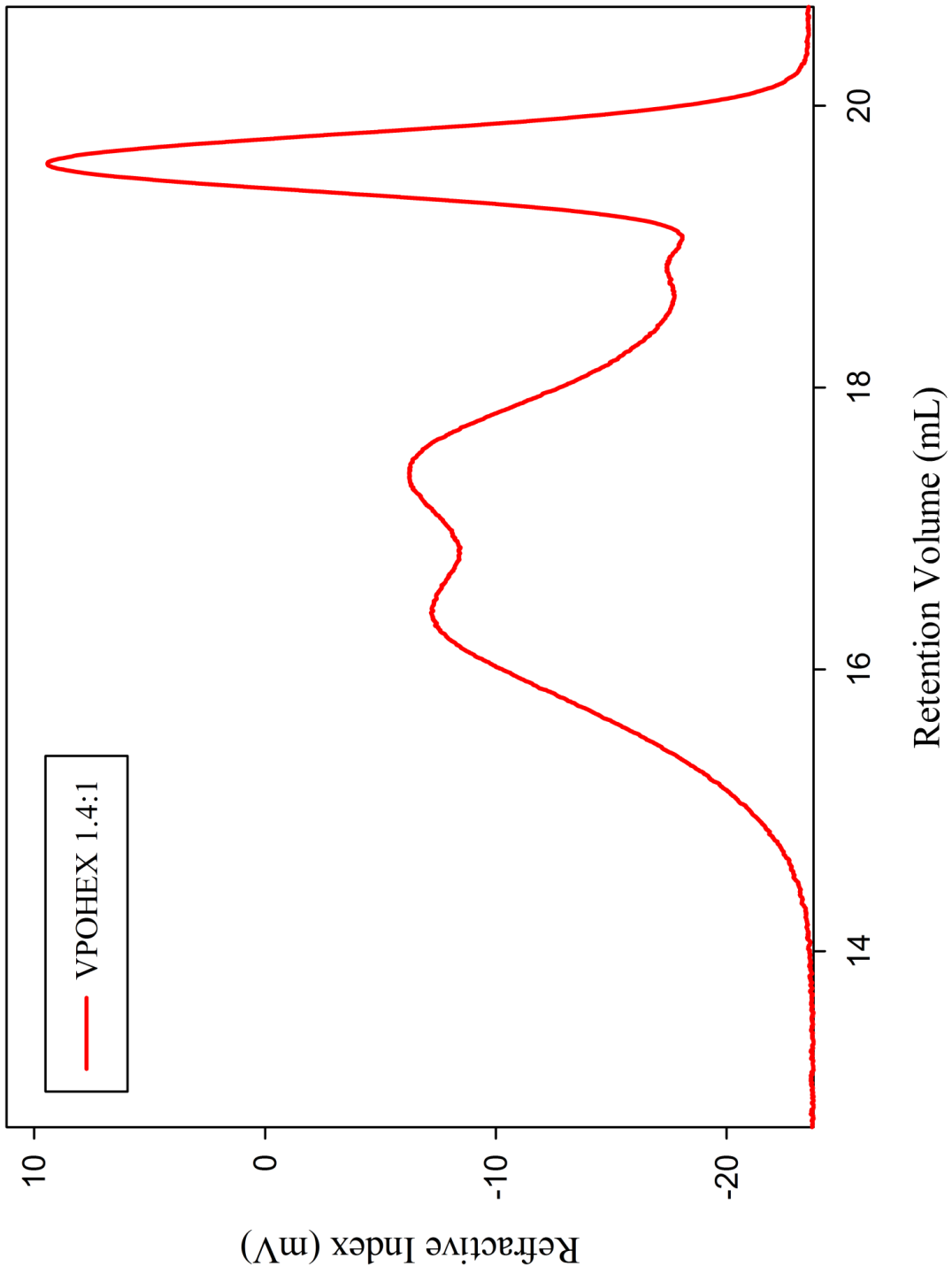

4.5.3 8-bis (4vinylphenoxy)octane (VPOOC)

DP_n100 branched, VPOOC, 0.97:1

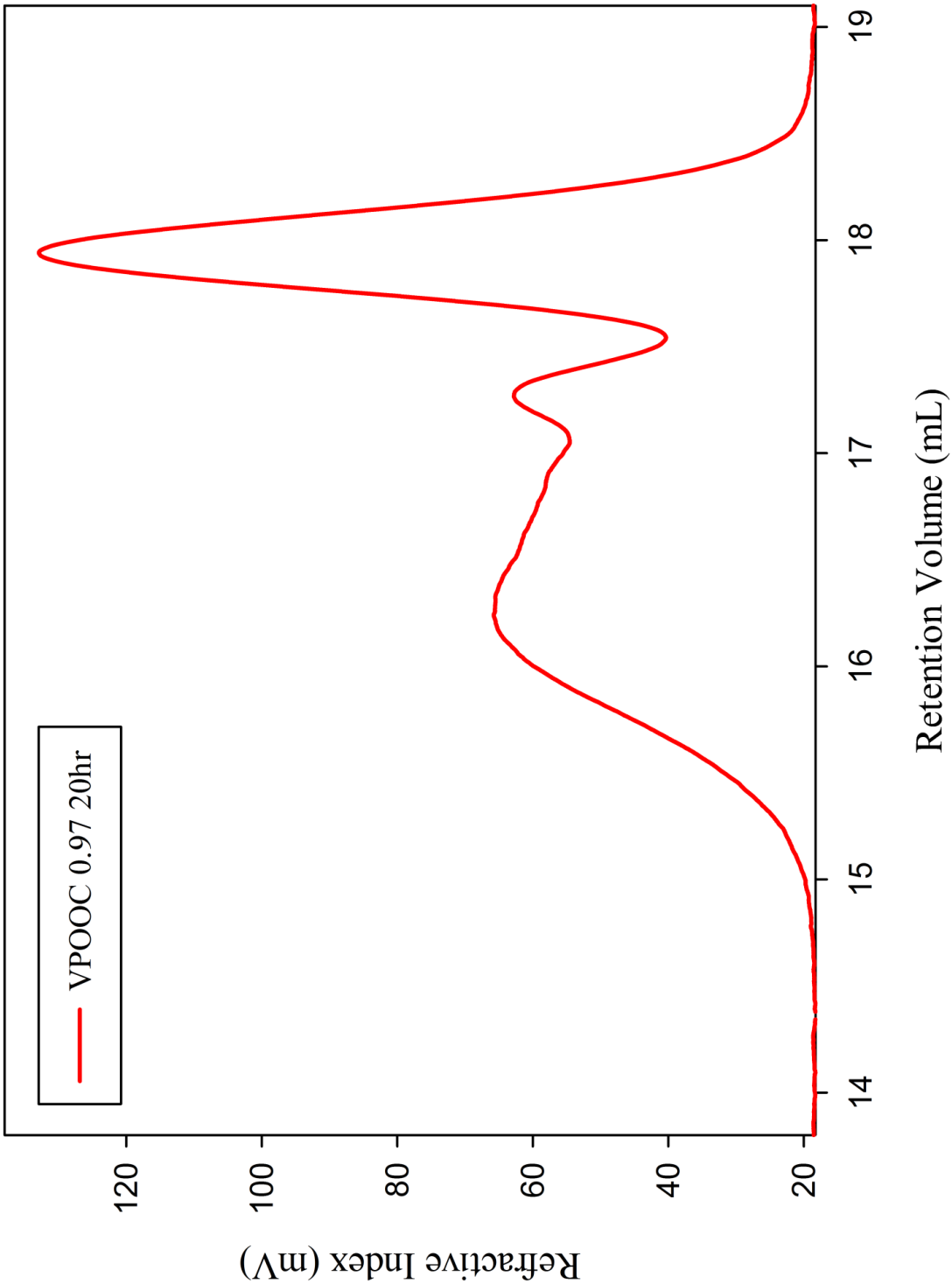

DP_n100 branched, VPOOC, 0.99:1

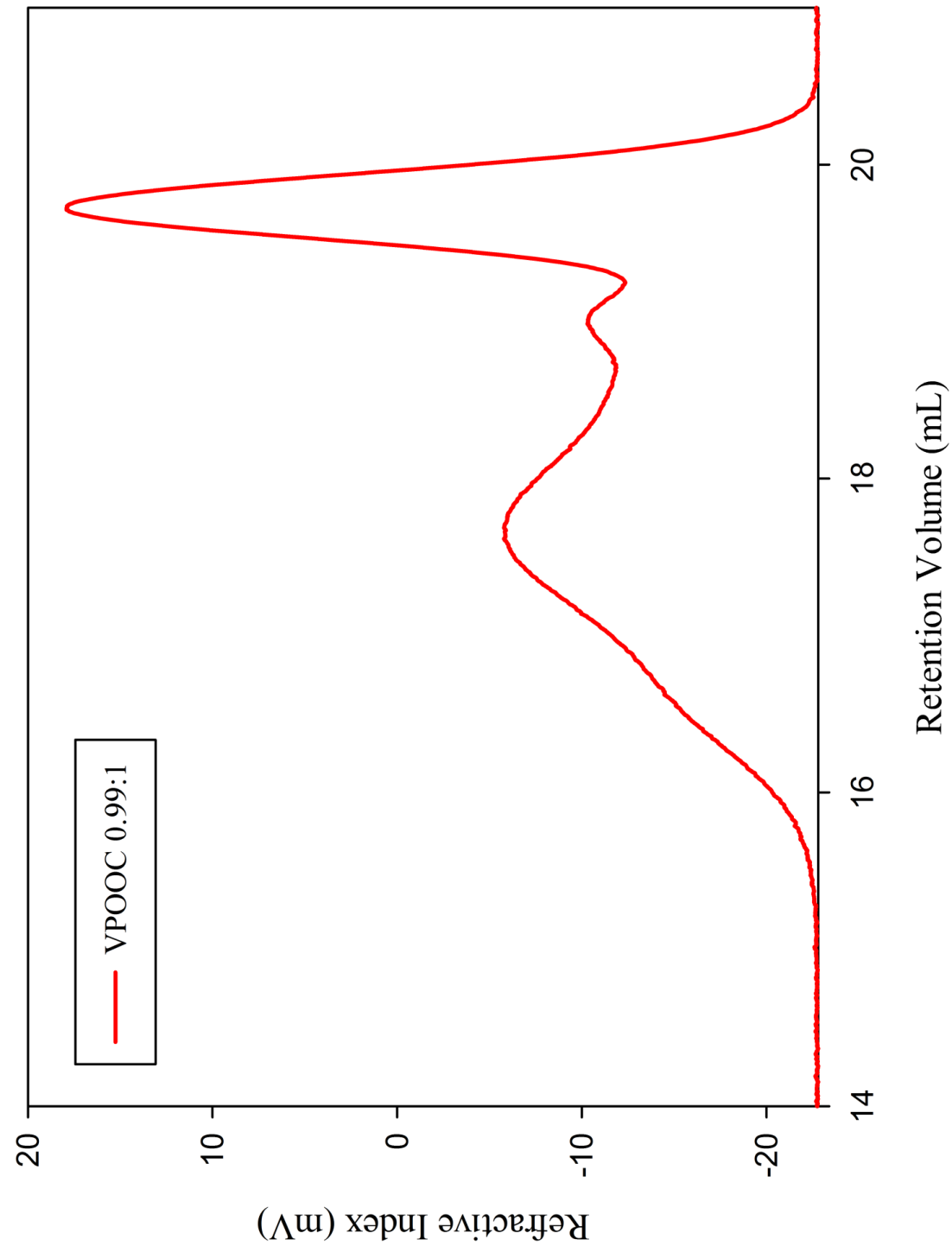

DP_n50 branched, VPOOC, 1.0:1

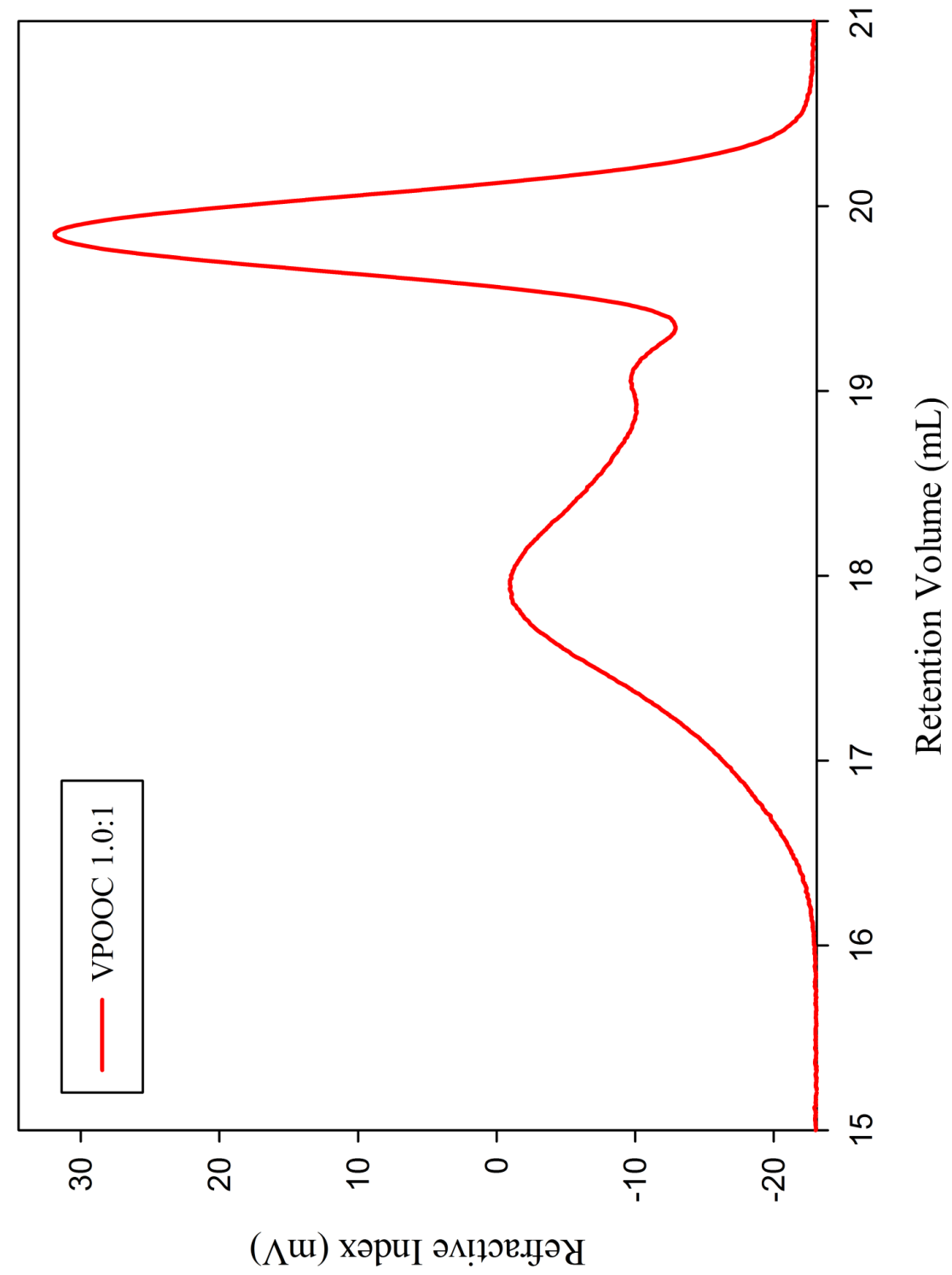

DP_n50 branched, VPOOC, 1.2:1

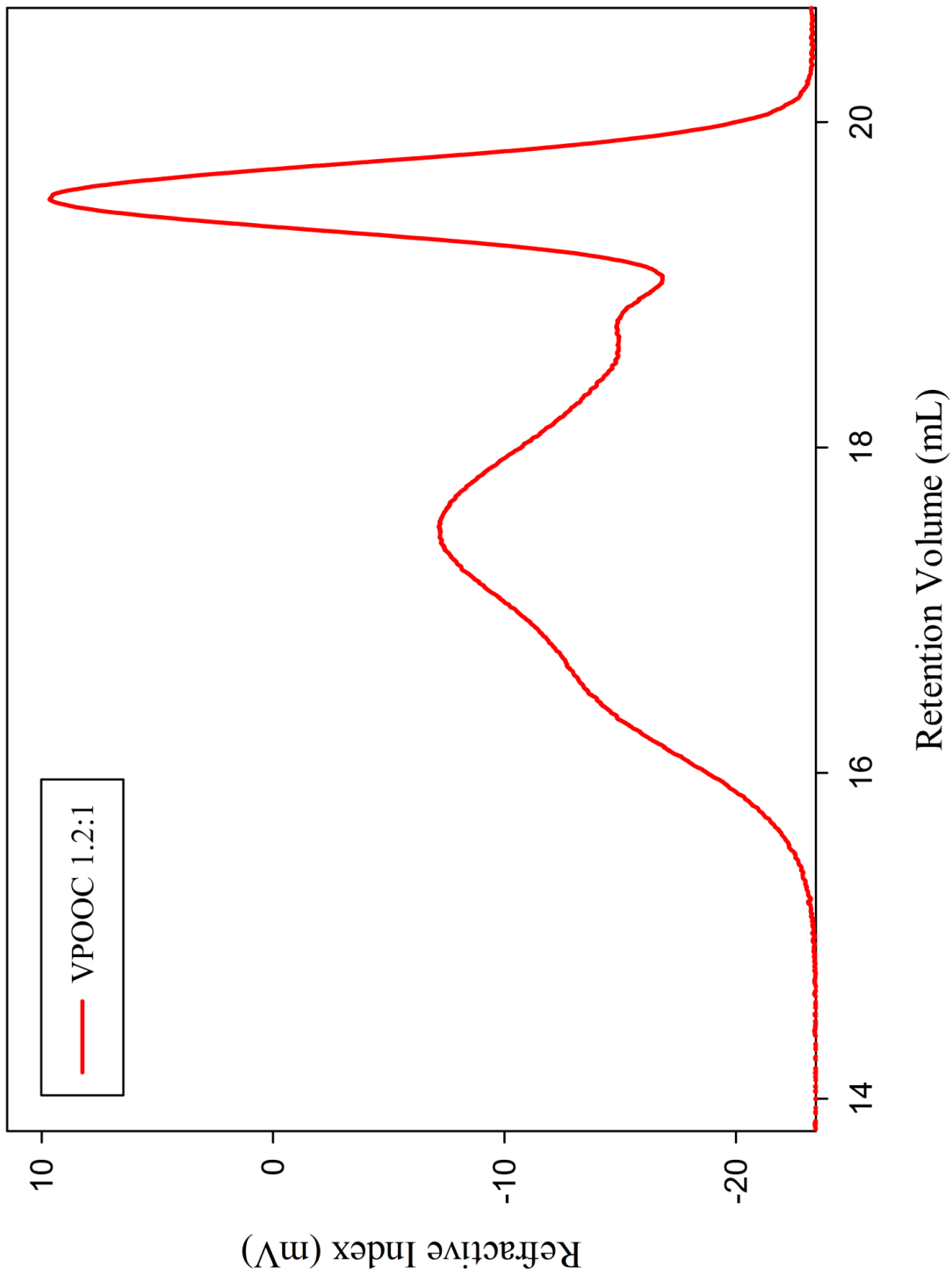

DP_n50 branched, VPOOC, 1.3:1

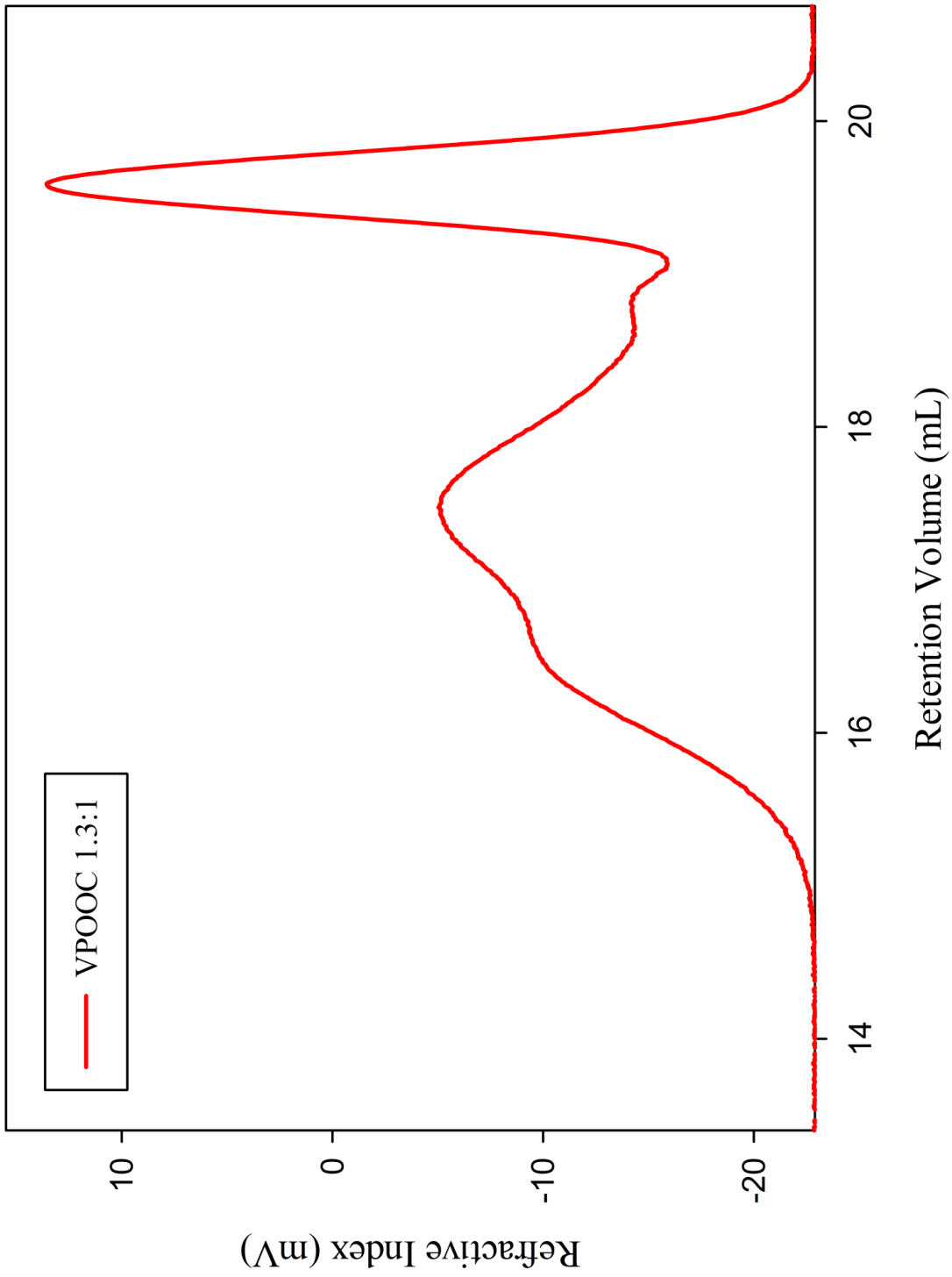

DP_n50 branched, VPOOC, 1.4:1

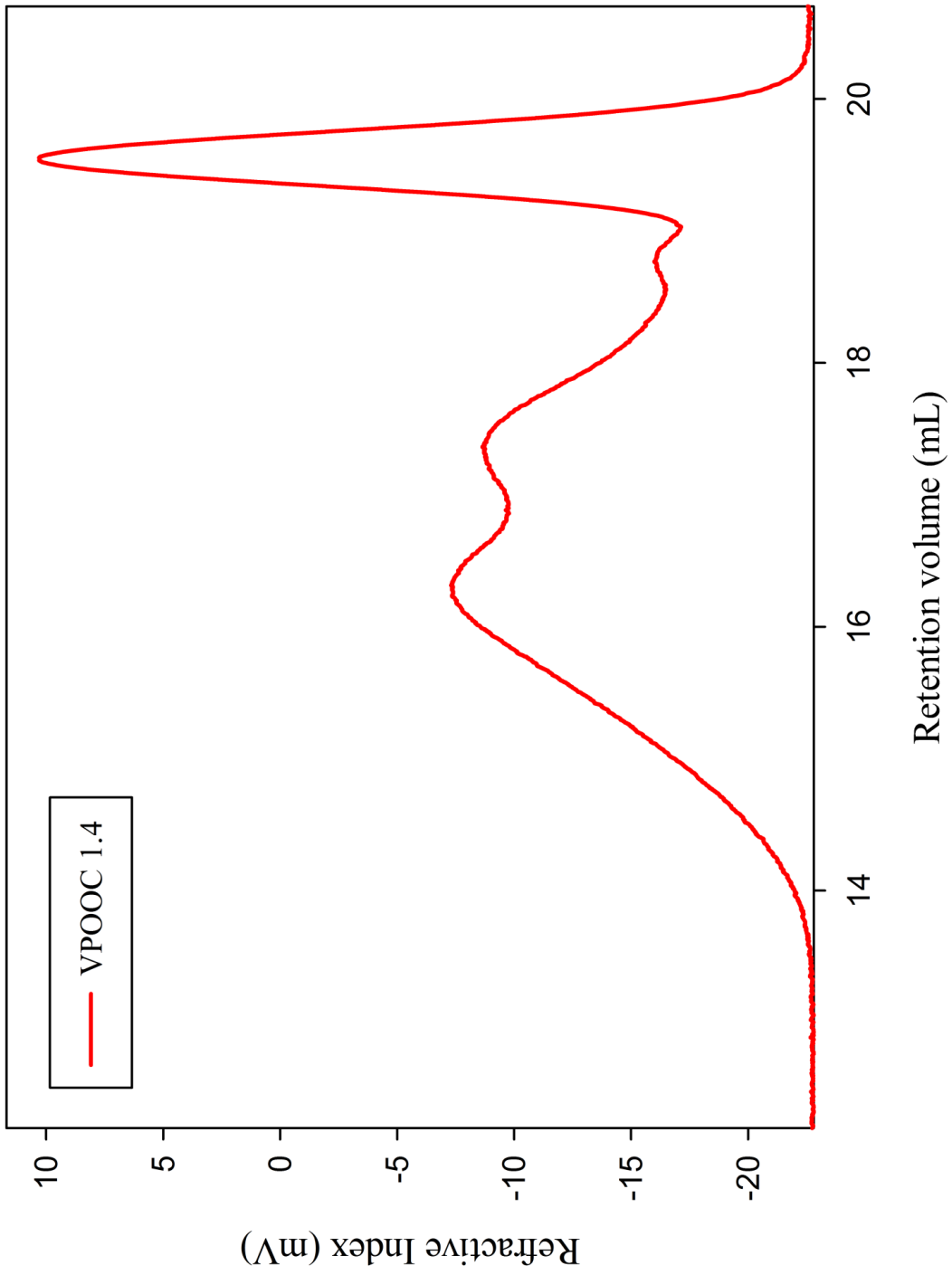

4.5.4 10-bis (4vinylphenoxy)decane (VPOT)

DP_n50 branched, VPOT, 0.98:1

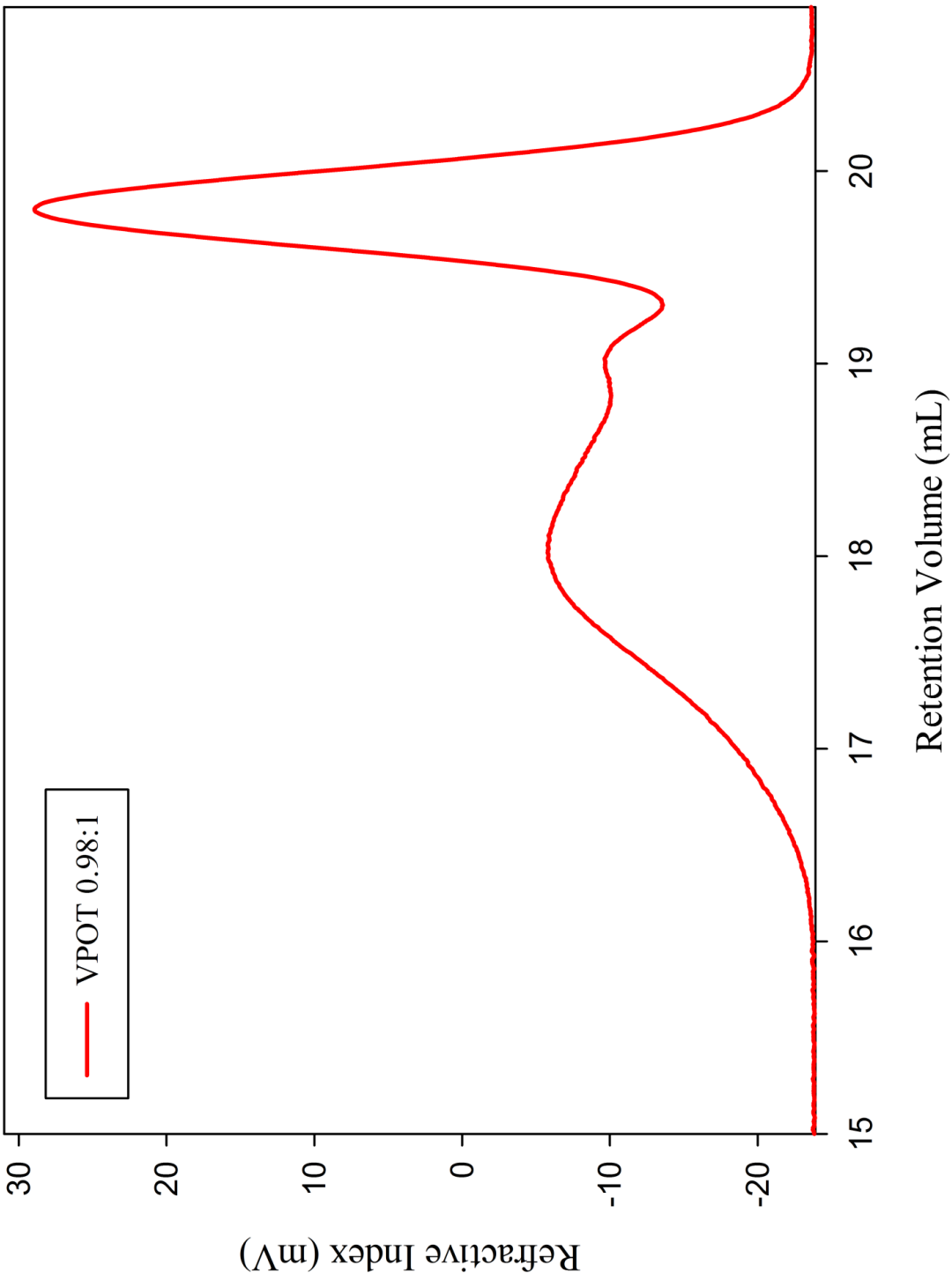

DP_n50 branched, VPOT, 1:1

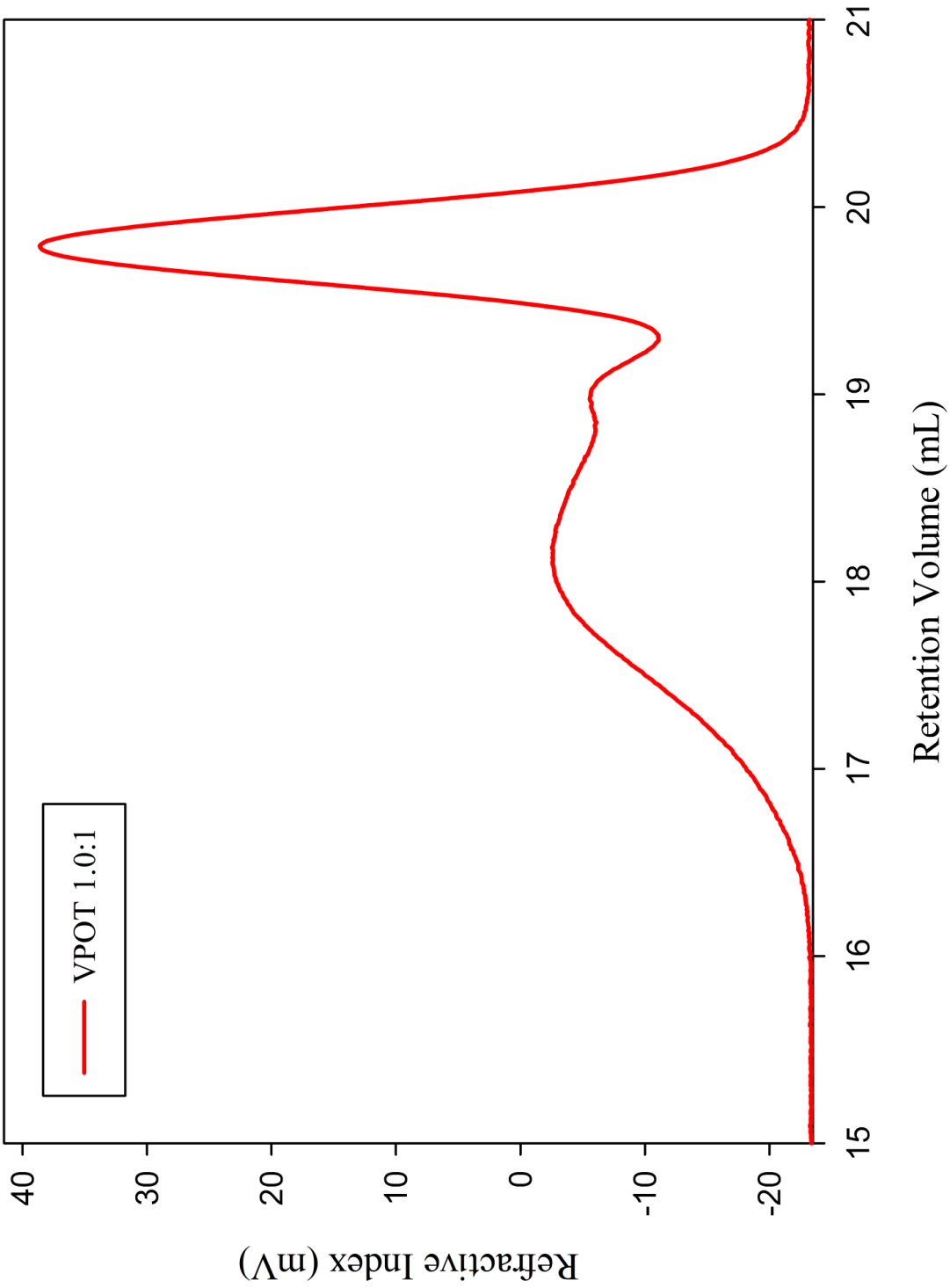

DP_n50 branched, VPOT, 1.2:1

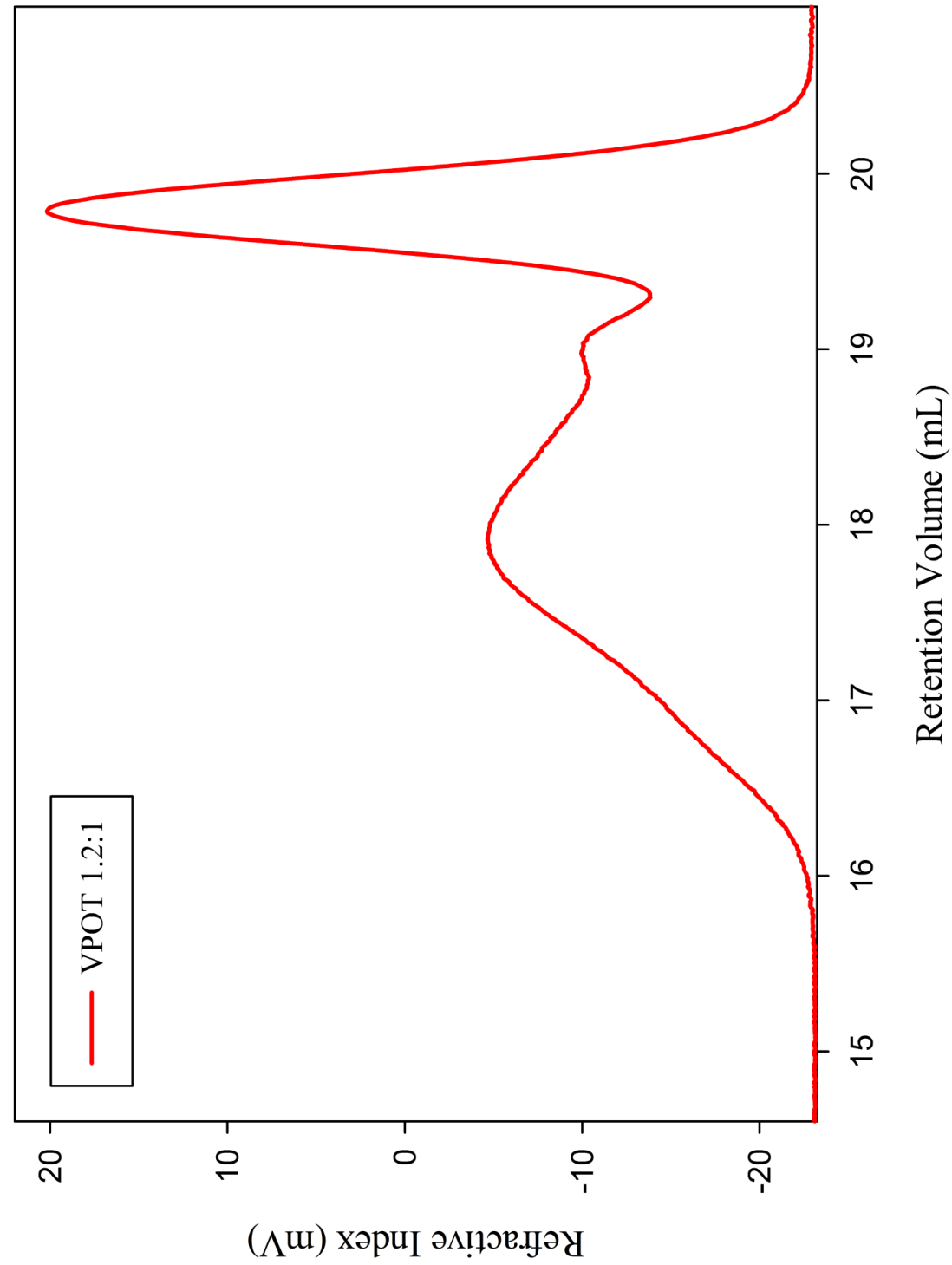

4.5.4 12-bis (4vinylphenoxy)dodecane (VPODD)

DP_n50 branched, VPODD, 0.90:1

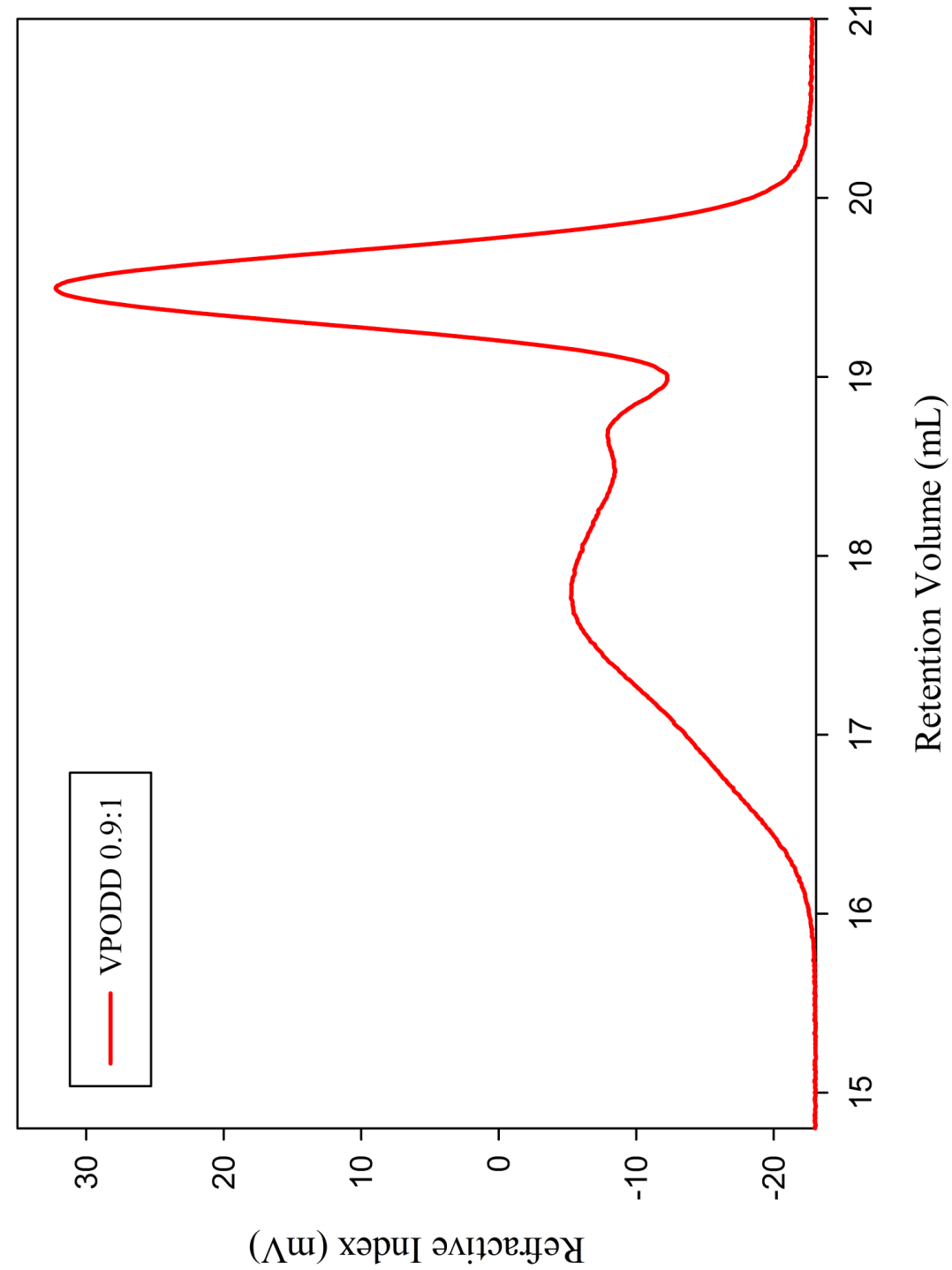

Chapter 5

5.1 Effect of primary chain length

DP_n10 branched

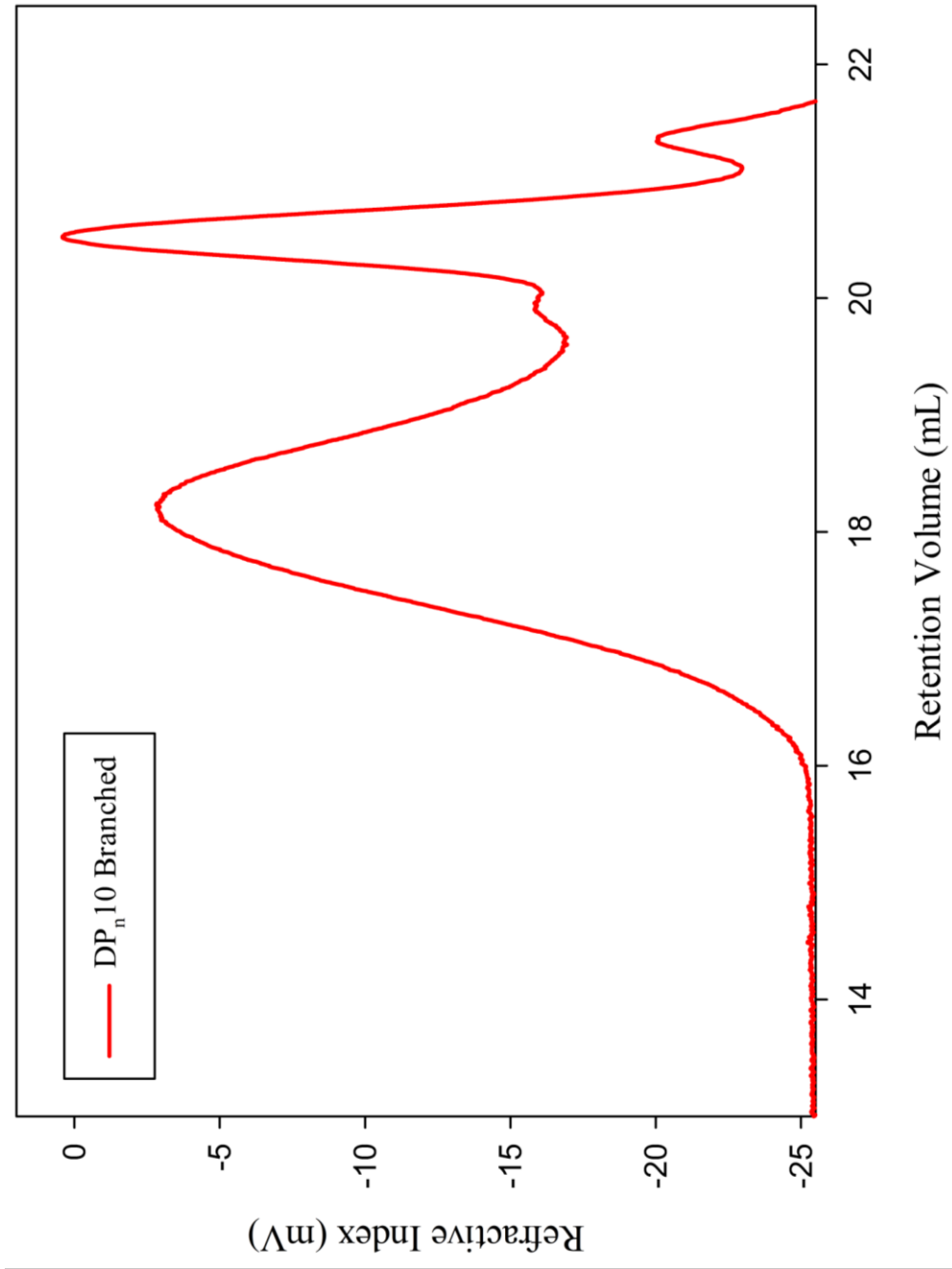

DP_n25 branched

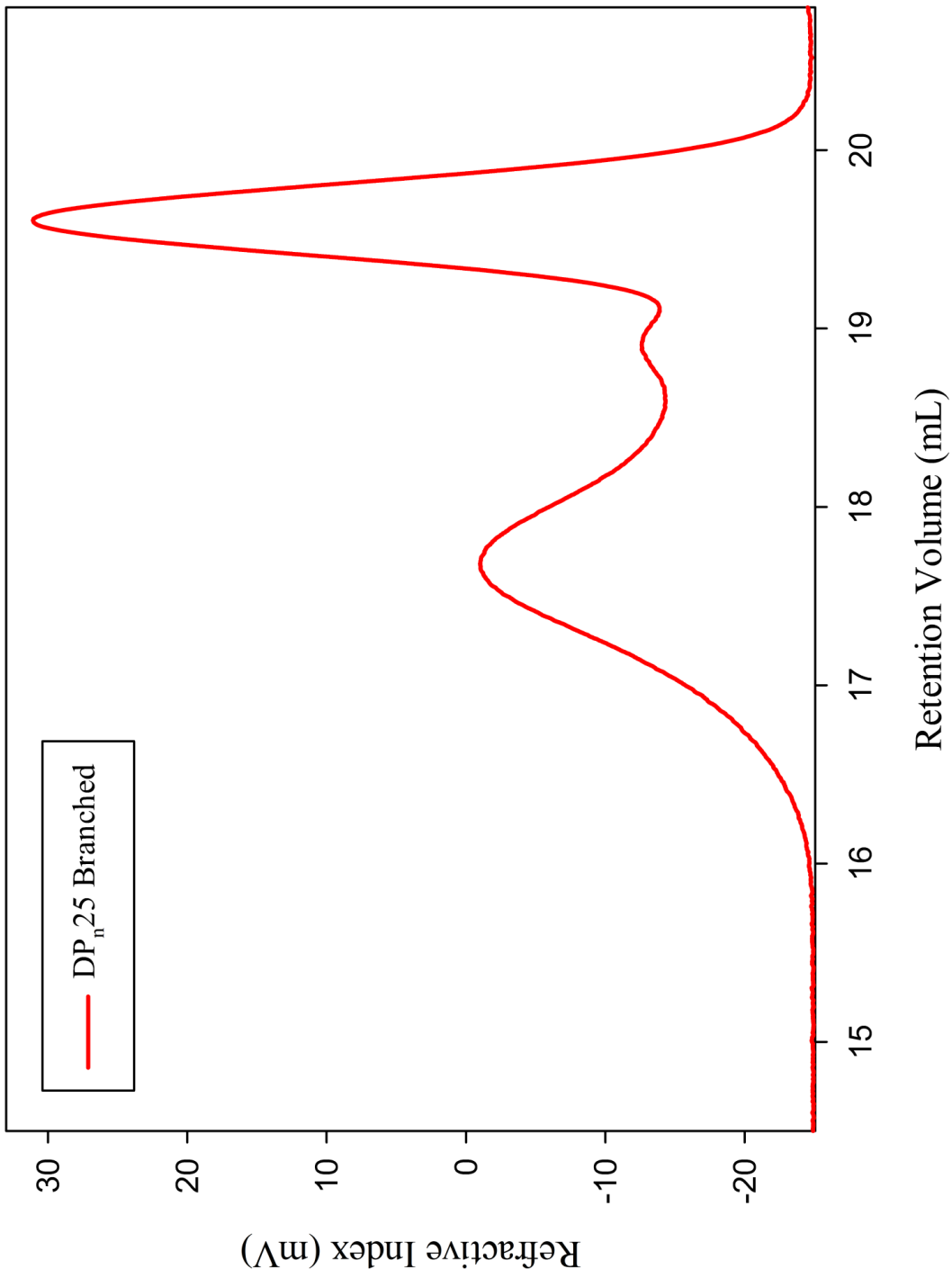

DP_n50 branched

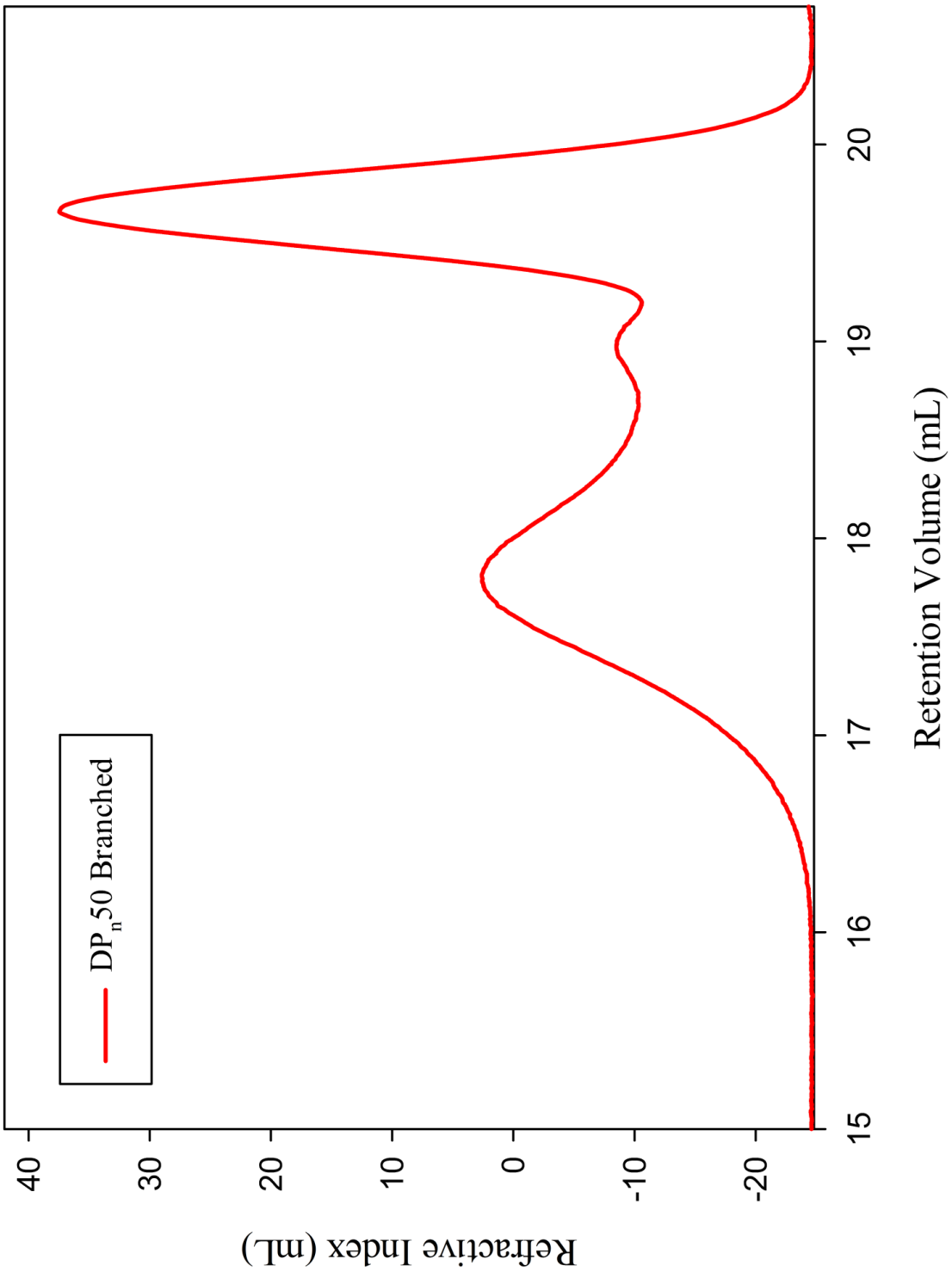

DP_n100 branched

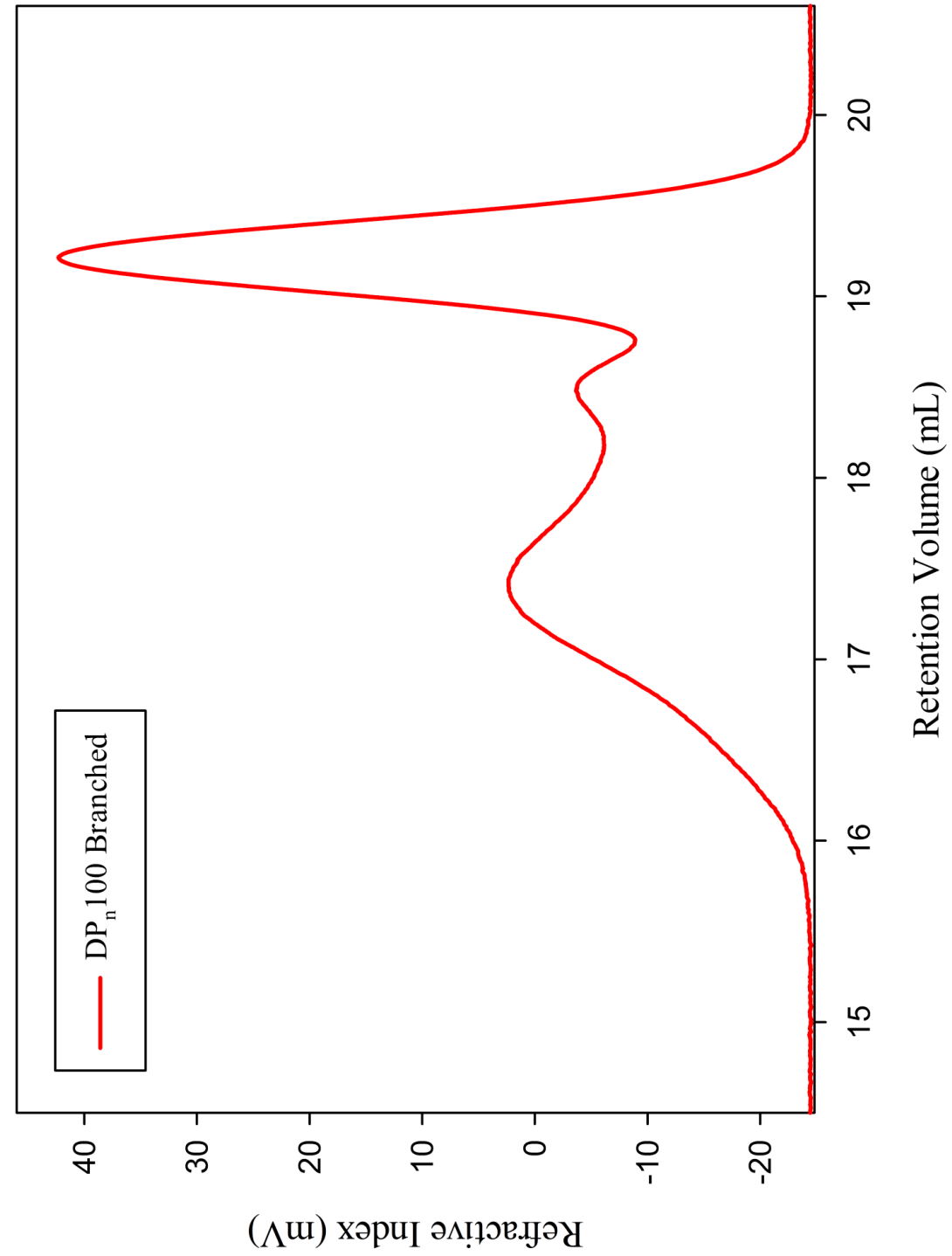

DP_n250 branched

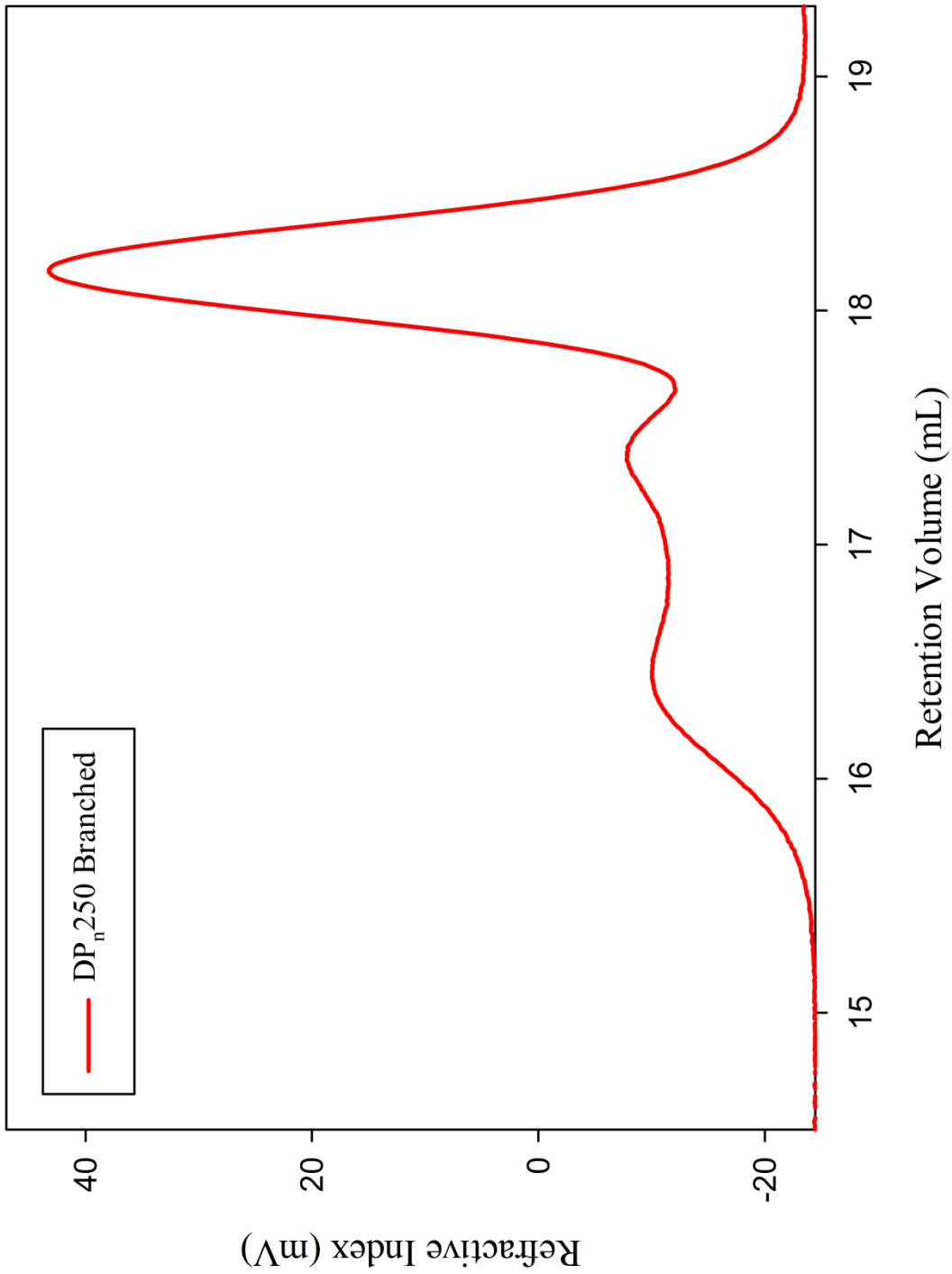

DP_n500 branched

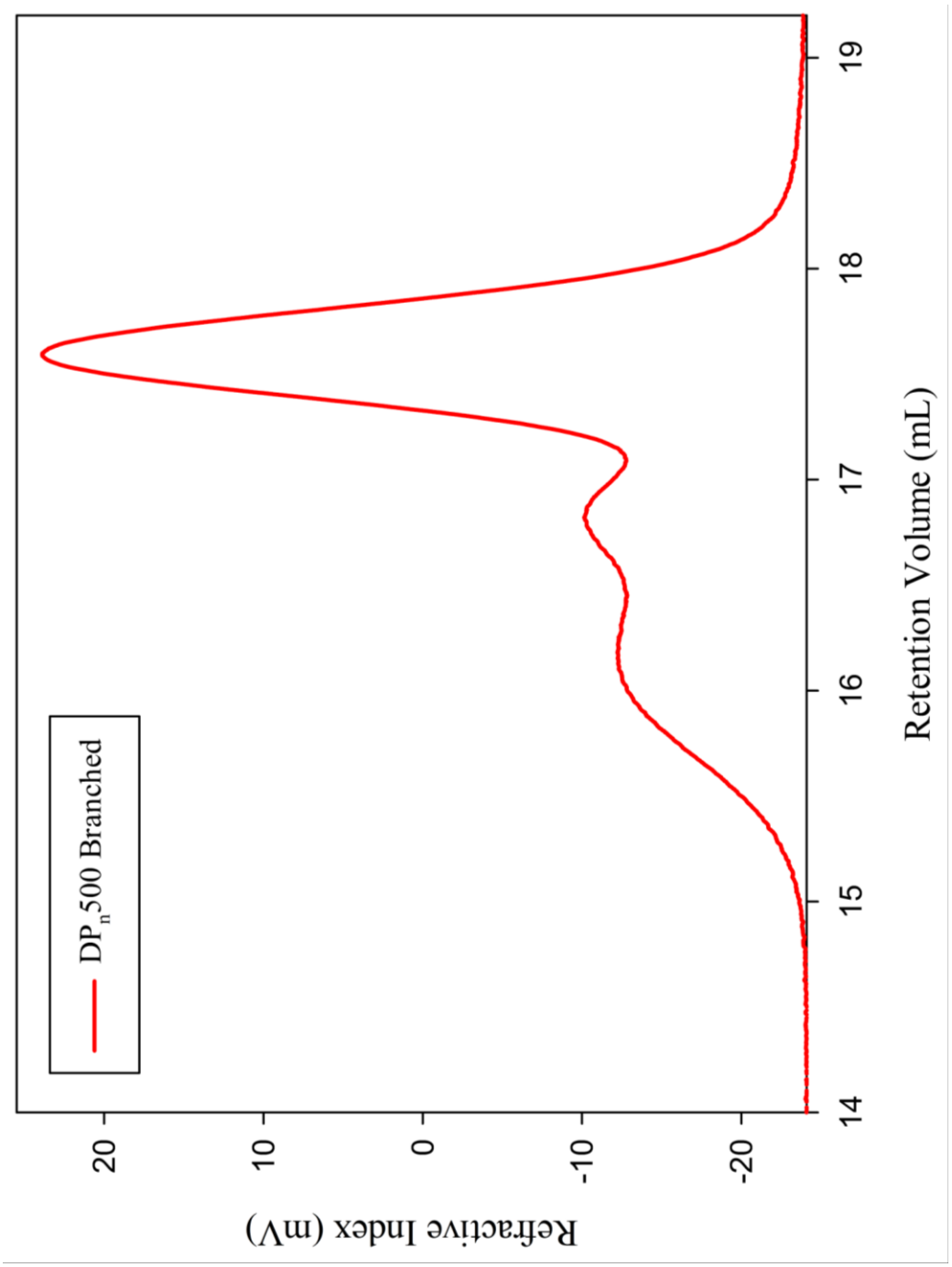

5.2 Chain extension of branched polymers

5.2.1 Equivalent to DPn100

DP_n10 branched plus DP_n90 linear

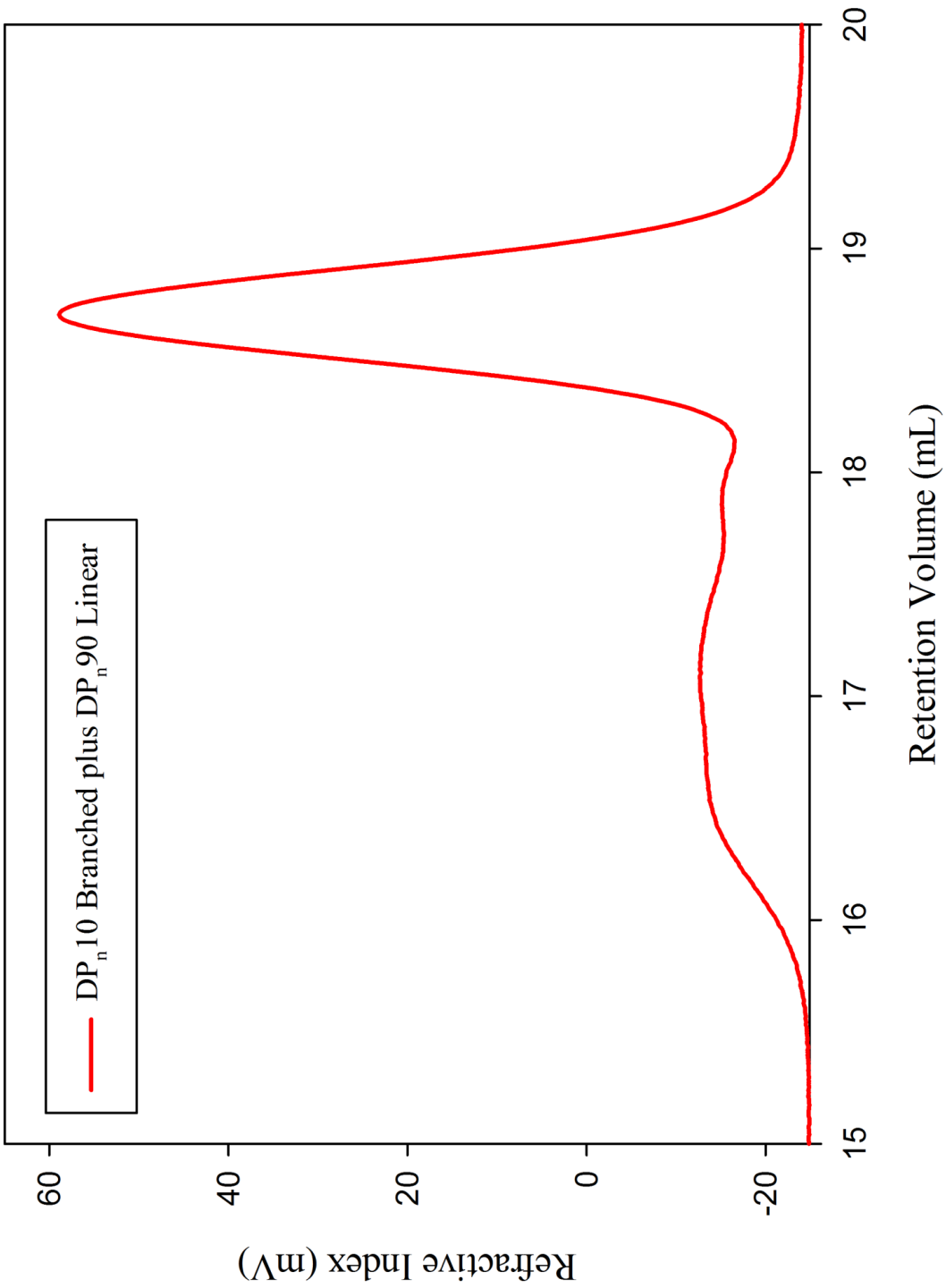

DP_n90 linear plus DP_n10 branched

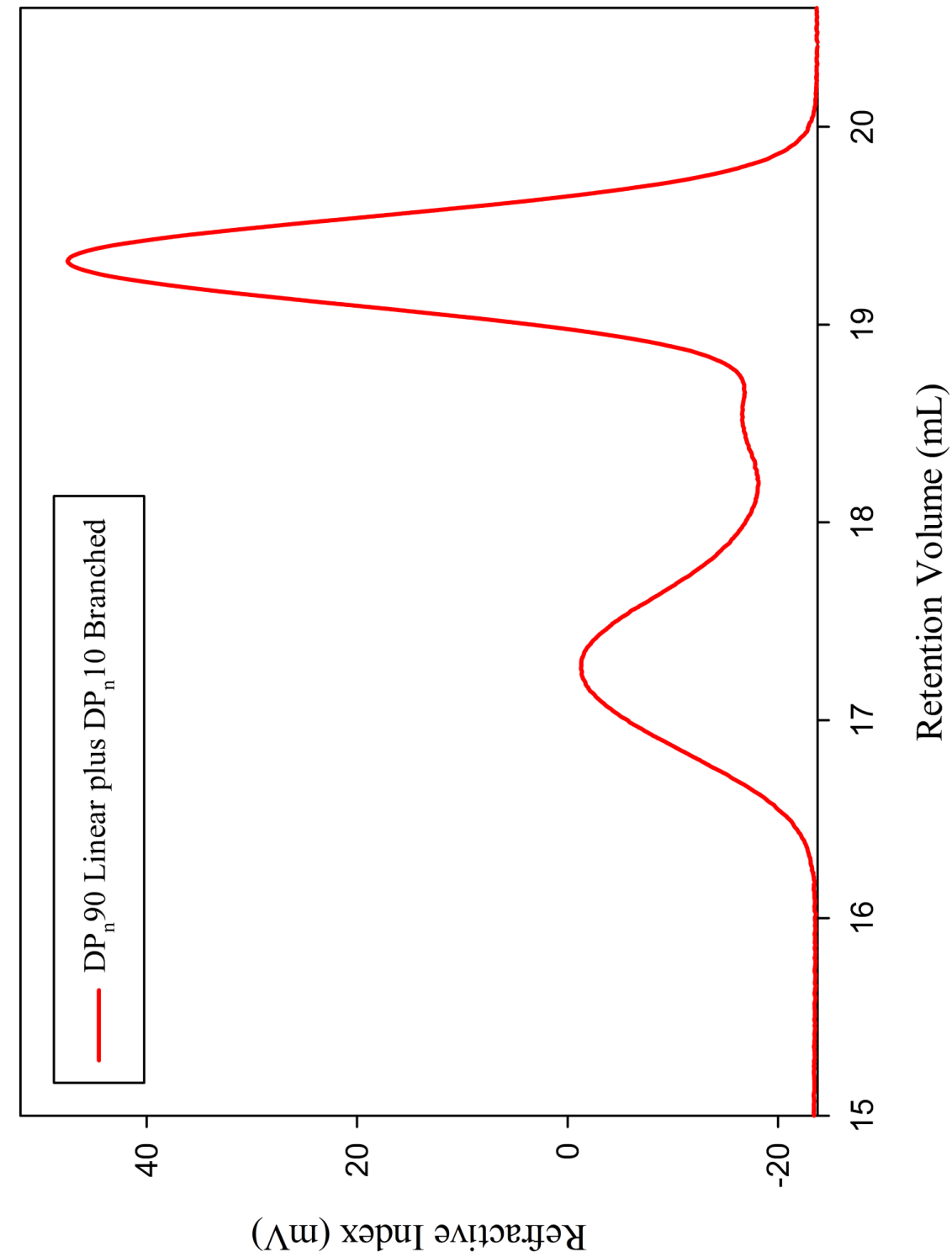

DP_n90 branched plus DP_n10 linear

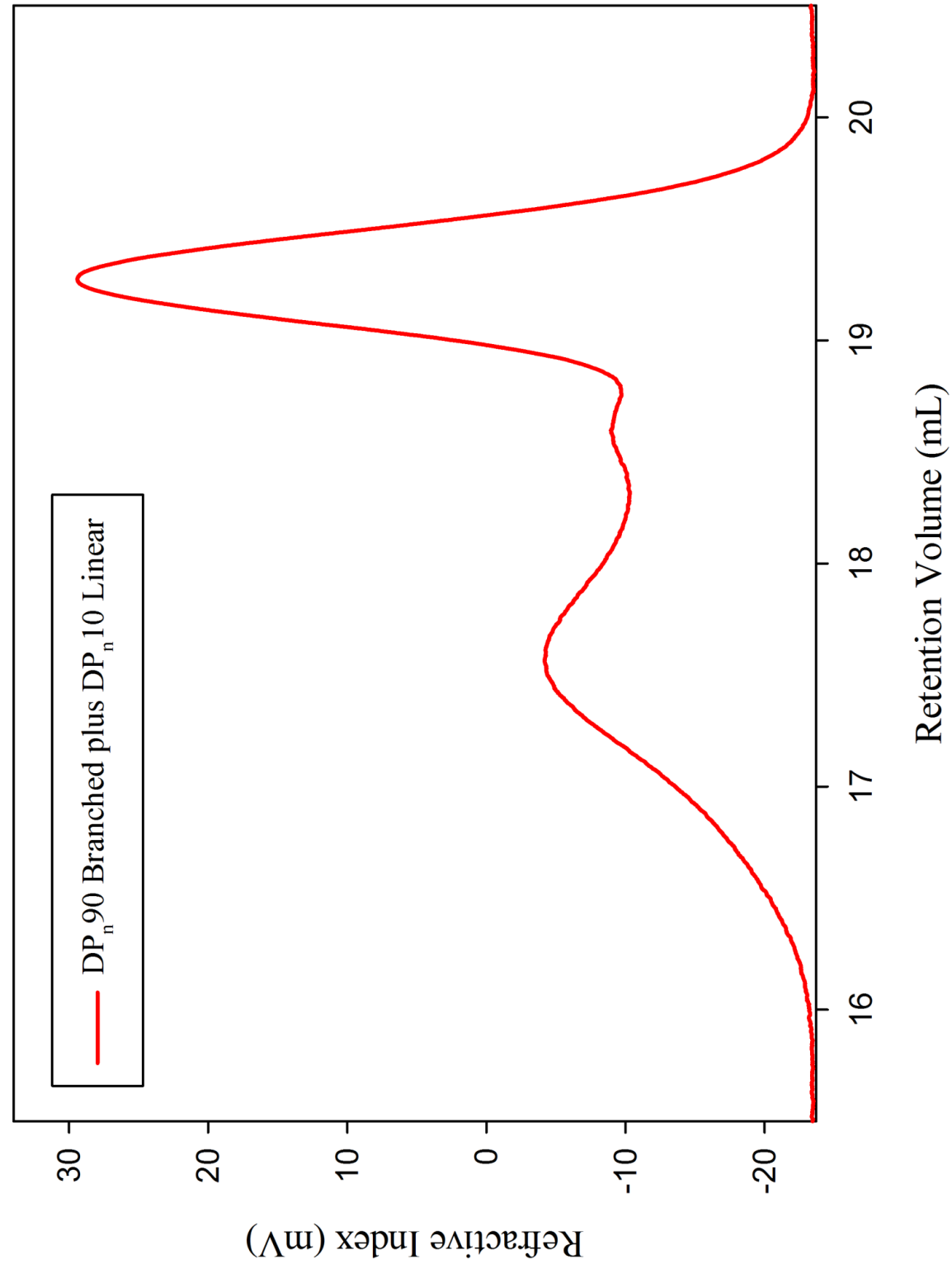

DP_n10 linear plus DP_n90 branched

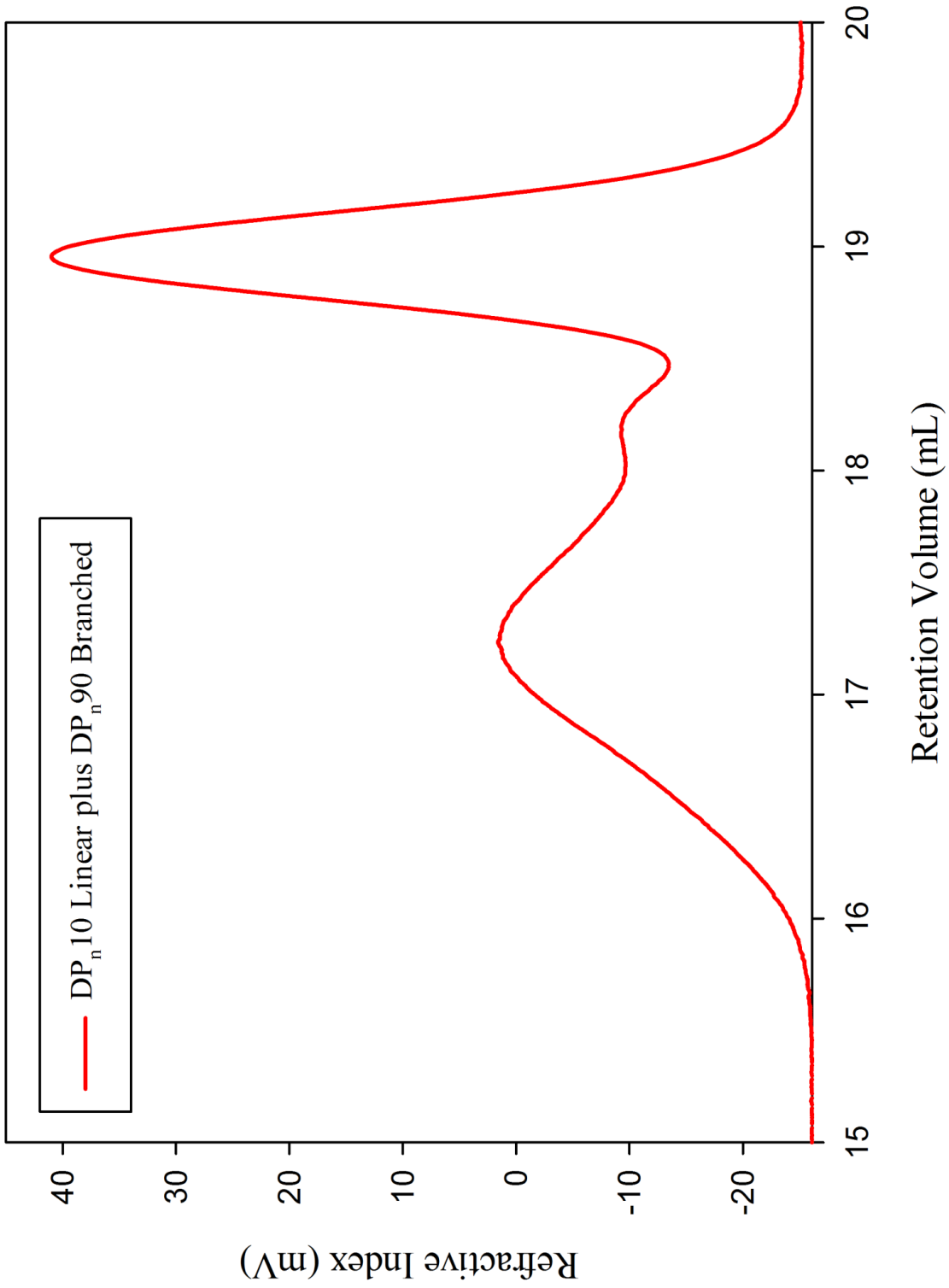

DP_n90 branched

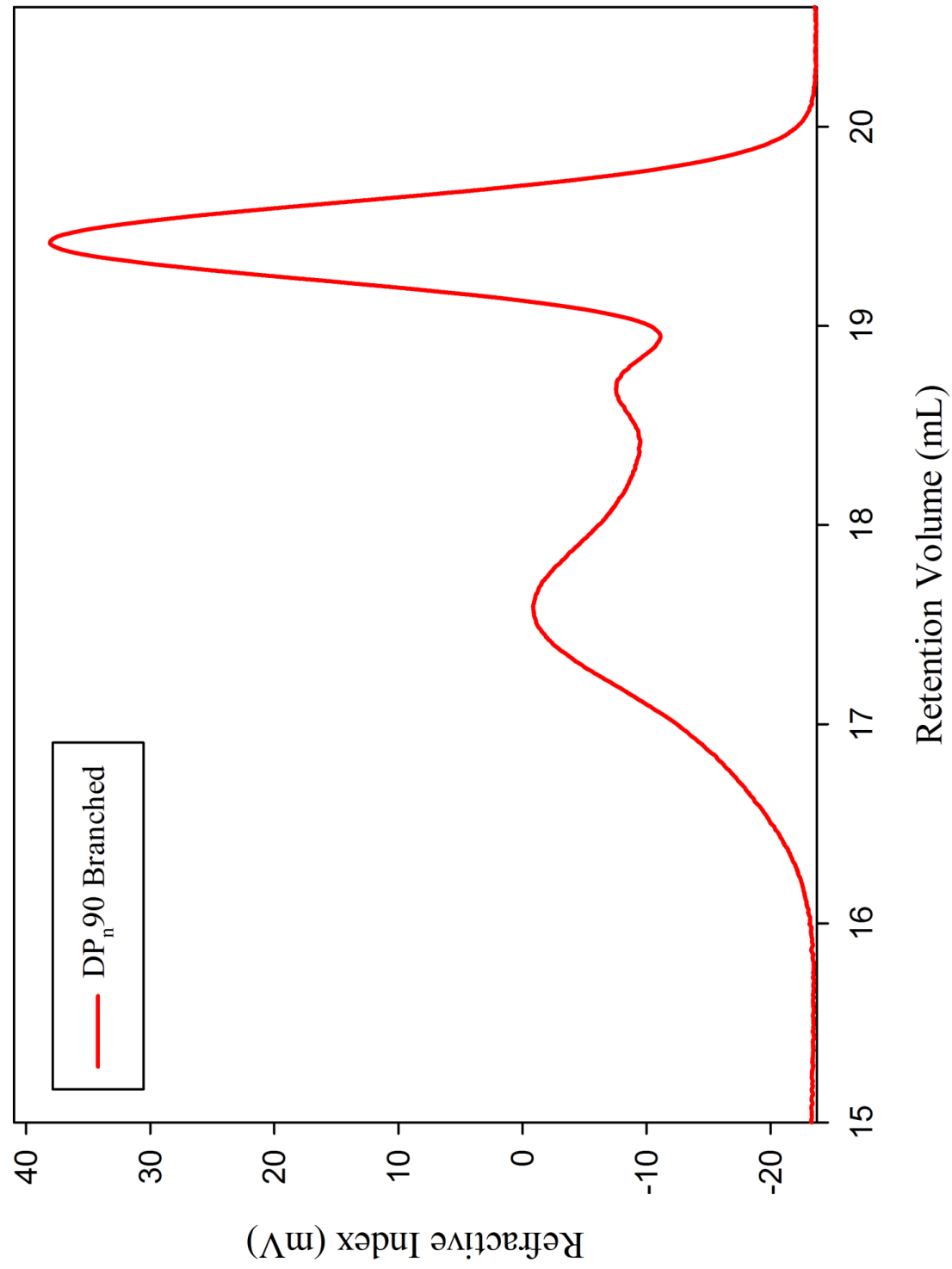

DP_n90 linear

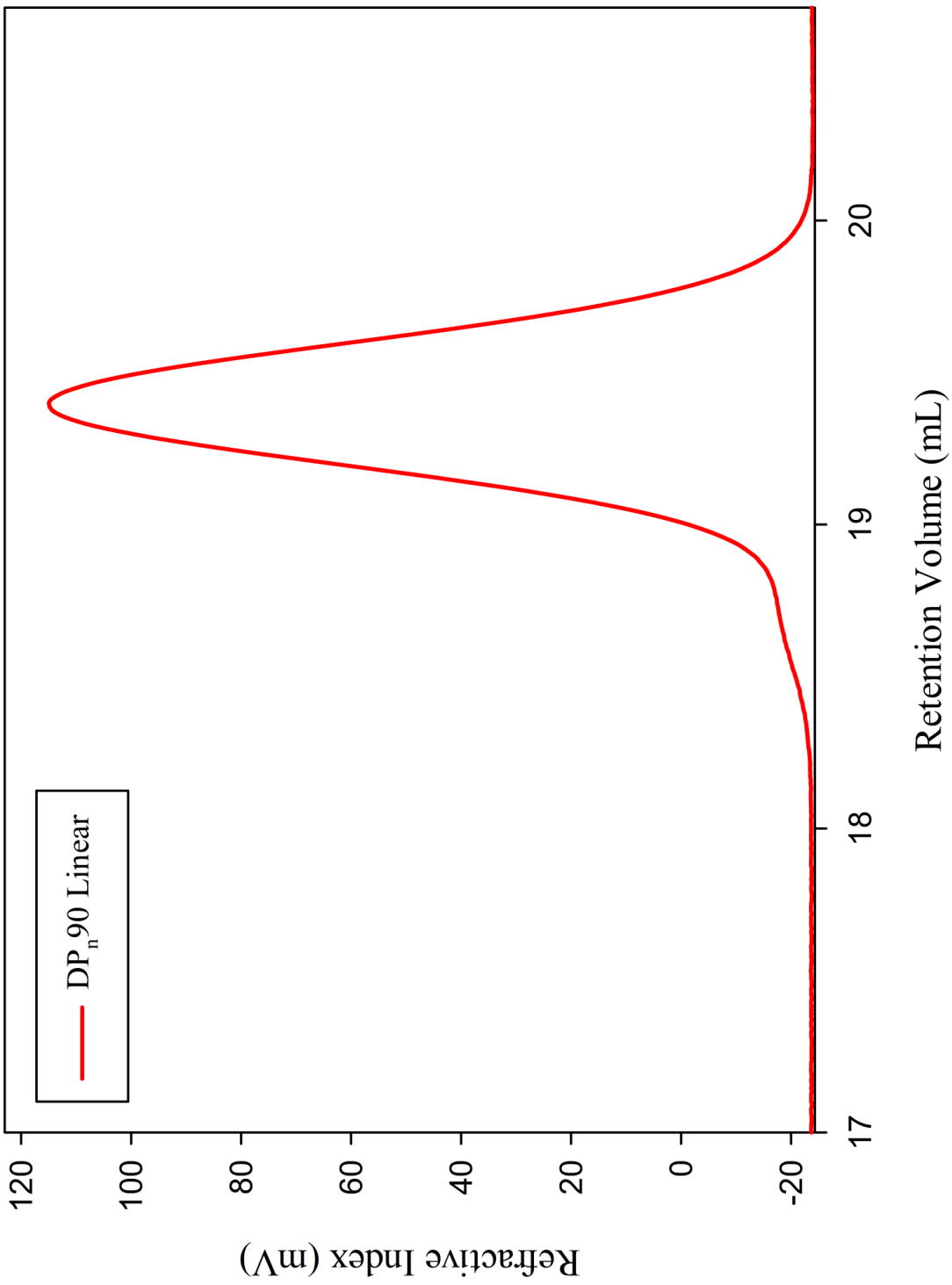

DP_n50 branched plus DP_n50 linear

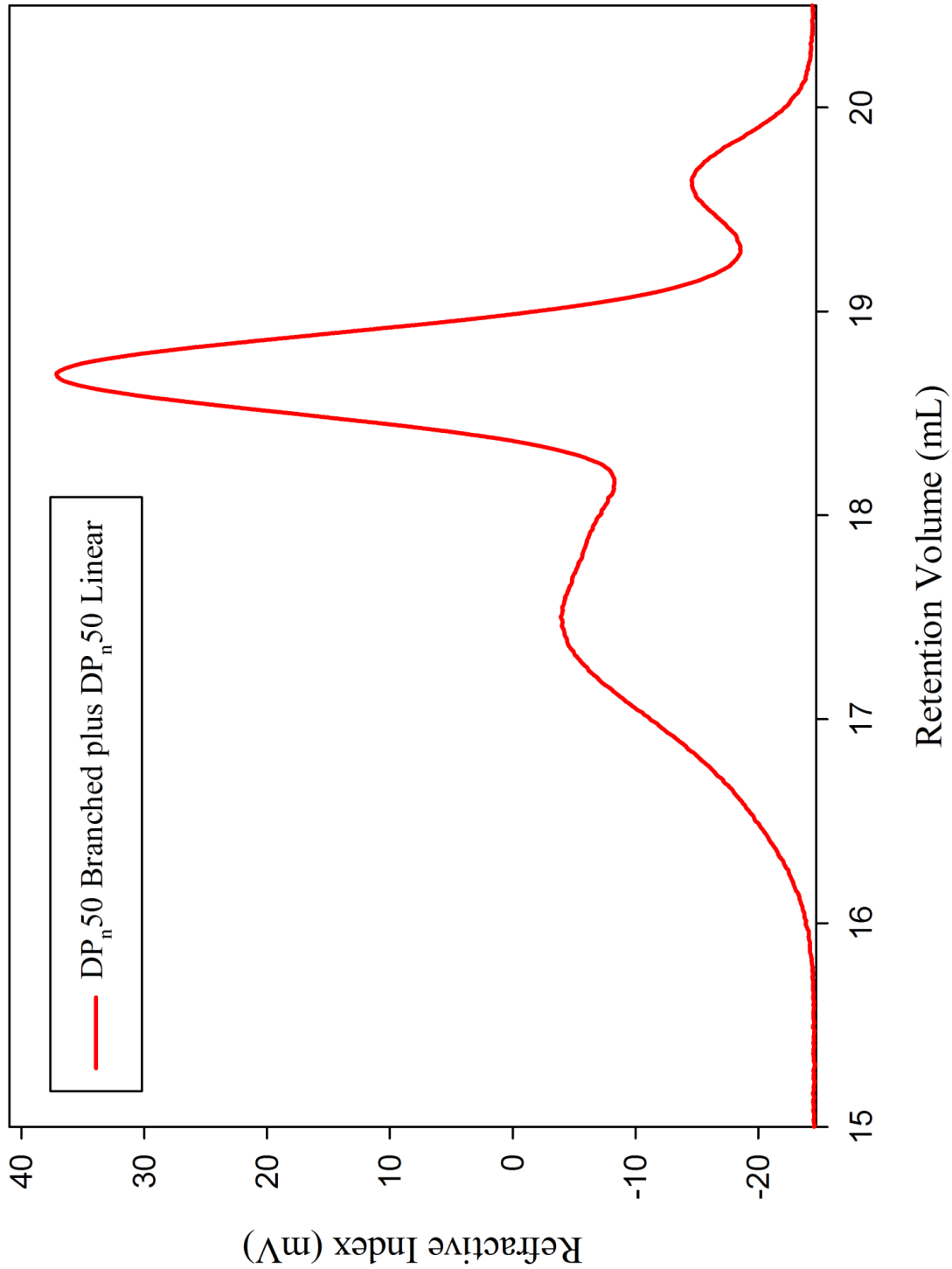

DP_n50 linear plus DP_n50 branched

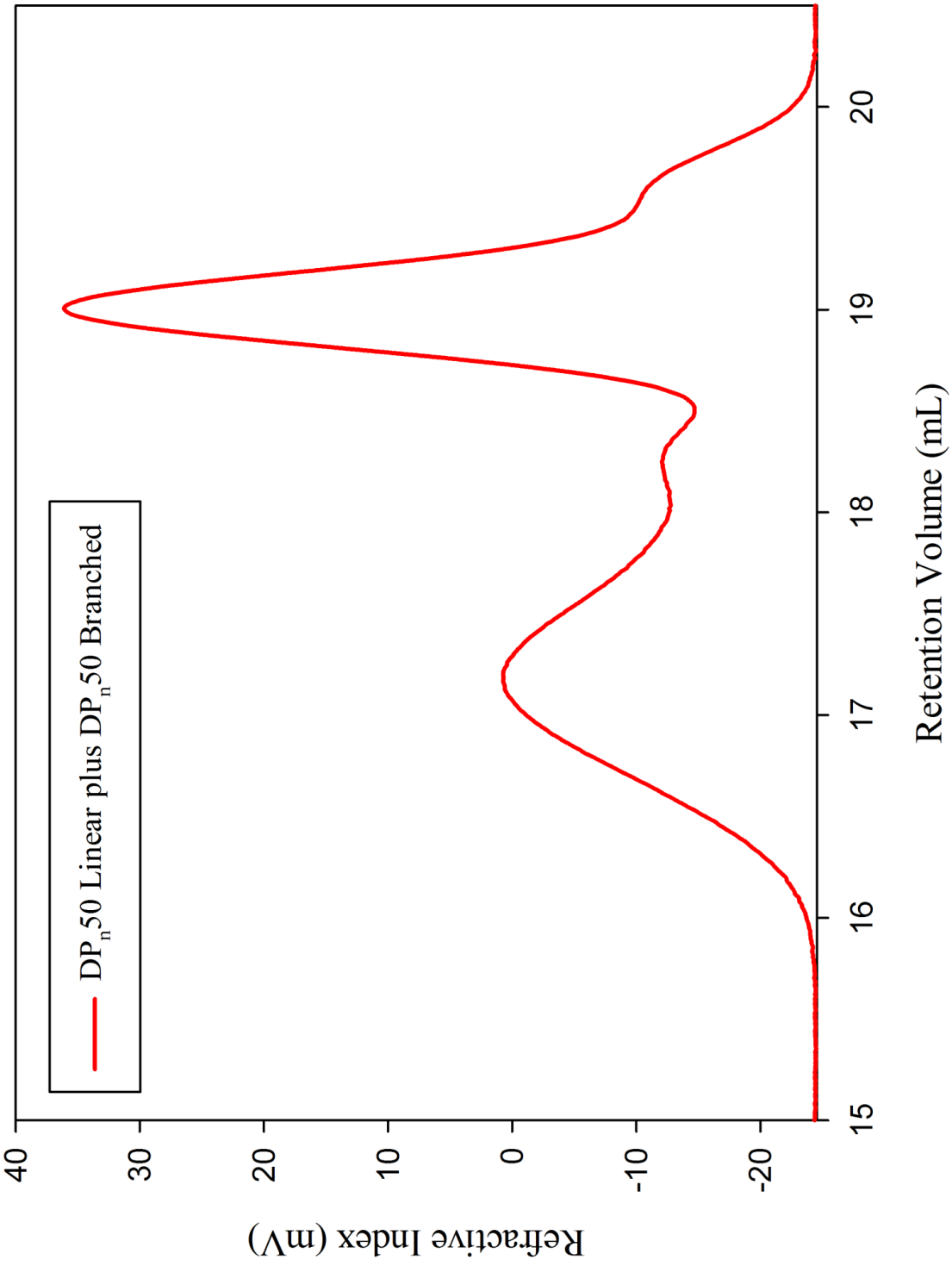

5.2 DP_n50 1:0.25 a

5.2.2 Equivalent to DPn50

5.1.2 DP_n10 branched plus DP_n40 linear

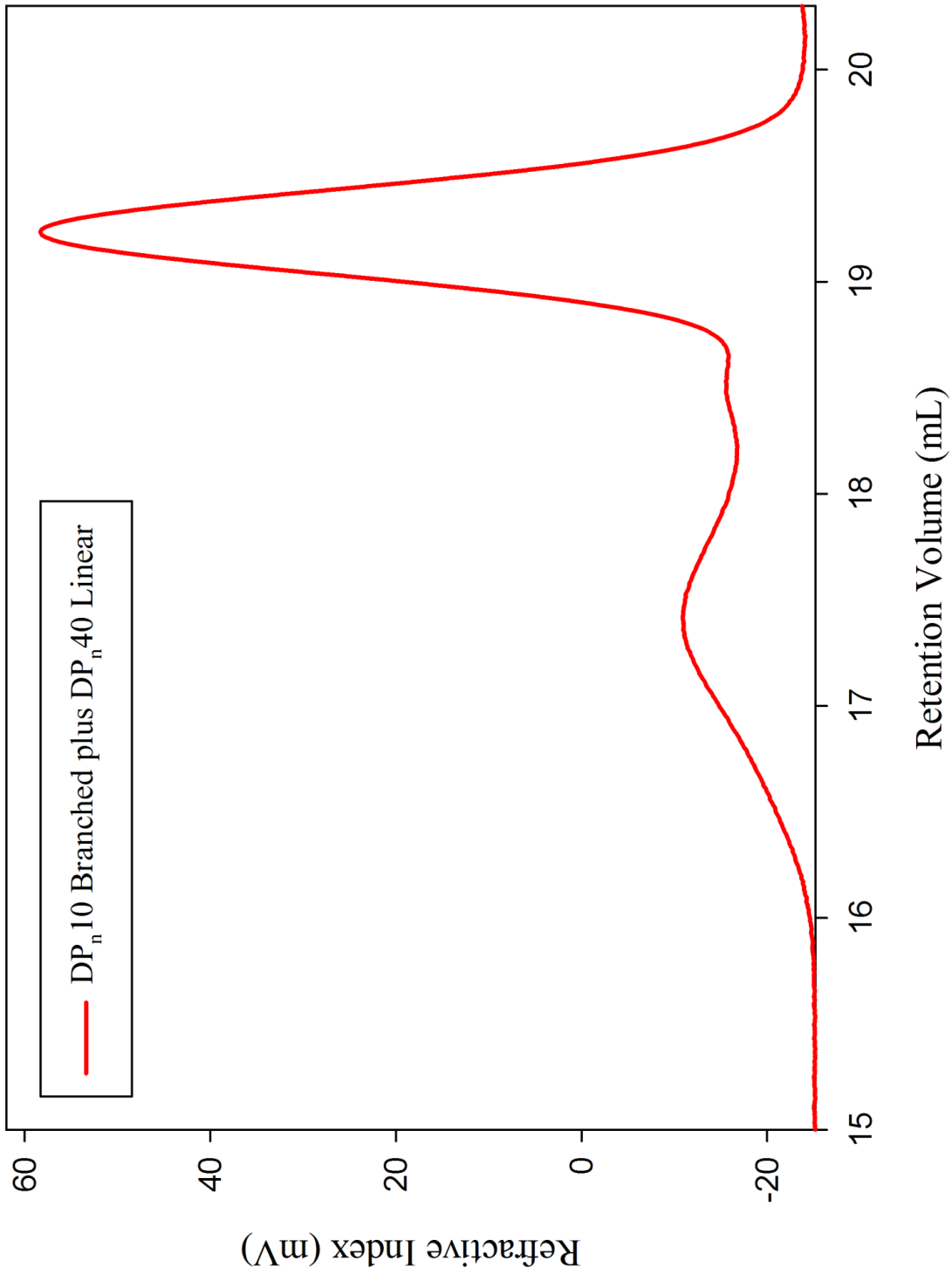

DP_n40 linear plus DP_n10 branched

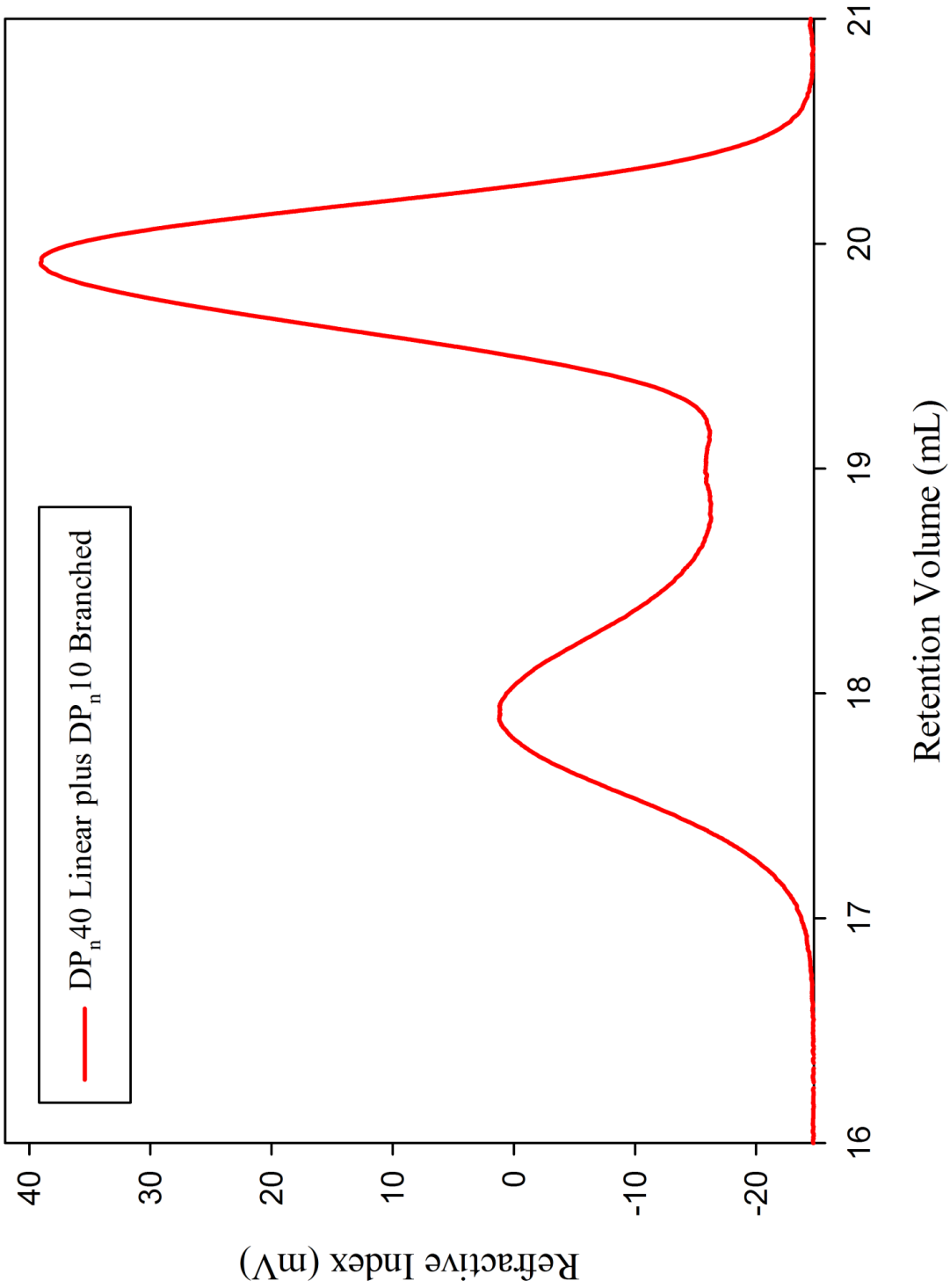

DP_n40 branched plus DP_n10 linear

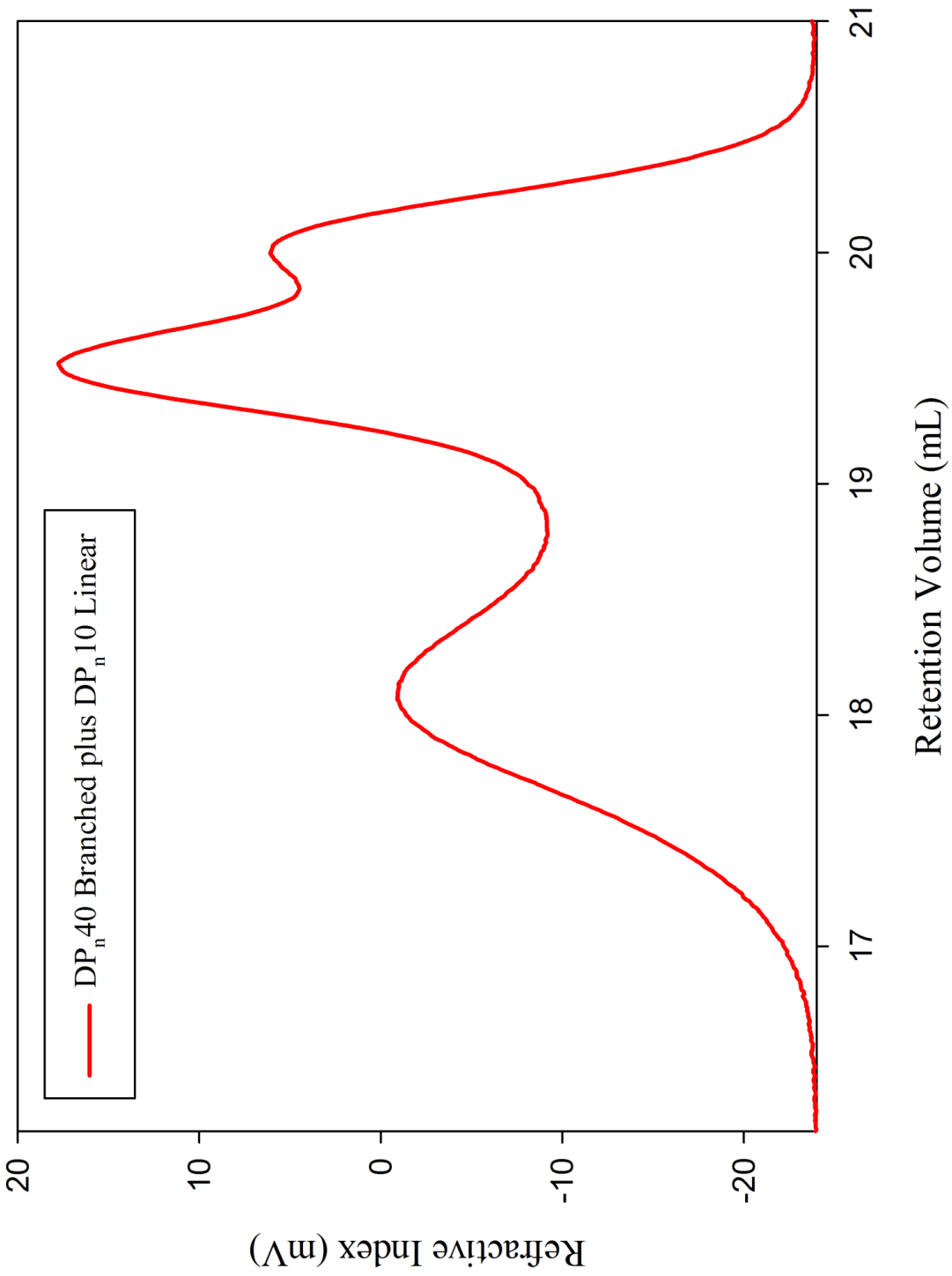

DP_n10 linear plus DP_n40 branched

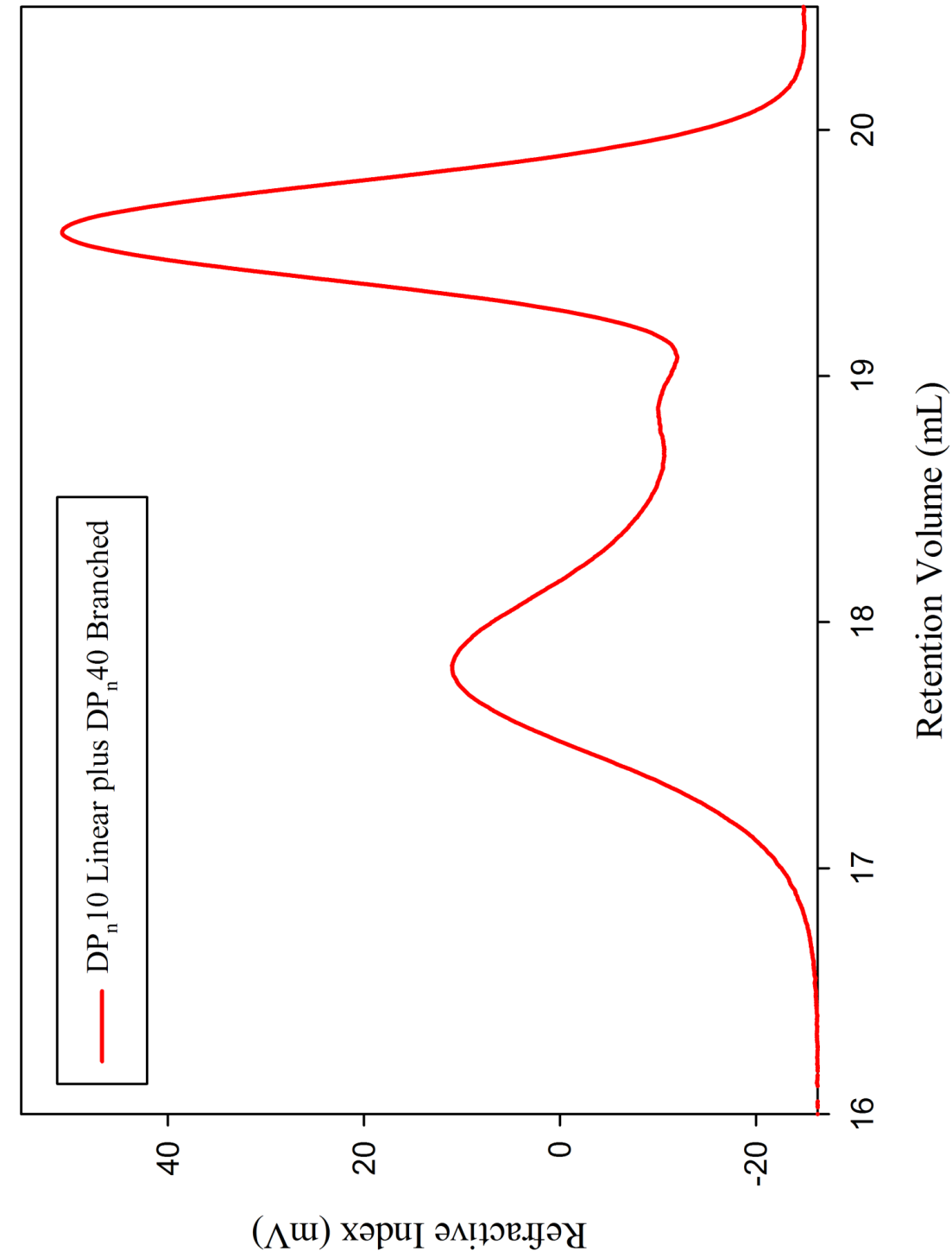

DP_n40 linear

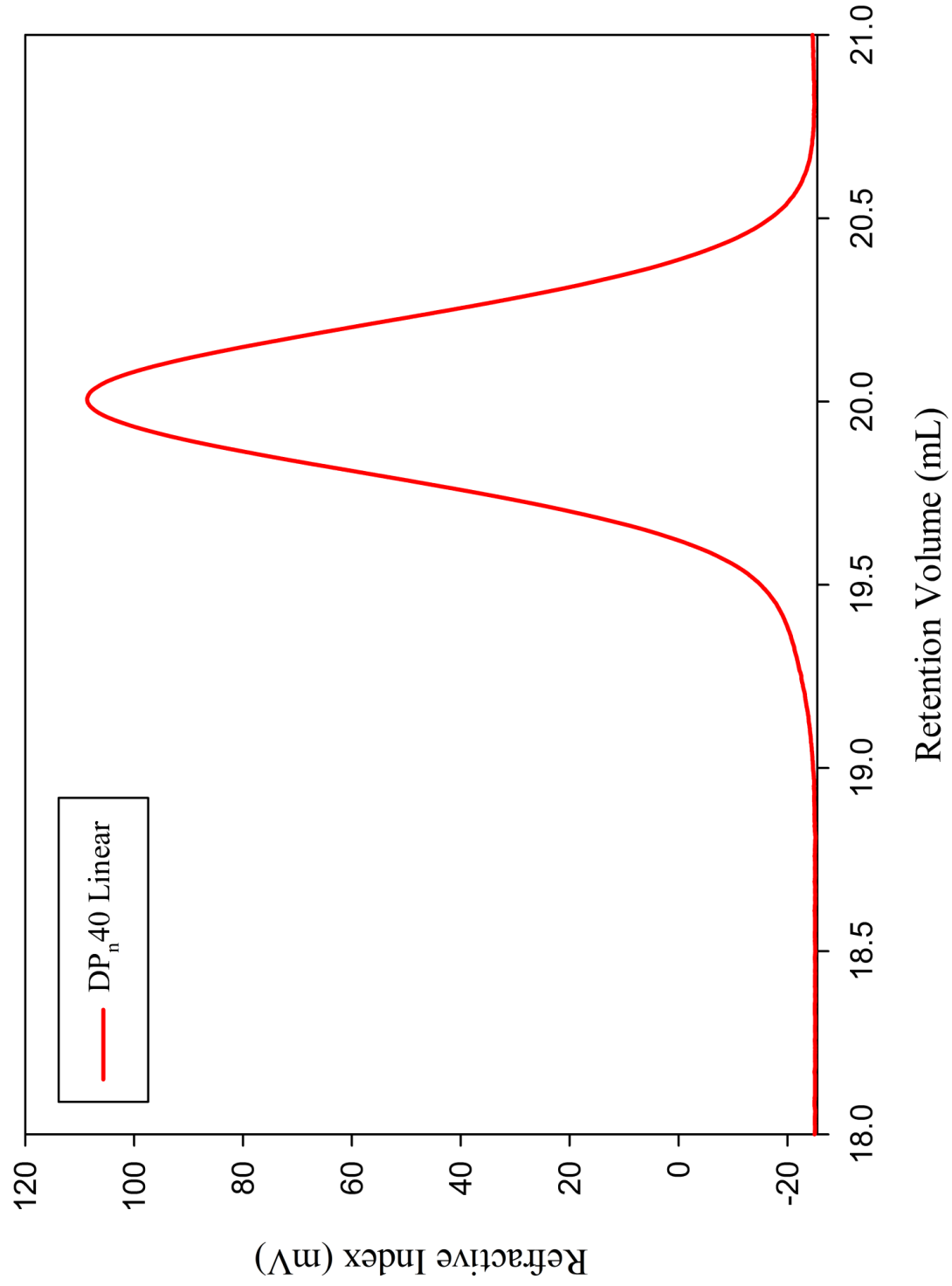

DP_n40 branched

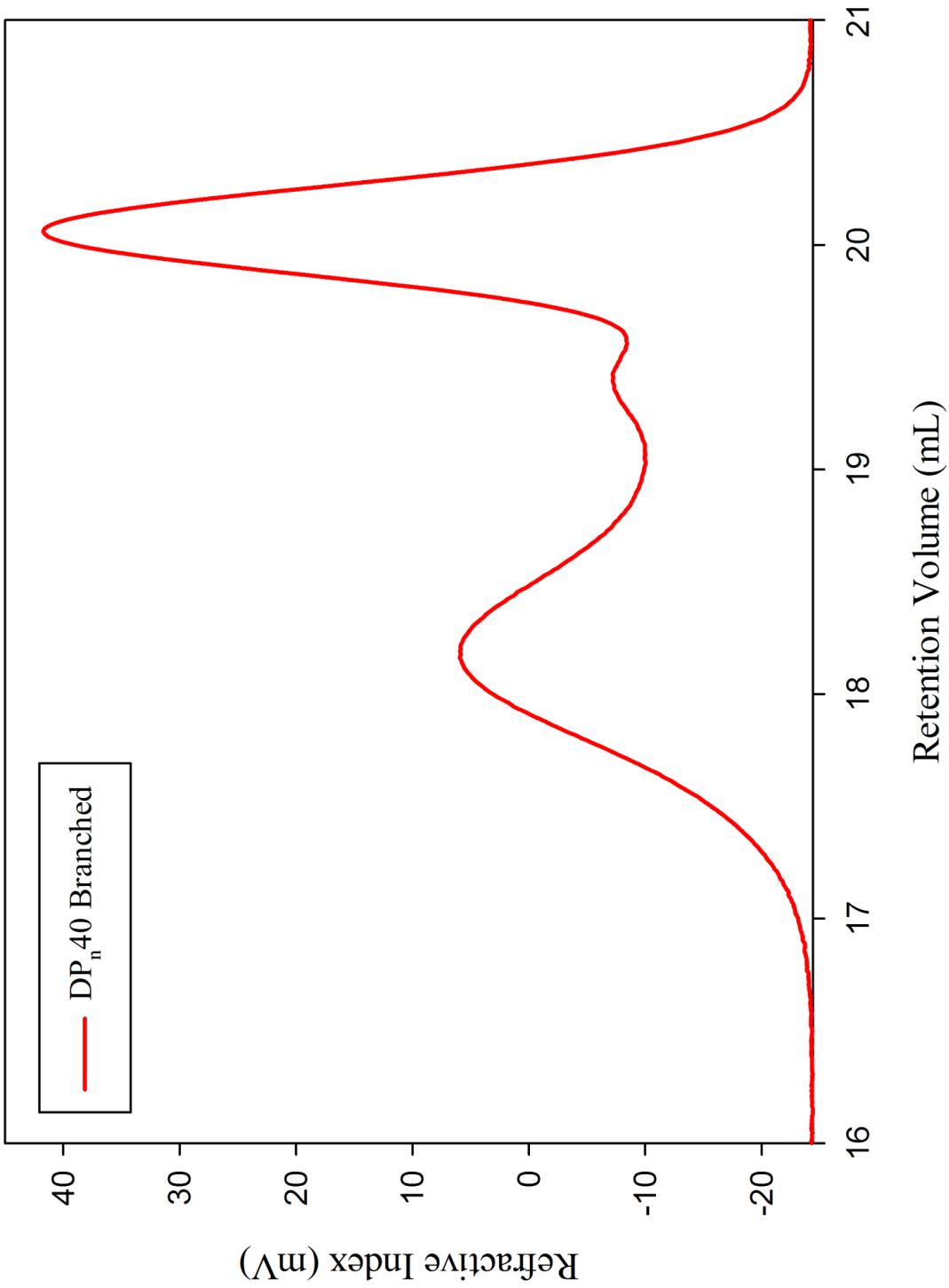

Chpater 8

Branched PS, VBC, Benzene solvent

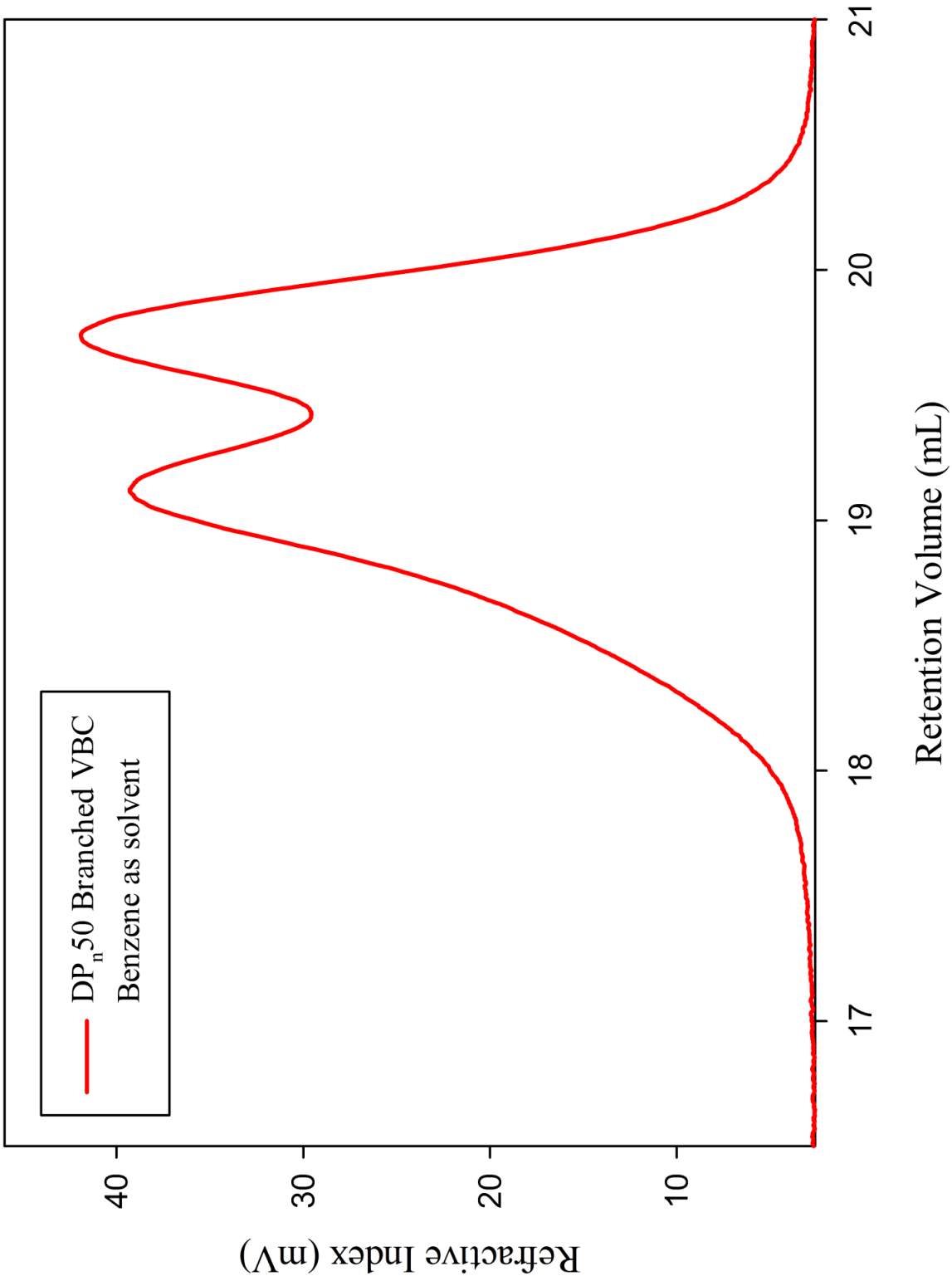

Branched PS, VBC, Benzene/THF solvent

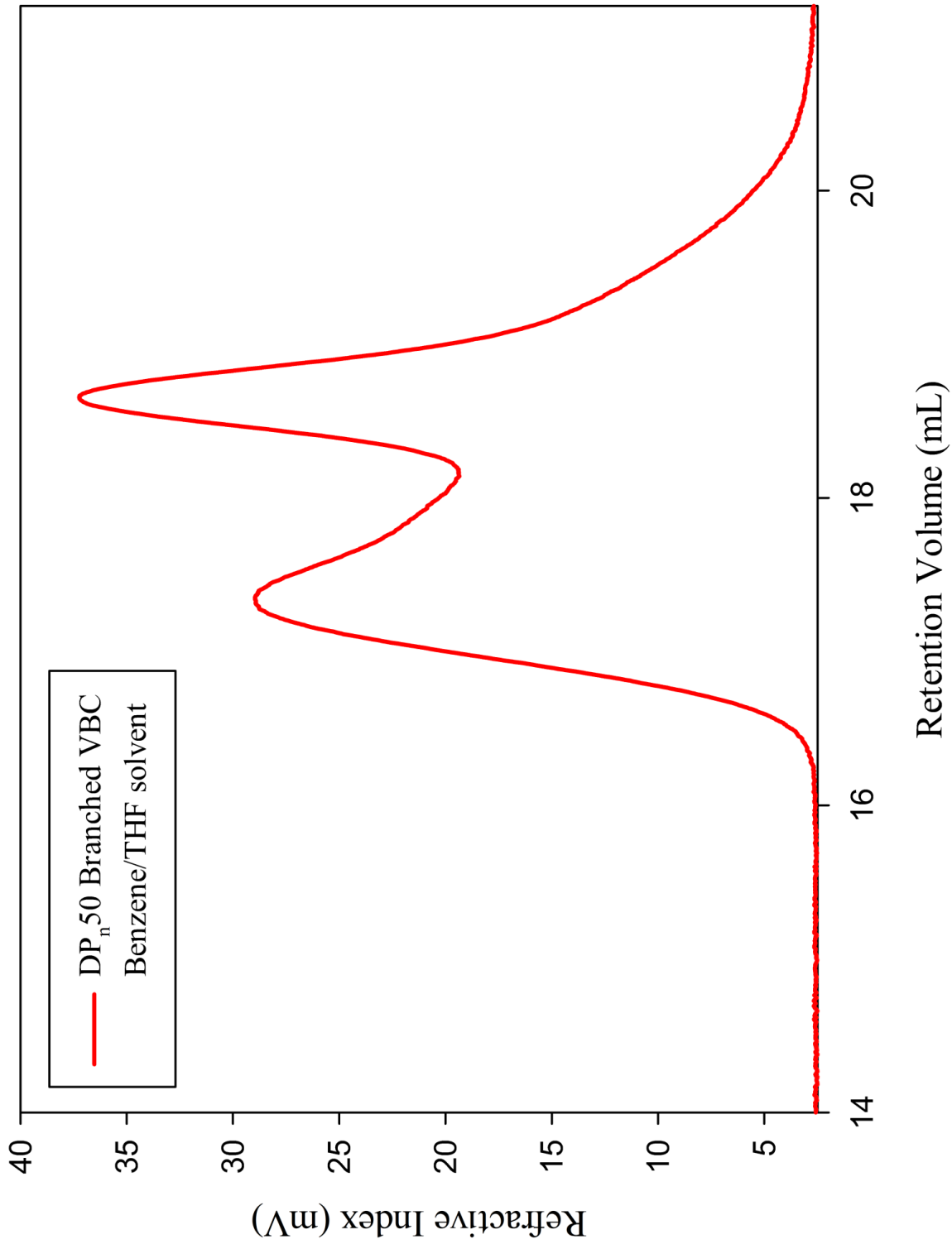

DP_n50 branched 1:0.25 a

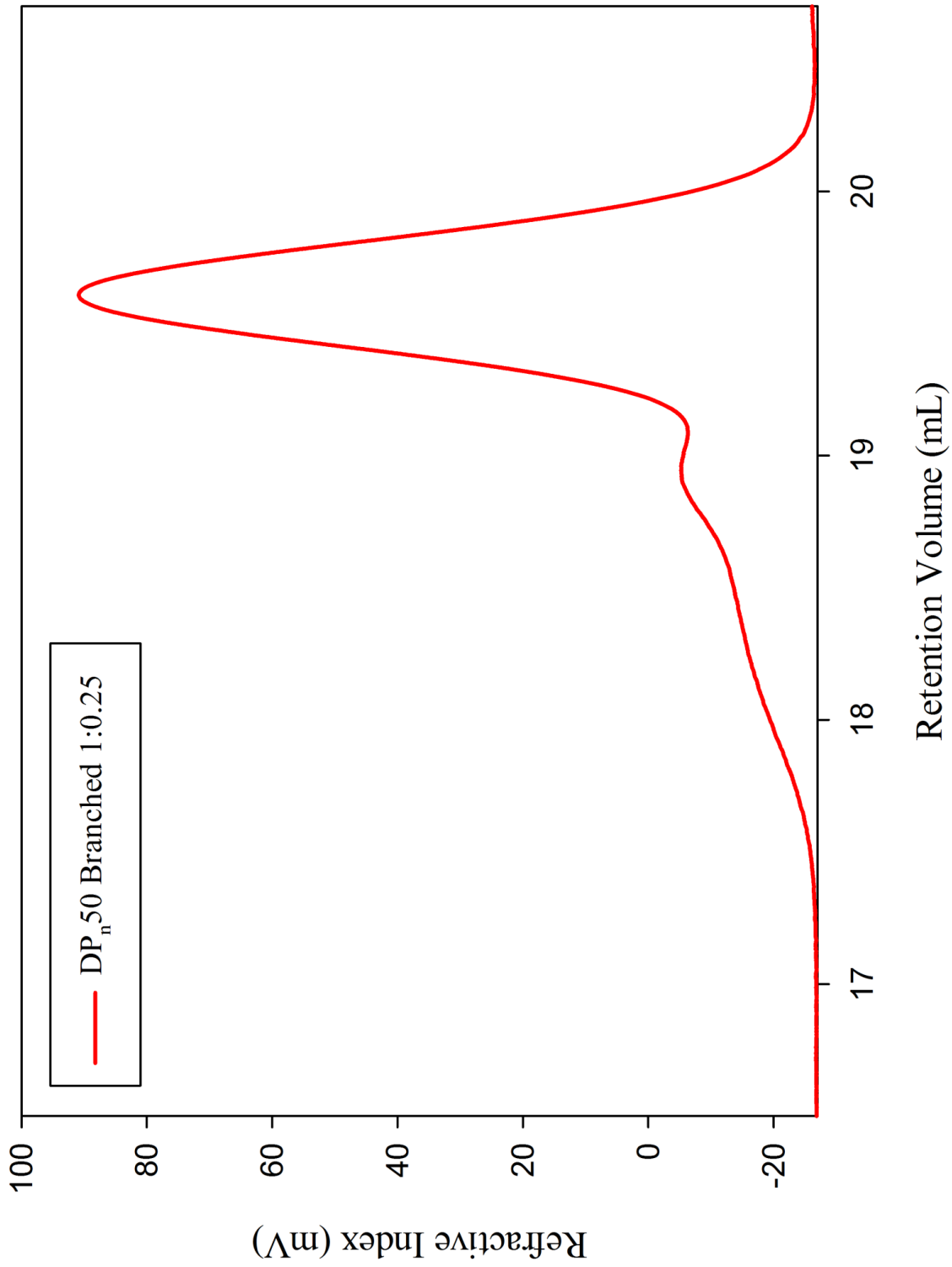

DP_n50 branched 1:0.25 plus DP_n50 1:1a

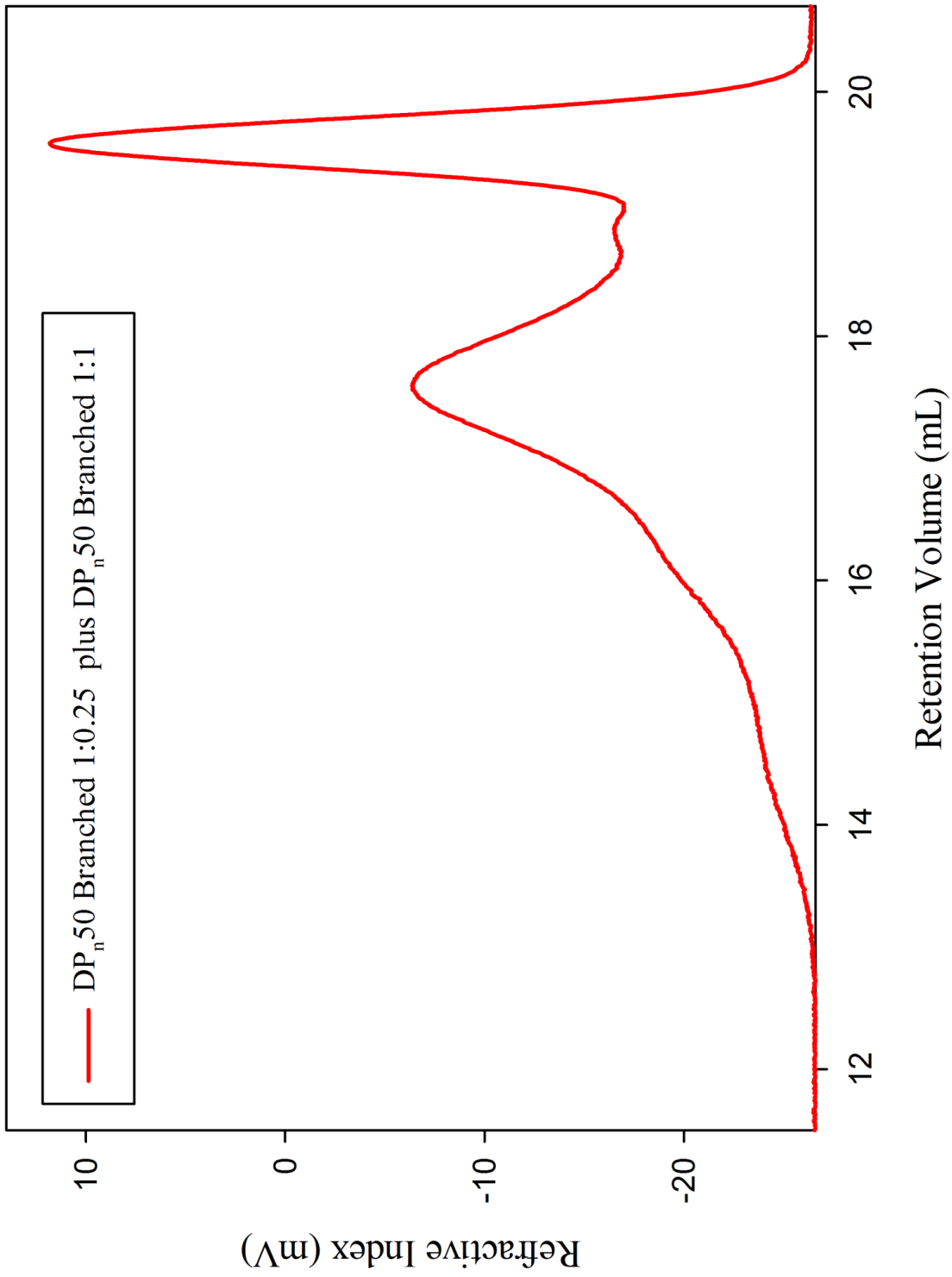

DP_n50 branched 1:0.25 plus DP_n50 branched 1:1 plus DP_n50 branched 1:0.25 a

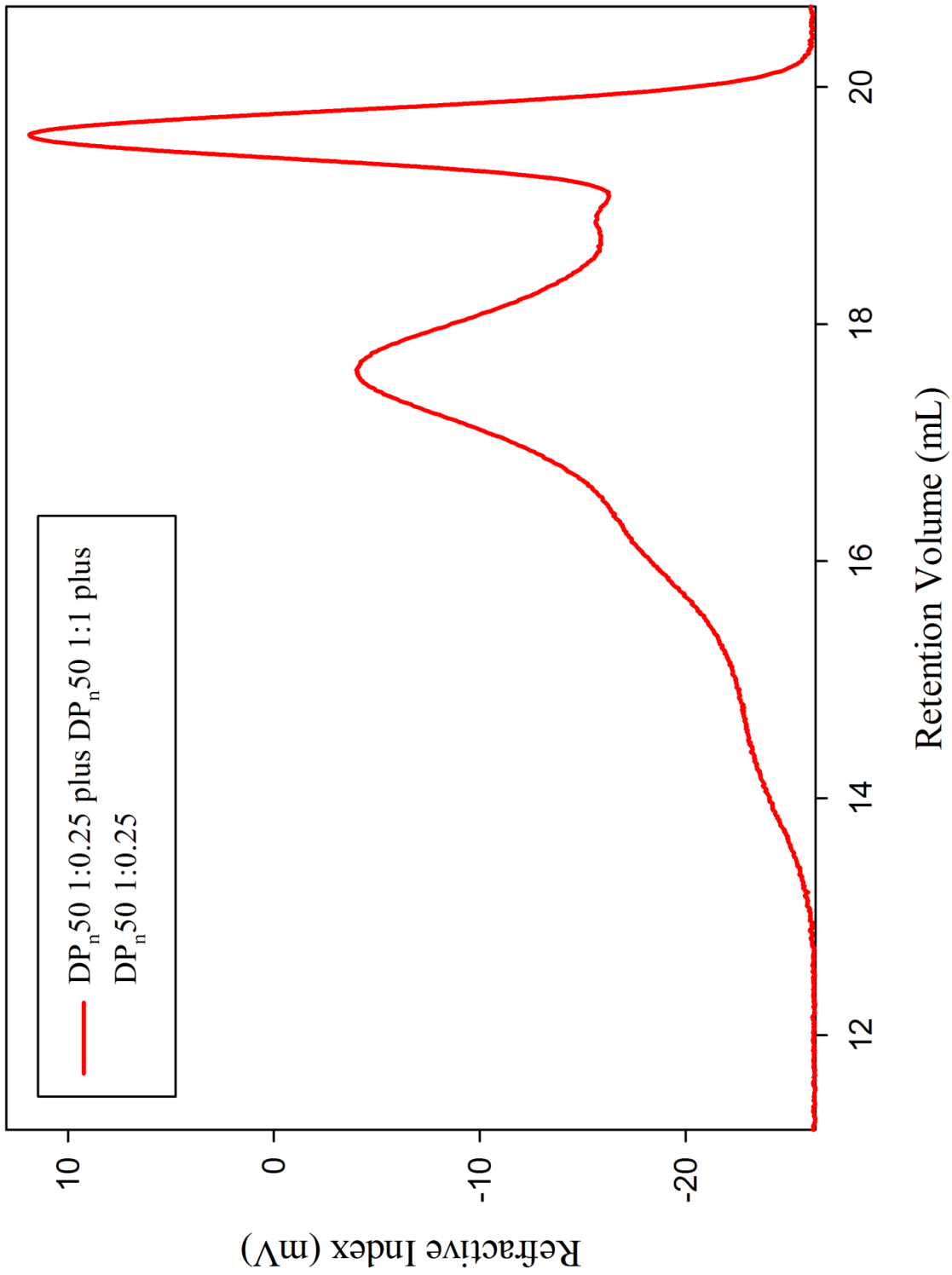

DP_n50 branched 1:0.25 b

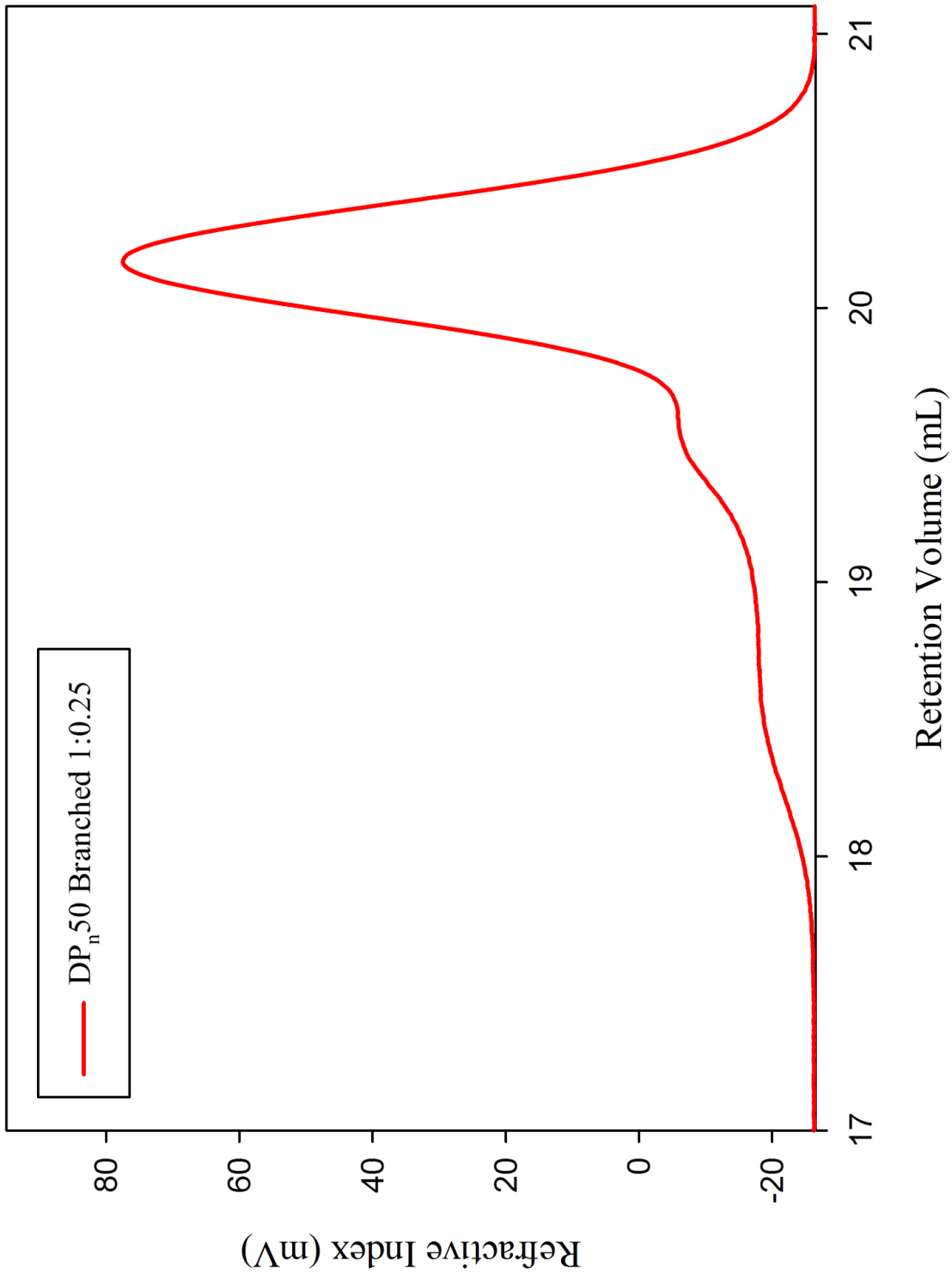

DP_n50 branched 1:0.25 plus DPn50 branched 1:1 b

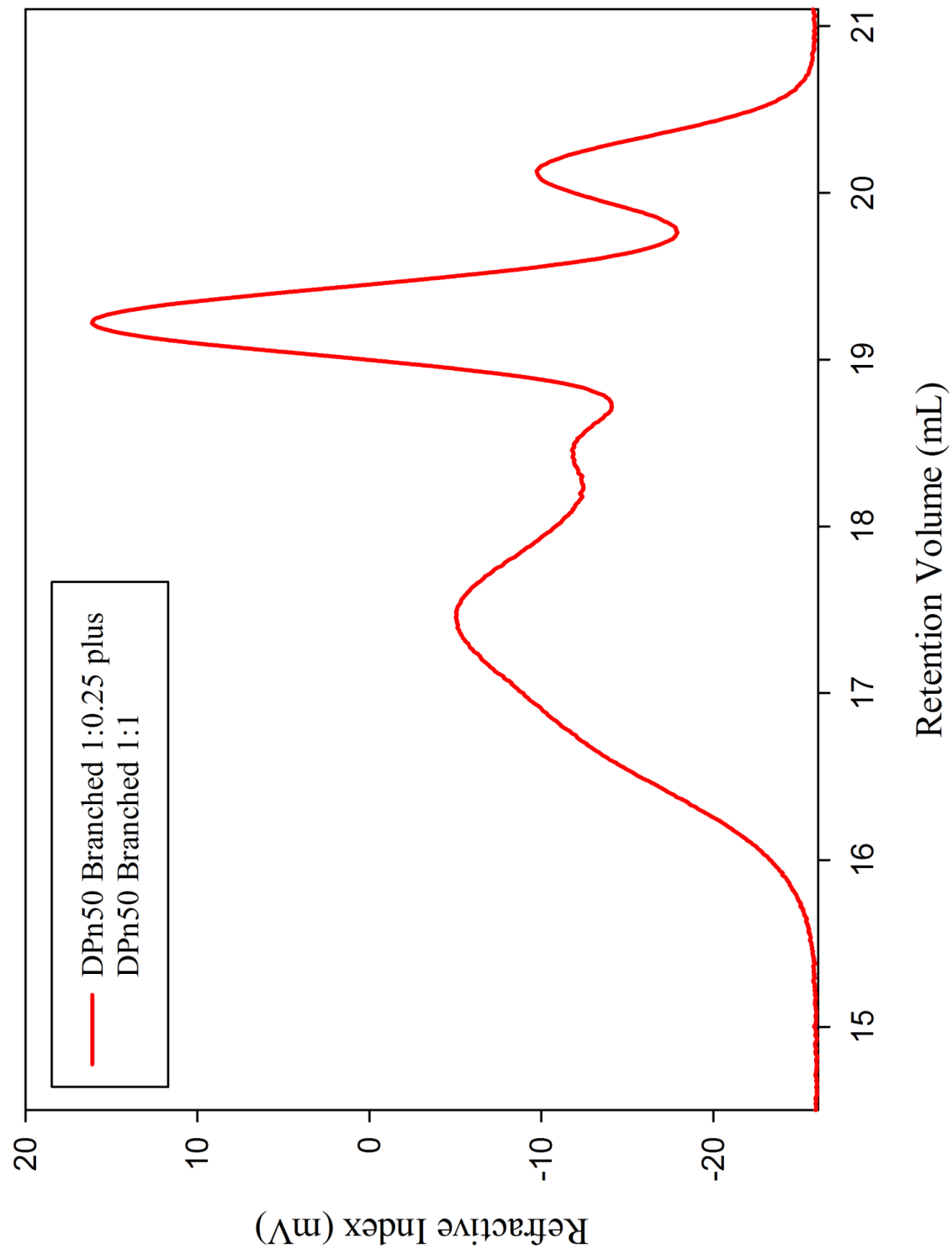

DP_n50 branched 1:0.25 plus DP_n50 branched 1:1 plus DP_n50 branched 1:0.25 b

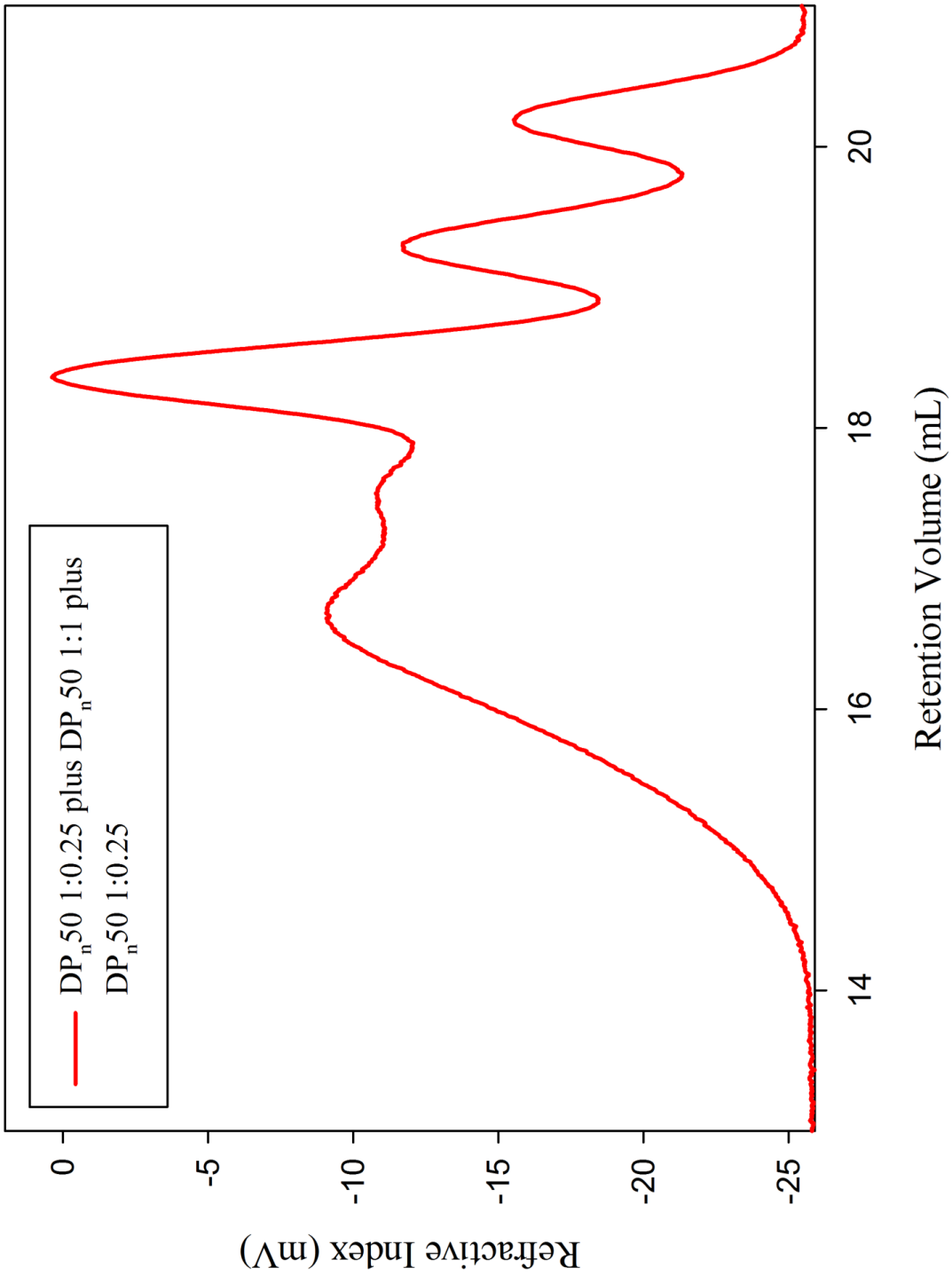

DP_n50 branched 1:1 (pre addition)

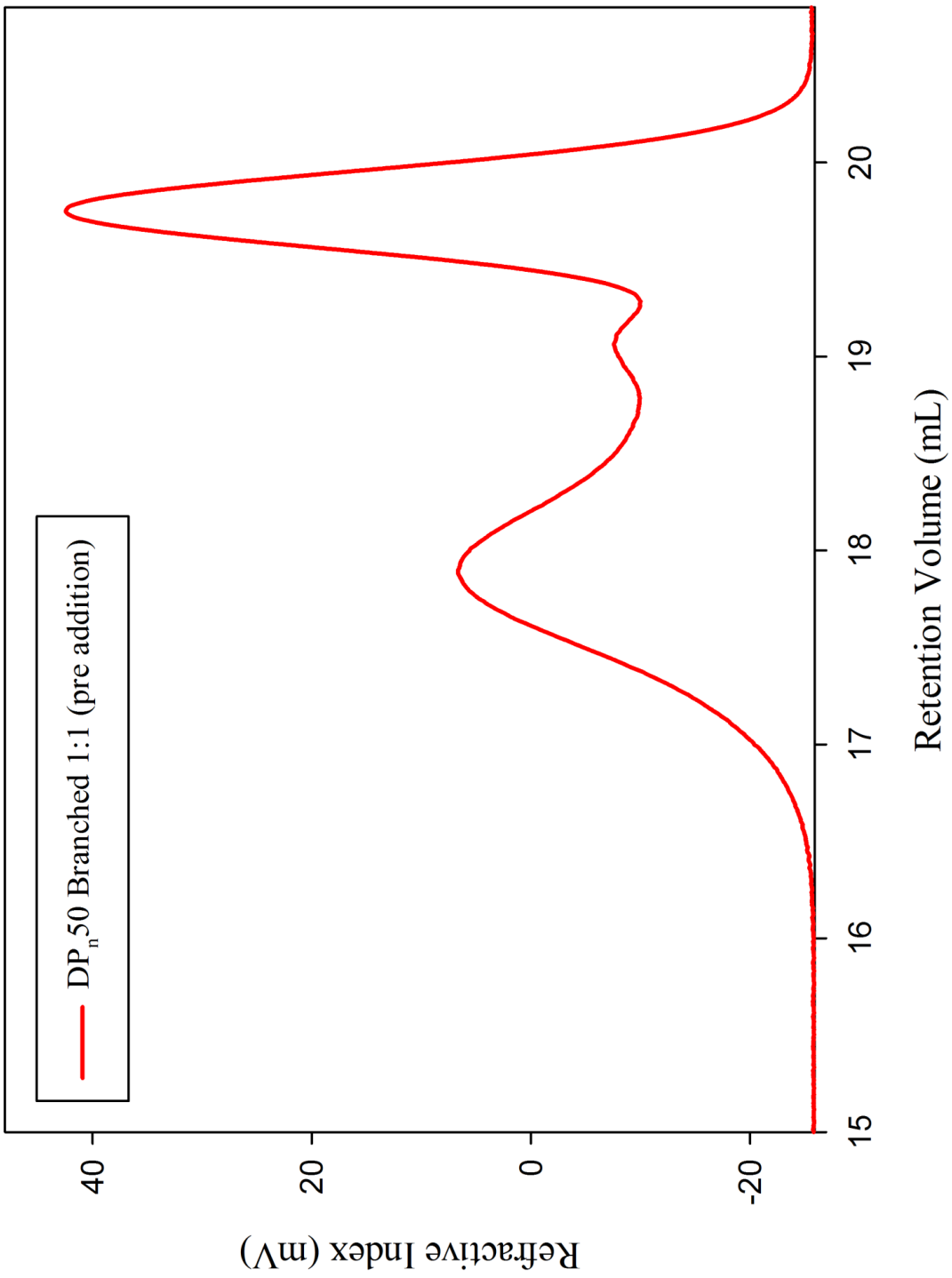

DP_n50 branched 1:1 plus DP_n50 branched 1:0.5

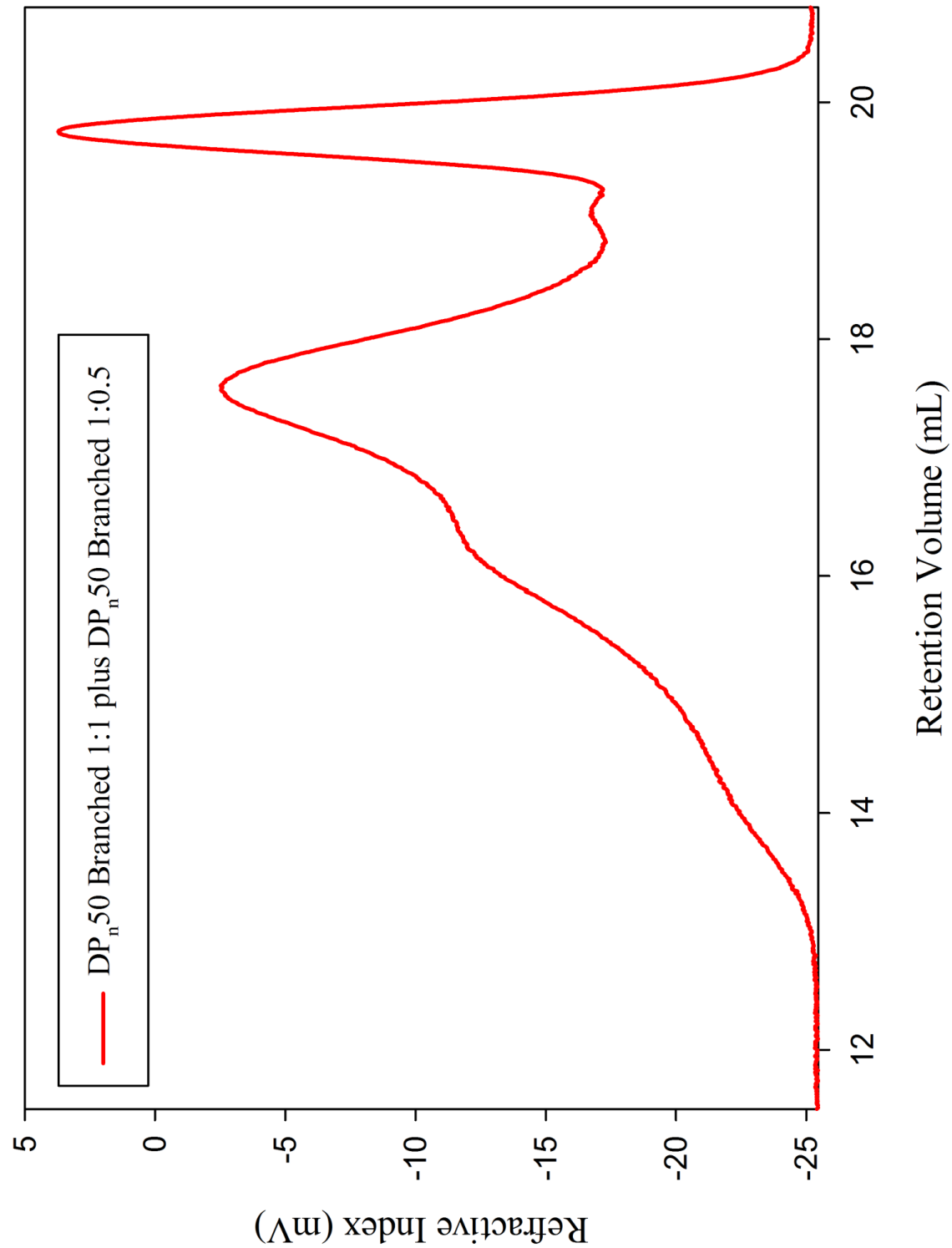

Appendix 2

DSC Thermograms

Chapter 6

6.3.1 T_g of linear polystyrenes

DP_n10 Linear

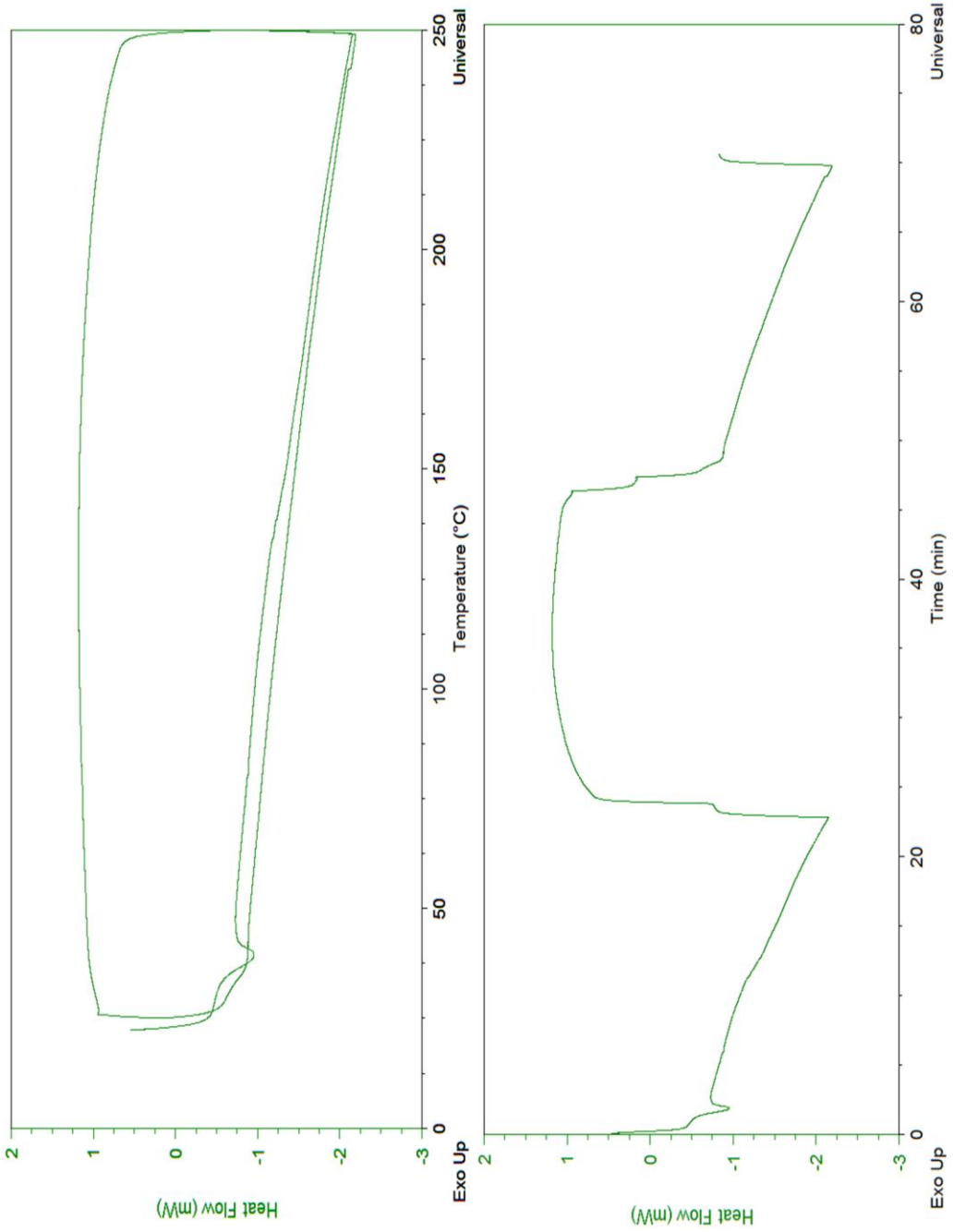

DP_n25 Linear

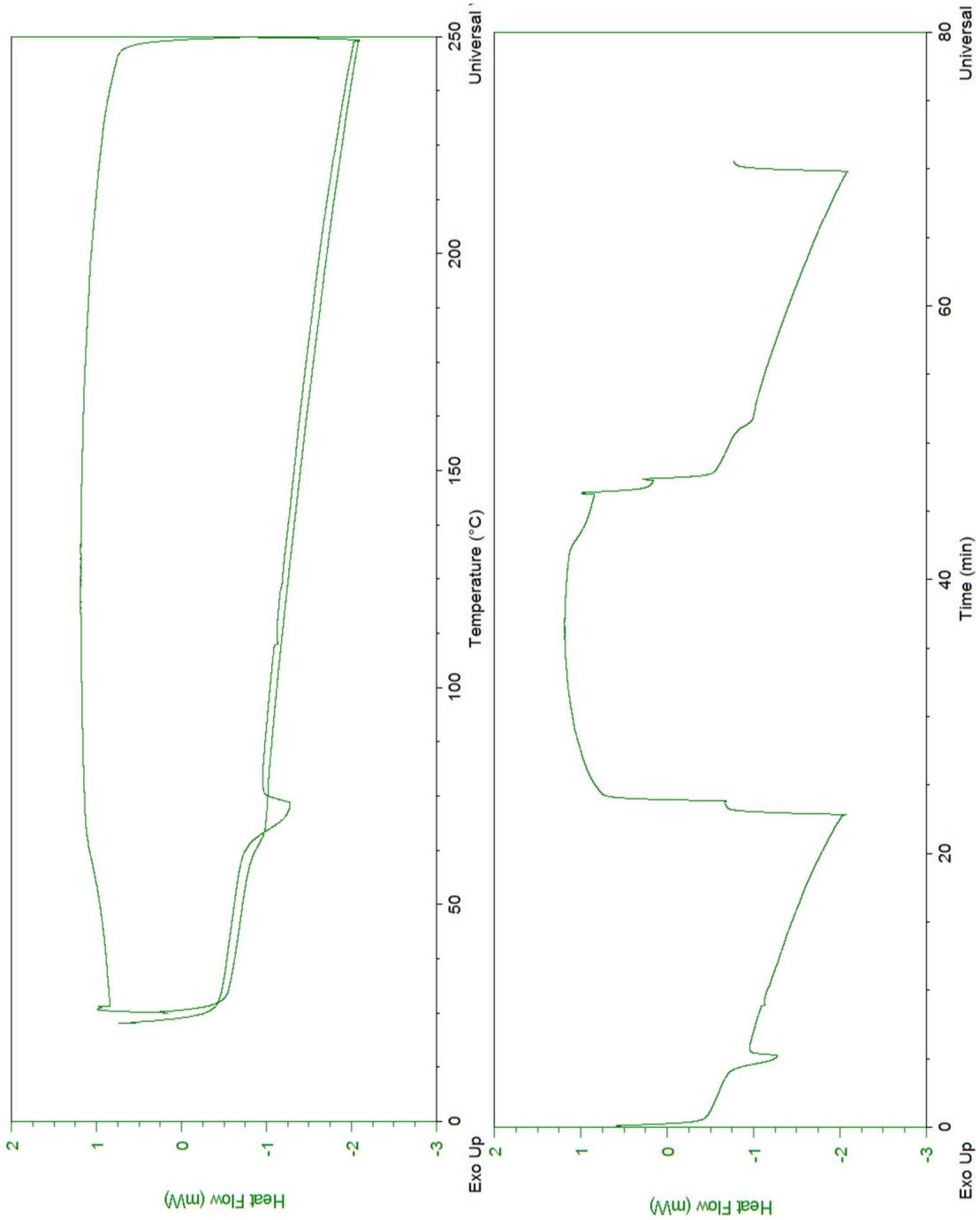

DP_n50 Linear

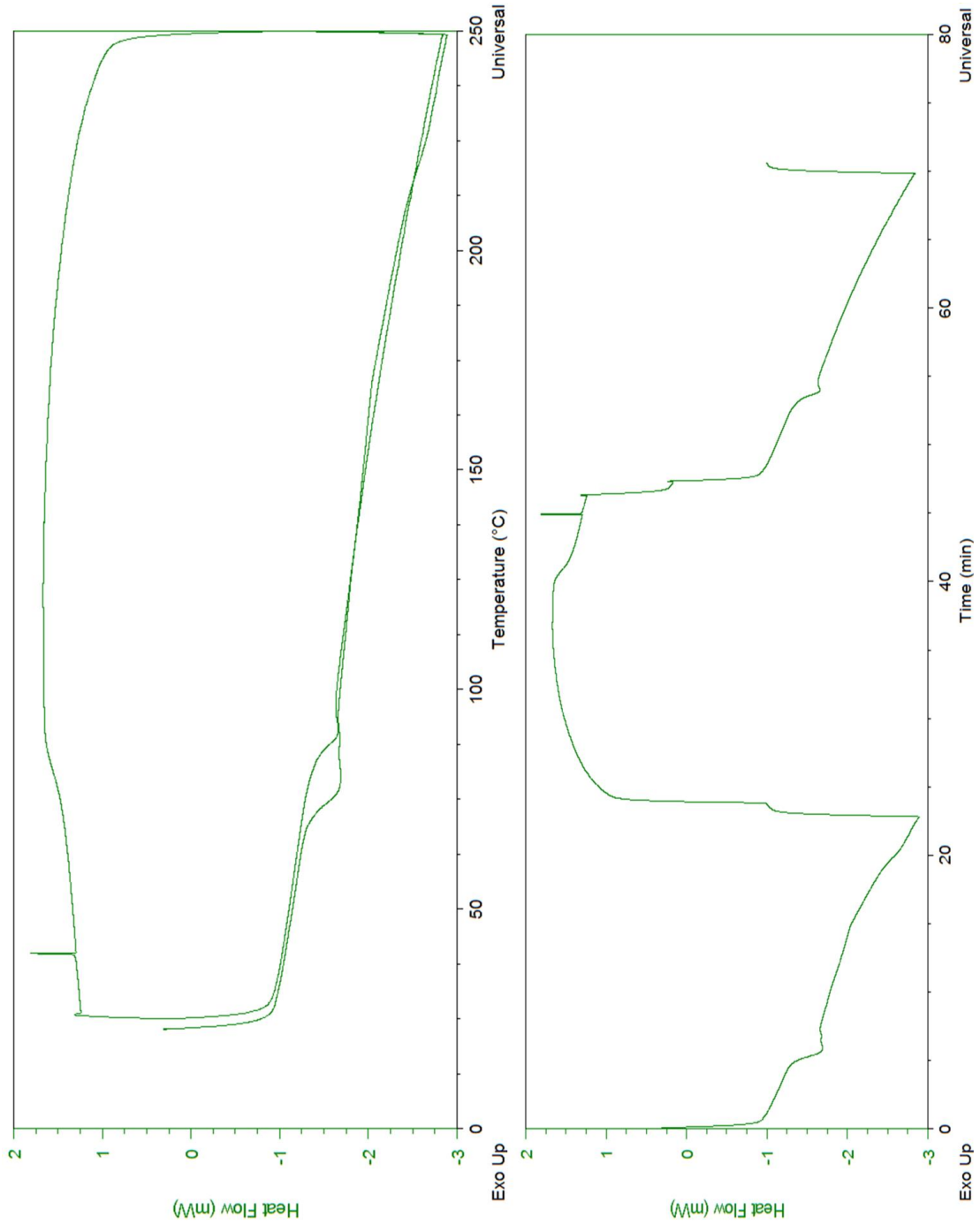

DP_n100 Linear

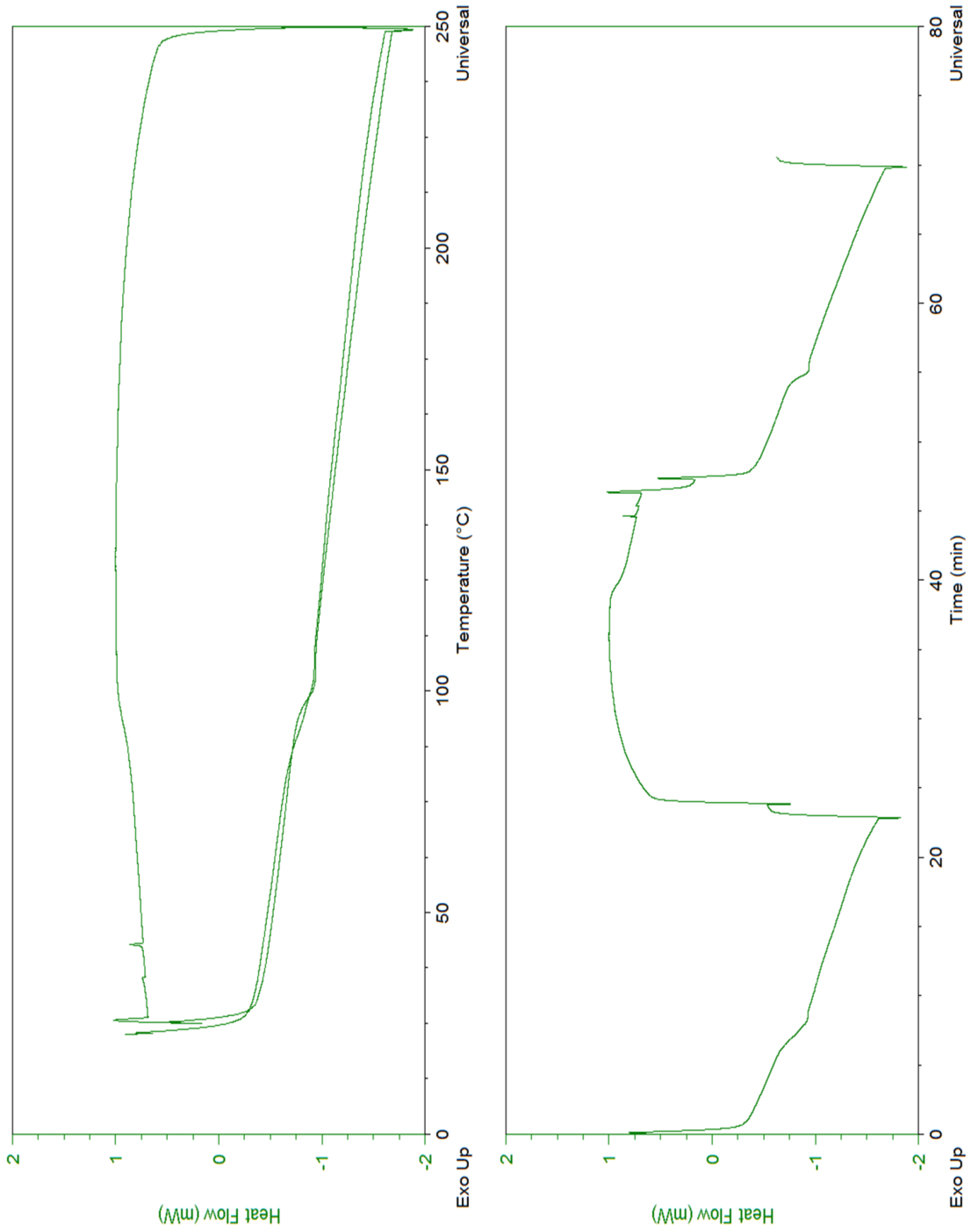

DP_n 500 Linear

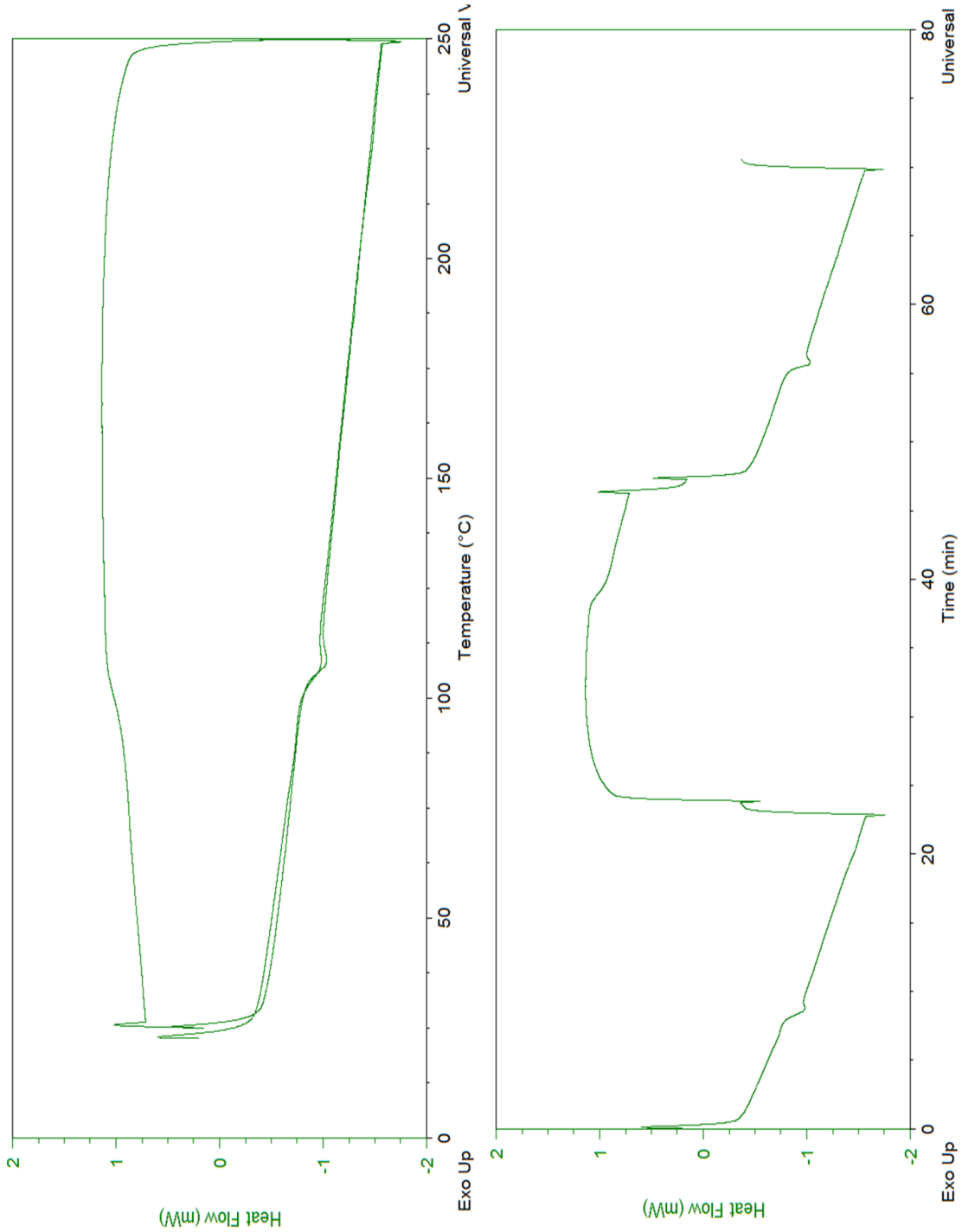

DP_n 10 Branched

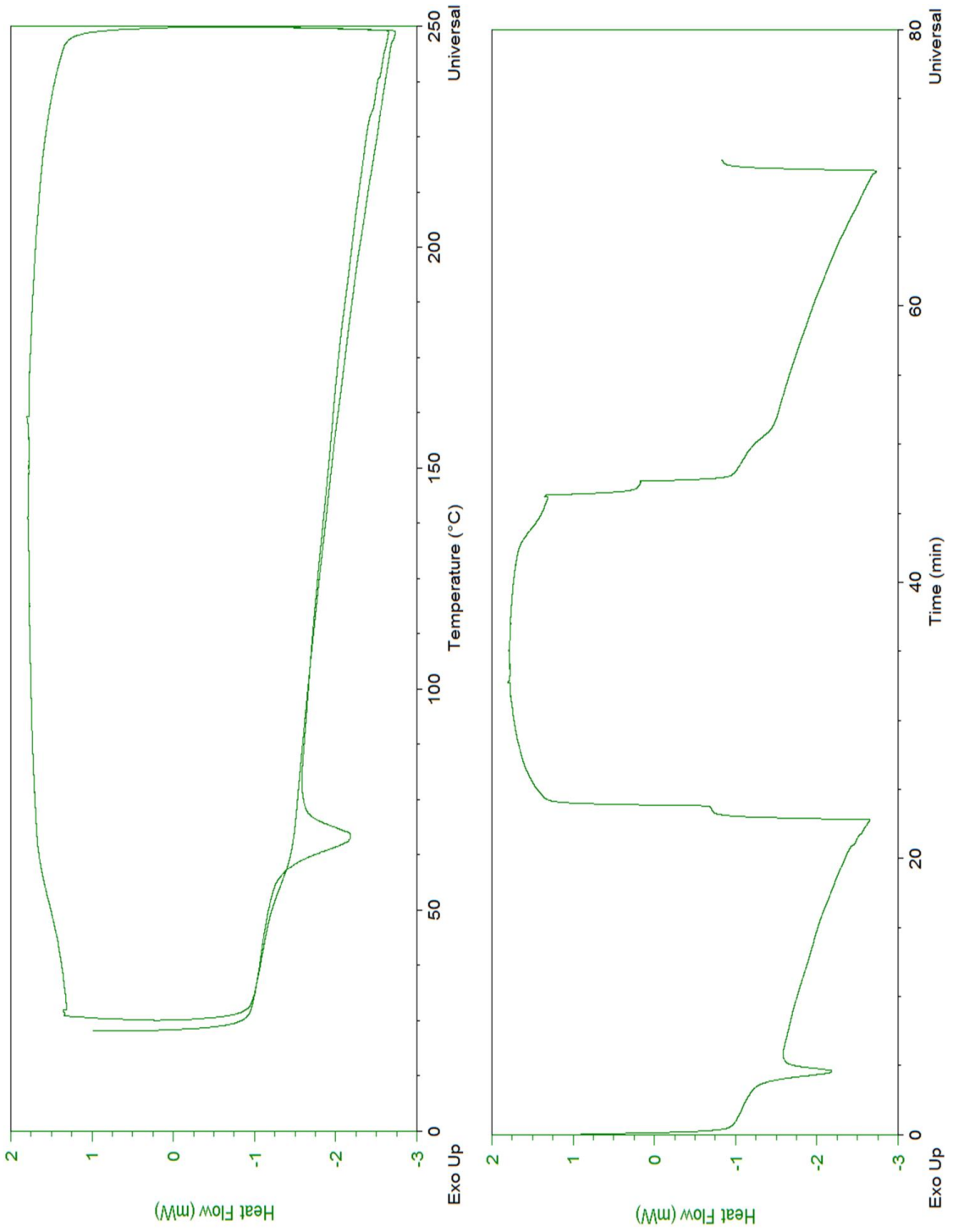

DP_n25 Branched

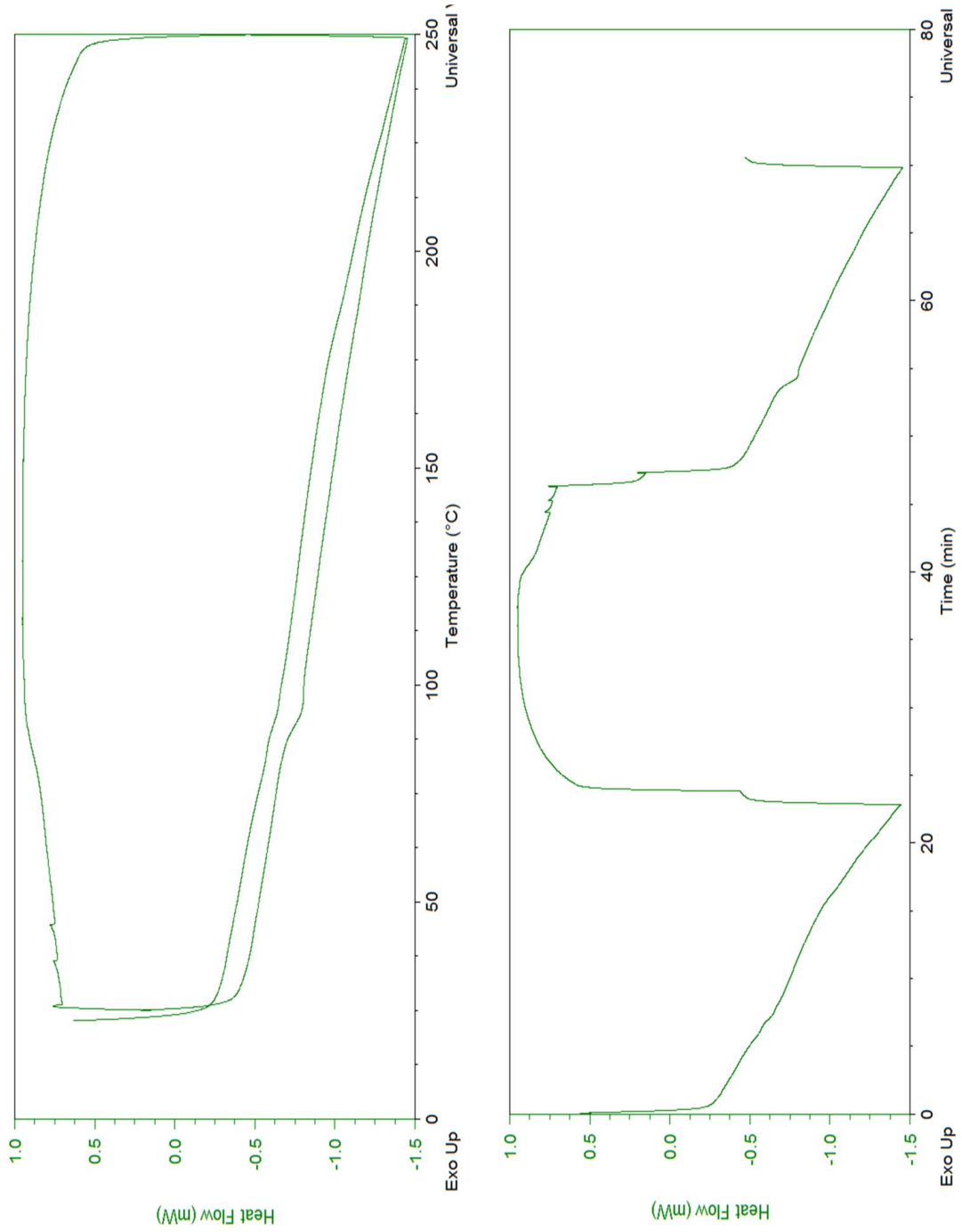

DP_n100 Branched

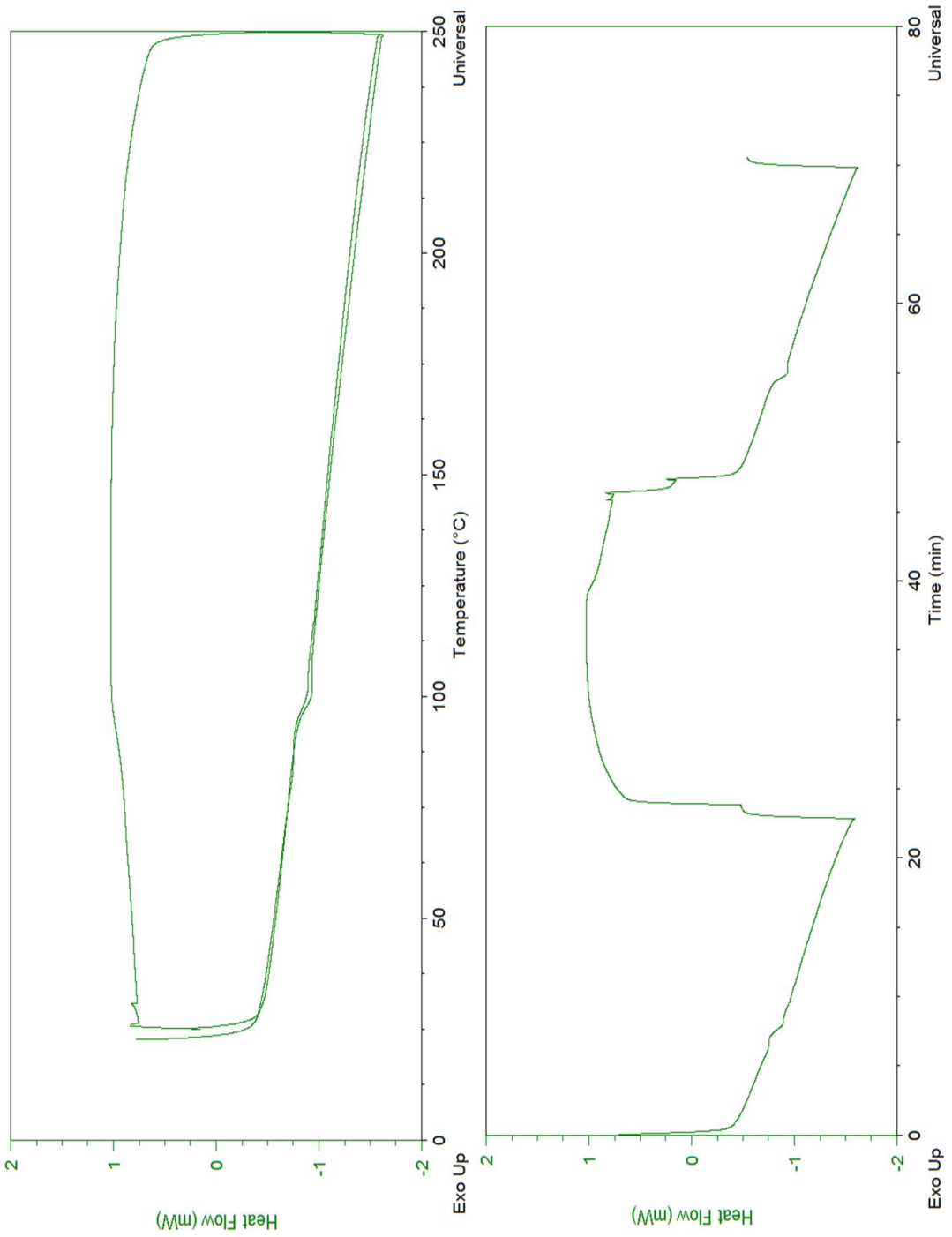

DP_n250 Branched

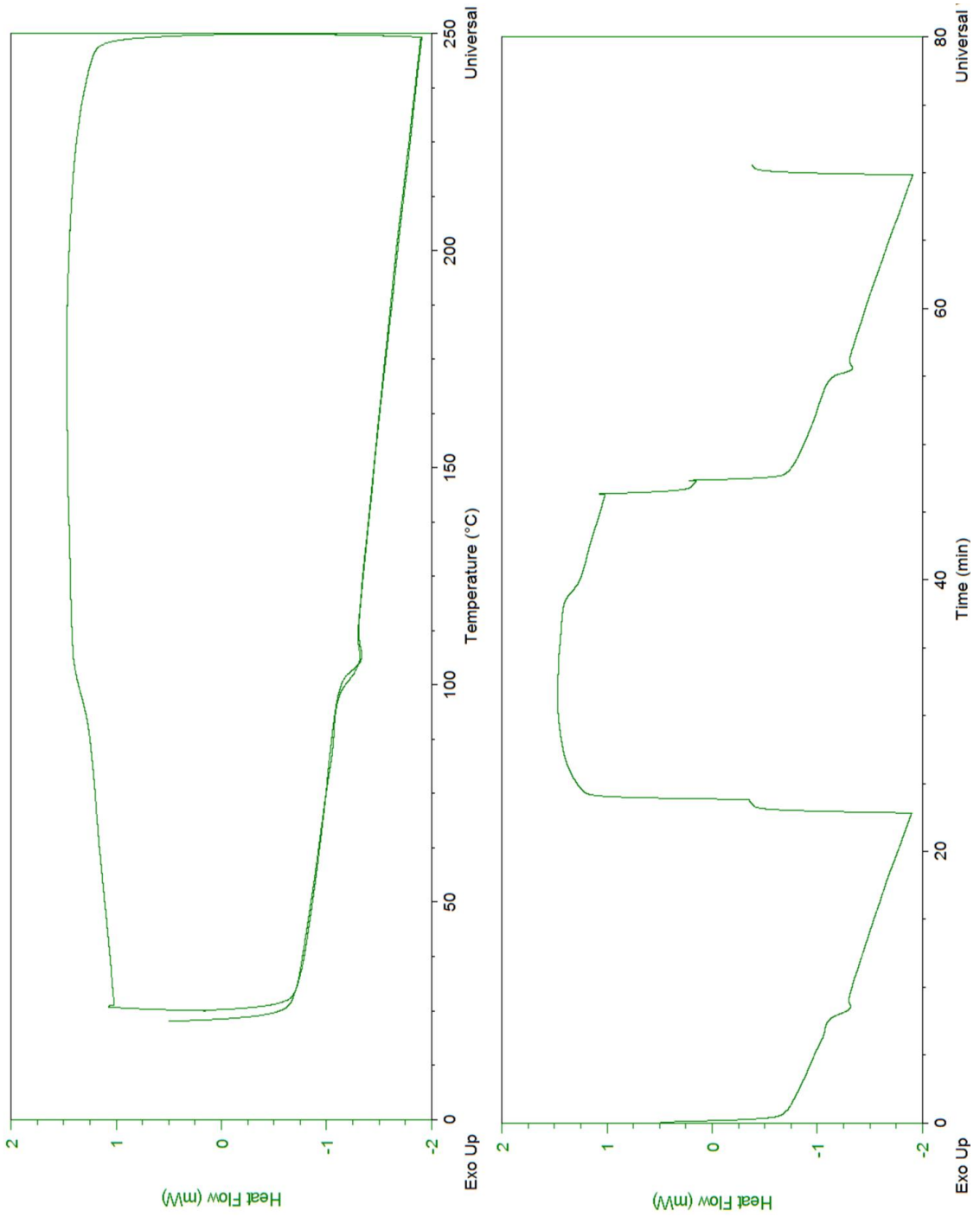

DP_n500 Branched

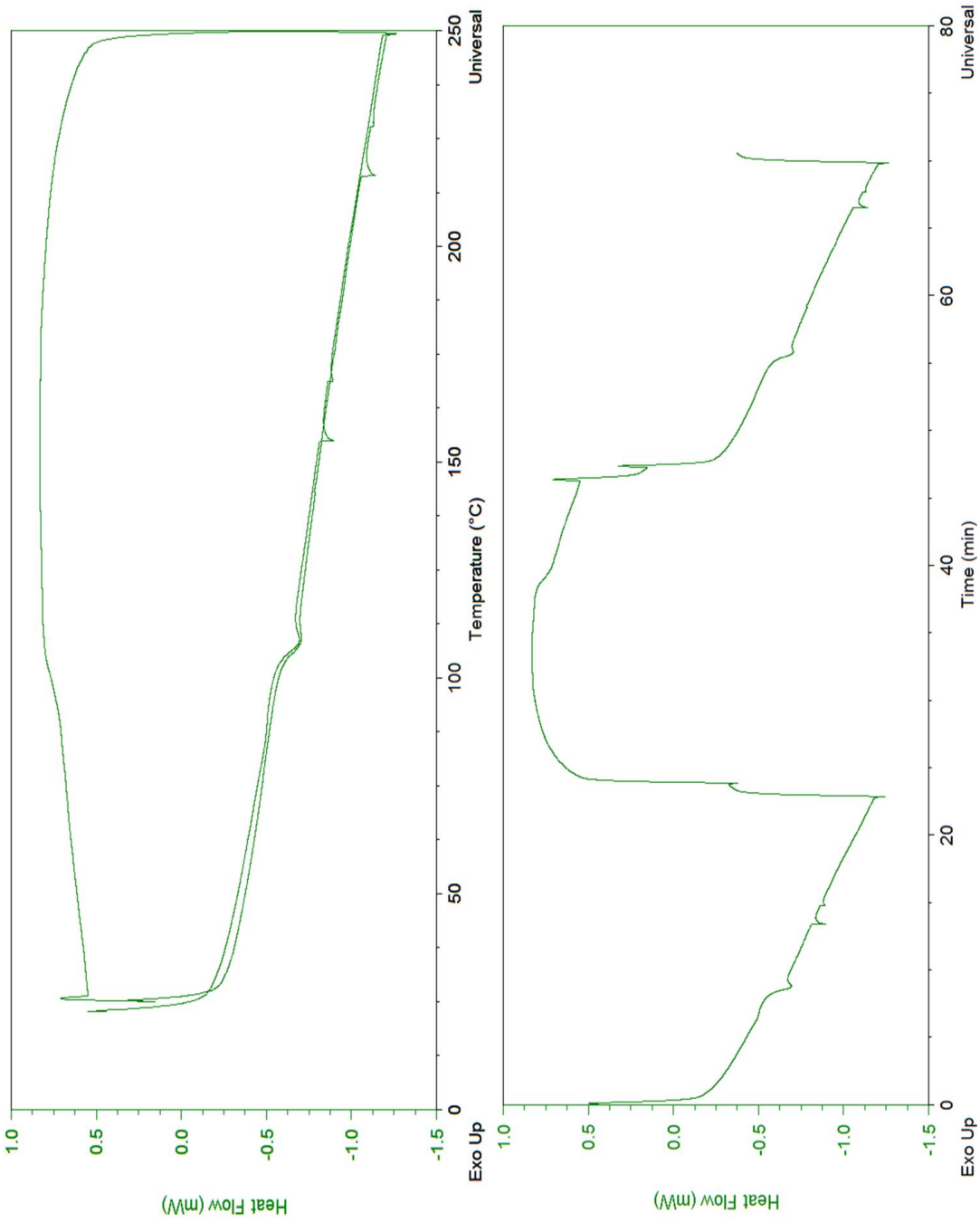

6.3.3 Effect of polymer architecture on T_g

DP_n10 branched plus DP_n90 linear

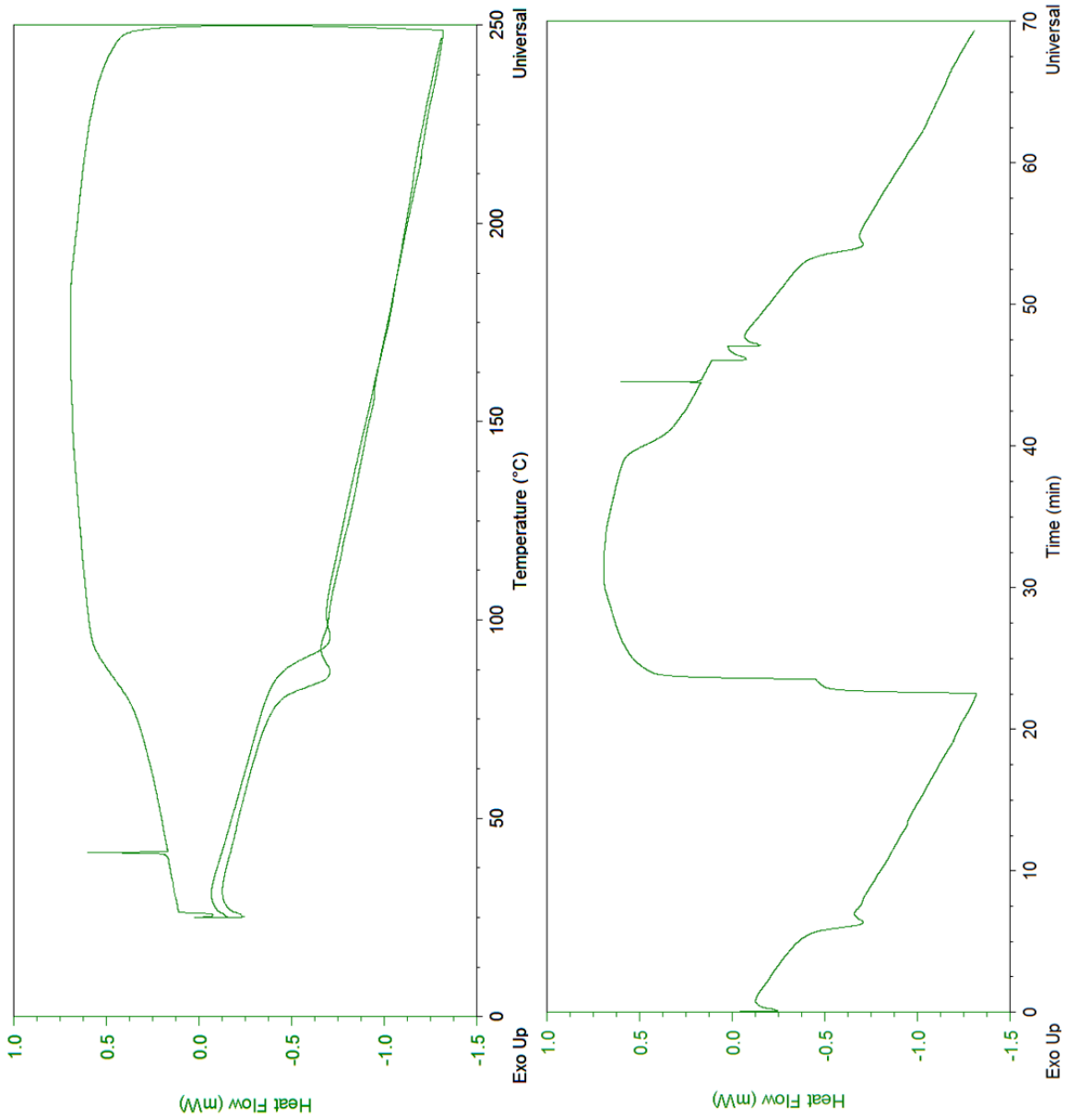

DP_n90 linear plus DP_n10 branched

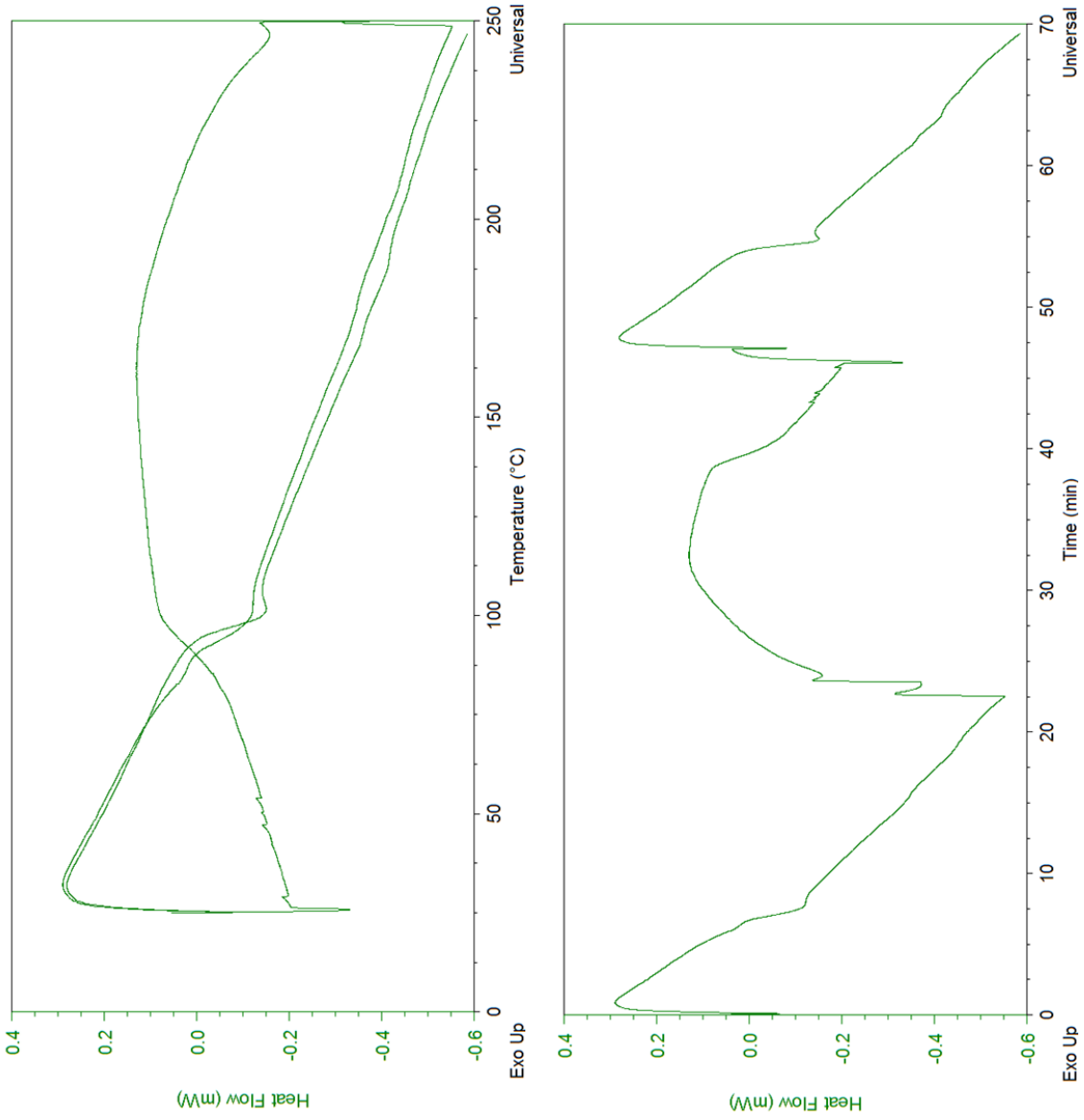

DP_n10 linear plus DP_n90 branched

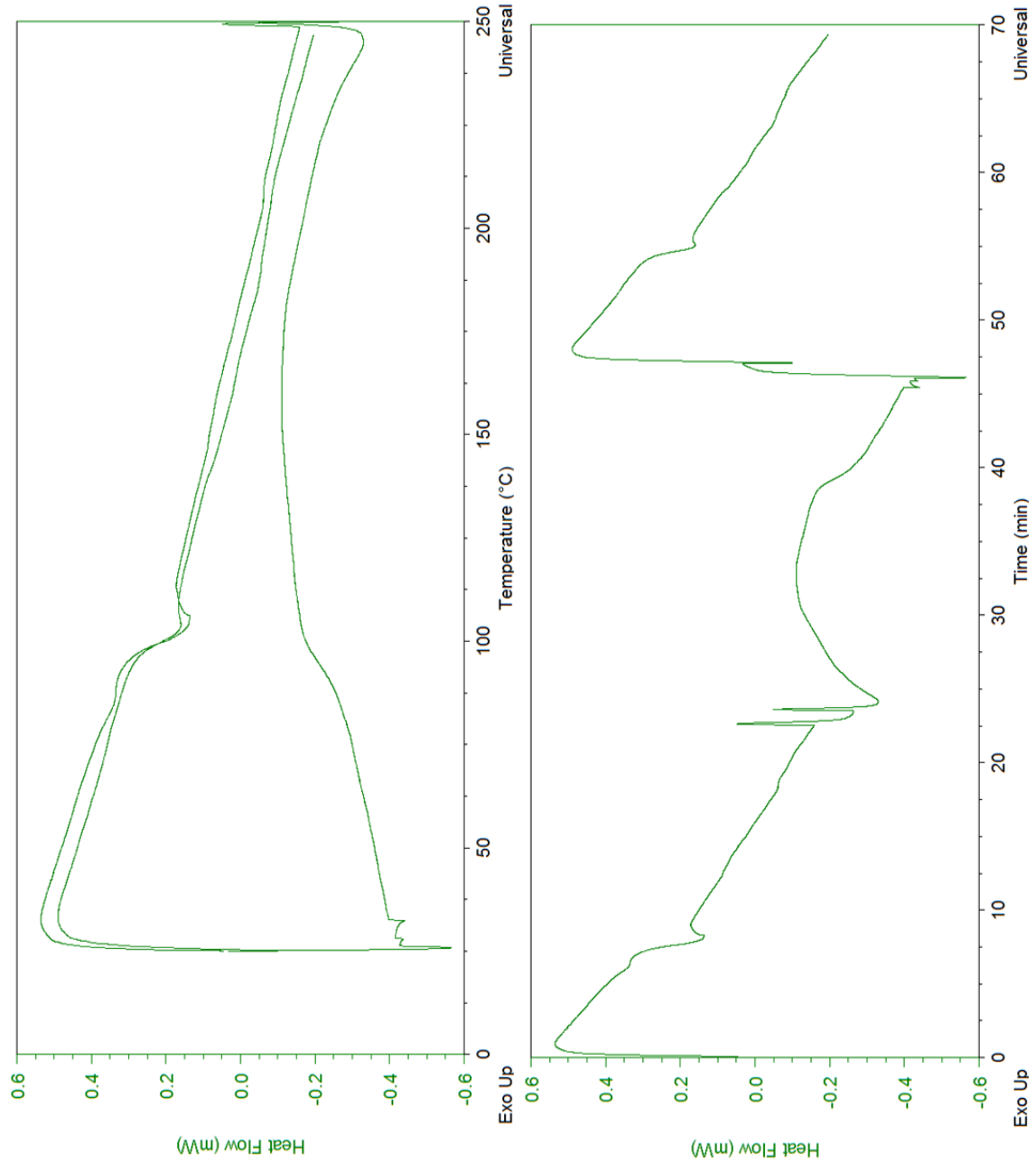

DP_n90 branched plus DP_n10 linear

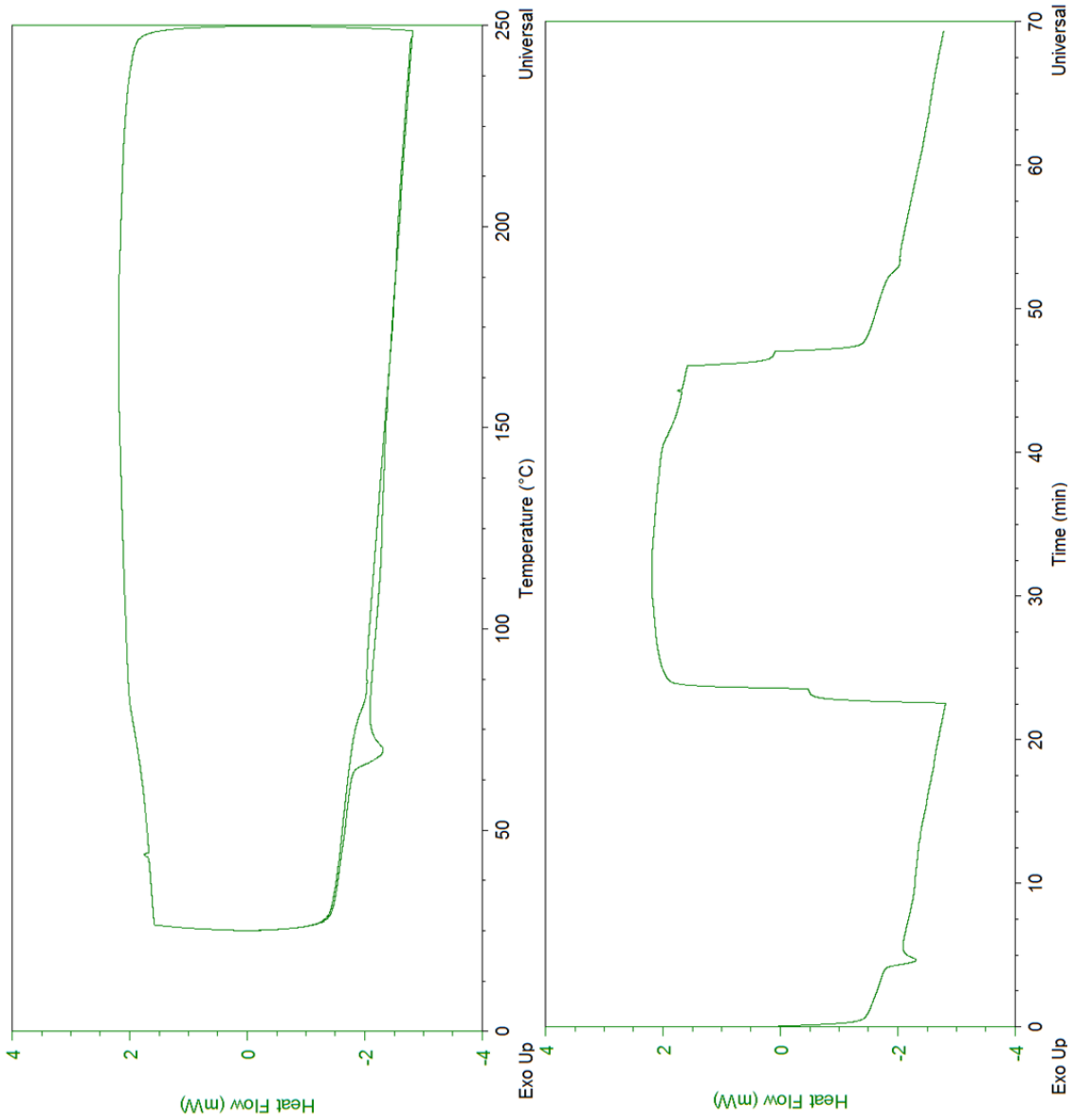

DP_n50 linear plus DP_n50 branched

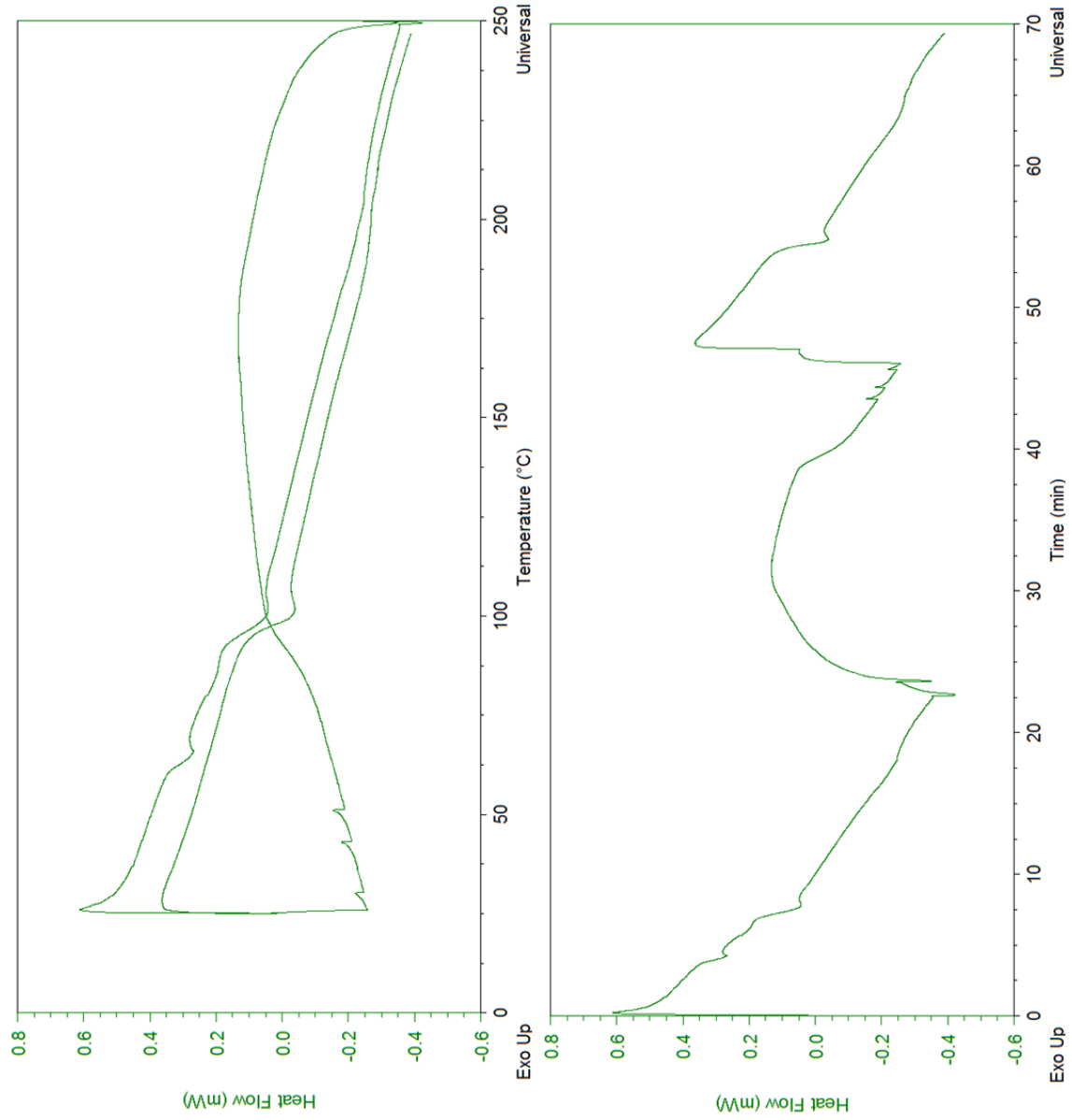

DP_n50 branched plus DP_n50 linear

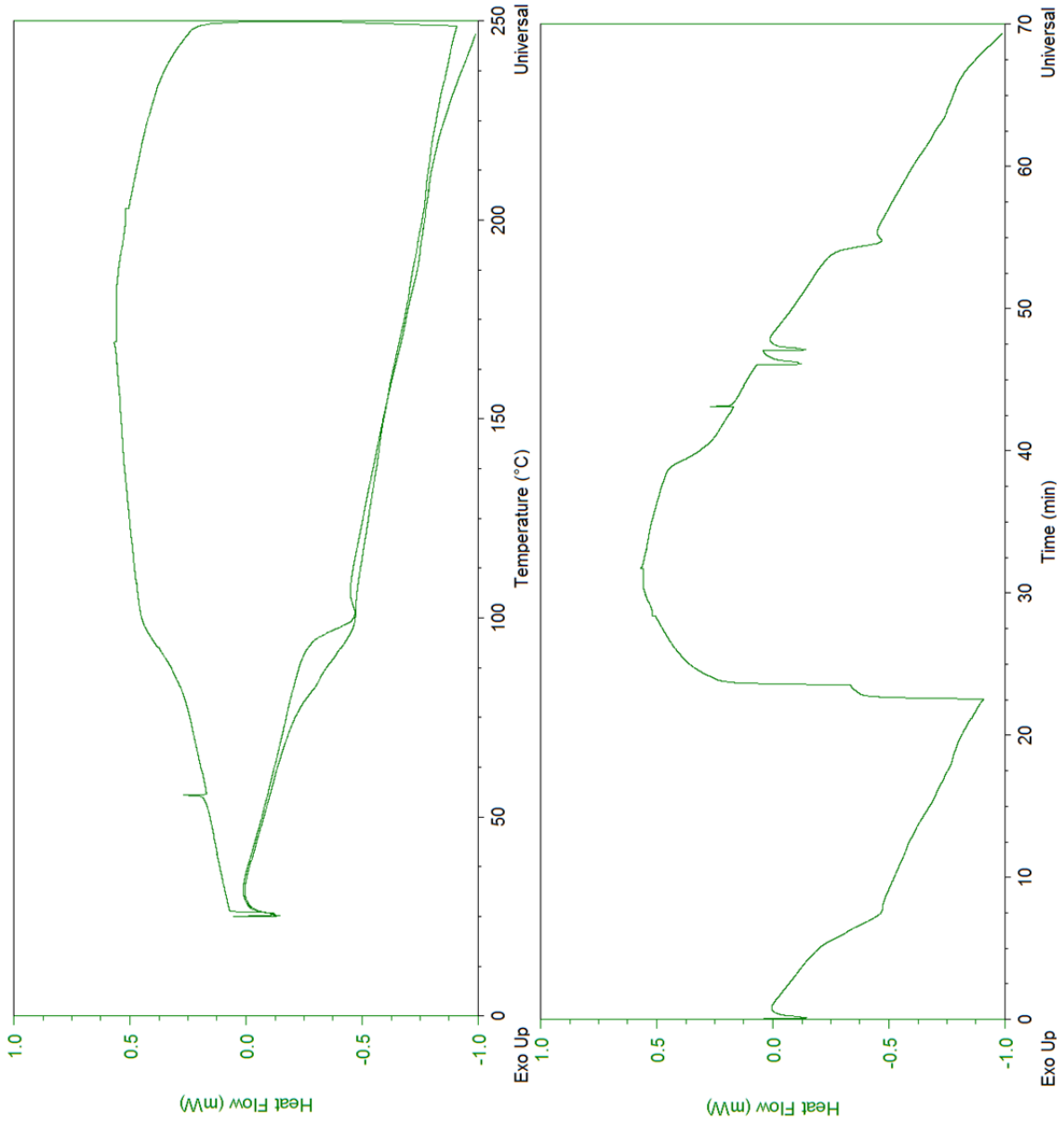

DP_n10 branched plus DP_n40 linear

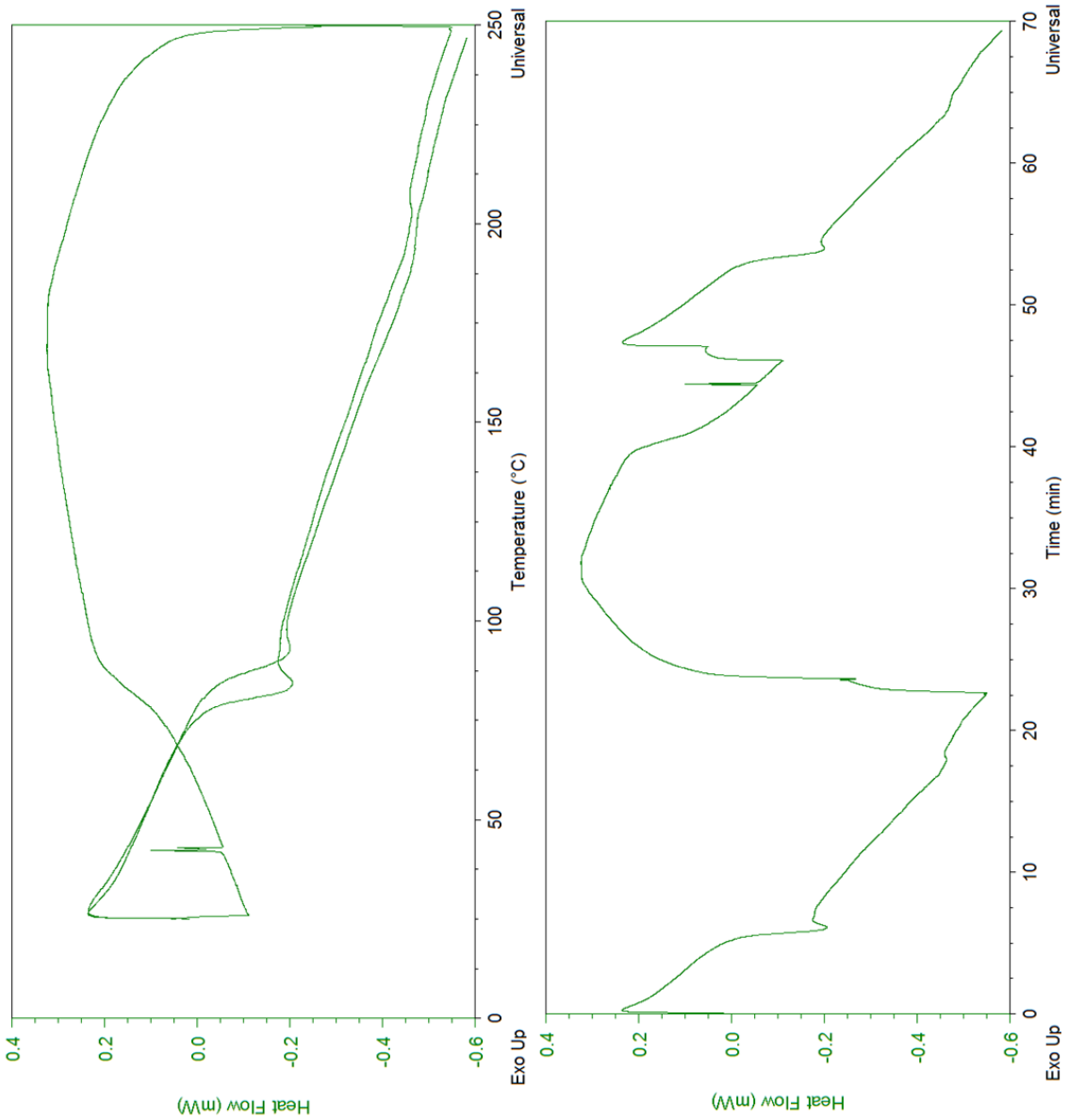

DP_n40 linear plus DP_n10 branched

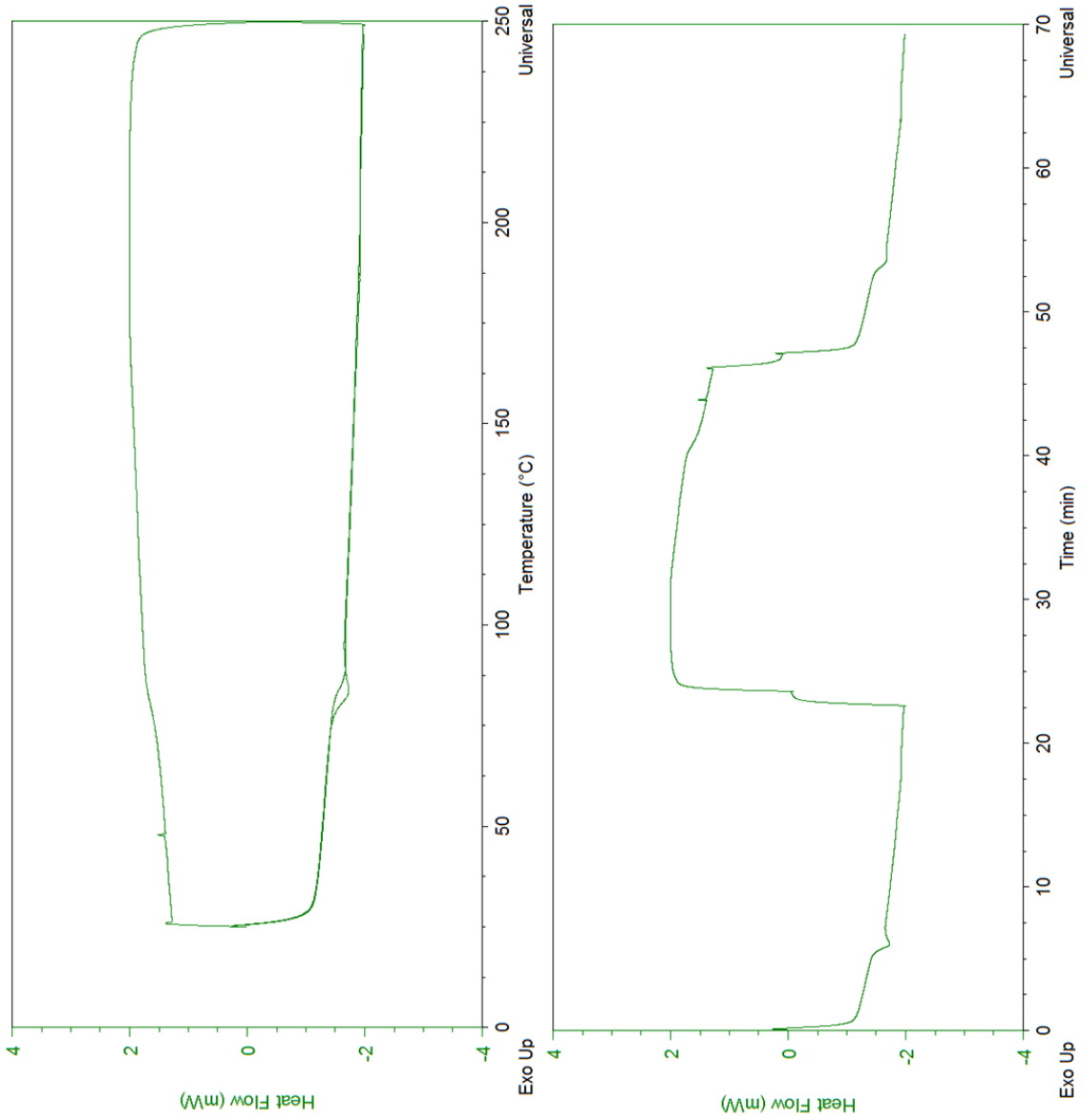

DP_n10 linear plus DP_n40 branched

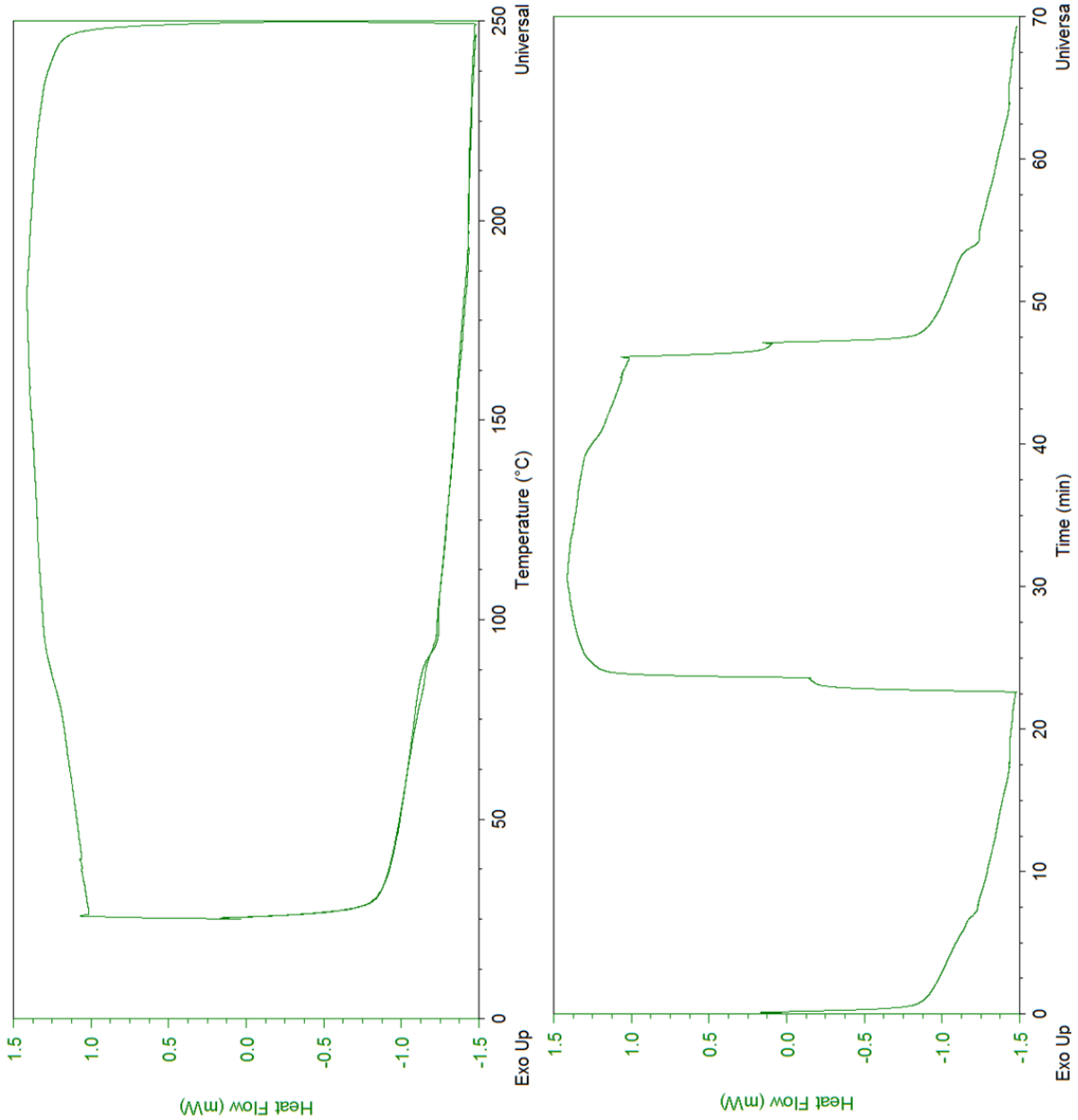

DP_n40 branched plus DP_n10 linear

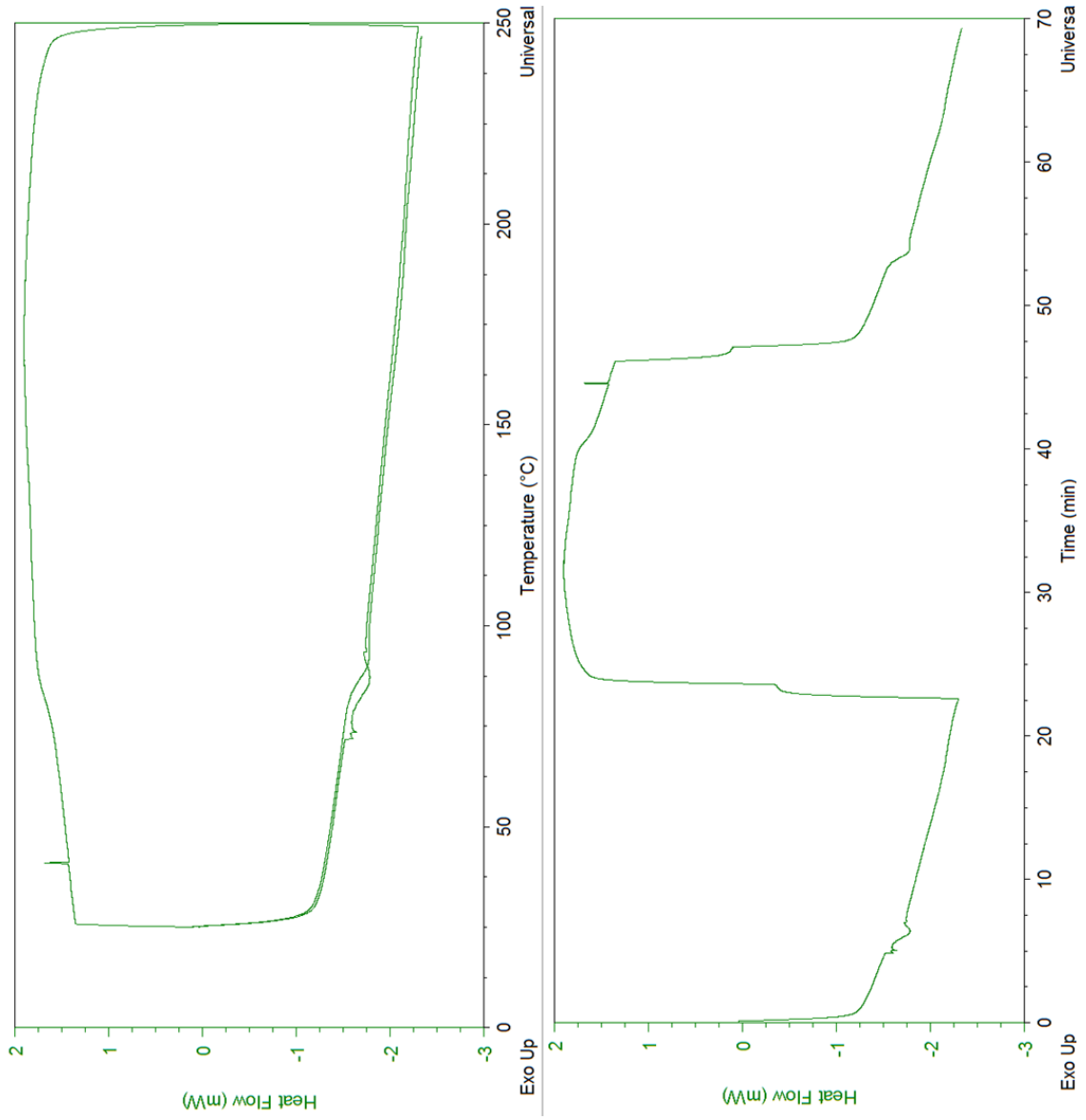

DP_n50 Branched, DVB, 1:1.6

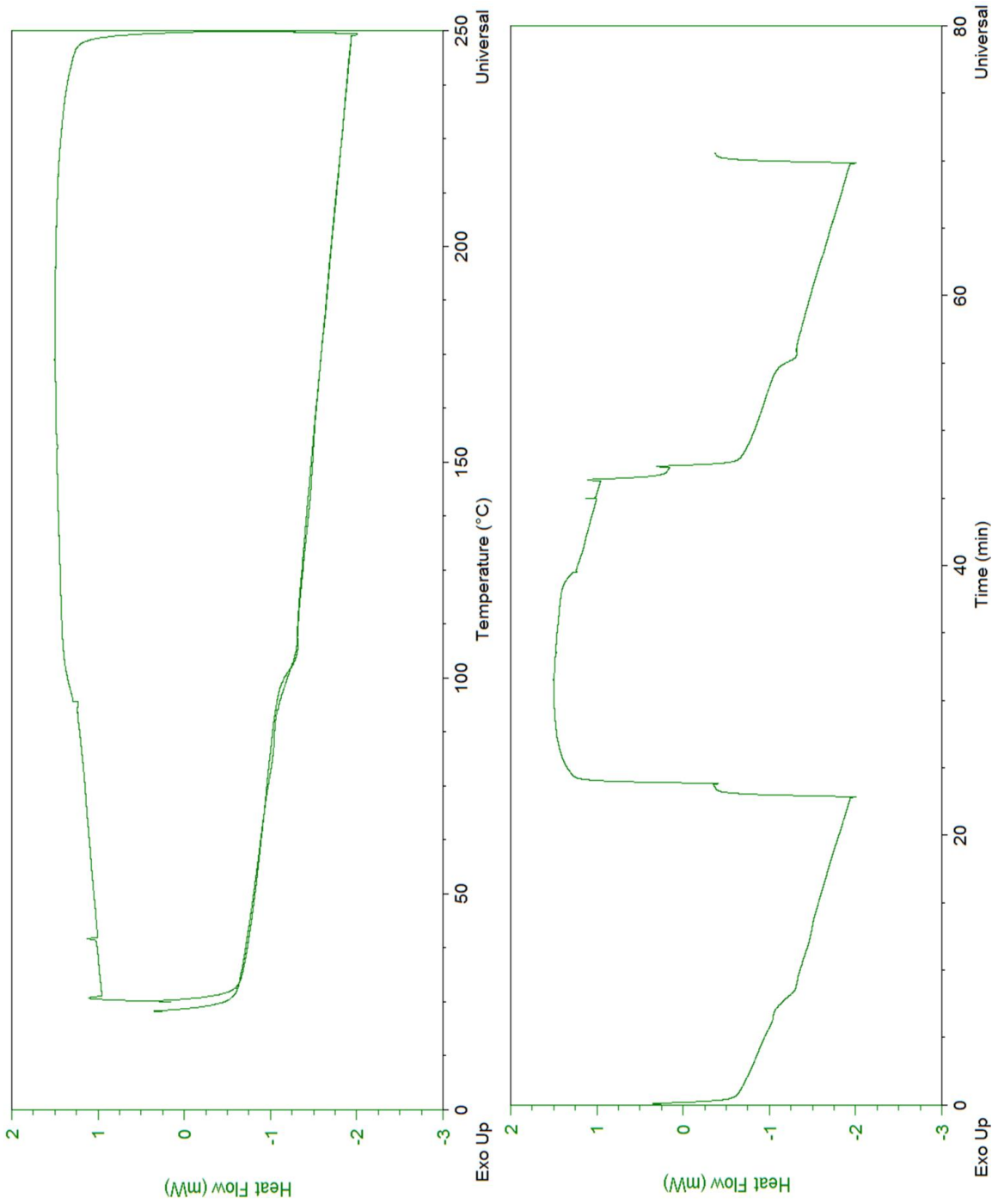

DPn50 Branched, VPOB 1:1.4

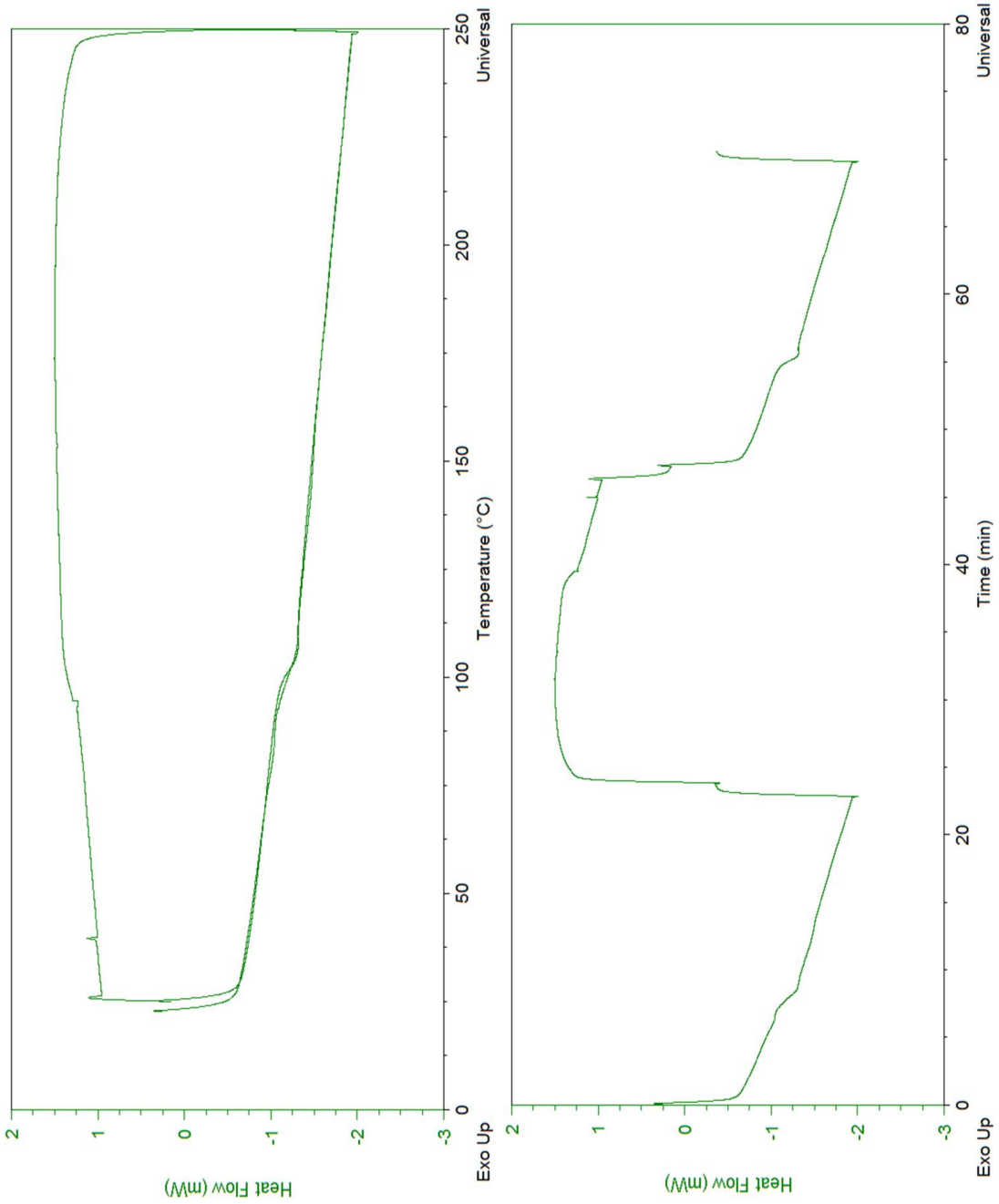

DP_n50 Branched VPOHEX, 1:1.4

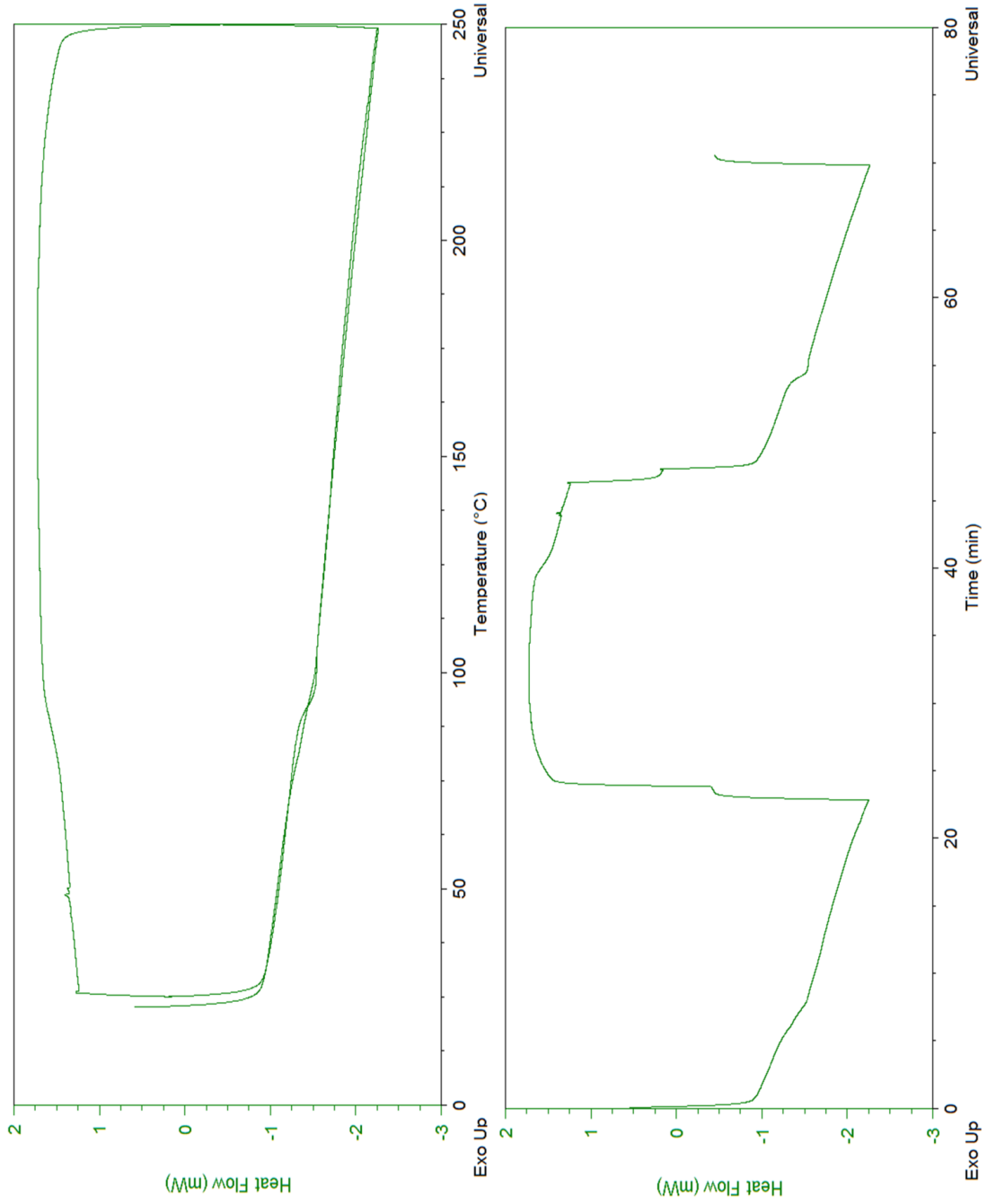

DPn50 Branched, VPOOC 1:1.4

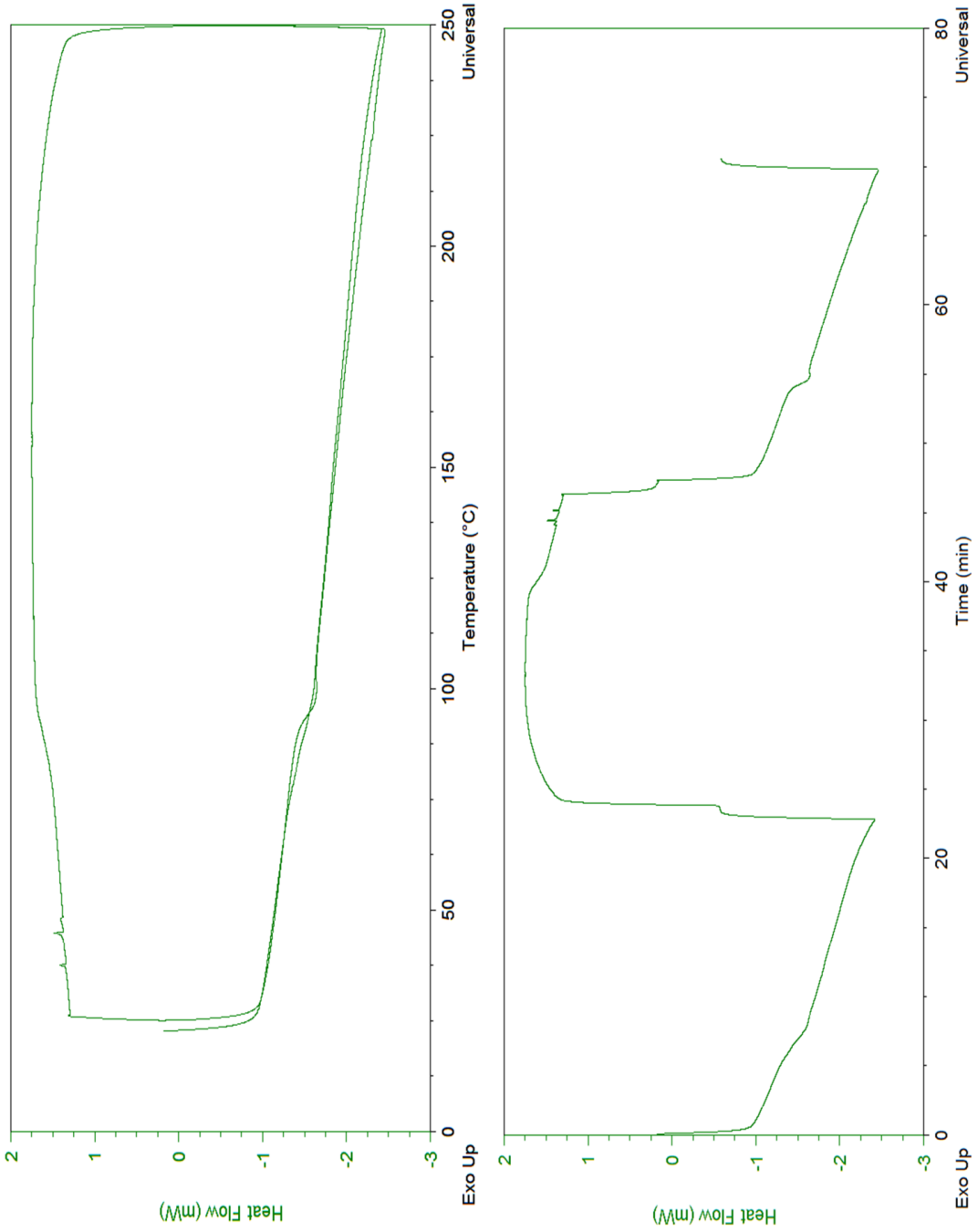

DPn50 Branched , VPOT, 1:1.2

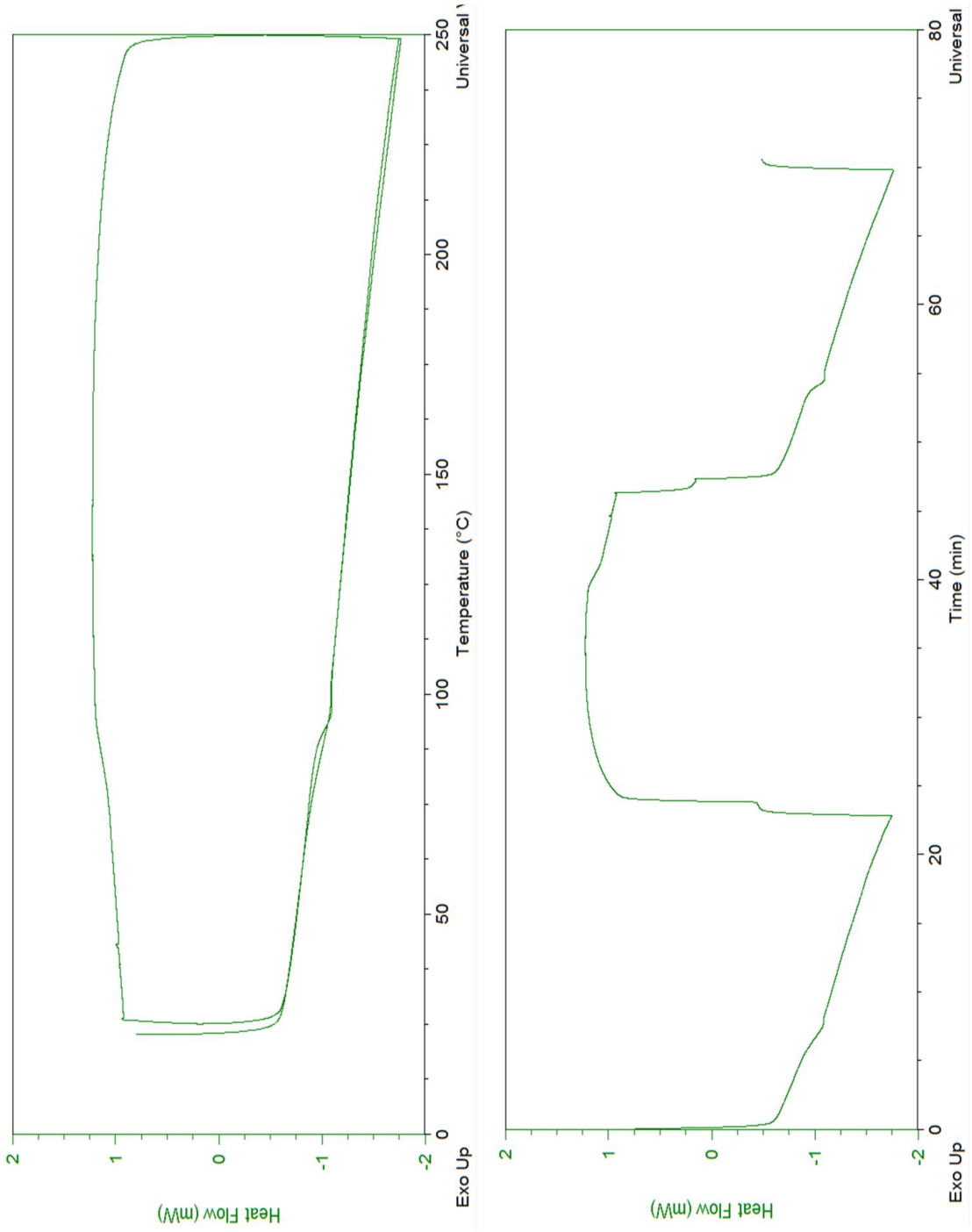

DPn50 Branched, VPODD, 1:0.9

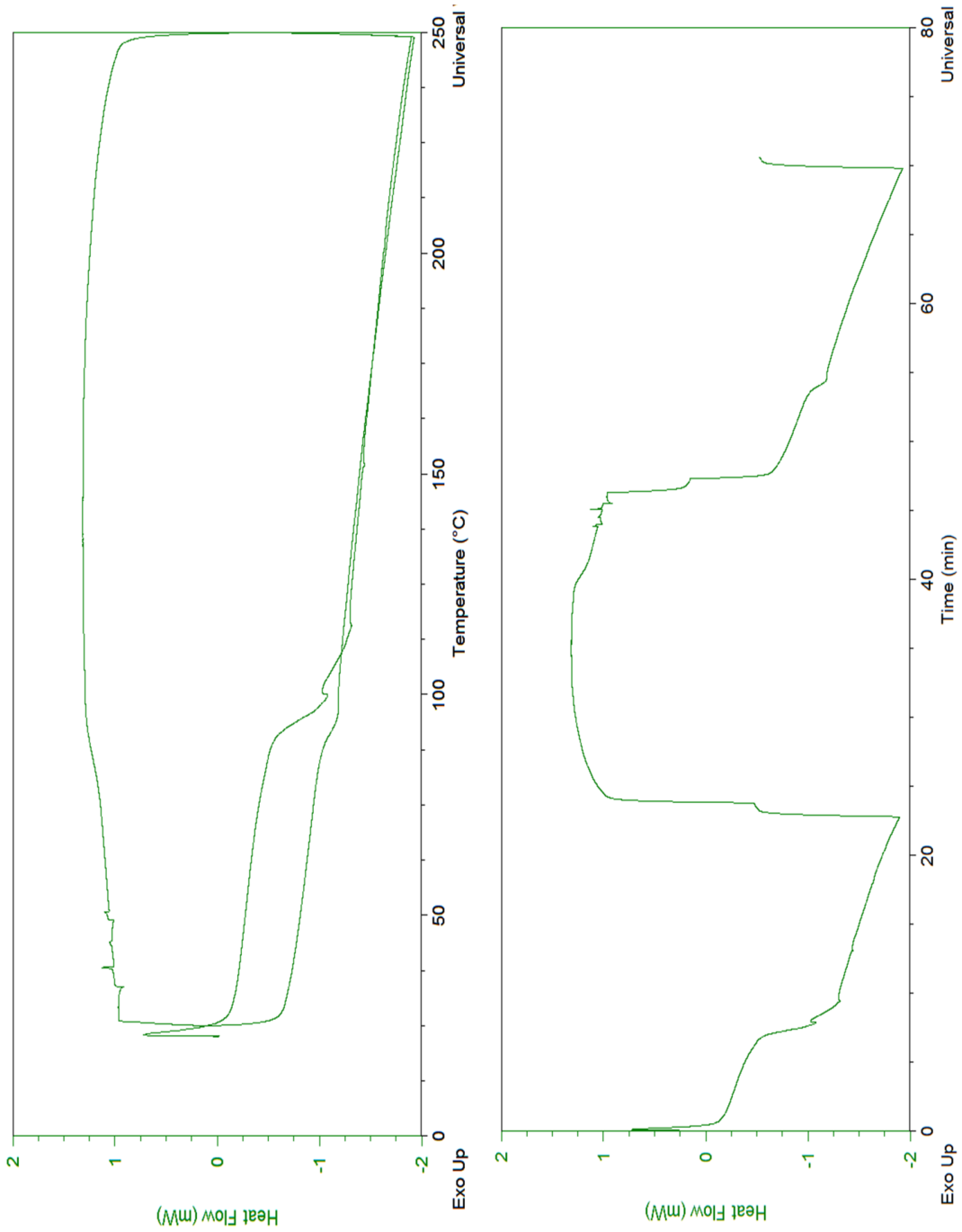

Appendix 3

^{13}C NMR Specta

Chapter 4

4.4 Branching with alternative dystyrl brancher compounds

^{13}C NMR spectrum of VPOB

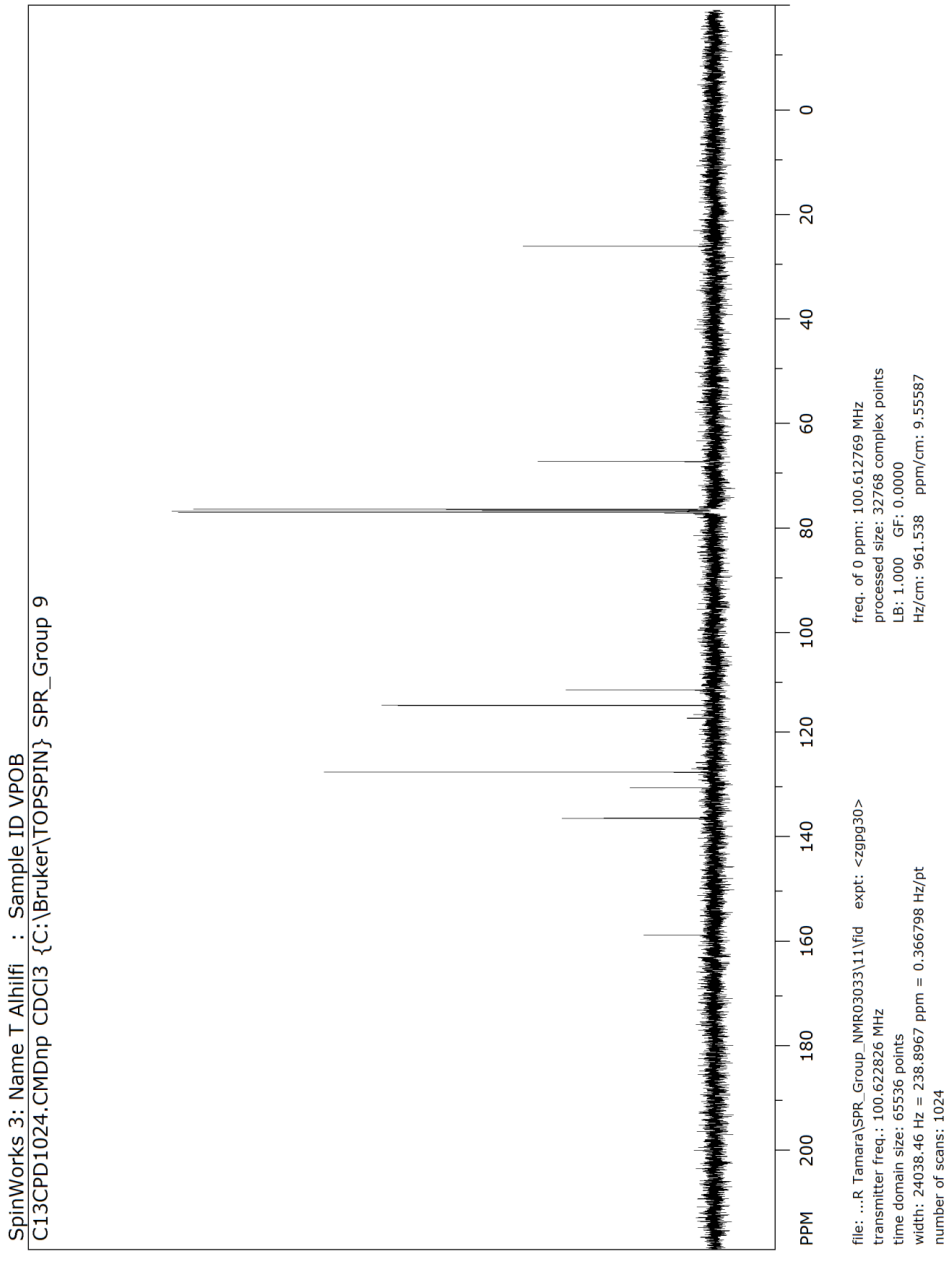

^{13}C NMR spectrum of VPOHEX

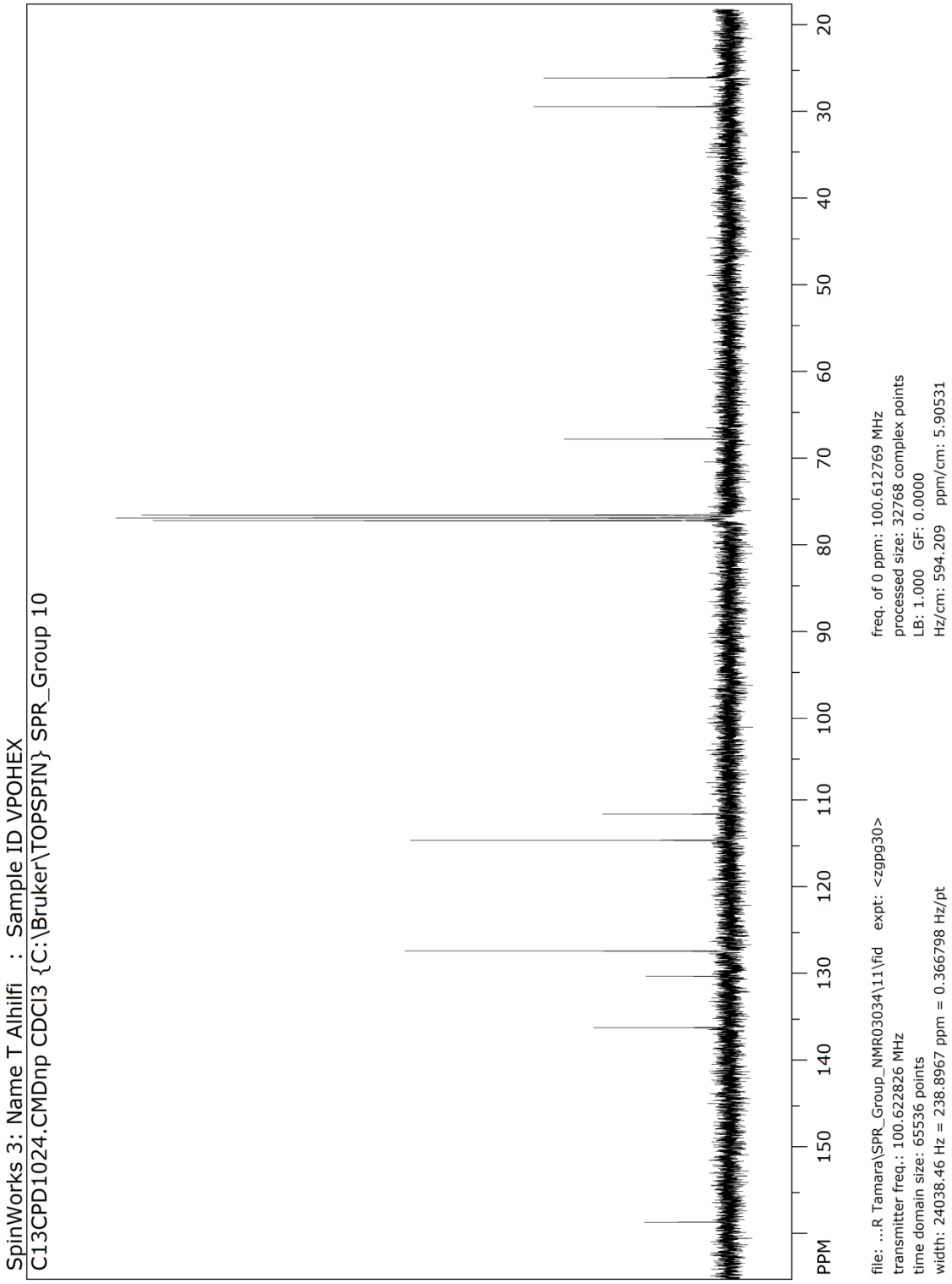

^{13}C NMR spectrum of VPOOC

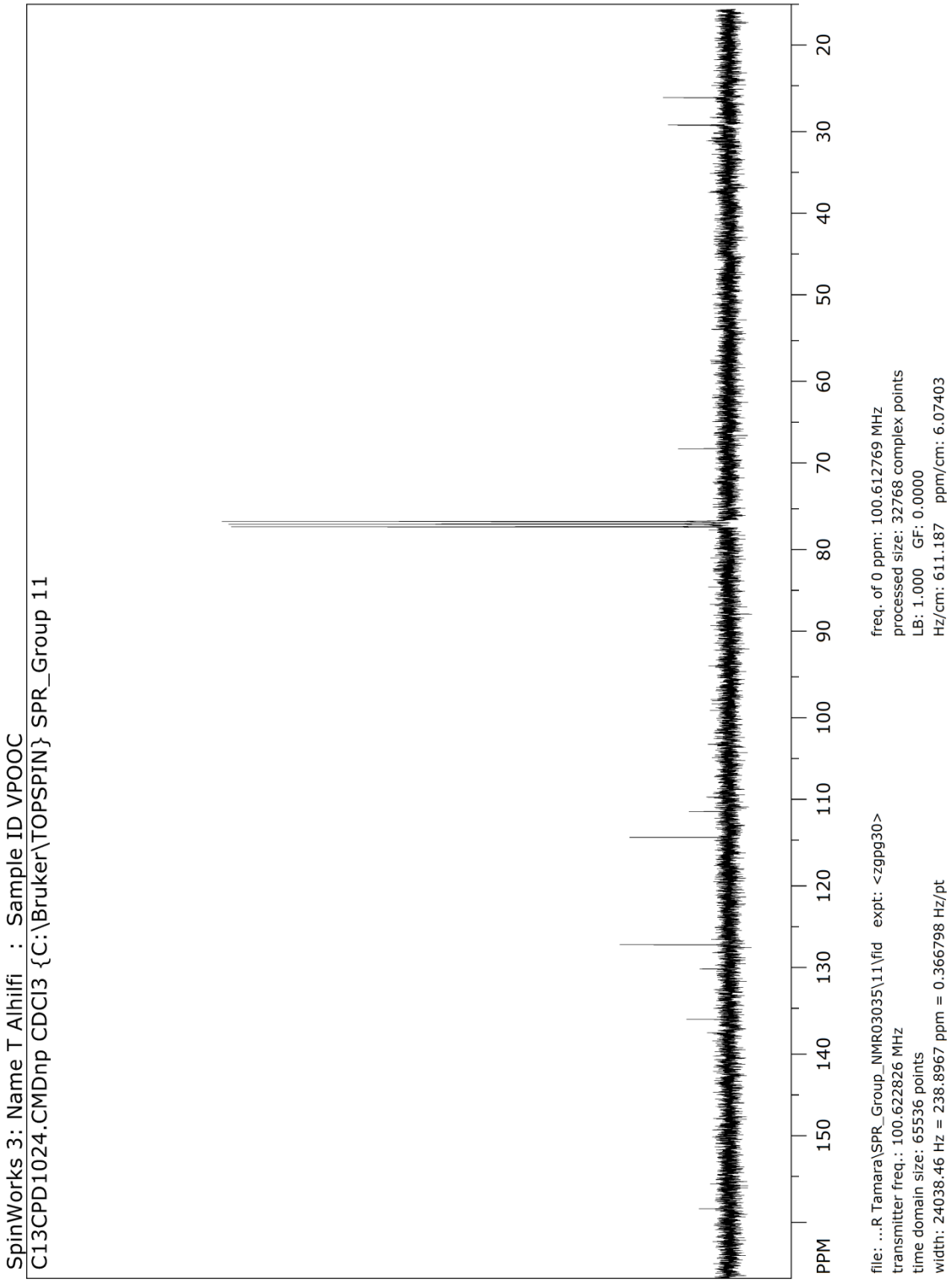

^{13}C NMR spectrum of VPOT

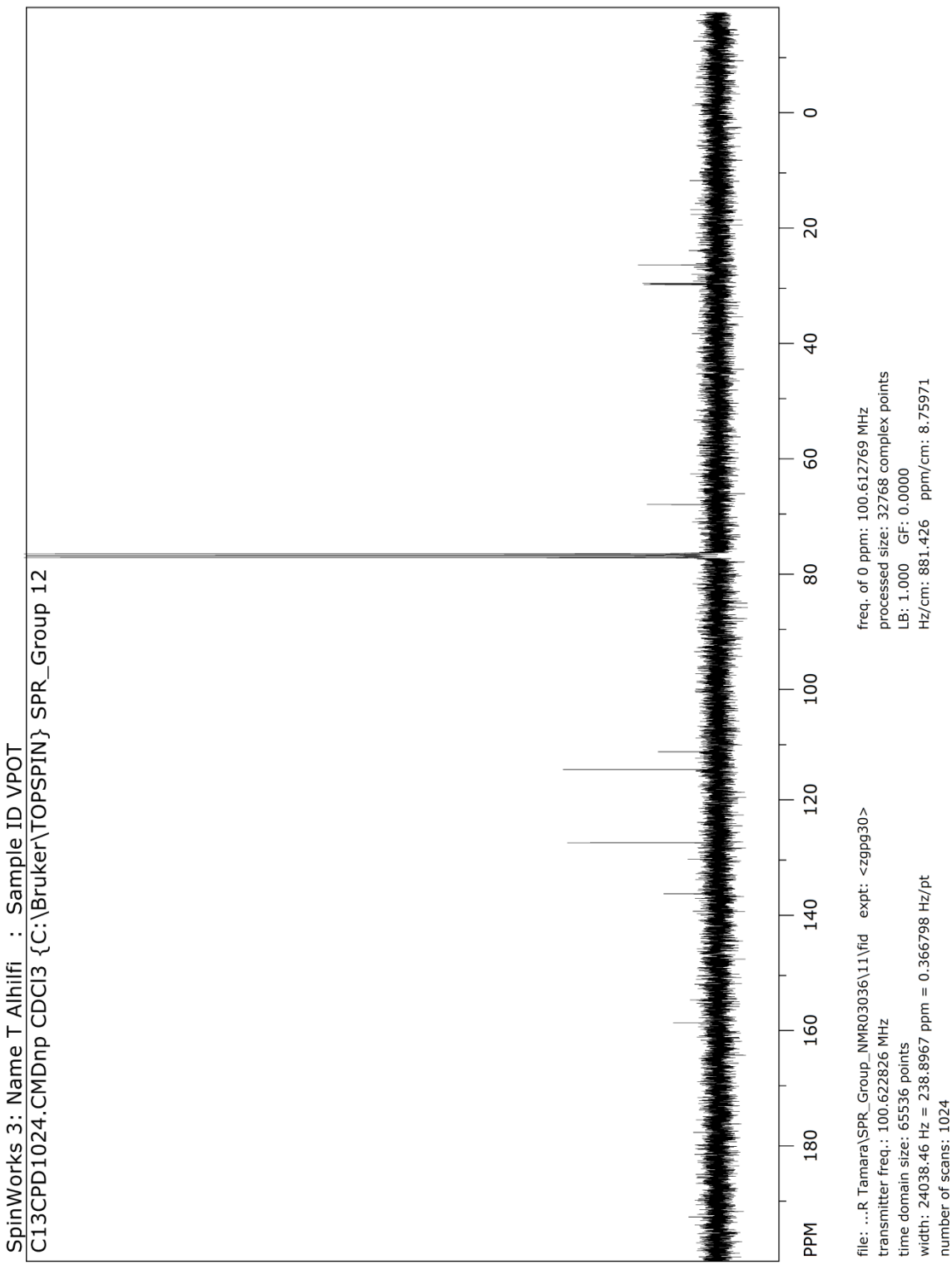

^{13}C NMR spectrum of VPODD